Complex Neurological Diseases:

Insights from genetics and neuroimaging

Hieab H.H. Adams

Acknowledgements:
Financial support for the publication of this thesis by STW, the Dutch Heart Foundation, MS Research, Alzheimer Nederland, and the departments of Epidemiology and Radiology of the Erasmus MC, is gratefully acknowledged.

ISBN: 978-94-6233-471-7

Cover: Concept and design by Hadie Adams, 3D printing by OMNIengineering, photography by Human Adams.

Layout: Hieab Adams.

Printing: Gildeprint, Enschede.

Complex neurological diseases:

Insights from genetics and neuroimaging

Complexe neurologische ziekten:

Inzichten vanuit de genetica en beeldvorming van de hersenen

Proefschrift

ter verkrijging van de graad van doctor aan de
Erasmus Universiteit Rotterdam
op gezag van de
rector magnificus

Prof.dr. H.A.P. Pols

en volgens besluit van het College voor Promoties.
De openbare verdediging zal plaatsvinden op

dinsdag 22 november 2016 om 15.30 uur

door

Hieab Adams
geboren te Heerlen, Nederland

Erasmus University Rotterdam

PROMOTIECOMMISSIE

Promotoren	Prof.dr. A. Hofman
	Prof.dr. A. van der Lugt
Overige leden	Prof.dr. S. Kushner
	Prof.dr. B. Franke
	Prof.dr. H.J. Grabe
Copromotoren	Dr. M.A. Ikram
	Dr. M.W. Vernooij
Paranimfen	Sirwan Darweesh
	Gennady Roshchupkin

To my family

TABLE OF CONTENTS

MANUSCRIPTS UPON WHICH THIS THESIS IS BASED

Chapter 2.1:**Adams HH**, Cavalieri M, Verhaaren BF, Bos D, van der Lugt A, Enzinger C, Vernooij MW, Schmidt R, Ikram MA. Rating method for dilated virchow-robin spaces on magnetic resonance imaging. *Stroke*. 2013;44:1732-1735

Chapter 2.2: **Adams HH**, Hilal S, Schwingenschuh P, Wittfeld K, van der Lee SJ, DeCarli C, Vernooij MW, Katschnig-Winter P, Habes M, Chen C, Seshadri S, van Duijn CM, Ikram MK, Grabe HJ, Schmidt R, Ikram MA. A priori collaboration in population imaging: The uniform neuro-imaging of virchow-robin spaces enlargement consortium. *Alzheimers Dement (Amst)*. 2015;1:513-520

Chapter 2.3: **Adams HH**, Adams H, Launer LJ, Seshadri S, Schmidt R, Bis JC, Debette S, Nyquist PA, Van der Grond J, Mosley TH, Yang J, Teumer A, Hilal S, Roshchupkin GV, Wardlaw JM, Satizabal CL, Hofer E, Chauhan G, Smith AV, Yanek LR, Van der Lee SJ, Trompet S, Chouraki V, Arfanakis KA, Becker JT, Niessen WJ, De Craen AJ, Crivello FF, Lin LA, Fleischman DA, Wong TY, Franco OH, Wittfeld K, Jukema JW, De Jager PL, Hofman A, DeCarli C, Rizopoulos D, Longstreth WT, Mazoyer BM, Gudnason V, Bennett DA, Deary IJ, Ikram MK, Grabe HJ, Fornage M, Van Duijn CM, Vernooij MW, Ikram MA. Partial derivatives meta-analysis: Pooled analyses when individual participant data cannot be shared. *bioRxiv*. 2016:038893

Chapter 2.4: Roshchupkin G, **Adams HH**, Vernooij M, Hofman A, van Duijn C, Ikram MA,** Niessen W.** Hase: Framework for efficient high-dimensional association analyses. *Scientific reports*. In press.

Chapter 2.5: **Adams HH**, Swanson SA, Hofman A, Ikram MA. Amyloid-β transmission or unexamined bias [quest]. *Nature*. 2016;537:E7-E9

Chapter 3.1.1: **Adams HH**,* Hibar DP,* Chouraki V,* Stein JL,* Nyquist PA,* Renteria ME,* Trompet S,* Arias-Vasquez A,* […], Launer LJ,** Schumann G,** Fornage M,** Franke B,** Debette S,** Medland SE,** Ikram MA,** Thompson PM.** Novel genetic loci underlying human intracranial volume identified through genome-wide association. *Nat Neurosci*. 2016

Chapter 3.1.2: Hibar DP,* **Adams HH**,* Jahanshad N,* Chauhan G,* Stein JL,* Hofer E,* Renteria ME,* Bis JC,* […], Schumann G,** Grabe HJ,** Franke B,** Launer LJ,** Medland SE,** Seshadri S,** Thompson PM,** Ikram MA.** Novel genetic loci underlying human intracranial volume identified through genome-wide association. *Nat Comm*. In press.

Chapter 3.1.3: Satizabal CL*, **Adams HH***, Hibar DP, CHARGE consortium, ENIGMA consortium, Thompson PM, Seshadri S**, Ikram MA**. Genetic Determinants of MRI subcortical brain structures: 20 novel loci identified through GWAS in 26,000 persons. *In preparation*.

Chapter 3.2.1: Ikram MA, Bersano A, Manso-Calderón R, Jia J, Schmidt H, Middleton L, Nacmias B, Siddiqi S, **Adams HH**. Genetics of Vascular Dementia: Consensus Report from the ICVD Working Group. *Submitted*.

Chapter 3.2.2: **Adams HH**, Ikram MA, Vernooij MW, van Dijk AC, Hofman A, Uitterlinden AG, van Duijn CM, Koudstaal PJ, Franco OH, van der Lugt A, Bos D. Heritability and genome-wide association analyses of intracranial carotid artery calcification: The rotterdam study. *Stroke*. 2016;47:912-917

Chapter 3.3.1: **Adams HH***, Teumer A*, Hibar DP*, Roshchupkin GV*, […], Niessen WJ**, Paul M Thompson**, Grabe HJ**, Ikram MA**. Genetic architecture of the human anterior commissure. *In preparation*.

Chapter 3.3.2: **Adams HH***, Verlinden VJ*, Callisaya ML, van Duijn CM, Hofman A, Thomson R, Uitterlinden AG, Vernooij MW, van der Geest JN, Srikanth V, Ikram MA. Heritability and genome-wide association analyses of human gait suggest contribution of common variants. *J Gerontol A Biol Sci Med Sci*. 2016;71:740-746

Chapter 3.3.3: Roshchupkin GV*, Gutman BA*, Vernooij MW, Jahanshad N, Martin NG, Hofman A, McMahon KL, Van der Lee S, Van Duijn CM, De Zubicaray G, Uitterlinden AG, Wright MJ, Niessen WJ, Thompson PM, Ikram MA**, **Adams HH****. Heritability of the shape of subcortical brain structures in the general population. *Nat Comm*. In press.

Chapter 3.3.4: Van der Lee S*, Roshchupkin GV*, **Adams HH***, Schmidt H, Hofer E, Saba Y, Schmidt R, Hofman A, Amin N, Van Duijn CM, Vernooij MW, Ikram MA, Niessen WJ. Grey matter heritability in family-based and population-based studies using voxel-based morphometry. *Submitted*.

Chapter 4.1.1: Chauhan G*, **Adams HH***, Bis JC, Weinstein G, Yu L, Toglhofer AM, Smith AV, van der Lee SJ, Gottesman RF, Thomson R, Wang J, Yang Q, Niessen WJ, Lopez OL, Becker JT, Phan TG, Beare RJ, Arfanakis K, Fleischman D, Vernooij MW, Mazoyer B, Schmidt H, Srikanth V, Knopman DS, Jack CR, Jr., Amouyel P, Hofman A, DeCarli C, Tzourio C, van Duijn CM, Bennett DA, Schmidt R, Longstreth WT, Jr., Mosley TH, Fornage M, Launer LJ, Seshadri S, Ikram MA, Debette S. Association of alzheimer's disease gwas loci with mri markers of brain aging. *Neurobiol Aging*. 2015;36:1765 e1767-1716

Chapter 4.1.2: Peymani A, **Adams HH**, Cremers LG, Krestin G, Hofman A, van Duijn CM, Uitterlinden AG, van der Lugt A, Vernooij MW, Ikram MA. Genetic determinants of unruptured intracranial aneurysms in the general population. *Stroke*. 2015;46:2961-2964

Chapter 4.1.3: Vojinovic D, **Adams HH**, van der Lee SJ, Ibrahim-Verbaas CA, Brouwer R, van den Hout MC, Oole E, van Rooij J, Uitterlinden A, Hofman A, van IWF, Aartsma-Rus A, van Ommen GB, Ikram MA, van Duijn CM, Amin N. The dystrophin gene and cognitive function in the general population. *Eur J Hum Genet*. 2015;23:837-843

Chapter 4.2.1: Roshchupkin GV*, **Adams HH***, van der Lee SJ*, Vernooij MW, van Duijn CM, Uitterlinden AG, van der Lugt A, Hofman A, Niessen WJ, Ikram MA. Fine-mapping the effects of alzheimer's disease risk loci on brain morphology. *Neurobiol Aging*. 2016;48:204-211

Chapter 4.2.2: **Adams HH**, Verhaaren BF, Vrooman HA, Uitterlinden AG, Hofman A, van Duijn CM, van der Lugt A, Niessen WJ, Vernooij MW, Ikram MA. Tmem106b influences volume of left-sided temporal lobe and interhemispheric structures in the general population. *Biol Psychiatry*. 2014;76:503-508

Chapter 4.2.3: **Adams HH**, Vernooij MW, Ikram MA. No evidence for a recessive effect of tmem106b rs1990622 variant in the general population. *Journal of Alzheimer's Disease*. 2015

Chapter 4.2.4: Ikram MA, Vernooij MW, Roshchupkin GV, *, Hofman A, Van Duijn CM, Uitterlinden AG, Niessen WJ, Hintzen RQ, **Adams HH**. Genetic susceptibility to multiple sclerosis: brain structure and cognitive function in the general population. *Submitted*.

Chapter 5.1.1: **Adams HH**, Schwingenschuh P, Wittfeld K, Hilal S, Ikram MA, Katschnig-Winter P, Habes M, Chen C, Seshadri S, van Duijn CM, Ikram MK, Grabe HJ, Schmidt R, Vernooij MW. Determinants of enlarged perivascular spaces in the general population: a pooled analysis of individual participant data in the UNIVRSE consortium**.** *In preparation*.

Chapter 5.1.2: Mutlu U, **Adams HH**, Hofman A, Lugt A, Klaver CC, Vernooij MW, Ikram MK, Ikram MA. Retinal microvascular calibers are associated with enlarged perivascular spaces in the brain. *Stroke*. 2016;47:1374-1376

Table of contents

Chapter 5.2.1: **Adams HH**, de Bruijn RF, Hofman A, Uitterlinden AG, van Duijn CM, Vernooij MW, Koudstaal PJ, Ikram MA. Genetic risk of neurodegenerative diseases is associated with mild cognitive impairment and conversion to dementia. *Alzheimers Dement*. 2015;11:1277-1285

Chapter 5.2.2: Darweesh SK*, Verlinden VJ*, **Adams HH***, Uitterlinden AG, Hofman A, Stricker BH, van Duijn CM, Koudstaal PJ, Ikram MA. Genetic risk of parkinson's disease in the general population. *Parkinsonism Relat Disord*. 2016;29:54-59

The complete references for these manuscripts can be found in the appendix.

Chapter 1

General introduction

INTRODUCTION

The brain is a highly interconnected organ, communicating both with itself as well as with other parts of the body. It is involved in many of our daily activities, from holding this thesis (motor function), seeing the individual words (processing sensory information), to understanding their meaning (cognitive function). As Michio Kaku put it: "Sitting on your shoulders is the most complicated object in the known universe."[1] While the complexity of the brain is a beautiful product of millions of years of evolution, at the same time it has left us with an organ that is highly vulnerable to damaging processes, with large clinical consequences. Among the most common and debilitating neurological diseases are those that are of a neurodegenerative or cerebrovascular nature, which are the primary focus of this thesis.

Research into the pathophysiology of neurological diseases seeks to determine what goes wrong in the brains of patients. Instrumental in this have been two fields of study: neuroimaging and genetics. On the one hand, neuroimaging technologies such as magnetic resonance imaging (MRI) have allowed researchers to non-invasively examine the brain of living individuals and visualize various structural and functional abnormalities. This has led to the identification of brain structures that are important for diseases, which in turn helped to better understand clinical symptoms. Furthermore, neuroimaging sometimes even shows signs of damage before a person has noticeable problems. Indeed, for many neurodegenerative and cerebrovascular diseases, evidence of an ongoing pathophysiological process can precede the moment of clinical presentation by years to even decades.[2-4] Even so, the exact neural substrate of these brain diseases remains unclear. Novel imaging markers have emerged from technical advances in the acquirement and processing of images and provide an opportunity to shed light on the pathophysiology of neurological disorders; for the majority of these markers, however, the clinical relevance has yet to be explored.

On the other hand, genetics has played an essential role in research on neurological diseases, which have varying degrees of heritability.[5-8] Early genetic discoveries in the field of neurodegenerative and cerebrovascular diseases stem mostly from monogenic forms of disease that aggregate in families. Examples of these include *APP* in Alzheimer's

disease,[9] *NOTCH3* in stroke,[10] *SNCA* in Parkinson's disease.[11] However, sporadic cases tend to have a more complex genetic architecture, with many genetic variants increasing risk only marginally. Genome-wide association studies (GWAS) in tens of thousands of individuals has resulted in the identification of hundreds of genetic variants.[12-19] While these findings have provided insight into the affected biological pathways, they have generally explained only a small amount of the variance in disease susceptibility. To uncover the so-called 'missing heritability',[20] studies are ongoing with even larger sample sizes and implementing next-generation sequencing technologies to capture more of the genetic variation.

Neuroimaging and genetics have, as individual fields, undeniably increased our understanding of neurological diseases. Nevertheless, recent advancements within each of these fields pave the way for further insights into disease by studying novel imaging markers and newly discovered genetic risk variants. Furthermore, the combination of both fields, also called 'imaging genetics', has even more potential. The effects of neurological disease genes are likely to be reflected in the brain and, conversely, observations on neuroimaging can have a substantial genetics basis. Imaging genetics tries to leverage these interrelations in order to gain knowledge about neurological diseases that would have been untapped by studying imaging or genetics separately.

METHODOLOGY

The innovative nature of both imaging and genetics, and more so of their combination, has resulted in analytical demands beyond our current capabilities. Chapter 2 of this thesis is dedicated to the development of methodology to enable such studies. First, I describe a method for assessing a novel neuroimaging marker, enlarged perivascular spaces on MRI – an emerging marker of cerebrovascular disease – (chapter 2.1) and the initiation of a global consortium to systematically investigate the clinical relevance of this marker (chapter 2.2). In chapter 2.3, I present a novel meta-analytical method that increases power and flexibility when individual participant data cannot be shared between sites, which is a common issue in genetic studies that require multi-site efforts. Chapter 2.4 covers a method to perform genome-wide and brain-wide association studies, a theoretical possibility in imaging genetics that is currently not feasible due to

computational and logistic limitations. Finally, chapter 2.5 highlights potential biases in a recent study on the transmissibility of amyloid-β , which can impact causal inference.

This methodological chapter is followed by three applied chapters.

GENETIC DISCOVERIES

Chapter 3 describes genetic discoveries of imaging markers. Those markers previously linked to neurodegeneration, mostly measures of the structure of the brain, are the focus of chapter 3.1. I describe GWAS of intracranial volume (chapter 3.1.1) , hippocampal volume (chapter 3.1.2), and the volumes of other subcortical brain structures (chapter 3.1.3) in the largest discovery samples to date, identifying 33 novel genetic variants in 25,000-34,000 individuals. Neuroimaging can also assess the burden of cerebrovascular disease, which is covered by chapter 3.2. Chapter 3.2.1 reviews our current knowledge of the genetics of cerebrovascular disease. Next, I describe the first heritability estimates and GWAS of intracranial carotid artery calcification in chapter 3.2.2.

In chapter 3.3 I study emerging imaging markers, which are not as established as those described earlier in this chapter. The anterior commissure is a recently proposed imaging marker for neurodegeneration, and I describe the first heritability and GWAS analyses in chapter 3.3.1. Similarly, the results in chapter 3.3.2 are the first comprehensive description of the genetic determinants of human gait, as imaged by an electronic walkway. Furthermore, emerging neuroimaging phenotypes can describe brain structure with great detail on a vertex- or voxel-wise level using thousands to millions of measures. For two of such phenotypes, we found them to be promising targets for genetic studies: the shape of subcortical brain structures (chapter 3.3.3) and the grey matter density using voxel-based morphometry (chapter 3.3.4).

UNDERSTANDING PATHOPHYSIOLOGY

Chapter 4 explores the effects of known disease genes on the brain. Chapter 4.1 considers disease variants in relation to candidate imaging markers: Alzheimer's disease variants and several key vascular and degenerative markers (chapter 4.1.1), intracranial

aneurysm variants and the presence and size of aneurysms (chapter 4.1.2), and the dystrophin gene and cognitive function (chapter 4.1.3). Contrary to the candidate markers of chapter 4.1, those in chapter 4.2 have been selected in an unbiased approach. This which includes brain-wide studies of genetics variants that increase the risk of Alzheimer's disease (chapter 4.2.1), frontotemporal lobar degeneration (chapter 4.2.2 and chapter 4.2.3), and multiple sclerosis (chapter 4.2.4).

EXPLORING CLINICAL RELEVANCE

Chapter 5 examines the clinical relevance of neuroimaging and genetics beyond making genetic discoveries and understanding pathophysiology. Given that many imaging markers are novel, their clinical relevance is yet unclear. In chapter 5.1, I determine clinical correlates of a variety of enlarged perivascular spaces, a novel imaging marker: I study various demographic and cardiovascular determinants of these enlarged perivascular spaces (chapter 5.1.1) and also their relation to the retinal microvasculature (chapter 5.1.2). Similarly, the clinical relevance of recently identified genetic variants that increase the risk for neurological diseases is largely unknown. This is explored in chapter 5.2, with a specific focus on the ability to improve prediction of symptoms and disease at an individual level. This was done for genetic risk factors of four neurodegenerative diseases in relation to mild cognitive impairment and incident dementia (chapter 5.2.1), and also for genetic risk of Parkinson's disease in relation to basic activities of daily living and incident Parkinson's disease (chapter 5.1.2).

GENERAL DISCUSSION

Both neuroimaging and genetics have expanded our knowledge of brain diseases. While these advances were largely driven by discoveries in each of these fields separately, joint analyses of imaging and genetics can yield even more insight into the pathophysiology of diseases and perhaps translate into useful tools for clinicians. In chapter 6, the findings described in this thesis are reflected upon from the broader perspective of complex diseases. I conclude with a discussion of the implications for future research.

REFERENCES

1. Egan J. *1000 historic quotes*. LULU Press; 2015.
2. Jack CR, *et al.* The Lancet Neurology. 2013
3. Vermeer, *et al.* NEJM. 2003
4. Wong TY, *et al.* Jama. 2002
5. Bevan S, *et al.* Stroke. 2012
6. Gatz M, *et al.* The Journals of Gerontology Series A: 1997
7. Keller MF, *et al.* Human molecular genetics. 2012
8. Sadovnick AD, *et al.* The Lancet. 1996
9. Mullan M, *et al.* Nature genetics. 1992
10. Joutel A, *et al.* Nature. 1996
11. Polymeropoulos, *et al.* Science. 1997
12. Fogh I, *et al.* Human molecular genetics. 2013
13. Lambert J-C, *et al.* Nature genetics. 2013
14. Nalls, *et al.* Nature genetics. 2014
15. CHARGE *et al.* The Lancet Neurology. 2016
16. IMSGC. Nat genetics. 2013
17. Gormley *et al.* bioRxiv. 2015
18. PGC. Nature. 2014
19. Van Deerlin VM, *et al.* Nature genetics. 2010
20. Manolio *et al.* Nature. 2009

.

Chapter 2

Methodology

Chapter 2.1

Rating method for enlarged perivascular spaces

ABSTRACT

Background and Purpose: Dilated Virchow-Robin spaces (dVRS) are an emerging neuroimaging biomarker, but their assessment on MRI needs standardization.

Methods: We developed a rating method for dVRS in four brain regions (centrum semi-ovale, basal ganglia, hippocampus and mesencephalon) and tested its reliability in a total of 125 MRI scans from two population based studies. Six investigators with varying levels of experience performed the ratings. Intraclass correlation coefficients (ICC) were calculated to determine intra- and inter-rater reliability.

Results: Intra-rater reliability was excellent for all four regions (ICC>0.8). Inter-rater reliability was excellent for the centrum semi-ovale and hippocampus (ICC>0.8) and good for the basal ganglia and mesencephalon (0.6–0.8). This did not differ between the cohorts or experience levels.

Conclusions: We describe a reliable rating method that can facilitate etiologic and prognostic research on dVRS using MRI.

INTRODUCTION

The study of imaging biomarkers plays an essential role in understanding brain aging as well as pathology, such as cognitive impairment, dementia, and cerebrovascular disease.[21] Structural imaging studies have already shown the importance of white matter lesions, infarcts and more recently cerebral microbleeds.[21] An emerging potential marker are Virchow-Robin spaces (VRS), spaces filled with interstitial fluid that surround the blood vessels in the brain.[22] VRS can increase in size and such dilated VRS (dVRS) can subsequently be found on brain imaging,[23] particularly in the mesencephalon, hippocampus, basal ganglia and centrum semi-ovale.[24, 25] Determinants of dVRS severity include age,[26] blood pressure[26] and inflammation.[27] The associated brain pathology is diverse, covering small vessel disease,[26 28,29] Alzheimer's disease[24,29,30] and CADASIL.[31]

Despite increasing literature on dVRS, a major limitation of current research is the lack of a robust and generalizable rating method on MRI. Current methods are restricted to studies that only use a single MRI protocol and focus on one or two brain regions.[23, 24, 26, 28, 29, 31] A method that can be applied to MRI protocols from different centers and scanners and evaluates the whole brain would strongly facilitate etiologic and prognostic research on dVRS. Here we propose a novel rating method for dVRS, which we apply in two population-based studies, encompassing three different scanning protocols.

METHODS

We aimed to develop a rating protocol meeting three preconditions. First, the method should be standardized and generalizable across various MRI protocols. Second, intra- and inter-rater agreement should be high, irrespective of rater experience. Third, the method should be easily applicable for other researchers without requiring complex image processing.

Setting

We used MRI-scans from two population-based cohort studies: the Austrian Stroke Prevention Study (ASPS)[32] and Rotterdam Scan Study (RSS).[33] The ASPS is a prospective community-based study investigating the effects of vascular risk factors on brain

structure and function in residents of Graz, Austria (aged ≥45 years). Between 1999-2003, a diagnostic work-up including MRI was done. Scans were obtained on a 1.5T Philips scanner. The MRI-protocol included axial T1-, T2-, proton-density-weighted and fluid attenuated inversion recovery (FLAIR) sequences. The study protocol was described previously.[32] The RSS investigates causes and determinants of chronic neurological diseases in the elderly (aged ≥45 years). Participants are residents of Ommoord, a suburb of Rotterdam, the Netherlands. Brain MRI was incorporated into the core study-protocol from 2005 onwards using a 1.5T GE MR unit. The protocol has been extensively described and includes axial T1-, T2-weighted and FLAIR sequences.[33] Earlier in 1995, a smaller MRI study was performed using a 1.5T Siemens system with the protocol including T1- and T2-weighted sequences.[33]

Rating Protocol

We developed and applied our rating method on scans from the ASPS and 2005 RSS, since these were acquired with the most up-to-date protocols available. The primary rating sequence was T2-weighted (ASPS: slice thickness 4.5mm, RSS: 1.6mm), which shows VRS as hyperintensities (Figure S1). VRS were identified by their linear, ovoid or round shape depending on the slice direction and considered dilated when their diameter was ≥1mm.[34] Also, since dVRS >3mm in shortest diameter may have a distinct etiology,[23] these large lesions were rated separately and not evaluated in the reliability analyses. For differential diagnosis with lacunar infarcts, symmetry of the lesions, sharp demarcation, and absence of a hyperintense rim on the FLAIR sequence supported rating them as dVRS.[34] White matter lesions (WML) are mostly confluent and were differentiated from dVRS by signal intensity not equivalent to cerebrospinal fluid on T2.

dVRS were scored in four brain regions: the centrum semi-ovale (CSO), basal ganglia (BG), hippocampus and mesencephalon. This choice was based on the pronounced presence of dVRS in these regions that was reported earlier and is known from own experience.[24, 25] Raters determined dVRS count for each region with a maximum of twenty per region. Because CSO and BG are visible on multiple slices, the rating was done on a single, predefined slice to decrease inter- and intra-rater variability. For CSO, this was the slice 1 cm above the lateral ventricles. For BG, this was the slice showing the anterior commissure or, when not visible, the first slice superior to it. In the

hippocampus and mesencephalon, all unique dVRS were counted (Figure 1). A blank rating form is provided as a supplement (File S1).

Reliability Assessment

To assess the intra-rater reliability, one rater (H.H.H.A.) scored 85 scans twice, blinded to his initial rating, separated by more than one month. Inter-rater reliability was assessed on 100 randomly selected scans and 5 additional scans in case of motion artifacts on the initial 100 (40 ASPS, 65 RSS). Every scan was rated independently by three to six investigators with varying degrees of experience (1-2 years: H.H.H.A., M.C., B.F.J.V., D.B., >10 years: C.E. and R.S.) who were blinded to all clinical data. The order of scans was randomized and different for each rater. Afterwards, we also assessed the reliability on 20 scans from the 1995 RSS MRI-protocol rated by three investigators (H.H.H.A., B.F.J.V., D.B.).

Intra-rater and inter-rater reliability was determined using intraclass correlation coefficients (ICC) for all raters combined. Secondary analyses were performed after stratifying by MRI-protocol (ASPS vs. RSS), experience level (1-2 years vs. 10 years) or co-existing brain pathology (WML, atrophy, lacunar infarcts). WML and brain volume were measured with automated software within each cohort and dichotomized at the median value to provide equally-sized groups. For lacunar infarcts, we restricted to participants without lacunar infarcts (n=8).

Table 1 | Study population characteristics.

	Total	RSS	ASPS
Demographics			
Number of participants, n (%)	105 (100)	65 (62)	40 (38)
Age in years, mean (SD)	65.8 (5.8)	66.9 (5.7)	64.0 (5.6)
Women, n (%)	54 (51)	34 (52)	20 (50)
MRI characteristics			
dVRS, mean (SD)			
Centrum semi-ovale	9.6 (6.8)	9.8 (6.5)	9.3 (7.3)
Basal Ganglia	5.3 (3.4)	5.7 (3.6)	4.7 (2.9)
Hippocampus	3.4 (3.1)	4.3 (3.3)	1.8 (2.1)
Mesencephalon	1.8 (1.7)	2.2 (1.9)	1.1 (1.2)
Participants with lacunar infarcts, n (%)	8 (8)	5 (8)	3 (8)
Brain volume as % of intracranial volume (SD)	-*	82.3 (3.5)	79.8 (2.7)
WML volume in mL, mean (SD)	-*	8.2 (1.0)	2.9 (4.7)

**WML and brain volume measures were not pooled because of differences in quantification between the two cohorts.*

Table 2 | Intraclass Correlation Coefficient values for inter-rater and intra-rater reliability.

		CSO	BG	HIP	MES
Intra-rater	Total	0.88	0.80	0.85	0.82
Inter-rater	Total	0.80	0.62	0.82	0.75
By protocol	Rotterdam Scan Study	0.78	0.65	0.81	0.78
	Austrian Stroke Prevention Study	0.85	0.68	0.74	0.74
By experience	1-2 years	0.76	0.64	0.79	0.82
	>10 years	0.74	0.58	0.70	0.83
	Between groups	0.67	0.64	0.77	0.78
By pathology	Small WML volume	0.76	0.65	0.82	0.68
	Large WML volume	0.81	0.57	0.83	0.80
	Small brain volume	0.82	0.67	0.86	0.75
	Large brain volume	0.74	0.59	0.73	0.76
	No lacunar infarct*	0.78	0.61	0.82	0.76

Values based on 105 MRI scans for inter-rater and 85 scans for intra-rater reliability.

**Eight persons with lacunar infarcts were excluded from this analysis.*

BG basal ganglia, CSO = centrum semi-vale, HIP = hippocampaus, MES = mesencephalon

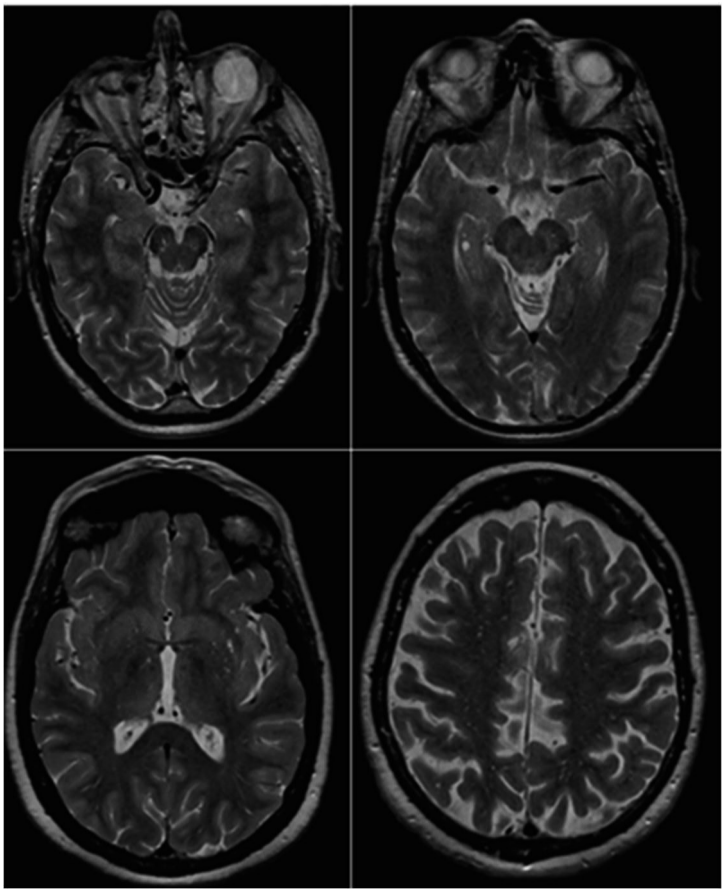

Figure 1 | Examples of the four regions used for rating dilated Virchow-Robin spaces.
A) The mesencephalon with four dVRS, B) hippocampus with two dVRS and one large lesion on the right side, C) basal ganglia with eleven dVRS and D) centrum semi-ovale with more than twenty dVRS.

RESULTS

Study population characteristics are shown in Table 1 (mean age 65.8 (SD 5.8) years, 54 (51%) women). The distribution of the average dVRS count showed most dVRS in the CSO (9.63 (SD 6.79), followed by the BG (5.30 (3.41)), hippocampus (3.35 (3.14)) and mesencephalon (1.78 (1.75)).

Intra-rater reliability for the 85 scans showed nearly perfect agreement (ICC>0.8) for all regions (Table 2). The ICC values for the 105 scans indicate good agreement between raters (ICC between 0.6-0.8) for the BG and mesencephalon and nearly perfect agreement for the CSO and hippocampus (Table 2). Calculating the ICC for RSS and ASPS scans separately gave similar values (Table 2). Furthermore, inter-rater reliability was independent of rater experience, WML burden and brain volume (Table 2). Excluding participants with lacunar infarcts (n = 8) also did not alter the results (Table 2). In the 20 additional scans from the 1995 RSS protocol, ICC values were >0.8 for each region (not shown).

DISCUSSION

We propose a newly developed rating method for dVRS in four brain regions, which shows good to nearly perfect inter-rater and intra-rater agreement, independent of rater experience and concomitant brain pathology. We applied this method to a total of 125 MRI scans acquired from three different scanners and protocols across two cohorts, and found comparable reliabilities.

The proposed rating has several strengths which can facilitate future dVRS research. We developed the protocol on a large dataset of images from different MRI scanners, with multiple raters of differing experience level, and performed secondary analyses for factors potentially affecting observer agreement. Also, we included the four brain regions with most prevalent dVRS, while rater instructions remained simple and time investment was minimal (~3min/scan). Moreover, regular transverse slices were used for scoring, thereby eliminating the need for complex planar reformatting of scans.

Whereas previous studies have only used upper limits in size for defining dVRS,[26, 29, 31] we also implemented a minimum diameter criterion to consider VRS dilated. This is because

the increasing resolution of new MRI scanners will enable detection of many VRS smaller than 1mm, which could inflate the dVRS rating and reduce comparability between studies if not excluded. Morphological criteria were used for differentiation between dVRS, lacunar infarcts and WML.[34] Although reliability of our method was not affected by concomitant brain pathology visible on MRI, the distinction between dVRS and lacunar infarcts in particular remains controversial.[34]

As an alternative to counting dVRS, we considered assigning a severity score to each region after comparison with a consensus-based template. Although preliminary analyses revealed good intra-rater agreement on 30 scans (average of regions: 0.70), inter-rater agreement was weak to moderate (0.48). We therefore did not pursue this approach further. Existing rating protocols were not evaluated, since there currently is no gold standard for quantifying dVRS burden. A future direction would be to compare the reliability across different rating protocols.

In conclusion, this study presents a generalizable rating method for dVRS in the mesencephalon, hippocampus, BG and CSO that has been tested in a multi-center setting. The protocol allows for better comparability between VRS research and is easy to implement by investigators.

REFERENCES

1. Gorelick PB, *et al.* Stroke. 2011
2. Ozturk MH, *et al.* J Comput Assist Tomogr. 2002
3. Groeschel S, *et al.* Neuroradiology. 2006
4. Chen W, *et al.* AJNR Am J Neuroradiol. 2011
5. Zhu YC, *et al.* AJNR Am J Neuroradiol. 2011
6. Zhu YC, *et al.* Stroke. 2010
7. Satizabal CL, *et al.* J Alzheimers Dis. 2013
8. Maclullich AM, *et al.* J Neurol Neurosurg Psychiatry. 2004
9. Patankar TF, *et al.* AJNR Am J Neuroradiol. 2005
10. Zhu YC, *et al.* J Alzheimers Dis. 2010
11. Cumurciuc R, *et al.* Eur J Neurol. 2006
12. Schmidt R, *et al.* Neurology. 1999
13. Ikram MA, *et al.* Eur J Epidemiol. 2011
14. Bokura H, *et al.* J Neurol. 1998

Chapter 2.2

Consortium investigating enlarged perivascular spaces

ABSTRACT

Background: Virchow-Robin spaces (VRS), or perivascular spaces, are compartments of interstitial fluid enclosing cerebral blood vessels and are potential imaging markers of various underlying brain pathologies. Despite a growing interest in the study of enlarged VRS, the heterogeneity in rating and quantification methods combined with small sample sizes have so far hampered advancement in the field.

Methods: The Uniform Neuro-Imaging of Virchow-Robin Spaces Enlargement (UNIVRSE) consortium was established with primary aims to harmonize rating and analysis (see www.uconsortium.org). The UNIVRSE consortium brings together 13 (sub)cohorts from 5 countries, totaling 16.000 subjects and over 25.000 scans. Eight different MRI protocols were used in the consortium.

Results: VRS rating was harmonized using a validated protocol that was developed by the two founding members, with high reliability independent of scanner type, rater experience, or concomitant brain pathology. Initial analyses revealed risk factors for enlarged VRS including increased age, sex, high blood pressure, brain infarcts, and white matter lesions, but this varied by brain region.

Conclusions: Early collaborative efforts between cohort studies with respect to data harmonization and joint analyses can advance the field of population (neuro)imaging. The UNIVRSE consortium will focus efforts on other potential correlates of enlarged VRS, including genetics, cognition, stroke, and dementia.

INTRODUCTION

Neuroimaging allows for the *in vivo* assessment of brain structure and function, thereby facilitating research on neurodegenerative, psychiatric and cerebrovascular diseases. In the past decades, magnetic resonance imaging (MRI) has identified both early and late markers of brain pathology that have greatly contributed to our understanding of the pathophysiology of neurological diseases. White matter lesions, for example, are now a well-established marker of cerebral small vessel disease, and hippocampal atrophy has even been translated into a diagnostic marker of Alzheimer's disease. For several neuroimaging markers, standardized definitions were recently proposed, but this was already after decades of research using considerably heterogeneous criteria.[1] Research on emerging neuroimaging markers would benefit from harmonization early on. This paper focuses on enlarged Virchow-Robin spaces (VRS), which hold great potential as an MRI marker for various pathologies in the brain but remain poorly studied. VRS are fluid-filled spaces enveloping the brain vasculature only to become visible on MRI after a substantial increase in volume. Enlargement of these VRS was traditionally thought to be an inconsequential finding on MRI, but this view has repeatedly been questioned in recent years through established links with cerebral small vessel disease, Alzheimer's disease and multiple sclerosis, among others. Several theories have been proposed for this enlargement, including brain atrophy, inflammation, hypertension, and microvascular obstruction (Figure 1).[2-9] Consequently, this resulted in the study of enlarged VRS in relation to a diverse range of diseases. However, the number of VRS studies almost equals the number of methods used for their assessment on MRI.[2-4, 10-13] This has led to the current inability to compare or pool results from different studies, which are already limited in number and size. Now, cohorts worldwide have joined efforts in trying to harmonize VRS research early on, in order to overcome these problems; an initiative which may be exemplary for future population neuroimaging research.

METHODS

In 2010, the Rotterdam Scan Study (RSS) and Austrian Stroke Prevention Study (ASPS), two large population-based studies in aging populations, entered a collaboration with

the goal to develop a robust VRS rating method that is reliable, incorporates relevant brain regions and can be easily applied by other researchers.[14] Briefly, enlarged VRS are rated primarily on an axial T2-weighted sequence, which shows VRS as hyperintensities, but this has now been extended to allow T1-weighted images, where VRS are hypointense, as the primary sequence. VRS are tubular structures that, depending on their orientation within the image, can be linear, ovoid, or round in shape. VRS are considered enlarged when their diameter is ≥1mm, to be able to distinguish 'enlarged' VRS from 'normal' VRS (Figure 2). The diameter is determined visually by the rater and not manually measured for every VRS since the latter would be too time-consuming. VRS are rated separately when these are larger than 3mm, since these large lesions potentially represent different pathology. The shape of the lesion and its intensity on the FLAIR sequence are additionally used to differentiate between enlarged VRS, lacunar infarcts, and white matter hyperintensities.

During the development of our visual rating scale, we focused on its reliability and ease of use. The number of enlarged VRS is determined in four relevant brain regions: the centrum semi-ovale, basal ganglia, hippocampus and mesencephalon. All unique enlarged VRS are counted in the hippocampus and mesencephalon, whereas only a single, predefined slice is used for the centrum semi-ovale and basal ganglia, which are large brain regions for which counting on all slices would be unfeasible. However, in a subset of 40 scans in which all VRS in the brain were counted, there was a high correlation (0.79) between the number from our single slice approach and the total number in that region, indicating that the VRS burden for the larger regions (centrum semi-ovale, basal ganglia) can be captured using only a single slice. We rate the actual counts for each region (either the whole region or a single slice), instead of categorizing this into a severity score, so that this information is not lost and can be analyzed continuously.

Furthermore, we are exploring the possibilities of an automated segmentation method for detecting enlarged VRS, similar to tools for white matter hyperintensities and hippocampal size. This would allow for the investigation of count and volume within the whole brain, as well as within regions of interest. Even though our visual rating method

and those of others have been shown to be reasonably reliable, we expect this objective, quantitative approach to greatly reduce noise and increase analytical opportunities. We believe automated detection will replace the visual rating as the method of choice for determining enlarged VRS load once this is ready to be applied within our consortium. A recent study showed that high-resolution images obtained from 7T scanners are better suited for automated segmentation,[16] although other efforts suggested that this might be feasible with weaker field strengths[15].

Since the publication of this method, the founding members have been joined by other cohorts that share an interest in VRS research and acknowledge that questions regarding their etiology and clinical relevance are best answered through a combined effort. The Uniform Neuro-Imaging of Virchow-Robin Spaces Enlargement (UNIVRSE) consortium was formally established in 2013 and intends to study enlarged VRS using a harmonized approach.

The UNIVRSE consortium currently consists of 13 (sub)cohorts from 5 countries and encompasses more than 16,000 persons with over 25,000 MRI scans (Table 1). It includes prospective, population-based cohort and family studies from various ethnicities and which have all previously been described in detail. A brief overview is provided below. Other cohorts that want to join the consortium are referred to the consortium website (www.uconsortium.org) for further details.

Rotterdam Scan Study

The Rotterdam Study is a Dutch prospective, population-based cohort study that aims to investigate causes and determinants of diseases in the elderly.[17] A total of 14,926 subjects aged 45 years or over at baseline were recruited in three subcohorts (1990, 2000 and 2006) and they are still being followed up. MRI scanning is performed on all participants from 2005 onwards as part of the Rotterdam Scan Study, and is repeated every 3-4 years.[18]

Austrian Stroke Prevention Study

The ASPS is a prospective cohort study on the effects of vascular risk factors on brain structure and function in cognitively normal middle-aged and elderly inhabitants of Graz, Austria.[19] In brief, 2007 subjects aged 50 to 75 years without neuropsychiatric disease were randomly selected from the official community register, of which a random subset of 1,076 participants underwent MRI in two panels (1991-1994 and 1999-2003). Between 2006 and 2013, the Austrian Stroke Prevention Family (ASPS-Fam) study was recruited as an extension of ASPS using identical inclusion criteria and diagnostic work-up with updated MRI protocols; ASPS-Fam included 381 members of the original ASPS cohort and their relatives.

Study of Health in Pomerania

The Study of Health in Pomerania (SHIP) is a longitudinal general population study from Greifswald, Germany that enrolled 4,308 middle-aged subjects in SHIP-0 (SHIP-0: 1997-2001; SHIP-1: 2003-2006; SHIP-2: 2008-2012). In addition to SHIP, a new cohort was started in 2008 (SHIP-TREND) with 4,420 subjects.[20] In SHIP-2 and SHIP-TREND whole body MRI scanning was performed in 3,317 subjects. The next follow-up starts in 2014/2015 and includes a follow-up MRI scan.

Framingham Heart Study

The Framingham Heart Study (FHS) is a single-site, community-based, prospective cohort study initiated in 1948 to investigate risk factors for cardiovascular disease and comprises three generations of participants. The original cohort of the Framingham Heart Study, Generation 1, consisted of 5,209 participants from Framingham MA who were enrolled into the study in 1948 (mean age 44 years). Generation 2 included 5,124 offspring of the original cohort and their spouses who were enrolled into the study in 1971 (mean age 36 years). Individuals from Generations 1 and 2 received an MRI of the brain between 1999-2004 and again between 2005-2011.[21, 22] The Generation 3 cohort was initiated in 2000 and all subjects were scanned between 2009 and March, 2013.[23]

Epidemiology of Dementia in Singapore Study

The Epidemiology of Dementia in Singapore (EDIS) Study draws participants from the Singapore Epidemiology of Eye Disease (SEED) Study, which is a population-based study among Chinese, Malays and Indians.[24] EDIS aims to examine the prevalence of and investigate risk factors for cognitive impairment and dementia in these three major ethnicities of Singapore. A total of 865 subjects aged 60 years and over have been recruited between 2010-2013. Cranial MRI is performed in all the individuals.

Erasmus Rucphen Family study

The Erasmus Rucphen Family (ERF) study is a family-based cohort study in a genetically isolated population from a community in the South-West of the Netherlands (Rucphen municipality) including 3,000 deeply phenotyped participants. Participants with brain MRI scanning in ERF aged 55–75 years and had hypertension to ensure a high prevalence of pathology.[25] Persons with a history of stroke or dementia or with MRI contraindications were excluded. Details about subject selection can be found elsewhere.[26, 27]

Epidemiological Prevention study Zoetermeer

The Epidemiological Prevention study Zoetermeer (EPOZ) is a population-based follow-up study that was initiated in 1975.[28] It includes 10,361 subjects between 5 and 91 years old and originally focused on determinants of various chronic diseases. Participants underwent baseline MRI scanning in 1995-1996 and were rescanned in 1999-2000 and 2008.[29, 30]

Statistical analyses

We will analyze enlarged VRS in a continuous manner when studying their potential determinants by employing negative binomial regression models that take into account the continuous nature of our visual rating scale. Depending on the specific research question, we will use the appropriate statistical tools to analyze the data (e.g., Cox regression models for time-to-event data, linear regression for continuous cognitive scores).

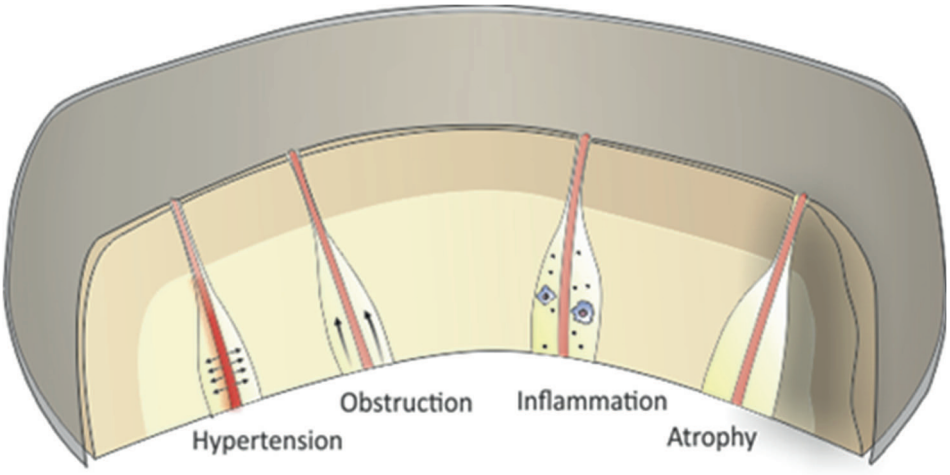

Figure 1 | Hypothesized etiologies for enlargement of Virchow-Robin spaces.

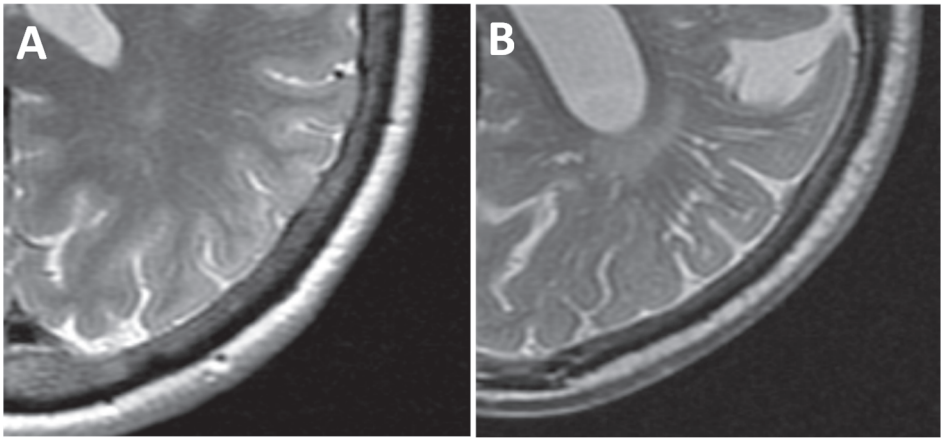

Figure 2 | Virchow-Robin spaces in the centrum semi-ovale of various sizes.

RESULTS

Study population

Table 1 summarizes basic demographics and MRI protocols for each study in the UNIVRSE consortium. The consortium includes participants from a wide age range (19-103 years), mainly sampled from a population-based setting. The RSS and ASPS have performed multiple rounds of MRI scanning and most of the other cohorts are still ongoing or reserve the possibility to perform an additional round of follow-up. Furthermore, participants were often part of other rounds of non-MRI data collection, since brain MRI was not always part of the core study protocol. For most cohorts, a wide range of measurements are available, of which the most relevant are summarized in Table 2.

Primary outcomes

We previously developed a rating method that evaluates four regions in the brain where enlarged VRS occur frequently: the centrum semi-ovale, the basal ganglia, the hippocampus and the mesencephalon. The method was rigorously tested by six raters ranging from medical students to experienced specialists using MRI data from three different scanners, and showed excellent reliability.[14] To promote the use of our VRS rating protocol, it has been made freely accessible through our website (www.uconsortium.org). Additionally, we have now extended the rating protocol to MRI data from the SHIP study: enlarged VRS were rated on the T1-weighted instead of the T2-weighted sequence, which is the primary sequence for VRS rating but was of too low resolution in SHIP for identifying VRS. In order to evaluate how this affects reliability, 25 scans from the RS with both good quality T1- and T2-weighted sequences were twice rated using each sequence separately, with good reliability (mean intraclass correlation coefficient = 0.8).

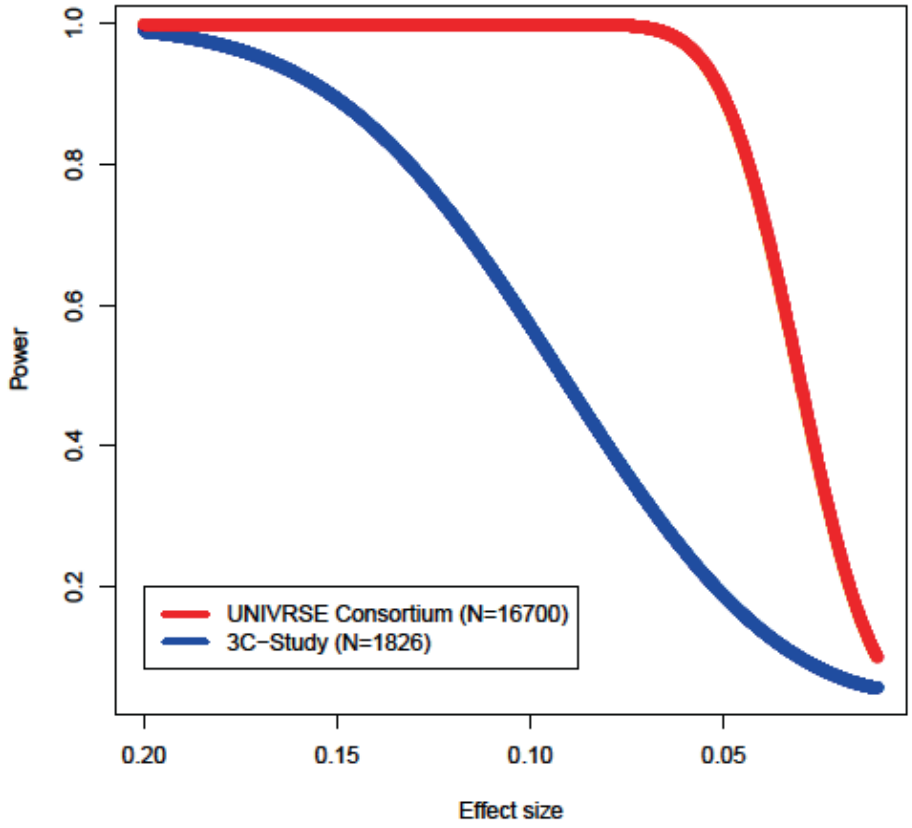

Figure 3 | Comparison of statistical power between the UNIVRSE consortium and the largest published study on Virchow-Robin spaces.

The UNIVRSE consortium aims to elucidate the etiology and clinical relevance of enlarged VRS. Therefore, it will first investigate potential determinants of enlarged VRS, including markers of cerebral small vessel disease, amyloid pathology, and genetic factors. Results of a preliminary analysis from only the founding members showed region-specific risk factors including sex, APOE genotype, and blood pressure, white matter hyperintensities, and lacunar infarcts.[31] Additionally, the consortium is determining how presence of enlarged VRS affects cognition,[3, 32, 33] and whether it is a useful marker for predicting diseases such as stroke[2, 34, 35] and Alzheimer's disease[6].

DISCUSSION

Here we present our initial experiences with data harmonization and joint analyses in a large consortium of population neuroimaging studies. We used a robust visual rating method for measuring enlarged VRS, which was rigorously tested in three studies prior to implementation in the consortium, to decrease heterogeneity and promote inter-study comparisons and collaboration. Importantly, this collaboration was initiated already in a relatively early phase of VRS research, with all the participating studies not having published separately using their own methodology, but instead first harmonizing ratings across sites and then jointly analyzing the data. For other imaging markers of cerebrovascular disease, such collaborative efforts typically follow decades of research using heterogeneous methods.[1] Initial joint analyses prove the value of this collaboration compared to separate, underpowered efforts.

While there is an abundance of VRS rating methods, they are usually restricted to studies using only a single MRI protocol and only rate the VRS in a limited number of regions. Additionally, rating reliability is not always reported and some methods require complex transformations of images to perform the actual rating. A crucial step in the development process was defining a lower limit for the diameter of VRS to be considered enlarged, which has not been done by any rating method before. We operationalized enlargement as VRS $\geq$ 1mm, while realizing this is an arbitrary threshold. However, counting all enlarged VRS, regardless of size, would mean that with increasing spatial resolution of the used MRI scanner, persons would have more "enlarged" VRS. Every study uses an implicit lower bound because of there is minimum size of enlarged VRS that can be detected, which is inherent to the field strength and protocol of the MRI scanner. Indeed, studies using a 3T MRI have found a 100% prevalence of enlarged VRS, in contrast with much lower prevalences on 1.5T images. Additionally, we found that using the T1-weighted images for the primary rating gave comparable results to T2-weighted images. This result further establishes our rating protocol as a method for reliably quantifying VRS burden, regardless of the sequence used for rating.

Table 1 | Overview of the UNIVRSE consortium members and their MRI protocol for Virchow-Robin spaces rating.

Cohort	Country	Sampling	Age range (years)	Baseline scans (N)	Follow-up scans (N)	Field strength (T)	Primary VRS rating sequence	Voxel size (mm)	Additional sequence(s)
ASPS									
ASPS original	Austria	Population-based	44-82	810	377	1.5	T2-weighted	0.9 x 0.9 x 5.5	T1, FLAIR
ASPS Family	Austria	Population-based	38-83	320	120	1.5	T2-weighted	0.8 x 0.8 x 3.0	T1, FLAIR
EPOZ	Netherlands	Population-based	60-94	514	687	1.5	T2-weighted	1.0 x 1.0 x 1.25	T1 and PD
ERF	Netherlands	Family study	55-75	129	-	1.5	T2-weighted	1.0 x 1.0 x 1.6	T1, FLAIR
FHS									
Generation 1	USA	Population-based	79-103	353	224	1.5	T2-weighted	0.95 x 0.95 x 4.0	T1, FLAIR
Generation 2	USA	Offspring	33-90	2749	2257	1.5	T2-weighted	0.95 x 0.95 x 4.0	T1, FLAIR
Generation 3	USA	Offspring	19-63	2008	-	1.5	T2-weighted	0.95 x 0.95 x 4.0	T1, FLAIR
RS									
RS-I	Netherlands	Population-based	68-100	1236	198	1.5	T2-weighted	1.0 x 1.0 x 1.6	T1, FLAIR
RS-II	Netherlands	Population-based	60-98	1493	1377	1.5	T2-weighted	1.0 x 1.0 x 1.6	T1, FLAIR
RS-III	Netherlands	Population-based	46-94	3075	3714	1.5	T2-weighted	1.0 x 1.0 x 1.6	T1, FLAIR
SHIP									
SHIP-2	Germany	Population-based	30-90	1163	Planned	1.5	T1-weighted	1.0 x 1.0 x 1.0	FLAIR
SHIP-TREND	Germany	Population-based	21-82	2154	Planned	1.5	T1-weighted	1.0 x 1.0 x 1.0	FLAIR
EDIS	Singapore	Population-based	60-85	865	-	3.0	T2-weighted	1.0 x 1.0 x 3.0	T1, FLAIR

Abbreviations: ASPS = Austrian Stroke Prevention Study, EPOZ = Epidemiological Prevention study of Zoetermeer, EDIS = Epidemiology of Dementia in Singapore, ERF = Erasmus Rucphen Family, FHS = Framingham Heart Study, RS = Rotterdam Study, SHIP = Study of Health in Pomerania.

Table 2 | Non-exhaustive list of measurements available across the UNIVRSE consortium member cohorts.

Phenotype	ASPS	ASPS-Family	EDIS	EPOZ	ERF	FHS	RS-I	RS-II	RS-III	SHIP-2	SHIP-TREND
Demographics											
Age	✓	✓	✓	✓	✓	✓	✓	✓	✓	✓	✓
Gender	✓	✓	✓	✓	✓	✓	✓	✓	✓	✓	✓
Education	✓	✓	✓	✓	✓	✓	✓	✓	✓	✓	✓
Lifestyle factors											
Smoking	✓	✓	✓	✓	✓	✓	✓	✓	✓	✓	✓
Alcohol	✓	✓	✓	✓	✓	✓	✓	✓	✓	✓	✓
Physical activity	✓	✓	✓	✓	✓	✓	✓	✓	✓	✓	✓
Cognitive function	✓	✓	✓	✓	✓	✓	✓	✓	✓	✓	✓
Blood chemistry											
Cholesterol	✓	✓	✓	✓	✓	✓	✓	✓	✓	✓	✓
Glucose	✓	✓	✓	✓	✓	✓	✓	✓	✓	✓	✓
CRP	✓	✓	✓	✓	✓	✓	✓	✓	✓	✓	✓
Cardiovascular											
Blood pressure	✓	✓	✓	✓	✓	✓	✓	✓	✓	✓	✓
Echocardiography	×	×	×	✓	✓	✓	✓	✓	✓	✓	✓
Brain MRI markers											
Intracranial volume	✓	✓	✓	✓	✓	✓	✓	✓	✓	✓	✓
Tissue-specific volumes	✓	✓	✓	✓	✓	✓	✓	✓	✓	✓	✓
Hippocampal volume	✓	✓	✓	✓	✓	✓	✓	✓	✓	✓	✓
Infarcts	✓	✓	✓	✓	✓	✓	✓	✓	✓	✓	✓
Microbleeds	×	✓	✓	✓	✓	✓	✓	✓	✓	×	×
Genetics											
Genome-wide SNP array	✓	✓	✓	✓	✓	✓	✓	✓	✓	✓	✓
Exome chip	×	✓	×	✓	×	✓	✓	×	×	✓	✓

Abbreviations: ASPS = Austrian Stroke Prevention Study, EDIS = Epidemiology of Dementia in Singapore, EPOZ = Epidemiological Prevention study of Zoetermeer, ERF = Erasmus Rucphen Family, FHS = Framingham Heart Study, RS = Rotterdam Study, SHIP = Study of Health in Pomerania.

Furthermore, we focused on the ease of use and speed of the method and rated VRS only a single slice for the two larger regions (basal ganglia and centrum semi-ovale). However, we have counted all VRS in the brain for 40 scans and compared this to the single slice that we used in the rating. This showed a high correlation between our single slice approach and the total number in that region. Although counting all VRS would be ideal, it is extremely time-consuming and given these results also seems unnecessary to capture the VRS burden. Still, we could have chosen the most severe slice instead of the pre-defined slice that we use now. We made this decision because of two reasons: 1) allowing the rater to choose the 'most severe' slice adds an additional layer of subjectivity to the method, and 2) it is currently unknown whether the spatial distribution of VRS is differentially related to pathology. If, for example, parietal VRS are related to amyloid depositions, it would introduce bias when only rating certain subjects with respect to that part of the brain.

Main strengths of the UNIVRSE consortium are: (i) the increased statistical power to detect associations, achieved by combining datasets; (ii) the harmonized approach of enlarged VRS rating, which facilitates the collaboration and allows for better comparisons; (iii) the inclusion of demographically diverse studies, with a broad range of phenotypic information available.

Although our rating protocol has several advantages in comparison to other scales, all methods still rely on the human assessment of VRS and are therefore subjective in nature and labor intensive. However, we are concurrently working on the development of an automated segmentation method, which is particularly difficult for VRS. Also, the selection of the brain regions is based mostly on prevalence and current knowledge of VRS; therefore, new research could for example increase the interest in other regions and studying different pathology might also require changes in the protocol.Our future research will include other determinants such as markers of cerebral small vessel disease, amyloid pathology, and genetic factors. Also, we aim to determine how presence of enlarged VRS affects cognition, and whether it is a useful marker for predicting diseases such as Alzheimer's disease and stroke.

CONCLUSIONS

The UNIVRSE consortium is a global initiative that was established in the young field of enlarged VRS research. It aims to implement at an early stage the hard-learned lessons on the value of data harmonization and joint analyses from decades of population imaging.

REFERENCES

1. Wardlaw *et al.* Lancet Neurol 2013
2. Zhu YC, *et al.* Stroke. 2010
3. Maclullich AM, *et al.* J Neurol Neurosurg Psychiatry. 2004
4. Patankar TF, *et al.* AJNR Am J Neuroradiol. 2005
5. Satizabal *et al.* J Alz Dis. 2012
6. Weller *et al.* Brain pathology. 2008
7. Zlokovic BV. Neuron. 2008
8. Kress BT, *et al.* Annals of neurology. 2014
9. Jessen NA, *et al.* Neuroch res 2015
10. Cumurciuc *et al.* EJN. 2006
11. Chen W, *et al.* AJNR Am J Neuroradiol. 2011
12. Groeschel S, *et al.* Neuroradiology. 2006
13. Potter GM, *et al.* Cerebrovascular Diseases. 2015
14. Adams HH, *et al.* Stroke. 2013
15. Cai K, *et al.* Journal of Neuroscience Methods. 2015
16. Hernández, *et al.* J of MRI. 2013
17. Hofman *et al.* EJE. 2015
18. Ikram *et al.* Eur J Epidemiol. 2011
19. Schmidt R, *et al.* Neurology. 1999
20. Volzke *et al.* Int J Epidemiol. 2011
21. DeCarli *et al.* NBA. 2005
22. Massaro JM, *et al.* Stat Med. 2004
23. Maillard P, *et al.* Lancet Neurol. 2012
24. Hilal S, *et al.* J Neurol Neurosurg Psychiatry. 2013
25. Schuur M, *et al.* J Neurol Neurosurg Psychiatry. 2011
26. Schuur *et al.* NBA. 2011
27. Vernooij MW, *et al.* NEJM. 2007
28. Hofman A, *et al.* Br Med J. 1979
29. de Leeuw FE, *et al.* Stroke. 2000
30. Prins ND, *et al.* Neurology. 2004
31. Adams HHH, *et al.* Alzheimer's & Dementia: The Journal of the Alzheimer's Association. Unpublished results
32. Hurford R, *et al.* JNNP. 2014
33. Yao M, *et al.* NBA. 2014
34. Doubal FN, *et al.* Stroke. 2010
35. Charidimou A, *et al.* JNNP. 2013

Chapter 2.3

Novel meta-analytical approach for pooled analysis

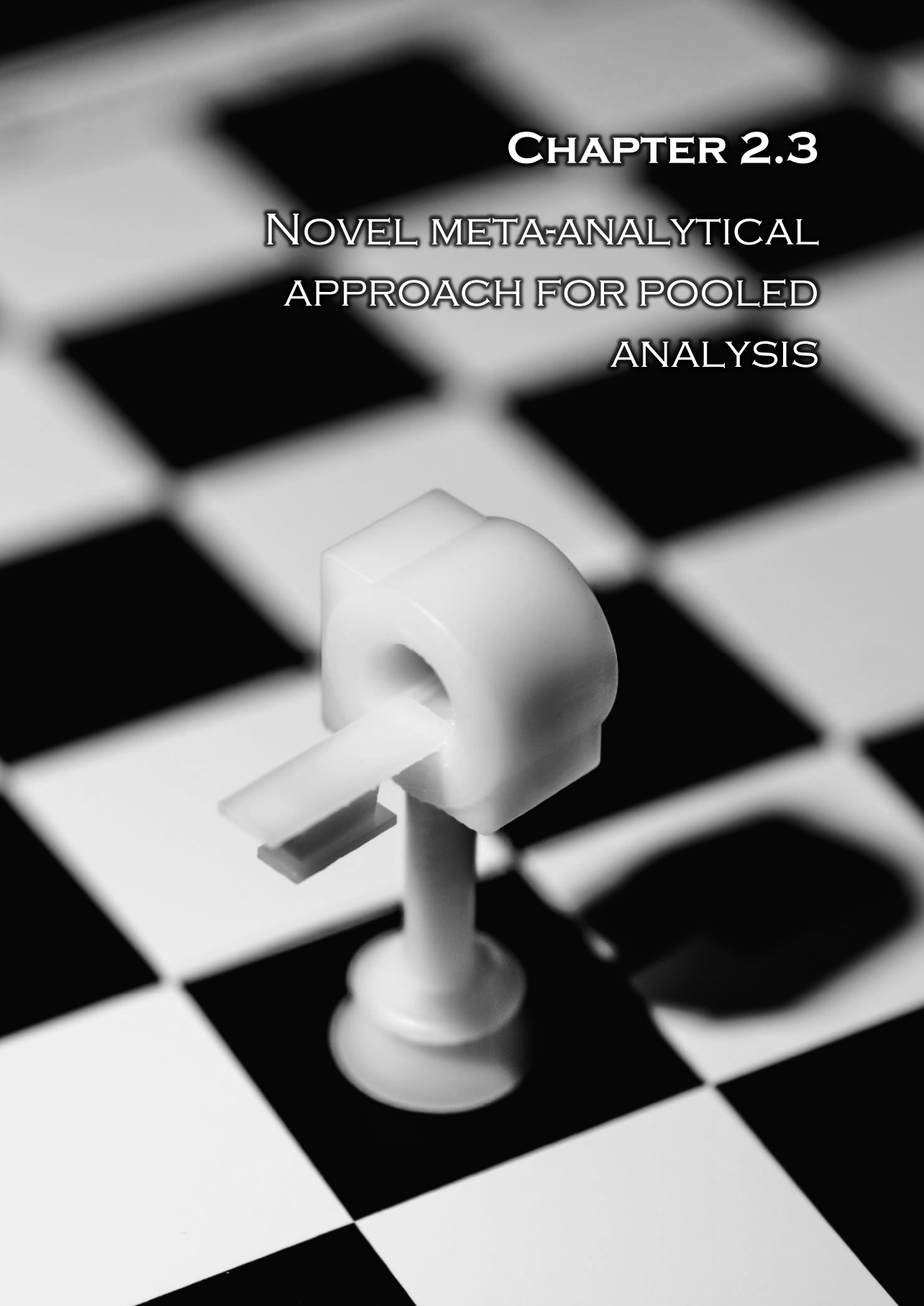

ABSTRACT

Joint analysis of data from multiple studies in collaborative efforts strengthens scientific evidence, with the gold standard approach being the pooling of individual participant data (IPD). However, sharing IPD often has legal, ethical, and logistic constraints for sensitive or high-dimensional data, such as in clinical trials, observational studies, and large-scale omics studies. Therefore, meta-analysis of study-level effect estimates is routinely done, but this compromises on statistical power, accuracy, and flexibility. Here we propose a novel meta-analytical approach, named partial derivatives meta-analysis, that is mathematically equivalent to using IPD, yet only requires the sharing of aggregate data. It not only yields identical results as pooled IPD analyses, but also allows post-hoc adjustments for covariates and stratification without the need for site-specific re-analysis. Thus, in case that IPD cannot be shared, partial derivatives meta-analysis still produces gold standard results, which can be used to better inform guidelines and policies on clinical practice.

INTRODUCTION

Science is an increasingly collaborative effort. The benefits of jointly investigating research questions, such as improved power to detect effects and generalizability of results,[1-3] have been known for long, but the recent technology-driven emergence of high-dimensional datasets, e.g. in the fields of genetics and imaging, has further underlined the need for collaboration.[4] The limited capacity of single studies to collect these data in sufficient numbers has resulted in the formation of numerous large consortia.[5-7]

Generally, joint analyses are performed by either pooling individual participant data (IPD) from multiple studies or by meta-analysing aggregate data that are derived from study-specific analyses. In pooled analyses, raw participant data are shared to produce combined datasets that are then analysed as a single study. In conventional aggregate data meta-analysis, only the study-specific effect estimates are provided or extracted from literature and these estimates are averaged to approximate the overall effect for all the studies combined. Although pooled analyses provide the highest power and accuracy,[4, 8, 9] several barriers exist to sharing IPD, including when local legislation prevents the release of collected data, when the process of sharing data presents logistic problems due to its size, or when the data, despite being anonymized, can lead to the identification of individuals and reveal sensitive medical information.[10] Even though the research community as well as funding agencies put considerable pressure on investigators to make datasets publicly available, in these conditions, IPD cannot be pooled for joint analysis.

Here we propose a novel meta-analytical approach, *partial derivatives meta-analysis*, which 1) provides the statistical and analytical benefits of pooled analyses for linear regression models, 2) uses aggregate data that cannot be traced back to individual participant data, and 3) is easily applicable in current research settings. We use examples from clinical trials, observational studies, and high-dimensional omics to illustrate the broad relevance of this approach.

METHODS

Regression analysis

Regression models estimate the effects of predictor variables on the outcome variable by determining the combination of effect estimates that correspond best to the data at hand. When performing a regression analysis, the IPD is converted into several intermediate statistics before arriving at the eventual results, i.e. the effect estimates (**Figure 1**). First, residual error terms are calculated for each individual. This error represents the difference between the actual outcome variable and its value predicted by the model. Second, the error terms are consolidated into a set of partial derivatives equations, which are the sum of all individual terms. Third, the partial derivatives equations are set to zero and solved, to find the best combination of effect estimates that minimize the error, i.e. give a predicted value as close to the actual outcome variable. The "fitting of the model" refers to this final step.

Partial derivatives meta-analysis

Although the partial derivatives are only intermediate statistics for calculating effect estimates, they have great potential for joint analyses, in particular with linear regression. In linear regression, partial derivatives are calculated by multiplying every variable with all the others, resulting in one value for every pair of variables. This is done separately for each participant in the analysis and these participant-specific values are subsequently summed together to obtain the partial derivatives (Figure 2A). The process of summation can be split for different groups of participants and combined afterwards, without compromising the end result. Extending from this concept, partial derivatives could be calculated separately for a group of participants (i.e., within different studies) and summed together at the meta-analytical stage—a strategy we term *partial derivatives meta-analysis* (Figure 2B; details in the Supplementary Material). Using these summed partial derivatives it is then possible to fit a (meta-analysed) model, which yields effect estimates that are mathematically identical to those from pooled analyses, without the sharing of IPD. Additionally, this approach allows for post-hoc changes in the covariate adjustments and stratified analyses without site-specific re-analyses.

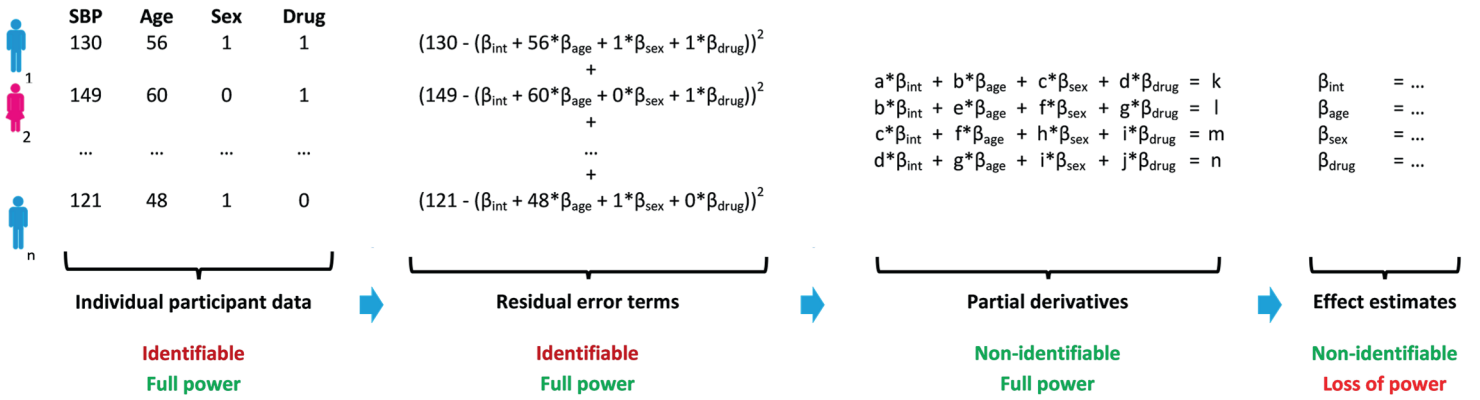

Figure 1 | Four stages of data in linear regression analysis and their meta-analytical properties when shared.

Schematic overview of four stages when performing a linear regression analysis for a study with n participants, where systolic blood pressure (SBP) is modelled using predictors age, sex, and a novel drug of interest. Starting with the individual participant data, the residual error terms are calculated for each individual separately. Subsequently, the partial derivatives are generated by adding up the residual error terms of all individuals. Finally, simultaneously solving the partial derivatives gives the effect estimates for each of the predictors and the intercept per study.

When sharing the individual participant data, residual error terms, or partial derivatives, it is possible to calculate meta-analysed effect estimates without the loss of power. Only by exchanging the partial derivatives or effect estimates, however, is the shared information not identifiable to a participant level.

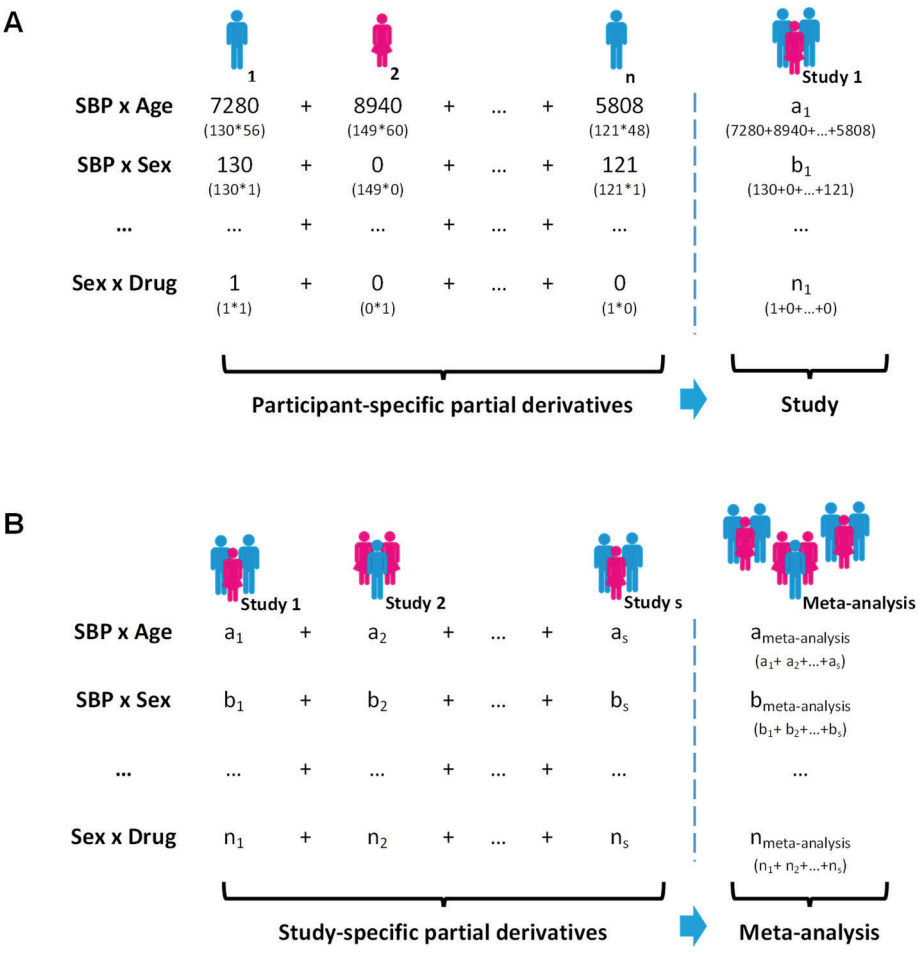

Figure 2 | Strategy for performing a partial derivatives meta-analysis.

Overview of calculation for a linear regression analysis for a meta-analysis of s studies, where systolic blood pressure (SBP) is modelled using predictors age, sex, and a novel drug of interest. For each of n participants in the first study, partial derivatives are calculated by multiplying the value of every variable with the value of all the others, resulting in a single value for every pair of variables (panel A, left side). The participant-specific values are subsequently summed together to obtain the partial derivatives of the whole first study (panel A, right side). Analogous to this, the partial derivatives can be calculated for each study separately (panel B, left side) and combined at the meta-analytical stage (panel B, right side). The resulting partial derivatives are mathematically equivalent to those that would have been obtained if all individual participant data was available and therefore provide identical results.

RESULTS

In this section, we show how partial derivatives meta-analysis can be applied in current research settings and compare this to the conventional methods, namely the sharing of IPD (gold standard) and the sharing of effect estimates. To illustrate the broad applicability of this approach, we use examples from clinical trials, observational studies, and omics studies.

Descriptive statistics

Papers describing investigations in humans generally start with a table containing the (baseline) characteristics of the study population. Using IPD, it is easy to generate these descriptive statistics, but this is not possible using the aggregated effect estimates. Instead, all contributing sites need to calculate their descriptive statistics locally, leading to a potential source of errors (e.g., using different individuals than for the main analysis).

The partial derivatives are a set of values, the exact number of which depends on the number of predictor variables in the chosen model (see Supplementary Material), and would for example equal 14 values when modelling 4 predictors. Interestingly, some of these values can be used to determine descriptive statistics, such as the sample size, but also the means and standard deviations of any of the variables, including the outcome. This therefore obviates the need for sites to provide these descriptive statistics separately.

Full statistical power: example using omics data

Statistical power to detect associations is important for all studies, but its relevance is perhaps most apparent for large-scale omics studies such as genome-wide association studies. Here, strict multiple testing correction for millions of tests and the small effect sizes of genetic variants make it difficult to identify true associations, and this has necessitated collaborative efforts. Pooling IPD is the gold standard and yields the greatest power, although conventional meta-analysis of effect estimates can provide similar results in specific cases.[11, 12] However, when some sites cannot share their IPD, this

leads to a smaller sample size than would be obtained using conventional meta-analysis, and this is even more detrimental to the statistical power. In comparison, partial derivatives meta-analysis has the potential to overcome both limitations.

First, using simulated data, we show that the effect estimates of partial derivatives meta-analysis are identical to those from a pooled IPD analysis, while this is not the case for conventional meta-analysis (Figure 3A). Additionally, partial derivatives meta-analysis increasingly outperformed conventional meta-analysis when, for a fixed total sample size, the number of studies were increased (i.e., the size of individual studies was smaller) (Figure 3B). For conventional meta-analysis, small sample sizes or complex models results in unstable (and eventually unobtainable) effect estimates within each site, which generally leads to the exclusion of these sites. Besides the statistical loss of power, this selection forms an epidemiological problem in the light of the biases associated with leaving out particular studies. In contrast, partial derivatives meta-analysis does not require a minimum number of participants and could theoretically even be performed on a single individual, although in this case the participant data would of course be identifiable.

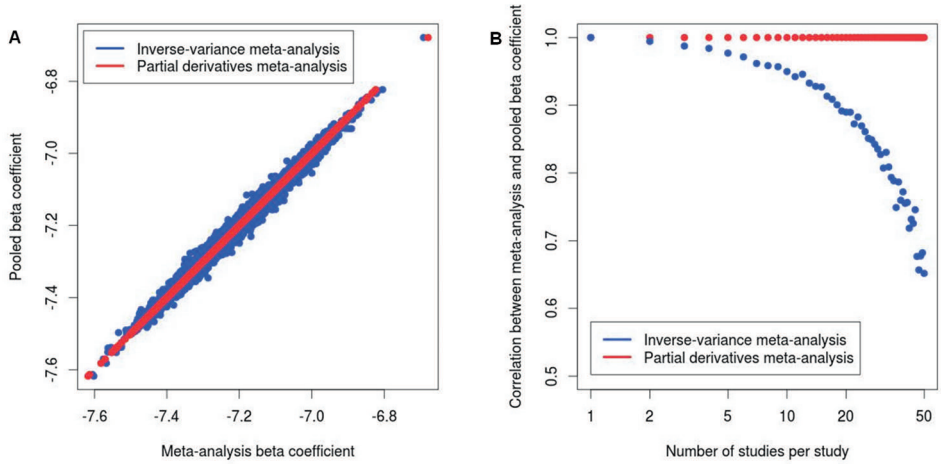

Figure 3 | Correlation of effect estimates from conventional and partial derivatives meta-analysis with effect estimates from a pooled analysis.

Panel A show a scatter plot of beta coefficients obtained from inverse-variance meta-analysis of effect estimates and pooled analysis (royal blue) and from partial derivatives meta-analysis and pooled analysis (firebrick red). Results were obtained from simulation with the following parameters: number of studies = 2, total sample size = 500, beta coefficient of predictor = -7.20, number of simulations = 10,000.

Panel B shows correlation coefficients of beta coefficients between inverse-variance meta-analysis of effect estimates and a pooled analysis (royal blue) and between partial derivatives meta-analysis and a pooled analysis (firebrick red), with a varying number of studies and study size. Simulation parameters were as follows: total sample size = 500, number of studies = 1 to 50, number of simulations = 10,000.

All simulations were performed in R (version 3.0.1)

Table 1 | Comparison of sharing conventional data and partial derivatives with respect to study site participation and analytical possibilities for a proof-of-principle study.

Characteristic	IPD	Partial derivatives	Effect estimates
Study characteristics			
Number of studies agreed to participate	7[§]	19	19
Number of participants	5,611	14,643	14,643
Country of origin			
Netherlands	5	5	5
United Kingdom	0	1	1
Germany	0	2	2
France	0	1	1
Austria	1	1	1
Iceland	0	1	1
Singapore	1	1	1
United States	0	7	7
Data sharing and analysis			
Sharing of non-identifiable data	No	Yes	Yes
Individual-level effect estimates	Yes	Yes	No
Stratified analyses	Yes	Yes	No
Post-hoc model adjustments	Yes	Yes	No
Number of required analyses per site[†]	0	1	21

† Calculated as number of analyses required for seven different models, for the complete sample as well stratified for sex.

§ These are the meta-analysis sites (Rotterdam Study 1-3), ASPS-Fam, EDIS, LLS, and PROSPER.

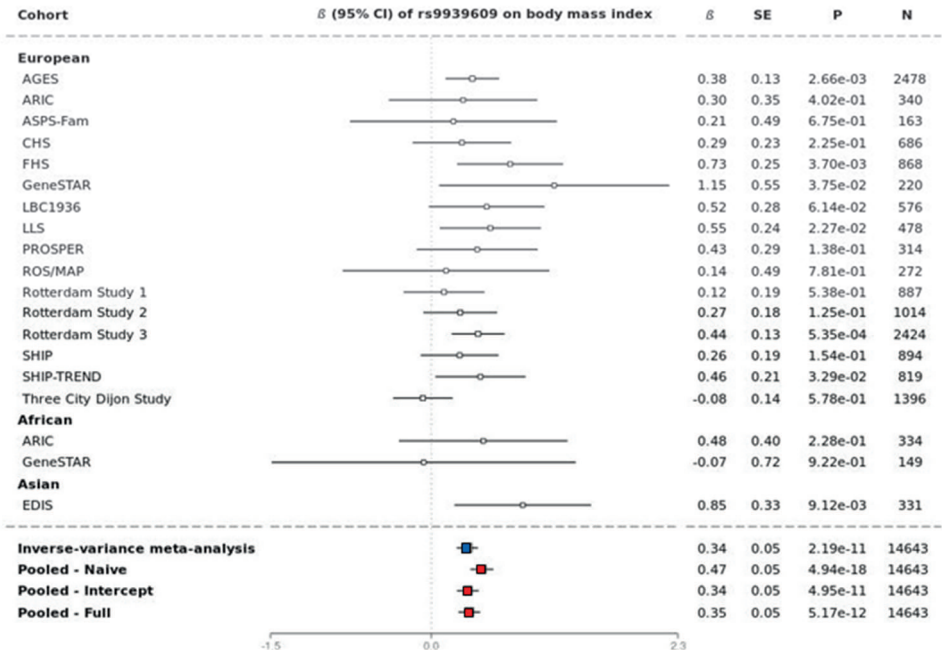

Figure 4 | Forest plot for the association of rs9939609 with body mass index.

Forest plots showing beta coefficients and 95% confidence intervals of individual cohorts as well as four different joint analyses, all obtained from the partial derivatives: Inverse-variance based meta-analysis of effect estimates, pooling without additional adjustments ("Naïve"), pooling with adjustment for cohort ("Intercept"), and pooling with adjustment for cohort and other cohort-specific covariates ("Full").

Second, using real data of 14,643 participants from 19 cohort studies from the HD-READY consortium (see Supplementary Material), we show that the anonymised nature of partial derivatives can overcome the data sharing obstacles related to IPD. Of the 19 participating studies, only 4 were able to share IPD with investigators from the meta-analytical site, resulting in a pooled IPD analysis of 5,611 individuals, less than 40% of the total sample (Table 1). In contrast, all studies were able to contribute partial derivatives. Studies sharing IPD did not need to perform any on-site analyses. For studies running partial derivatives (which were all studies), all site-specific data could be generated through a single analysis. Studies sharing effect estimates needed to perform additional analyses for every model, thus increasing the analytical burden.

Third, using the data from these 19 studies, we compared the different meta-analytical methods to investigate the association between an established genetic risk variant (rs9939609, *FTO/IRX3* locus) and body mass index (Figure 4). Conventional meta-analysis of effect estimates showed a genome-wide significant association (ß = 0.34, P = 2.19 x 10^{-11}). Next, we confirmed that partial derivatives meta-analysis indeed yields identical results as pooled analyses in the subset of participating cohorts that were able to share their IPD. We then used the partial derivatives to calculate the effect estimates under various scenarios of pooled analyses. Naïve pooling of samples, which assumes a completely homogeneous population, resulted in biased estimates (ß = 0.47, P = 4.94 x 10^{-18}), whereas controlling for study site using an intercept for each cohort resolved this issue (ß = 0.34, P = 4.95 x 10^{-11}). Modelling cohort-specific effects for all the covariates in the model (intercept, age, and sex) provided a slightly larger effect estimate that was more significant than conventional meta-analysis (ß = 0.35, P = 5.17 x 10^{-12}). At first sight, this improvement over the conventional meta-analysis is modest. However, large-scale omics studies routinely involve millions of analyses, and the increase in power for such investigations will thus be cumulative.

Post-hoc adjustment of the model: example using observational data

Although the increase in power of partial derivatives meta-analysis is advantageous, the increased flexibility of the method is particularly appealing. Similar to an IPD analysis, partial derivatives meta-analysis allows for adjustments of statistical models without the need for each contributing study to reanalyse its data and share new results. All predictors of interest, including those to be added or removed in a later stage, can simply be included when generating the partial derivatives; when fitting the model on the meta-analytical level, the decision can be made about what specific predictors to include. For conventional meta-analysis, post-hoc adjustments are not possible, as this would require re-analyses from each site. We illustrate this application using data from three observational cohorts (total N = 5,431), where the aim of the study is to understand how body height relates to general cognitive function.

In this study, we defined general cognitive function as the common variance between multiple cognitive tests, as previously described.[13] The pooled age- and sex-adjusted analysis showed a strong association between body height and cognitive function (ß = 0.016, P = 3.03 x 10^{-15}). However, given that body height is an indicator of educational attainment and this in turn is related to cognitive function, it remains unclear whether this association is independent of education. With the partial derivatives, education can be added to the model at the meta-analytical level to test this and thereby provide more information for correct inference of the results. Adjustment for education resulted in an attenuated, but still significant, effect estimate of height (ß = 0.010, P = 9.78 x 10^{-8}).

Naively pooling IPD from all cohorts together does not sufficiently account for any underlying heterogeneity that may exist between the cohorts.[14, 15] For example, the education variable was not on the same scale for all three cohorts due to the use of a different questionnaire, and it might not be appropriate to treat them the same. Conventional meta-analysis, on the other hand, assumes complete heterogeneity among the cohorts for all variables in the model. However, using partial derivatives, these assumptions can be formally tested and modelled on the meta-analytical stage. It is possible to determine the study-specific effects for all variables, and also determine whether some studies cluster together. In our example, we found that the effects of education were indeed significantly different between the cohorts, whereas the intercept did not differ between two of the cohorts, which were demographically similar.

Stratified analyses: example using clinical trial data

Another application of partial derivatives is the possibility to perform stratified analyses. For a comparative clinical trial, stratification in the form of subgroup analyses provides means of investigating whether certain patient groups are likely to respond differently to a treatment. Consider randomized, clinical trials that aim to determine the efficacy of a novel blood pressure lowering medication. If the treatment is found to be successful, it might be interesting to see if the benefit is the same for men and women. In case of a negative trial, it could be informative to find that persons with kidney disease do not tolerate the treatment, whereas there is a beneficial effects in those without. If the subgroups are pre-specified, the partial derivatives will contain the necessary

information to perform these joint analyses of the clinical trials without exchanging the IPD.

DISCUSSION

We show that sharing of partial derivatives among studies is sufficient to calculate meta-analysed effect estimates for linear regression models that are mathematically equivalent to a pooled analysis, the gold standard, without the need to share IPD. Partial derivatives meta-analysis outperforms conventional meta-analysis, in particular for complex models and with an increasing number of (smaller) studies. Furthermore, partial derivative meta-analysis has additional advantages over conventional meta-analysis, including the ability to perform post-hoc adjustments of the model and detailed subgroup analyses, as well as the possibility to include small studies in a meta-analysis that would otherwise have been excluded. For the specific case of high-dimensional data, sharing of partial derivatives is in fact more efficient than sharing IPD given the size of the data.

Thus, the partial derivatives are in fact 'pluripotent' since not only IPD effect estimates can be calculated, but also those from conventional meta-analysis. Additionally, this approach enables the examination of each of the predictors separately and for different combinations of studies that might cluster together. Therefore, in cases where naïve pooling of IPD might not be appropriate, a different analytic approach will be possible using the same partial derivatives. The increased flexibility of sharing partial derivatives also requires increased caution. Just as with sharing of IPD and effect estimates, the partial derivatives can be used for analyses other than those of the primary research question. Subgroup analyses in clinical trials require rigorous reporting,[16, 17] and we suggest to follow these standards to prevent secondary hypothesis testing not considered in the primary analysis plan.

A main focus when developing this method was its ease of use for other researchers. To promote the dissemination of partial derivatives meta-analysis, we provide examples for calculating the partial derivatives with commonly used statistical software (R, SPSS,

Excel, SAS, and STATA). Additionally, we have implemented partial derivatives meta-analysis in HASE, a software package for genome-wide association studies.[18]

Here we described a meta-analytical approach for continuous outcomes using linear regression analysis, but additional work is needed for applying this approach to binary outcomes and time-to-event data. The usual method for parameter estimation in generalized linear models and proportional hazards models is through multiple rounds of individual-level calculations to find the maximum likelihood numerically; a non-iterative approach would therefore be more feasible to reduce demands on contributing studies. Other proposed solutions for pooling of individual-level data include projects such as BioSHaRE and DataSHIELD.[17, 19, 20] In these projects, for each analysis, summary statistics are continuously exchanged between servers of different sites until an adequate model is fit. Although this is promising from a methodological perspective, it does require rigorous data harmonization and subsequent linking of the data to external servers using dedicated software packages. The high level of collaboration needed between the studies and the time-investment for preparation of the data could potentially explain the limited implementation by other researchers.

Also, using DataSHIELD or conventional aggregate data, published results cannot be re-used for calculating effect estimates identical to IPD meta-analysis. With partial derivatives meta-analysis however, the partial derivatives can be provided and, with new studies, added to get new estimates. We therefore propose publishing of partial derivatives in addition to the conventional effect estimates, while retaining IPD within host institutions of participating studies when this cannot be made available too.

Interestingly, many of the partial derivatives values correspond to descriptive statistics already being published on a frequent basis (e.g. sample size, mean age, number of women), along with the effect estimates for the variables of interest. This raises the intriguing possibility of using published results to recalculate the partial derivatives and subsequently perform a pooled analysis. Not all values of the partial derivatives are available, however, so some assumptions would need to be made about the correlation between variables (e.g., by using data from an available sample). This possibility is

especially interesting for published data for which it is not feasible to request re-analysis, e.g. when investigators are not reachable or they do not wish to participate.

Another potentially useful avenue is for computationally intensive analyses that are common in the omics field, such as genome-wide association studies. Partial derivatives meta-analysis only requires a "partial" regression to be performed within each site, since the partial derivatives are needed for sharing, but it is not necessary to subsequently calculate the effect estimates. The fitting of the model will be done only once, after combining all the partial derivatives from the contributing sites, thereby shifting part of the computational burden to the stage of the meta-analysis. Also, it is possible to use the same partial derivatives to perform exploratory analyses, for instance additional adjustments for potential confounders, which are particularly time-consuming for large-scale omics studies, and therefore are often not performed. However, since these exploratory analyses can be instrumental for the correct causal inference of findings, the use of partial derivatives meta-analysis could facilitate the completion of scientific efforts and potentially accelerate scientific discoveries. Furthermore, in addition to the usual difficulties accompanying the exchange of IPD, the sharing of aggregate data actually outperforms the sharing of IPD with respect to the time needed for transferring the files,[21] making this approach more efficient and perhaps less costly.

Ultimately, sharing IPD is still superior with respect to flexibility and insight into data. However, until such sharing is adopted by the scientific community as a whole, partial derivatives meta-analysis could provide a way forward while using only aggregate data.

REFERENCES

1. Button et al. Power failure: Why small sample size undermines the reliability of neuroscience. *Nat Rev Neuro*. 2013;14:365-376
2. Seminara et al. The emergence of networks in human genome epidemiology: Challenges and opportunities. *Epidemiology*. 2007;18:1-8
3. Thompson A. Thinking big: Large-scale collaborative research in observational epidemiology. *EJE* 2009;24
4. Ioannidis et al. Meta-analysis of individual participants' data in genetic epidemiology. *AJE* 2002;156:204-210
5. Budin-et al. Data sharing in large research consortia:. *EJHG*. 2013
6. Psaty et al Cohorts for heart and aging research in genomic epidemiology consortium.. *Circ C Gen* 2009
7. Thompson et al. Imaging genomics. *Current opinion in neurology*. 2010;23:368
8. Lambert et al. A comparison of summary patient-level covariates in meta-regression with individual patient data meta-analysis. *J clin epi*. 2002;55:86-94
9. Riley RD, Lambert PC, Abo-Zaid G. Meta-analysis of individual participant data: Rationale, conduct, and reporting. *BMJ:* 2010:521
10. Lumley et al. Potential for revealing individual-level information in genome-wide association studies. *JAMA*. 2010;303:659-660
11. Lin et al. On the relative efficiency of using summary statistics versus individual-level data in meta-analysis. *Biometrika*. 2010;97:321-332
12. Lin et al. Meta analysis of genome wide association studies: *Gen epi* 2010;34:
13. Davies et al. Genetic contributions to variation in general cognitive function:. *M Psy* 2015
14. Liu et al. Meta-analysis of gene-level tests for rare variant association. *Nat Genet*. 2014;46:200-204
15. Higgins et al. Quantifying heterogeneity in a meta analysis. *Statistics in medicine*. 2002;21:1539
16. Wang et al. Reporting of subgroup analyses in clinical trials. *NEJM* 20074
17. Wolfson et al. Datashield: . *IJE* 2010;39:1372-1382
18. Roshchupkin et al. HASE: . Sci Rep. 2016
19. Doiron et ak. The bioshare project. *Em th epi* 2013;
20. Jones et al. Datashield. *Norsk epidemiologi*. 2012;21
21. Willer CJ, Li Y, Abecasis GR. Metal:.*Bioinformatics*. 2010

Chapter 2.4

Software for performing high-dimensional association studies

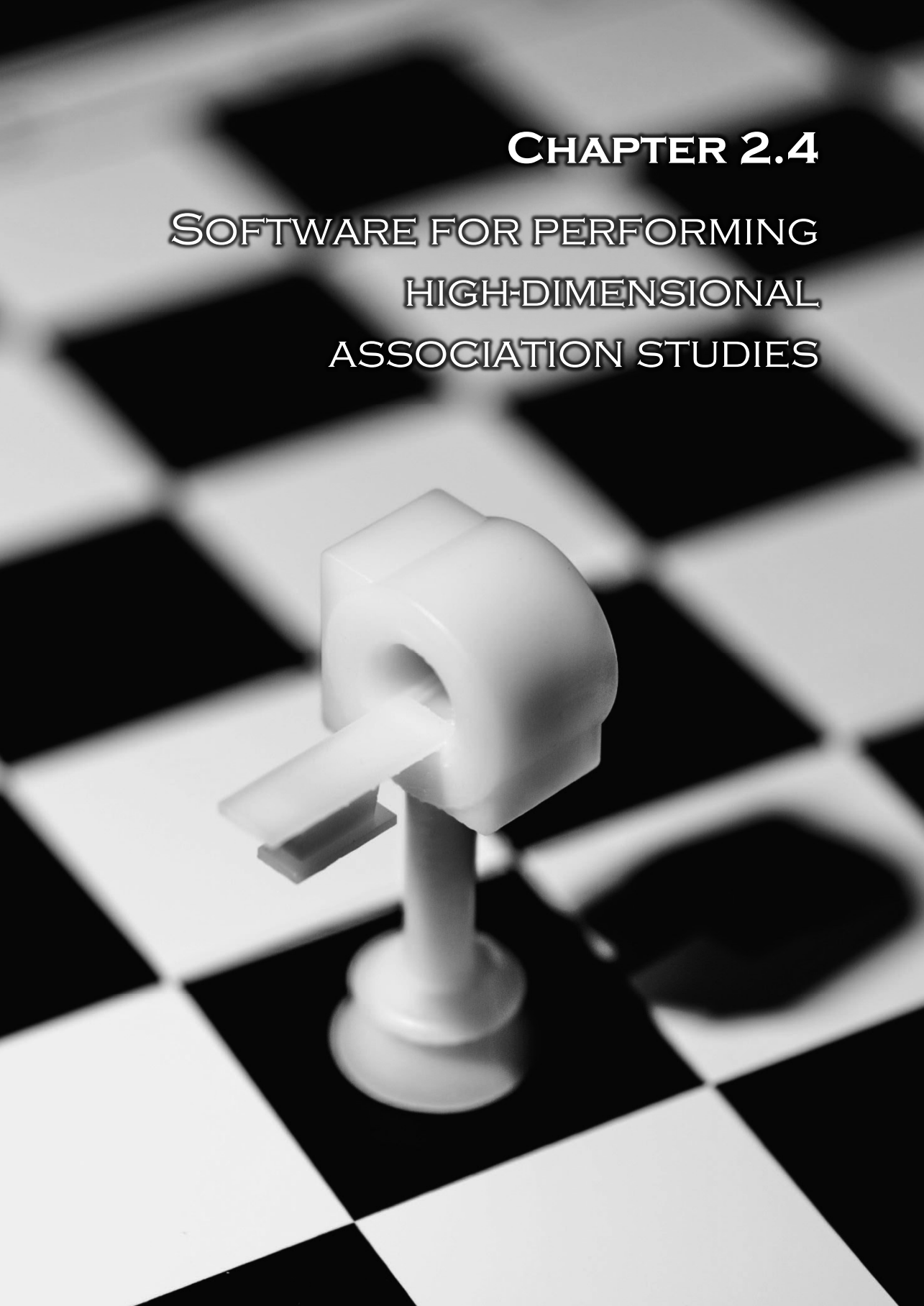

ABSTRACT

High-throughput technology can now provide rich information on a person's biological makeup and environmental surroundings. Important discoveries have been made by relating these data to various health outcomes in fields such as genomics, proteomics, and medical imaging. However, cross-investigations between several high-throughput technologies remain impractical due to demanding computational requirements (hundreds of years of computing resources) and unsuitability for collaborative settings (terabytes of data to share). Here we introduce the HASE framework that overcomes both of these issues. Our approach dramatically reduces computational time from years to only hours and also requires several gigabytes to be exchanged between collaborators. We implemented a novel meta-analytical method that yields identical power as pooled analyses without the need of sharing individual participant data. The efficiency of the framework is illustrated by associating 9 million genetic variants with 1.5 million brain imaging voxels in three cohorts (total N=4,034) followed by meta-analysis, on a standard computational infrastructure. These experiments indicate that HASE facilitates high-dimensional association studies enabling large multicenter association studies for future discoveries.

INTRODUCTION

Technological innovations have enabled the large-scale acquisition of biological information from human subjects. The emergence of these big datasets has resulted in various 'omics' fields. Systematic and large-scale investigations of DNA sequence variations (genomics)[1], gene expression (transcriptomics)[2], proteins (proteomics)[3], small molecule metabolites (metabolomics)[4], and medical images (radiomics)[5], among other data, lie at the basis of many recent biological insights. These analyses are typically unidimensional, i.e. studying only a single disease or trait of interest.

Although this approach has proven its scientific merit through many discoveries, jointly investigating multiple big datasets would allow for their full exploitation, as is increasingly recognized throughout the 'omics' world[5–8]. However, the high-dimensional nature of these analyses makes them challenging and often unfeasible in current research settings. Specifically, the computational requirements for analyzing high-dimensional data are far beyond the infrastructural capabilities for single sites. Furthermore, it is incompatible with the typical collaborative approach of distributed multi-site analyses followed by meta-analysis, since the amount of generated data at every site is too large to transfer.

Some studies have attempted to combine multiple big datasets[5,8–10], but these methods generally rely on reducing the dimensionality or making assumptions to approximate the results, which leads to a loss of information.

Here we present the framework for efficient high-dimensional association analyses (HASE), which is capable of analyzing high-dimensional data at full resolution, yielding exact association statistics (i.e. no approximations), and requiring only standard computational facilities. Additionally, the major computational burden in collaborative efforts is shifted from the individual sites to the meta-analytical level while at the same time reducing the amount of data needed to be exchanged and preserving participant privacy. HASE thus removes the current computational and logistic barriers for single- and multi-center analyses of big data. The HASE software is available at our website www.imagene.nl/HASE/.

RESULTS

Overview of the methods

The methods are described in detail in the Methods. Essentially, HASE implements a high-throughput multiple linear regression algorithm that is computationally efficient when analyzing high-dimensional data of any quantitative trait. Prior to analysis, data are converted to an optimized storage format to reduce reading and writing time. Redundant calculations are removed and the high-dimensional operations are simplified into a set of matrix operations that are computationally inexpensive, thereby reducing overall computational overhead. While deriving summary statistics (e.g., beta coefficients, p-values) for every combination in the high-dimensional analysis would be computationally feasible at individual sites with our fast regression implementation, it would be too large to share the intermediate results (>200GB per thousand phenotypes) in a multi-center setting. Therefore, extending from a recently proposed method, partial derivatives meta-analysis[17], we additionally developed a method that generates two relatively small datasets (e.g. 5GB for genetics data of 9 million variants and 20MB of thousand phenotypes for 4000 individuals) that are easily transferred and can subsequently be combined to calculate the full set of summary statistics, without making any approximation. This meta-analysis method additionally reduces computational overhead at individual sites by shifting the most expensive calculation to the central site. The total computational burden thus becomes even more efficient relative to conventional methods with additional sites.

Table 1 | Comparison of complexity and speed between the HASE framework and a classical workflow.

Stage	Complexity[c]		Time[a,b] (hours)			
			n_p=1		n_p=10^6	
	Classical workflow	HASE	Classical workflow	HASE	Classical workflow	HASE
Single site analysis	$O(n_i n_p n_t)$	$\max(O(n_i n_p), O(n_i n_t))$	2.46	0.63	2.46×10^6	0.70
Data transfer	$O(n_p n_t)$	$O(n_i n_p + n_i n_t)$	0.04	0.07*	4×10^4	11.6
Meta-Analysis	$O(n_p n_t)$	$O(n_i n_p n_t)$	0.06	0.03	6×10^4	1.7×10^3

[a] Based on a model with three covariates and 9 million genetic variants, for a total of 4034 participants from three sites. For the classical workflow we used the PLINK software for single site analysis and METAL for the meta-analysis.

[b] For single site analysis and meta-analysis the time is given in CPU hours; for the data transfer stage this is in hours using an average network speed of 10Mbps.

[c] Complexity for CPU hours is given in terms of classical computation time complexity; complexity for data transfer is shown in terms of how the size of the to be transferred data depends on the size of the input data.

** This time is derived from the transfer of partial derivatives only, because for an association analysis with relatively few phenotypes it is not necessary to transfer encoded data.*

$\mathbf{n_i}$ *- number of individuals in the study;* $\mathbf{n_p}$ *- number of phenotypes of interest;* $\mathbf{n_t}$ *- number of tests (genetic variants);* $\mathbf{N_s}$ *- number of sites in the meta-analysis. In standard analysis* $\mathbf{n_i << n_p}$ *and* $\mathbf{n_i << n_t}$

Comparison of complexity and speed

We compared the complexity and speed of HASE with a classical workflow, based on linear regression analyses with PLINK (version 1.9)[11] followed by meta-analysis with METAL[12]; two of the most popular software packages for these tasks.

Table 1 shows that HASE dramatically reduces the complexity for the single site analysis and data transfer stages. For conventional methods, the single site analysis and data transfer have a multiplicative complexity (dependent on the number of phenotypes and determinants), whereas this is only additive for HASE. Our approach requires 3.500-fold less data to transfer for a high-dimensional association study. Additionally, the time for single site analysis does not increase significantly from analyzing a single phenotype to a million phenotypes (Table 1). This is due to the fact that speed is determined by the highest number of either the determinants or phenotypes. Therefore, in this case with nine million genetic variants, the complexity of $\boldsymbol{O}(\boldsymbol{n_i n_p})$ is the primary factor influencing the speed,whereas $\boldsymbol{O}(\boldsymbol{n_i n_t})$ plays a secondary role.

This drastic increase in performance is made possible through the shift of the computationally most expensive regression operation to the meta-analytical stage. For the meta-analytical stage, the HASE complexity is therefore slightly higher. However, it outperforms the classical meta-analysis using METAL (total computation time reduced 35 times), owing to the efficient implementation of our algorithm.

Additionally, HASE can be used as a standard tool for high-dimensional association studies of a single site, i.e without subsequent meta-analysis or to prepare summary statistics for sharing with the central site as in a classical workflow. Although PLINK is a very popular tool for association analysis, it is not optimized for high-dimensional data sets. Therefore we compared the speed of such analyses to the recently developed tool RegScan[13], which was developed for doing GWAS on multiple phenotypes and outperformed state-of-the-art methods. We conducted several experiments within the Rotterdam Study by varying the number of phenotypes and subjects, while keeping the number of variants fixed at 2.172.718 since the complexity of both programs is linear

with respect to number of variants. HASE outperformed RegScan and the difference becomes larger for increasing numbers of subjects and phenotypes (Figure 1).

Application to real data

We used HASE to perform a high-dimensional association study in 4,034 individuals from the population-based Rotterdam Study. In this proof of principle study, we relate 8,723,231 million imputed genetic variants to 1,534,602 million brain magnetic resonance imaging (MRI) voxel densities (see Supplementary Note). The analysis was performed on a small cluster of 100 CPUs and took 17 hours to complete.

To demonstrate the potential of such high-dimensional analyses, we screened all genetic association results for both hippocampi (7,030 voxels) and identified the voxel with the lowest p-value. The most significant association (rs77956314; $p = 3 \times 10^{-9}$) corresponded to a locus on chromosome 12q24 (Figure 2), which was recently discovered in a genome-wide association study of hippocampal volume encompassing 30,717 participants[14].

Additionally, we performed the high-dimensional association studies separately in three subcohorts of the Rotterdam Study (RSI = 841, RSII = 1003, RSIII = 2190, Supplementary Notes) and meta-analyzed the results using the HASE data sharing approach, as a simulation of a standard multicenter association study. This experiment required two steps. First, for each subcohort we generated intermediate data (matrices A, B and C from the Methods section). It took on average 40 minutes on a single CPU for all genetic variants and voxels. Second, the meta-analysis, which consist of merging intermediate data and running regressions, was performed on the same cluster and took 17 hours to complete using 100 cores. We compared the association results of the pooled analysis with the meta-analysis. Figure 3 shows that the results are identical as it was predicted by theory (see Methods). We would like to point out that for the classical approach with inverse-variance meta-analysis such an experiment would be not possible to conduct, as it would require generating and sharing hundreds of terabytes of summary statistics.

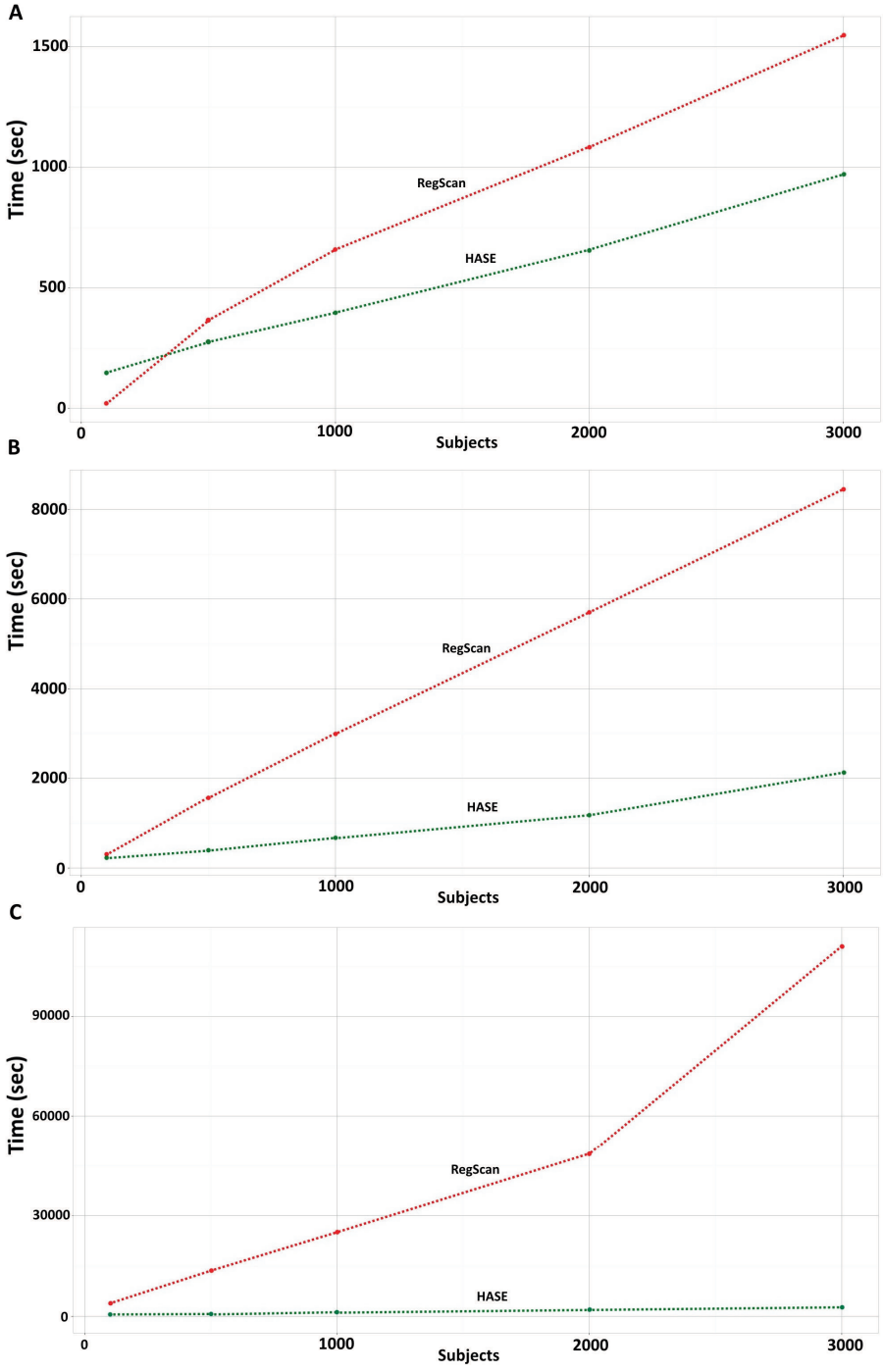

Figure 1 | Analysis time (HASE versus RegScan) with 2.172.718 variants.

A – for 1 phenotype; B – for 100 phenotypes; C- for 1000 phenotypes.

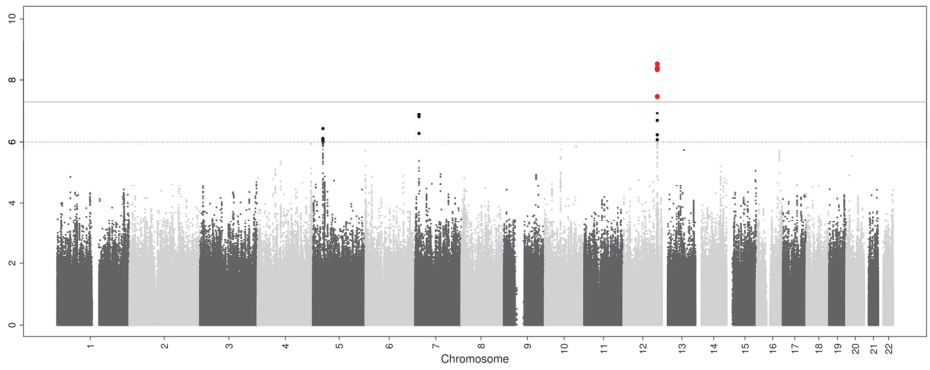

Figure 2 | Manhattan plot of the hippocampus voxel with the most significant association after screening all 7030 hippocampal voxels.
The most significant association (rs77956314; p = 3 x 10-9) corresponded to a previously identified locus on chromosome 12q24. Such voxel-wise hippocampus screening would take less than 8 hours on standard laptop.

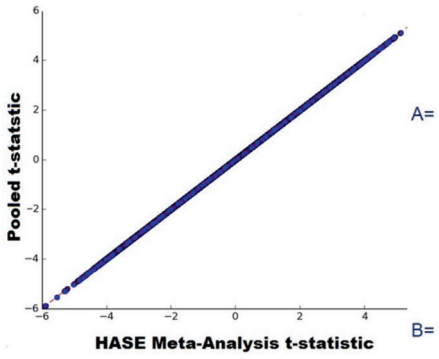

Figure 3 | Correlation plot of voxel GWAS t-statistic estimated from pooled together data and voxel GWAS t-statistic estimated from meta-analysis of partial derivatives and encoded matrix.
It took 40 min for single site to pre-compute data instead of 280 years to compute summary statistics.

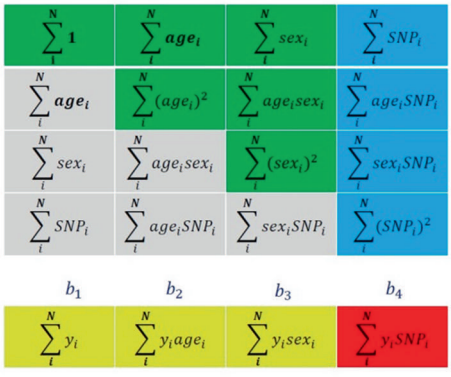

Figure 4 | Explanation of the achieved speed reduction in HASE framework by removing redundant computations.
In HASE multi-dimensional A and B matrices need to be calculated to perform GWAS studies. In the figure grey color means elements are parts of the matrix that are not necessary to calculate, as the A matrix is symmetric. The green color indicates elements that need to be calculated only once. Blue elements only have to be calculated for every SNP and yellow only for every phenotype. The red color indicates the most computationally expensive element, which needs to be calculated for every combination of phenotype and genotype. N denotes the number subjects in study.

DISCUSSION

We describe a framework that allows for (i) computationally-efficient high-dimensional association studies within individual sites using standard computational infrastructure and (ii) facilitates the exchange of compact summary statistics for subsequent meta-analysis for association studies in a collaborative setting. Using HASE, we performed a genome-wide and brain-wide search for genetic influences on voxel densities (more than 1.5 million GWAS analysis in total), and illustrate both its feasibility and potential for driving scientific discoveries.

A large improvement in efficiency comes from the reduced computational complexity. High-dimensional analyses contain many redundant calculations, which were removed in the HASE. Also, we were able to further increase efficiency by simplifying the calculations to a set of matrix operations, which are computationally inexpensive, compared to conventional linear regression algorithms. Furthermore, the implementation of partial derivatives meta-analysis allowed us to greatly reduce the size of the summary statistics that need to be shared for performing a meta-analysis. Another advantage of this approach is that it only needs to calculate the partial derivatives for each site instead of the parameter estimates (i.e., beta coefficients and standard errors). This enabled us to develop within HASE a reduction approach that encodes data prior to exchange between sites, while yielding the exact same results after meta-analysis as if the original data were used. The encoding is performed such that tracing back to original data is impossible. This guarantees protection of participant privacy and circumvents restrictions on data sharing that are unfortunately common in many research institutions.

When using HASE, it is first necessary to convert the multi-dimensional data to «HDF5[18]» format that is optimized for fast reading and writing. This particular format is not dependent on the architecture of the file system and can therefore be implemented on a wide range of hardware and software infrastructures. To facilitate this initial conversion step, we have built-in tools within the HASE framework for processing common file format of such big data. HDF5 allows direct access to the data matrix row/column from the disk through an index without reading the whole file(s) into memory. Additionally, it

requires much less disk space to store data (Supplementary Notes).This is easily generalizable to other large omics datasets in general and we foresee this initial conversion step not to form an obstacle for researchers to implement HASE.

Alternative methods for solving the issues with high-dimensional data take one of two approaches. One approach is to reduce the dimensionality of the big datasets by summarizing the large amount of data into fewer variables[2]. Although this increases the speed, it comes at the price of losing valuable information, which these big data were primarily intended to capture. The second approach is to not perform a full analysis of all combinations of the big datasets, but instead make certain assumptions (e.g., a certain underlying pattern, or a lack of dependency on potential confounders) that allow for using statistical models that require less computing time. Again, this is a tradeoff between speed and accuracy, which is not necessary in the HASE framework, where computational efficiency is increased without introducing any approximations.

Unidimensional analyses of big data, such as genome-wide association studies, have already elucidated to some extent the genetic architecture of complex diseases and other traits of interest[1,15–17], but much remains unknown. Cross-investigations between multiple big datasets potentially hold the key to fulfill the promise of big data in understanding of biology[7]. Using the HASE framework to perform high-dimensional association studies, this hypothesis is now testable.

METHODS

HASE

In high-dimensional associations analyses we test the following simple regression model:

$$Y = X\beta + \varepsilon \quad (1)$$

where $\mathbf{Y}$ is a $n_i \times n_p$ matrix of phenotypes of interest, n_i denotes the number of samples in the study, n_p the number of phenotypes of interest, and ε denotes the residual effect. $\mathbf{X}$ is a three dimensional matrix $n_i \times n_c \times n_t$ of independent variables, with n_c representing

the number of covariates, such as the intercept, age, sex and, for example genotype as number of alleles, and $\mathbf{n_t}$ the number of independent determinants.

In association analyses we are interested in estimating the p-value to test the null hypothesis that β=0. The p-values can be directly derived from the t-statistic of our test determinants. We will rewrite the classical equation for calculating t-statistics for our multi-dimensional matrices, which will lead to a simple matrix form solution for high-dimensional association analysis:

$$RSS(\beta) = (Y - X\beta)^T(Y - X\beta) \tag{2}$$

$$\frac{\partial RSS}{\partial \beta} = -2X^T(Y - X\beta) \tag{3}$$

$$\hat{\beta} = (X^T X)^{-1} X^T Y \tag{4}$$

$$RSS(\beta) = Y^T Y \ - Y^T X (X^T X)^{-1} X^T Y \tag{5}$$

$$T = \frac{\beta}{SE} = \frac{\beta}{\sqrt{diag((X^T X)^{-1}) \frac{RSS}{df}}} \tag{6}$$

$$= \frac{(X^T X)^{-1} X^T Y}{\sqrt{diag((X^T X)^{-1}) \frac{Y^T Y \ - Y^T X (X^T X)^{-1} X^T Y}{df}}}$$

Where **T** is $\mathbf{n_p} \times \mathbf{n_c} \times \mathbf{n_t}$ matrix of t-statistics and **df** is degree of freedom of our regression model. Let's define $\mathrm{A} = \mathrm{X^T X}$, $\mathrm{B} = \mathrm{X^T Y}$ and $\mathrm{C} = \mathrm{Y^T Y}$, so that we can write our final equation for t-statistics:

$$\mathrm{T} = A^{-1}\mathrm{B} \sqrt{\frac{df}{diag(A^{-1})(C \ - \ B^T A^{-1} B)}} \tag{7}$$

The result of this derivation is that, rather than computing all combinations of covariates and independent determinants, we only need to know three matrices: A, B and C, to calculate t-statistics and perform the full analysis. These results will be used in the section about meta-analysis.

The most computationally expensive operations here are the two multi-dimensional matrix multiplications $(\boldsymbol{A^{-1}\mathbf{B}})$ and $(\boldsymbol{B^T A^{-1} B})$, where $\boldsymbol{A^{-1}}$ is a three dimensional matrix $\mathbf{n_c \times n_c \times n_t}$ and $\mathbf{B}$ is three dimensional matrix $\mathbf{n_c \times n_p \times n_t}$. Without knowledge of the data structure of these matrices, the simplest way to write the results of their multiplication would be to use Einstein's notation for tensor multiplication:

$$(A^{-1}\mathrm{B})^{i}{}_{\mathrm{jk}} = (A^{-1})^{i}{}_{ck} B^{c}{}_{jk} \tag{8}$$

$$(B^T A^{-1} B)^{j}{}_{k} = (B^T)_{i}{}^{jk} (A^{-1}\mathrm{B})^{i}{}_{\mathrm{jk}} \tag{9}$$

$$where\ i = \overrightarrow{1, n_c};\ j = \overrightarrow{1, n_p};\ k = \overrightarrow{1, n_t} and\ c = \overrightarrow{1, n_c}$$

As you can see, the result is two matrices of $\mathbf{n_c \times n_p \times n_t}$ and $\mathbf{n_p \times n_t}$ elements respectively. Despite the seemingly complex notation, the first matrix just represents the beta coefficients for all combinations of covariates ($\mathbf{n_c}$ by $\mathbf{n_p \times n_t}$ combinations) and the second is fitting values of the dependent variable for every test ($\mathbf{n_p \times n_t}$ independent determinants).

However, insight into the data structure of **A** and **B** can dramatically reduce the computational burden and simplify operations. First of all, matrix **A** depends only on the covariates and number of determinants, making it unnecessary to compute it for every phenotype of interest, so we just need to calculate it once. Additionally, only the last covariate (i.e., the variable of interest) is different between tests, meaning that the $\mathbf{(n_p - 1) \times (n_p - 1) \times n_t}$ part of matrix **A** remains constant during high-dimensional analyses. Matrix **B** consists of the dot product of every combination of the covariate and phenotype of interest. However, as we mentioned before, there are only $\mathbf{(n_t + n_c\ 1)}$ different covariates, and thus we can split matrix **B** in two low dimensional matrices: the first includes dot products of non-tested covariates - $\mathbf{(n_c - 1) \times n_p}$ elements; the second

includes the dot products only of the tested covariates - $n_p \times n_t$ elements. Removing all these redundant calculations reduces the complexity of this step from $O(n_c^2 \cdot n_i \cdot n_p \cdot n_t)$ to $O(n_p \cdot n_t)$. All this allows us to achieve a large gain in computational efficiency and memory usage. In **Figure 3** we show a 2D schematic representation of these two matrices for standard genome association study with the covariates being an intercept, age, sex, and genotype. This example could be easily extrapolated to any linear regression model.

Applying the same splitting operation to $\boldsymbol{B^T}$ it is possible to simplify tensor multiplication equation **(8, 9)** to a low-dimensional matrix operation and rewrite the equation for t-statistics:

$$(A^{-1}\mathrm{B})^{i}{}_{\mathrm{jk}} = (A^{-1})^{i}{}_{\delta k} B^{\delta}{}_{j} + (A^{-1})^{i}{}_{\theta k} B^{\theta}{}_{jk} \tag{10}$$

$$(B^T A^{-1} B)^{j}{}_{k} = (B^T)_{\delta}{}^{j} (A^{-1}\mathrm{B})^{\delta}{}_{\mathrm{jk}} + (B^T)_{\theta}{}^{jk} (A^{-1}\mathrm{B})^{\theta}{}_{\mathrm{jk}} \tag{11}$$

$$\begin{aligned} \mathrm{T} = ((A^{-1})^{i}{}_{\delta k} B^{\delta}{}_{j} + (A^{-1})^{i}{}_{\theta k} B^{\theta}{}_{jk}) \sqrt{\frac{df}{diag(A^{-1})}} \times \\ (C - \Big((B^T)_{\delta}{}^{j} \big((A^{-1})^{i}{}_{\delta k} B^{\delta}{}_{j} + (A^{-1})^{i}{}_{\theta k} B^{\theta}{}_{jk} \big)^{\delta}_{jk} \\ + (B^T)_{\theta}{}^{jk} \big((A^{-1})^{i}{}_{\delta k} B^{\delta}{}_{j} \\ + (A^{-1})^{i}{}_{\theta k} B^{\theta}{}_{jk} \big)^{\theta}_{jk} \Big))^{-\frac{1}{2}} \end{aligned} \tag{12}$$

Then, to compute t-statistics for high-dimensional association analyses we just need to perform several matrix multiplications.

Meta-analysis

In classical meta-analysis, summary statistics such as beta coefficients and p-values are exchanged between sites. For 1.5 million phenotypes, this would yield around 400TB of data at each site, making data transfer to a centralized site impractical.

In the previous section we showed that, to compute all statistics for an association study, we just need to know the **A, B** and **C** matrices. As we demonstrated before[17], by exchanging these matrices between sites, it is possible to gain the same statistical power as with a pooled analysis, without sharing individual participant data, because these matrices consist of aggregate data (**Figure 4**). However, in high-dimensional association analyses, matrix **B** grows very fast, particularly the part that depends on the number of determinants and phenotypes ($\mathbf{b_4}$ in **Figure 3**).

If **Y** is a $\mathbf{n_i \times n_p}$ matrix of phenotypes of interest and **G** is a $\mathbf{n_i \times n_t}$ matrix of determinants which we want to test (e.g., a genotype matrix in GWAS), then $\mathbf{b_4 = Y^T \times G}$. These two matrices, **Y** and **G**, separately are not so large, but their product matrix has $\mathbf{n_p \times n_t}$ elements, which in a real application could be $10^6 \times 10^7 = 10^{13}$ elements and thus too large to share between sites. We propose to create a random $\mathbf{n_i \times n_i}$ nonsingular square matrix **F** and calculate its inverse matrix $\mathbf{F^{-1}}$. Then by definition $\mathbf{F \times F^{-1} = I}$, where **I** is a $\mathbf{n_i \times n_i}$ elements identity matrix with ones on main diagonal and zeros elsewhere. Using this property, we can rewrite the equation for $\mathbf{b_4}$:

$$b_4 = Y^T \times G \tag{13}$$

$$b_4 = Y^T \times (F \times F^{-1}) \times G \tag{14}$$

$$b_4 = (Y^T \times F) \times (F^{-1} \times G) \tag{15}$$

$$b_4 = {Y_F}^T \times G_F \tag{16}$$

where Y_F and G_F are matrices carrying phenotypic and determinant information in encoded form respectively.Therefore, instead of transferring TBs of intermediate statistics ($\mathbf{b_4}$), each side just needs to compute **A, C,** $\mathbf{Y_F}$ **and** $\mathbf{G_F}$. Sharing just the encoded matrices does not provide information on individual participants and without knowing matrix **F** it is impossible to reconstruct the real data. However, it will be possible to calculate $\mathbf{b_4}$, perform a high-dimensional meta-analysis, and avoid problems with data transfer. Additionally, this method dramatically reduces computation time by shifting all

complex computations to central site, where the HASE regression algorithm should be used to handle the association analysis in a time efficient way.

REFERENCE

1. Wood, A. R. *et al.* Defining the role of common variation in the genomic and biological architecture of adult human height. *Nat. Genet.* **46,** (2014).
2. Goel, et al. Spatial patterns of genome-wide expression profiles reflect anatomic and fiber connectivity architecture of healthy human brain. *HBM* (2014).
3. Stunnenberg, H. G. & Hubner, N. C. Genomics meets proteomics: Identifying the culprits in disease. *Hum. Genet.* **133,** 689–700 (2014).
4. Krumsiek,. *et al.* A Systems Approach to Metabolite Identification Combining Genetic and Metabolic Information. *PLoS Gen* (2012).
5. Parmar, C. *et al.* Radiomic feature clusters and Prognostic Signatures specific for Lung and Head & Neck cancer. *Sci. Rep.* (2015).
6. Medland, S. E., Jahanshad, N., Neale, B. M. & Thompson, P. M. Whole-genome analyses of whole-brain data : working within an expanded search space. *Nat. Publ. Gr.* (2014).
7. Robinson, M. R., Wray, N. R. & Visscher, P. M. Explaining additional genetic variation in complex traits. *Trends Genet.* **30,** 124–32 (2014).
8. Zou, F. *et al.* Brain Expression Genome-Wide Association Study (eGWAS) Identifies Human Disease-Associated Variants. *PLoS Genet.* (2012).
9. Stein, J. L. *et al.* Voxelwise genome-wide association study (vGWAS). *Neuroimage* **53,** 1160–74 (2010).
10. Huang, M. *et al.* FVGWAS: Fast voxelwise genome wide association analysis of large-scale imaging genetic data. *Neuroimage* **118,** (2015).
11. Purcell, *et al.* PLINK: *Am. J. Hum. Genet.* **81,** (2007).
12. Willer, C. J., Li, Y. & Abecasis, G. R. METAL: Fast and efficient meta-analysis of genomewide association scans. *Bioinformatics* (2010).
13. Haller, T. RegScan:. *Brief. Bioinform.* (2013).
14. Hibar, D. P. *et al.* Common genetic variants influence human subcortical brain structures. *Nature* **8,** (2015).
15. Purcell, S. M. *et al.* Common polygenic variation contributes to risk of schizophrenia and bipolar disorder. *Nature* **460,** (2009).
16. Polychronakos, C. & Alriyami, M. Diabetes in the post-GWAS era. *Nat. Genet.* (2015).
17. Adams, H.H.H. *et al.* Partial derivatives meta-analysis: BioRxiv (2016).
18. HDF5 Group, "HDF5" (2006)

Chapter 2.5

Amyloid-β transmission or unexamined bias?

ABSTRACT

Jaunmuktane and colleagues reported on eight persons of short stature who had been treated with preparations of human-derived growth hormone and subsequently developed iatrogenic Creutzfeldt–Jakob disease (CJD)[1]. On autopsy, the authors found marked deposition of parenchymal and vascular amyloid-β (Aβ), which was unexpected given the relatively young age (36–51 years) of the patients. The selected comparator group included patients with sporadic CJD, who were not of short stature and did not receive any growth hormone treatment. These sporadic cases did not show marked Aβ pathology. Although the authors make an interesting case for iatrogenic transmission of Aβ pathology, their findings could also be explained by two notable differences between the eight growth-hormone-treated patients and the comparator group: the indication for growth hormone treatment and the treatment itself.

MAIN TEXT

The eight patients at the centre of this study received growth hormone treatment for various reasons, including panhypopituitarism (numbers 1, 2, 7), mental retardation (number 2), microcephaly (number 2), craniopharyngioma (number 5), and idiopathic short stature (numbers 3, 4, 6, 8). The cases with marked Aβ deposition (numbers 4, 5, 6, 8) were generally of short stature owing to unknown causes. Common to this heterogeneous group of patients is the lack of endogenous growth hormone, a hormone that plays an important role in learning and memory, synaptic plasticity, neurogenesis, and is considered as a treatment for patients with cognitive impairment resulting from its deficiency[2]. Insulin-like growth factor-1 (IGF-1) is one of the main downstream targets regulated by growth hormone and supports cell survival and growth at multiple levels, with IGF-1 being important in the brain. It plays a well-documented role in many aspects of neurodegeneration, including Alzheimer's disease[3,4], and IGF-1 promotes Aβ production[5,6]. Lack of IGF-1 has been proposed to cause neurodegenerative disorders such as Alzheimer's disease owing to the disturbed trophic support to neurons (for a review, see ref. 7). Absence or reductions in IGF-1 can thus promote neurodegeneration and, particularly worrying for the conclusion of Jaunmuktane *et al.* increase Aβ depositions. This mechanism is similar to the lack of insulin seen in type 1 diabetes. In other words, the underlying disease state, which was the indication to start growth hormone treatment, can act as a shared cause of Aβ deposition and — through treatment with human-derived growth hormone — CJD. This should therefore be considered a confounder of the effect under study (that is, confounding by the indication of growth hormone treatment). The comparator group presented by Jaunmuktane *et al.* does not allow for confounding adjustment, as all exposed (that is, growth-hormone-treated) individuals are growth-hormone deficient (and of short stature) and all unexposed individuals are not, which means any differences between the comparator groups could also be explained by growth hormone deficiency.

Furthermore, growth hormone treatment itself should have been considered as an important alternative cause of the Aβ deposition. Although this might seem

counterintuitive, as increased IGF-1 levels should increase Aβ clearance, this alternative explanation is not without support. Both low and high levels of IGF-1 have been observed in neurodegenerative diseases, and this is also the case for Alzheimer's disease[8,9]. It has been proposed that this is due to an abundance of IGF-1 that reduces the sensitivity of the cells[7]. Given the long-term treatment of patients with growth hormone, where the complex circadian and age-dependent rhythm of growth hormone secretion is not taken into account, it is plausible that this led to cell resistance to IGF-1. This mechanism is similar to the increased levels of insulin (to which patients are resistant) seen in type 2 diabetes. Therefore, growth hormone treatment could possibly lead to the development of Aβ depositions in individuals at an earlier age than if untreated. Similar to the previous point, this would also confound the authors' interpretation, in this case confounding by growth hormone treatment.

The authors mention prion disease as an improbable cause for their findings, for example, through protein cross-seeding or clearance overload, which they attempt to rule out by comparing the iatrogenic CJD patients to sporadic cases. On the basis of the lack of marked Aβ depositions in the sporadic cases, the authors concluded that prion disease does not predispose to Aβ depositions and thus another factor must cause these deposits. This conclusion does not appear fully warranted as the excess of Aβ in iatrogenic CJD compared to sporadic CJD does not indicate whether prion disease causes Aβ depositions (independently of this other factor). In other words, by restricting the study to patients who all have prion disease, the effect of prion disease compared to no prion disease cannot be examined. A comparison of persons with CJD to those without CJD but who are similar with regard to important confounders (for example, age, sex, other medical conditions and treatments) would better inform such an effect, as has been done in a previous study[10]. Although the greater deposition of Aβ in the iatrogenic CJD cases compared to the sporadic CJD therefore does not prove or disprove prion disease as a cause for this, we agree with the authors that this points to a factor other than prion disease causing the additional Aβ deposits. We have already mentioned the indication for growth hormone treatment and the growth hormone treatment itself as two plausible causes for Aβ deposits; the authors focus on the potential human transmissibility. On the basis of the data presented by the authors

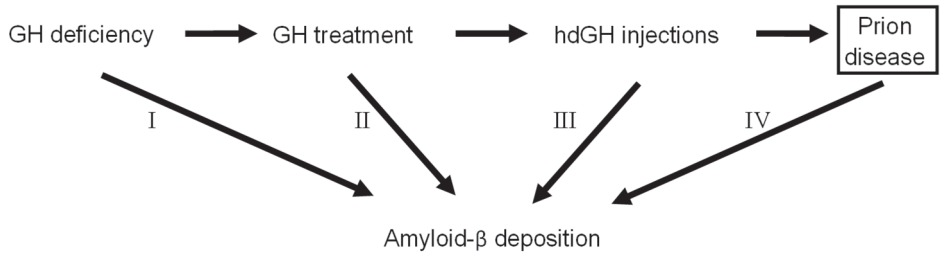

Figure 1 | Causal diagram showing the proposed causal pathway, the authors' interpretation, the two confounding biases and the inappropriate conditioning on presence of prion disease.

Horizontal arrows depict the known causal pathway of growth hormone deficiency being the indication for growth hormone treatment, which is administered using human-derived growth hormone injections, which in turn can cause CJD if contaminated with prions. The numbered arrows indicate possible effects on Aβ deposition. From their data, the authors conclude (see below) that CJD could not have a direct effect, that is, that the arrow IV is not present. The authors then conclude that the shared cause must lie in the human-derived growth hormone injections (arrow III), which they infer contained infectious prions as well as infectious amyloid. However, there are two alternative shared causes for the co-occurrence of prion disease and amyloid, namely the indication of growth hormone treatment (arrow I) and the treatment itself (arrow II). In the current study design, these alternative explanations are therefore confounders of the proposed arrow III if arrows I and/or II are present. The authors sought to rule out arrow IV by comparing iatrogenic CJD patients with sporadic CJD patients. However, in this comparison all included patients have prion disease, which thus entails conditioning on the exposure (indicated with the square box around prion disease). While this comparison may suggest that another factor is causing additional Aβ (e.g, arrows I–III), it does not inform about prion disease causing Aβ deposition; that is, arrow IV cannot be proven or ruled out. Finally, for simplicity, the causal diagram above does not include additional unmeasured shared causes; in particular, if prion disease and Aβ deposition shared other causes beyond those described here, then additional confounding and/or selection biases invalidating the authors' interpretation may also be present.

alone, it is not possible to determine which factor or factors are actually causal; their findings are consistent with multiple explanations.

Given that the results of Jaunmuktane *et al.* are inconclusive in this respect, what data would help to disentangle the hypothesized transmissibility from these competing explanations? One study design option would entail comparing persons of short stature who received synthetic versus human-derived growth hormone, as the synthetically produced treatment could not transmit any infectious agent from another person. We understand the difficulty concerning persons treated with synthetic hormone as a comparator group, as they have longer expected lifespans than those with (iatrogenic)

Table 1 | Four potential causes of marked Aβ deposition in persons of short stature treated with human growth hormone and subsequently developing iatrogenic CJD.

Potential cause of Aβ deposition*	Consistency of the purported causal effect with findings	Stated conclusions from the authors
Short stature (vs normal stature)	Yes	Not discussed
GH treatment (vs no GH treatment)	Yes	Not discussed
Human-derived GH (vs synthetic GH)	Inconclusive†	Causal
Prion disease (vs no prion disease)	Inconclusive‡	Not causal

The first column shows four potential causes for the observed Aβ deposition in persons of short stature who were treated with human-derived growth hormone and developed CJD as a result of prion transmission (and their causal contrasts in parentheses). The second column indicates whether the causes are consistent with the findings of Jaunmuktane et al., whereas the third column contains the conclusions of the authors.

CJD. Although neuropathology in a comparable age group will therefore be relatively difficult to obtain, non-invasive methods to quantify Aβ depositions in the brain, for example using positron emission tomography (PET) imaging, might be useful. Four possible causes of the marked deposition of Aβ are summarized in Table 1 along with, for each of these factors, consistency with the findings of Jaunmuktane *et al.*, and the emphasized conclusion of the authors. Figure 1 depicts the suspected confounding biases in the current study design[11].

In conclusion, the study presented by Jaunmuktane *et al.* is consistent with multiple explanations for the marked deposition of Aβ. However, the authors emphasize one hypothesis indirectly supported by the data over other hypotheses, although a considerable body of previous empirical evidence argues in favour of these alternative explanations. Furthermore, the improbable explanation of CJD cross-seeding was disregarded on the basis of experiments that provide no such evidence, and was subsequently discussed at length whereas the plausible alternatives have not been mentioned. For these reasons, and in particular given the public health implications incited by the publicity of the Jaunmuktane *et al.* study[12], it is imperative to carefully consider confounders and study design[13,14] when weighing the possibility of human transmissibility of Aβ.

REFERENCES

1. Jaunmuktane, Z. *et al.* Evidence for human transmission of amyloid-β pathology and cerebral amyloid angiopathy. *Nature* **525,** 247–250 (2015).
2. Nyberg, F. & Hallberg, M. Growth hormone and cognitive function. *Nat. Rev. Endocrinol.* **9,** 357–365 (2013).
3. Gasparini, L. & Xu, H. Potential roles of insulin and IGF-1 in Alzheimer's disease. *Trends Neurosci.* **26,** 404–406 (2003).
4. Westwood, A. J. *et al.* Insulin-like growth factor-1 and risk of Alzheimer dementia and brain atrophy. *Neurology* **82,** 1613 (2014).
5. Carro, et al. Serum insulin-like growth factor I regulates brain amyloid-β levels. *Nat. Med.* **8** (2002).
6. Araki, et al. *Biochem. Biophys. Res. Commun.* **380,** (2009).
7. Trejo. et al. Role of insulin-like growth factor I signaling in neurodegenerative diseases. *J. Mol. Med. (Berl.)* **82** 2004.
8. Mustafa, A. *et al.* Decreased plasma insulin-like growth factor-I level in familial Alzheimer's disease patients carrying the Swedish APP 670/671 mutation. *Dement. Geriatr. Cogn. Disord.* **10,** 446–451 (1999).
9. Tham, A. *et al.* Insulin-like growth factors and insulin-like growth factor binding proteins in cerebrospinal fluid and serum of patients with dementia of the Alzheimer type. *J. Neural Transm. Park. Dis. Dement. Sect.* **5,** 165 (1993).
10. Hainfellner, J. A. *et al.* Coexistence of Alzheimer-type neuropathology in Creutzfeldt–Jakob disease. *Acta Neuropathol.* **96,** 116–122 (1998).
11. Greenland, et al. Causal diagrams for epidemiologic research. *Epidemiology* **10** (1999).
12. Abbott, A. The red-hot debate about transmissible Alzheimer's. *Nature* **531,** 294 (2016).
13. Rothman, K. J., Greenland, S. & Lash, T. L. *Modern epidemiology*. (Lippincott Williams & Wilkins, 2008).
14 Hernán, M. A. & Robins, J. M. *Causal Inference*. (Boca Raton: Chapman & Hall/CRC) In press.

Chapter 3

Genetic discoveries

Chapter 3.1

Neurodegenerative markers

Chapter 3.1.1

Genome-wide association study of intracranial volume

ABSTRACT

Intracranial volume reflects the maximally attained brain size during development, and remains stable with loss of tissue in late life. It is highly heritable, but the underlying genes remain largely undetermined. In a genome-wide association study of 32,438 adults, we discovered five novel loci for intracranial volume and confirmed two known signals. Four of the loci are also associated with adult human stature, but these remained associated with intracranial volume after adjusting for height. We found a high genetic correlation with child head circumference ($\rho_{genetic}$=0.748), which indicated a similar genetic background and allowed for the identification of four additional loci through meta-analysis ($N_{combined}$ = 37,345). Variants for intracranial volume were also related to childhood and adult cognitive function, Parkinson's disease, and enriched near genes involved in growth pathways including PI3K-AKT signaling. These findings identify the biological underpinnings of intracranial volume and their link to physiological and pathological traits.

INTRODUCTION

The intricate genetic control of the human brain, complemented by environmental factors, leads to the observed variations in brain size in human populations[1]. Intracranial volume is closely related to brain volume in early life as the brain grows.[2,3] However, it becomes stable after the brain has fully developed and remains unaffected by later age-related changes such as brain atrophy[4,5], thus representing the maximal attained brain size. Discovering genetic variants that influence intracranial volume can contribute to our understanding of brain development and related diseases, but prior studies have only identified two influential genetic loci[6-9].

Here, we performed genome-wide association studies in populations from the Cohorts for Heart and Aging Research in Genomic Epidemiology (CHARGE)[10] and Enhancing NeuroImaging Genetics through Meta-Analysis (ENIGMA)[11] consortia on intracranial volume measured by magnetic resonance imaging. Genotypes were imputed to the 1000 Genomes reference panel (phase 1, version 3). Meta-analysis revealed five novel loci associated with intracranial volume. We also discovered genome-wide overlap between intracranial volume and other key traits including height, cognitive ability, and Parkinson's disease. Furthermore, we found relatively enriched patterns of association for certain functional categories of variants and near genes that are involved in specific pathways.

RESULTS

Genome-wide association studies

Detailed information on the population characteristics, image acquisition and processing, and genetic quality control can be found in the Online Methods and Supplementary Tables S1-3.

The discovery meta-analysis (N = 26,577) yielded seven genome-wide significant ($p < 5 \times 10^{-8}$) loci, five of them novel (Figures 1-2; Table 1). The quantile-quantile plot showed inflation ($\lambda = 1.092$; Figure S1), which we determined to be mainly due to polygenicity rather than cryptic relatedness or population stratification using LD score regression[12]. Next we analyzed European samples (N = 2,362; not included in the discovery sample) and generalization samples with African (N = 938), Asian (N = 955), and Hispanic (N = 1,605) ancestries (Table 1). All variants had the same direction of effect in the additional European samples (*sign test*, $P = 0.0078$), and three variants replicated, at nominal significance. Although sample sizes were small for the non-Europeans, here too, the direction of effect was generally concordant (*sign test,* $P = 0.039$). Five nominally significant associations were detected across all three ethnicities.

Next we were able to map the association to novel variants for two previously identified loci at 17q21 (rs199525; $P = 3.8 \times 10^{-21}$) and 6q22 (rs11759026; $P = 2.2 \times 10^{-20}$)[6,7]. The five novel loci were on 6q21 (rs2022464; $P = 3.7 \times 10^{-11}$), 10q24 (rs11191683; $P = 1.1 \times 10^{-10}$), 3q28 (rs9811910; $P = 2.0 \times 10^{-9}$), 12q14 (rs138074335/ rs7312464; $P = 6.2 \times 10^{-9}$), and 12q23 (rs2195243; $P = 1.5 \times 10^{-8}$). Functional annotation of the variants and those in LD ($r^2 > 0.8$) can be found in Table S4**.**

Table 1 | Association of genome-wide significant loci for intracranial volume in European, African, Asian, and Hispanic populations.

						European discovery (N=26,577)		European replication (N=2,363)		African generalization (N=938)		Asian generalization (N=955)		Hispanic generalization (N=1605)	
Genetic variant	Locus	Position	A1	A2	Freq	β	P	β	P	β	P	β	P	β	P
rs199525	17q21	44847834	T	G	0.80	.102	$3.8x10^{-21}$	.024	0.407	.358	$1.3x10^{-3}$	.264	0.406	.035	0.493
rs11759026	6q22	126792095	A	G	0.76	-.095	$2.2x10^{-20}$	-.019	0.528	-.131	0.194	-.071	0.123	-.046	0.209
rs2022464	6q21	108945370	A	C	0.30	-.063	$3.7x10^{-11}$	-.090	$5x10^{-3}$	-.060	0.233	-.105	0.035	-.088	0.013
rs11191683	10q24	105170649	T	G	0.33	.059	$1.1x10^{-10}$	.040	0.174	.187	0.021	.085	0.075	-.005	0.911
rs9811910	3q28	190670902	C	G	0.08	.096	$2.0x10^{-9}$	.075	0.010	.346	0.020	.101	0.621	-.148	0.187
rs138074335	12q14	66374247	A	G	0.59	.051	$6.2x10^{-9}$	.106	$3x10^{-4}$	-.016	0.735	-.004	0.951	.001	0.984
rs2195243	12q23	102922986	C	G	0.22	-.059	$1.5x10^{-8}$	-.044	0.132	.037	0.585	-.020	0.774	-.093	0.101

Abbreviations: A1 = effect allele, A2 = reference allele, Freq = frequency of the effect allele, SE = standard error, N = sample size.

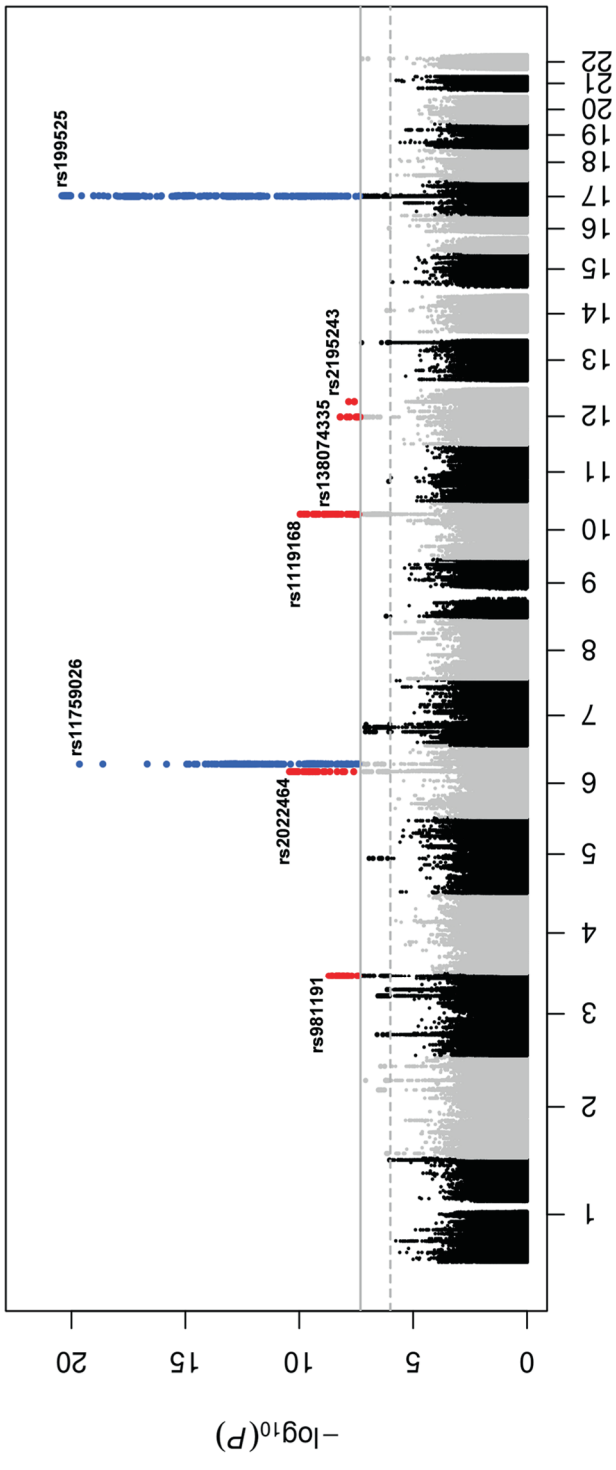

Figure 1 | Common genetic variants associated with intracranial volume.

Manhattan plot where every point represents a single genetic variant plotted according to its genomic position (x-axis) and its –log10(p-value) for association with intracranial volume (y-axis). Variants in blue are genome-wide significant in a previously known locus, whereas red variants reach genome-wide significant for the first time in that locus. The dashed horizontal line represents a significance threshold of p-value < 10^{-6} and the full horizontal line represents genome-wide significance of p-value < 5×10^{-8}. Variants surpassing these thresholds are indicated by larger points.

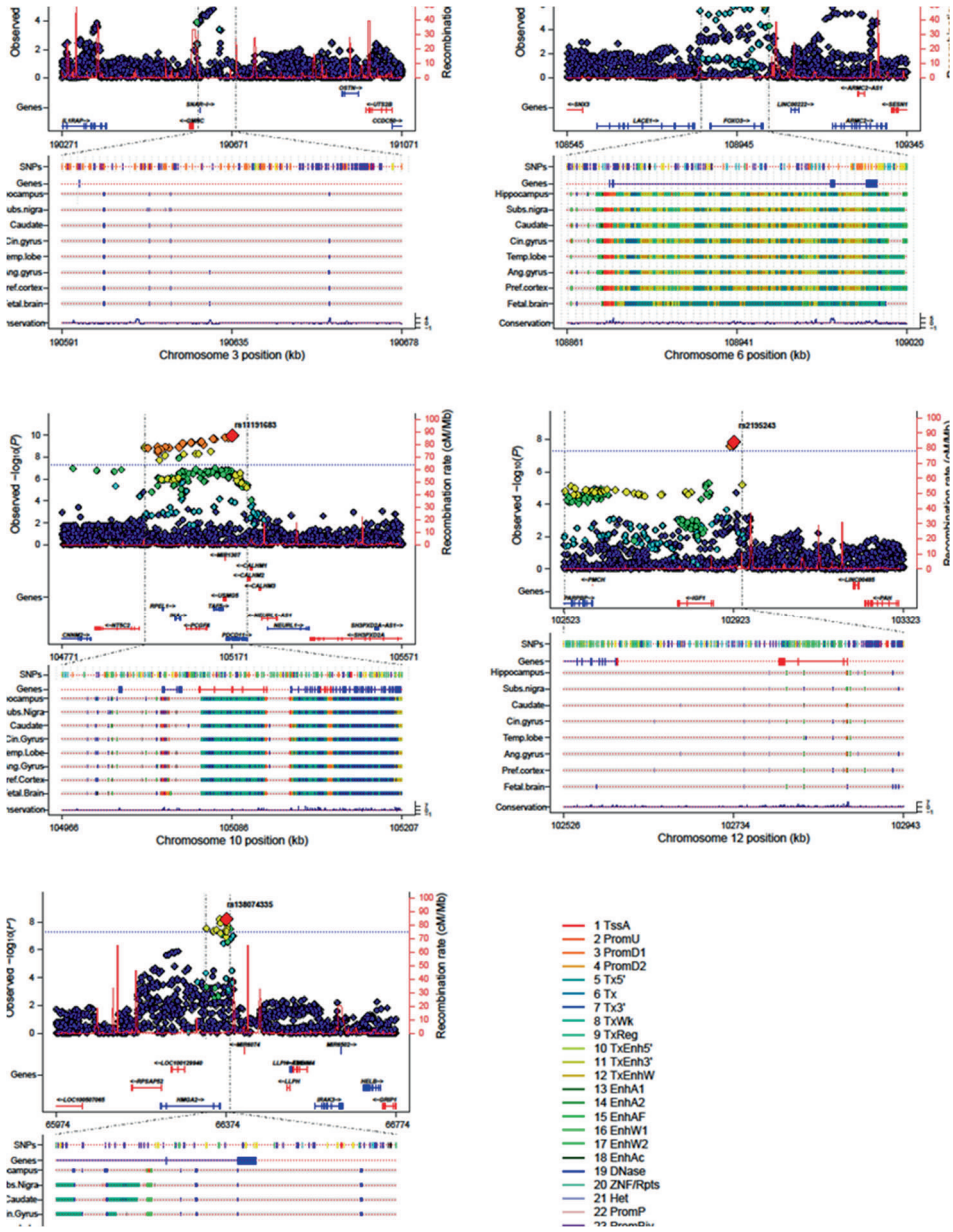

Figure 2 | Regional association and functional annotation of novel genome-wide significant loci.

Regional association plots for the five novel genome-wide significant loci of intracranial volume with gene models below (GENCODE version 19). Annotation tracks below from the Roadmap Epigenomics Consortium[57] highlight the genomic region that likely harbors the causal variant(s) (r2 > 0.8 from the top SNP). See ***Methods*** *for detailed track information. Generated using LocusTrack (http://gump.qimr.edu.au/general/gabrieC/LocusTrack/).*

Height-adjusted analyses

Four of the seven loci for intracranial volume were previously discovered for height (17q21, 6q22, 6q21, and 12q14), prompting us to investigate genome-wide overlap between the two traits. As height and intracranial volume are correlated (weighted average Pearson's $r = 0.556$; Supplementary Table S5) and this could drive association signals, we performed a GWAS of intracranial volume adjusted for height in the studies that had measured height ($N = 21,875$). Findings were compared to the corresponding subset of studies without adjustment ($N = 22,378$). Using LD score regression (Online Methods), we found that there is considerable genetic correlation between intracranial volume and height ($\rho_{genetic} = 0.241$, $P = 2.4 \times 10^{-10}$), which disappears after adjusting for height ($\rho_{genetic} = 0.049$, $P = 0.21$) (Table 2). The associations of the seven intracranial volume loci, however, remained significant after adjusting for height (Supplementary Table S6). To investigate whether more height loci were associated with intracranial volume independently of height, we analyzed all 697 genome-wide significant height variants[13]. An additional 73 variants (10.7%; 14 variants not available) showed nominally significant associations with intracranial volume but were not attenuated after adjustment for height, although none survived Bonferroni correction (Supplementary Table S7). For some variants, the direction of effect was discordant, i.e. positive for height and negative for intracranial volume. Furthermore, a polygenic score of the 697 variants predicted intracranial volume, and this was also the case after adjustment for height in a subset of the studies (Supplementary Table S8).

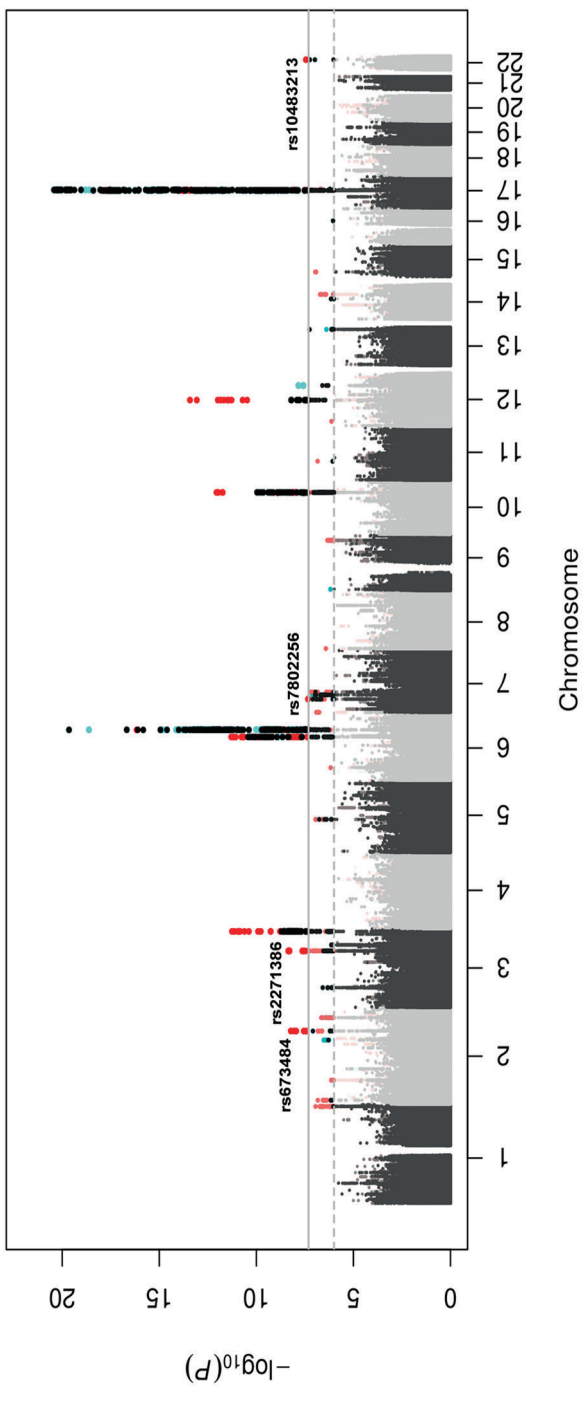

Figure 3 | Meta-analysis of intracranial volume and child head circumference.
A 'twin' Manhattan plot shows every variant twice: once for the discovery analysis and once for the combined discovery plus replication analysis. The least significant association of the variant-pair is plotted in grey (alternating light and dark between chromosomes). The most significant association of the variant-pair is plotted in red if is from the combined analysis (i.e., the association became more significant after meta-analyzing with the child head circumference GWAS) and in turquoise if it is from the discovery analysis (i.e., the association became less significant after meta-analyzing with the child head circumference GWAS). The dashed horizontal line represents a significance threshold of p-value < 10^{-6} and the full horizontal line represents genome-wide significance of p-value < 5×10^{-8}. Variants surpassing these thresholds are indicated by larger and brighter

Table 2 | Genetic correlation between intracranial volume and other anthropometric traits, cognitive function, and neurodegenerative diseases.

				Intracranial volume Full sample (N=26,577)			Intracranial volume Height subset (N=22,378)			Intracranial volume Height adjusted (N=21,875)		
Phenotype	**N_{total}**	**N_{cases}**	**Mean χ^2**	**$\rho_{genetic}$**	**SE**	**P**	**$\rho_{genetic}$**	**SE**	**P**	**$\rho_{genetic}$**	**SE**	**P**
Anthropometric traits												
Adult height	253,280	-	2.98	.249	.037	**$1.4x10^{-11}$**	.241	.038	**$2.4x10^{-10}$**	.049	.039	0.21
Child head circumference	10,768	-	1.04	.748	.121	**$5.5x10^{-10}$**	.758	.124	**$1.1x10^{-9}$**	.750	.126	**$2.5x10^{-9}$**
Birth length	28,459	-	1.07	.296	.087	**$6.7x10^{-4}$**	.278	.087	**$1.3x10^{-3}$**	.192	.088	**0.029**
Birth weight	26,836	-	1.06	.285	.081	**$4.4x10^{-4}$**	.219	.082	**$7.9x10^{-3}$**	.160	.086	0.062
Neurological traits												
Childhood cognitive function	12,441	-	1.08	.277	.090	**$2.2x10^{-3}$**	.277	.091	**$2.5x10^{-3}$**	.257	.090	**$4.2x10^{-3}$**
Adult cognitive function	53,949	-	1.15	.202	.059	**$6.3x10^{-4}$**	.205	.060	**$6.0x10^{-4}$**	.198	.059	**$6.9x10^{-4}$**
Alzheimer's Disease	54,162	17,008	1.11	-.070	.097	0.47	-.049	.097	0.61	-.043	.098	0.66
Parkinson's Disease	108,990	13,708	1.10	.315	.063	**$6.6x10^{-7}$**	.316	.070	**$5.5x10^{-6}$**	.335	.072	**$3.0x10^{-6}$**
White matter lesions	17,936	-	1.07	.112	.075	0.13	.111	.078	0.16	.096	.079	0.23
Psychiatric traits												
Autism	10,263	4,949	1.07	-.011	.069	0.87	-.036	.074	0.63	.026	.071	0.72
Bipolar disorder	11,810	6,990	1.14	.070	.071	0.33	.007	.075	0.93	-.004	.076	0.95
Major depressive disorder	16,610	9,227	1.07	.002	.100	0.98	.025	.098	0.80	.005	.096	0.96
Schizophrenia	17,115	9,379	1.23	.054	.056	0.33	.017	.058	0.77	-.009	.058	0.87
Extraversion	63,030	-	1.08	-.041	.092	0.65	-.101	.095	0.29	-.097	.092	0.29
Neuroticism	63,661	-	1.06	-.017	.109	0.87	.035	.106	0.74	.070	.111	0.53

Genetic correlation between various phenotypes and intracranial volume in the complete discovery sample ("Full sample"), adjusted for height in the studies that had measured height ("Height adjusted"), and the corresponding subset of studies without adjustment ("Height subset").

Abbreviations: SE = standard error.

Genetic correlation

In addition to height, we examined the genome-wide genetic overlap between intracranial volume and other anthropometric traits, cognitive function, and neurodegenerative diseases (Table 2). We found a strong genetic correlation with child head circumference ($\rho_{genetic}$ = 0.748), which validates intracranial volume as a measure of brain growth during early development. Since this high correlation indicates that the genetic determinants of intracranial volume and child head circumference are largely shared, we aimed to leverage this information by performing a meta-analysis of both traits. The meta-analysis (combined N = 37,345) led to the identification of four novel loci (Figure 3; Supplementary Table S9).

Weaker correlations were found with birth length and weight ($\rho_{genetic}$ < 0.3), which attenuated after adjusting for height. Additionally, intracranial volume was genetically correlated with cognitive function in childhood ($\rho_{genetic}$ = 0.277, P = $2.2x10^{-3}$) as well as general cognitive function in middle-aged and older adults ($\rho_{genetic}$ = 0.202, P = $6.3x10^{-4}$). Furthermore, we found a positive genetic correlation with Parkinson's disease ($\rho_{genetic}$ = 0.315, P = 6.6 x 10^{-7}), but there was no significant genetic overlap with Alzheimer's disease, white matter lesions, and psychiatric traits.

Enrichment analyses

Next, we assessed whether particular subsets of genetic variants were enriched for association with intracranial volume using partitioned heritability and pathway analyses (Online Methods). Overall, we found that common variants genotyped from across the whole genome explained 25.42% (S.E. 2.73%) of the variation in intracranial volume. Partitioning heritability by chromosome showed that chromosome 22 contributed twofold more to variation in intracranial volume than would be expected by its size (Figure 4A), which was not seen for any of the other complex traits from the genetic correlation analysis (Supplementary Figure S2). Partitioning by functional elements showed an enrichment for introns and several histone codes that are found in actively transcribed promoters (Figure 4B). The enrichment for intronic variants was specific to intracranial volume, whereas the other functional classes were also enriched in other

complex traits (Supplementary Figure S3). We also found that loci associated with intracranial volume cluster around genes involved in specific pathways, with 94 pathways significantly enriched (Figure 4C; full list in Supplementary Table S10). These pathways included all cell cycle components – the M-, G1-, S-, and G2-phases – and various growth factor signaling pathways, including PI3K-AKT.

Head growth trajectories

Although intracranial volume reflects brain development until maturation, and we identified influences of many growth-related processes contributing to its variation, all loci were still discovered via cross-sectional associations in adults. Therefore, we tested whether a polygenic score of the 7 loci could predict head growth in a longitudinal cohort of 2,824 children of European ancestry followed prenatally until 6 years of age (Online Methods). We found that a higher polygenic score, representing a genetically larger intracranial volume in adults, was also associated with a larger child head circumference ($\beta = .031$ per SD, $P = 0.010$). Furthermore, the effect of the polygenic score was age-dependent and more prominent in older children ($\beta = 0.0080$ per SD polygenic score per year age, $P_{interaction} = 0.0091$). When investigating the individual loci separately, both 17q21 and 12q14 showed significant associations with child head circumference, but they influenced the trajectories of head growth differently (Figure 4A-B). For 17q21, the negative impact of the G allele on head circumference becomes apparent postnatally and increases towards six years, whereas the 12q14 locus exerts an effect from early pregnancy to one year of age, but is less prominent later in life.

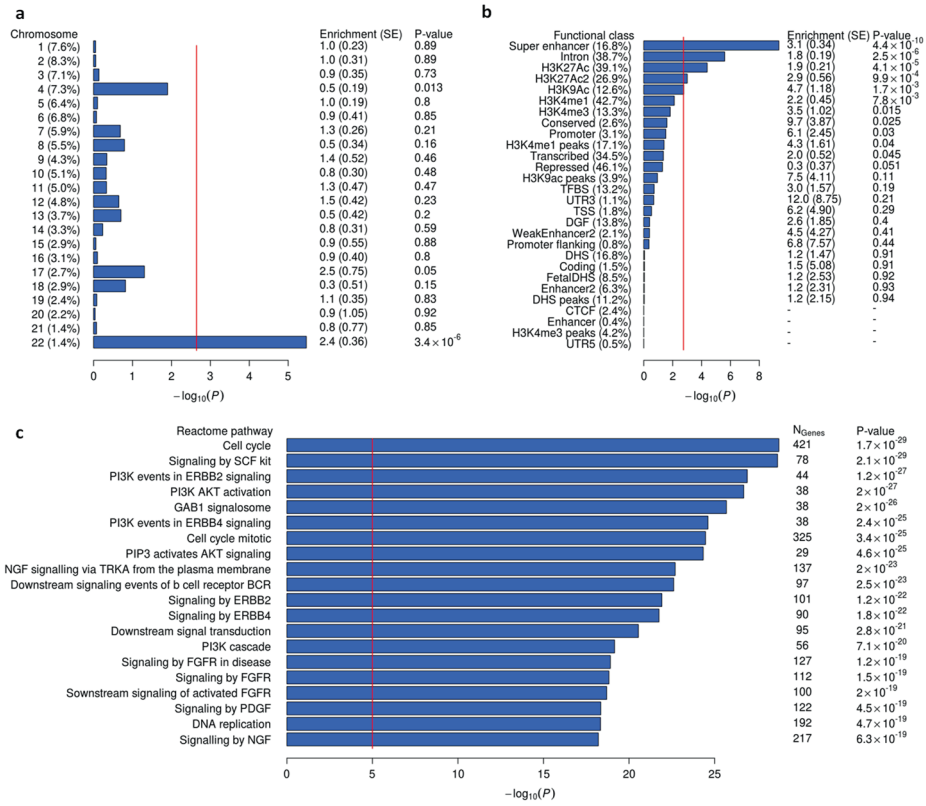

Figure 4 | Enrichment analyses of common variants associated with intracranial volume.
Enrichment of subsets of variants for association with intracranial volume: A) by chromosomes, B) by functional subtype, and C) by pathway. See ***Online Methods*** *for additional information.*

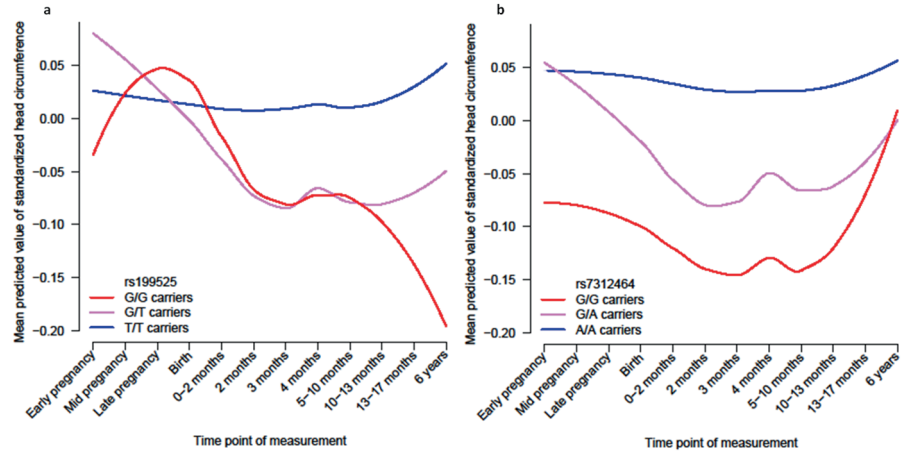

Figure 5 | Temporal trends of intracranial volume loci during pre- and postnatal brain development.

Mean predicted values of standardized head circumference using linear mixed models with age, sex, and the rs199525 or rs138074335 variants. The blue line represents children not carrying the risk allele, purple only a single risk allele, and red with two risk alleles. See ***Online Methods*** *for additional information. Total sample size is 2,824.*

DISCUSSION

Genes contributing to variation in the size of the human brain remain challenging to discover. In a worldwide project of unprecedented scale, we performed the largest-ever meta-analysis of genome-wide association studies of intracranial volume. We discovered five novel genetic loci associated with intracranial volume, and replicated two known signals. The discovery sample included Europeans only, but the direction of effect was similar in other ethnicities. The genes in these loci provide intriguing links between maximal brain size and various processes, including neural stem cell proliferation (*FOXO3*), neurodegeneration (*MAPT*), bone mineralization (*CENPW*), growth signaling (*IGF1, HMGA2*), DNA replication (*GMNC*), and rRNA maturation (*PDCD*). On a genome-wide scale, we discovered evidence of genetic correlation between intracranial volume and other key traits such as height and cognitive function, and also with Parkinson's disease, indicating that the genes underlying brain development have far-reaching effects well beyond the initial years of life.

The 17q21 locus tags a 1Mb inversion that is under positive selection in Caucasians[14]. It contains multiple genes including the *MAPT* and *KANSL1.* The *MAPT* gene is consistently implicated in various neurodegenerative disorders including Parkinson's disease, Alzheimer's disease, and frontotemporal dementia[15,16], and microduplications have been reported to cause microcephaly[17]. *KANSL1* causes the reciprocal 17q21.31 microdeletion syndrome - a multisystem disorder with intellectual disability, hypotonia and distinctive facial features[18]. The signal at 6q22 is intergenic to *CENPW* and *RSPO3*, but now lies 172kb closer to *CENPW*. Interestingly, multiple variants at this locus independently influence bone mineral density[19,20], and our signal particularly overlaps with the variant showing high specificity for the skull[20].

The significant variants at chr 6q21 span *FOXO3*, a gene associated with longevity[21], height[13], and serum IGF1 levels[22]. *FOXO3* regulates the proliferation of neural stem cells, and knockout mice show larger brains resulting from increased proliferation immediately after birth[23], followed by a decrease in adult neural stem cell renewal[23,24]. The rs3800229 variant in strong LD with our top variant ($r^2 = 0.84$) contains chromatin promoter marks in the fetal brain (Supplementary Table S4), and regulates serum IGF1

levels in infants[25]. This provides a link to the genome-wide significant locus on chr12q23 near *IGF1*, pointing to a potential mechanism through which these loci may affect brain growth. Chr12q23 lies 20Mb from one of two loci previously detected for head circumference in children[26], but that region was not associated with intracranial volume in our study (rs7980687; P = 0.06). The other reported child head circumference locus, however, corresponded to our chr12q14 signal, with the top variant lying 14kb downstream of *HMGA2*, and already showed suggestive association with intracranial volume in a previous report[7]. It has also previously been associated with height[13] and is essential for growth[27]. The chr10q24 LD-block covers multiple genes, but an intronic variant within *PDCD11* is most significant. *PDCD11* encodes an NF-kappa-B-binding protein required for rRNA maturation and generation of 18S rRNA[28]. A variant in LD (rs7894407) has recently been identified in a GWAS of cerebral white matter hyperintensities[29]. The top chr3q28 variant is located upstream of *GMNC*, which codes for the geminin coiled-coil domain-containing protein essential for DNA replication[30].

Prior efforts to identify variants affecting intracranial volume were much smaller and critically did not adjust for height[6-9]. We found that 4 out of 7 loci were already discovered for height[13], but also that over 10% of the known 'height loci' actually affect intracranial volume, even after regressing out height. Interestingly, some variants showed discordant associations for height and intracranial volume - in line with the recent finding that different height loci disproportionally affect either leg length or spine/head length[31] and may be a marker for pathological development[32]. Also, height might thus serve as a proxy phenotype for intracranial volume, with the tenfold larger sample of the height GWAS giving greater power to detect associations. Neural genes are also enriched in pathway analyses of height[13]. However, to fully disentangle whether these identified genes are 'height genes', 'brain volume genes', or 'growth genes' (i.e., pleiotropic), a large collaborative effort is needed that examines the association of these variants with both intracranial volume and height under various models.

When investigating genome-wide overlap with other traits, we found a strong correlation with child head circumference, underlining that intracranial volume is valid measure for maximal attained brain size. We were able to leverage this genetic link by

meta-analyzing both traits, which led to the identification of four additional loci (2q32.1, 3q23, 7p14.3, 22q13.2). The correlations with birth length and weight were weaker and decreased further after adjusting for height, so a similar phenotypic correlation between head size and body size at younger age may drive these correlations. Intracranial volume was also genetically associated with cognitive function in childhood as well as general cognitive function in middle-aged and older individuals. This indicates that variation in maximally attained brain size during development shares a genetic basis with cognitive ability later in life and supports intracranial volume as a measure of brain reserve[5].

The brain reserve hypothesis states that premorbid brain size can modify resilience to age-related brain pathology[33], but there was no indication of a genome-wide overlap with Alzheimer's disease. However, we found a positive genetic correlation with Parkinson's disease that rather points to a brain "overgrowth" hypothesis. Interestingly, the IGF1 and the PI3K-AKT pathways, key factors in both growth signaling and our current study of intracranial volume, are neuroprotective in a model system of Parkinson's disease[34]. There were no correlations with other neurological or psychiatric traits, indicating that this finding might be specific to Parkinson's disease. However, it is important to note that there is a certain extent of variation in the sample size and power of these studies, and larger GWAS might reveal genetic correlation with other traits as well.

It is not yet known if variance in intracranial volume, within the normal range, contributes to disease risk or brain reserve. There is no doubt that in the pathological extremes of the distribution, size can matter, as in disorders such as microcephaly or macrocephaly. Here we found evidence for a shared genetic background between intracranial volume and cognitive function, and risk of Parkinson's disease. While not definitive, these are novel pieces of empirical evidence in the debate on whether or not whole brain size matters.

The pathway analyses highlight cellular growth and proliferation and included all components of the cell cycle (M-, G1-, S-, and G2-phase) and various growth factor signaling pathways. PI3K-AKT signaling has a well described role in brain overgrowth disorders[35,36], and was the only significant pathway using a different pathway analysis

method (Supplementary Table S11). Interestingly, *AKT3* intronic variants showed suggestive evidence for association with intracranial volume (rs7538011; $P = 9.2 \times 10^{-7}$). Deletions of *AKT3* cause microcephaly syndromes[37], whereas duplications give rise to macrocephaly[38]. Similar to *FOXO3*, it is part of the IGF1 signaling pathway, which is important for human longevity[39]. The PI3K-AKT signaling pathway seems to have an important role in brain growth, not only in pathological extremes, but also for normal variation at a population level. Other pathways enriched for association with intracranial volume highlight neuronal functions such as neurotransmission and axon guidance.

We identified novel loci all influencing intracranial volume and, at a genome-wide level, there seem to be common pathways, but our longitudinal study reveals that their developmental effects are complex. The loci influenced trajectories of head growth differently; it also would be interesting to investigate whether their spatial profiles of effects are distinct, where certain loci promote growth of particular brain regions.

Here we identified key genetic loci implicated in intracranial volume within a global collaborative effort, followed by computational analyses to determine the important biological pathways and functional elements. While the majority of the genetic variants are yet to be discovered, it is clear that these will provide better insight into brain development, but also into related neuropsychiatric traits such as cognitive functioning and even for neurodegeneration late in life. Uncovering the remaining heritability will advance our understanding of the brain's complex genetic architecture.

METHODS

Study population

This study reports data on 32,438 subjects from 52 study sites that are part of the Cohorts for Heart and Aging Research in Genomic Epidemiology (CHARGE)[10] consortium and Enhancing NeuroImaging Genetics through Meta-Analysis (ENIGMA)[11] consortium. Briefly, the CHARGE consortium is a collaboration of predominantly population-based cohort studies that investigate the genetic and molecular underpinnings of age-related complex diseases, including those of the brain. The ENIGMA consortium brings together numerous studies, mainly with a case-control design, which performed neuroimaging in

a range of neuropsychiatric or neurodegenerative diseases, as well as healthy normative populations. Studies participated in either the discovery cohort of European ancestry, the replication in European ancestry, or the generalization to other ethnicities. An overview of the demographics and type of contribution for each cohort is provided in Supplementary Table S1. Written informed consent was obtained from all participants. Each study was approved by the respective Institutional Review Board or Local Ethics Committee.

Genetics

Genotyping was performed using a variety of commercial arrays across the contributing sites. Both samples as well as variants underwent similar quality control procedures based on genetic homogeneity, call rate (less than 95%), minor allele frequency (MAF < 0.01), and Hardy-Weinberg Equilibrium (HWE p-value less than 1×10^{-6}). Good quality variants were used as input for imputation to the 1000 Genomes reference panel (phase 1, version 3) using validated software packages (MaCH/minimac, IMPUTE2, BEAGLE, GenABLE). Variants that were poorly imputed ($R^2 < 0.5$) or uncommon (MAF < 0.5%) were removed prior to meta-analysis. Full details on the site-specific genotyping and quality control may be found in Supplementary Table S2.

Imaging

Magnetic resonance imaging (MRI) was obtained from scanners with a diversity of manufacturers, field strengths, and acquisition protocols. Images were used to estimate milliliters of intracranial volume from automated segmentations generated by freely available or in-house methods that have been described and validated earlier. Most sites measured intracranial volume for each participant by multiplying the inverse of the determinant of the transformation matrix required to register the subject's MRI scan to a common template by the template volume (1,948,105 mm3), using the FreeSurfer software. Visual inspections were performed to identify and remove poorly segmented images. Either all scans were visually inspected, or sites generated histogram plots to identify any outliers, which were defined as individuals with a volume more than three standard deviations away from the mean. Statistical outliers were only excluded if the

segmentations were deemed improper. . More site-specific information related to the imaging is available in Supplementary Table S3.

Genome-wide association studies

Genome-wide association studies of intracranial volume were performed for each site separately, controlling for age, sex, and, when applicable, age^2, population stratification variables (MDS / principal components), study site (for multi-site studies only), diagnosis (for case-control studies only). Studies of unrelated individuals performed a linear regression analyses whereas studies of related individuals (ASPSFam, BrainSCALE, ERF, GeneSTAR, GOBS, NeuroIMAGE, NTR-Adults, OATS, QTIM, SYS) used linear mixed models to account for familial relationships. Summary statistics, including the effect estimates of the genetic variant with intracranial volume under an additive model, were exchanged to perform a fixed-effects meta-analysis weighting for sample size in METAL[40]. After the final meta-analysis, variants were excluded if they were only available for fewer than 5,000 individuals. Meta-analyses were stratified by race and done separately for discovery, replication, and generalization samples. Beta coefficients were recalculated from Z-scores, allele frequencies, and the sample, as described earlier[41] Site-specific quantile-quantile plots were generated to inspect the presence of genomic inflation. The variance explained by all variants in the GWAS was estimated using LD score regression[12,42]. Sensitivity analyses were performed by excluding patients.

Functional annotation

All tracks of the regional association plots were taken from the UCSC Genome Browser Human hg19 assembly. *SNPs (top 5%)* shows the top 5% associated variants within the locus and are colored by their correlation to the top variant. *Genes* shows the gene models from GENCODE version 19. The tracks give the predicted chromatin states based on computational integration of ChIP-seq data for 12 chromatin marks in various human tissues derived from the Roadmap Epigenomics Consortium[43]. Additionally, we used HaploReg version 3 for annotation of the top variants and all variants in LD (> 0.80) (http://www.broadinstitute.org/mammals/haploreg/haploreg_v3.php).

Genetic correlation

The genetic correlation analyses were also performed using LD score regression. The GWAS meta-analysis of intracranial volume, as well as the height adjusted and height subset meta-analyses, were correlated with published GWAS of the following traits: Child head circumference[26], birth weight[44], birth length[45], adult height[13], childhood cognitive function[46], adult cognitive function[47], Alzheimer's disease[48], Parkinson's disease[49], white matter lesions[50], psychiatric disorders[51], neuroticism[52], and extraversion[53].

Enrichment analyses

To determine whether the intracranial volume association results were enriched for certain types of genetic variants, we employed two strategies: partitioned heritability and pathway analyses.

Partitioned heritability was calculated using a previously described method[42]. This was done by partitioning variants by chromosome and by 28 functional classes: coding, UTR, promoter, intron, histone marks H3K4me1, H3K4me3, H3K9ac5 and two versions of H3K27ac, open chromatin DNase I hypersensitivity Site (DHS) regions, combined chromHMM/Segway predictions, regions that are conserved in mammals, super-enhancers and active enhancers from the FANTOM5 panel of samples (Finucane et al. page 4)[42]. Multiple testing thresholds were calculated accordingly: P_{thresh} = 0.05/(22 chromosomes) = 2.27 x 10^{-3} for the chromosomes and P_{thresh} = 0.05/(28 classes) = 1.79 x 10^{-3} for the functional classes.

Pathway analyses were performed using the KGG2.5[54] and MAGENTA[55] software packages. LD was calculated based with the 1000 Genomes Project European samples as a reference (see URLs). Variants were considered to be within a gene if they were within 5 kb of the 3'/5' UTR based on chromosome positions (hg19) coordinates. Gene-based tests were done with the GATES test[54] without weighting *P*-values by predicted functional relevance. Pathway analysis was performed using the HYST test of association[56]. A multiple testing threshold accounting for the number of pathways tested resulting in a significance threshold of P_{thresh} = 0.05/(671 pathways) = 7.45 x 10^{-5}.

Head growth trajectories

Head growth trajectory analyses were done within the Generation R study, a longitudinal cohort study situated in Rotterdam, the Netherlands. For this analysis we included 2,824 children of European ancestry followed prenatally until 6 years of age. Head size was measured at the following points: prenatally (using echo) during the first, second, and third trimester, and postnatally (measuring head circumference) at 0-2 months, 2 months, 3 months, 4 months, 5-10 months, 10-13 months, 13-17 months, and 5 years of age. We tested whether a polygenic score of the 7 loci, as well as the 7 loci themselves separately, were related to head growth using linear mixed models and included an interaction term between time and the genetic score/variant (SAS software). Next, the predicted values were calculated for each person and plotted over time, stratified by genotype (0/1/2 risk alleles) using the R software package.

URLs

ftp://pricelab:pricelab@ftp.broadinstitute.org/LDSCORE/

http://enigma.ini.usc.edu/protocols/genetics-protocols/

http://genenetwork.nl/bloodeqtlbrowser/

http://gump.qimr.edu.au/general/gabrieC/LocusTrack/).

REFERENCES

1 Bartley et al. Genetic variability of human brain size and cortical gyral patterns. *Brain* **120**, 257-269 (1997).

2 Davis et al.. *Neuropathology and applied neurobiology* **3**, (1977).

3 Sgouros, et al. Intracranial volume change in childhood. *Journal of neurosurgery* **91**, (1999).

4 Buckner et al.. *Neuroimage* **23**, (2004).

5 Farias, S. T. *et al.* Maximal brain size remains an important predictor of cognition in old age, independent of current brain pathology. *Neurobiology of aging* **33**, 1758-1768 (2012).

6 Ikram, M. A. *et al.* Common variants at 6q22 and 17q21 are associated with intracranial volume. *Nat Genet* **44**, 539-544, doi:10.1038/ng.2245 (2012).

7 Stein, J. L. *et al. Nat Genet* **44**, 552-561, doi:10.1038/ng.2250 (2012).

8 Hibar, D. P. *et al. Nature*, doi:10.1038/nature14101 (2015).

9 Paus, T. *et al.* KCTD8 gene and brain growth in adverse intrauterine environment: a genome-wide association study. *Cerebral Cortex* **22**, (2012).

10 Psaty, B. M. *et al.. Circulation: Cardiovascular Genetics* **2** (2009).

11 Thompson, P. M. *et al.. Brain imaging and behavior* **8**, (2014).

12 Bulik-Sullivan, B. K. *et al. Nat Genet* **47**, 291-295,.

13 Wood. *et al.. Nat Genet* (2014).

14 Stefansson, H. *et al.. Nat Genet* (2005).

15 Spillantini, M. G. & Goedert, M. Tau. *The Lancet Neurology* **12**, 609-622 (2013).

16 Desikan, R. *et al.. Molecular psychiatry* (2015).

17 Kirchhoff, et al. *European journal of medical genetics* **50**, 256-263, doi:10.1016/j.ejmg.2007.05.001 (2007).

18 Koolen, D. A. *et al.. Nature genetics* **44**, 639-641 (2012).

19 Estrada, K. *et al. Nature genetics* **44**, 491-501 (2012).

20 Kemp, J. P. *et al. PLoS genetics* **10**, e1004423 (2014).

21 Broer, L. *et al. The Journals of Gerontology Series A: Biological Sciences and Medical Sciences* **70**, 110-118 (2015).

22 Kaplan, R. C. *et al. Human molecular genetics* **20**, (2011).

23 Paik, J.-h. *et al.. Cell stem cell* **5**, 540-553 (2009).

24 Renault, V. M. *et al.* FoxO3 regulates neural stem cell homeostasis. *Cell stem cell* **5**, 527-539 (2009).

25 Rzehak, P. *et al.* Associations of IGF-1 gene variants and milk protein intake with IGF-I concentrations in infants at age 6months—Results from a randomized clinical trial. *Growth hormone & IGF research* **23**, 149-158 (2013).

26 Taal, H. R. *et al.* Common variants at 12q15 and 12q24 are associated with infant head circumference. *Nat Genet* **44**, 532-538, doi:10.1038/ng.2238 (2012).

27 Lynch, S. A. *et al.* The 12q14 microdeletion syndrome: six new cases confirming the role of HMGA2 in growth. *European Journal of Human Genetics* **19**, 534-539 (2011).

28 Sweet, T., Yen, W., Khalili, K. & Amini, S. Evidence for involvement of NFBP in processing of ribosomal RNA. *Journal of cellular physiology* **214**, 381-388 (2008).

29 Verhaaren, B. F. *et al.* Multi-Ethnic Genome-Wide Association Study

of Cerebral White Matter Hyperintensities on MRI. *Circulation: Cardiovascular Genetics*, CIRCGENETICS. 114.000858 (2015).
30 Balestrini, A., Cosentino, C., Errico, A., Garner, E. & Costanzo, V. GEMC1 is a TopBP1-interacting protein required for chromosomal DNA replication. *Nature cell biology* **12**, 484-491 (2010).
31 Chan, Y. *et al.* Genome-wide Analysis of Body Proportion Classifies Height-Associated Variants by Mechanism of Action and Implicates Genes Important for Skeletal Development. *The American Journal of Human Genetics* (2015).
32 Fukumoto, A. *et al.* Head circumference and body growth in autism spectrum disorders. *Brain and Development* **33**, 569-575 (2011).
33 Stern, Y. Cognitive reserve in ageing and Alzheimer's disease. *The Lancet Neurology* **11**, 1006-1012 (2012).
34 Quesada, A., Lee, B. Y. & Micevych, P. E. PI3 kinase/Akt activation mediates estrogen and IGF 1 nigral DA neuronal neuroprotection against a unilateral rat model of Parkinson's disease. *Developmental neurobiology* **68**, 632-644 (2008).
35 Hevner, R. F. in *Seminars in perinatology.* 36-43 (Elsevier).
36 Rivière, J.-B. *et al.* De novo germline and postzygotic mutations in AKT3, PIK3R2 and PIK3CA cause a spectrum of related megalencephaly syndromes. *Nature genetics* **44**, 934-940 (2012).
37 Boland, E. *et al.* Mapping of deletion and translocation breakpoints in 1q44 implicates the serine/threonine kinase AKT3 in postnatal microcephaly and agenesis of the corpus callosum. *The American Journal of Human Genetics* **81**, 292-303 (2007).
38 Wang, D., Zeesman, S., Tarnopolsky, M. A. & Nowaczyk, M. J. Duplication of AKT3 as a cause of macrocephaly in duplication 1q43q44. *American Journal of Medical Genetics Part A* **161**, 2016-2019 (2013).
39 Pawlikowska, L. *et al.* Association of common genetic variation in the insulin/IGF1 signaling pathway with human longevity. *Aging cell* **8**, 460-472 (2009).
40 Willer, C. J., Li, Y. & Abecasis, G. R. METAL: fast and efficient meta-analysis of genomewide association scans. *Bioinformatics* **26**, 2190-2191, doi:Doi 10.1093/Bioinformatics/Btq340 (2010).
41 Chauhan, G. *et al.* Association of Alzheimer disease GWAS loci with MRI-markers of brain aging. *Neurobiology of aging* (2015).
42 Finucane, H. K. *et al. Partitioning heritability by functional category using GWAS summary statistics*. (2015).
43 Roadmap Epigenomics, C. *et al.* Integrative analysis of 111 reference human epigenomes. *Nature* **518**, 317-330, doi:10.1038/nature14248 (2015).
44 Horikoshi, M. *et al.*. *Nature genetics* **45**, 76-82 (2013).
45 van der Valk, R. J. P. *et al.* A novel common variant in DCST2 is associated with length in early life and height in adulthood. *Human molecular genetics* **24**, 1155-1168 (2015).
46 Benyamin, B. *et al.* Childhood intelligence is heritable, highly polygenic and associated with FNBP1L. *Molecular Psychiatry* **19**, 253-258 (2014).
47 Davies, G. *et al.* Genetic contributions to variation in general cognitive function: a meta-analysis of genome-wide association studies in the CHARGE consortium (N = 53 949). *Molecular Psychiatry* (2015).

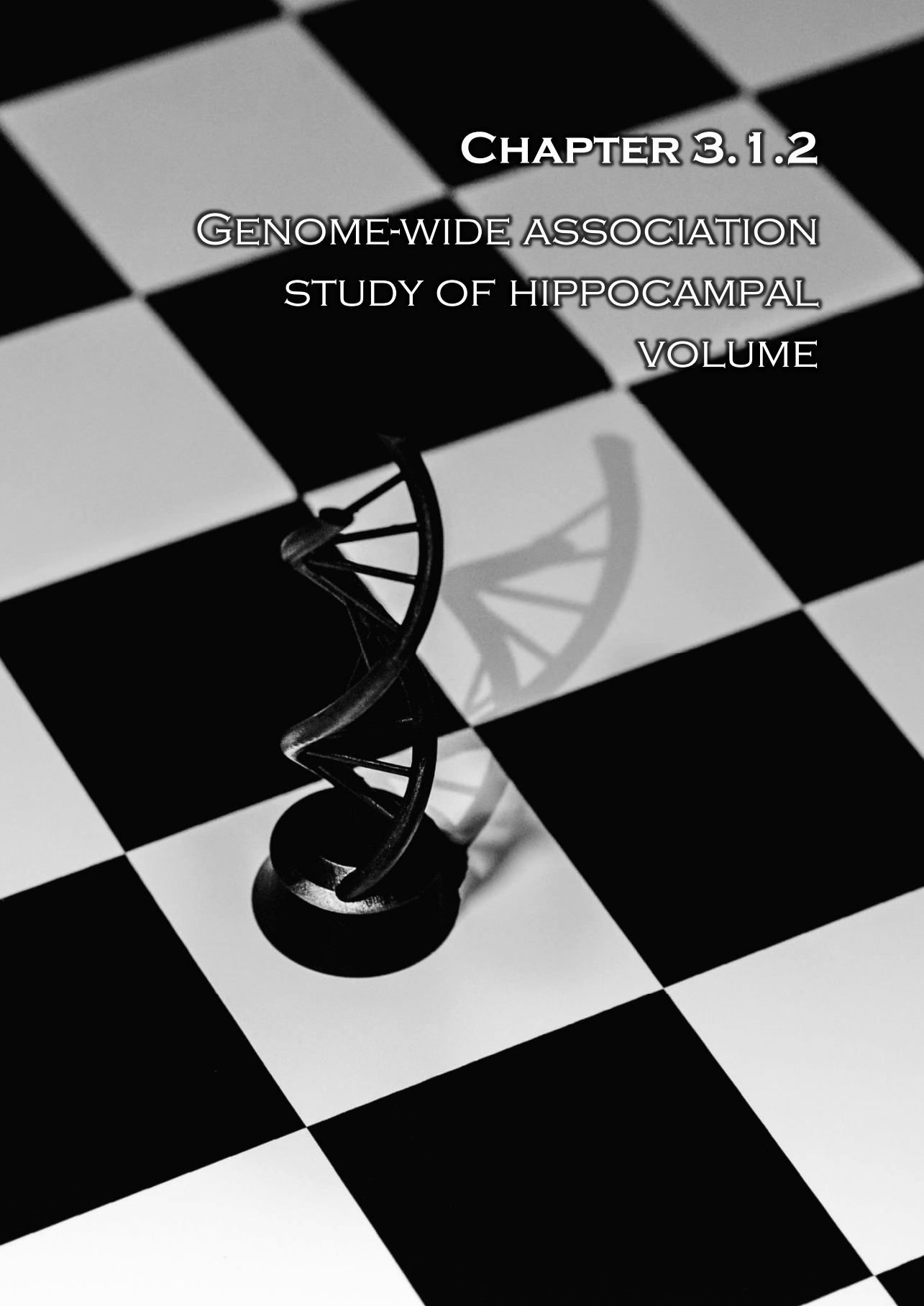

Chapter 3.1.2

Genome-wide association study of hippocampal volume

ABSTRACT

The hippocampal formation is a brain structure integrally involved in episodic memory, spatial navigation, cognition, and stress responsiveness. Structural abnormalities in hippocampal volume and shape are found in several common neuropsychiatric disorders. To identify the genetic underpinnings of hippocampal structure here we perform a genome-wide association study (GWAS) of 33,536 individuals and discover six independent loci significantly associated with hippocampal volume, four of them novel. Of the novel loci, three lie within genes (ASTN2, DPP4, MAST4) and one is found 200kb upstream of SHH. A hippocampal subfield analysis shows that a locus within the MSRB3 gene shows evidence of a localized effect along the dentate gyrus, subiculum, CA1, and fissure. Further, we show that genetic variants associated with decreased hippocampal volume are also associated with increased risk for Alzheimer's disease (r_g=-0.155). Our findings suggest novel biological pathways through which human genetic variation influences hippocampal volume and risk for neuropsychiatric illness.

INTRODUCTION

Brain structural abnormalities in the hippocampal formation are found in many complex neurological and psychiatric disorders including temporal lobe epilepsy[1], vascular dementia[2], Alzheimer's disease[3], major depression[4], bipolar disorder[5], schizophrenia[6], and post-traumatic stress disorder[7], among others. The diverse functions of the hippocampus, including episodic memory[8], spatial navigation[9], cognition[10], and stress responsiveness[11] are commonly impaired in a broad range of diseases and disorders of the brain that are associated with insults to the hippocampal structure. Further, the cytoarchitectural subdivisions (or 'subfields') of the hippocampus are associated with distinct functions. For example, the dentate gyrus (DG) and sectors 3 and 4 of the cornu ammonis (CA) are involved in declarative memory acquisition[12], the subiculum and CA1 play a role in disambiguation during working memory processes[13], and the CA2 is implicated in animal models of episodic time encoding[14] and social memory[15]. The anterior hippocampus, which includes the fimbria, CA subregions, and HATA, may be involved in the mediation of cognitive processes including imagination, recall, and visual perception[16] and anxiety-related behaviors[17].

Environmental factors, such as stress, affect the hippocampus[18], but genetic differences across individuals account for most of the population variation in its size; the heritability of hippocampal volume is high at around 70%[19-21]. High heritability and a crucial role in healthy and diseased brain function make the hippocampus an ideal target for genetic analysis. We formed a large global partnership to empower the quest for mechanistic insights into neuropsychiatric disorders associated with hippocampal abnormalities and to chart, in depth, the genetic underpinnings of the hippocampal structure.

Here we perform a GWAS meta-analysis of mean bilateral hippocampal volume in 33,536 individuals scanned at 65 sites around the world as a joint effort between the Enhancing Neuroimaging Genetics through Meta-analysis (ENIGMA) and the Cohorts for Heart and Aging Research in Genomic Epidemiology (CHARGE) consortia. Our primary goal is to find common genetic determinants of hippocampal volume with previously unobtainable power. We make considerable efforts to coordinate data analysis across all sites from both consortia in order to maximize the comparability of both genetic and

imaging data. Standardized protocols for image analysis and genetic imputation are freely available online. In the most powerful imaging study of the hippocampus to date, we shed light on the common genetic determinants of hippocampal structure and allow for a deepened understanding of the biological workings of the brain's memory center. We confirm previously identified loci influencing hippocampal volume, identify four novel loci, and determine gross genetic overlap with Alzheimer's disease.

RESULTS

Novel genome-wide markers forippocampal volume

Our combined meta-analysis (n = 26,814 individuals of European ancestry) revealed six independent, genome-wide significant loci associated with hippocampal volume (Figure 1; Table 1). Four are novel: with index SNPs rs11979341 (7q36.3; P=1.42x10^{-11}), rs7020341 (9q33.1; P=3.04x10^{-11}), rs2268894 (2q24.2; P=5.89x10^{-11}), and rs2289881 (5q12.3; P=2.73x10^{-8}). The other two loci have been previously characterized in detail: with index SNPs rs77956314 (12q24.22, P=2.06x10^{-25}), in linkage disequilibrium (LD) (r^2=0.901 in European samples from the 1000 Genomes Project, Phase 1v3) with our previously identified variant at this locus (rs7294919) and rs61921502 (12q14.3, P=1.94x10^{-19}), in LD (r^2=0.459) with previous top locus rs17178006[22-24] (Figure 2a-f). In addition to these SNPs, we identified nine independent loci with a statistically suggestive influence on hippocampal volume (P < 1x10^{-6}; Supplementary Data 4). All pathway results and gene-based p-values are summarized in Supplementary Data 6 and 7.

Table 1 | Genetic variants at six loci were significantly associated with hippocampal volume.

RSID	Chr	Pos	Nearest Gene	A1	A2	Freq	Z-score	N	P-value
rs77956314	12	117323367	4 kb 5′ to *HRK*	T	C	0.92	-10.48	26814	2.06x10^{-25}
rs61921502	12	65832468	intron of *MSRB3*	T	G	0.85	9.017	26814	1.94x10^{-19}
rs11979341	7	155797978	200 kb 5′ to *SHH*	C	G	0.68	-6.755	24484	1.42x10^{-11}
rs7020341	9	119247974	intron of *ASTN2*	C	G	0.36	6.645	26700	3.04x10^{-11}
rs2268894	2	162856148	intron of *DPP4*	T	C	0.54	-6.546	26814	5.89x10^{-11}
rs2289881	5	66084260	intron of *MAST4*	T	G	0.35	-5.558	26814	2.73x10^{-8}

The allele frequency (Freq) and effect size (Z-score) are given with reference to Allele 1. Effect sizes are additive effects for each copy of Allele 1 given as a Z-score. Additional validation was attempted in non-European ancestry generalization samples (shown in Supplementary Data 5).

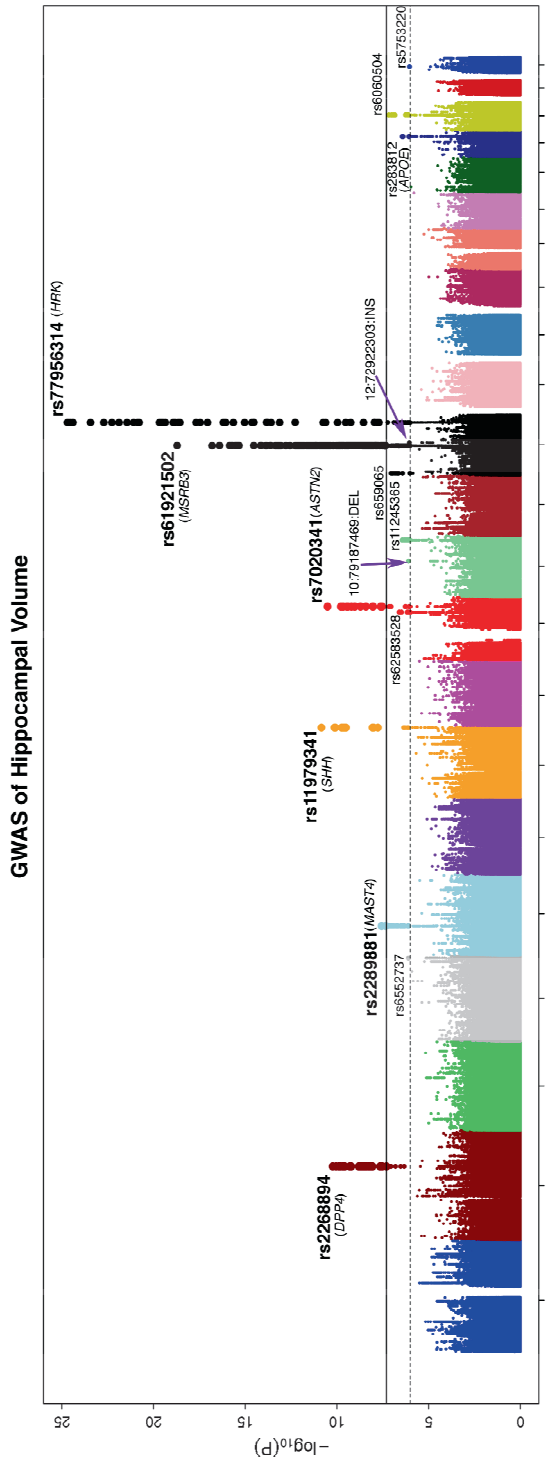

Figure 1 | Common genetic variants associated with hippocampal volume (N=26,814 of European ancestry).
A Manhattan plot displays the association P-value for each single nucleotide polymorphism (SNP) in the genome (displayed as $-log_{10}$ of the P-value). Genome-wide significance is shown for the $P = 5x10^{-8}$ threshold (solid line) and also for the suggestive significance threshold of $P = 1x10^{-6}$ (dotted line). The most significant SNP within an associated locus is labeled. For the significant loci and age-dependent loci (Chromosome 19) we labeled the nearest gene, which is not necessarily the gene of action.

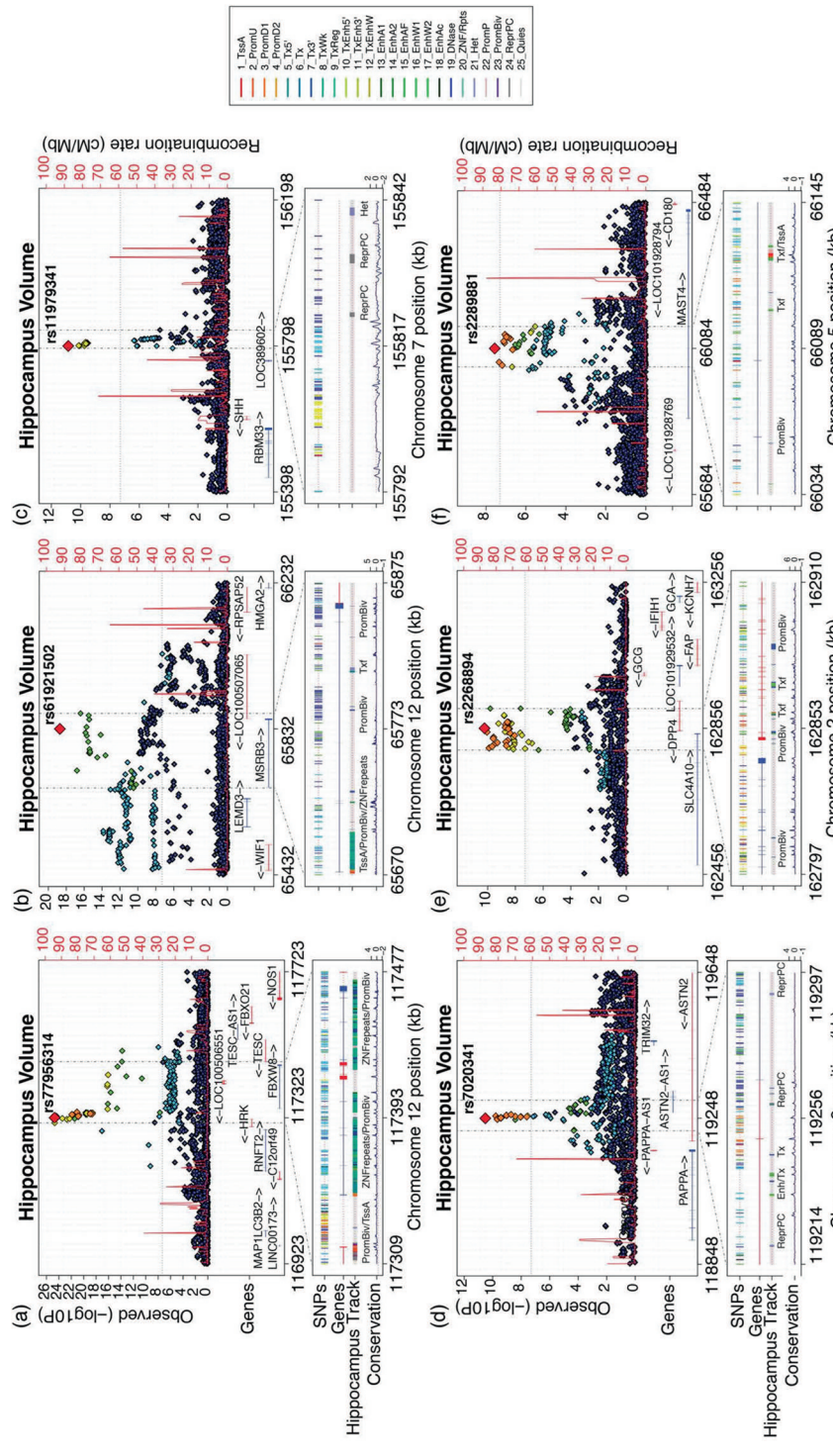

Figure 2 | Functional annotation within genome-wide significant loci.
*For each panel, zoomed-in Manhattan plots (+/- 400 kb from top SNP) are shown with gene models below (GENCODE v19). Plots below are zoomed to highlight the genomic region that likely harbors the causal variant(s) ($r^2 > 0.8$ from the top SNP). Genomic annotations from the Roadmap Epigenomics Consortium[53] are shown to indicate potential functionality (see **Methods** for detailed track information). Plots were made with*

Variance explained by common variants

Common variants genotyped from across the whole genome explained as much as 18.76% (S.E. 1.56%) of the observed variance in human hippocampal volume, based on LDSCORE regression[25] (Supplementary Fig. 3). Common genetic variants account for around a quarter of the overall heritability, estimated in twin studies to be around 70%[19-21]. Further partitioning the genome into functional categories using LDSCORE[26] revealed significant over-representation of regions evolutionarily conserved in mammals (*P*=0.0026): 2.6% of the variants accounted for 43.3% of the 18.76% variance explained (Figure 3).

Effects of top variants on hippocampal subfield volume

To test for differential effects on individual subfields of the hippocampal formation, we examined the six significant variants influencing whole hippocampal volume in a large cohort (n = 5,368). We found that the top SNP from our primary analysis, rs77956314, has a broad, nonspecific effect on hippocampal subfield volumes with the greatest effect in the right hippocampal tail ($P = 1.27x10^{-8}$). rs61921502 showed strong lateral effects across right hippocampal subfields with the largest effect in the right hippocampal fissure ($P = 6.45x10^{-9}$). rs7020341 showed greatest effects bilaterally in the subiculum (left: $P = 1.59x10^{-8}$; right: $P = 1.42x10^{-8}$). rs2268894 show left-lateralized effects across hippocampal subfields with the strongest effect in the left hippocampal tail ($P = 1.76x10^{-5}$). The remaining two variants (rs11979341 and rs2289881) did not show significant evidence of association across any of the hippocampal subfields. See Supplementary Data 8 for the full results.

Genetic overlap with hippocampal volume

We used LDSCORE[27] regression to quantify the degree of common genetic overlap between variants influencing the hippocampus and those influencing Alzheimer's disease. We found significant evidence of a moderate, negative relationship whereby variants associated with a decrease in hippocampal volume are associated with an increased risk for Alzheimer's disease (r_g=-0.155 (S.E. 0.0529), P=0.0034; see Methods).

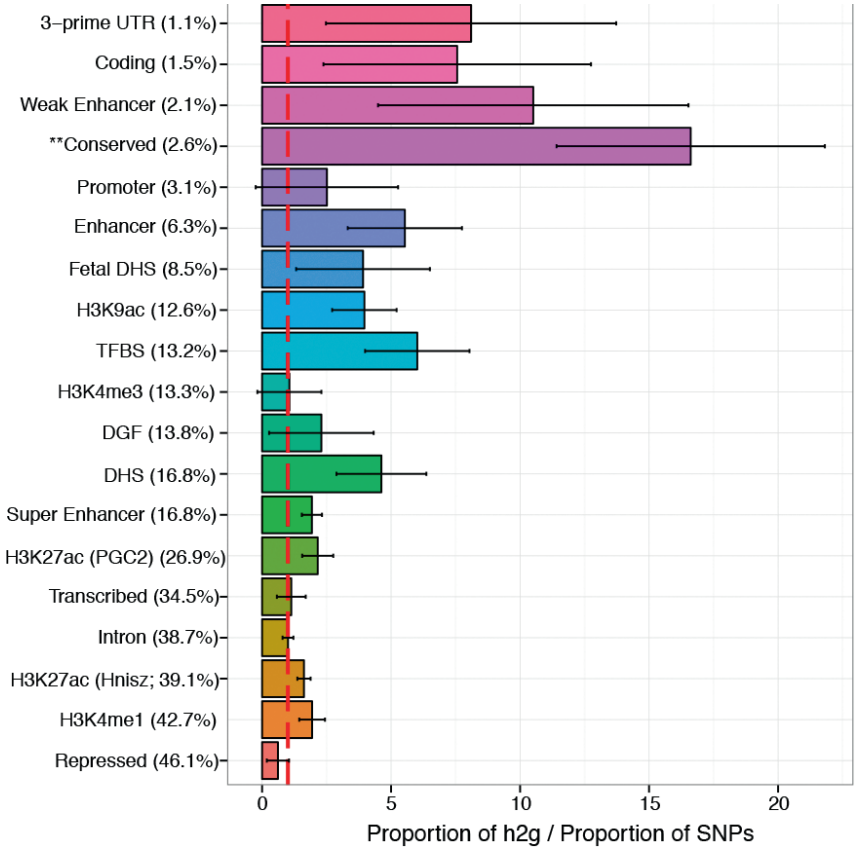

Figure 3 | Analysis of variance explained by functional annotations.
*LDSCORE regression analysis for different functional annotation categories. Plotted values are the proportion of h^2_g explained divided by the proportion of SNPs in a given functional category. Values are over- or under-represented if they differ significantly from 1. Values are plotted with a standard error calculated with a jackknife in LDSCORE. Evolutionarily conserved regions across mammals significantly contributed to the heritability of hippocampal volume (indicated by **).*

DISCUSSION

We identified six genome-wide significant, independent loci associated with hippocampal volume in 26,814 subjects of European ancestry. Of the six loci, four were novel: rs11979341 (7q36.3; P=1.42x10^{-11}), rs7020341 (9q33.1; P=3.04x10^{-11}), rs2268894 (2q24.2; P=5.89x10^{-11}), and rs2289881 (5q12.3; P=2.73x10^{-8}). We previously discovered two of the novel loci, rs7020341 and rs2268894[24], but in this higher-powered analysis they now surpassed the genome-wide significance. In addition to the four novel loci, we replicated two loci associated with hippocampal volume: rs7492919 and rs17178006[23, 24]. Hibar et al. (2015) previously reported additional support for the rs17178006 association with hippocampal volume[22].

Each novel locus identified has unique functions and has previously been linked to diseases of the brain. Variant rs7020341 lies within an intron of the *astrotactin 2* (*ASTN2*) gene (Figure 2d) which encodes for a protein involved in glial-mediated neuronal migration in the developing brain[28]. Rare deletions overlapping this locus near the 3' end of *ASTN2* have been observed in patients with autism spectrum disorder and attention-deficit/hyperactivity disorder[29]. Common variants near this site are associated with autism spectrum disorders[29] and migraine[30]. Variant rs2268894 is located in an intron of *DPP4* (Figure 2e) that encodes dipeptidyl peptidase IV; an enzyme regulating response to the ingestion of food[31], and an established target of a treatment for type 2 diabetes mellitus (vildagliptin)[32]. In addition, rs2268894 is in strong LD (r^2 = 0.83) with a genome-wide significant locus associated with a decreased risk for schizophrenia (rs2909457)[33]; however, the allele that increases risk for schizophrenia also increases hippocampal volume even though patients with schizophrenia show decreased hippocampal volume relative to controls[6]. Variant rs11979341 lies in an intergenic region (Figure 2c) around 200 kb upstream of the *sonic hedgehog* (*SHH*) gene, crucial for neural tube formation[34]. Adult brain expression data provide some evidence that rs11979341-C increases the expression of *SHH* in adult human hippocampus[35] (P=0.0089). Finally, variant rs2289881 lies within an intron of the *microtubule-associated serine/threonine kinase family member 4* (*MAST4*) gene (Figure 2f). The protein product of *MAST4* modulates the

microtubule scaffolding; the gene has been linked to susceptibility for atherosclerosis in HIV-infected men[36], and atypical frontotemporal dementia[37].

Effect sizes from the full sample were almost identical to those obtained from a subset meta-analysis (Pearson's $r^2 > 0.99$; $n = 22{,}761$) that removed all patients diagnosed with a neuropsychiatric disorder. Observed effects are therefore not likely to be driven by inclusion of patients with brain disorders. All significant loci are tabulated in Table 1. We found little evidence that these effects could be generalized to populations of African, Japanese, and Mexican-American ancestry, which could be due to the limited power from smaller non-European sample sizes available (see Supplementary Data 5).

We estimated that 18.76% (S.E. 1.56%) of the variance in hippocampal volume could be explained by genotyped common genetic variation. This effect was only tested within populations of European ancestry and does not necessarily reflect the level of explained variance in other populations worldwide. This is a substantial fraction of the overall genetic component of variance determined by twin heritability studies, and the heritability of hippocampal volume is relatively high at around 70%[19-21]. With the same LDSCORE method, we estimated the amount of variance explained by common gene variants belonging to known functional cell categories.[26] We discovered enrichment of genomic regions conserved across mammals, which may have a strong evolutionary role in the hippocampal formation, a structure much more extensively developed in mammals than in other vertebrates[38]. Given that hippocampal atrophy is a hallmark of Alzheimer's disease pathology[39], we were motivated to examine common genetic overlap between hippocampal volume and Alzheimer's disease risk. We found a significant negative relationship (r_g=-0.155 (S.E. 0.0529), P=0.0034), through which loci associated with decreased hippocampal volume also increase risk for AD. This confirms a shared etiological component between AD and hippocampal volume whereby genetic variants influencing hippocampal volume also modify the risk for developing AD.

As the hippocampal formation is a complex structure comprised of diverse functional units, we sought to examine the genetic variants identified in our analysis for focal effects on hippocampal subfield volumes. When assessing 13 subfields of the hippocampus (26 total, left and right) we found that two of the top variants from our

analysis (rs77956314 and rs7020341) had largely non-specific effects: most of the subfield volumes showed significant evidence of association (Supplementary Data 8). The variant rs61921502 showed a lateralized effect across the body of the right hippocampal formation, which includes the DG, subiculum, CA1, and fissure. Volume losses are frequently observed across the hippocampal body in AD[40], major depression[41], bipolar disorder[42], and temporal lobe epilepsy[43]. Prior pathway analyses have implicated the rs61921502 with *MSR3B*, a gene related to oxidative stress[24]. Genetic variation at *MSR3B* may influence neurogenesis specifically within the dentate regions of the hippocampal body, where cell proliferation is known to continue into adulthood in healthy humans[44]. However, further functional validation is required to test this hypothesis. Finally, the variant rs2268894 was associated with volume differences in the left hippocampal tail, a subfield that has previously shown shape abnormalities[45] and volume differences[46] in schizophrenia.

Here we identified four novel loci associated with hippocampal volume and examined each variant for localized effects in hippocampal subfields. When partitioning the full genome-wide association results into functionally annotated categories, we discovered that SNPs in evolutionarily conserved regions were significantly over-represented in their contribution to hippocampal volume. Further, we found significant evidence of shared genetic overlap between hippocampal volume and Alzheimer's disease. This large international effort shows that by mapping out the genetic influences on brain structure, we may begin to derive mechanistic hypotheses for brain regions causally implicated in the risk for neuropsychiatric disorders.

METHODS

Subjects and sites

High-resolution MRI brain scans and genome-wide genotyping data were available for 33,536 individuals from 65 sites in two large consortia: the ENIGMA Consortium and the CHARGE Consortium. Full details and demographics for each participating cohort are given in Supplementary Data 1. All participants (or their legal representatives) provided written informed consent. The institutional review board of the University of Southern California and the local ethics board of Erasmus MC University Medical Center approved this study.

Imaging analysis and quality control

Hippocampal volumes were estimated using the automated and previously validated segmentation algorithms, FSL FIRST[47] from the FMRIB Software Library (FSL) and FreeSurfer[48]. Hippocampal segmentations were visually examined at each site, and poorly segmented scans were excluded. Sites also generated histogram plots to identify any volume outliers. Individuals with a volume more than three standard deviations away from the mean were visually inspected to verify proper segmentation. Statistical outliers were included in analysis if they were properly segmented; otherwise, they were removed. Average bilateral hippocampal volume was highly correlated across automated procedures used to measure it (Pearson's $r = 0.74$)[22]. A measure of head size - intracranial volume (ICV) - was used as a covariate in these analyses to adjust for volumetric differences due to differences in head size alone. Most sites measured ICV for each participant using the inverse of the determinant of the transformation matrix required to register the subject's MRI scan to a common template and then multiplied by the template volume (1,948,105 mm^3). Full details of image acquisition and processing performed at each site are given in Supplementary Data 2.

Genetic imputation and quality control

Genetic data were obtained at each site using commercially available genotyping platforms. Prior to imputation, genetic homogeneity was assessed in each sample using

multi-dimensional scaling (MDS). Ancestry outliers were excluded by visual inspection of the first two components. The primary analysis and all data presented in this main text were derived from subjects with European ancestry. Replication attempts in subjects of additional ancestries are presented in Supplementary Data 5. Data were further cleaned and filtered to remove single nucleotide polymorphisms (SNPs) with low minor allele frequency (MAF < 0.01), deviations from Hardy-Weinberg Equilibrium (HWE P < $1x10^{-6}$), and poor genotyping call rate (<95%). Cleaned and filtered datasets were imputed to the 1000 Genomes Project reference panel (phase 1, version 3) using freely available and validated imputation software (MaCH/minimac, IMPUTE2, BEAGLE, GenABLE). After imputation, genetic data were further quality checked to remove poorly imputed SNPs (estimated R^2 < 0.5) or low MAF (<0.5%). Details on filtering criteria, quality control, and imputation at each site may be found in Supplementary Data 3.

Genome-wide association analysis

Genome-wide association scans (GWAS) were performed at each site, as follows. Mean bilateral hippocampal volume ((left + right)/2) was the trait of interest, and the additive dosage value of a SNP was the predictor of interest, while controlling for 4 MDS components, age, age^2, sex, intracranial volume, and diagnosis (when applicable). For studies with data collected from multiple centers or scanners, additional covariates were also included in the model to adjust for any scanning site effects. Sites with family data (NTR-Adults, BrainSCALE, QTIM, SYS, GOBS, ASPSFam, ERF, GeneSTAR, NeuroIMAGE, OATS, RSIx) used mixed-effects models to account for familial relationships, in addition to covariates stated previously. The primary analyses for this paper focused on the full set of individuals, including datasets with patients, to maximize power. We re-analyzed the data excluding patients to verify that detected effects were not due to disease alone. The regression coefficients for SNPs with $P < 1x10^{-5}$ in the model including all patients were almost perfectly correlated with the regression coefficients from the model including only healthy individuals (Pearson's $r = 0.996$). Full details for the software used at each site are given in Supplementary Data 3.

The GWAS of mean hippocampal volume was performed at each site, and the resulting summary statistics uploaded to a centralized site for meta-analysis. Prior to meta-

analysis, GWAS results from each site were checked for genomic inflation and errors using Quantile-Quantile (QQ) plots (Supplementary Fig. 1-2). GWAS results from each site were combined using a fixed-effects sample size-weighted meta-analysis framework as implemented in METAL[49]. Data were meta-analyzed first in the ENIGMA and CHARGE Consortia separately and then combined into a final meta-analyzed result file. After the final meta-analysis, SNPs were excluded if the SNP was available for fewer than 5,000 individuals.

Variance explained and genetic overlap in hippocampal volume

The common genetic overlap, total variance explained by the GWAS, and the partitioned heritability analyses were estimated using LDSCORE[25, 26]. Following from the polygenic model, an association test statistic at a given locus includes signal from all linked loci. Given a heritable polygenic trait, a SNP in high linkage disequilibrium (LD) with, or tagging, a large number of SNPs is on average likely to show stronger association than a SNP that is not. The magnitude of information conveyed by each variant (a function of the number of SNPs tagged taking into account the strength of the tagging) is summarized as an LD score. By regressing the LD scores on the test statistics, we estimated the proportion of variance in the trait explained by the variants included in the analysis. As an extension, two LD score models for two separate traits can be used to estimate the covariance (and correlation) structure to yield an estimate of the common genetic overlap (r_g) between any two trait pairs. Here we estimated the common genetic overlap between hippocampal volume and Alzheimer's disease[50]. Standard errors were estimated using a block jackknife.

Genomic partitioning into functional categories

As well as estimating the total variance explained, the genomic heritability (h^2_g) can be partitioned into specific subsets of variants. The functional annotation partitioning used the pre-prepared LDSCORE and annotation (.annot) files available online (see URLs) following the method of Finucane et al.[26]. These analyses use the following 24 functional classes not specifically unique to any cell type: coding, UTR, promoter, intron, histone

marks H3K4me1, H3K4me3, H3K9ac5 and two versions of H3K27ac, open chromatin DNase I hypersensitivity Site (DHS) regions, combined chromHMM/Segway predictions, regions conserved in mammals, super-enhancers and active enhancers from the FANTOM5 panel of samples (Finucane et al., page 4)[26]. Annotated coordinates are determined by a combination of all cell types from ENCODE. As in Finucane et al[26], to avoid bias, we included the 500bp windows surrounding the variants included in the functional classes. The chromosome-partitioned analyses were conducted using LDSCOREs calculated for each chromosome. Following the method of Bulik-Sullivan et al.[25], these analyses focus on the variants within HapMap3 as these SNPs are typically well imputed across cohorts. Enrichment of a given partition is calculated as the proportion of h^2_g explained by that partition divided by the proportion of variants in the GWAS that fall into that partition. All LDSCORE analyses used non-genomic controlled meta-analyses.

Gene annotation and pathway analysis

Gene annotation, gene-based test statistics, and pathway analysis were performed using the KGG2.5 software package[51] (Supplementary Data 6 and 7). LD was calculated based on RSID numbers using the 1000 Genomes Project European samples as a reference (see URLs). For annotation, SNPs were considered "within" a gene, if they fell within 5 kb of the 3'/5' UTR based on human genome (hg19) coordinates. Gene-based tests were performed using the GATES test[51] without weighting *P*-values by predicted functional relevance. Pathway analysis was performed using the HYST test of association[52]. For all gene-based tests and pathway analyses, results were considered significant if they exceeded a Bonferroni correction threshold accounting for the number of pathways tested such that $P_{thresh} = 0.05/(671 \text{ pathways}) = 7.45 \times 10^{-5}$.

Annotation of SNPs with epigenetic factors

In Figure 2, all tracks were taken from the UCSC Genome Browser Human hg19 assembly. *SNPs (top 5%)* shows the top 5% associated SNPs within the locus and are colored by their correlation to the top SNP. *Genes* shows the gene models from GENCODE version 19. *Hippocampus* gives the predicted chromatin states based on

computational integration of ChIP-seq data for 18 chromatin marks in human hippocampal tissue derived from the Roadmap Epigenomics Consortium[53]. The 18 chromatin states from the *hippocampus* track are as follows: TssA (Active TSS), TssFlnk (Flanking Active TSS), TssFlnkU (Flanking TSS Upstream), TssFlnkD (Flanking TSS Downstream), Tx (Strong transcription), TxWk (Weak transcription), EnhG1 (Genic Enhancers 1), EnhG2 (Genic Enhancers 2), EnhA1 (Active Enhancers 1), EnhA2 (Active Enhancers 2), EnhWk (Weak Enhancers), ZNF/Rpts (ZNF genes & repeats), Het (Heterochromatin), TssBiv (Bivalent/Poised TSS), EnhBiv (Bivalent Enhancer), ReprPC (Repressed PolyComb), ReprPCWk (Weak Repressed PolyComb), Quies (Quiescent/Low). Additional information about the 18 state chromatin model is detailed elsewhere[53]. *Conservation* is the basewise conservation score over 100 vertebrates estimated by PhyloP from the UCSC Genome Browser Human hg19 assembly.

Analysis of hippocampal subfields

We segmented the hippocampal formation into 13 subfield regions: CA1, CA3, CA4, fimbria, Granule Layer + Molecular Layer + Dentate Gyrus Boundary (GC_ML_DG), hippocampal-amygdaloid transition area (HATA), hippocampal tail, hippocampal fissure, molecular layer (HP), parasubiculum, presubiculum, and subiculum using a freely available, validated algorithm distributed with the FreeSurfer image analysis package[54]. We measured the hippocampal subfield volumes within the Rotterdam (n = 4,491) and HUNT (n = 877) cohorts. Volumes from the 26 subfield regions (13 in each hemisphere) were the phenotypes of interest and individually assessed for significance with the top variants from our primary analysis while correcting for the following nuisance variables: 4 MDS components, age, age^2, sex, intracranial volume. Association statistics from each of the tests in the Rotterdam and HUNT cohorts were meta-analyzed using a fixed-effects inverse variance-weighted model yielding the final results. We declare an individual test significant if the P-value is less than a Bonferroni-corrected P-value threshold accounting for the total number of tests: $P_{thresh} = 0.05/(26 \text{ subfields} * 6 \text{ SNPs}) = 3.21 \times 10^{-4}$.

Data availability

The genome-wide summary statistics that support the findings of this study are available upon request from the corresponding authors MAI and PMT. The data are not publicly available due to them containing information that could compromise research participant privacy/consent.

REFERENCES

1. Van Paesschen et al. Quantitative hippocampal mri and intractable temporal lobe epilepsy. *Neurology*. 1995;45:2233-2240
2. Kim GH, et al. Hippocampal volume and shape in pure subcortical vascular dementia. *Neurobiol Aging*. 2015;36:485-491
3. Thompson et al. N*euroImage*. 2004;22:1754-1766
4. Schmaal et al. Subcortical brain alterations in major depressive disorder: Findings from the enigma major depressive disorder working group. *Mol Psychiatr*. 2015
5. Hibar. Robust subcortical volumetric reductions in bipolar disorder: *Jama Psychiat*. 2014
6. van Erp et al. Subcortical brain volume abnormalities in 2028 individuals with schizophrenia and 2540 healthy controls via the enigma consortium. *Mol Psych*. 2015
7. Smith ME. Bilateral hippocampal volume reduction in adults with post-traumatic stress disorder: A meta-analysis of structural mri studies. *Hippoc* 2005
8. Bliss et al. A synaptic model of memory: Long-term potentiation in the hippocampus. *Nature*. 1993
9. Maguire et al. Knowing where and getting there: A human navigation network. *Science*. 1998
10. Vinogradova OS. *Hippocampus*. 2001
11. McEwen et al Stress and anxiety: Structural plasticity and epigenetic regulation as a consequence of stress. *Neu.ph*2012
12. Coras et al. Differential influence of hippocampal subfields to memory formation. *Brain*. 2014
13. Newmark et al. Contributions of the hippocampal subfields and entorhinal cortex to disambiguation during working memory. *Hippocampus*. 2013
14. Navratilova Z, Battaglia FP. Ca2: It's about time-and episodes. *Neuron*. 2015;85:8-10
15. Hitti et al. *Nature*. 2014;508:88-92
16. McCormick et al. *Cereb Cortex*. 2015;25:1297-1305
17. Strange et al. F *Nat Rev Neu* 2014
18. Lupien et al. *Nat Rev Neurosci*. 2009;10:434-445
19. Renteria et al. Genetic architecture of subcortical brain regions. *Genes, brain, behavior*. 2014
20. Kremen et al. Genetic and environmental influences on the size of specific brain regions in midlife: *NeuroImage*. 2010
21. den Braber et al. Heritability of subcortical brain measures: *NeuroImage* 2013
22. Hibar et al. Common genetic variants influence human subcortical structures. *Nature*. 2015
23. Stein J et al. Identification of common variants associated with human hippocampal and intracranial volumes. *Nat gen* 2012
24. Bis et al.*Nature genetics*. 2012;44:545-+
25. Bulik-Sullivan et al. *Nat Genet*. 2015;47:291-295
26. Finucane et al. *Partitioning heritability by functional category using gwas summary statistics*. 2015.
27. Bulik-Sullivan et al. *An atlas of genetic correlations across human diseases and traits*. 2015.

28. Wilson et al. Astn2, a novel member of the astrotactin gene family, regulates the trafficking of astn1 during glial-guided neuronal migration. *J Neuroscience*. 2010
29. Lionel et al.. *Hum Mol Genet*. 2014;23:2752-2768
30. Freilinger et al. Genome-wide association analysis identifies susceptibility loci for migraine without aura. *Nat gen*. 2012;
31. Pratley RE et al. Inhibition of dpp-4. *Curr Med Res Opin*. 2007
32. Pratley RE, Jauffret-Kamel S, Galbreath E, Holmes D. . *Horm Metab Res*. 2006;38:423-428
33. Schizophrenia Working Group of the Psychiatric Genomics C. *Nature*. 2014;511:421-427
34. Dessaud E, McMahon AP, Briscoe J. *Development*. 2008;135:2489-2503
35. Ramasamy et al. *Nature Neuroscience*. 2014;
36. Shrestha et al. *Aids*. 2010
37. Martins-de-Souza D et al. *Journal of proteome research*. 2012;11:2533-2543
38. Garcia-Verdugo JM, Ferron S, Flames N, Collado L, Desfilis E, Font E. The proliferative ventricular zone in adult vertebrates: A comparative study using reptiles, birds, and mammals. *Brain Res Bull*. 2002;57:765-775
39. Apostolova et al. *Archives of neurology*. 2006;63:693
40. Mueller SG, Weiner MW. Selective effect of age, apo e4, and alzheimer's disease on hippocampal subfields. *Hippocampus*. 2009;19:558-564
41. Huang Y et al. *Biol Psychiatry*. 2013;74:62-68
42. Haukvik et al. *Biol Psychiatry*. 2015;77:581-588
43. Schoene et al. I. *Hum Brain Mapp*. 2014;35:4718-4728
44. Erickson et al. E. *Proc Natl Acad Sci U S A*. 2011;108:3017-3022
45. Styner et al. Boundary and medial shape analysis of the hippocampus in schizophrenia. *Med Image Anal*. 2004;8:197-203
46. Maller et al. *Hippocampus*. 2012;22:9-16
47. Patenaude B et al. *NeuroImage*. 2011;56:907-922
48. Fischl B et al *Neuron*. 2002;33:341-
49. Willer CJ et al. *Bioinformatics*. 2010;26:2190-
50. Lambert Jet al. *Nat Genet*. 2013;45:1452-1458
51. Li et al. *American journal of human genetics*. 2011;88:283-293
52. Li et al. *American journal of human genetics*. 2012;91:478-488
53. Roadmap Epigenomics et al. I. *Nature*. 2015;518:317-
54. Iglesias et al. *NeuroImage*. 2015;115:117-137
55. Cuellar-Partida et al *Source code for biology and medicine*. 2015;10:1

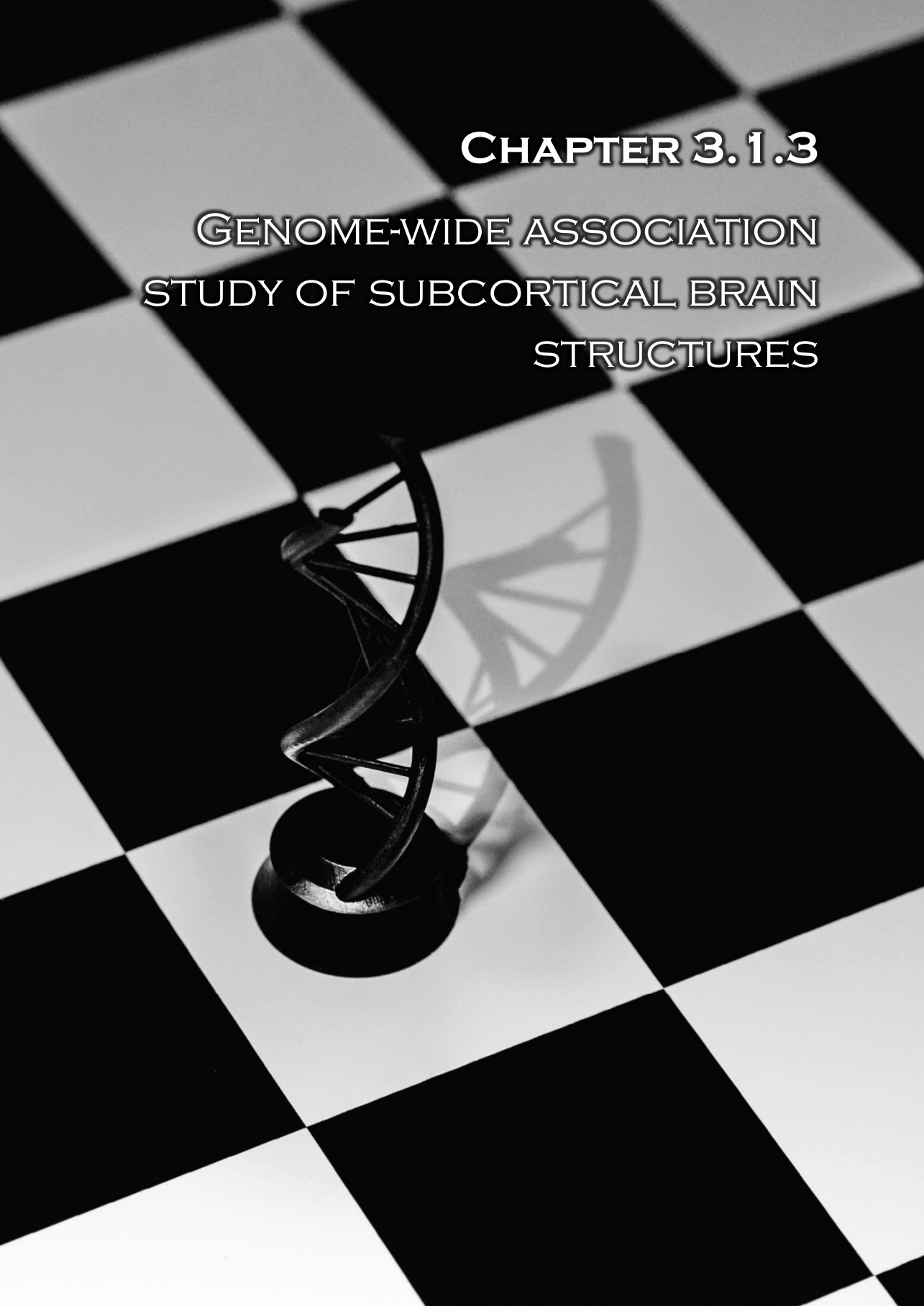

Chapter 3.1.3

Genome-wide association study of subcortical brain structures

ABSTRACT

Subcortical brain structures are essential for the control of autonomic and sensorimotor functions,[1,2] modulation of cognitive processes involved in learning, memory and decision-making,[3,4] as well as emotional reactivity[5,6] and consciousness,[7] acting through networks influencing input to and output from the cerebral cortex.[8,9] The pathology of many cognitive, mood and movement disorders is restricted to, begins in, or prominently involves subcortical brain structures and related circuitries.[10] A recent investigation described five novel genetic loci influencing the volumes of the putamen and the caudate, which pointed to genes controlling neuronal growth, apoptosis and learning.[11] However, this study did not detect genome-wide significant signals in other structures. Furthermore, the genetic variation associated with brainstem volume has not been explored. Identifying novel genetic determinants of subcortical structures, including the brainstem, should therefore improve our understanding of brain development and disease. We sought to identify novel genetic variants underlying the volumes of seven subcortical structures (i.e. nucleus accumbens, amygdala, caudate, putamen, globus pallidus, thalamus and brainstem) through genome-wide association analyses (GWAS) in 26,319 persons from 39 studies in the Cohorts of Heart and Aging Research in Genomic Epidemiology (CHARGE) and the Enhancing Neuro Imaging Genetics through Meta-Analysis (ENIGMA) consortia.

Novel genetic discoveries in this unpublished manuscript have been anonymized or removed following consortium-wide practices. As a result, the text will not go in-depth about gene functions and the identified pathways.

RESULTS

Heritability

We estimated heritability of subcortical brain volumes in the Framingham Heart Study (FHS), a population-based cohort including three generations of participants.[12] All volumes were moderately to highly heritable, ranging from 0.34 for the amygdala, 0.54 for the thalamus, 0.60 for the globus pallidus, 0.66 for the nucleus accumbens, 0.71 for the caudate, 0.79 for the putamen, to 0.86 for the brainstem (See Figure 1). Heritability results were similar in a familial Austrian cohort[13] (See Supplementary Methods).

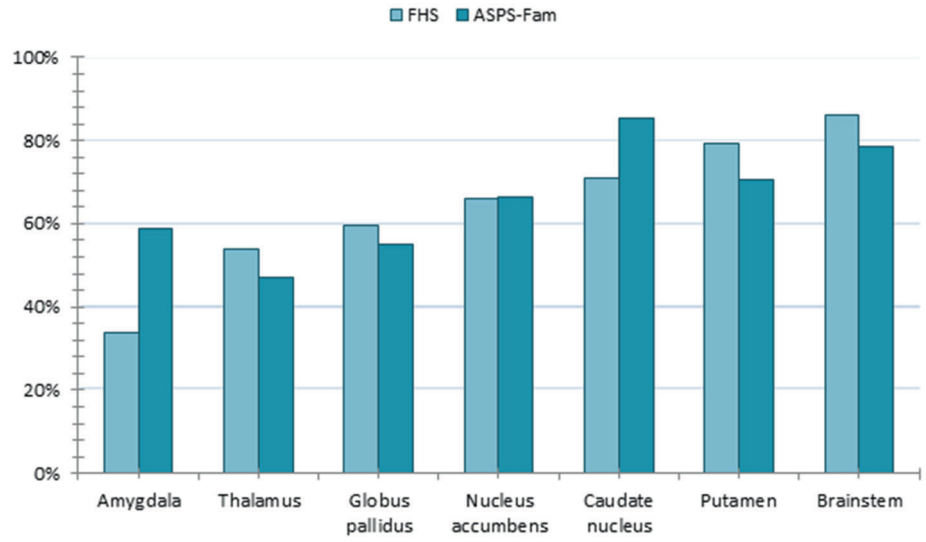

Figure 1 | Heritability of subcortical brain structures in the Framingham Heart Study (FHS) and Austrian Stroke Prevention Study (ASPS).

Analysis was performed with SOLAR in the Framingham Heart Study (FHS in light blue, n=895) and the Austrian Stroke Prevention Study-Family (ASPS-Fam in darker blue, n=370) Models were adjusted for sex, age, age squared, total intracranial volume and PC1-PC3.

Meta-analysis of GWAS results

We undertook a 1000G imputed GWAS on the MRI volumes of subcortical brain structures. Our discovery sample comprised a total of 25,587 persons of European ancestry from 39 studies in CHARGE and ENIGMA. Each study related common and less frequent genetic variants (>1% minor allele frequency) to the volume of subcortical structures (sum of left and right) using additive genetic models adjusted for age, age^2, sex, total intracranial volume and population structure. Adjustment for study site or accounting for family structure was additionally performed if needed. After quality control processing, GWAS results were meta-analyzed using sample-size weighting. Overall we found 25 genome-wide significant associations ($P < 5 \times 10^{-8}$), 20 of which are novel, across all the subcortical structures in our discovery sample (See Table 1 and Figure 2).

Ten novel (single nucleotide polymorphisms) SNPs were associated with brainstem volume, six of which are intronic, one lies in a UTR3, one is in a non-coding transcript SNP and four are intergenic. Two novel SNPs influenced the thalamus volume. One of these was a missense variants, whereas the other was an intronic variant. Of the five loci associated with the putamen, four have been previously reported.[11] The strongest association was found for a locus in LD with the gene Kinectin-1 (KTN1, rs8017172, 6.69×10^{-34}), a kinesin-binding protein involved in the transport of cellular components along microtubules.[14] Impairment of these molecular motors has been increasingly recognized in neurological diseases with a subcortical component.[15] The second finding is an intronic SNP in the DCC Netrin-1 Receptor (*DCC*, rs62097986, 1.31×10^{-13}), that when coupled with netrin-1 helps guide axonal growth and promotes tumor cell apoptosis.[16] More recently, DCC has been related to PD,[17] schizophrenia,[18] and development of prefrontal cortex in adolescence.[19] Third, we found an intronic SNP in the Bcl-2-like protein 1 (BCL2L1, rs1484994, 1.52×10^{-12}), a protein that regulates cell survival and neuronal development.[20,21]. Another intronic SNP was found in the Discs, Large Homolog 2 gene (DLG2, rs512556, 7.06×10^{-12}), a scaffolding protein involved in glutamatergic-mediated synaptic signaling and cell polarity.[22] Mutations in this gene have been associated with schizophrenia[23] and cognitive impairment.[24] Finally, one novel intronic SNP was associated with putamen volume. For the caudate, we replicated one of the

SNPs previously reported[11] near the FAT Atypical Cadherin 3 (FAT3, rs2845878, 1.02×10^{-10}), a large molecule that mediates neuronal morphogenesis and cell migration in the fetal brain.[25] We found three other novel intergenic loci related to caudate volume located near genes influencing brain development. Our results confirm previously reported borderline significant loci influencing the size of the globus pallidus near KTN1,[11] which also relate to putamen volume. Three additional novel loci were found for this structure. We identified no genome-wide significant SNP related to nucleus accumbens volume, the structure with the lowest heritability. Finally, for the amygdala we found one significant intergenic SNP near a microRNA on chromosome 2. Additional look-up revealed that many of the loci related to one subcortical structure in our genome-wide analysis are also associated with other subcortical structures (Table S1).

Genetic correlations

We explored the genetic correlations among subcortical structures as well as with a range of anthropometric, neurological and psychiatric traits using LD score regression methods.[26] We observed a strong genetic overlap among all subcortical structures (Table 2), consistent with our findings indicating that the loci identified are associated with the size of several subcortical structures (Table S1).

Furthermore, strong genetic correlations were found for the nucleus accumbens with bipolar disorder and height; the amygdala with AD and intracranial volume (ICV); the brainstem with PD, cognitive function, ICV and height; the caudate with the burden of white matter hyperintensities, PD, bipolar disorder and ICV, the globus pallidus with PD and ICV; the putamen with AD; and the thalamus with cognitive function, PD, ICV and height.

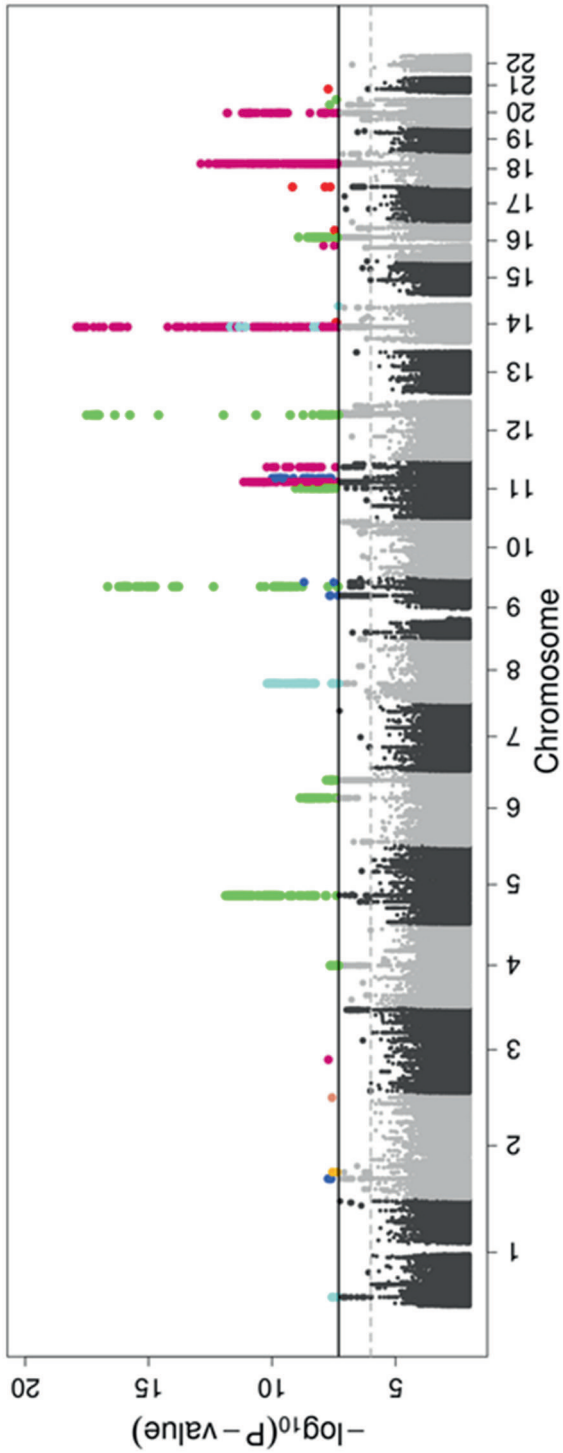

Figure 2 | Genome-wide association results for subcortical brain structures in European descent populations.

Manhattan plot showing the associations between genetic variants and the subcortical brain structures. Genome-wide significant associations are colored: green for brainstem, deep pink for brainstem, red for thalamus, yellow for amygdala, royal blue for caudate, and light blue for pallidum. The accumbens had no significant variants.

Table 1 | Genome-wide association results for subcortical brain structures in European descent populations.

Structure	Chromosome	Function	A1 / A2	Frequency A1	N	Z-score	P-value	I^2
Amygdala	2	intergenic	t/c	0.62	25,400	-5.553	2.81E-08	0
Brainstem	12	intergenic	a/c	0.52	19,930	8.706	3.14E-18	0
	9	intronic	a/g	0.39	19,930	8.482	2.22E-17	0
	5	UTR3	t/c	0.74	19,930	-7.092	1.32E-12	68.4
	11	intergenic	a/g	0.48	19,769	6.127	8.98E-10	65
	16	intergenic	d/i	0.37	19,205	6.082	1.18E-09	0
	6	intronic	t/c	0.34	19,930	-6.058	1.38E-09	33.3
	6	intronic	d/i	0.32	18,552	5.65	1.60E-08	29.1
	20	intronic	d/i	0.21	19,205	-5.597	2.18E-08	0
	4	intergenic	a/g	0.60	19,930	-5.59	2.28E-08	0
	20	non-coding transcript	a/g	0.33	16,943	-5.489	4.05E-08	81
Caudate nucleus	*11*	*intergenic*	*c/g*	*0.33*	*25,563*	*-6.464*	*1.02E-10*	*0*
	9	*intergenic*	*a/g*	*0.58*	*25,449*	*-6.001*	*1.96E-09*	*0*
	2	intergenic	a/g	0.40	25,563	-5.623	1.88E-08	0
	9	intergenic	a/t	0.08	25,445	5.599	2.15E-08	0
Globus pallidus	14	intergenic	t/c	0.54	25,534	7.058	1.69E-12	0.1
	8	intergenic	a/g	0.58	25,534	6.536	6.31E-11	18.2
	1	intronic	t/c	0.67	25,335	-5.561	2.68E-08	0
Putamen	*14*	*intergenic*	*a/g*	*0.42*	*25,393*	*-12.137*	*6.69E-34*	*82.2*
	18	*intronic*	*a/c*	*0.44*	*25,393*	*7.406*	*1.31E-13*	*75.7*
	20	*intronic*	*a/g*	*0.71*	*24,113*	*7.072*	*1.52E-12*	*50.3*
	11	*intronic*	*a/c*	*0.64*	*25,393*	*-6.857*	*7.06E-12*	*0*
	11	intronic	c/g	0.80	25,393	6.54	6.14E-11	0
Thalamus	17	missense	t/c	0.18	22,864	-6.172	6.73E-10	31.7
	21	intronic	a/c	0.57	25,585	5.623	1.88E-08	66.8

DISCUSSION

In the largest GWAS to date, we identified 20 novel genetic loci for subcortical brain structures. For many structures, these are the first ever described genetic findings that surpass the strict genome-wide significance threshold: the amydala, brainstem, globus pallidus, and thalamus. The nucleus accumbens was the only structure for which no loci were identified. These results correspond well to the heritability analyses, where we found that there some evolutionarily older deep and subcortical structures are more strongly heritable, such as the brainstem, and these also yielded the most significant loci.

Additionally, we find evidence that these novel and to be discovered variants, at a genome-wide scale, are also influencing other traits. Most notably, we see several genetic correlations with cognitive function (brainstem and thalamus volume) and bipolar disorder (accumbens and caudate volume), Parkinson's disease (brainstem, caudate, pallidum, and thalamus volume), and Alzheimer's disease (amygdala and putamen volume). This points to biological and clinical relevance of our findings. Follow-up analyses of these loci could provide insight into the pathophysiology of common neuropsychiatric disorders.

Finally, we show that the approach of increasing sample sizes for GWAS discovery can lead to the identification of novel variants. However, even at a sample size of 25,000 we were unable to identify a single significant locus for the nucleus accumbens volume. While even larger may ultimately lead to such discoveries, another approach may be to refine the phenotype by looking at more detailed phenotypes such as the accumbens shape or at a voxel-wise level.

In conclusion, we were able to identify novel genetic loci for subcortical structures, which may have relevance for cognitive function and neuropsychiatric diseases.

Table 2 | Genetic correlations among subcortical brain structures and other anthropometric, neurological and behavioral traits.

Phenotypic traits	Nucleus accumbens		Amygdala		Brainstem		Caudate		Globus pallidus		Putamen		Thalamus	
	ρ (SE)	P-value	ρ (SE)	P-value	ρ (SE)	P-value	ρ (SE)	P-value	ρ (SE)	P-value	ρ (SE)	P-value	ρ (SE)	P-value
Subcortical brain structures														
Nucleus accumbens			0.28	7.15E-02	0.12	1.76E-01	0.52	6.92E-13	0.40	4.60E-04	0.50	1.24E-14	0.36	3.33E-05
Amygdala	0.28	7.15E-02			0.04	7.69E-01	0.13	3.72E-01	0.23	1.41E-01	0.38	1.59E-03	0.31	4.10E-02
Brainstem	0.12	1.76E-01	0.04	7.69E-01			0.08	2.02E-01	0.43	9.20E-09	0.08	2.64E-01	0.57	4.45E-17
Caudate nucleus	0.52	6.92E-13	0.13	3.72E-01	0.08	2.02E-01			0.28	4.00E-04	0.35	1.63E-06	0.06	4.54E-01
Globus pallidus	0.40	4.60E-04	0.23	1.41E-01	0.43	9.20E-09	0.28	4.00E-04			0.57	4.73E-14	0.47	6.55E-09
Putamen	0.50	1.24E-14	0.38	1.59E-03	0.08	2.64E-01	0.35	1.63E-06	0.57	4.73E-14			0.27	3.54E-05
Thalamus	0.36	3.33E-05	0.31	4.10E-02	0.57	4.45E-17	0.06	4.54E-01	0.47	6.55E-09	0.27	3.54E-05		
Hippocampus	0.24	1.68E-02	0.65	1.15E-05	0.21	1.26E-02	0.01	9.49E-01	0.35	2.69E-03	0.16	2.84E-02	0.41	1.00E-06
Anthropometrics														
Intracranial volume	0.08	3.18E-01	0.25	3.63E-02	0.16	2.82E-02	0.14	2.55E-02	0.20	2.15E-02	0.13	5.87E-02	0.24	6.40E-04
Height	0.11	1.54E-02	0.12	8.96E-02	0.08	1.47E-02	-0.01	7.50E-01	0.08	5.30E-02	0.03	3.00E-01	0.17	5.54E-06
BMI														
Neurological														
Alzheimer's disease	-0.23	1.10E-01	-0.40	2.44E-02	-0.14	1.84E-01	-0.03	7.86E-01	-0.13	3.19E-01	-0.23	2.95E-02	-0.10	3.64E-01
Parkinson's disease	0.19	2.71E-02	-0.01	9.50E-01	0.16	1.77E-02	0.15	3.82E-02	0.22	2.48E-02	0.13	8.16E-02	0.15	4.45E-02
Cognitive function	0.15	4.74E-02	0.11	3.08E-01	0.13	2.51E-02	0.04	5.20E-01	0.14	5.38E-02	0.11	7.42E-02	0.19	3.94E-03
White matter burden	0.07	5.06E-01	0.20	1.72E-01	-0.08	3.09E-01	0.20	1.04E-02	-0.08	4.56E-01	0.05	4.67E-01	0.11	2.58E-01
Stroke														
Psychiatric disorders														
Bipolar disorder	-0.28	5.48E-03	-0.12	4.73E-01	-0.05	5.23E-01	-0.17	3.02E-02	-0.09	3.02E-01	-0.07	3.47E-01	-0.11	2.74E-01
Schizophrenia	0.03	7.26E-01	0.08	5.17E-01	-0.04	5.16E-01	-0.04	5.75E-01	-0.05	4.75E-01	0.07	2.51E-01	-0.04	5.60E-01

REFERENCES

1 Marsden, C. D. The mysterious motor function of the basal ganglia: the Robert Wartenberg Lecture. *Neurology* **32**, 514-539 (1982).

2 Yin, H. H. & Knowlton, B. J. The role of the basal ganglia in habit formation. *Nature reviews. Neuroscience* **7**, 464-476, doi:10.1038/nrn1919 (2006).

3 McDonald, A. J. & Mott, D. D.. *Journal of neuroscience research*, doi:10.1002/jnr.23709 (2016).

4 Hikosaka, O., Kim, H. F., Yasuda, M. & Yamamoto, S.. *Annual review of neuroscience* **37**, 289-306, doi:10.1146/annurev-neuro-071013-013924 (2014).

5 Salzman, C. D. & Fusi, S.. *Annual review of neuroscience* **33**, 173-202, doi:10.1146/annurev.neuro.051508.135256 (2010).

6 Floresco, S. B. T. *Annual review of psychology* **66**, 25-52, doi:10.1146/annurev-psych-010213-115159 (2015).

7 Fabbro, F., Aglioti, S. M., Bergamasco, M., Clarici, A. & Panksepp, J. E. *Frontiers in human neuroscience* **9**, 157, doi:10.3389/fnhum.2015.00157 (2015).

8 Alexander, G. E., DeLong, M. R. & Strick, P. L.. *Annual review of neuroscience* **9**, 357-381, doi:10.1146/annurev.ne.09.030186.002041 (1986).

9 Jahanshahi, M., Obeso, I., Rothwell, J. C. & Obeso, J. A. . *Nature reviews. Neuroscience* **16**, 719-732, doi:10.1038/nrn4038 (2015).

10 Shepherd, G. M. Corticostriatal connectivity and its role in disease. *Nature reviews. Neuroscience* **14**, 278-291, doi:10.1038/nrn3469 (2013).

11 Hibar, D. P. *et al.*. *Nature* **520**, 224-229, doi:10.1038/nature14101 (2015).

12 Tsao, C. W. & Vasan, R. S. . *International journal of epidemiology* **44**, 1800-1813, doi:10.1093/ije/dyv337 (2015).

13 Schmidt, R. *et al.* Assessment of cerebrovascular risk profiles in healthy persons: definition of research goals and the Austrian Stroke Prevention Study (ASPS). *Neuroepidemiology* **13**, 308-313 (1994).

14 Santama, N., Er, C. P., Ong, L. L. & Yu, H. Distribution and functions of kinectin isoforms. *Journal of cell science* **117**, 4537-4549, doi:10.1242/jcs.01326 (2004).

15 Liu, X. A., Rizzo, V. & Puthanveettil, S. V. . *Translational neuroscience* **3**, 355-372, doi:10.2478/s13380-012-0044-7 (2012).

16 Finci, L., Zhang, Y., Meijers, R. & Wang, J. H.. *Progress in biophysics and molecular biology* **118**, 153-160, doi:10.1016/j.pbiomolbio.2015.04.001 (2015).

17 Kim, J. M. *et al.* SNPs in axon guidance pathway genes and susceptibility for Parkinson's disease in the Korean

population. *Journal of human genetics* **56**, 125-129, doi:10.1038/jhg.2010.130 (2011).

18 Grant, A., Fathalli, F., Rouleau, G., Joober, R. & Flores, C. A. *Schizophrenia research* **137**, 26-31, doi:10.1016/j.schres.2012.02.023 (2012).

19 Manitt, C. *et al.* dcc orchestrates the development of the prefrontal cortex during adolescence and is altered in psychiatric patients. *Translational psychiatry* **3**, e338, doi:10.1038/tp.2013.105 (2013).

20 Shacka, J. J. & Roth, K. A. Bcl-2 family and the central nervous system: from rheostat to real complex. *Cell death and differentiation* **13**, 1299-1304, doi:10.1038/sj.cdd.4401974 (2006).

21 Lindsten, T., Zong, W. X. & Thompson, C. B. *The Neuroscientist : a review journal bringing neurobiology, neurology and psychiatry* **11**, 10-15, doi:10.1177/1073858404269267 (2005).

22 Zhu, J., Shang, Y. & Zhang, M. *Nature reviews. Neuroscience* **17**, 209-223, doi:10.1038/nrn.2016.18 (2016).

23 Ingason, A. *et al.*. *Translational psychiatry* **5**, e656, doi:10.1038/tp.2015.151 (2015).

24 Nithianantharajah, J. *et al. Nature neuroscience* **16**, 16-24, doi:10.1038/nn.3276 (2013).

25 Deans, M. R. *et al.* Control of neuronal morphology by the atypical cadherin Fat3. *Neuron* **71**, 820-832, doi:10.1016/j.neuron.2011.06.026 (2011).

26 Bulik-Sullivan, B. *et al.* An atlas of genetic correlations across human diseases and traits. *Nature genetics* **47**, 1236-1241, doi:10.1038/ng.3406 (2015).

Chapter 3.2

Cerebrovascular markers

Chapter 3.2.1

Review on the genetics of vascular dementia

ABSTRACT

Vascular dementia is a common disorder resulting in considerable morbidity and mortality. Determining the extent to which genes play a role in disease susceptibility and their pathophysiological mechanisms could improve our understanding of vascular dementia, leading to a potential translation of this knowledge to clinical practice. In this consensus report, we discuss what is currently know about the genetics of vascular dementia. The identification of causal genes remains limited to monogenic forms of the disease, with findings for sporadic vascular dementia being less robust. However, progress in genetic research on associated phenotypes such as cerebral small vessel disease, Alzheimer's disease, and stroke, have the potential to inform on the genetics of vascular dementia. We conclude by providing an overview of future developments in the field and how such work could impact patients and clinicians.

INTRODUCTION

While vascular dementia (VaD) is the second most common form of dementia,[1] studies on its genetic basis are scarce. It is well established that the risk of VaD can be modified by various lifestyle factors, physiological risk factors, and comorbidities.[1] However, its genetic component remains poorly understood, especially when compared to other causes of dementia such as Alzheimer's disease (AD), Parkinson's disease, and frontotemporal lobar degeneration. Only a single study in 24 twins has attempted to determine the heritability of VaD, but it was unable to identify a significant genetic component.[2] While this could suggest the environment plays a larger role, a careful interpretation is warranted given the limited sample size and the heterogeneity in VaD definitions. Furthermore, several lines of evidence actually indicate that VaD might have a substantial genetic component.

In this consensus report we summarize the current knowledge of the genetics of VaD and provide an overview of future developments in genetic research on VaD. Besides the diagnosis of VaD, we extend our report to include several associated phenotypes. These include AD, stroke, as well as cerebral small vessel disease (CSVD), which can be considered as a precursor or a distinct form of VaD (see dedicated consensus report in this volume[3]). These have all been shown to be significantly heritable and potentially share predisposing genetic factors.

METHODS

This consensus report is based on the 9th International Congress on Vascular Dementia (ICVD), which took place in Ljubljana, Slovenia, on 16-18 October 2015. The ICVD meeting was structured in several Working Groups that focused on specific topics within the field of VaD. The current report is based on the work of the 'Genetics of Vascular Dementia' Working Group.

Here, we provide a narrative review on the genetic aspect of VaD, which is divided in the four sections. First, we provide an overview of monogenic disorders that results in VaD. Second, we review our current knowledge of the genetic background of sporadic VaD, which remains obscure. Third, we point to future developments in the field that are likely to shed light on the role of genetics. Finally, we discuss how a proper understanding of genetics can have clinical implications for VaD.

MONOGENIC DISORDERS

The most apparent evidence for a genetic basis of VaD is the fact that dysfunction of single genes can lead to the development of VaD. Several of these monogenic disorders have been described and are summarized in Table 1, along with their clinical and neuroimaging features relevant to VaD. Below, we highlight the most important of these disorders.

A well-known monogenic disorder is Cerebral Autosomal Dominant Arteriopathy with Subcortical Infarcts and Leukoencephalopathy (CADASIL). which is the most frequent heritable cause of VaD. It results from mutations of the *NOTCH3* gene on chromosome 19q12 that cluster in exons 3 and 4. Common manifestations are migraine headaches, recurrent subcortical ischaemic events, cognitive impairment, mood disorders, and seizures.[4] This disorder is the subject of another consensus report from its respective ICVD working group.

Another monogenic form, first described in 1989, is Fabry disease (FD) an X-Linked lysosomal disease due to a mutation of the *GLA* gene (Xq22), resulting in an absent or reduced a-galactosidase activity that finally leads to accumulation of glicosphingolipid

(globotriaosilceramide) in different organs. Stroke or transient ischemic attack (TIA), renal disease, and cardiomyopathy have been observed in FD patients.[5-7] FD has been described as potential cause of young stroke (mostly lacunar but also large vessel and cardioembolic) in a percentage ranging from 0.4 to 11%.[8,9]

Other more rarely described single-gene disease entities are the *COL4A1-A2* gene-related arteriopathy, which is a possible cause of small vessel arteriopathy and intracranial haemorrhages,[10] and Retinal Vasculopathy with Cerebral Leukodystrophy (RVCL), which now subsumes three previously considered separate entities (cerebroretinal vasculopathy, hereditary endotheliopathy, retinopathy, nephropathy and stroke and hereditary vascular retinopathy). The typical features of RVCL are retinal vasculopathy, cognitive impairment, migraine, psychiatric abnormalities, seizures as well as hepatic and renal dysfunction.[11,12] The disease is due to the *TREX1* gene and associated both with CSVD neuroimaging features and, in some cases, pseudotumoral lesions surrounded by vasogenic oedema.[13-15]

Table 1 | Monogenic disorders associated with cerebral small vessel disease (modified from Bersano et al., 2012).

Disease	CADASIL	Fabry Disease	RVCL	COL4A1	CARASIL
OMIM	#125310	#301500	#192315	#120130	#60142
Pattern of inheritance	Autosomal dominant	X-linked recessive	Autosomal dominant	Autosomal dominant	Autosomal recessive
Gene	*NOTCH3*	α-GAL A (GLA)	TREX1	COL4A1	HTRA1
Locus	19p13	Xq22	3p21.3-p21.2	13q34	10q25
Gene product	Notch 3 receptor	Alpha galactosidase A enzyme	DNA specific 3'-5' exonuclease DNase III	Type IV collagen 1	HTRA1 serine peptidase/protease 1
Clinical manifestations					
Stroke					
Age at onset (yrs)	20-70	M:33-46/F:40-52	40-50	14-49	20-40
Stroke subtype					
Small vessel disease	+	+	+	+	+
Large vessel disease	-	+	-	-	-
Cardioembolic	-	+	-	-	-
Haemorrhagic	Rare	Rare	-	+	-
Other neurological manifestations					
Psychiatric disturbance	+	+	+	+	+
Migraine with/without aura	+	-	+	+	-
Seizures	+		+	+	
Cognitive impairment	+	±	+	+	+
Extra-neurological manifestations					
Neuropathy	-	+(80%)	+/-	+	-
Myopathy	-	-	+	+	+
Renal disease	-	+	+	+	-
Skin involvement	-	+	-	-	-

Table 1 continued.

Ocular involvement	+/- Retinal arteriolar narrowing	+ Cornea verticillata	+ Retinopathy	+ Cataracts, retinopathy	+ Retinopathy
Gastrointestinal involvement	-	+	+/-	+	-
Cardiac involvement	-	+	-	+	-
Others		Acroparhestesia, hypoacusia	Raynaud phenomena (80%), hepatopathy	Poroencephaly, prenatal bleeding, infantile hemiparesis	Alopecia, spondylosis deformans, acute lumbago
Radiological findings					
White matter lesions	+	+	+	+	+
Lacunar lesions	+	+	+	+	+
Cortical-subortical lesions	-	+	+/-	-	-
ICH	+	+	-	+	+
Aneurysms	-	+	-	+	-
Peculiar findings	Temporal lobe hyperintensities, external capsule involvement	Pulvinar hyperintensities on T1-wheighted images	Subcortical contrast-enhancing lesions with oedema	Porencephaly, ICH	-
Pathological findings					
	Granular Osmiophilic Material (GOM) around vascular smooth muscle cells	Cytoplasmatic Gb3 inclusions in vascular endothelial cells and smooth muscle cells	Multilaminated vasculare basement membranes	Interruption and thickening of basement membrane	Degeneration in vascular smooth muscle cells

Finally, the Cerebral Autosomal Recessive Arteriopathy with Subcortical Infarcts and Leukoencephalopathy (CARASIL), due to mutations in the *HTA1* gene has been described in Asians and recently in some European cases. Clinically, the disease is characterized by recurrent lacunar strokes associated with a rapidly progressive cognitive impairment, seizures and psychiatrics disturbance.[16-20]

Although the above described single gene disorders are believed to account for a small proportion of cases, their prevalence is probably underestimated; systematic studies on well-defined phenotypes and larger series are needed since these diseases are expected to play a crucial role in our understanding of the pathogenesis of VaD and CSVD.[21]

SPORADIC VASCULAR DEMENTIA

Compared to these monogenic forms, it is reasonable to assume that sporadic VaD might have a more complex mode of inheritance, in which multiple genetic variants with small effects predispose to disease (similar to other causes of dementia). Additionally, many of the risk factors for VaD such as hypertension, dyslipidemia, and smoking habits are partly genetically determined and this may further complicate the picture.[22] To identify genetic risk factors for VaD, two genome-wide association studies (GWAS) have been reported: a retrospective study in Koreans (84 VaD patients, 200 controls) did not detect any genetic association,[23] while a prospective study in the Netherlands (67 patients, 5700 controls) identified an association with the variant rs12007229 near the androgen receptor gene on the X chromosome, which was replicated in a German population (221 cases, 213 controls).[24] However, large-scale hypothesis-free studies are lacking, thereby hampering gene discovery in VaD. Instead, most of our current genetic understanding is based on candidate genes for stroke and AD and on GWAS findings for CSVD endophenotypes.

Candidate gene studies

The candidate genes for association studies may encompass both genes implicated in stroke and Alzheimer disease and genes that affect critical biological processes to VaD. Given the multitude of candidate gene studies and the common failure of replicating

the findings, we focus only on candidates that show consistent effect in two or more published studies.

From a pathophysiological view, the genes involved in lipid metabolism, especially the apolipoprotein E (*APOE*), have been the focus of genetic research over the last two decades. Several meta-analyses, including a recent one which consists of 44 studies (2481 cases, 7490 controls), found a significant association between ε4 allele carriers and increased risk of VaD, irrespective of ethnicity.[25,26] However, there was no difference in risk for VaD between ε2 and ε3 allele carriers nor in the *APOE* promoter T-427C[2]. Two polymorphisms (Q192R and L55M) of *PON1* were associated with a higher risk of VaD in Indian and French populations,[27-29] but these findings for Q192R were not confirmed in two other studies on Caucasian populations.[30,31] Several genes related to inflammation have also been related to VaD, including two polymorphisms in the *TNF-α* in Caucasians[32] and Asians.[33] In addition, an association between VaD and *TGF-β1* was described in two Asian reports.[34,35]

However, candidate genes studies have not identified robust associations for various features of sporadic CSVD, such as lacunar infarction, intracerebral hemorrhage, or white matter hyperintensities. Methodological issues, particularly related to inaccurate or heterogeneous phenotyping and insufficient sample sizes, have been invoked as possible reasons for this.[6]

Genome-wide association studies

A more recent line of research has been to consider genes that have been identified through GWAS of stroke and AD. With respect to stroke, the Cohorts of the Heart and Aging Research in Genetic Epidemiology (CHARGE) consortium,[36,37] International Stroke Genetics Consortium (ISGC),[38,39] NINDS Stroke Genetics Network (SiGN)[39] and Wellcome Trust Case Control Consortium 2 (WTCCC2)[38] have conducted separate studies totaling tens of thousands of stroke patients and hundreds of thousands of controls. A variant near *FOXF2* was found to increase risk of all-stroke, and was also associated with white matter hyperintensities. Furthermore, multiple robust associations have been reported in an apparent subtype-specific manner: *TSPAN2* was associated with large artery atherosclerosis-related stroke, *PITX2* and *ZFHX3* with cardioembolic stroke, *HDAC9* with

large artery atherosclerosis stroke, and *ALDH2* with small artery stroke. However, these genes have yet to be investigated for their relation with VaD. Currently, even larger GWAS on stroke are underway. Linking all these novel genes with VaD would crucially advance our knowledge of its genetic architecture. Similarly, the International Genomics of Alzheimer's Project (IGAP) has identified various genes for AD through GWAS,[40] but these have yet to be associated with VaD. Interestingly though, not all these novel genes fit into known AD pathways involving amyloid or tau processing.[41] Indeed, several genes have been implicated in cardiometabolic pathways, most notably *APOE*, *CLU*, and *ABCA7*, which are related to lipid metabolism.[41]

In contrast to the candidate gene studies, GWAS have recently been carried out successfully to identify novel genes underlying CSVD. For white matter hyperintensities, for instance, five loci have been identified by studying over 21,000 individuals from the CHARGE consortium.[42] Interestingly, genes at these loci are implicated in both AD and in (hemorrhagic) stroke.[42] Earlier findings have been replicated in independent population-based[43,44] and clinical[45] samples. The CHARGE consortium also investigated whether genetic influences could be detected for the progression of white matter hyperintensities over time.[46] While a very small genetic contribution was identified, larger sample sizes and improved methods for assessing change could yield more results.[46] GWAS of MRI-defined brain infarcts have been less robust, with an identified association in the *MACROD2* gene showing inconsistent effects.[47]

Instead of restricting genetic overlap to the top genes, an exciting alternative approach is to test for genetic overlap between clinical endpoints on a genome-wide scale. Novel methods, including linkage disequilibrium score regression,[48] now make such investigations possible. Currently, a study is ongoing for stroke and AD and, if the results are positive, this will provide important evidence of a causal link between these two clinical distinct entities, which overlap clinically in the realm of VaD.

FUTURE DEVELOPMENTS

Despite the initial successes of GWAS, it is important to keep in mind that the explained variance of these genetic associations is limited, indicating that the largest proportion of

the heritability of CSVD still remains to be elucidated. A common message from all genetic studies in the field of VaD is that we need larger sample size. The genetic complexity is such that there are likely thousands of unknown variants, each with a modest contribution to disease. Sufficient power can only be achieved by jointly analyzing all data together and will likely even necessitate cross-consortia efforts. Furthermore, many consortia have progressed to novel technologies, such as next generation sequencing (NGS) that permit further identification of multiple causal variants, including rare variants.[49]

Another important aspect of gaining power is by improving phenotype definitions, which are currently quite heterogeneous for VaD. Also, mixed pathologies are common above the age of 75 and require careful statistical handling. While GWAS of clinical phenotypes has started to provide robust association with current sample sizes over hundreds of thousands participants in VaD and other complex diseases, the endophenotypes approach has shown promising results with much smaller sample sizes. The focus has so far been on white matter hyperintensities and brain infarcts, but other neuroimaging traits have yet to be analyzed. Particularly, brain microbleeds (from T2*-weighted or susceptibility-weighted imaging), enlarged perivascular spaces, and white matter integrity (from diffusion imaging) would be important phenotypes for VaD. Brain microbleeds and enlarged perivascular spaces are markers for both ischemic and hemorrhagic pathology,[50,51] and elucidating genetic factors that are common to both pathways can also shed light on VaD. Also, white matter integrity as measured by diffusion imaging provides a much more complete assessment of the burden of CSVD, since it precedes many of the 'end stage' findings such as white matter hyperintensities.[52]

CLINICAL IMPLICATIONS OF UNDERSTANDING THE GENETICS OF VASCULAR DEMENTIA

An important implication of unravelling the genetic causes of VaD would be a biological understanding of its origin. However, what genetic studies have actually demonstrated so far is that clinical definitions are rather heterogeneous; one of the primary challenges

will be to create robust definitions of VaD phenotypes, along with the selection of appropriate controls and replication in independent samples.[53]

Understanding the causal genes and their underlying disease mechanisms can also lead to the identification of pathways. These can provide attractive targets for intervention and subsequently stimulate drug development, for which the related field of AD provides a good example. The identification of causative mutations in *APP*, *PSEN1* and *PSEN2* in familial AD cases has led to the amyloid cascade hypothesis that changes in the *APP* gene and its processing results in the aggregation and deposition of amyloid-β (Aβ), and this presumably leads to disease. In GWAS of sporadic AD, the identification of *APOE* (initially also through linkage) and more recently a variety of other genes that are known to be implicated in pathways such as immune response, endyctosis, and lipid metabolism may lead to novel directions in drug discovery.[41]

Also, *APOE* is already used for the selection and stratification of trial participants in drug development studies for AD by using ε4 allele carriers as a high risk group. The variability in the length of an intronic poly-T repeat of the *TOMM40*, which is in linkage disequilibrium with *APOE* on chromosome 19, has been shown to also have a predictive value for disease risk[54] and an algorithm combining both *APOE* and *TOMM40* is now used in the TOMMORROW randomized control trial.[55] The identification of more genetic variants can thus lead to improved selection of persons for clinical trials.

Furthermore, the variability of response to drugs among individuals remains a key challenge of the pharmaceutical drug research and in clinical practice, both in terms of efficacy and adverse effects. This differential response of individuals is thought to be related to genetic and non- genetic factors. Pharmacogenetics (PGX) refers to the inter-individual genome-wide DNA variations and potential interactions that correlate with drug response and toxicity.[56] With the addition of new omics translational tools and technologies, the term now also encompasses alterations in gene expression and post-translational modifications (e.g. proteomics and metabolomics) that also correlate with drug response and drug toxicity. PGX studies are typically differentiated into two broad types, namely safety PGX studies and efficacy PGX studies. Safety PGX involves genes affecting drug absorption, distribution, metabolism and excretion. Variations in these

genes may affect pharmacokinetic and pharmacodynamic responses that may ultimately result into adverse effects. Extensive sequencing data of such genes are increasingly being used in various discovery stages by pharmaceutical companies, as complementary tools of clinical pharmacology databases for key decision making processes. Efficacy PGX includes studies involving genes that are known to encode "druggable" targets. Variants within these genes may affect target engagement, thus alter efficacy. On the other hand, disease susceptibility genes, identified though large scale GWAS analyses and meta-analyses on cases and controls, serve for the generation of new discovery hypotheses and for target validation, as well as for the selection and/or stratification of patients in phase II clinical trials. Ideally, assuming appropriate samples and ethics approvals are in place for PGX and other biomarker studies, positive efficacy signals may correlate with genetic variants in responders to the active drug and not to the placebo; then these markers could inform the much larger (and considerably more expensive) phase III trials to increase their probability of success through PGX/ biomarker enriched trial designs for the drug or several drugs at a time. Such approaches have been successfully applied in cancer, but regrettably not in most other therapy areas, including vascular dementia.

REFERENCES

1 Gorelick, P. B. *et al.* o. *Stroke* **42**, 2672-2713 (2011).

2 Bergem, A. L. M., Engedal, K. & Kringlen, E. *Archives of General Psychiatry* **54**, 264-270 (1997).

3 Heiss', W. D., Rosenberg, G. A., Thiel, A., Berlot, R. & De Reuck, J. Neuroimaging in Vascular Cognitive Impairment: A State-of-the-art Review.

4 Chabriat, H., Joutel, A., Dichgans, M., Tournier-Lasserve, E. & Bousser, M.-G. Cadasil. *The Lancet Neurology* **8**, 643-653 (2009).

5 Pastores, G. M. & Lien, Y.-H. H. B. *Journal of the American Society of Nephrology* **13**, S130-S133 (2002).

6 Clarke, J. T. R. Narrative review: Fabry disease. *Annals of internal medicine* **146**, 425-433 (2007).

7 Bersano, A. *et al.* Neurological features of Fabry disease: clinical, pathophysiological aspects and therapy. *Acta Neurologica Scandinavica* **126**, 77-97 (2012).

8 Shi, Q., Chen, J., Pongmoragot, J., Lanthier, S. & Saposnik, G. *Journal of Stroke and Cerebrovascular Diseases* **23**, 985-992 (2014).

9 Rolfs, A. *et al.* Acute Cerebrovascular Disease in the Young The Stroke in Young Fabry Patients Study. *Stroke* **44**, 340-349 (2013).

10 Lanfranconi, S. & Markus, H. S.. *Stroke* **41**, e513-e518 (2010).

11 Winkler, D. T. *et al.*. *Journal of neurology* **255**, 77-88 (2008).

12 Siveke, J. T. & Schmid, H. *American Journal of Medical Genetics Part A* **123**, 309-309 (2003).

13 Richards, A. *et al. Nature genetics* **39**, 1068-1070 (2007).

14 Weil, S. *et al. Neurology* **53**, 629-629 (1999).

15 DiFrancesco, J. C. *et al. Neurological Sciences* **36**, 323-330 (2014).

16 Fukutake, T.*Journal of Stroke and Cerebrovascular Diseases* **20**, 85-93 (2011).

17 Nozaki, H. *et al.* Characteristic features and progression of abnormalities on MRI for CARASIL. *Neurology* **85**, 459-463 (2015).

18 Nozaki, H., Nishizawa, M. & Onodera, O.. *Stroke* **45**, 3447-3453 (2014).

19 Cordeiro, I. M. *et al.* S. *Stroke* **46**, 1110-1112 (2015).

20 Bianchi, S. *et al.* Two novel HTRA1 mutations in a European CARASIL patient. *Neurology* **82**, 898-900 (2014).

21 Tan, R. Y. Y. & Markus, H. S. Monogenic causes of stroke: now and the future. *Journal of neurology* **262**, 2601-2616 (2015).

22 Bersano, A. *et al.* The genetics of small-vessel disease. *Current medicinal chemistry* **19**, 4124-4141 (2012).

23 Kim, Y., Kong, M. & Lee, C. . *The World Journal of Biological Psychiatry* **14**, 220-226 (2013).

24 Schrijvers, E. M. C. *et al.* Genome-wide association study of vascular dementia. *Stroke* **43**, 315-319 (2012).

25 Yin, Y.-W. *et al. Neuroscience letters* **514**, 6-11 (2012).

26 Zeng, L. *et al.* Can Chinese Herbal Medicine Adjunctive Therapy Improve Outcomes of Senile Vascular Dementia? Systematic Review with Meta analysis of Clinical Trials. *Phytotherapy Research* **29**, 1843-1857 (2015).

27 Alam, R. *et al.* . *American journal of Alzheimer's disease and other dementias*, 1533317514539541 (2014).

28 Dantoine, T. F. *et al.*. *Annals of the New York Academy of Sciences* **977**, 239-244 (2002).

29 Helbecque, N., Cottel, D., Codron, V., Berr, C. & Amouyel, P. Paraoxonase 1 gene polymorphisms and dementia in humans. *Neuroscience letters* **358**, 41-44 (2004).

30 Zuliani, G. *et al.* Genetic polymorphisms in older subjects with vascular or Alzheimer's dementia. *Acta Neurologica Scandinavica* **103**, 304-308 (2001).

31 Bednarska-Makaruk, M. E. *et al.*. *Folia Neuropathol* **51**, 111-119 (2013).

32 McCusker, S. M. *et al. The Lancet* **357**, 436-439 (2001).

33 Fung, H. C. *et al.*. *Dementia and geriatric cognitive disorders* **20**, 1-7 (2005).

34 Kim, Y. & Lee, C. The gene encoding transforming growth factor β1 confers risk of ischemic stroke and vascular dementia. *Stroke* **37**, 2843-2845 (2006).

35 Peila, R. *et al.* A TGF-β1 *Neurobiology of aging* **28**, 1367-1373 (2007).

36 Ikram, M. A. *et al.* Genomewide association studies of stroke. *New England Journal of Medicine* **360**, 1718-1728 (2009).

37 of the Cohorts, N. W. G., Network, S. G. & International Stroke Genetics, C. Identification of additional risk loci for stroke and small vessel disease: a meta-analysis of genome-wide association studies. *The Lancet Neurology* (2016).

38 Bellenguez, C. *et al.* Genome-wide association study identifies a variant in HDAC9 associated with large vessel ischemic stroke. *Nature genetics* **44**, 328-333 (2012).

39 Network, N. S. G. & International Stroke Genetics, C. L. *The Lancet Neurology* (2015).

40 Lambert, J.-C. *et al. Nature genetics* **45**, 1452-1458 (2013).

41 Karch, C. M. & Goate, A. M. Alzheimer's disease risk genes and mechanisms of disease pathogenesis. *Biological psychiatry* **77**, 43-51 (2015).

42 Verhaaren, B. F. J. *et al. Circulation: Cardiovascular Genetics*, CIRCGENETICS. 114.000858 (2015).

43 Verhaaren, B. F. J. *et al.*. *Stroke* **42**, 3297-3299 (2011).

44 Tabara, Y. *et al.*. *European Journal of Neurology* **20**, 860-862 (2013).

45 Traylor, M. *et al.*. *Neurology* **86**, 146-153 (2016).

46 Hofer, E. *et al.* White Matter Lesion Progression Genome-Wide Search for Genetic Influences. *Stroke* **46**, 3048-3057 (2015).

47 Debette, S. *et al.* G. *Stroke* **41**, 210-217 (2010).

48 Bulik-Sullivan, B. K. *et al.* LD Score regression distinguishes confounding from polygenicity in genome-wide association studies. *Nat Genet* **47**, 291-295, doi:10.1038/ng.3211 (2015).

49 Bersano, A. *et al. Journal of Stroke and Cerebrovascular Diseases* **24**, 759-765 (2015).

50 Akoudad, S. *et al.*. *Cerebrovascular Diseases* **37**, 382-388 (2014).

51 Charidimou, A. *et al.*. *Journal of Neurology, Neurosurgery & Psychiatry* **84**, 624-629 (2013).

52 de Groot, M. *et al.* Changes in normal-appearing white matter precede development of white matter lesions. *Stroke* **44**, 1037-1042 (2013).

53 Hachinski, V. *et al. Stroke* **37**, 2220-2241 (2006).

54 Roses, A. D. *et al.* A TOMM40 variable-length polymorphism predicts the age of late-onset Alzheimer's disease. *The pharmacogenomics journal* **10**, 375-384 (2010).

55 Roses, A. D. *et al.* New applications of disease genetics and pharmacogenetics to drug development. *Current opinion in pharmacology* **14**, 81-89 (2014).

56 McCarthy, A. D., Kennedy, J. L. & Middleton, L. T. Pharmacogenetics in drug development. *Philosophical Transactions of the Royal Society B: Biological Sciences* **360**, 1579-1588 (2005).

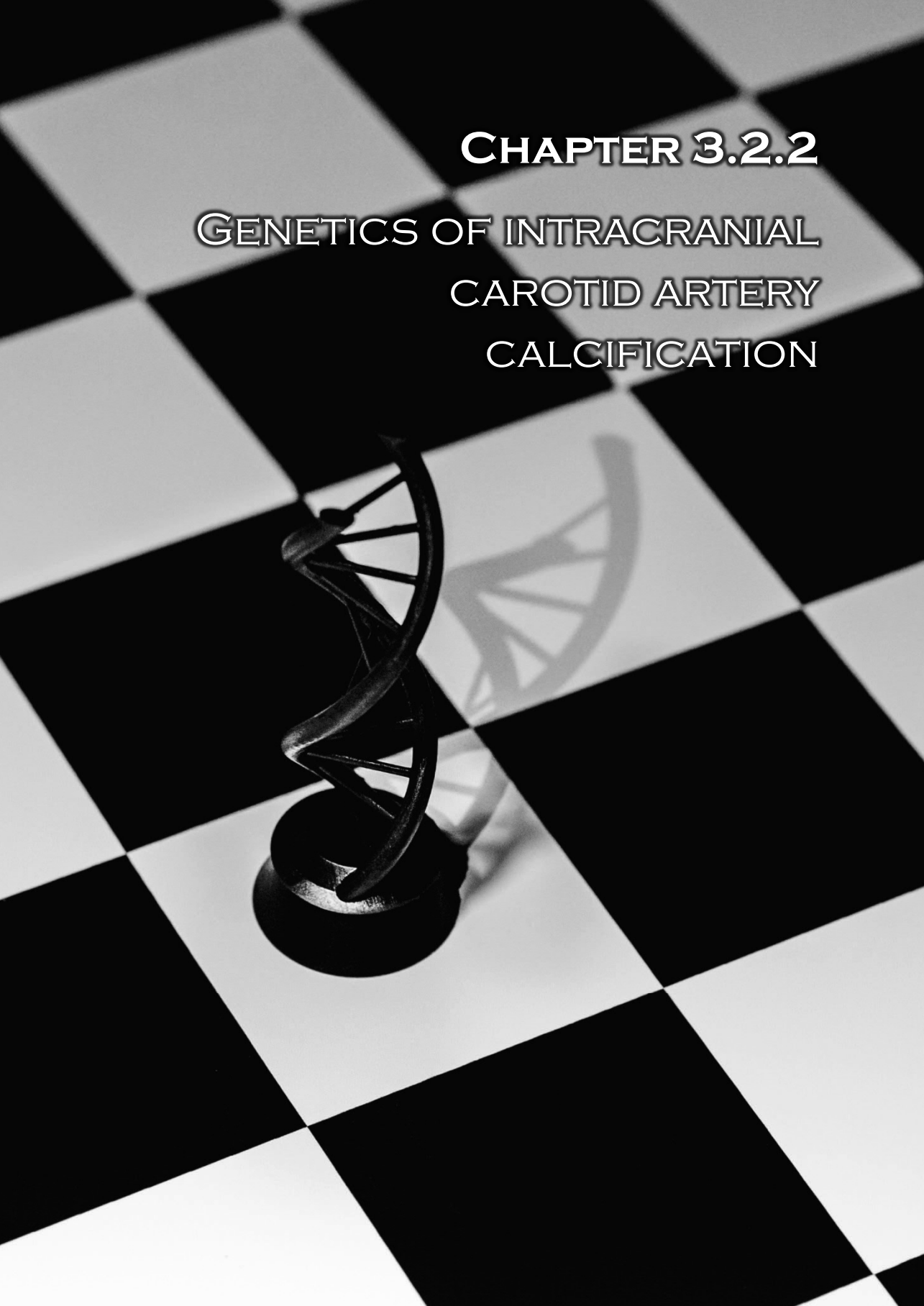

Chapter 3.2.2

Genetics of intracranial carotid artery calcification

ABSTRACT

Background: Intracranial carotid artery calcification (ICAC) is one of the most important risk factors for stroke. Although several environmental risk factors for ICAC have been identified, its genetic background remains unclear.

Methods: Between 2003 and 2006, 2403 participants from the prospective population-based Rotterdam Study (mean age: 69.6 ± 6.8 years; 51.7% female) underwent computed tomography to quantify vascular calcification in the intracranial internal carotid artery. Blood samples were drawn for genotyping. Genotypes of the participants were imputed to the 1000-Genomes reference panel to generate genetic relationship matrices for the estimation of the heritability of ICAC volume. Adjustments were made for age and sex. Subsequently, genome-wide association analyses were performed to identify specific variants.

Results: The age- and sex-adjusted heritability (h^2) of ICAC was 47% (standard error (SE): 19%, P=0.009). Genome-wide association analyses identified a variant on chromosome 9p21.3 (rs1537372; N=2034; $P=4.75x10^{-9}$) and one variant on chromosome 11p11.2 (rs11038042, N=2034; $P=3.27x10^{-8}$), that were significantly associated with ICAC volume. Rs1537372 replicated in an independent sample of 716 stroke patients ($P_{combined} =1.38x10^{-10}$).

Conclusions:ICAC volume is a heritable trait which is partly explained by common genetic variation. We identified specific genetic variants associated with ICAC, which given the importance of ICAC in stroke risk, needs replication in larger-scale studies to further elucidate its genetic basis.

INTRODUCTION

Intracranial carotid artery calcification (ICAC) is a leading risk factor for stroke.[1-3] Various established environmental and lifestyle factors such as smoking and diabetes mellitus are known to contribute substantially to the formation of ICAC.[1,2,4] Yet, it remains unknown to what extent genetics play a role in the development of ICAC.

For the last decade, genetic research of atherosclerotic calcification has mainly focused on the coronary arteries given strong relations with coronary morbidity and mortality. Recently, this has led to the identification of three common genetic variants strongly related to the presence and amount of coronary artery calcification.[5] Yet, preliminary evidence suggests that these variants are not associated with calcification in other vessels.[6] This suggests that although arterial calcification is a systemic process, there are important vessel-specific differences in its etiology.[7,8] Given that other risk factors such as diabetes and smoking are generally thought to exert a systemic effect on the formation of arterial calcification, genetic information may be crucial for explaining location-specific differences.

Against this background, it is vital to elucidate the genetic susceptibility underlying the development of ICAC. This information may ultimately aid in the development of therapeutic or preventive interventions for stroke.

Therefore, in the current study, we quantified ICAC,[3] determined its heritable component, and performed a genome-wide association analysis including independent replication of top hits.

METHODS

Discovery cohort

This study was embedded in the Rotterdam Study,[9] a prospective population-based study investigating the determinants and consequences of age-related diseases in older adults. The original cohort consisted of 7,983 participants 55 years or older and was extended in 2000-2001 by 3,011 persons. At study entry and every 3 to 4 years, all participants are re-examined in a dedicated research center. The Rotterdam Study represents a relatively stable, homogeneous middle-class population, largely of European descent. The Rotterdam Study has been approved by the medical ethics committee according to the Population Screening Act: Rotterdam Study, executed by the Ministry of Health, Welfare and Sports of the Netherlands. All participants provided written informed consent.

Between September 2003 and February 2006, we invited all participant who visited the research center to undergo non-enhanced computed tomography (CT) scanning to quantify calcification in the intracranial carotid arteries (as part of a large project on quantification of vascular calcification in multiple vessel beds).[10,11]Due to errors in image acquisition or image artefacts, 29 CT examinations from the 2,524 were not gradable, leaving a total of 2,495 persons with a gradable CT examination for ICAC. Of these 2,495 persons, 2,034 were successfully genotyped.

Assessment of ICAC

Non-contrast CT images were obtained using a 16-slice (n=724) or 64-slice (n=1,689) multidetector CT (MDCT) scanner (Somatom Sensation 16 or 64, Siemens, Forchheim, Germany). We performed two scans: a cardiac scan and a scan that reached from the aortic arch to the circle of Willis. Using these scans, we imaged the coronary arteries, the aortic arch, the extracranial part of the internal carotid arteries, and intracranial part of the internal carotid arteries. Detailed information on the imaging parameters of the scans is described elsewhere.[8,11]

As marker of intracranial atherosclerosis, we measured ICAC in both internal carotid arteries from the horizontal petrous bone segment up to its top.[3,4] To quantify ICAC, we

used a semi-automated scoring method which is described in detail elsewhere.[4,12] In short, all calcifications in the trajectory of the intracranial internal carotid artery were manually delineated in consecutive MDCT-slices while making sure that bony structures were not included. Next, the number of pixels above 130 Hounsfield units was determined and the calcification volume (mm^3) was calculated by multiplying the number of pixels, pixel-size and the increment. Calcification volumes in the coronary arteries, aortic arch, and extracranial carotid arteries, were quantified using dedicated commercially available software (Syngo CalciumScoring, Siemens, Germany).[8] All calcification volumes are expressed in mm^3.

Genotyping

All study participants were genotyped with the 550K, 550K duo, or 610 quad Illumina arrays. We removed samples with a call rate below 97.5%, gender mismatch, excess autosomal heterozygosity (>0.336), duplicates or family-relations and ethnic outliers. Moreover, we removed those variants with call rates below 98.0%, failing missingness tests, Hardy-Weinberg equilibrium p-values < 10^{-6}, and minor allele frequencies (MAF) of less than 0.1%. Genotypes were imputed using MACH/minimac software to the 1000 Genomes phase I version 3 reference panel (entire population).

Heritability analysis

We used Genome-wide Complex Trait Analysis (GCTA) to estimate heritability in our sample of unrelated individuals.[13] This method is based on comparing the genetic similarity between individuals to their phenotypic similarity, and the heritability estimates refer to the proportion of variance explain by the variants on the genome-wide chip. As previously described,[14] the 1000 Genomes imputed genotypes were filtered on imputation quality (R^2 < 0.5) and allele frequency (MAF < 0.01). We calculated pairwise genetic relatedness between all individuals and removed one person for pairs with more than 0.02 genotype similarity.

We performed heritability analyses for calcification volume in the four vessel beds separately. Moreover, we assessed the proportion of shared heritability between intracranial carotid artery calcification and calcification in the other three vessel beds

using the bivariate REML function of GCTA. Because calcification volume had a skewed distribution, we used natural log-transformed values and added 1.0 mm^3 to the non-transformed values in order to deal with calcium volumes of zero [Ln(calcification volume + 1.0 mm^3)]. We adjusted the analyses for age and sex.

Genome-wide association analyses

We conducted genome-wide association analyses (GWAS) on calcification in the four vessel beds using the R-package ProbABEL (version 0.4.4).[15] Given that measures of subclinical atherosclerosis in the coronary arteries, aortic arch, and carotid artery bifurcation have already been studied in larger GWAS (in some instances also including this sample),[5,16,17] the main focus was on ICAC. Calcification measures were analyzed under an additive model with linear regression, while adjusting for age and sex. The results were adjusted for genomic control and meta-analyzed using the METAL software.[18] Variants with an $R^2 < 0.5$ and a MAF < 0.05 were removed. Genome-wide significance was established at $p < 5x10^{-8}$. Manhattan-plots and regional association plots were generated in R. For the top variants ($p < 10^{-7}$) and those in linkage disequilibrium ($r^2 > 0.2$) we checked HaploReg (v4.1, www.broadinstitute.org/mammals/haploreg/) for indications of functionality (eQTLs, promotor and enhancer histone marks, and conservation).Next, we investigated the association of the top variants from the GWAS on ICAC with calcification volume in the other vessel beds.

Table 1. Characteristics of the study population.

Characteristic	Value
Sample size	2034
Female sex, %	50.7
Age, mean (SD), years	69.8 (6.8)
ICAC prevalence, %	83.0
CAC prevalence, %	81.6
AAC prevalence, %	92.3
ECAC prevalence, %	74.0
ICAC volume, median (IQR), mm^3	46.0 (8.0 – 148.0)
CAC volume, median (IQR), mm^3	53.8 (2.0 – 283.6)
AAC volume, median (IQR), mm^3	267.8 (46.8 – 924.5)
ECAC volume, median (IQR), mm^3	26.2 (0.0 – 126.4)

SD: standard deviation, ICAC: intracranial carotid artery calcification, IQR: interquartile range, CAC: coronary artery calcification, AAC: aortic arch calcification, ECAC: extracranial carotid artery calcification

Replication

Replication of genome-wide significant variants was attempted in the Erasmus Stroke Study (ESS), a clinical TIA and stroke registry, in which stroke-patients were enrolled between December 2005 and September 2010, in the Erasmus MC, Rotterdam, the Netherlands and which is described in detail elsewhere.[19] For the current study, we used all patients with complete information on ICAC (as assessed by contrast-enhanced MDCTA) and in whom blood samples were taken (n = 776). Of these 776, 716 were successfully genotyped for rs1537372, and 743 for rs1103842. The stroke subtypes according to the TOAST-criteria of these participants were as follows: 1) large vessel disease: 17%, 2) cardio-embolism: 12%, 3) small vessel disease: 24%, 4) other: 6%, 5) undetermined: 42%. Participants were genotyped using Taqman Allelic Discrimination (Thermo Fisher Scientific Inc.). Reactions were performed according to manufacturer's protocol with minor adjustments.

RESULTS

Study population

The characteristics of the study population are shown in Table 1. The mean age of the study population was 69.6 ± 6.8 years, and 51.7% were females.

Heritability of ICAC

We found an age- and sex-adjusted heritability for ICAC volume of 47% [heritability estimate (h^2): 0.47 (standard error (SE): 0.19, $p = 0.009$)]. In comparison, the age- and sex-adjusted heritability estimates for coronary artery calcification, aortic arch calcification, and extracranial carotid artery calcification were 0.52 (SE: 0.20, $p = 0.004$), 0.36 (SE: 0.19, $p = 0.024$), and 0.17 (SE: 0.19, $p = 0.186$), respectively. We found a shared heritability of intracranial carotid artery calcification with coronary artery calcification of 77% (h^2: 0.47, $p = 0.006$). For aortic arch calcification and extracranial carotid artery calcification this was 9% and 78% (h^2: 0.09, $p = 0.400$, and h^2: 0.78, $p = 0.077$), respectively.

GWAS of ICAC

We performed a GWAS for ICAC volume. Figure 1 plots the p-values for this trait. For ICAC volume, 28 variants from a single locus at 9p21.3 (top variant rs1537372; MAF = 0.41; $p = 4.75 \times 10^{-9}$) and one variant from a locus at 11p11.2 (rs11038042; MAF = 0.78; $p = 3.27 \times 10^{-8}$) reached genome wide significance. We also found one variant at 2q14.1 (rs34008603; MAF = 0.97, $p = 1.91 \times 10^{-7}$) that showed a suggestive association with ICAC. Figure 2 shows the regional plots for 9p21.3 and 11p11.2. Table 2 shows the top genetic variants at three loci associated with ICAC volume of with $p < 1 \times 10^{-7}$. For the 9p21 locus, there is a considerable body of literature on potential functional mechanisms. The top variant of 11p11.2 shows enhancer histone marks in muscle and stomach cell lines. For 2q14.1, several variants in LD overlap with promotor or enhancer marks, or affect gene expression (Supplementary Table S1).

Given the known association of the 9p21 locus with ischemic stroke,[20] we performed a sensitivity analysis in which we excluded participants with prevalent clinical stroke from the sample (n = 85). This did not attenuate the association of rs1537372 with ICAC

volume (beta = 0.18, p = 9.50x10^{-9}). We also repeated the analyses after excluding persons without any calcifications, but this did not materially affect the results (Supplementary Table 2). Furthermore, we did not identify any interaction with sex.

When investigating associations the three top variants for ICAC with calcification volume in three other vessel beds, namely the coronary, aortic and extracranial carotid artery. We found that rs1537372 and rs11038042 were related to calcification in at least two of the other vessel beds, whereas rs34008603 showed only a single nominally significant association with the extracranial carotid artery (Table 3).

Replication of top variants for ICAC

We were able to replicate our top variant rs1537372 from the locus at 9p21.3 (n = 716; beta = 0.13, p = 5.19x10^{-3}). Rs11038042 at 11p11.2 did not replicate in the independent sample (n = 731; beta = -0.06, p = 0.304). Yet, the direction of the effect was similar to that in the discovery cohort. After meta-analyzing both samples we found a more significant p-value for rs1537372 (n = 2750; p = 1.38x10^{-10}) and a less significant p-value for rs11038042 (n = 2765; p = 2.99x10^{-7}).

DISCUSSION

In this population-based study, we examined the contribution of common genetic variants to ICAC, for which the genetic basis is currently unknown. We found a high heritability of ICAC volume and identified two loci that influence ICAC, one of which replicated in an independent cohort of stroke-patients.

Strengths of our study are the quantitative assessment of ICAC volume, and the fact that the results remained unchanged after excluding participants with a previous clinical stroke. There are also methodological considerations to take into account. First, it is important to keep in mind that calcification is thought to represent atherosclerosis, but represents only a part of the total atherosclerotic plaque. With non-enhanced CT, it is not possible to visualize the non-calcified plaque components. Yet, extensive evidence demonstrates that calcification volume is an adequate indicator of the total underlying atherosclerotic burden.[21,22] Second, our analyses were performed on relatively small

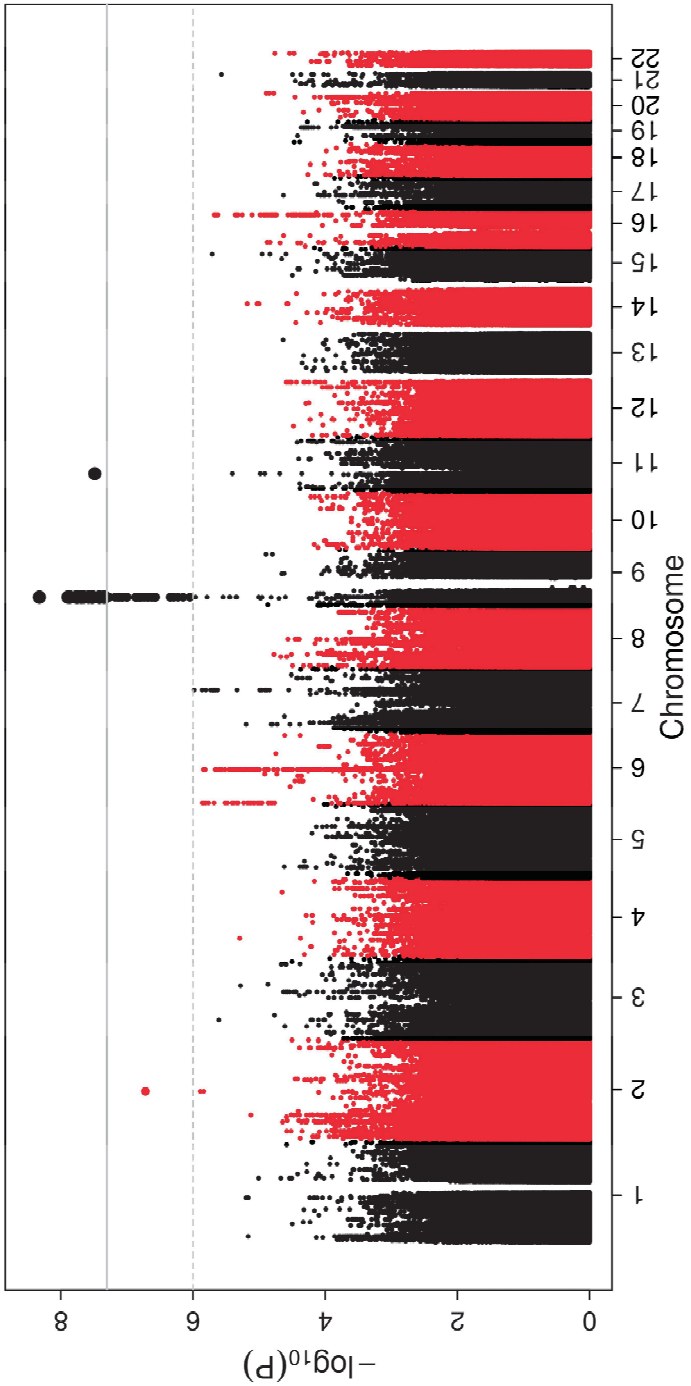

Figure 1 | Common genetic variants associated with intracranial carotid calcification.

Manhattan-plot of demonstrating genetic variants associated with intracranial carotid artery calcification.

Table 2 | Top genetic variants at three loci associated with ICAC volume ($p<1x10^{-7}$)

							Discovery sample		
Variant	**Locus**	**Position**	**Closest gene(s)**	**A1**	**A2**	**Freq**	**β (SE)**	**P**	**N**
rs1537372	9p21.3	22103183	CDKN2A/CDKN2B	T	G	0.41	0.18 (0.03)	$4.75x10^{-9}$	2034
rs11038042	11p11.2	44539107	CD82	A	G	0.78	-0.21 (0.04)	$3.27x10^{-8}$	2034
rs34008603	2q14.1	116125800	DPP10	T	G	0.97	0.51 (0.10)	$1.91x10^{-7}$	2034

Table 3 | Top genetic variants for ICAC volume ($p<1x10^{-7}$) and their association with calcification in other vessel beds.

					ICAC (N=2034)		Aortic arch (N=2048)		Coronary (N=1982)		ECAC (N=2050)	
Variant	**Locus**	**A1**	**A2**	**Freq**	**β (SE)**	**P**	**β (SE)**	**P**	**β (SE)**	**P**	**β (SE)**	**P**
rs1537372	9p21.3	T	G	0.41	0.18 (0.03)	$4.75x10^{-9}$	0.09 (0.03)	$2.32x10^{-3}$	0.12 (0.03)	$5.38x10^{-5}$	0.12 (0.03)	$1.65x10^{-4}$
rs11038042	11p11.2	A	G	0.78	-0.21 (0.04)	$3.27x10^{-8}$	-0.05 (0.04)	0.234	-0.16 (0.04)	$2.74x10^{-5}$	-0.11 (0.04)	$3.50x10^{-3}$
rs34008603	2q14.1	T	G	0.97	0.51 (0.10)	$1.91x10^{-7}$	0.19 (0.10)	0.054	0.02 (0.10)	0.8761	0.23 (0.10)	0.020

Table 4 | Shared heritability between ICAC volume and calcification in other vessel beds.

	ICAC	
Trait	**$r_{genetic}$ (SE)**	**P**
Aortic arch	0.09 (0.34)	0.403
Coronary	0.77 (0.20)	0.0055
ECAC	0.78 (0.41)	0.077

Abbreviations. ECAC: extracranial carotid artery calcification, ICAC: intracranial carotid artery calcification, A1: effect allele, A2: reference allele, SE:

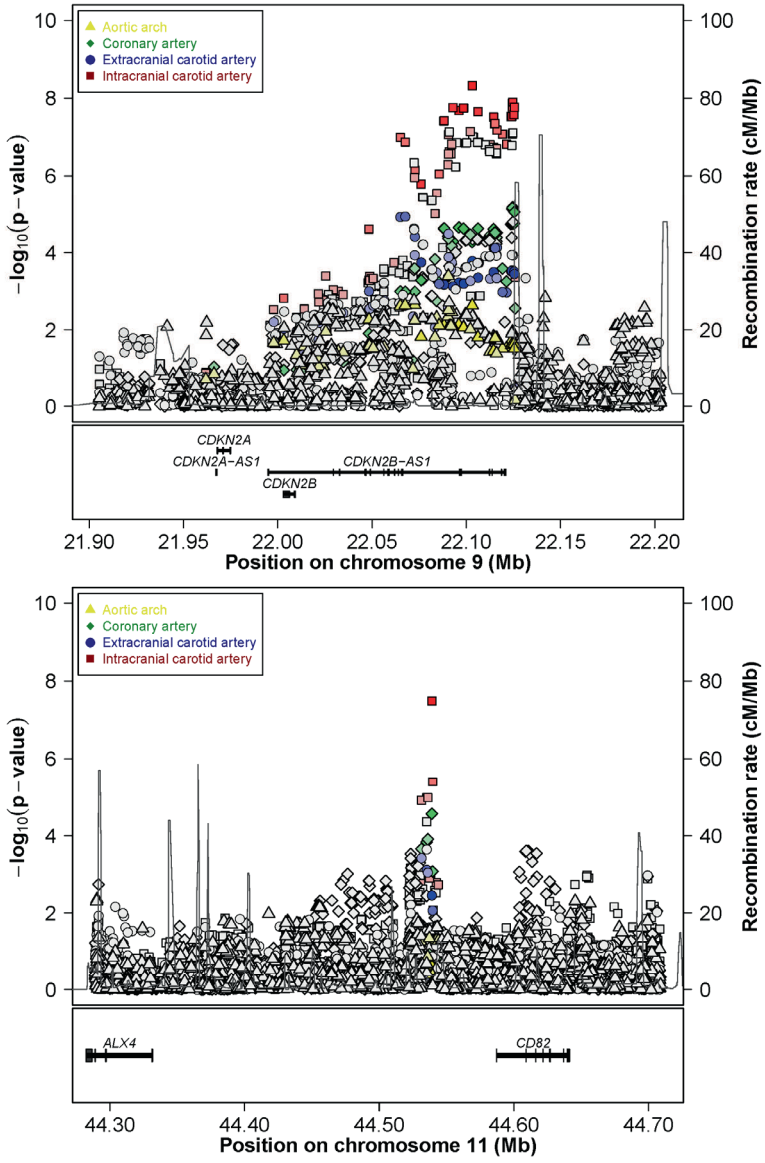

Figure 2 | Regional plots of loci 9p21 and 11p11 associated with intracranial carotid artery calcification

Upper panel: plot of the genetic variants on locus 9p21.3 which are associated with intracranial carotid artery calcification volume. Lower panel: plot of the genetic variants on locus 11p11.2 associated with intracranial carotid artery calcification volume. Figures were created using the Locuszoom software (http://locuszoom.sph.umich.edu/locuszoom/)

samples, both the discovery and replication sample. Yet, this is a direct consequence of the lack of other studies that have quantitatively assessed ICAC as well as performed genome-wide genotyping and that could have been used to increase the study population and hence the statistical power of the association. Nonetheless, we were able to obtain genome-wide significant variants and heritability estimates for intracranial atherosclerosis. A final consideration is that we used the GCTA to determine the heritability estimates, which are measures of the additive heritability, representing narrow-sense heritability.[13] This directly means that only the additive effects of the genes are taken into account, leaving non-additive effects unstudied.

We found a heritability of over 47% for ICAC, which is comparable to the heritability of coronary artery calcification which we found to be 52%. One previous report on the heritability of coronary artery calcification quantity showed a heritability of 44%.[23] In contrast, we found that for calcification in the carotid artery bifurcation only 17% was attributable to genetic factors, and aortic arch calcification was heritable for 36%. These differences in genetic contribution to the development of calcification in different vessel beds provide more insight into the etiology of the previously reported considerable variation in atherosclerotic burden across various vessel beds.[7,8,24]

In addition to its high heritability, we also identified multiple genome-wide significant variants for ICAC at two loci. The first locus, on which we found 28 variants that were associated with ICAC, was located on chromosome 9, near the *CKDN2a/CKDN2b* genes. In the METASTROKE Collaboration,[20] the 9p21.3 locus has previously been implicated in ischemic strokes which were classified as strokes due to large-vessel disease on the basis of the TOAST-criteria. Although even using tens of thousands of samples, this did not reach genome-wide significance even. Remarkably, we robustly identify a very strong signal in only 2000 individuals and show that this locus likely increases risk of stroke through calcifications in the intracranial carotid artery. Future large-collaborative research is needed to clarify this further. Besides its associations with stroke, variants at 9p21 have been related to coronary artery calcification volume and myocardial infarction.[5] In fact, the top variant found in the GWAS on these traits, rs1333049, was in our study also strongly associated ($p = 1.70 \times 10^{-8}$) with ICAC volume. Earlier, we found

that this variant was also associated with aortic arch calcification and calcification in the carotid artery bifurcation.[6] Also, associations with the 9p21 locus have been found for vascular stiffness,[25] and aneurysms of the abdominal aorta,[26] suggesting a broad influence on arterial disease. Of particular note is a recent publication on how 9p21.3 risk variants disrupt specific transcription factor-dependent TGF-β regulation of p16 expression in human aortic smooth muscle cells.[27] An interesting hypothesis would be that this same mechanism is responsible for vascular disease in other vessel beds by affecting smooth muscle cells locally, such as in the carotid arteries, providing a potential mechanism on how the risk variants influence vascular disease.

We identified another variant in the 11p11.2 region on chromosome 11 that associated with ICAC volume. Although we were unable to replicate this finding, this was an interesting association, especially because this 11p11.2 locus is not known for associations with subclinical vascular disease or cardiovascular events. However, this region has been linked to fasting glucose homeostasis and a higher risk of type 2 diabetes.[28] Interestingly, diabetes is one of the strongest known risk factors for ICAC.[4,29]

Finally, we identified a variant on 2q14.1 which showed a suggestive association with ICAC. The *DPP10* gene, which is closely located to the variant that we identified, is primarily known for its influence on asthma.[30] The exact mechanisms underlying the associations of these loci with ICAC need further elucidation from future studies.

In summary, ICAC volume is a heritable trait, which is explained by common genetic variation. Moreover, we identified and replicated one variant at locus 9p21.3 which is known for its contribution to ischemic stroke. Given the importance of ICAC in the development of stroke, larger-scale studies to further elucidate the genetic basis of intracranial atherosclerosis are needed.

REFERENCES

1. Chimowitz MI, Caplan LR. Is calcification of intracranial arteries important and how? *JAMA Neurol*. 2014;71:401-402
2. Qureshi AI, Caplan LR. Intracranial atherosclerosis. *Lancet*. 2014;383:984-998
3. Bos D, Portegies ML, van der Lugt A, Bos MJ, Koudstaal PJ, Hofman A, et al. *JAMA Neurol*. 2014;71:405-411
4. Bos D, van der Rijk MJ, Geeraedts TE, Hofman A, Krestin GP, Witteman JC, et al.. *Stroke*. 2012;43:1878-1884
5. O'Donnell CJ, Kavousi M, Smith AV, Kardia SL, Feitosa MF, Hwang SJ, et al. *Circulation*. 2011;124:2855-2864
6. Bos D, Ikram MA, Isaacs A, Verhaaren BF, Hofman A, van Duijn CM, et al.. *Circ Cardiovasc Genet*. 2013;6:47-53
7. Allison MA, Criqui MH, Wright CM. Patterns and risk factors for systemic calcified atherosclerosis. *Arterioscler Thromb Vasc Biol*. 2004;24:331-336
8. Odink AE, van der Lugt A, Hofman A, Hunink MG, Breteler MM, Krestin GP, et al. Association between calcification in the coronary arteries, aortic arch and carotid arteries: The rotterdam study. *Atherosclerosis*. 2007;193:408-413
9. Hofman A, Brusselle GG, Darwish Murad S, van Duijn CM, Franco OH, Goedegebure A, et al. The rotterdam study: 2016 objectives and design update. *Eur J Epidemiol*. 2015;30:661-708
10. Elias-Smale SE, Wieberdink RG, Odink AE, Hofman A, Hunink MG, Koudstaal PJ, et al. *Eur Heart J*. 2011;32:2050-2058
11. Odink AE, van der Lugt A, Hofman A, Hunink MG, Breteler MM, Krestin GP, et al. Risk factors for coronary, aortic arch and carotid calcification; the rotterdam study. *J Hum Hypertens*. 2010;24:86-92
12. de Weert TT, Cakir H, Rozie S, Cretier S, Meijering E, Dippel DW, et al. *AJNR Am J Neuroradiol*. 2009;30:177-184
13. Yang J, Lee SH, Goddard ME, Visscher PM. Gcta: A tool for genome-wide complex trait analysis. *Am J Hum Genet*. 2011;88:76-82
14. Adams HH, Verlinden VJ, Callisaya ML, van Duijn CM, Hofman A, Thomson R, et al. *J Gerontol A Biol Sci Med Sci*. 2015
15. Aulchenko YS, Struchalin MV, van Duijn CM.. *BMC Bioinformatics*. 2010;11:134
16. O'Donnell CJ, Cupples LA, D'Agostino RB, Fox CS, Hoffmann U, Hwang SJ, et al. *BMC Med Genet*. 2007;8 Suppl 1:S4
17. Bis JC, Kavousi M, Franceschini N, Isaacs A, Abecasis GR, Schminke U, et al. *Nat Genet*. 2011;43:940-947
18. Willer CJ, Li Y, Abecasis GR. Metal: Fast and efficient meta-analysis of genomewide association scans.

Bioinformatics. 2010;26:2190-2191
19. van Dijk AC, Fonville S, Zadi T, van Hattem AM, Saiedie G, Koudstaal PJ, et al.. *Stroke*. 2014;45:728-733
20. Traylor M, Farrall M, Holliday EG, Sudlow C, Hopewell JC, Cheng YC, et al.. *Lancet Neurol*. 2012;11:951-962
21. Rumberger JA, Simons DB, Fitzpatrick LA, Sheedy PF, Schwartz RS.*Circulation*. 1995;92:2157-2162
22. Sangiorgi G, Rumberger JA, Severson A, Edwards WD, Gregoire J, Fitzpatrick LA, et al. . *J Am Coll Cardiol*. 1998;31:126-133
23. Peyser PA, Bielak LF, Chu JS, Turner ST, Ellsworth DL, Boerwinkle E, et al. Heritability of coronary artery calcium quantity measured by electron beam computed tomography in asymptomatic adults. *Circulation*. 2002;106:304-308
24. Lopez-Cancio E, Galan A, Dorado L, Jimenez M, Hernandez M, Millan M, et al. *Stroke*. 2012;43:2712-2719
25. Bjorck HM, Lanne T, Alehagen U, Persson K, Rundkvist L, Hamsten A, et al. Association of genetic variation on chromosome 9p21.3 and arterial stiffness. *J Intern Med*. 2009;265:373-381
26. Thompson AR, Golledge J, Cooper JA, Hafez H, Norman PE, Humphries SE. S. *Eur J Hum Genet*. 2009;17:391-394
27. Almontashiri NA, Antoine D, Zhou X, Vilmundarson RO, Zhang SX, Hao KN, et al. *Circulation*. 2015;132:1969-1978
28. Dupuis J, Langenberg C, Prokopenko I, Saxena R, Soranzo N, Jackson AU, et al. *Nat Genet*. 2010;42:105-116
29. Lopez-Cancio E, Dorado L, Millan M, Reverte S, Sunol A, Massuet A, et al. T. *Atherosclerosis*. 2012;221:221-225
30. Allen M, Heinzmann A, Noguchi E, Abecasis G, Broxholme J, Ponting CP, et al.. *Nat Genet*. 2003;35:258-263

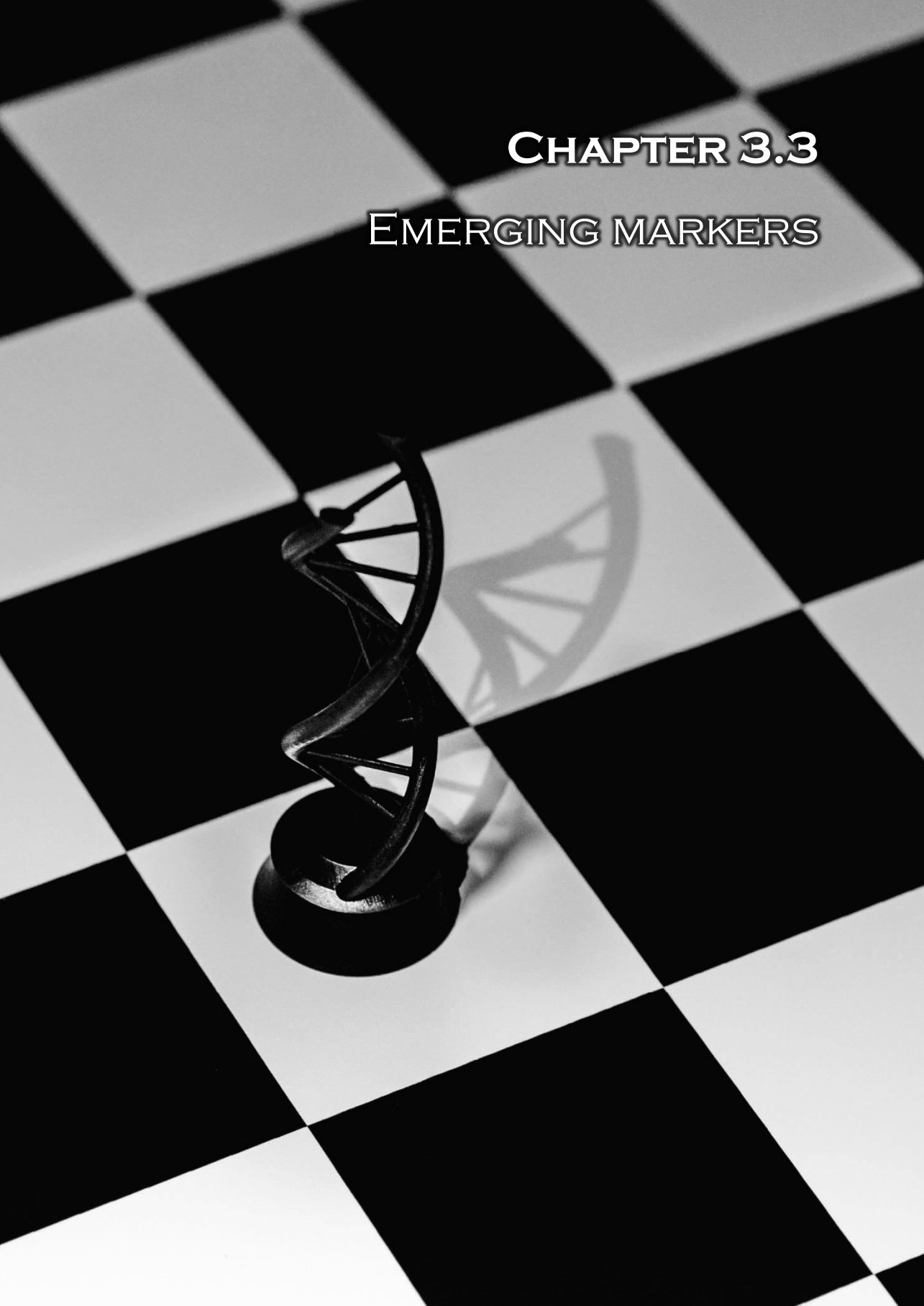

Chapter 3.3

Emerging markers

Chapter 3.3.1

Genome-wide association study of the anterior commissure

ABSTRACT

The anterior commissure is a nerve fiber bundle that interconnects the brain's hemispheres and is important for higher-order cognitive functions, but its genetic architecture remains elusive. This is particularly compelling in view of its presumed role in neurodegeneration. Uncovering the underlying genes could aid understanding of its development and it potentially provides mechanistic insight into diseases that results from its dysfunction. We performed genome-wide association studies (N = 18,828) of the size of the anterior commissure and identified six independent variants at four loci (p-values ranging from 4.1×10^{-8} to 9.4×10^{-22}). Using in silico and in vitro approaches, we mapped the loci to probable causal genes involved in axon guidance (EPHA3 and SEMA6A), cognitive disorders (CTNND2), and growth factor signaling (RIT2). Also, voxel-based morphometry revealed distinct associations of the variants with connected grey matter regions in the brain. While these loci accounted for less than 1% of the variance in the anterior commissure, 30% could be explained by many additional loci that have yet to be discovered. Genome-wide analyses revealed an enrichment for H3K4me1 peaks (marking enhancer sites), introns, and conserved sequences, as well as cell-type-specific annotations from the central nervous system and cardiovascular system. Furthermore, we identify pleiotropy between genes known to increase risk of neurodegenerative diseases and loci of the anterior commissure, including frontotemporal lobar degeneration gene TMEM106B. These combined imaging and genetics analyses shed light on the genetic architecture of commissural tracts and establish the size of the anterior commissure as a relevant marker of neurodegeneration.

INTRODUCTION

Commissural structures in the brain facilitate the cross-talk between the cerebral hemispheres. As such, they are essential for coordinating bilateral sensory and motor functions,[1-4] as well as for integrating lateralized cognitive and behavioral functions.[1,5-7] The white matter of the brain as a whole is highly heritable,[8] but the commissural tracts in particular are under tight genetic control.[9,10]

Most of our genetic understanding of brain commissures stems from studies of model organisms. These studies, mainly in mice and fruit flies, show an important role for several families of axon guidance proteins, including Ephrins, Semaphorins, Robos, Slits, and Netrins.[11-15] By contrast, genes influencing the commissures in humans remain elusive. Some mutations leading to midline crossing defects have been identified in axon guidance proteins, hinting at a similarity with animal models.[16] Additionally, these proteins are active beyond brain development with roles in neuronal repair and regeneration,[17] and could therefore also be important for neurological disorders in adults.[18]

To advance our understanding of the genes influencing brain commissures in humans, we performed genome-wide association studies in 18,828 persons who underwent brain magnetic resonance imaging. We focused on the size of the anterior commissure, the second largest commissure in humans, which connects frontal, temporal, and occipital cortical regions as well as the olfactory bulbs and amygdalae.[19] The identified genes underlying variation in the size of the anterior commissure highlight axon guidance (*EPHA3* and *SEMA6A*) as well as pleiotropy with neurodegenerative diseases (*TMEM106B*).

Table 1 | Genetic loci associated with the anterior commissure cross-sectional area.

						Discovery (N = 7,935)		Combined (N = 18,828)		Heterogeneity (N = 17)	
Locus	Lead variant	Position	A1	A2	Freq	β	P	β	P	I^2	P
3p11.1	rs7650184	89530057	A	C	0.40	-.149	2.0×10^{-6}	-.172	2.5×10^{-19}	0	0.75
5p15.2	rs11748929	11370494	C	G	0.70	-.095	5.0×10^{-3}	-.114	4.1×10^{-8}	0	0.48
5q23.1	rs11948331	116673915	T	G	0.61	-.226	8.2×10^{-12}	-.187	9.4×10^{-22}	20.4	0.22
5q23.1	rs148925592	117348902	A	T	0.96	-.437	2.8×10^{-6}	-.333	5.8×10^{-9}	45.8	0.024
18q12.3	rs346205	40013715	A	G	0.64	-.110	8.2×10^{-4}	-.119	1.1×10^{-9}	10.8	0.33
7p21.3	*rs3807865*	*12250402*	*A*	*G*	*0.41*	*.179*	*1.7* x 10^{-8}	*.095*	*6.2* x 10^{-7}	*52.1*	*0.0079*
8q24.22	*rs1159153*	*132617311*	*T*	*C*	*0.32*	*.182*	*3.4* x 10^{-8}	*.058*	*4.8* x 10^{-3}	*46.2*	*0.022*

[a] Variant missing in some cohorts due to insufficient imputation quality.

Abbreviations: A1 = effect allele, A2 = reference allele, Freq = frequency of the effect allele, I^2 = …, N = sample size.

RESULTS

Genome-wide association studies

After determining that the AC cross-sectional area was significantly heritable (population-based h2 = 36%, p = 3.0 x 10^{-4}; family-based h2 = 32%, p = 6.1 x 10^{-25}; see Online Methods), we performed a two-stage meta-analysis of genome-wide association studies. The discovery sample consisted of seven cohorts (N = 7,935) and was subsequently meta-analyzed with ten replication cohorts (N = 10,893; total N = 18,828), all of European ancestry (Supplementary Table S1).

Both the discovery and replication results are shown in a single 'Manhat-twin' plot (Figure 1A). Four loci reached genome-wide significance in the combined sample (in red; 3p11.1, 5p15.2, 5q23.1, and 18q12.3; Figures 1B-E, respectively), whereas two loci were no longer significant after adding the replication sample (in turquoise; 7p21.3 and 8q24.22; Supplementary Figures S1A-B, respectively). To determine whether these associations were confounded by disease status, we repeated all analyses after excluding persons with stroke and dementia (N = 1,240; remaining N = 17,588), but this did not affect the findings. More details on all six loci are provided in Table 1.

Functional characterization

To elucidate potential mechanisms underlying these genetic associations we investigated the functional role of variants at the four significant loci. For each locus, we examined all genes lying within a 2 Mb window of the lead variant and prioritized genes based on their spatial expression patterns in six human brains (Figure 2A, Supplementary Figure S3; see Online Methods). Of particular interest were genes expressed in the white matter and in the grey matter of frontal, temporal, and central structures (Figure 2B). Next, we investigated whether the lead variants and those in linkage disequilibrium (LD) were quantitative trait loci (QTL) or predicted to be damaging by searching publicly available databases (Supplementary Table S2, see Online Methods). Finally, we screened the putative causal genes for (rare) functional variants using exome sequencing (N = 1,479) and a dedicated exome chip (N = 8,087) in subsamples of our study populations (Supplementary Table S3, see Online Methods).

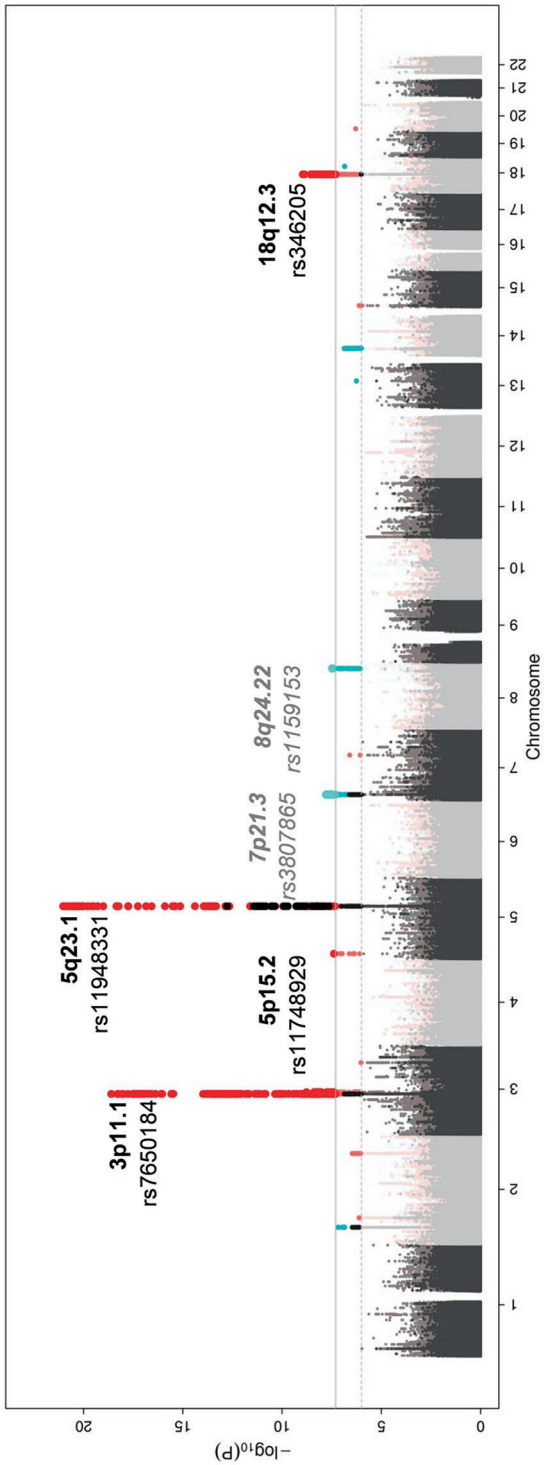

Figure 1 | Genome-wide and regional association plots showing four loci significantly associated with anterior commissure cross-sectional area in the combined discovery and replication (N = 18,828).

Panel A (above) | A 'twin' Manhattan plot shows every variant twice: once for the discovery analysis and once for the combined discovery plus replication analysis. The least significant association of the variant-pair is plotted in grey (alternating light and dark between chromosomes). The most significant association of the variant-pair is plotted in red if is from the combined analysis (i.e., the association replicated) and in turquoise if it is from the discovery analysis (i.e., the association became less significant after combining with the replication).

Panels B-E (next page) | Regional association plots of the four significant loci: 3p11.1 (B), 5p15.2 (C), 5q23.1 (D), and 18q12.3 (E).

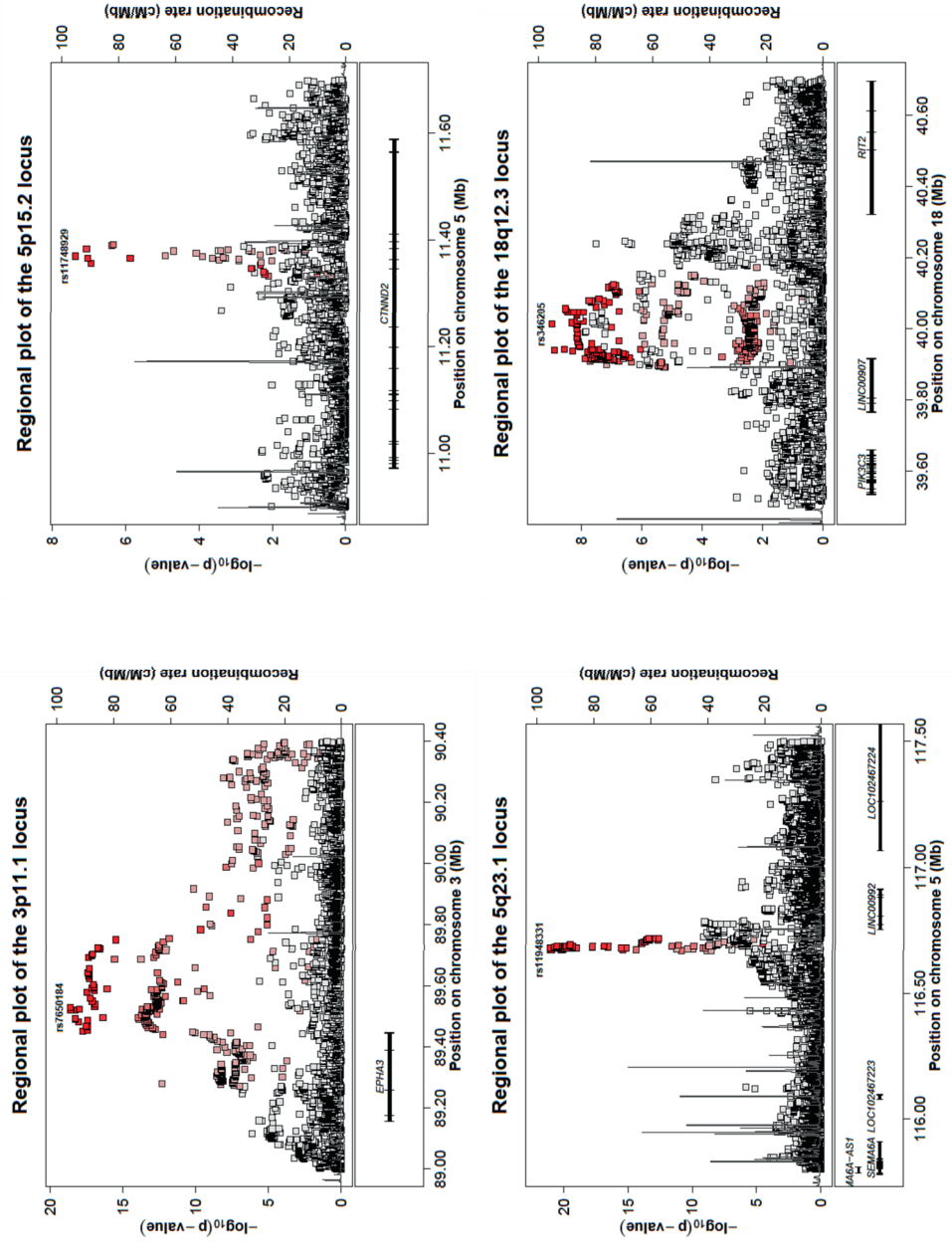
Regional plot of the 5p15.2 locus
rs11748929
CTNND2
−log10(p−value)
Recombination rate (cM/Mb)
Position on chromosome 5 (Mb)
Regional plot of the 18q12.3 locus
rs346205
PIK3C3
LINC00907
RIT2
−log10(p−value)
Recombination rate (cM/Mb)
Position on chromosome 18 (Mb)
Regional plot of the 3p11.1 locus
rs7650184
EPHA3
−log10(p−value)
Recombination rate (cM/Mb)
Position on chromosome 3 (Mb)
Regional plot of the 5q23.1 locus
rs11948331
MAP4K4-AS1
SEMA6A
LOC102467223
LINC00992
LOC102467224
−log10(p−value)
Recombination rate (cM/Mb)
Position on chromosome 5 (Mb)

3p11.1 and EPHA3

The 3p11.1 signal surrounds the *EPHA3* gene and its downstream region (Figure 1B), with no other genes in close proximity of the lead variant. *EPHA3* belongs to the Eph family of receptor tyrosine kinases, which is one of the five canonical families of axon guidance proteins. The mouse homolog EphA3 mediates segregation and pathfinding of callosal axons.[20] In humans, it is expressed in grey matter structures of the brain that are connected by the anterior commissure, including the piriform cortex (Figures 2A-B). The lead variant rs7650184 lies in the 3'-UTR and influences expression of *EPHA3* in brain tissue obtained from the temporal cortex ($p = 3.3 \times 10^{-7}$). Also, the missense variant rs35124509 is in high linkage disequilibrium ($r^2 = 0.93$; $D' = 0.99$). Exome analyses of the *EPHA3* region supported the association of another variant in the 3'-UTR (rs73139148; $p = 3.3 \times 10^{-7}$), but did not reveal any additional functional variants (Supplementary Table S3).

5p15.2 and CTNND2

For 5p15.2, the signal is located in a narrow region inside the *CTNND2* gene (Figure 1C). The lead variant rs11748929 and those in LD are all intronic and have enhancer histone marks (H3K4me1, H3K27ac, and H3K9ac) almost exclusively in brain tissues (Supplementary Table S2). The *CTNND2* gene is also expressed in the brain (Figure 2A-B), but largely undetected in other parts of the body.[21] *CTNND2* encodes a neuron-specific member armadillo protein, also known as δ-Catenin or NPRAP, that is a member of the β-catenin superfamily. It was initially discovered as an interaction partner of Presenilin-1,[21,22] mutations of which cause familial Alzheimer's Disease. Subsequently, *CTNND2* has been related to various cognitive disorders, including Cri-du-Chat syndrome,[23] reading problems and mild intellectual disability,[24] and a variety of psychiatric disorders.[25] Zebrafish knockdowns show migration defects of neuron subpopulations,[24] and mice mutants reveal that *CTNND2* is critical for cognitive function *in vivo*.[26] Exome sequencing of *CTNND2* identified a rare, but synonymous exonic variant (chr5:10973781; minor allele frequency (MAF) = 0.4%; $p = 9.2 \times 10^{-4}$).

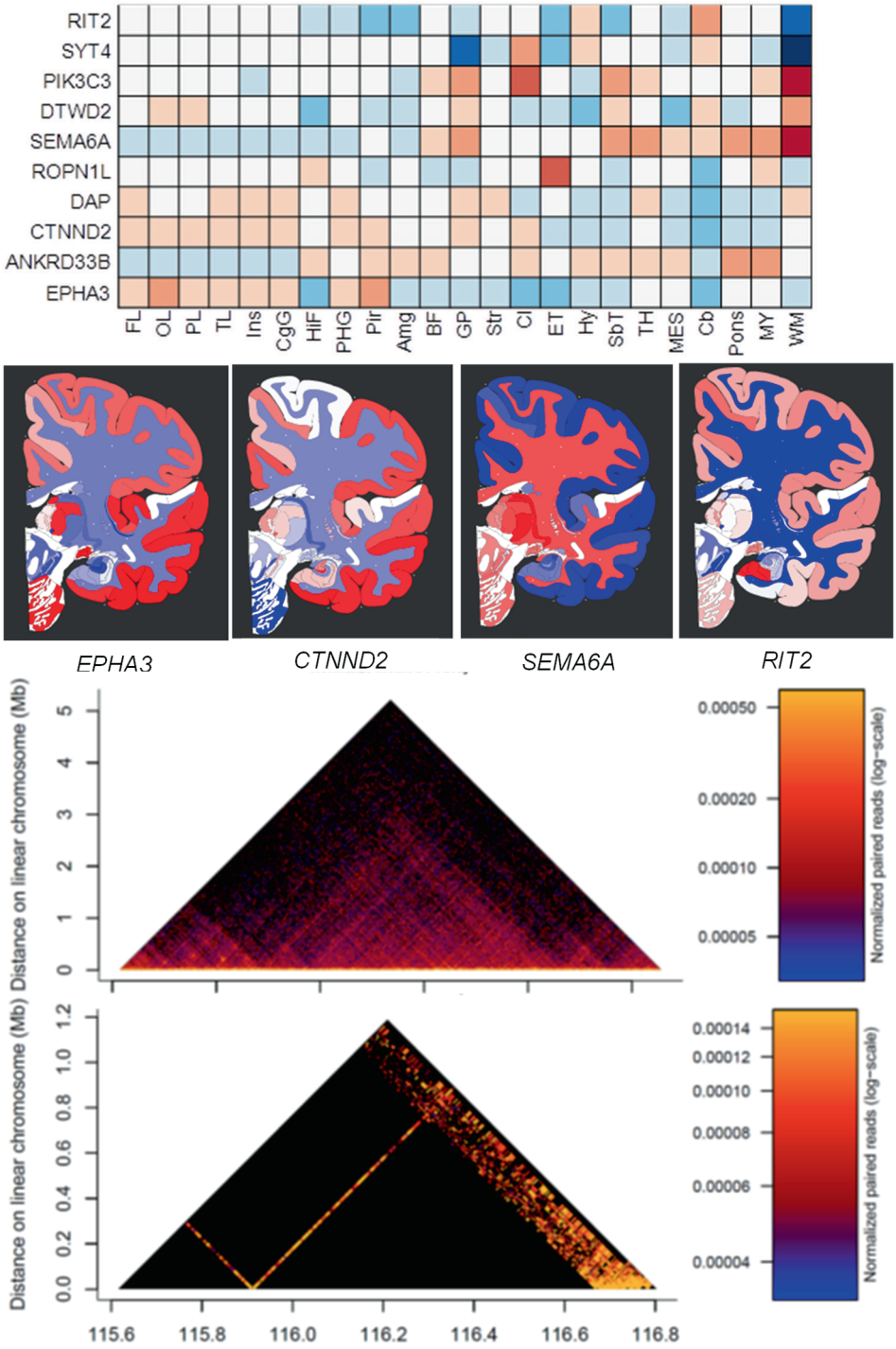

Figure 2 | Functional characterization of the genome-wide significant loci.

5q23.1 and SEMA6A

Also on chromosome 5, we find the strongest signal of our genome-wide association study at 5q23.1 (Figure 1D). The lead variant rs11948331 lies close to *LINC00992*, a long non-coding RNA on which little is known. Additionally, there was an apparent second signal on 5q23.1 from a less common variant (rs148925592; minor allele frequency = 4%; $r^2 = 0.002$; D' = 0.21). Therefore, we performed conditional analyses in a subset of studies, and found this to be an independent signal (Supplementary Table S4). This variant has an almost two-fold larger effect and lies within another long non-coding RNA, *LOC102467224*, which remains uncharacterized.

The nearest coding gene to the primary signal is *SEMA6A*, which is 762 kb further in the proximal direction. *SEMA6A* is highly expressed in the human brain, particularly in the white matter (Figure 2A-B). Interestingly, murine Sema6a is crucial for neurons to cross the midline, and misrouted axons of the anterior commissure are still present in adult mice mutants.[27] However, we found no evidence for QTLs nor any enhancer marks that might implicate the identified variants in regulating the expression of *SEMA6A* or other genes. One rare exonic nonsynonymous variant with a predicted damaging effect was nominally significant (rs200578077, MAF = 1.0%, p=0.046), but it was not in LD with rs11948331 and thus unlikely to explain its effect. However, given the expression pattern of *SEMA6A* and the phenotype of Sema6a mutants, but lack of a direct link with our association signal, we hypothesized there might exist long-distance interaction between the region harboring the associated variants and the *SEMA6A* promotor. We first searched a curated database of genome-wide chromosome interaction and found that two long-distance interactions were described using Hi-C for both regions, but these did not include interaction with the promotor (Table S5).[28] Since none of the available cell lines for Hi-C were derived from the brain, we performed Targeted Chromatin Capture (T2C)[29] in human neural progenitor cells to selectively interrogate the 5q23.1 region at a high resolution. We identified three topological associated domains (TADs) in a 5 Mb region surrounding the variants of interest (Figure 2D). The larger TAD contains both the *SEMA6A* promotor and the associated variants, indeed showing that, three-dimensionally, these genomic regions are in close proximity (Figure 2E).

18q12.3 and RIT2

The final locus spans an intergenic region on chromosome 18 that is flanked by two recombination hotspots (Figure 1E). Conditional analyses revealed that, independent of the lead variant rs346205, there was another association at 18q12.3 with rs144695388 (Supplementary Table S4). The lead variant lies inside the long non-coding RNA *LINC00907* and between the coding genes *PIK3C3* and *RIT2*. Brain expression data shows *PIK3C3* is highly expressed in the white matter (Figure 2A-B), whereas *RIT2* as well as the more distal gene *SYT4* have a particularly low expression (Figure 2A). Putative functional variants in LD have enhancer marks in the brain and some acting as expression QTLs (Supplementary Table S2), including rs346212 that influences *RIT2* expression in the anterior cingulate cortex ($p = 8.6 \times 10^{-7}$). *RIT2* belongs to the Ras superfamily of small guanosine triphosphate binding proteins and expressed in neurons, particularly in the substantia nigra.[30] A large GWAS of Parkinson's disease (PD) discovered rs12456492,[31] which is 660 kb distal of our lead variant, but it was not associated with the anterior commissure ($p = 0.30$). Through exome analyses of all nearby genes a rare missense mutation was found in *RIT2* (rs142911081; MAF = 1.5%; $p = 1.0 \times 10^{-3}$) that was evolutionarily constrained and had an active transcription start site chromatin state in all samples taken from the brain, but in none of the other tissues (Table S5).

Neural substrate

Next, we set out to gain insight into the neural effects of the identified loci. The anterior commissure contains multiple fiber tracts that connect various cortical and subcortical grey matter regions. Therefore, we aimed to determine which grey matter regions are connected by the anterior commissure using voxel-based morphometry in the discovery sample (N = 9,934; includes individuals without genotyping). A larger anterior commissure cross-sectional area was associated with more tissue in the many subcortical and cortical regions, particularly the thalamus, insula, and the posterior temporal lobe (Figure 3A; Supplementary Table S6).Next, we explored the effect of the four loci on grey matter within these regions that are presumably connected by the anterior commissure (N = 7,579; Figure 3B; Supplementary Table S6). Regions that were significantly associated with both the anterior commissure and the individual loci ($p <$

3.0×10^{-7}) included the anterior temporal lobe (3p11.1, 5p15.2, 18q12.3), insula (5q23.1), superior frontal gyrus (5p15.2, 5q23.1, 18q12.3), putamen (5p15.2, 5q23.1), and caudate (3p11.1, 5p15.2).

Epistasis

Since all loci affect the same brain structure, i.e. the anterior commissure, we investigated whether there were more interrelations. The first approach was by determining the presence of epistasis, i.e. interaction between risk variants from different loci beyond the expected additive effect. Using partial derivatives meta-analysis (see Online Methods), we performed a pooled analysis of the various gene-by-gene interactions but did not identify any significant effects for the various combinations (Supplementary Figure 4A). Then, we used the brain expression data from all genes in a 2 Mb window from the lead variants to identify genes with a similar expression, especially between different loci (Supplementary Figure 4B). The strongest interlocus correlations were for *EPHA3* (3p11.1) with *CTNND2* (5p15.2) and *SEMA6A* (5q23.1) with *PIK3C3* (18q12.3).

Enrichment analyses

Besides studying the top loci, we also investigated genome-wide trends using the GWAS meta-analyses. We detected inflation that was not the result of population stratification but rather due to a true enrichment from polygenicity (Supplementary Figure 5A), similar to other complex traits. Of the total variance in the anterior commissure cross-sectional area, 30% could be explained by common variants. Next, we investigated whether certain groups of variants were contributing disproportionately to this observed signal. We found significant enrichment for a variety of functional groups, most notably variants in enhancers (marked by H3K4me1 peaks), introns, and conserved regions (Supplementary Figure 5B). Furthermore, there were cell-type-specific enrichments for the central nervous system ($p = 0.014$) and cardiovascular system (0.0048) (Supplementary Figure 5C). However, the proportion of heritability explained was divided fairly homogenously across chromosomes (Supplementary Figure 5D).

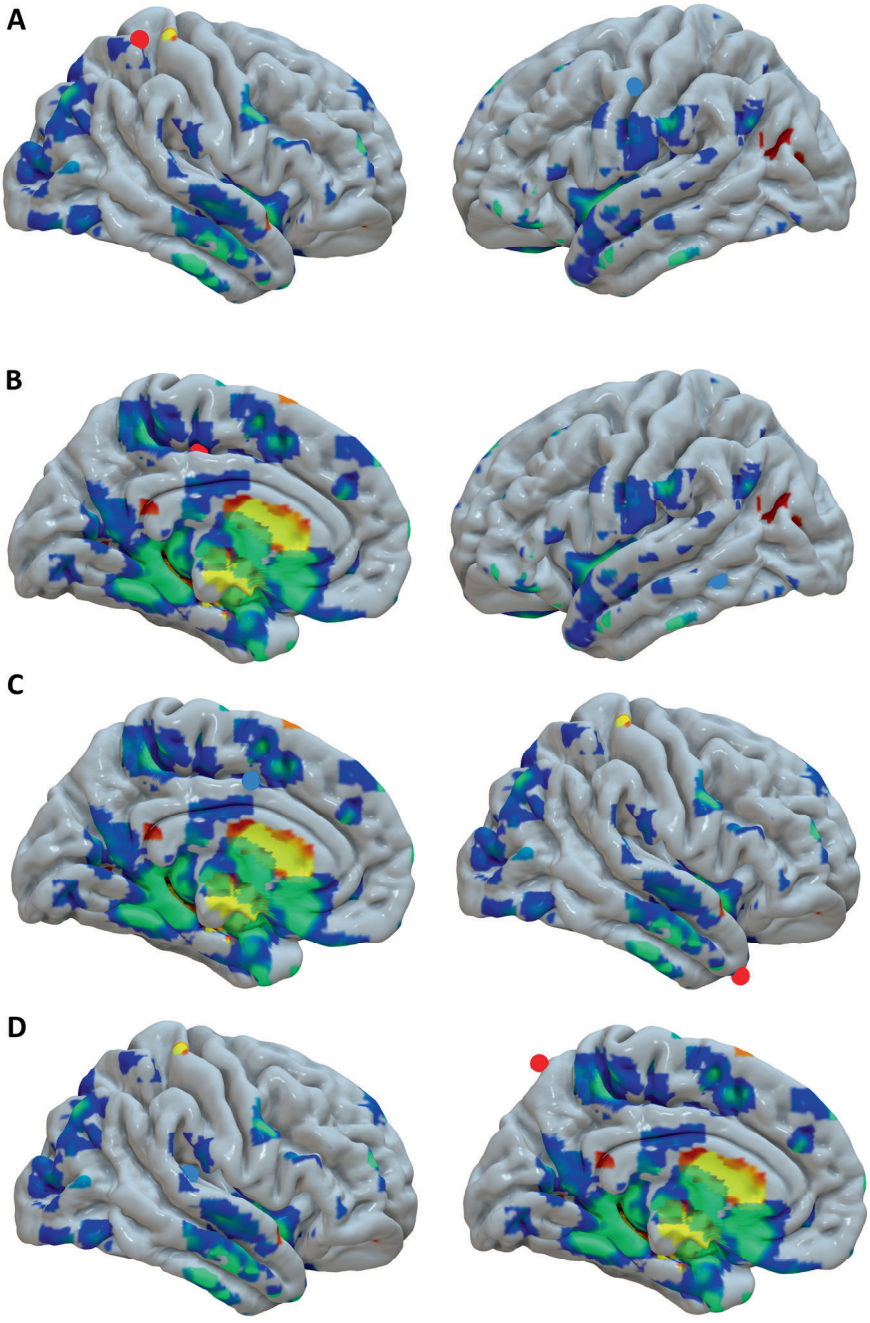

Figure 3 | Grey matter regions affected by the anterior commissure and genetic loci.
Projection of voxel-based morphometry results on cortical surface. Significant association with anterior comissure surface shown in green-blue scale for negative association, red-yellow for positive; For four discovered loci the centers of the most significant clusters were extracted and plotted as spheres. A - rs346205; B- rs11948331; C - s1174892; D - rs7650184.

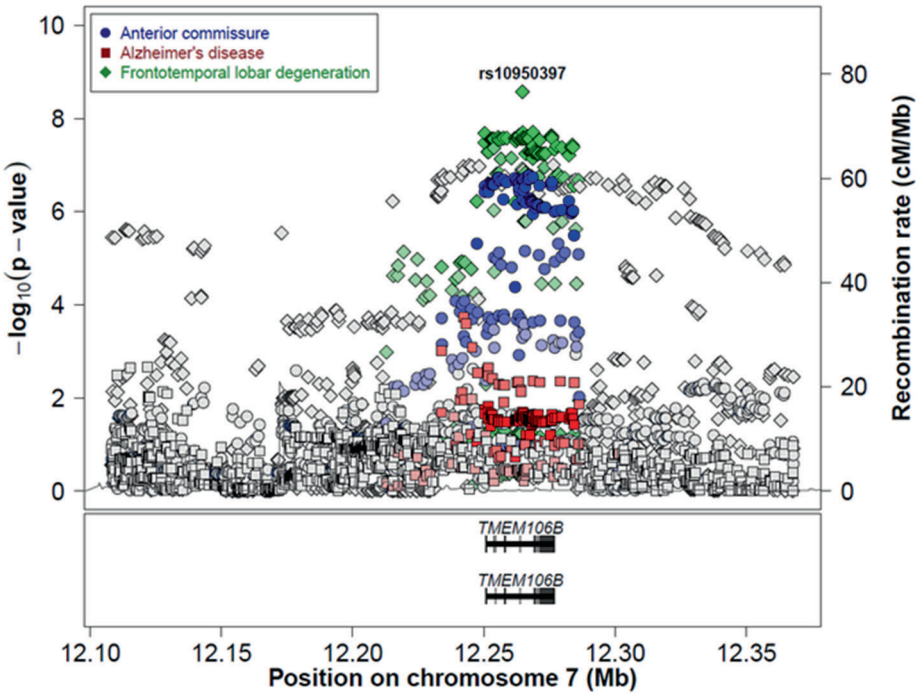

Figure 4 | Genetic pleiotropy between the anterior commissure and neurodegenerative diseases at *TMEM106B*.

Regional plot showing the association signals of variants in the TMEM106B locus, with the anterior commissure cross-sectional area (blue), frontotemporal lobar degeneration (green), and Alzheimer's disease (red).
Gene tracks Refflat from http://hgdownload.cse.ucsc.edu/goldenPath/hg19/database/

Pleiotropy with neurodegenerative diseases

Given the relevance of commissural tracts and their connected brain regions for neurodegeneration, we determined whether genetic loci for AC show pleiotropy with neurodegenerative diseases. We used published genome-wide association studies of AD (n_{cases} / $N_{controls}$ =17,008 / 37,154),[32] PD (13,708 / 95,282),[31] and frontotemporal lobar degeneration (FTLD; 567 / 3,380)[33]. Here we focus on the 7p21.3 locus, which was genome-wide significant at the discovery stage (Table 1) and previously reported to be associated with FTLD.[33] Interestingly, it was significant not only for the combination with FTLD, but also for AD. A regional association plot shows that the signal of all three traits overlaps and spans the *TMEM106B* gene (Figure 4). Since the 7p21.3 association with the AC was attenuated after addition of the replication samples and there was significant

heterogeneity across the cohorts (Table 1), we set out to identify factors underlying these apparent inconsistencies. We previously showed that the effect of 7p21.3 increases with age (in a subset of the discovery sample; N = 4,413),[34] and the mean age within the cohorts was indeed related to the magnitude of the effect in a meta-regression analysis (Supplementary Figure 6A). Additionally, restricting to the discovery cohorts with a mean age > 65 years considerably increased the signal even though the sample size was much smaller (N = 3,015; $p = 3.8 \times 10^{-11}$). Furthermore, we formally tested the presence of a gene-by-age interaction for the 7p21.3 locus by modelling an interaction term between age and the lead variant, rs3807865. Initially, we performed these analyses within each cohort separately and subsequently meta-analyzed the results. This did not show a significant interaction (p = 0.87), which we hypothesized was due to the limited age range within each cohort as this would obscure a potential interaction in a conventional meta-analysis (compared to a pooled analysis). Since exchanging individual participant data was not possible due to restrictions in data sharing, we performed a partial derivatives meta-analysis, which provides identical results as a pooled analysis while only using summary statistics. Indeed, this showed a significant interaction between rs3807865 and age (N = 7,459; $p = 7.0 \times 10^{-3}$).

DISCUSSION

We elucidated the genetic architecture of the human anterior commissure in this comprehensive study, which extended from large-scale population imaging and genetics to *in silico* and *in vitro* experiments. We identified robust associations of six variants at four distinct loci for which we assign the most likely causative genes, and show the remaining genetic component can be explained by many additional common variants with small effects. Across the whole genome, there is enrichment for variants in regulatory regions, and those in genomic sequences with functional marks specific to the central nervous system and cardiovascular cell lines. Finally, we found that loci affecting the anterior commissure in the general population have clear links to neurodegenerative diseases, highlighting the genetic pleiotropy.

Brain circuitry develops through complex processes that include cell fate specification and migration, axon guidance, and synaptogenesis.[35] These processes are tightly

regulated by genetics, especially for the brain's commissural tracts. We therefore studied the size of the anterior commissure in order to uncover how of the variance is due to genetics and which specific factors are important. Similar to other brain structures,[36] we find that the anterior commissure has a polygenic architecture, with most of the variance remaining unexplained by the four identified loci. Larger GWAS will likely shed light on the additional loci that involved, as has been successfully achieved for other complex traits.

The combined meta-analysis of the discovery and replication cohorts yielded four genome-wide significant loci. Although GWAS only points to genomic regions associated with a trait, we subsequently performed *in silico* and *in vitro* analyses aimed at determining the causal genes. First, we prioritized genes that are particularly expressed in the white matter of the brain and in cortical and subcortical grey matter regions that are connected by the anterior commissure. Although this pointed to certain genes in some instances (*EPHA3* and *SEMA6A*), the results were ambiguous for 18q12.3, where multiple genes have plausible expression pattern. As a second step, however, we investigated whether our specific variants (or those in high LD) themselves affect gene expression. We found that variants at two loci show direct evidence of influencing expression of *EPHA3* (3p11.1) and *RIT2* (18q12.3) in brain tissue samples. No eQTL effects were observed for 5p15.2 or 5q23.1, but indirect evidence indicates these might be regulatory regions as well. The 5p15.2 locus contains enhancer marks in neural cell lines, whereas the T2C experiment in neural stem cells showed that 5q23.1 and the *SEMA6A* promotor are in close proximity. The third approach to identify causal genes was by studying the exomes of the nearby genes, allowing the study of variants not captured by genotyping chips nor well imputed using 1000 Genomes reference panel. This could reveal (functional) coding variants that drive the primary GWAS signal or, alternatively, independent risk variants that would further implicate putative causal genes. For 3p11.1, exome analyses supported the variant discovered through GWAS, suggesting that this locus indeed exerts its affect by influencing expression of *EPHA3*. Screening of the other loci revealed other, rare variants with nominally significant effects on the anterior commissure. Most notably was the missense mutation in *RIT2* that also showed pronounced functional marks exclusively in brain tissue.

While gene expression and eQTL analyses provided valuable functional information on the identified loci, an important limitation is that white matter tissue is underrepresented in most expression and chromatin state databases. The candidate gene of our top locus, *SEMA6A*, is expressed in the white matter but we found no evidence of eQTL effects in any of the brain tissue samples, which were mostly obtained from grey matter structures. However, other evidence indicated that this region might interact with distant genomic regions, and we hypothesized this could be with the *SEMA6A* promotor. Using T2C, a high-resolution method to investigate these interaction, we indeed found that the region harboring the risk variants is in close proximity with the *SEMA6A* promotor. These experiments were done in human neural stem cells, which can be cultured to a sufficient scale. Besides the spatial gene expression in the brain, it is also important to consider differential temporal expression, which is particularly crucial for axon guidance. Further explorations of this *SEMA6A* and the effect of the common variants in this locus should take these factors into account.

The identified loci highlight the concordance between animal models and findings in humans. In mice and fruit flies, experimental studies have revealed gene families that are crucial for the development of commissural tracts. Interestingly, two of our four loci are likely to regulate genes from these families, namely the Semaphorin *SEMA6A* and the Ephrin *EPHA3*. However, while there are similarities with model systems, each of the families contains many members and it is unclear which are relevant for humans. Here we specifically identify genes for the human anterior commissure. It is not remarkable that human genes have remained elusive, since it is currently not feasible to study this complex organization of brain circuitry *in vitro*. Genetic studies thus rely on *in* vivo imaging, an approach requiring large sample sizes that has only become attainable in the past years with the formation of imaging genetics consortia such as CHARGE and ENIGMA.

We did not restrict our analyses to the top variants of the GWAS, but also examined genome-wide trends. The most apparent enrichment was for genomic regions with H3K4me1 peaks (marking enhancer sites), introns, and conserved sequences, with a large proportion of heritability being explained by variants in these regions. This

indicates that, genetically, the size of the anterior commissure is predominantly determined by regulatory regions throughout the genome. Also, we find an enrichment for cell-type specific annotations, specifically from the central nervous system, but interestingly also from the cardiovascular system. The development of nerves and blood vessels is thought to have shared genes, and our results support a similar link in humans.

Our measure of interest was the cross-sectional area of the anterior commissure, which we used as a proxy for the amount of fibers crossing through the anterior commissure. Theoretically, a larger area could be due to an increase in the total number of fibers or, alternatively, due to more space between the fibers. However, the density of callosal fibers has been shown not to correlate with the callosal area, thus making the area a good proxy for the total amount of fibers.[37] Another consideration is that a smaller area might not necessarily translate into less interhemispheric connections, but could also correspond to a different anatomical organization, e.g. fibers instead passing through the corpus callosum. Furthermore, although for example *SEMA6A* is expressed in the white matter, some of the proposed causative genes are expressed in the grey matter (*EPHA3* and *CTNND2*), in regions connected by the anterior commissure, as we have shown in our voxel-based morphometry analyses. It is therefore possible that not all identified loci are directly affecting the anterior commissure, but some might influence it secondarily by their effect on related cortical and/or subcortical grey matter regions.

Regardless of the underlying mechanism through which genes affect the anterior commissure, there seems to be pleiotropy with various neurodegenerative diseases. Genetic variants for AD, PD, and FTLD have been shown to jointly affect cognitive status,[38] and some have been reported to be shared risk factors for disease. We now find an additional link through the anterior commissure. While commissures are formed during development by axon guidance molecules, these molecules remain important for adults with roles in neuronal repair and regeneration. Furthermore, commissural genes seem relevant for adult neurological disorders, as evidenced by the presence of misrouted fibers in AD and PD[39] Here, we found the *TMEM106B* affecting the anterior commissure, a locus previously identified for FTLD, a disease affecting the anterior commissure as well as frontal and temporal brain regions interconnected by it. Both of

these loci have been found to also associate with other diseases. Systematic studies of pleiotropy between the anterior commissure and FTLD might reveal additional loci. Focusing on older population might be a fruitful approach for neurodegenerative diseases given the gene-by-age interaction of the *TMEM106B* locus. The pronounced effect at older age indicates that variation in the anterior commissure size is more due to neurodegeneration rather than developmental differences, allowing us to pick up effects of risk loci for FTLD, AD, and PD. Since the (dys)function of the anterior commissure remains understudied in humans, its relevance could very well extend to other neurological or psychiatric disorders, for which different study populations are more informative.

We demonstrated that the combination of imaging and genetics can be powerful to yield insight into the biological underpinnings of complex human traits that are not easily studied or manipulated experimentally. Our results will hopefully lead to additional follow-up laboratory work aimed at characterizing the identified candidate genes. As a potential clinical application, though the size of the anterior commissure itself is not (yet) a diagnostic or predictive tool for a disease, it might serve as a marker of the underlying disease process, e.g. as an endophenotype. A quantitative measure could be statistically more powerful to detect genetic risk loci compared to a dichotomous diagnosis of disease. Indeed, we were able to identify the *TMEM106B* locus, which was originally discovered in a GWAS of FTLD (567 cases and 3,380 controls; $p = 2.7 \times 10^{-9}$), at a higher level of significance and a lower total sample size when restricting to older cohorts only ($N = 3{,}015$; $p = 3.8 \times 10^{-11}$). Particularly for rare diseases such as FTLD, where samples are obtained with difficulty, this approach could be helpful. Furthermore, the identification of risk genes for multiple disorders makes them attractive targets for pharmacological intervention.

In conclusion, we show that the anterior commissure has a considerable polygenic basis and we identified loci that begin to unravel this complex genetic architecture. The successful approach of imaging genetics to understanding developmental biology and disease pathophysiology paves the way for applications to other brain structures.

REFERENCES

1 Paul, L. K. *et al.*. *Nature Reviews Neuroscience* **8**, 287-299 (2007).

2 Fabri, M. *et al.* . *Cognitive Brain Research* **24**, 73-80 (2005).

3 Berlucchi, G.. *Progress in brain research* **144**, 77-93 (2004).

4 Zaidel, D. & Sperry, R. W. Some long-term motor effects of cerebral commissurotomy in man. *Neuropsychologia* **15**, 193-204 (1977).

5 Häberling, I. S., Badzakova-Trajkov, G. & Corballis, M. C. Callosal tracts and patterns of hemispheric dominance: a combined fMRI and DTI study. *Neuroimage* **54**, 779-786 (2011).

6 Schulte, T. & Müller-Oehring, E. M. *Neuropsychology review* **20**, 174-190 (2010).

7 Schutter, D. J. L. G. & Harmon-Jones, E. *Neuroscience & Biobehavioral Reviews* **37**, 2481-2488 (2013).

8 Posthuma, D. *et al. Nature neuroscience* **5**, 83-84 (2002).

9 Kochunov, P. *et al. Neuroimage* **53**, 1109-1116 (2010).

10 Jahanshad, N. *et al.* . *Neuroimage* **81**, 455-469 (2013).

11 Okada, A. *et al.* Boc is a receptor for sonic hedgehog in the guidance of commissural axons. *Nature* **444**, 369-373 (2006).

12 Brankatschk, M. & Dickson, B. J. Netrins guide Drosophila commissural axons at short range. *Nature neuroscience* **9**, 188-194 (2006).

13 Eichmann, A., Makinen, T. & Alitalo, K. Neural guidance molecules regulate vascular remodeling and vessel navigation. *Genes & development* **19**, 1013-1021 (2005).

14 Dickson, B. J. & Gilestro, G. . *Annu. Rev. Cell Dev. Biol.* **22**, 651-675 (2006).

15 Dickson, B. J. & Senti, K.-A. Axon guidance: growth cones make an unexpected turn. *Current biology* **12**, R218-R220 (2002).

16 Izzi, L. & Charron, F. Midline axon guidance and human genetic disorders. *Clinical genetics* **80**, 226-234 (2011).

17 Curinga, G. & Smith, G. M. Molecular/genetic manipulation of extrinsic axon guidance factors for CNS repair and regeneration. *Experimental neurology* **209**, 333-342 (2008).

18 Van Battum, E. Y., Brignani, S. & Pasterkamp, R. J. Axon guidance proteins in neurological disorders. *The Lancet Neurology* **14**, 532-546 (2015).

19 Berlucchi, G.. *Cortex* **56**, 1-13 (2014).

20 Nishikimi, M., Oishi, K., Tabata, H., Torii, K. & Nakajima, K. *The Journal of Neuroscience* **31**, 16251-16260 (2011).

21 Zhou, J. *et al.* Presenilin 1 interaction in the brain with a novel member of the Armadillo family. *Neuroreport* **8**, 2085-2090 (1997).

22 Levesque, G. *et al.. Journal of neurochemistry* **72**, 999-1008 (1999).
23 Medina, M., Marinescu, R. C., Overhauser, J. & Kosik, K. S. *Genomics* **63**, 157-164 (2000).
24 Hofmeister, W. *et al. Journal of medical genetics* **52**, 111-122 (2015).
25 Nivard, M. G. *et al.. Genes, Brain and Behavior* **13**, 195-201 (2014).
26 Israely, I. *et al. Current biology* **14**, 1657-1663 (2004).
27 Rünker, A. E. *et al. International Journal of Developmental Neuroscience* **28**, 690 (2010).
28 Li, M. J., Wang, L. Y., Xia, Z., Sham, P. C. & Wang, J. *Nucleic acids research*, gkt456 (2013).
29 Kolovos, P. *et al.. Epigenetics Chromatin* **16**, 10 (2014).
30 Zhou, Q., Li, J., Wang, H., Yin, Y. & Zhou, J. I. *Neurobiology of aging* **32**, 313-326 (2011).
31 Nalls, M. A. *et al.. Nature genetics* (2014).
32 Lambert, J.-C. *et al.. Nature genetics* **45**, 1452-1458 (2013).
33 Van Deerlin, V. M. *et al.. Nature genetics* **42**, 234-239 (2010).
34 Adams, H. H. H. *et al.. Biological psychiatry* **76**, 503-508 (2014).
35 Jessell, T. M. & Sanes, J. R. Development: The decade of the developing brain. *Current opinion in neurobiology* **10**, 599-611 (2000).
36 Hibar, D. P. *et al.. Nature* (2015).
37 Aboitiz, F., Scheibel, A. B., Fisher, R. S. & Zaidel, E. *Brain research* **598**, 143-153 (1992).
38 Adams, H. H. *et al.. Alzheimers Dement*, doi:10.1016/j.jalz.2014.12.008 (2015).
39 Hoogland, P. V., Van Den Berg, R. & Huisman, E.. *Neuropathology and applied neurobiology* **29**, 303-311 (2003).
40 Winter, T. J. & Franz, E. A.. *Frontiers in psychology* **5** (2014).
41 Adams, H. H. H. *et al.. Biological psychiatry* (2014).

Chapter 3.3.2

Heritability and genome-wide association study of human gait

ABSTRACT

Human gait is a complex neurological and musculoskeletal function, of which the genetic basis remains largely unknown. To determine the influence of common genetic variants on gait parameters, we studied 2946 participants of the Rotterdam Study, a population-based cohort of unrelated elderly individuals. We assessed 30 gait parameters using an electronic walkway, which yielded 7 independent gait domains after principal component analysis. Genotypes of participants were imputed to the 1000 Genomes reference panel for generating genetic relationship matrices to estimate heritability of gait parameters, and for subsequent genome-wide association scans to identify specific variants. Gait domains with the highest age- and sex-adjusted heritability were Variability (h^2 = 61%), Rhythm (37%), and Tandem (32%). For other gait domains, heritability estimates attenuated after adjustment for height and weight. Genome-wide association scans identified a variant on 1p22.3 that was significantly associated with single support time, a variable from the Rhythm domain (rs72953990; N = 2946; β (SE) = .0069 (.0012), p = 2.30×10^{-8}). This variant did not replicate in an independent sample (N = 362; p = 0.78). In conclusion, human gait has highly heritable components that are explained by common genetic variation, which are partly attributed to height and weight. Collaborative efforts are needed to identify robust single variant associations for the heritable parameters.

INTRODUCTION

The planning and execution of gait requires a delicate integration of sensory information and motor commands [1]. Consequently, gait in humans is affected by a wide range of diseases, including disorders of the brain, muscles, and joints [1-5]. Problems in gait strongly increase the risk of adverse health outcomes, including morbidities (e.g. falls) and death [3]. Although it is known that various environmental factors contribute to variation in gait, it remains unclear to what extent genetics plays a role.

Variation in gait is associated with age and sex, but also with several complex traits such as height, weight and cognitive function, which are all highly polygenic and heritable [6-8]. Walking speed was found to be heritable in two twin studies, suggesting that gait follows a similar genetic pattern [9-11]. However, walking speed alone does not capture the complexity of human gait, which consist of many more measurable components [12]. Additionally, to our knowledge, no genome-wide association scan (GWAS) has been performed to identify genetic variants that are associated with gait.

Here, we comprehensively assessed gait using an electronic walkway and determined the heritabilty of the various parameters comprising gait, followed by genome-wide association scans for the heritable parameters.

MATERIAL AND METHODS

Setting

The Rotterdam Study is a prospective, population-based study that investigates 14 926 inhabitants of Rotterdam aged 45 years or over [13]. Subjects were enrolled during three recruitment phases (1990, 2000, and 2006) and visit the research center every 3-4 years for various medical examinations. Genotyping was successfully performed on 11 496 subjects. In March 2009, gait assessment was introduced in the study protocol. The Rotterdam Study has been approved by the medical ethics committee according to the Population Study Act Rotterdam Study, executed by the Ministry of Health, Welfare and Sports of the Netherlands. A written informed consent was obtained from all participants.

Gait assessment

A 5.79-m long pressure-activated walkway (GAITRite Platinum; CIR systems, Sparta, NJ: 4.88-m active area; 120-Hz sampling rate) was used to accurately measure gait parameters, as described previously [14,15]. Participants performed standardized walking protocols over the walkway. First, participants walked eight times across the walkway at their own pace (normal walk). Second, participants walked at their usual pace, turned halfway, and returned to the starting position (turning). Third, participants walked tandem (i.e., heel-to-toe) over a line on the walkway (tandem walk). The first normal walk was considered a practice walk and not included in the analysis. All other recordings were visually inspected and individual footsteps were identified and marked for further processing by the walkway software, from which 30 spatiotemporal (gait) parameters were derived. Principal component analysis identified 7 independent components with eigenvalues of 1 or higher, representing the following gait domains: Rhythm, Phases, Variability, Pace, Tandem, Turning and Base of Support [14,15]. Varimax rotation was used to provide domains that are uncorrelated to each other.

Study population

Between March 2009 and March 2012, 3651 people were invited for gait assessment. Of these, 129 did not complete gait assessment for the following reasons: 69 for physical problems, 45 for technical reasons, 13 for refusal, and 2 for other reasons. Additionally, we excluded 34 participants for performing less than 16 steps in normal walking, lowering validity of the gait parameters; 3 for using walking aids on the walkway; and 1 for not following instructions. Of 3484 remaining participants, 2946 were genotyped. Since not all participants completed all walking conditions, the numbers of participants included vary for the individual variables (where we included the maximal sample size to increase power), but are identical for all the domains since these are derived from principal component analysis, which does not allow for any missing values in the 30 variables.

Genotyping

The three subcohorts of the Rotterdam Study were genotyped with the 550K (cohort 1),

550K duo (cohort 2) and 610K (cohort 3) Illumina arrays. We removed samples with a call rate below 97.5%, gender mismatch, excess autosomal heterozygosity, duplicates or family relations and ethnic outliers, and variants with call rates below 95.0%, failing missingness tests, Hardy–Weinberg equilibrium p-values<10^{-6}, and minor allele frequencies<1%. Genotypes were imputed using MACH/minimac software to the 1000 Genomes phase I version 3 reference panel (all populations).

Heritability analysis

To estimate heritability in our sample of unrelated individuals, we used Genome-wide Complex Trait Analysis (GCTA) [16]. This method compares genotypic similarity between individuals to their phenotypic similarity. The 1000 Genomes imputed genotypes were filtered on imputation quality (R^2 < 0.5) and allele frequency (MAF < 0.01). Pairwise genetic relatedness between all individuals was calculated, and for pairs with more than 0.02 genotype similarity one person was removed.

Heritability analyses were performed for the 7 gait domains and (secondarily) for all 30 variables separately. Adjustments were made for age, sex, and the first 10 principal components of population stratification (model 1), and additionally for height (model 2) and weight (model 3). For the Tandem domain, step count and step length during the tandem walk were also included as covariates.

Polygenic scores

Polygenic scores were created from variants associated with height (N=180) and BMI (N=32) at genome-wide significance [6,17]. Variants were weighted by multiplying the beta coefficient for the corresponding trait with the number of alleles. For each individual, the weighted allele scores were added together to generate the polygenic score.

Genome-wide association scan

Genome-wide association analyses were conducted in the three subcohorts separately using the R package ProbABEL (version 0.42). Gait parameters were analyzed under an additive model with linear regression, covarying for age and sex, height, weight, and first two principal components. The results were adjusted for genomic control and meta-

analyzed using the METAL software [18]. Variants with an $R^2 < 0.5$ and a minor allele frequency (MAF) < 0.01 were removed. Subsequently, a more stringent filter for MAF < 0.05 was added to remove remaining false-positive signals, resulting in 6.2 million variants included in the analyses. Genome-wide significance was established at $p < 5x10^{-8}$. Manhattan and quantile-quantile plots were generated in R (version 3.1.0).

Functional annotation of genetic variants

Genetic variants showing evidence of association with gait parameters were further examined for potential biological function using publicly available databases: Regulomedb, GWASdb, rSNPBase, HaploReg, and SNVrap.

Replication

For genome-wide significant variants replication was attempted in the Tasmanian Study of Cognition and Gait (TASCOG), which investigates cerebrovascular mechanisms underlying gait, balance and cognition. TASCOG comprises a population-based sample of 395 people aged 60–86 years living in Southern Tasmania, Australia [19]. They were randomly selected from the electoral roll between 2006 and 2008, but excluded if they lived in a nursing home, had a contraindication for magnetic resonance scanning or were unable to walk without a gait aid. Participants were genotyped using Illumina Hap370CNV chips and completed 6 walks at their preferred walking speed over a 4.6 meter computerized GaitRite walkway. Participants started 2 meters before and finished 2 meters after the walkway.

Statistical analysis

Cohort-specific results were meta-analyzed using inverse variance meta-analysis. Polygenic scores were transformed into z-scores so that effects are expressed per standard deviation increase for each score. A Bonferroni correction for 14 tests (2 polygenic scores and 7 gait domains) was applied, resulting in a significance threshold of $p < 0.0036$. For the candidate gene analyses, a Bonferroni correction for 1484 tests (212 variants and 7 gait domains) was applied where $p < 3.37 \times 10^{-5}$ was considered significant. Association analyses of the polygenic scores with gait domains were performed in SPSS version 22, IBM.

RESULTS

Study population

Mean (SD) age in the Rotterdam Study was 68.2 (9.5) years, ranging from 50 to 97 years, and 1604 (54.4%) were women. Table 1 shows basic demographic and anthropometric characteristics of the total study population as well as the population with all gait measurements available, which were similar.

Heritability of gait parameters

The Variability, Rhythm and Tandem domains showed the highest age- and sex-adjusted heritability, which remained after correction for height and weight, but decreased slightly for Rhythm after including height. The Variability domain was more heritable than any of its constituting parameters. For Rhythm, most parameters had higher estimates than the domain score, which was most pronounced for single support time and swing time ($\rho = .99$). The other gait domains had a smaller heritable component (<.25) and were strongly attenuated after adjustment for height (Pace) and weight (Base of Support, Phases).

To explore whether these decreases in heritability after adjustment for height and weight were due to specific genetic variants related to these traits, polygenic scores of height and body mass index (BMI) were studied in relation to gait (Table 3). Indeed, the polygenic height score was associated with Rhythm and Pace, but not after adjustment for height itself. The BMI score did not associate with any gait domain after multiple testing correction, but showed a nominally significant effect on Turning that became stronger after adjustment for weight.

GWAS of gait traits

GWASs were performed for the three gait domains showing moderate to high heritability (Variability, Rhythm, and Tandem) and their highest heritable parameter (stride length SD, single support time, and sum of the sidestep distance, respectively). Figure 1 shows the Manhattan plots for these traits, with all loci having variants with a p-value < $1x10^{-6}$ summarized in Table 4. Eight variants from a single locus at 1p22.3

Table 1 | Study population characteristics.

Characteristic	Rotterdam Study – total population (N=2946)	Rotterdam Study – sub-population (N=2588)	Tasmanian Study of Cognition and Gait (N=362)
Age in years, mean (SD)	68.2 (9.5)	67.3 (9.1)	72.1 (7.1)
Women, n (%)	1604 (54.4%)	1396 (53.9%)	148 (40.9%)
Height in cm, mean (SD)	169.2 (9.3)	169.5 (9.2)	167.5 (9.1)
Weight in kg, mean (SD)	78.6 (14.3)	78.8 (14.2)	78.2 (15.0)
MMSE score, mean (SD)	28.0 (2.0)	28.1 (1.8)	–

Abbreviations: MMSE = Mini-Mental State Examination, SD = standard deviation.

reached genome-wide significance for single support time (top variant rs72953990; minor allele frequency (MAF) = 0.14; $p = 2.30x10^{-8}$), and were also associated with the Rhythm domain ($p = 2.43x10^{-7}$). No variants reached genome-wide significance for the other gait traits.

Intronic variants in *PTPRD* (rs71321217; 9p23; $p = 7.65x10^{-7}$) and *PRKG1* (rs10823991; 10q21; $p = 9.72x10^{-7}$) showed suggestive association with Rhythm. For Variability a variant in *DGCR5* (rs11914070; 22q11.21; $p = 1.64x10^{-7}$), and for stride length SD two variants at 9q22.1 and 11p14.3 were found, of which 11p14.3 showed significant heterogeneity across the three cohorts. The most reliable signal for Tandem and sum of the sidestep distance was located on 1p32.1 in *KIF14*, with top variant rs10800713 showing evidence of transcription factor binding affinity.

Replication of 1p22.3 with single support time

For the genome-wide significant variant for single support time (rs72953990) replication was attempted in the TASCOG study (N = 362), where a similar Rhythm domain was constructed (Table 5). The variant associated with the parameters in the opposite direction, reaching nominal significance with the Rhythm domain ($p = 0.039$).

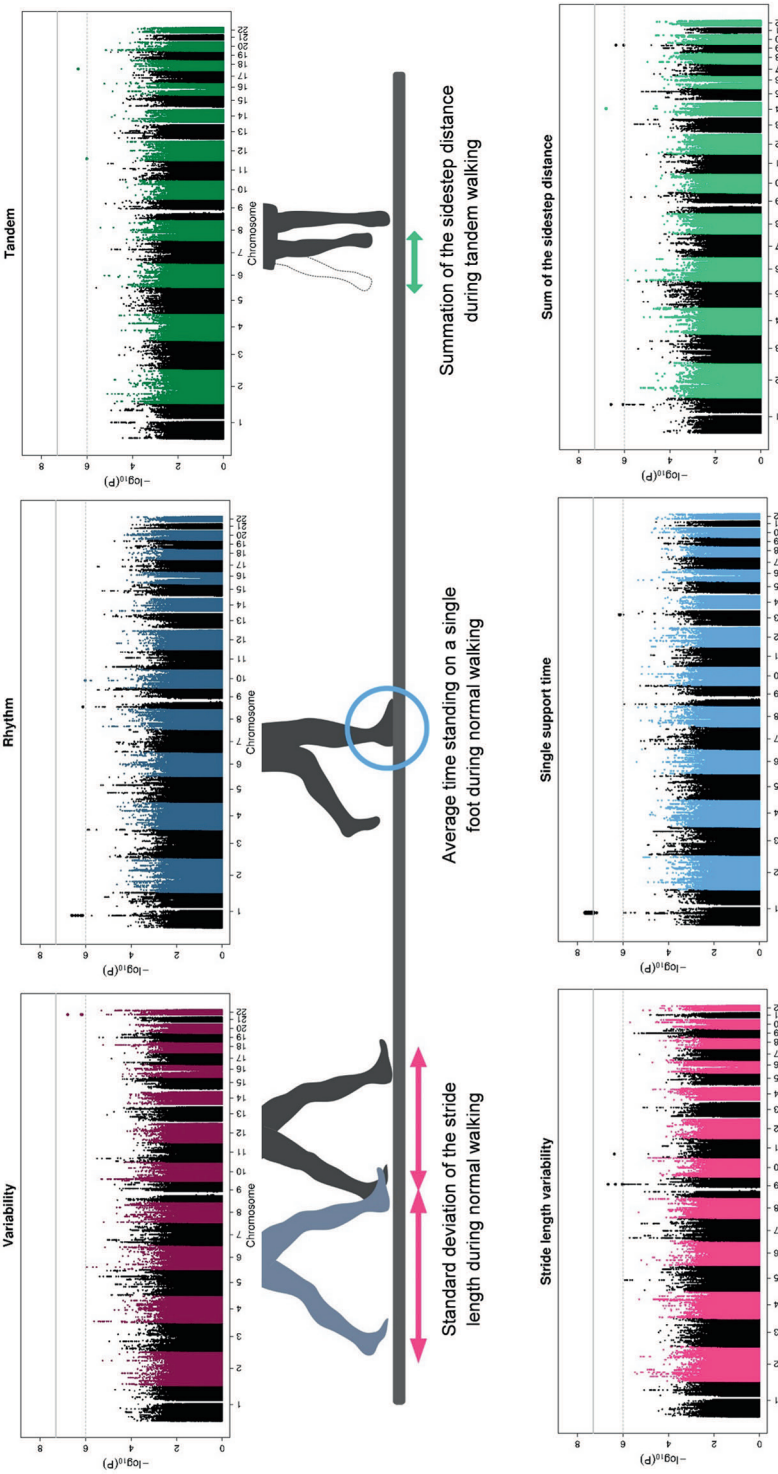

Figure 1 | Common genetic variants associated with the three most heritable gait domains and their highest heritable parameters. *Manhattan plots of the three most heritable gait domains (Variability, Rhythm, and Tandem) and their highest heritable parameters (Stride length variability, Single support time, and Sum of the sidestep distance, respectively). Every dot represents a single genetic variant plotted according to its genomic position (x-axis) and its –log10(p-value) for association with the respective gait variable (y-axis).*

Table 2 | Heritability estimates of gait domains and parameters, adjusted for age, sex, height and weight.

Gait domain (PVE) / parameter	Mean (SD)	Correlation with factor	Heritability estimate (SE)		
			Model 1	Model 2	Model 3
Variability (20%)			.61 (.23)	.63 (.23)	.58 (.23)
Stride length SD (cm)	4.58 (1.67)	-0.88	.42 (.21)	.43 (.21)	.42 (.21)
Step length SD (cm)	2.86 (0.94)	-0.86	.39 (.21)	.38 (.21)	.37 (.21)
Stride velocity SD (cm/s)	5.91 (1.97)	-0.87	.33 (.21)	.34 (.21)	.28 (.21)
Stride time SD (s)	0.03 (0.02)	-0.77	.22 (.21)	.24 (.21)	.26 (.21)
Step time SD (s)	0.02 (0.01)	-0.75	.24 (.21)	.24 (.21)	.28 (.21)
Stance time SD (s)	0.03 (0.01)	-0.76	.32 (.21)	.34 (.21)	.37 (.21)
Swing time SD (s)	0.02 (0.01)	-0.65	.01 (.21)	.01 (.21)	.01 (.21)
Single support time SD (s)	0.02 (0.01)	-0.65	.01 (.21)	.01 (.21)	.01 (.21)
Double support time SD (s)	0.02 (0.01)	-0.52	.35 (.22)	.36 (.22)	.36 (.22)
Rhythm (21.5%)			.37 (.24)	.28 (.24)	.27 (.24)
Single support time (s)	0.42 (0.04)	-0.96	.56 (.21)	.45 (.21)	.44 (.22)
Swing time (s)	0.42 (0.04)	-0.96	.56 (.21)	.45 (.21)	.44 (.22)
Step time (s)	0.55 (0.05)	-0.94	.38 (.21)	.30 (.21)	.34 (.21)
Stride time (s)	1.10 (0.10)	-0.94	.41 (.21)	.33 (.21)	.37 (.21)
Cadence (steps/min)	109.8 (9.5)	0.94	.42 (.21)	.32 (.21)	.35 (.21)
Stance time (s)	0.67 (0.07)	-0.83	.20 (.21)	.15 (.21)	.23 (.21)
Tandem (7.2%)			.32 (.23)	.32 (.23)	.34 (.23)
Sum of sidestep distance (cm)	9.56 (17.0)	-0.90	.35 (.22)	.35 (.22)	.36 (.22)
Sum of sidestep surface (fraction)	0.32 (0.64)	-0.91	.28 (.22)	.28 (.22)	.32 (.23)
Double step (n)	0.07 (0.28)	-0.54	.07 (.23)	.07 (.23)	.06 (.23)
Pace (9.8%)			.22 (.23)	.02 (.23)	.03 (.23)
Stride length (cm)	130.9 (18.2)	0.85	.26 (.21)	.15 (.21)	.18 (.21)
Step length (cm)	65.2 (9.13)	0.85	.26 (.21)	.15 (.21)	.18 (.21)
Velocity (cm/s)	119.5 (20.1)	0.72	.26 (.21)	.27 (.21)	.31 (.21)

Table 2 continued.

Base of Support (3.7%)			.20 (.23)	.21 (.23)	.11 (.23)
Stride width SD (cm)	2.40 (0.84)	-0.73	.15 (.21)	.16 (.21)	.15 (.21)
Stride width (cm)	10.3 (4.02)	0.67	.24 (.20)	.23 (.20)	.21 (.20)
Phases (19%)			.13 (.23)	.13 (.23)	.01 (.23)
Single support (%GC)	38.6 (1.87)	0.97	.18 (.21)	.21 (.21)	.06 (.21)
Swing (%GC)	38.6 (1.87)	0.97	.18 (.21)	.21 (.21)	.07 (.21)
Stance (%GC)	61.4 (1.87)	-0.97	.18 (.21)	.22 (.21)	.07 (.21)
Double support (%GC)	23.0 (3.75)	-0.97	.19 (.21)	.23 (.21)	.07 (.21)
Double support time (s)	0.25 (0.06)	-0.85	.14 (.21)	.18 (.21)	.05 (.21)
Turning (6.1%)			.10 (.24)	.10 (.24)	.07 (.24)
Turning step count (n)	4.94 (0.91)	-0.92	.03 (.23)	.03 (.23)	.03 (.23)
Turning time (s)	2.83 (0.63)	-0.85	.25 (.22)	.27 (.23)	.26 (.23)

Adjustments were made for age, sex, and the first 10 principal components of population stratification (model 1), and additionally for height (model 2) and weight (model 3).
Abbreviations: GC = gait cycle time, PVE = percentage of variance explained, SD = standard deviation, SE = standard error.

DISCUSSION

Here we determined the contribution of common genetic variants to an extensive range of gait parameters, for which the genetic basis is largely unknown. Subsequently, we performed a genome-wide association scan to identify specific loci influencing gait. We found that the heritability of gait varies across domains and we identified a variant influencing single support time that did not replicate in a small, independent sample.

Table 3 | Associations of polygenic scores of height and weight with gait domains, before and after adjusting for height and weight.

Polygenic score	Variability		Rhythm		Tandem		Pace		Base of Support		Phases		Turning	
	β (SE)	P	β (SE)	P	β (SE)	P	β (SE)	P	β (SE)	P	β (SE)	P	β (SE)	P
Height score, unadjusted for height	-.024 (.019)	.212	*-.057 (.018)*	*.002*	.002 (.019)	.922	*.049 (.016)*	*.003*	-.015 (.019)	.450	.021 (.017)	.208	.008 (.020)	.688
Height score, adjusted for height	.002 (.019)	.915	-.013 (.018)	.465	.003 (.020)	.872	-.003 (.016)	.857	.012 (.020)	.542	-.006 (.017)	.726	.001 (.020)	.942
BMI score, unadjusted for weight	.023 (.019)	.224	.016 (.017)	.350	-.005 (.019)	.775	-.003 (.016)	.832	.003 (.019)	.864	-.032 (.019)	.089	.049 (.020)	.013
BMI score, adjusted for weight	.021 (.019)	.260	.015 (.017)	.401	-.004 (.019)	.822	-.003 (.016)	.862	.000 (.019)	.985	-.016 (.017)	.332	.052 (.020)	.008

All analyses were adjusted for age, sex, height, and weight, unless otherwise stated. For Tandem, additional adjustments were made for the step count and step length during the tandem walk. Betas are expressed per standard deviation of the polygenic score. Associations surviving multiple testing ($p<0.0036$) are indicated in italic.

Abbreviations: BMI = body mass index, SE = standard error.

Table 4 | Genetic variants at 12 loci associated with heritable gait domains Variability, Rhythm, Tandem, or their highest heritable parameters ($p<1x10^{-6}$).

									Discovery sample			Heterogeneity	
Gait parameter	Variant	Locus	Position	Closest gene(s)	Type	A1	A2	Freq	β (SE)	P	N	I^2	P
Variability	rs11914070	22q11.21	18965628	*DGCR5*	Intronic	T	C	0.39	-.136 (.026)	$1.64x10^{-7}$	2588	0.0	.85
Stride length SD	rs6560039	9q22.1	90474946	*XXyac-YM21GA2.4*	Upstream	T	C	0.22	-.230 (.044)	$2.22x10^{-7}$	2946	0.0	.97
Stride length SD	rs7932614	11p14.3	26045601	*ANO3*	Intergenic	A	G	0.57	-.246 (.049)	$4.19x10^{-7}$	2946	70.6	.03
Rhythm	rs72953990	1p22.3	88064857	*LMO4*	Intergenic	A	G	0.14	-.192 (.037)	$2.43x10^{-7}$	2588	48.0	.15
Rhythm	rs71321217	9p23	10036568	*PTPRD*	Intronic	I	R	0.27	.144 (.029)	$7.65x10^{-7}$	2588	45.8	.16
Rhythm	rs10823991	10q21.1	53794532	*PRKG1*	Intronic	A	T	0.27	.138 (.028)	$9.72x10^{-7}$	2588	0.0	.85
Single support time	rs72953990	1p22.3	88064857	*LMO4*	Intergenic	A	G	0.14	.0069 (.0012)	$2.30x10^{-8}$	2946	0.0	.71
Single support time	rs80092143	13q31.3	91057759	*MIR622*	Intergenic	C	G	0.89	-.0065 (.0013)	$6.88x10^{-7}$	2946	17.4	.30
Tandem	rs11054786	12p13.2	12458665	*MANSC1, LRP6*	Intergenic	T	C	0.90	.590 (.121)	$9.89x10^{-7}$	736[a]	-	-
Tandem	rs77292326	18p11.21	11737231	*GNAL*	Intronic	A	T	0.06	-.294 (.058)	$4.10x10^{-7}$	2588	70.8	.03
Sum sidestep distance	rs10800713	1q32.1	200548745	*KIF14*	Intronic	A	T	0.73	-2.431 (.472)	$2.62x10^{-7}$	2736	0.0	.71
Sum sidestep distance	rs146647518	14q23.3	67529620	*GPHN*	Intronic	A	G	0.06	8.183 (1.561)	$1.58x10^{-7}$	1346[a]	-	-
Sum sidestep distance	rs80050017	19q13.33	51383200	*KLK2*	3prime UTR	T	G	0.06	5.213 (1.031)	$4.24x10^{-7}$	2736	82.7	0.003

[a] *Variant missing in some cohorts due to insufficient imputation quality.*

Abbreviations: A1 = effect allele, A2 = reference allele, Freq = frequency of the effect allele, SD = standard deviation, SE = standard error, N = sample size

Table 5 | Associations between rs72953990 and the Rhythm domain and parameters in the TASCOG replication sample (N=362).

Gait domain (PVE) / parameter	Mean (SD)	Correlation with factor	β (SE)	P-value
Rhythm (28.3%)			.107 (.052)	.039
Single support time (s)	0.42 (0.04)	-0.69	-.001 (.004)	.775
Swing time (s)	0.42 (0.04)	-0.69	-.001 (.004)	.775
Step time (s)	0.55 (0.06)	-0.88	-.008 (.007)	.213
Stride time (s)	1.11 (0.12)	-0.87	-.016 (.013)	.213
Cadence (steps/min)	109.6 (10.6)	0.91	1.37 (1.15)	.235
Stance time (s)	0.68 (0.09)	-0.83	-.015 (.01)	.135

Betas are expressed per minor allele (A) increase of rs72953990 in relation to the respective dependent variable (i.e., gait domain or parameter).
Abbreviations: PVE = percentage of variance explained, SD = standard deviation, SE = standard error.

Gait is an important indicator of health [3]. Identifying factors that contribute to variation in gait could aid our understanding of gait dysfunction and its associated diseases. Given the highly complex cooperation of multiple organ systems that is required for gait, it is not surprising that we found a genetic architecture that is similar to other complex traits (i.e., height, cognition), which are partly determined by multiple common genetic variants, each with a small effect. Others have studied the heritability of walking speed, which mainly forms the Pace domain, [9-11] and found estimates between 16% and 60%. Similar to Pajala *et al.*, we found walking speed to be only moderately heritable (17%). However, the comprehensive and quantitative gait assessment in our study enabled us to investigate the genetic influence on the gait pattern in more detail than walking speed alone. Interestingly, we found the genetic influence to be much larger on several other gait domains, particularly Variability, Rhythm and Tandem.

Variability in gait was found to be the most heritable (58%). It captures the irregularity in walking and is believed to be particularly related to cognitive functioning [15]. Interestingly, none of the individual parameters comprising Variability had a heritability >42%, suggesting that the principal component analysis extracted a true genetic (and

biological) construct. Although Variability had the highest heritability, no genome-wide significant variants were identified. Importantly, we did not have enough power to detect small effects. However, this does not preclude the possibility of a different genetic architecture. For example, Variability could be influenced by numerous variants with only a small effect that jointly have a large influence but make identification of specific variants difficult. Furthermore, it is possible that the gait parameters comprising this domain each have distinct genetic determinants with larger effects, but that these signals become diluted when analyzing the domain as a whole. However, no genome-wide significant variants were detected for the highest heritable parameter, stride length variability.

We did identify a variant that reached significance in the GWAS of single support time, the highest heritable gait parameter of Rhythm. Replication of the variant was attempted in an independent sample (N = 362), but this failed to show an association with single support time. Whether this represents a false-positive finding or a combination of the winner's curse and a small replication sample can only be clarified by additional studies. This underlines that, in order to detect robust genetic associations for gait, more researchers in the field of human gait need to obtain DNA samples and large genetic collaborations should introduce phenotyping of gait.

This increase in sample size seems particularly promising for Variability, Rhythm, or Tandem. Other gait domains initially showed small to moderate heritability, but the estimates strongly attenuated after adjusting for height and weight. To investigate whether the reduction in heritability was due to genetic variants that primarily associate with these traits, but not with gait, we explored the effect of established variants for height and BMI in relation to gait. Indeed, the polygenic score of height was associated with the same gait domains that showed attenuation after adjustment for height. The BMI score did not show significant associations with the gait domains. Given the lower number of variants for BMI (32) compared to height (180), it is likely that the polygenic score of BMI is less powerful to detect effects. This is underlined by the fact that the BMI score was not convincingly associated with BMI in our sample ($p = 0.056$), contrary to the height score with height ($p = 6.5 \times 10^{-47}$). As a whole, our analyses thus seem to suggest

that Pace, Base of support, and Phases are potentially not very heritable beyond their correlation with height and weight, and the polygenic score of height adds an additional line of evidence to this finding.

Important to note is that the heritability estimates calculated using GCTA represent narrow-sense heritability, and thus only take into account the additive genetic portion of the phenotypic variance while leaving out non-additive effects. Furthermore, GCTA only uses the variants provided as input for determining the genetic similarity. However, causal variants that are not in included (e.g., rare variants) but are in linkage disequilibrium with those that are in the analysis will also be indirectly used. Another limitation that is inherent to GCTA analyses is the dependence on unrelated individuals, which produces relatively large standard errors for the heritability estimates in our sample of less than 3000 persons. This emphasizes the main limitation of our study, namely its low power. Although it is well known that the largest effect sizes typically explain less than 1% of the phenotypic variance of similar quantitative traits [20], we performed this study for several reasons: First, we provide estimates of genetic influence on a comprehensive set of gait parameters, which could serve to direct future genetic studies of gait and as an incentive for larger initiatives. Second, we excluded to a reasonable degree the possibility of genetic variants having large effects on gait. Third, we are not aware of additional studies that have both quantitatively assessed gait and genome-wide genotyping, making this in fact the largest available sample for genetic studies on gait.

In conclusion, we found that human gait is comprised of various heritable domains. A large number of variants remain to be identified for gait, but this will require large-scale collaborative efforts.

REFERENCES

1. Sahyoun C, Floyer-Lea A, Johansen-Berg H, Matthews P (2004) T Neuroimage 21: 568-575.
2. Maki BE (1997) r. Journal of the American geriatrics society 45: 313-320.
3. Studenski S, Perera S, Patel K, Rosano C, Faulkner K, et al. (2011) Gait speed and survival in older adults. Jama 305: 50-58.
4. Blin O, Ferrandez A-M, Serratrice G (1990) Journal of the neurological sciences 98: 91-97.
5. Kaufman KR, Hughes C, Morrey BF, Morrey M, An K-N (2001) Journal of biomechanics 34: 907-915.
6. Allen HL, Estrada K, Lettre G, Berndt SI, Weedon MN, et al. (2010) Nature 467: 832-838.
7. Yang J, Manolio TA, Pasquale LR, Boerwinkle E, Caporaso N, et al. (2011) Nature genetics 43: 519-525.
8. Davies G, Tenesa A, Payton A, Yang J, Harris SE, et al. (2011). Molecular psychiatry 16: 996-1005.
9. Pajala S, Era P, Koskenvuo M, Kaprio J, Alén M, et al. (2005) The Journals of Gerontology Series A: Biological Sciences and Medical Sciences 60: 1299-1303.
10. Ortega-Alonso A, Pedersen NL, Kujala UM, Sipilä S, Törmäkangas T, et al. (2006) The Journals of Gerontology Series A: Biological Sciences and Medical Sciences 61: 1082-1085.
11. Ortega Alonso A, Sipilä S, Kujala UM, Kaprio J, Rantanen T (2009) Scandinavian journal of medicine & science in sports 19: 669-677.
12. Bilney B, Morris M, Webster K (2003). Gait & posture 17: 68-74.
13. Do R, Willer CJ, Schmidt EM, Sengupta S, Gao C, et al. (2013) Nat Genet 45: 1345-1352.
14. Verlinden VJA, van der Geest JN, Hoogendam YY, Hofman A, Breteler MMB, et al. (2013) Gait patterns in a community-dwelling population aged 50 years and older. Gait & posture 37: 500-505.
15. Verlinden VJA, van der Geest JN, Hofman A, Ikram MA (2013). Alzheimer's & Dementia.
16. Yang J, Lee SH, Goddard ME, Visscher PM (2011) The American Journal of Human Genetics 88: 76-82.
17. Speliotes EK, Willer CJ, Berndt SI, Monda KL, Thorleifsson G, et al. (2010) Nature genetics 42: 937-948.
18. Willer CJ, Li Y, Abecasis GR (2010) Bioinformatics 26: 2190-2191.
19. Srikanth V, Beare R, Blizzard L, Phan T, Stapleton J, et al. (2009) Stroke 40: 175-180.
20. Park J-H, Gail MH, Weinberg CR, Carroll RJ, Chung CC, et al. (2011). Proceedings of the National Academy of Sciences 108: 18026-18031.

Chapter 3.3.3

Heritability of the shape of subcortical structures

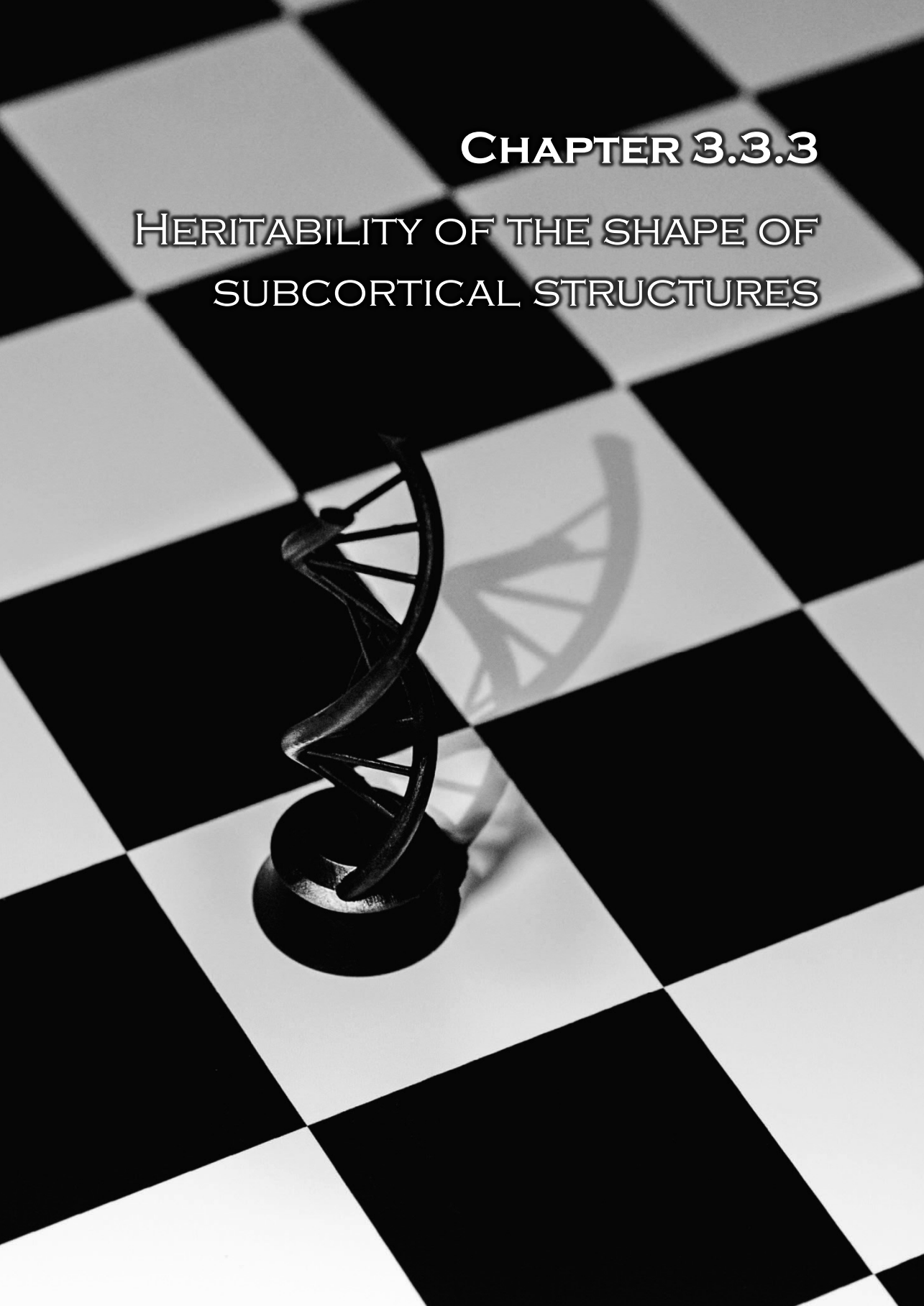

ABSTRACT

The volumes of subcortical brain structures are highly heritable, but genetic underpinnings of their shape remain relatively obscure. Here we determine the relative contribution of genetic factors to individual variation in the shape of 7 bilateral subcortical structures: the nucleus accumbens, amygdala, caudate, hippocampus, pallidum, putamen and thalamus. In 3,686 unrelated individuals aged between 45 and 98 years, brain magnetic resonance imaging and genotyping was performed. The maximal heritability of shape varied from 32.7% to 53.3% across the subcortical structures. Genetic contributions to shape extend beyond influences on intracranial volume and the gross volume of the respective structure. The regional variance in heritability was related to the reliability of the measurements, but could not be accounted for by technical factors only. These findings could be replicated in an independent sample of 1040 twins. Differences in genetic contributions within a single region reveal the value of refined brain maps to appreciate the genetic complexity of brain structures..

INTRODUCTION

Subcortical brain regions are important for a multitude of biological processes, including cognitive and motor functions.[1,2] There is substantial structural variation in these regions, both within the normal range[3] and in the context of various neuropsychiatric diseases.[4,5] Factors driving individual variation could provide insight into brain development, healthy aging, and pathological states, but these remain largely unknown. Variation in subcortical brain structures is affected by environmental factors, such as education, diet and stress, but a considerable proportion of the variation is determined by genes.[6,7] A recent twin study of gross subcortical volumes found heritability estimates ranging between 0.44 and 0.88,[8] which were especially high for the caudate and thalamus.

Even so, aggregate measures such as volume do not capture the complexity of subcortical structures. The hippocampus, for example, is made up of several subfields, each with partially independent functional roles. More recently, image processing methods have been developed to characterize brain structure beyond purely volumetric measures, and yielding a range of shape descriptors.[9-13] The high-dimensionality allows the detection of more localized differences in brain structure, and shape can provide relevant biological information in addition to aggregate measures.[14-17] Several genetic variants that influence the volume of subcortical structures have been identified,[18-20] but their effect could be localized to certain sub-regions using shape analyses.[19,20] However, the extent to which genes contribute to the variability in shape of subcortical structures has yet to be determined.

Here, we quantify genetic influences on shape variability of 14 subcortical brain structures in 3,686 unrelated individuals from the population-based Rotterdam Study. We compare the heritability of vertex-wise shape measures to gross volumes as well as other aggregate measures of shape obtained through dimension-reduction techniques. We show that the shape of subcortical structures is under genetic control, and investigate the relation of the resulting profiles with the gross volume and measures of reproducibility.

METHODS

Study population

This work was performed in the Rotterdam Study,[21] a population-based cohort study in the Netherlands including a total of 14,926 participants (aged 45 years or over at enrollment). The overall aim of the study is to investigate causes and determinants of chronic diseases in elderly people, the participants were not selected for the presence of diseases or risk factors. Since 2005, all participants underwent brain magnetic resonance imaging (MRI) to examine the causes and consequences of age-related brain changes.[22] Between 2005 and 2013, a total of 5,691 unique persons were scanned. The Rotterdam Study has been approved by the Medical Ethics Committee of the Erasmus MC and by the Ministry of Health, Welfare and Sport of the Netherlands, implementing the Wet Bevolkingsonderzoek: ERGO (Population Studies Act: Rotterdam Study). All participants provided written informed consent to participate in the study and to obtain information from their treating physicians.

Replication was performed in 1040 healthy young adult twins from the Queensland Twin IMaging (QTIM) project [de Zubicaray et al. 2008]. All participants of the imaging sample were Caucasian and right-handed for throwing and writing (Annett's Handedness Questionnaire). The genetic analyses were conducted in the 350 complete twin pairs (n = 700): 148 monozygotic (100 male), 120 dizygotic (39 male), and 82 opposite-sex pairs. Self-reported data was used to screen participants for contraindications for imaging as well as any significant medical, psychiatric or neurological conditions, history of substance abuse and current use of psychoactive medication. The study was approved by the Human Research Ethics Committees of the Queensland Institute of Medical Research, the University of Queensland, and Uniting Health Care, Wesley Hospital. Informed consent was obtained from each participant and parent or guardian for participants under 18 years of age.

Genotyping and imputation

Genotyping in the Rotterdam Study was performed using the Illumina 550K and 550K duo arrays.[21] Subsequently, we removed samples with call rate below 97.5%, gender

mismatch, excess autosomal heterozygosity, duplicates or family relations and ancestry outliers, and variants with call rate below 95.0%, failing missingness test, Hardy–Weinberg equilibrium p-value < 10^{-6}, and minor allele frequency < 1%. Genotypes were imputed using MACH/minimac software[23] to the 1000 Genomes phase I version 3 reference panel (all population).

For QTIM, genotyping of nine markers was used to determine the zygosity of same-sex twins, which was later confirmed for >92% of the sample with the Illumina 610K SNP array.

Image acquisition

For the Rotterdam Study, MRI scanning was done on a 1.5-T MRI unit with a dedicated eight-channel head coil (GE Healthcare). The MRI protocol consisted of several high-resolution axial sequences, including a T1-weighted sequence (slice thickness 0.8 mm), which was used for further image processing. In addition, 85 persons were rescanned within days to weeks after the first scan to estimate the reproducibility of imaging-derived measures. A detailed description of the MRI protocol was presented by Ikram *et al.*[22]

The twin pairs of QTIM were scanned on a 4T Bruker Medspec (Bruker, Germany) whole body MRI system paired with a transverse electromagnetic (TEM) head coil. Structural T1-weighted 3D images were acquired (TR=1500ms, TE=3.35ms, TI=700ms, 240mm FOV, 0.9mm slice thickness, 256 or 240 slices depending on acquisition orientation (86% coronal (256 slices), 14% sagittal (240 slices)).

Image processing

The T1-weighted MRI scans were processed using FreeSurfer[24] (v5.1) to obtain segmentations and volumetric summaries of 7 subcortical structures for each hemisphere: nucleus accumbens, amygdala, caudate, hippocampus, pallidum, putamen, and thalamus (Figure 1A). Next, segmentations were processed using a previously described shape analysis pipeline.[9,10] Briefly, a mesh model was created for the boundary of each structure. Subcortical shapes were registered using the "Medial Demons" framework, which matches shape curvatures and medial features to a pre-computed

template.[25,26] To do this, a medial model of each individual surface model is fit following Gutman *et al.*[27], and medial as well as intrinsic features of the shape drive registration to a template parametrically on the sphere. To minimize metric distortion, the registration was performed in the fast spherical demons framework.[10] The templates and mean medial curves were previously constructed and are distributed as part of the ENIGMA-Shape package (http://enigma.ini.usc.edu/ongoing/enigma-shape-analysis/).

The resulting meshes for the 14 structures consist of a total of 27,120 vertices (Figure 1A). For these vertices, two measures were used to quantify shape: the radial distance and the natural logarithm of the Jacobian determinant. The radial distance represents the distance of the vertex from the medial curve of the structure (Figure 1B). The Jacobian determinant captures the deformation required to map the subject-specific vertex to a template and indicates surface dilation due to sub-regional volume change (Figure 1C).

Finally, we performed 28 principal component analyses: for each of the 14 subcortical structures and for both types of shape measures (radial distance and Jacobian determinant), we computed the full set of components. This yielded the same number of principal components as the original number of vertices that were describd shape (Figure 1A). The components were sorted in descending order of the eigenvalues, which corresponds to the amount of explained variance of shape.

Heritability estimation

We used Massively Expedited Genome-wide Heritability Analysis (MEGHA)[28] to estimate heritability in our sample of unrelated individuals. This method allows fast and accurate estimates of heritability across thousands of phenotypes based on genome-wide genotype data of common genetic variants from unrelated individuals. As previously described,[28] a genetic relationship matrix was constructed using the 1000 Genomes imputed genotypes, filtered on imputation quality ($R^2 < 0.5$) and allele frequency (MAF < 0.01). We calculated pairwise genetic relatedness between all individuals. We removed one person for pairs with more than 0.025 genotype similarity, resulting in a final study population of 3,686 subjects.

Twin-based heritability was estimated using maximum-likelihood variance components methods implemented in the SOLAR software (version 6.6.2). [29] To test the hypothesis that no variance can be explained genetically, log likelihoods of models with no genetic components were compared to those with genetic and environmental components. As twice the log likelihood is distributed as a mixture of chi-squared distributions, the hypothesis test and p-value can be derived parametrically.[29]

To correct for multiple comparisons across all vertices and all structures, we used the standard False Discovery Rate (FDR) threshold at q=0.05 to localize regions of significant heritability within each of the subcortical structures.[30]

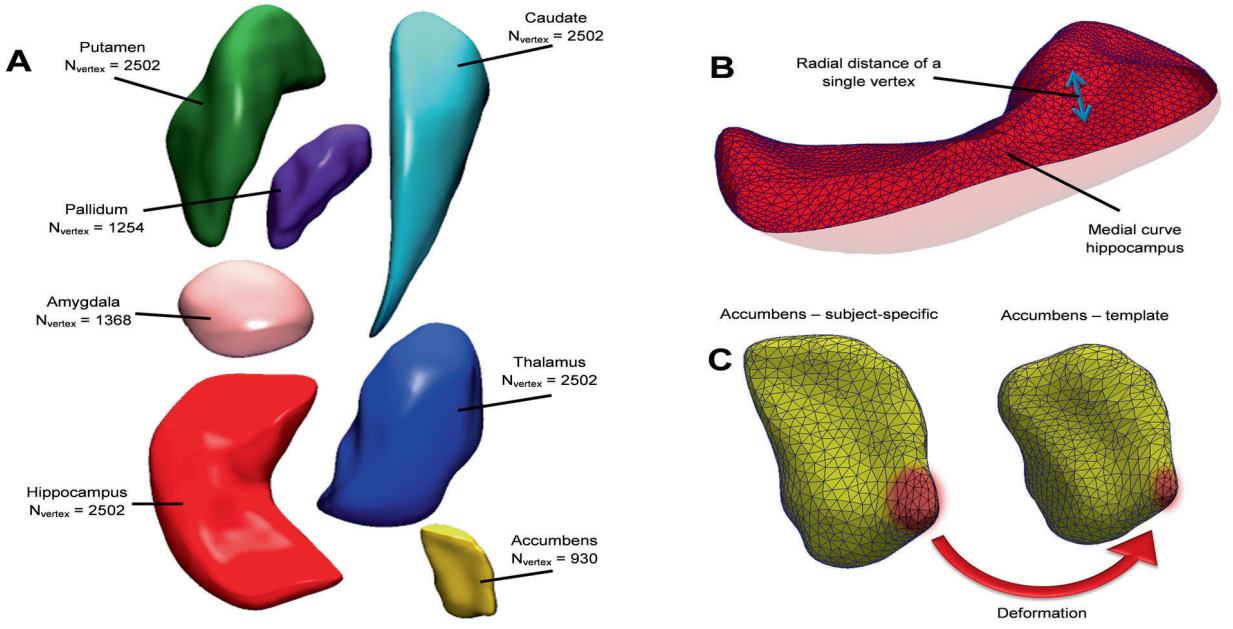

Figure 1 | Subcortical brain structures and the derivation of shape measures.

Overview of the subcortical brain structures studied in this manuscript and the derivation of the shape measures. Panel A shows the seven structures with corresponding number of vertices: accumbens, amygdala, caudate, hippocampus, pallidum, putamen, and thalamus. Panels B and C illustrate the two vertex-wise measures of shape: the radial distance is defined as the distance of a vertex to the medial curve of the structure, e.g. the hippocampus in Panel B. The Jacobian determinant captures the deformation that is needed to map a subject-specific shape to a template, which is shown with an example of the accumbens in Panel C.

Table 1 | Characteristics of the study population.

Characteristic	Rotterdam Study (N = 3,686)	QTIM (N = 1,040)
Age, mean (SD), years	65.9 (10.9)	22.9 (2.8)
Female sex, n (%)	2,029 (55.0%)	641 (61.6%)
Intracranial volume, mean (SD), cm^3	1478.6 (161.3)	1484 (157.1)
Left hemisphere, mean (SD), cm^3		
Accumbens	0.56 (0.10)	0.83 (0.15)
Amygdala	1.31 (0.21)	1.84 (0.25)
Caudate	3.40 (0.56)	3.76 (0.50)
Hippocampus	3.84 (0.62)	4.32 (0.46)
Pallidum	1.47 (0.24)	1.61 (0.25)
Putamen	4.62 (0.68)	6.60 (0.72)
Thalamus	6.25 (0.79)	7.82 (0.89)
Right hemisphere, mean (SD), cm^3		
Accumbens	0.49 (0.09)	0.79 (0.11)
Amygdala	1.39 (0.22)	1.88 (0.25)
Caudate	3.51 (0.58)	3.92 (0.53)
Hippocampus	3.85 (0.59)	4.32 (0.46)
Pallidum	1.41 (0.25)	1.53 (0.18)
Putamen	4.45 (0.65)	6.00 (0.65)
Thalamus	6.25 (0.79)	7.43 (0.88)

Abbreviation: SD = standard deviation.

RESULTS

Study population

The characteristics of the study population are shown in Table 1. The mean age of the Rotterdam study population was 65.9 ± 10.9 years, and 55.0% were women. For the 14 subcortical structures, the mean volumes were between 0.49 and 6.25 mL. For the QTIM study, mean age was 22.9 ± 2.8 years, and 61.6% were women. Mean subcortical volumes were higher than in the Rotterdam study across the board, ranging from 0.79 and 7.82 mL.

Heritability of subcortical structures: volume and shape

The structure of subcortical brain regions was quantified by calculating their gross volume as well as two measures of their shape. Age- and sex-adjusted heritability estimates for the gross volume of each of the subcortical structures were between 1.6% and 43.4% (Table 2). For the two vertex-wise shape measures, the maximal heritability estimates per structure ranged from 32.7% to 53.3% (Table 2). Both the radial distance (Figure 2A-C) and the Jacobian determinant (Figure 2D-F) showed clusters of high heritability under various models. Further adjustment for intracranial volume did not influence results (Figure 2), and estimates were highly correlated between both models (Supplementary Figure 1). The addition of the structure-specific gross volume to the model, however, did affect the heritability distribution across the structures (Figure 2), particularly for the shape measures that are highly correlated with the gross volume (Supplementary Figure 2).

Table 2 | Heritability estimates of various structural measures of subcortical brain regions.

Region	Gross volume		Radial distance		Jacobian determinant		PCA radial distance		PCA Jacobian determinant	
	h^2	p	h^{2*}	p	h^{2*}	p	h^{2*}	p	h^{2*}	p
Left hemisphere										
Amygdala	8.1	0.18	47.7	1.72×10^{-6}	35.4	2.85×10^{-4}	29.9	4.40×10^{-4}	27.9	9.30×10^{-4}
Accumbens	11.6	0.099	34.0	4.71×10^{-4}	33.7	5.11×10^{-4}	28.7	7.04×10^{-4}	42.0	1.45×10^{-6}
Caudate	33.7	8.6×10^{-5}	49.9	6.33×10^{-7}	52.9	1.40×10^{-7}	42.4	1.20×10^{-6}	35.1	4.73×10^{-5}
Hippocampus	10.8	0.12	32.7	7.32×10^{-4}	29.2	2.23×10^{-3}	28.9	6.59×10^{-4}	29.6	5.03×10^{-4}
Pallidum	32.2	1.7×10^{-4}	39.6	5.75×10^{-5}	44.1	8.65×10^{-6}	30.8	2.96×10^{-4}	27.0	1.33×10^{-3}
Putamen	43.4	6.8×10^{-7}	49.4	7.43×10^{-7}	52.7	1.45×10^{-7}	34.1	7.16×10^{-5}	40.7	2.92×10^{-6}
Thalamus	34.1	7.4×10^{-5}	53.3	1.05×10^{-7}	45.3	5.07×10^{-6}	30.2	3.78×10^{-4}	29.4	5.26×10^{-4}
Right hemisphere										
Amygdala	20.4	0.012	33.5	5.45×10^{-4}	31.5	1.08×10^{-3}	30.5	3.45×10^{-4}	27.7	1.03×10^{-3}
Accumbens	1.6	0.43	33.1	6.30×10^{-4}	35.1	3.13×10^{-4}	34.5	5.99×10^{-5}	31.7	2.10×10^{-4}
Caudate	34.7	5.4×10^{-5}	46.7	2.86×10^{-6}	47.5	1.95×10^{-6}	29.9	4.45×10^{-4}	33.8	8.75×10^{-5}
Hippocampus	8.0	0.19	33.7	5.26×10^{-4}	17.7	4.23×10^{-2}	30.8	3.00×10^{-4}	28.9	6.44×10^{-4}
Pallidum	36.6	2.3×10^{-5}	46.4	3.12×10^{-6}	44.5	7.22×10^{-6}	41.4	1.97×10^{-6}	29.2	5.77×10^{-4}
Putamen	37.1	1.8×10^{-5}	42.6	1.70×10^{-5}	37.5	1.32×10^{-4}	32.7	1.36×10^{-4}	33.4	1.01×10^{-4}
Thalamus	30.8	3.0×10^{-4}	46.2	3.50×10^{-6}	50.4	4.50×10^{-7}	37.1	1.78×10^{-5}	31.8	2.02×10^{-4}

**Estimate indicates highest heritability among all vertices or principal components.*

Abbreviations: h^2 = heritability estimate in %, PCA = principal component analysis.

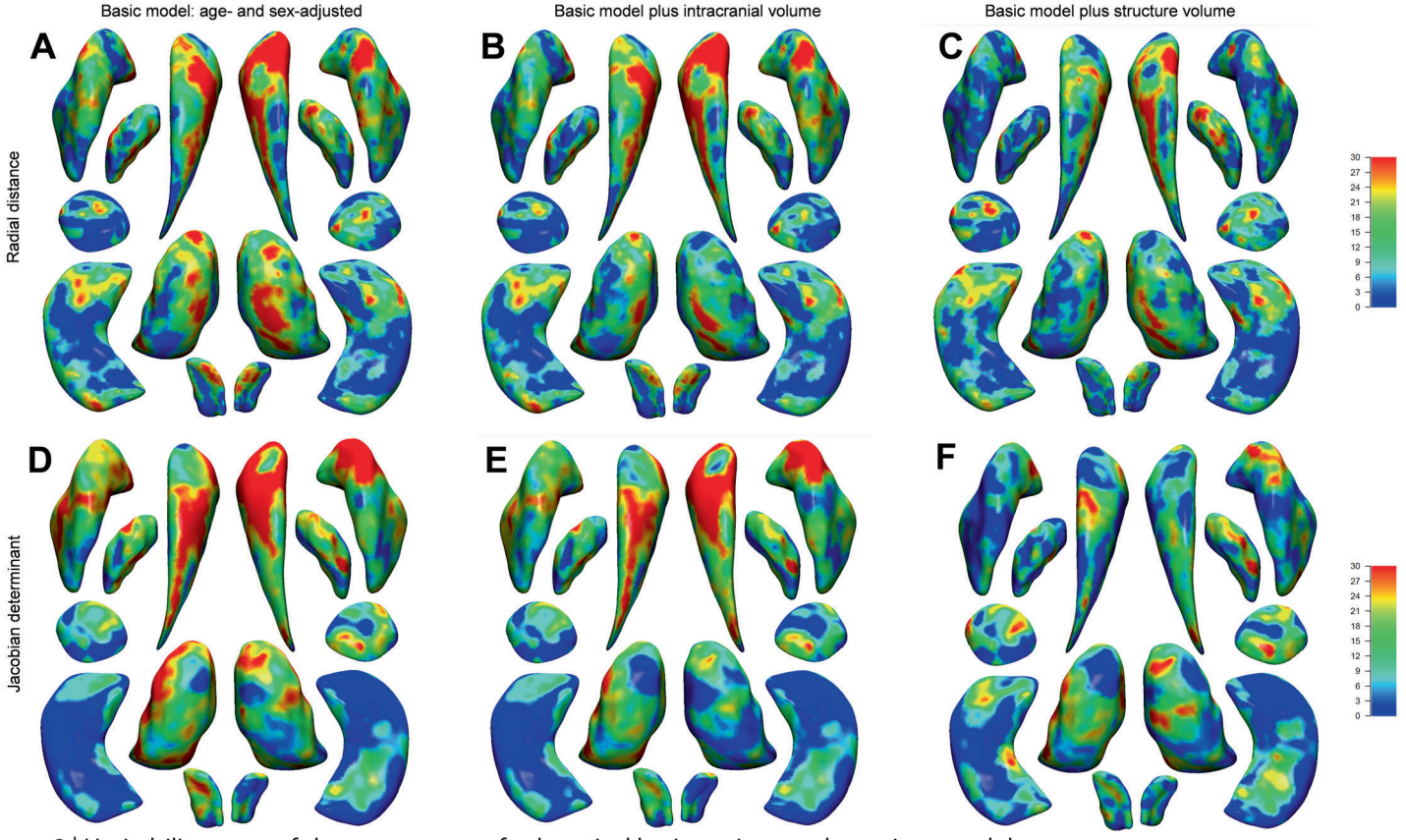

Figure 2 | Heritability maps of shape measures of subcortical brain regions under various models.

Maps show the heritability of 7 bilateral subcortical structures for the shape measures of radial distance (Panels A-C) and the Jacobian determinant (Panels D-F). Heritability estimates were obtained using three different statistical models: a basic model with age and sex (Panels A and D), and additionaly adjusting for either intracranial volume (Panels B and E) or the volume of the specific structure (Panels C and F).

Reproducibility of subcortical shape

Next, we investigated the relation between our heritability estimates and the reproducibility of subcortical shape. In a subset of 83 persons who were scanned twice within 1-9 weeks, we quantified the reproducibility by calculating intraclass correlation coefficients for the vertex-wise shape measures (Supplementary Figure 3). There was considerable overlap between heritability and reproducibility (Figure 3A-B), and both were correlated within hemisphere (Figure 3C-D). Poorly reproducible shape measures were generally not heritable, whereas high reproducibility included the full range of heritability estimates (Figure 3C-D).

Heritability of shape measures through data reduction

Finally, we explored whether high-dimensional shape data could be reduced to a smaller set of variables with a larger genetic contribution. We performed principal component analyses on the two vertex-wise shape measures for each structure and computed the heritability of the resulting components. Except for the Jacobian determinant of both hippocampi, the maximal heritability was lower than for the vertex-wise measures (Table 2). Similarly, the components were in general less heritable than the vertex-wise measures (Figure 4). Furthermore, the order of the components based on the eigenvalues did not correlate well with the order based on the heritability (ρ ranges from -0.038 to 0.096; Supplementary Table 1).

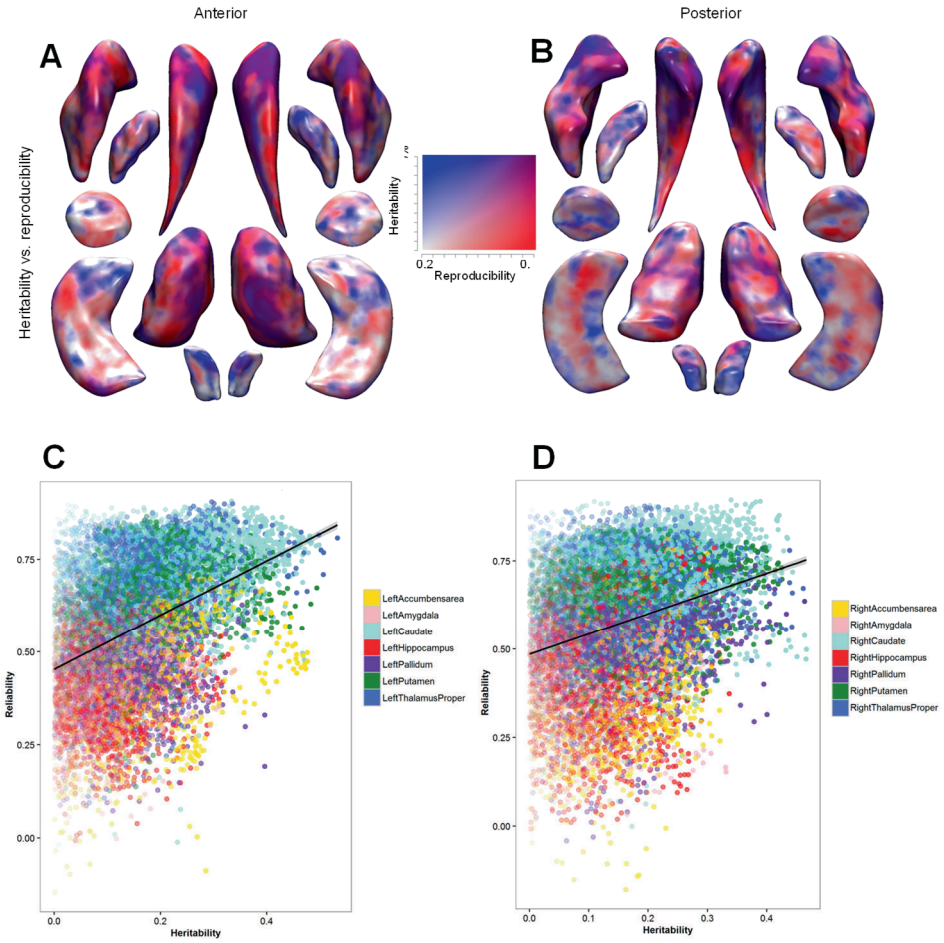

Figure 3 | Concordance between the heritability of subcortical shape and reproducibility of the measures.

Figure showing the concordance between the heritability of the shape (radial distance) ofsubcortical structures and the reproducibililty of these measures. Maps illustrate heritability (high is red) and reproducibility (high is blue) and their overlap (purple) from the anterior (Panel A) and posterior (Panel B) direction. Scatter plots between heritability and reprodcubility of the left (Panel C) and right (Panel D) hemisphere for the 7 subcortical structures. Colors indicate the different structures (see figure legends).

Replication of heritability in twins

The maximum heritability estimates for the two vertex-wise shape measures per structure ranged from 48.9% to 78.3%. Both the radial distance (Supplementary Figure 4A-C) and the Jacobian determinant (Supplementary Figure 4D-F) showed clusters of high heritability under various models. Further adjustment for intracranial volume did not influence the results (Supplementary Figure 4C, E). The addition of the structure-specific gross volume to the model, however, did affect the heritability distribution across the structures (Supplementary Figure 4C, F). Comparing the results of the twin-based and population study, we found a considerable overlap and significant correlation (p-value = 3.03×10^{-306}) in estimated heritability (Supplementary Figure 5).

DISCUSSION

Here we show that, in a general population of middle-aged and elderly individuals, the shapes of subcortical structures are under genetic control. The vertex-wise heritability is higher than for aggregate measures such as volume and principal components. Moreover, the heritability pattern underlines the importance of reproducibility in deriving shape measures, but also reveals that the extent of genetic influences is not uniformly distributed across subcortical structures. We confirmed our findings in an independent cohort of twins, suggesting that the genetic architecture of subcortical shapes is similar across populations, despite differences in the sample, the study design, scanner types, and methods to compute the heritability.

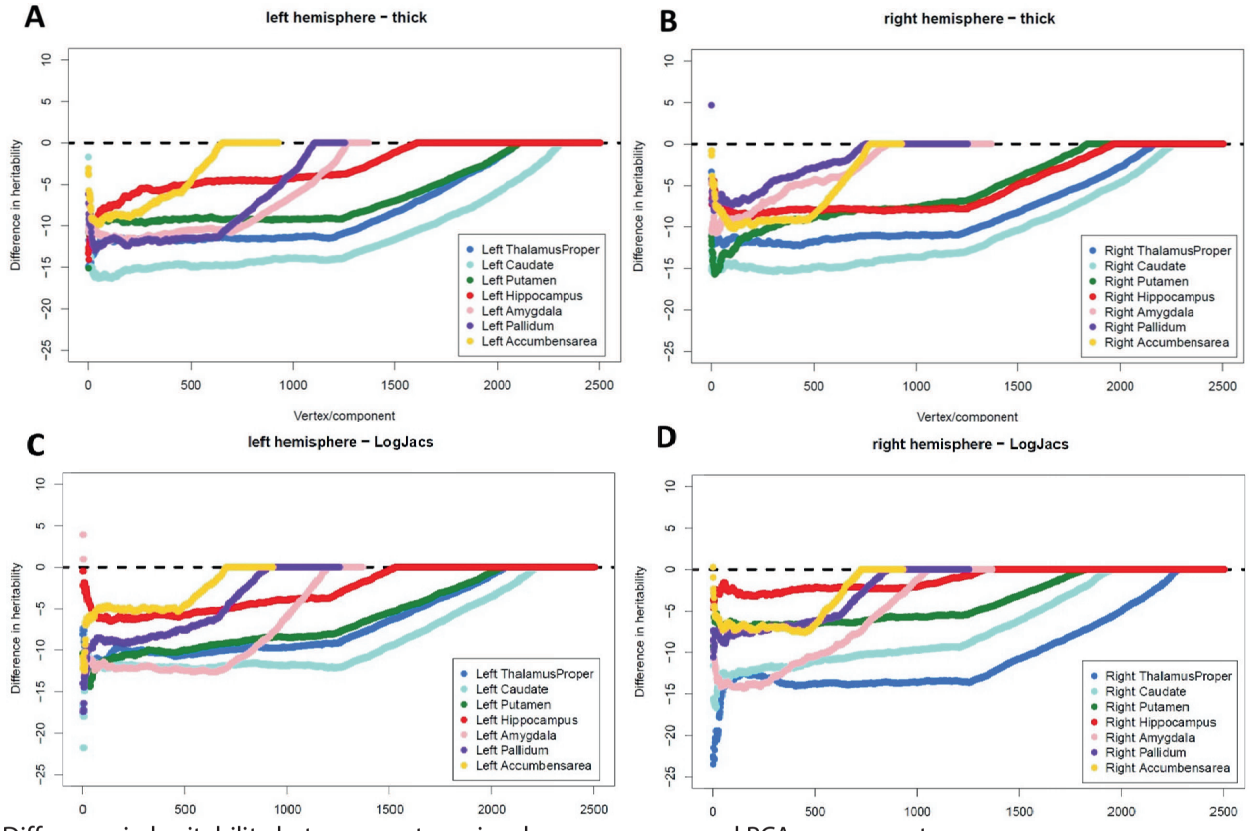

Figure 4 | Difference in heritability between vertex-wise shape measures and PCA components.

The difference between heritability estimates obtained from the vertex-wise shape measures and the heritability of the components obtained through principal component analysis for 7 bilateral subcortical structures. Separate panels are provided for the shape measures of radial distance (A-B) and the Jacobian determinant (C-D) and the left (A,C) and right (B,D) hemisphere. All vertex-wise shape measures and principal components were first sorted in descending order of heritablility, and the vertex-wise measures were substracted from the corresponding component's

The higher vertex-wise heritability could reflect true biological differences in the degree of genetic contribution to the variability in shape. For the cerebral cortex, it has already been shown that different genes influence distinct parts of the brain and that the heritability also differs between regions.[31-33] Subcortical structures are also heterogeneous and consist of functionally diverging sub-regions, such as the nuclei of the pallidum or the head and tail of the caudate. Our results are in line with a recent study by Whelan *et al.* showing that hippocampal subfields differ in their heritability.[34] However, methodological reasons for this difference in heritability should also be considered. Particularly, a lower signal-to-noise ratio in some of the measures might have influenced the results, leading to low heritability estimates. Issues in the segmentation or registration steps will thus obscure true biological differences if these systematically affect certain sub-regions of a structure. We investigated whether this plays a role by overlapping our heritability maps with maps of the technical reproducibility. Indeed, shape measures that could be poorly reproduced were not heritable. However, while high reproducibility was required for detecting a substantial genetic component, it did not necessarily translate into a high heritability. For example, for the shape measures with a high reproducibility (intraclass correlation coefficients > 0.75), a wide range of heritability estimates was observed (0% to 53%). Thus, even when the signal-to-noise ratio was comparable, we still observed regional differences in the degree of genetic contribution. The highly heritable measures are interesting targets for more in-depth genetic studies.

Heritability estimates calculated in our analysis represent both upper and low bounds of narrow-sense heritability. Our results are consistent with the theory that twin-based heritability tends to be higher than population-based estimates. However, we did not find a high correlation between the results, which could be due to several factors. Our population study consisted of relatively older individuals, which may impact the heritability: the effects of non-genetic factors on subcortical structures (e.g., lifestyle factors) accumulate over an individual's lifetime and the overall contribution of genes might be reduced compared to younger individuals. Causal variants not captured on the genotyping array or through subsequent imputation also could lead to a different distribution of the heritability. Additionally, apart from array limitations, non-additive

genetic factors are not taken into account when computing population based heritability. These factors should be taken into account when interpreting our results.

An important question for future research on shape is which variables need to be controlled for in a regression analysis. Here, we aimed to provide an answer by studying two controversial adjustment variables: the total intracranial volume and the gross volume of the structure under study. For the heritability estimates of shape, adjustment for intracranial volume did not affect the results, suggesting that the genes regulating shape are not general brain growth genes, but rather more specific for a structure or its sub-regions. The volume adjustments did change some of the results, but more so for vertices whose shape measures correlate most with the gross volume of the structure. Likely, the genes underlying a structure's gross volume are largely driven by these vertices as they typically represent the widest parts of a structure (highest mean radial distance), where radial measures tend to be highly correlated with its volume. Our results are in agreement with previous work,[35] where the heritability of region-specific measures was reduced after adjustments for the total cortical surface area and thickness.

The detailed information provided by shape measures being their most attractive feature, the increase in dimensionality is potentially counterproductive, especially in the case of genetic homogeneity across a structure. We therefore also performed principal component analyses to demonstrate that the amount of variability explained by the components did not seem related to the heritability: near-zero correlations were found between the order of the components based on the eigenvalues and the heritability estimates. Although the principal component analysis captures most of the variation using fewer variables, methods, which are based on the genetic correlation, may lead to biologically more meaningful results.

While heritability provides an estimate of how much of the variance is determined by genetics, it does not point to specific genetic loci. The most commonly accepted method for gene discovery is to perform an unbiased screen of all genetic variants, i.e. genome-wide association study (GWAS) in order to identify specific genetic factors. However, such efforts require large-scale collaborations in the order of tens of thousands of individuals in order to identify a robust association[18-20,39]. Furthermore, additional

multiple testing correction should be considered when performing GWAS of 54,000 shape measures. This could lead to a loss of power if the effects are homogeneous across a structure. However, if the effects are localized and mostly affect specific vertices, then a GWAS of shape measures may actually increase power since the effect sized will be larger compared to a GWAS of an aggregate volume.

Data reduction methods always rely on assumptions and are often aimed at resolving computational issues. However, with the advent of big data collection, methods have been developed to analyze such large datasets efficiently. Software packages designed for high-dimensional data include MEGHA,[36] for heritability analyses, BOLT-LMM,[37] for genetic correlation analyses, and HASE,[38] for genome-wide association studies. These improvements in software, and also hardware, now pave the way for full-scale analyses without reliance on data reduction methods.

In conclusion, our work demonstrates that the shape of subcortical brain structures is a relevant phenotype for genetic studies, complementary to aggregated measures. Fine-scale maps of genetic influences on the brain are likely to reveal a complex mosaic of genetic modules, with partially divergent sets of genes that drive them.

REFERENCES

1 Bressler, S. L. & Menon, V. *Trends in cognitive sciences* **14**, (2010).
2 Doyon, J. & Benali. *Current opinion in neurobiology* **15**, (2005).
3 Andreasen. *et al.. American Journal of Psychiatry* **150**, 130-130 (1993).
4 Tekin, S. & Cummings, J. L. *Journal of psychosomatic research* (2002).
5 Verstraete, E., Veldink, J. H., den Berg, L. H. & den Heuvel, M. P. *Human brain mapping* **35** (2014).
6 Blokland, et al . *Twin Research and Human Genetics* **15**, (2012).
7 Peper, J. S. *et al. Human brain mapping* **28**, 464-473 (2007).
8 den Braber, A. *et al. Neuroimage* **83**, 98-102 (2013).
9 Gutman. *et al.* in *Info Processing in Medical Imaging* 205-218 (2015).
10 Gutman et al. in *Multimodal Brain Image Analysis* Vol. 8159 Ch. 24,
11 Reuter, M., Wolter, F.-E. & Peinecke, N. *Comput. Aided Des.* **38**, 342-366, (2006).
12 Wang, Y. *et al.* Surface-based *Neuroimage* **56**, 1993-2010,
13 Yonggang, S. *et al.* Metric *Medical Imaging, IEEE Transactions on* **33**, 1447-1463, (2014).
14 Cole, J. H. *et al.. PloS one* (2015).
15 Wade, B. S. C. *et al.* in *SPIE Medical Imaging.* 94171S-94171S-94178
16 McKeown. *et al. BMC Neurol* 2008.
17 Bron, E. E. *et al. Neuroimage* **111**, 562-579 (2015).
18 Bis, J. C. *et al. Nat Genet* **44**, 2012.
19 Stein, J. L. *et al. Nature genetics* **44**, 552-561 (2012).
20 Hibar, D. P. *et al. Nature* **520**, 224,
21 Hofman, A. *et al. EJE* **28**, 889-926,.
22 Ikram, M. A. *et al. EJE* **26**, 811-824,
23 Howie, et al. *Nature genetics* **44**, 955-959 (2012).
24 Fischl, B. *et al. Neuroimage* **23 Suppl 1**, S69-84 (2004).
25 Gutman, B. A. *et al. Neuroimage* **70**, 386-401,(2013).
26 Gutman, B. A. *et al.* in *Biomedical Imaging (ISBI), 2015*.
27 Gutman, et al. in *Biomedical Imaging (ISBI), 2012 9*.
28 Adams. *et al. J Gerontol A Biol Sci Med Sci* (2015).
29 Almasy, L. & Blangero, J. *AJHGs* **62**, 1198-1211 (1998).
30 Benjamini, Y. & Hochberg, Y. *Journal of the Royal Statistical Society. Series B*, 289-300 (1995).
31 Chen, C.-H. *et al. Science* **335**, 1634-1636 (2012).
32 Chen, C.-H. *et al. Neuron* **72**, 537-544 (2011).
33 Chen, C.-H. *et al. PNAs* **110**, 17089-17094 (2013).
34 Whelan, C. D. *et al. Neuroimage* **128**, 125-137 (2016).
35 Eyler, L. T. *et al. Twin Research and Human Genetics* **15**, (2012).
36 Ge, T. *et al. PNA* **112**, (2015).
37 Loh, P.-R. *et al.. Nature genetics* **47**, 284-290 (2015).
38 Roshchupkin, G. *et al.. Scientific Reports* (2016)
39 Adams H.H.H. et al., *Nature Neuroscience* (2016), in press

.

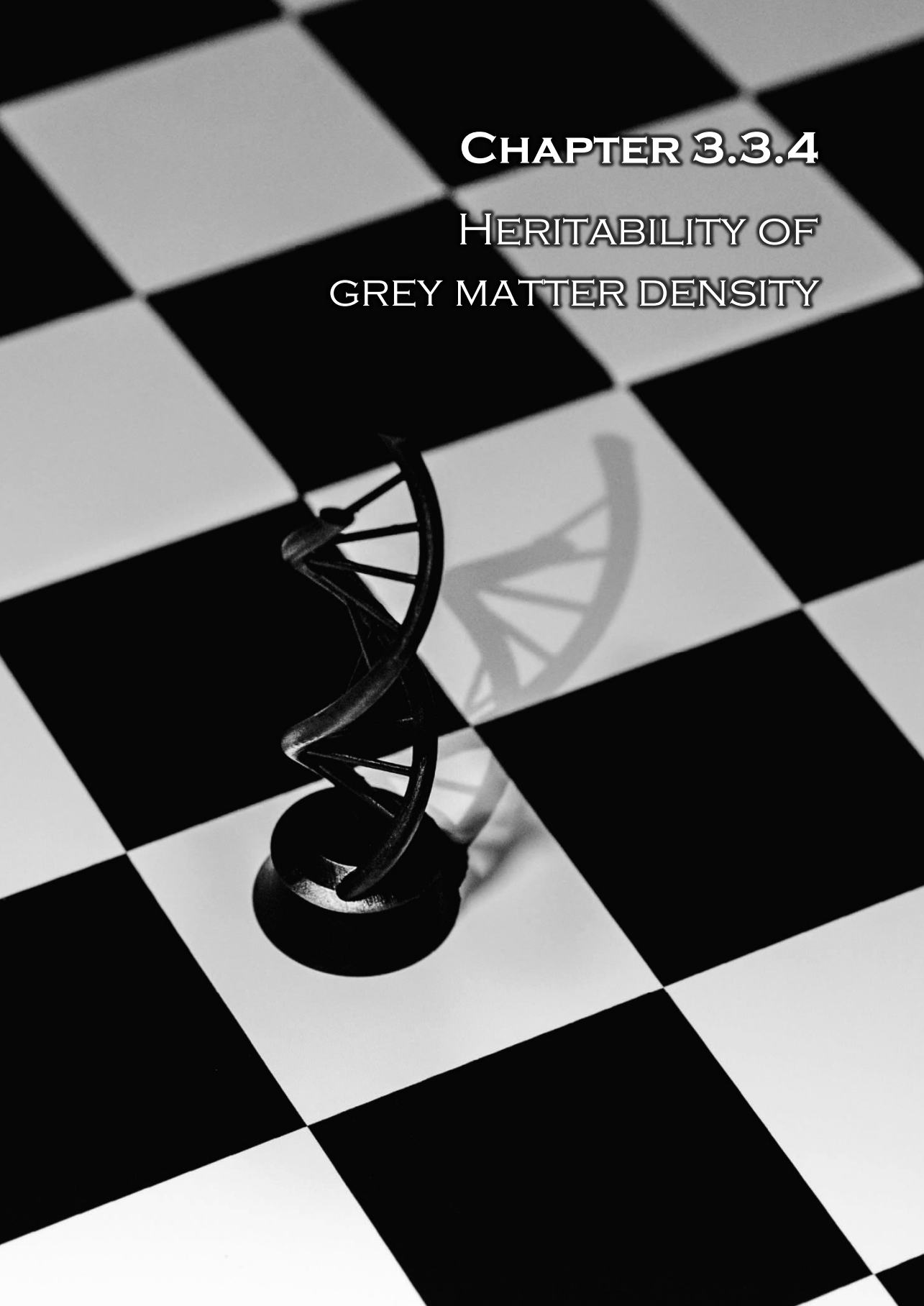

Chapter 3.3.4

Heritability of grey matter density

ABSTRACT

Background: The combination of genetics and imaging has improved our understanding of the brain through studies of aggregate measures obtained from high-resolution structural imaging. Voxel-wise analyses have the potential to provide more detailed information of genetic influences on the brain. Here we report a large-scale study of the heritability of grey matter at voxel resolution (1×1×1mm).

Methods: Validated voxel-based morphometry (VBM) protocols were applied to process MRI data of 3239 unrelated subjects from a population-based study and 491 subjects from two family-based studies. Genome-wide genetic data was used to estimate voxel-wise gray matter heritability of the unrelated subjects and pedigree-structure was used to estimate heritability in families. We subsequently determined whether restricting to the most heritable voxels would enhance association signals for two known genetic variants for subcortical brain volumes.

Results: Voxels significantly heritable in both estimates mapped to subcortical structures, but also voxels in the language areas of the left hemisphere were found significantly heritable, and family-based estimates were higher than population-based estimates. However, regional consistency of the heritability measures across study designs was high (correlation =0.73, $p=2.6\times10^{-13}$). Furthermore, the association signal of known genetic loci for subcortical volume improved by using only the most heritable voxels.

Conclusion: Grey matter voxel-wise heritability can be reliably estimated with different methods. Combining heritability estimates from multiple studies is feasible to construct reliable heritability maps of grey matter voxels.

INTRODUCTION

The human brain shows large inter-individual variation, which could be explained by genetic and environmental influences. Studying these influences is essential in better understanding brain structure and function. The degree to which genetics explains phenotypic variation, in other words heritability, depends on many factors: the actual genetic contribution to the trait, environmental effects, measurement error, study design and sample characteristics [1-3]. Recently an overview was published of fifty years of worldwide heritability research in twins encompassing thousands of traits, showing heritability studies are highly informative on how large the genetic contribution to a trait is [4]. Heritability studies could aid future genetic research to focus on particular regions of interest in the brain. For example, large scale genetic studies of brain structures with the highest heritability typically yield the most findings [5]. When studying the multitude of measures of voxel based magnetic resonance imaging (MRI), limiting genetic studies to the most heritable traits could be feasible in light of multiple testing. Recent studies have focused on heritability of detailed MRI measures at a voxel level [6-12]. Different study designs showed comparably high estimates for white matter tract heritability in twin pairs [9, 12], sib-pairs [7] and extended pedigrees (heritability = 50-90%) [10]. The heritability of grey matter was studied by voxel-based morphometry (VBM) previously [13-15], but the studies were relatively small and relatively large voxels were studied. Moreover, heritability of grey matter VBM has not been estimated in population-based studies.

Table I | Descriptive statistics.

	ERF	ASPS-Fam	RS	p-value
Country	Netherlands	Austrian	Netherlands	
Study type	Family-based	Family-based	Population-based	
Minimum-maximum age	56-76	38-86	46-98	
Age (± SD)	64.3 ± 4.5	64.9 ± 10.7	64.7 ± 10.7	0.86‡
Percentage females	52.5%	60.4%	55.3%	0.13†
N participants with MRI	122	369	3239*	
Total relatives in pedigrees	880	718	-	

*Descriptive statistics of the included studies. ‡ p calculated with one-way ANOVA, † p calculated chi-squared test. *The total number of participants with brain magnetic imaging and genetics data in the Rotterdam study was 4071, but for pairs with more than 0.02 genotype similarity one person was removed ($N_{removed}$ = 832). MRI = Magnetic Resonance Imaging, ERF = Erasmus Rucphen Family study, ASPS-Fam = Austrian Stroke Prevention Family Study, RS = Rotterdam Study, SD= standard deviation.*

Here, we perform a large multi-site study to estimate the voxel-wise heritability of grey matter. We calculate pedigree-based heritability in two family-based studies and heritability based on genome-wide genetic data in a large population-based study of unrelated subjects. Using these approaches, we created two grey matter heritability maps and described which regions contain significantly heritable voxels in both designs. We also estimated overall regional consistency of the heritability measures across study designs and explored if usage of our heritability maps could potentially enhance association signals of two genetic variations, previously discovered by genome-wide association studies [5,16,17].

METHODS

Study subjects and imaging protocol

Rotterdam Study – The Rotterdam Study is a population-based cohort study among inhabitants of a district of Rotterdam (Ommoord), The Netherlands, and aims to examine the determinants of disease and health in the elderly with a focus on neurogeriatric, cardiovascular, bone, and eye disease [18]. In 1990 to 1993, 7983 persons participated and were re-examined every 3 to 4 years (RS-I). In 2000 to 2001 the cohort was expanded by 3011 persons who had not yet been part of the Rotterdam Study (RS-II). All participants had DNA extracted from blood at their first visit. In 2006-2008 a second expansion (RS-III) of 3,932 persons aged 45 and over was realized. Genotyping was performed at the Human Genotyping Facility, Genetic Laboratory Department of Internal Medicine, Erasmus MC, Rotterdam. Genotypes were imputed to the 1000 genomes phase I version 3 reference panel, using standard methods and software [19]. From 2005 onwards MRI is part of the core protocol of the Rotterdam study [20]. For this study a total of 4071 unique study participants had both MRI and genetic data and were available for analysis. The Rotterdam Study has been approved by the Medical Ethics Committee of the Erasmus MC and by the Ministry of Health, Welfare and Sport of the Netherlands, implementing the Wet Bevolkingsonderzoek: ERGO (Population Studies Act: Rotterdam Study). All participants provided written informed consent to participate in the study and to obtain information from their treating physicians.

Erasmus Rucphen Family (ERF) – The ERF study is a family-based cohort study in a genetically isolated population from a community in the South-West of the Netherlands (Rucphen municipality) including 3000 participants. Participants are all descendants of a limited number of founders living in the 19th century, and all of Caucasian European descent. Extensive genealogical data is available for this population. The study population is described in detail elsewhere [21]. In a follow-up analysis, non-demented hypertensive (systolic blood pressure ≥ 160, diastolic blood pressure ≥ 100 or use of antihypertensive medication) subjects aged 55-75 years were included for a new battery of tests, including MRI scanning [22]. These 122 participants from the ERF were related to each other in one large pedigree. This large pedigree was split into multiple small

pedigrees for heritability calculations (pedcut version 1.19 http://mga.bionet.nsc.ru/soft/). Participants related to each other in 27 families with in total 880 relatives. The average size of the pedigrees was 32.6 relatives (range 20-44) with on average 4.5 participants with MRI per family. All participants gave informed consent to participate in the study and to obtain information from their treating physicians. The study was approved by the medical ethics committee at Erasmus MC University Medical Center, Rotterdam, The Netherlands.

MRI scanning for ERF and the Rotterdam Study was done on the same 1.5 T MRI unit (GE Healthcare, Milwaukee, USA, Signa Excite software version 11×) fitted with a dedicated 8-channel head coil. The T1-weighted, proton density-weighted (PDw) and fluid-attenuated inversion recovery (FLAIR) sequences were used [20]. For the purpose of segmentation, the T1w scan is acquired in 3D at high in-plane resolution and with thin slices (voxel size < 1 mm3 [20].

Austrian Stroke Prevention Study (ASPS) – The ASPS study is a single-center, prospective follow-up study on the effects of vascular risk factors on brain structure and function in the normal elderly population of the city of Graz, Austria. The procedure of recruitment and diagnostic work-up of study participants has been described previously [23, 24]. Between 2006 and 2013 the study was extended for the Austrian Stroke Prevention Family Study (ASPS-Fam) [25]. Study participants of the ASPS and their first grade relatives were invited to enter ASPS-Fam. Inclusion criteria were no history of previous stroke or dementia and a normal neurological examination. In total 176 families connecting a total of 719 relatives, among which 369 were study participants with brain-MRI. The average size of the pedigrees was 4 (range 1-10) relatives with on average 2.4 participants with MRI per family. The diagnostic work-up was identical to the original study. The study protocol was approved by the ethics committee of the Medical University of Graz, Austria, and written and informed consent was obtained from all subjects. MRI scanning of the ASPS-Fam was done on a 3.0 T Tim Trio (Siemens, Erlangen). T1-MPRAGE 1×1×1mm was used for image processing [25].

Image processing

Prior to analysis, a number of pre-processing steps were performed. For multispectral image analysis, the different scans were spatially registered using rigid registration [20]. Subsequently, the brain was extracted from the scan. Hereto a manually segmented brain mask, which excludes cerebellum, eyes and skull, was non-rigidly registered to the T1-weighted image using Elastix [20]. Finally, scans were corrected for intensity non-uniformity using the N3 method; non-uniformity correction was carried out within the brain mask [20]. All T1-weighted images were segmented into supra-tentorial grey matter (GM), white matter (WM) and cerebrospinal fluid (CSF). For the Rotterdam Study and ERF, we used a previously described k-Nearest-Neighbor (kNN) algorithm, which was trained on six manually labeled atlases [26]. For the ASPS-Fam study a Quantib BV tissue segmentation tool was applied (www.quantib.org). Quantib® software implements the same algorithm, which we then used for tissue segmentation in the Rotterdam Study and ERF. There are thus no methodological differences between the methods, both of them based on kNN-based segmentation training on manually labeled subjects for segmenting GM, WM and CSF.

Voxel-based morphometry (VBM) was performed by the same optimized VBM protocol in all three studies [27]. FSL software [28] was used for VBM data processing. First, all GM density maps were non-linearly registered to the standard GM probability template. For this study we chose the MNI152 GM template (Montreal Neurological Institute) with a 1×1×1 mm voxel resolution [29]. The MNI152 standard-space T1-weighted average structural template image is derived from 152 structural images, which have been warped and averaged into the common MNI152 coordinate system after high-dimensional nonlinear registration. A spatial modulation procedure was used to avoid differences in absolute grey matter volume due to the registration. This involved multiplying voxel density values by the Jacobian determinants estimated during spatial normalization. To decrease signal to noise ratio, all images were smoothed using a 3 mm (FWHM 8 mm) isotropic Gaussian kernel. Thus all results are in MNI space. Brain regions were segmented using atlas-based segmentation based on the Hammer atlas [30]. The modulation step in the VBM pipeline preserves the volume of a particular tissue within a voxel. The multiplication of the voxel values in the segmented images by the Jacobian

determinants derived from the spatial normalization step allows us to calculate volumes by aggregating voxels. In total we estimated heritability for 1,405,508 grey matter voxels in all three studies.

Heritability analysis

Population-based heritability estimates were calculated using Genome-wide Complex Trait Analysis (GCTA v1.24) [31] (http://cnsgenomics.com/software/gcta/) in the population-based Rotterdam Study. GCTA implements REML (restricted maximum likelihood) analysis, this method compares genotypic similarity between individuals to their phenotypic similarity. Formula's underlying the GCTA method to determine heritability estimates are described elsewhere [3] and thoroughly explained in a commentary by the authors [32]. The 1000 Genomes imputed genotypes (Imputation quality (Rsq) > 0.5 and minor allele frequency (MAF) > 0.01) were used to create a genetic relationship matrix (GRM) in GCTA [33]. The power of GCTA analysis is determined by pair-wise genetic relationships in the studied population [3, 32]. Therefore the three cohorts of the Rotterdam study were combined and analyzed as one in the voxel-wise heritability analysis. Pairwise genetic relatedness between all individuals (N=4071) was calculated and for pairs with more than 0.02 genotype similarity [33] one person was removed ($N_{removed}$ = 832). REML analysis was then performed in the remaining 3239 unrelated subjects using the GRM correcting for age and sex. All grey matter heritability was estimated once.

Family-based heritability was estimated using maximum-likelihood variance components methods implemented in the SOLAR (version 6.6.2) [34] software. Formulas for the calculation of heritability estimates are described in detail elsewhere [34]. Briefly, the algorithms in SOLAR employ maximum likelihood variance decomposition methods. The covariance matrix Ω for a pedigree of individuals is given by:

$$\Omega = 2 \cdot \Phi \cdot \sigma_g^2 + I \cdot \sigma_e^2$$

where σ^2_g is the genetic variance due to the additive genetic factors, Φ is the kinship matrix representing the pair-wise kinship coefficients among all individuals, σ^2_e is the

variance due to individual-specific environmental effects, and I is an identity matrix (under the assumption that all environmental effects are uncorrelated among family members). Narrow sense heritability is defined as the fraction of phenotypic variance σ^2_P attributable to additive genetic factors:

$$h^2 = \frac{\sigma_g^2}{\sigma_P^2}.$$

The variance parameters are estimated by comparing the observed phenotypic covariance matrix with the covariance matrix predicted by kinship (Almasy and Blangero, 1998). Significance of heritability is tested by comparing the likelihood of the model in which σ^2_g is constrained to zero with that of a model in which σ^2_g is estimated. Twice the difference between the $\log_e$ likelihoods of these models yields a test statistic, which is asymptotically distributed as a ½:½ mixture of a χ^2 variable with 1 degree-of-freedom and a point mass at zero. SOLAR outputs the heritability value, the significance value (p), and the standard error for each voxel [8, 34].

ERF study and ASPS-Fam were not jointly analysed because ERF subjects were scanned on a 1.5T MRI and ASPS-Fam subjects on a 3.0T MRI. Instead inverse variance meta-analysis using heritability and heritability standard errors was performed in METAL [35] to boost power and improve stability of heritability estimates [6]. Heritability estimates were calculated in both studies with age and sex as covariates. Variance component methods implemented in SOLAR are vulnerable for inflation if phenotypes have a leptokurtic to distribution. Therefore we applied inverse normal transformations in SOLAR to all voxels, but some voxels still violated the distribution of too high residual kurtosis (kurtosis >0.9) and were therefore excluded [36]. Heritability estimates of 0 with invalid standard errors were also excluded from the meta-analysis. In the family-based studies some voxels had valid p-values and a heritability of 1, but missing standard errors. These voxels were located in the middle of voxel-clusters with high heritability (online viewer reference) (close to 1). Therefore standard errors for such voxels were imputed to retain these voxels for meta-analysis. In practice this resulted in imputation of the standard error for 6.4% of voxels in ERFand a negligible percentage in ASPS(<0.001%).

Enhancement of association signal

We explored whether voxel heritability information could enhance the association of genetic variants with brain structures. The genetic variants most significantly associated with hippocampal volume (rs77956314 on 12q24.22, near the gene *HRK*) and putamen volume (rs945270 on 14q22.3, downstream of the gene *KTN1*) were selected from a recently published genome-wide association study on subcortical structures [5]. To select the most heritable voxels in the hippocampus and putamen, we ordered them using three approaches. First, we ranked the voxels from low to high family-based heritability estimates. Second, we ranked them from low to high population-based heritability estimates. In the third approach we summed the ranks obtained from both the family- and population-based estimates and used the sum of the ranks to prioritize the voxels. Using these three approaches we excluded the voxels in a step-wise manner by removing the 5% least heritable voxels. For each step we computed the volume by summing the values of the remaining voxels. As a voxel represents grey matter density in 1 mm^3, the sum of voxels gives the volume of grey matter. We determined the association of the two genetic variants in an additive model with the volumes in linear regression analyses (adjusted for age, sex, and the first three principal components) and compared this to association of the volume derived from all voxels mapped to the structure (i.e. the total VBM-volume of the hippocampus or putamen). The p-value of the association of the genetic variants with the subsets of voxels divided by the p-value of the association of the genetic variants with the total VBM-volume was calculated to measure change in the strength of the association. Genetic effects were calculated in the three cohorts of the Rotterdam study separately (RS-I = 844, RS-II = 1003, RS-III = 2190) and were combined using an inverse variance weighted meta-analysis in METAL [35].

Statistical analysis

Descriptive statistics were compared using one-way ANOVA and chi-squared tests. To estimate the significance of heritability results we estimated the FDR p-value threshold [37] for both population ($p<2.78\times10^{-3}$) and family heritability ($p<1.91\times10^{-2}$) maps separately.

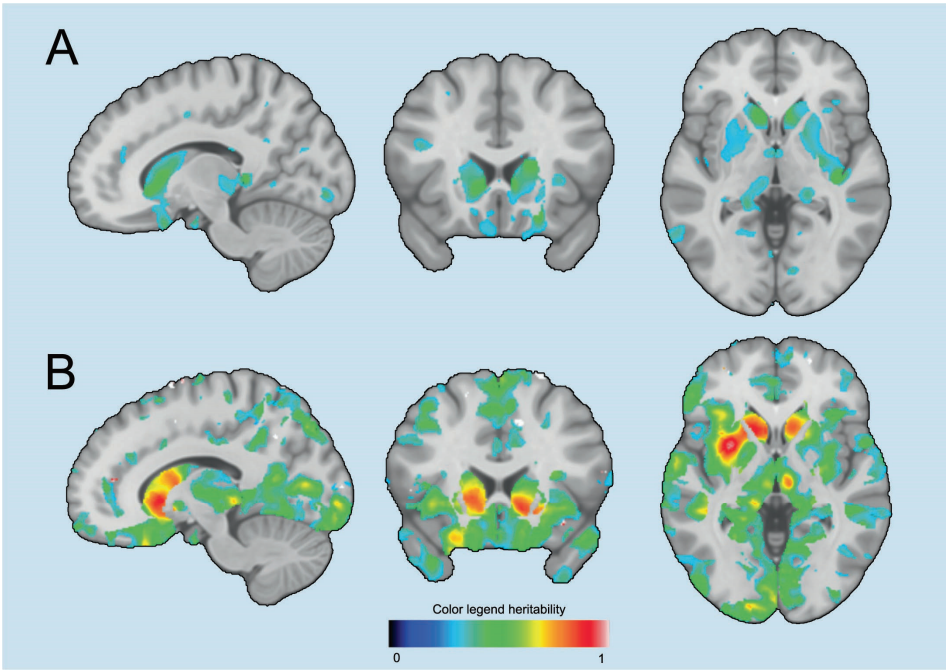

Figure 1 | Example of FDR-Significant voxels in both population-based (A) and family-based (B) estimates.

Significant voxels cluster in subcortical structures, such as the caudate nucleus. All results can be interactive accessed (www.imagene.nl/heritability) and downloaded from the website.

RESULTS

Population characteristics

Characteristics of the study population are shown in Table 1. The spread of the age of subjects in the ERF study (age range 55-76) was smaller compared to ASPS-Fam (38-86) and the Rotterdam Study (46-98) due to the fact that inclusion criteria for scanning was restricted to midlife (Table 1). However, the average age at the time of MRI-scanning of the cohorts was very similar, ranging from 64.3 (± 4.5) years in the ERF study, 64.9 (± 10.7) years in ASPS and 64.9 (± 10.7) in the Rotterdam Study ($p = 0.86$). The percentage of women was 52.5% in ERF, 60.4% in ASPS-Fam and 55.3% in the Rotterdam study, these differences were non-significant ($p = 0.13$) (Table 1).

Heritability estimates

In total 454,184 (33.3% of all voxels) were FDR-significant in the family-based estimates. Mean heritability of significant voxels was 0.44 ± 0.12 SD (all voxels 0.29 ± 0.17 SD), with heritability estimates ranging from 0.23 to 1. In total 68,616 (4.9% of all voxels) were FDR-significant in the population-based estimates. Mean heritability of the significant voxels was 0.34 ± 0.04 SD (all voxels 0.11 ± 0.10), with heritability estimates ranging from 0.25 to 0.56. We found heritability of 44,349 voxels (3.2% of all voxels) to be FDR significant in the family- as well as the population-based heritability estimates. These significantly heritable voxels were clustered, mostly within subcortical brain structures (Figure 1). Table 2 shows the percentage of voxels that were significantly heritable of the total of voxels in a structure in both estimates, as well as the average regional heritability, considering all voxel-wise heritability estimates. Highest percentage of significantly heritable in both estimates voxels were located in the caudate nucleus (right 72.4% and left 68.6%) followed by the putamen (right 57.5% and left 32.6%). Other subcortical structures with a large percentage of significantly heritable voxels were; left pallidum (32.2%), left nucleus accumbens (29.7%), right pallidum (28.5%), left amygdala (21.4%), left hippocampus (17.9%), left thalamus (14.4%), right amygdala (12.8%) and the right insula (11.4%). Apart from the subcortical structures, parts of the right lateral occipitotemporal gyrus (gyrus fusiformis) (10.4%), left straight gyrus (gyrus rectus) (10.4%), left subcallosal area (8.0%) and the left lingual gyrus (7.9%) harbored a

proportion significantly heritable voxels. In the parietal lobe and the frontal lobe the number of voxels that was significantly heritable in both estimates was low. (Table 2 and Figure 1).

When comparing regional heritability, estimates calculated in families was always higher than the population-based estimates ($p<0.001$) (Figure 2 A) and the difference in heritability between family-based estimates and population-based estimates was relatively stable (mean difference of regional heritability = 0.21 ± 0.08) (Table 2). Therefore, the regional heritability pattern of the family-based estimates significantly predicted the regional pattern of heritability in the population-based study (Pearson's correlation coefficient = 0.73, $p = 2.6 \times 10^{-13}$) (Figure 2 B).

Enhancement of association signal

We explored if applying our heritability map could enhance the statistical association signal of previously discovered genome-wide significant loci. As expected the T-allele of rs77956314 (*HRK*) associated with a smaller total volume of the hippocampus ($p = 5.1 \times 10^{-7}$) and the C-allele of rs945270 (*KTN1*) significantly associated with larger total volume of the putamen ($p = 4.3 \times 10^{-3}$). When excluding the less heritable voxels the average heritability in the remaining voxels increased (Figure 3 A and 3B). With rising average heritability we observed a gradual decrease in p-values (Figure 3 C), thus a more significant association of *HRK* with hippocampal volume. The maximum enrichment of association was reached when the 10% most significantly heritable voxels when combining heritability information from family-based and population-based studies was used. This increase corresponds to a 95.9 times more significant association, as the *p*-value decreased from $p=5.1 \times 10^{-7}$ to $p = 5.4 \times 10^{-9}$. Using only the family-based estimates the association was 12.9 times more significant. A less substantial decrease in p-value was observed for the effect of *KTN1* on putamen (Figure 3 D). The p-value decreased when restricting to voxels that belong to the 25% most heritable voxels from the only the family-based study. This corresponds to a 5.5 times more significant association (*p*-value decrease from $p = 4.3 \times 10^{-3}$ to $p = 7.9 \times 10^{-4}$).

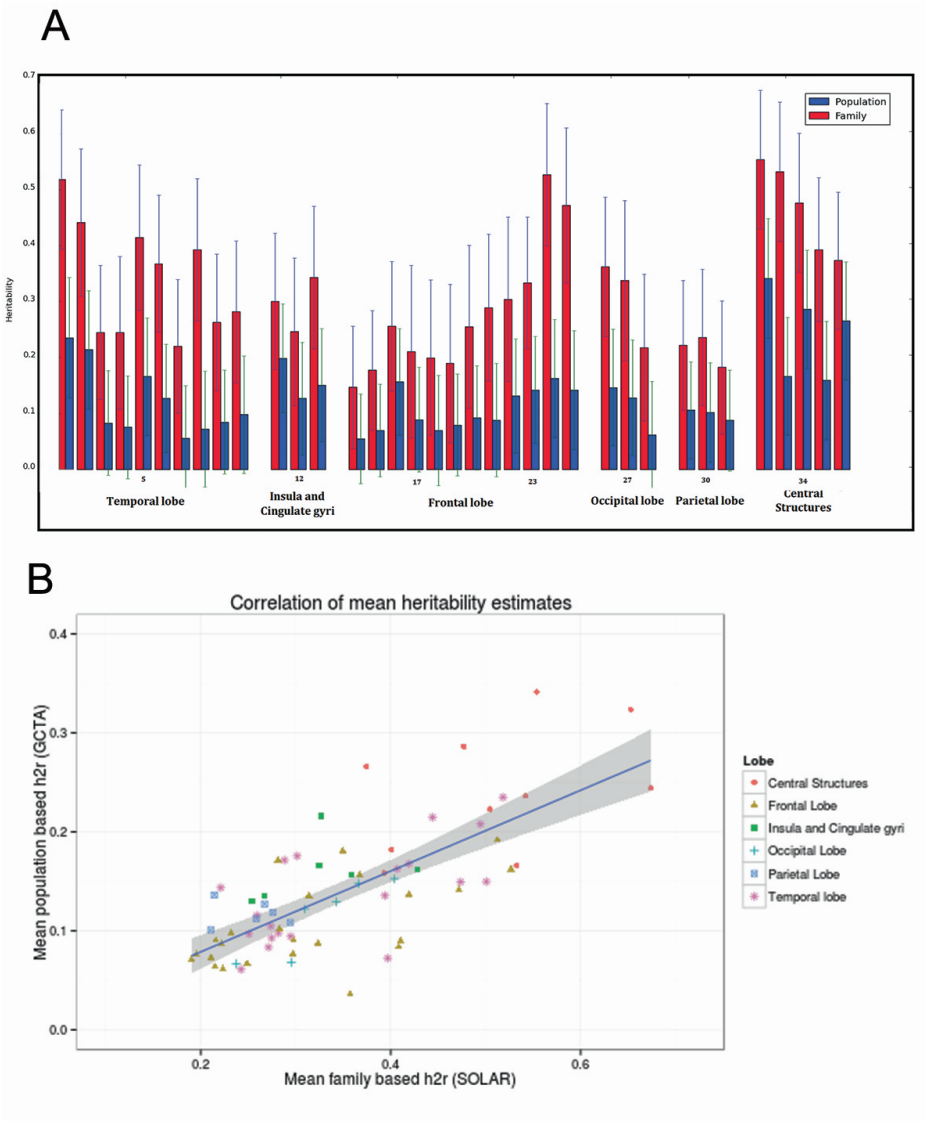

Figure 2 | A bar plot showing regional brain heritability.

Structures that are in both the left as well as the right hemisphere were averaged for this figure. It can clearly be seen that the heritability from family-based studies is higher than heritability form the unrelated population (P<0.001). B Scatter plot of the average regional heritability of all brain structures. The correlation of the family-based and population-based estimates was high (Pearson's correlation coefficient = 0.73, $p = 2.6 \times 10^{-13}$). Data points per structure correspond to family and population heritability in table 2.

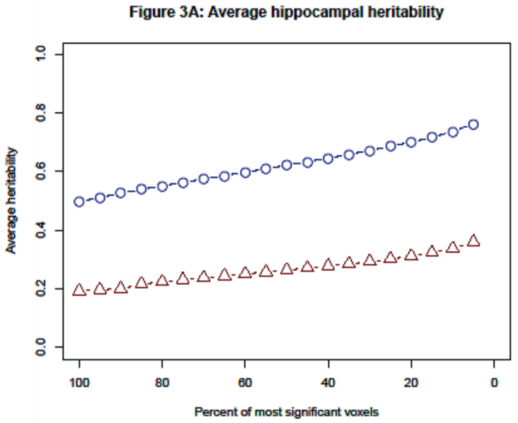

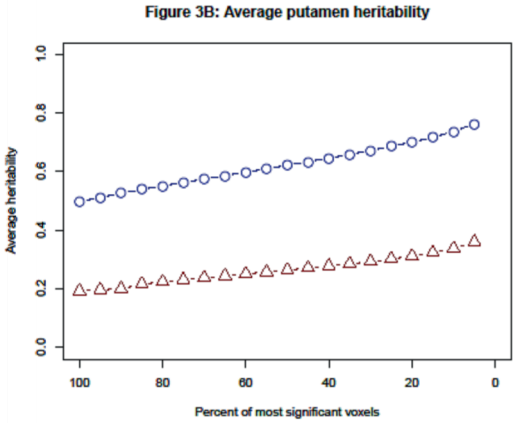

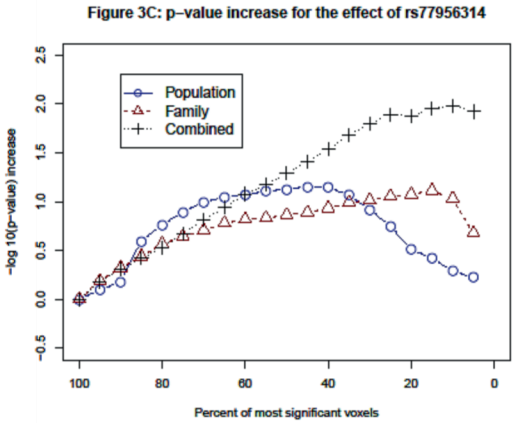

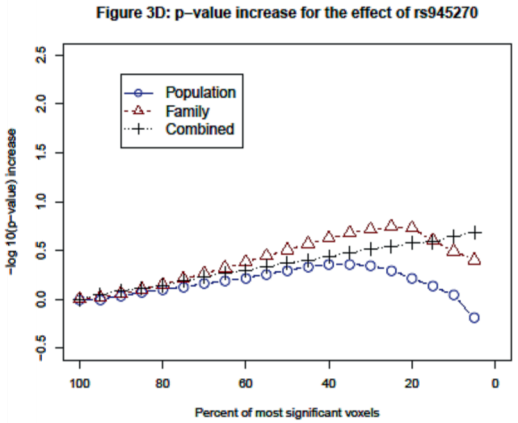

Figure 3 | Enhancement of the association signal of variants with the most heritable voxels of the hippocampus and putamen.

A,B: Average heritability (y-axis) of the voxels in hippocampus (A) and putamen (B) given a percentage of the most heritable voxels in that region (x-axis) in steps of 5%. C,D: The -log(p-value) increase comparing the p-value of association with subsets of the most heritable voxels and all voxels in the region. The –log(p-value) increase for association of hippocampal with rs77956314 (HRK gene) and putamen voxels with rs945270 (KTN1 gene) is shown. Associations were corrected for age, sex, and the first three principal components.

DISCUSSION

In this study we presented grey matter voxel heritability maps at resolution of 1×1×1 mm from population- and family-based studies. First we found that clusters of voxels that are significantly heritable in family-based heritability estimates as well as in an unrelated population-based study are predominantly located in subcortical regions. Second, when comparing the overall regional patterns of voxel-wise heritability the family-based estimates were always higher compared to population-based estimates and predicted the population-based heritability estimates. Lastly, we showed that the heritability estimates from our studies could be used to enhance the association signal of two genetic variants with subcortical volumes.

Voxels with significant heritability formed clusters within mainly the subcortical structures. This is in line with the findings of previous studies that the volumes of subcortical structure are among the most heritable in the brain [38]. The average heritability of voxels in brain structures was comparable with the volume-based heritability estimates from previous studies. For instance the average voxel-based heritability of the hippocampus was approximately 0.52 in our family-based estimate and 0.21 population-based estimates (Figure 2). Volume-based estimates from family-based ranged from 0.4 to 0.7 [39] and in a population-based study it was 0.12 [95% CI 0.08-0.16] [5]. There are multiple explanations for this consistent finding. First, subcortical structures probably are under tight genetic control as they exert vital functions within the brain. Second, subcortical structures are technically better registered compared to other parts of the brain as they are smaller and have a more uniform shape over individuals than cortical foldings. This reduces measurement error and therefore increases estimated heritability. Finally, environmental effects could have a larger effect on cortical grey matter compared to subcortical structures. Differences in training of the brain and the occurrence of disease can lead to differences in an individuals' size and shape of grey matter, decreasing heritability. As the effects of non-genetic factors (e.g. lifestyle factors) accumulate over an individual's lifetime and the overall contribution of genes might be reduced compared to younger individuals [39]. We studied relatively old

participants (~65 years), therefore study participants might have reduced estimated heritability because of their older age.

Apart from the subcortical structures, we found three cortical regions in the left hemisphere, the dominant hemisphere in over 95% of individuals, involved in speech production and word processing to have more than 5% significant voxels; the subcallosal area (also called Broca area), central part of the superior temporal gyrus (contains Wernicke's area) and the lingual gyrus. Moreover, their right counterparts contained less significant voxels compared to the left side. Language skills[40] and brain networks [41] are thought to be under tight genetic control and the left hemisphere language areas have been found more heritable than the right hemisphere before [14]. Regions with significant heritability could in theory be connected by white matter connections, which in turn then also are under high genetic control, suggesting a common genetic architecture. In a recent report evidence for this theory was found [42]. Cortical thickness in some regions with high heritability, were connected by heritable white matter connections. These connections and the cortical regions were anatomically distant but showed significant genetically correlation [42].

We found a relatively stable difference in the regional patterns of the total additive genetic heritability. The heritability calculated from familial relations was always higher than the total additive variance explained by all autosomal variants calculated in unrelated subjects. This known difference between family and population-based heritability estimates has been extensively described [43, 44]. The difference can in part be explained by overestimation of heritability in families due to sharing of environmental factors within the family. These factors are interpreted as genetic effects and cause the overestimation of heritability in twin and nuclear family studies [45]. Subjects in multi-generational families share less environmental factors. Therefore multi-generational families, as ASPS-Fam and especially the ERF study, are more likely to yield an unbiased estimate of heritability. However, we assumed that all environmental factors affecting brain voxel volume are uncorrelated among family members (unique environmental effects) therefore some unassessed common environmental effects might be causing the higher heritability in our family-based estimates. At the same time an

underestimation of the heritability calculated from genetic data in unrelated populations could occur because of an incomplete coverage of the causal variants and exclusion of rare variants. We used imputed data to increase coverage of the causal variants. Imputed data provide a much denser coverage of the genome than only genotyped variants, but we did exclude rare variants (MAF<0.01) which may in part be responsible for some missing heritability.

The overall regional patterns of heritability from families strongly predicted the population-based heritability. This suggests that the regional pattern of variance explained by additive genetic effects is similar across populations, despite different ways to measure heritability, study design and scanner types. On the website (http://www.imagene.nl/heritability) both the population-based estimates and the family-based estimates can be viewed separately and can be downloaded. Combining current maps with results from other studies will further increase accuracy of the heritability estimates.

Heritability in genetic studies

Within the putamen and hippocampus we observed highly heritable clusters of grey matter voxels alternating with parts of the subcortical structures that were less heritable. Differences in heritability within structures might be due to technical limitations (e.g. voxels that are difficult to measure) or due to genetic or functional correlations. We hypothesized that studying the genetics of only highly heritable voxels could enhance signals in imaging genetics, either through reducing signal to noise ratio or through studying a more genetically homogeneous trait. We picked two genetic variants with a proven and strongly replicated biological effect, identified through genome-wide association studies, on the subcortical structure volume (hippocampus, putamen) to explore if enhancement was possible [5]. We show enhancement of the statistical signal of almost hundred-fold for the association of HRK (rs77956314) with hippocampal volume and a five-fold increase for the association of KTN1 (rs945270) with putamen volume From Figure 3 we can deduct that for future genetic studies this translates to the maximum power for association analyses using voxels with a heritability over 30% from the population-based heritability estimates and a heritability over 70% from family-

based heritability estimates. Despite these encouraging results there are limitations of our analysis. First, we only tested two genetic variants in two subcortical structures. While we expect that the increased signal of genetic variants with more heritable voxels will not be limited to the two variants tested in current study, future studies applying this method should be performed to determine whether this truly is the case. Second, we calculated heritability estimates and genetic association of HRK and KTN1 variants with voxels in the same subjects of the Rotterdam Study. As voxels with a large (technical) measurement error have lower heritability and therefore were excluded first in our analysis, the decreased measurement error of the more heritable voxels could result in the more significant association of genetic variants. In other words, the enhancement of signal is a reflection of a higher signal to noise ratio. Also a higher test re-test reliability of the highly heritable voxels, reduce signal to noise ratio. Third, we used the same data for the calculation of population-based heritability estimates and genetic testing, resulting in a possible inflation of the increase in signal due to non-independence [46]. However, when only the family-based heritability estimates were used to select the voxels for genetic associations in the population-based study (Figure 3 C, D) the analyses were independent. . In these analyses, we still observed an increase in the signal – and the enhancement was actually even stronger for the putamen – arguing against inflation due to non-independence. However, for the hippocampus the best enhancement was achieved using the combined sample when restricting to 50% or less of the most significant voxels. While this could be due to non-independence, that is contradicted by the fact that the population-only results (i.e., fully dependent) are in fact worse. An explanation other than non-independence could be that the combined sample provides more accurate heritability estimates and therefore results in a better enhancement. Last, highly heritable voxels which are in close proximity of each other could share their genetic background. However finding a cluster of heritable voxels does not directly prove genetic correlation.

Strengths and limitations

Major strengths of this study are the large sample size of the population based study and unified imaging processing. Subjects from ERF and the Rotterdam Study subjects

were scanned using the same 1.5T scanner, identical MRI protocols and images were processed with exactly the same software. The ASPS-Fam was scanned on a 3T scanner, but segmented using similar protocols and VBM processing was performed in the same way as ERF and the Rotterdam Study. Important to note is that softwares used for tissue segmentation are different, but both implement the same kNN algorithm [26]. The ERF and the Rotterdam Study both are both from the Netherlands, a genetically homogeneous country [47]. The ASPS-Fam study is from Austria, Austrians likely have slightly different genetic architecture than the Dutch. The estimation of the heritability parameters uses maximum likelihood iterative optimization, which is prone to convergence failures (i.e. heritability = 0 and missing standard error). The methods used for population-based estimation of heritability always output an estimate. The percentage of voxels that did not converge was 9% in ASPS-Fam ($N_{participants}$ = 369) and 36% in ERF ($N_{participants}$ = 122). It has been shown that not converging occurs frequently in small datasets in SOLAR producing conservative estimates [45, 48]. We further note that using only VBM to assess heritability of brain morphology is a limitation of the current study. Cortical thickness, surface area and other MRI measures, including tensor-based (i.e. deformation) morphometry (TBM) [49, 50] and shape analysis are all potentially interesting for future heritability and genetic studies. The differences between measures have been attributed both to biology [51, 52] and methodology [53, 54]. Most probably, these measures reflect a different genetic architecture [51] and should therefore be studied separately.

Future perspectives

Genetic associations with subsets of voxels within an anatomical structure could be biologically relevant as it shows an important genetic contribution to this subregion of the brain, and these subregions could have clinical significance. It was shown previously that different parts of anatomically defined brain regions contribute differently to clinical outcomes, for example the hippocampal subfields[55, 56]. If only highly heritability brain voxels are studied in future voxel-wise genome-wide association studies we do not expect statistical signals to be uniformly enhanced. However, for the tested genetic variant that was identified for putamen volume, we did find statistical enhancement. High heritability estimates capture a variety of sources that can affect power to detect associations, including lower signal to noise ratios and higher genetic homogeneity (i.e.

genetic correlation). Using these benefits to increase statistical signal is desirable, irrespective of the underlying cause. Ideally we envision selecting groups of voxels for genetic studies based on high heritability and measured high genetic correlation. Genetic correlation can be calculated for any of the commonly used MRI-measures, but it would still require genetic testing of sufficiently powered (large) studies. A promising future direction would be to enable the calculation of genetic correlations, genetic association (millions of voxels times millions of genetic variants) and meta-analyses of these associations. Programs which make the calculation of genetic correlation and genetic association computationally possible in sufficiently powered studies (i.e. meta-analyses) are essential to the field. Currently these programs tailored to large scale genetic studies are developed and genetic studies started. The results of these studies will be able to prove to which extend clusters of heritable voxels have a common genetic architecture.

CONCLUSIONS

Heritability estimates can be reliably estimated using different methods and on different cohorts and combining heritability estimates from multiple studies leads to the construction of a reliable heritability map of grey matter. These maps can be used to prioritize highly heritable regions in future genetic imaging studies.

REFERENCES

1. Visscher PM, Hill WG, Wray NR. *Nat Rev Genet*. 2008;9:255-266
2. Visscher PM, Medland SE, Ferreira MA, Morley KI, Zhu G, Cornes BK, et al.. *PLoS Genet*. 2006;2:e41
3. Yang J, Benyamin B, McEvoy BP, Gordon S, Henders AK, Nyholt DR, et al.. *Nat Genet*. 2010;42:565-569
4. Polderman TJ, Benyamin B, de Leeuw CA, Sullivan PF, van Bochoven A, Visscher PM, et al.. *Nat Genet*. 2015;47:702-709
5. Hibar DP, Stein JL, Renteria ME, Arias-Vasquez A, Desrivieres S, Jahanshad N, et al. *Nature*. 2015;520:224-
6. Jahanshad N, Kochunov PV, Sprooten E, Mandl RC, Nichols TE, Almasy L, et al. *Neuroimage*. 2013;81:455-
7. Jahanshad N, Lee AD, Barysheva M, McMahon KL, de Zubicaray GI, Martin NG, et al. *Neuroimage*. 2010;52:455-469
8. Kochunov P, Jahanshad N, Marcus D, Winkler A, Sprooten E, Nichols TE, et al. *Neuroimage*. 2015;111:300-
9. Kochunov P, Glahn DC, Lancaster JL, Winkler AM, Smith S, Thompson PM, et al. *Neuroimage*. 2010;53:1109-1116
10. Ganjgahi H, Winkler AM, Glahn DC, Blangero J, Kochunov P, Nichols TE. *Neuroimage*. 2015;115:256-268
11. Kochunov P, Fu M, Nugent K, Wright SN, Du X, Muellerklein F, et al. *Hum Brain Mapp*. 2016;37:525-535
12. Brouwer RM, Mandl RC, Peper JS, van Baal GC, Kahn RS, Boomsma DI, et al. *Neuroimage*. 2010;53:1085-
13. Hulshoff Pol HE, Schnack HG, Posthuma D, Mandl RC, Baare WF, van Oel C, et al. Genetic contributions to human brain morphology and intelligence. *J Neurosci*. 2006;26:10235-10242
14. Thompson PM, Cannon TD, Narr KL, van Erp T, Poutanen VP, Huttunen M, et al. Genetic influences on brain structure. *Nat Neurosci*. 2001;4:1253-1258
15. Peper JS, Schnack HG, Brouwer RM, Van Baal GC, Pjetri E, Szekely E, et al. Heritability of regional and global brain structure at the onset of puberty: A magnetic resonance imaging study in 9-year-old twin pairs. *Hum Brain Mapp*. 2009;30:2184-2196
16. Bis JC, DeCarli C, Smith AV, van der Lijn F, Crivello F, Fornage M, et al. Common variants at 12q14 and 12q24 are associated with hippocampal volume. *Nat Genet*. 2012;44:545-551
17. Stein JL, Medland SE, Vasquez AA, Hibar DP, Senstad RE, Winkler AM, et al. Identification of common variants associated with human hippocampal and intracranial volumes. *Nat Genet*. 2012;44:552-561
18. Hofman A, Brusselle GG, Darwish Murad S, van Duijn CM, Franco OH, Goedegebure A, et al. The rotterdam study: 2016 objectives and design update. *Eur J Epidemiol*. 2015;30:661-708
19. Willer CJ, Sanna S, Jackson AU, Scuteri A, Bonnycastle LL, Clarke R, et al. Newly identified loci that influence lipid concentrations and risk of coronary artery disease. *Nat Genet*. 2008;40:161-169
20. Ikram MA, van der Lugt A, Niessen WJ, Koudstaal PJ, Krestin GP, Hofman A, et al. The rotterdam scan study: Design update 2016 and main findings. *Eur J Epidemiol*. 2015;30:1299-1315
21. Sayed-Tabatabaei FA, van Rijn MJ, Schut AF, Aulchenko YS, Croes EA, Zillikens MC, et al. Heritability of the

function and structure of the arterial wall: Findings of the erasmus rucphen family (erf) study. *Stroke*. 2005;36:2351-2356
22. Ibrahim-Verbaas CA, Zorkoltseva IV, Amin N, Schuur M, Coppus AM, Isaacs A, et al. Linkage analysis for plasma amyloid beta levels in persons with hypertension implicates abeta-40 levels to presenilin 2. *Hum Genet*. 2012;131:1869-1876
23. Schmidt R, Lechner H, Fazekas F, Niederkorn K, Reinhart B, Grieshofer P, et al. Assessment of cerebrovascular risk profiles in healthy persons: Definition of research goals and the austrian stroke prevention study (asps). *Neuroepidemiology*. 1994;13:308-313
24. Schmidt R, Fazekas F, Kapeller P, Schmidt H, Hartung HP. Mri white matter hyperintensities: Three-year follow-up of the austrian stroke prevention study. *Neurology*. 1999;53:132-139
25. Seiler S, Pirpamer L, Hofer E, Duering M, Jouvent E, Fazekas F, et al. Magnetization transfer ratio relates to cognitive impairment in normal elderly. *Front Aging Neurosci*. 2014;6:263
26. Vrooman HA, Cocosco CA, van der Lijn F, Stokking R, Ikram MA, Vernooij MW, et al. Multi-spectral brain tissue segmentation using automatically trained k-nearest-neighbor classification. *Neuroimage*. 2007;37:71-81
27. Good CD, Johnsrude IS, Ashburner J, Henson RN, Friston KJ, Frackowiak RS. A voxel-based morphometric study of ageing in 465 normal adult human brains. *Neuroimage*. 2001;14:21-36
28. Smith SM, Jenkinson M, Woolrich MW, Beckmann CF, Behrens TE, Johansen-Berg H, et al. Advances in functional and structural mr image analysis and implementation as fsl. *Neuroimage*. 2004;23 Suppl 1:S208-219
29. Fonov V, Evans AC, Botteron K, Almli CR, McKinstry RC, Collins DL, et al. Unbiased average age-appropriate atlases for pediatric studies. *Neuroimage*. 2011;54:313-327
30. Hammers A, Allom R, Koepp MJ, Free SL, Myers R, Lemieux L, et al. *Hum Brain Mapp*. 2003;19:224-247
31. Yang J, Lee SH, Goddard ME, Visscher PM. Gcta: A tool for genome-wide complex trait analysis. *Am J Hum Genet*. 2011;88:76-82
32. Visscher PM, Yang J, Goddard ME. . (2010). *Twin Res Hum Genet*. 2010;13:517-524
33. Adams HH, Verlinden VJ, Callisaya ML, van Duijn CM, Hofman A, Thomson R, et al. Heritability and genome-wide association analyses of human gait suggest contribution of common variants. *J Gerontol A Biol Sci Med Sci*. 2015
34. Almasy L, Blangero J. Multipoint quantitative-trait linkage analysis in general pedigrees. *Am J Hum Genet*. 1998;62:1198-1211
35. Willer CJ, Li Y, Abecasis GR. Metal: Fast and efficient meta-analysis of genomewide association scans. *Bioinformatics*. 2010;26:2190-2191
36. Blangero J, Williams JT, Almasy L. Variance component methods for detecting complex trait loci. *Adv Genet*. 2001;42:151-181
37. Benjamini Y, Hochberg Y.. *J Roy Stat Soc B Met*. 1995;57:289-300
38. Blokland GA, de Zubicaray GI, McMahon KL, Wright MJ. Genetic and environmental influences on neuroimaging phenotypes: A meta-

analytical perspective on twin imaging studies. *Twin Res Hum Genet*. 2012;15:351-371
39. Batouli SA, Trollor JN, Wen W, Sachdev PS. The heritability of volumes of brain structures and its relationship to age: A review of twin and family studies. *Ageing Res Rev*. 2014;13:1-9
40. Gayan J, Olson RK. Reading disability: Evidence for a genetic etiology. *Eur Child Adolesc Psychiatry*. 1999;8 Suppl 3:52-55
41. Budisavljevic S, Dell'Acqua F, Rijsdijk FV, Kane F, Picchioni M, McGuire P, et al. Age-related differences and heritability of the perisylvian language networks. *J Neurosci*. 2015;35:12625-12634
42. Shen KK, Dore V, Rose S, Fripp J, McMahon KL, de Zubicaray GI, et al. *Hum Brain Mapp*. 2016
43. Zuk O, Hechter E, Sunyaev SR, Lander ES. The mystery of missing heritability: Genetic interactions create phantom heritability. *Proc Natl Acad Sci U S A*. 2012;109:1193-1198
44. Zuk O, Schaffner SF, Samocha K, Do R, Hechter E, Kathiresan S, et al. Searching for missing heritability: Designing rare variant association studies. *Proc Natl Acad Sci U S A*. 2014;111:E455-464
45. Koran ME, Thornton-Wells TA, Jahanshad N, Glahn DC, Thompson PM, Blangero J, et al.. *J Med Imaging (Bellingham)*. 2014;1:014005
46. Kriegeskorte N, Simmons WK, Bellgowan PS, Baker CI.. *Nat Neurosci*. 2009;12:535-540
47. Boomsma DI, Wijmenga C, Slagboom EP, Swertz MA, Karssen LC, Abdellaoui A, et al. The genome of the netherlands: Design, and project goals. *Eur J Hum Genet*. 2014;22:221-227
48. Blangero J, Diego VP, Dyer TD, Almeida M, Peralta J, Kent JW, Jr., et al. *Adv Genet*. 2013;81:1-31
49. Brun CC, Lepore N, Pennec X, Lee AD, Barysheva M, Madsen SK, et al. Mapping the regional influence of genetics on brain structure variability--a tensor-based morphometry study. *Neuroimage*. 2009;48:37-49
50. Yoon U, Perusse D, Lee JM, Evans AC.. *Neurosci Lett*. 2011;493:8-13
51. Winkler AM, Kochunov P, Blangero J, Almasy L, Zilles K, Fox PT, et al. Cortical thickness or grey matter volume? The importance of selecting the phenotype for imaging genetics studies. *Neuroimage*. 2010;53:1135-1146
52. Voets NL, Hough MG, Douaud G, Matthews PM, James A, Winmill L, et al. Evidence for abnormalities of cortical development in adolescent-onset schizophrenia. *Neuroimage*. 2008;43:665-675
53. Hutton C, Draganski B, Ashburner J, Weiskopf N. g. *Neuroimage*. 2009;48:371-380
54. Blankstein U, Chen JYW, Mincic AM, McGrath PA, Davis KD. The complex minds of teenagers: Neuroanatomy of personality differs between sexes. *Neuropsychologia*. 2009;47:599-603
55. Schroeder C, Park MT, Germann J, Chakravarty MM, Michels L, Kollias S, et al. Hippocampal shape alterations are associated with regional abeta load in cognitively normal elderly individuals. *Eur J Neurosci*. 2016
56. Kuhn S, Musso F, Mobascher A, Warbrick T, Winterer G, Gallinat J. Hippocampal subfields predict positive symptoms in schizophrenia: First evidence from brain morphometry. *Transl Psychiatry*. 2012;2:e127

Chapter 4

Understanding pathophysiology

Chapter 4.1

Candidate phenotypes

Chapter 4.1.1

Alzheimer disease genes and markers of brain aging

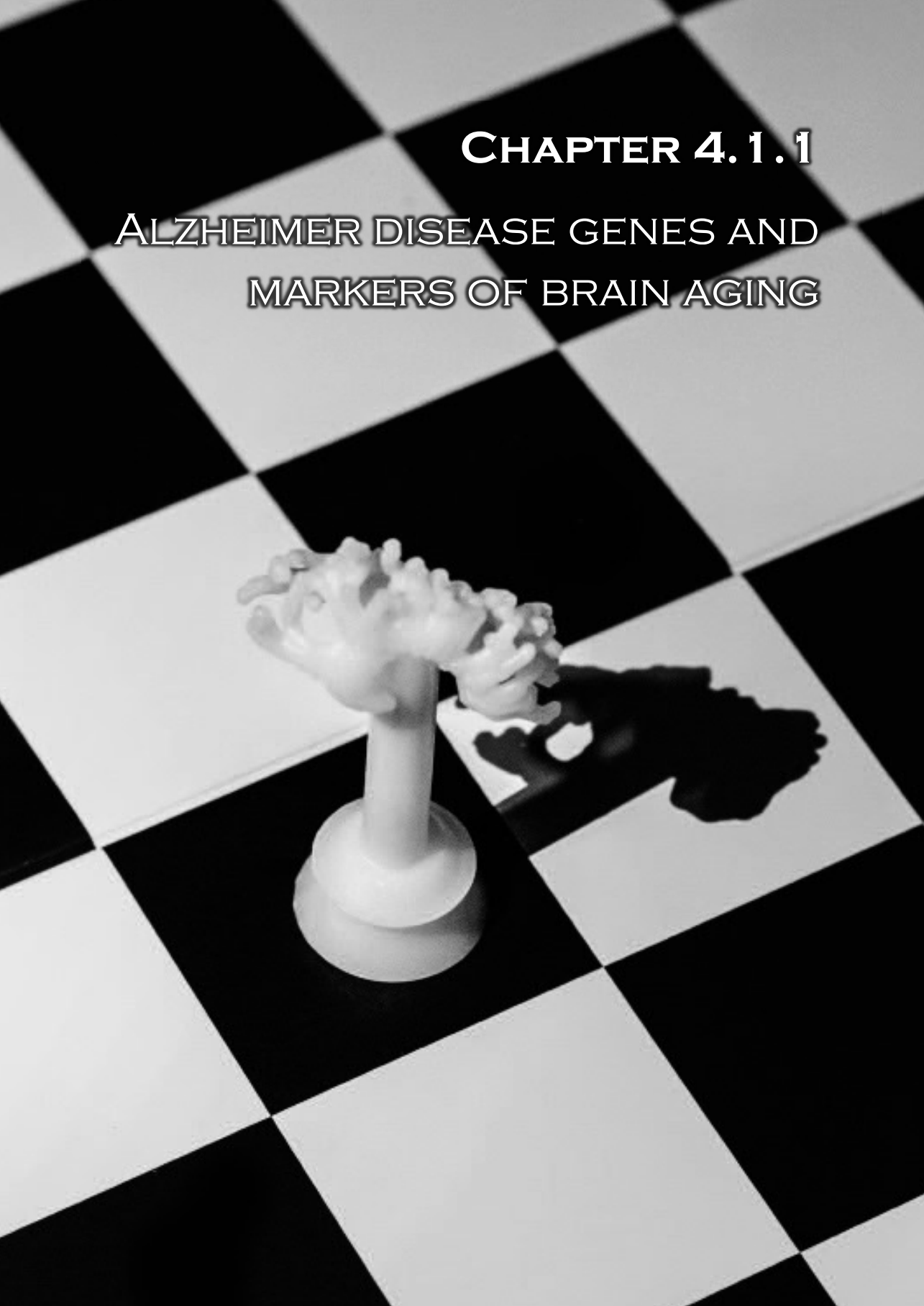

ABSTRACT

Whether novel risk variants of Alzheimer's disease (AD) identified through genome-wide association studies (GWAS) also influence MRI-based intermediate phenotypes of AD in the general population is unclear. We studied association of 24 AD risk loci with intra-cranial volume (ICV), total brain volume (TBV), hippocampal volume (HV), white matter hyperintensity (WMH) burden, and brain infarcts in a meta-analysis of genetic association studies from large population-based samples (N=8,175-11,550). In single-SNP based tests, AD risk alleles of APOE (rs2075650) was associated with smaller HV (p=0.0054) and CD33 (rs3865444) with smaller ICV (p=0.0058) In gene-based tests, there were associations of HLA-DRB1 with TBV (p=0.0006) and BIN1 with HV (p=0.00089). A weighted AD genetic risk score was associated with smaller HV (beta±SE=-0.047±0.013, p=0.00041), even after excluding the APOE locus (p=0.029).However, only association of AD genetic risk score with HV, including APOE, was significant after multiple testing correction (including number of independent phenotypes tested). These results suggest that novel AD genetic risk variants may contribute to structural brain aging in non-demented older community persons.

INTRODUCTION

Alzheimer's disease (AD) is the leading cause of dementia and represents a major public health burden [1]. Converging evidence suggests that pathological processes leading to this progressive neurodegenerative disorder start many years before clinical diagnosis of dementia [2]. MRI-markers of brain aging, including total brain volume (TBV) and hippocampal volume (HV), and markers of vascular brain injury, including white matter hyperintensities (WMH) and brain infarcts, are powerful predictors of dementia and may, at least in part, represent intermediate markers reflecting pathological processes leading to AD [2-7]. Intracranial volume (ICV), an imaging marker reflecting brain growth during development and maturation, was suggested to be correlated with resilience to brain damage [8].

Recently, large scale genome-wide association studies (GWAS) and candidate gene based studies have identified novel susceptibility loci for late-onset AD [9-18]. These AD risk variants have recently been used to examine the genotypic overlap between AD and other types of dementia [19]. Some of these variants have been studied with respect to various MRI measures in a mixed study sample of AD patients, mildly cognitive impaired and healthy controls [20, 21]. They could also be implemented to explore the impact of genetic determinants of AD on MRI-markers of structural brain changes in non-demented community persons. Indeed, this could provide important information on the disease mechanisms through which these genes affect the risk of AD, and could be of interested for the design of preventative interventions. Whether all previously and newly discovered AD risk loci influence brain structure in advance of clinically detectable dementia has never been systematically investigated in large community samples to our knowledge. Our aim was to study association of known AD GWAS loci with ICV, TBV, HV, WMH burden and brain infarcts in non-demented participants from 10 population-based studies.

MATERIALS AND METHODS

Population

Analyses were performed on 8,175 to 11,550 dementia free participants of European ancestry with quantitative brain MRI and genome-wide genotypes (N=8,175 for ICV, N=8,673 for TBV, N=11,550 for HV, N=9,361 for WMH burden and N=9,401 for brain infarcts), from up to 10 population-based cohort studies participating in the Cohorts of Heart and Aging Research in Genomic Epidemiology (CHARGE) consortium: Aging Gene-Environment Susceptibility (AGES)–Reykjavik Study, Atherosclerosis Risk in Communities Study (ARIC), Austrian Stroke Prevention Study (ASPS), Cardiovascular Health Study (CHS), Framingham Heart Study (FHS), Rotterdam Study (RS), Erasmus Rucphen Family (ERF) study, Religious Order Study (ROS) & Rush Memory and Aging Project (MAP), Tasmanian Study of Cognition and Gait (TASCOG) and the 3C-Dijon study. Each study secured approval from institutional review boards, and all participants provided written informed consent for study participation, brain MRI, and use of DNA for genetic research. Individual studies are described in the Supplementary Appendix.

MRI scans

In each study, MRI scans were performed and interpreted in a standardized fashion, without reference to clinical or genetic information. Details on MRI parameters and phenotype definition are provided in the Supplementary Appendix. Briefly, automated or semi-quantitative post-processing software was used to measure ICV and TBV. TBV was expressed as percentage of ICV to correct for differences in head size [22]. HV was evaluated using operator-defined boundaries drawn on serial coronal sections or automated methods [23]. WMH burden was estimated on a quantitative scale using custom-written computer programs in AGES-Reykjavik, ASPS, FHS, and RS; in ARIC and CHS, WMH burden was estimated on a semi-quantitative scale [24]. Brain infarcts were defined as areas of abnormal signal intensity in a vascular distribution that lacked mass effect, $\geq$ 3-4 mm, distinct from dilated perivascular spaces [25].

AD GWAS loci

We manually scanned the GWAS catalog (www.genome.gov/gwastudies) and Alzgene (www.alzgene.org/) for GWAS on AD. We only chose studies performed on European subjects, including a replication stage, examining single marker based associations and having loci reaching genome wide significance ($P<5.0\times10^{-8}$). This led to the identification of 24 independent loci. Effect estimates for SNPs with the lowest p-value in each locus (defined as the index SNP of the locus) are presented in Supplementary Table 1. We included the *CD33* locus (rs3865444) despite absence of replication in the latest AD GWAS meta-analysis;[15] this locus was previously replicated in several AD GWAS,[13, 14] and recent functional studies provide strong evidence for involvement of rs3865444 and *CD33* in AD pathology [26]. For the *APOE*-ε polymorphism we used rs2075650 as a proxy (r^2=0.48 with rs429358, the *APOE*-ε SNP), because *APOE*-ε genotypes cannot be reliably imputed on commercial genome-wide chips. The AD risk variants near *HLA-DRB1*[15], *ATP5H/KCTD2* [16], in *TREM2,*[18], and *APP*[17] were not included for single-SNP based association and genetic risk score based association as no index SNP or proxy (r^2>0.3) was available among the genome-wide genotypes for MRI-markers of brain aging.

Power calculation

Quanto software [27, 28] was used to compute power of of the five MRI marker studies assuming additive model of inheritance at α=0.0025 (Supplementary Figure 1). Power for the quantitative traits (ICV, TBV, HV, WMH burden) was computed for different percentage variance explained while for brain infarcts, a dichotomous trait, it was computed for different odds ratios at different allele frequencies.

Correlation between phenotypes

Correlation between the five MRI phenotypes in 3C-Dijon and FHS was calculated based on Pearson's correlation using the "rcorr" function in R. These correlations were used to compute the equivalent number of independent phenotypes using the online tool matSpDlite (neurogenetics.qimrberghofer.edu.au/matSpDlite/). MatSpDlite which is based on the same principles used to identify number of independent SNPs in a locus, gives the equivalent number of independent variables in a correlation (r) matrix,

depending upon the ratio of observed eigenvalue variance (after spectral decomposiiton) to its theoretical maximum [29].

Association Analyses

Three analytical approaches were taken to examine the associations of interest.

Single-SNP based association analysis

We tested for association of AD GWAS loci with MRI-markers of brain aging using association estimates obtained from meta-analyses of GWAS for ICV[22], TBV[22], HV[23], WMH burden [24] and brain infarcts [25] using genotypes imputed on the HapMap2 CEU reference panel. AD risk alleles, as described in the latest AD GWAS meta-analysis,[15] were modeled as the effect alleles for associations with MRI-markers of brain aging. Logistic (brain infarcts) or linear (ICV, TBV, HV and WMH burden) regression was performed within each study, adjusting for age, gender, and principal components of population stratification, and for familial relationships or study center if relevant. For WMH burden, data was log transformed to achieve normal distribution and associations were additionally adjusted for ICV (except for studies measuring WMH burden on a semi-quantitative visual scale, visual grades being inherently normalized for brain size)[24]. For most phenotypes (ICV, TBV, HV, and brain infarcts) meta-analyses were performed using fixed effects inverse variance weighted meta-analysis. For WMH burden, meta-analysis was performed using effective sample size weighted meta-analysis, because WMH burden was measured on different scales across studies. If the lead SNP at a specific AD GWAS locus was not available, a proxy SNP (r^2>0.70 in 1000G CEU) of the lead SNP was used to check single-SNP based association results (Supplementary Table 1).After Bonferroni correction for testing 20 independent loci, $p<0.0025$ was considered significant for single-SNP based associations. However, application of a more stringent threshold additionally accounting for the number of independent phenotypes tested led to a Bonferroni correction of $p<0.000625$.

Gene-based association analysis

Gene-based association tests can be more powerful in comparison to single-SNP based association tests when there are many causal variants in a gene with small effects [30].

Single-SNP based association results from the respective MRI-marker GWAS meta-analysis were used to compute gene-based association results using the Versatile Gene-Based Association Study2 (VEGAS2) software (https://vegas2.qimrberghofer.edu.au/) [30]. The gene annotations and LD calculation in VEGAS2 are based on 1000 genomes (phase 1 version 3). This tool annotated all but one gene (*MS4A4E*) within 50KB of the index SNPs. The test incorporates information from all markers within a gene and accounts for linkage disequilibrium (LD) between markers by using simulations from the multivariate normal distribution. Gene-based association analyses were performed for all protein coding genes (N=65 genes) which lie within a 50kb distance of index SNP of the AD risk loci. Gene boundaries were defined as 50kb upstream and downstream of the start and end of gene [30]. The choice of 50 KB boundary to cover a gene was chosen as a trade-off between a longer boundary which would have caused excess overlap between nearby genes and a shorter boundary which would have ignored potential regulatory regions [30]. Maximum permutation limits were set to 1000,000. After correcting for the number of genes (N=65) tested the multiple testing threshold was $p<0.00077$. A more stringent correction additionally accounting for number of independent phenotypes (N=4) tested, lead to a multiple testing threshold of $p< 0.00019$ for gene based association.

Construction of genetic risk score

We constructed a genetic risk score comprising all selected AD risk variants from 20 independent AD risk loci to estimate joint effect of these SNPs on MRI-markers of brain aging. Methods have been recently developed to apply a genetic risk score to meta-analysis summary estimates without requiring access to raw data from individual studies [31]. For each MRI-marker of interest, the beta-coefficient for a given SNP, as obtained from the GWAS meta-analysis for this MRI-marker, was weighted with the published AD beta-coefficient for the given SNP. The weighted sum of beta-coefficients for all 20 SNPs (Formula-i(a)) was used as the beta-coefficient of the genetic risk score. Similarly, for each MRI-marker of interest, the inverse of the variance for a given SNP (from the GWAS meta-analysis for this MRI-marker) was weighted by the square of the published AD beta-coefficient for the given SNP. These weighted inverse of variances were then summed and the inverse of this sum was used as the variance of the genetic risk score (Formula-i(b)). The Wald statistic was used to test for significance of associations

between the genetic risk score and each MRI-marker [31]. For WMH burden, betas and standard errors were estimated from Z-statistics provided by the effective sample size weighted meta-analysis using Formula-ii. AD beta-coefficients used as weights for the score were all drawn from the discovery stage of the recent largest AD GWAS meta-analysis (17,008 AD cases and 37,154 controls, Supplementary Table 1) [15]. Associations with p<0.05 were considered significant for genetic risk score based associations.

$$\beta_{grs} = \frac{\sum_1^m w\beta SE^{-2}}{\sum_1^m w^2 SE^{-2}} \qquad Formula - i(a)$$

$$SE^2{}_{grs} = \frac{1}{\sum_1^m w^2 SE^{-2}} \qquad Formula - i(b)$$

β_{grs}=beta of genetic risk score; SE_{grs}=SE of genetic risk score; *w*=weight applied (=SNP-specific beta of AD GWAS); β=SNP specific beta of association with MRI-phenotype; SE= SNP-specific SE of association with MRI-phenotype

$$SE\sim = \sqrt{VP/(ES \times 2pq)} \qquad Formula - ii(a)$$

$$Beta = SE \times Z \qquad Formula - ii(b)$$

VP=phenotypic variance (approximated to 1); ES=Effective sample size; p=Minor allele frequency; q=Major allele frequency.

After correcting for four independent phenotypes tested, the multiple testing threshold for genetic risk score association was P<0.0125.

RESULTS

Correlation and heritability of the five MRI traits

Based on data from two studies which were part of the original meta-analysis the two MRI markers of structural brain aging, ICV and TBV showed high correlation with each other but were only moderately correlated with HV (Supplementary Table 2). The two MRI markers of vascular brain aging WMH burden and brain infarcts showed low correlation with each other and very little or no correlation with the three markers of structural brain aging. Depending upon this correlation the equivalent number of independent phenotypes calculated using matSpDlite was four for both studies. Published literature showed that the five MRI markers had moderate to high heritability (Supplementary Table 3).

Single-SNP based associations

In total 9 out of 20 AD risk variants that could be analyzed showed association with at least one MRI-marker at $p<0.05$ (Table 1). With only 2 exceptions (*CD33* locus with brain infarcts ($p=0.048$) and *PTK2B* locus with ICV ($p=0.028$)), betas were in the expected direction i.e. the AD risk allele was associated with increased risk for brain infarcts and with lower ICV, TBV and HV. The most significant associations were for *APOE*-rs2075650 with HV (beta±SE=-0.042±0.015, $p=0.0054$) and *CD33*-rs3865444 with ICV (beta±SE=-5.209±1.886, $p=0.0058$) (Table 1). However, none of the single-SNP based associations were significant after correcting for multiple testing. None of the AD risk variants showed associations with WMH burden.

Table 1 | Single-SNP based association of the AD loci with MRI markers of brain aging

Index SNP[a] (Proxy)	Closest gene	Chr:position[b]	Intra-Cranial Volume (in cm^3)			Total Brain Volume (in % ICV)			Hippocampal Volume (cm^3)			WMH burden[d]		Brain Infarcts (yes/no)		
			β	SE	p	β	SE	p	β	SE	p	Z-statistics	p	β	SE	p
rs2075650	*APOE*	19:45395619	4.405	2.605	0.091	-0.1	0.072	0.168	-0.042	0.015	0.0054	1.089	0.276	-0.081	0.062	0.195
rs9331896 (rs2279590)	*CLU*	8:27467686	-3.112	1.795	0.083	-0.104	0.051	0.04	-0.009	0.011	0.416	-1.546	0.122	-0.012	0.043	0.771
rs10792832	*PICALM*	11:85867875	0.763	1.681	0.65	0.064	0.047	0.18	-0.001	0.01	0.863	1.243	0.214	0.003	0.04	0.932
rs6656401	*CR1*	1:207692049	-2.834	2.19	0.196	0.023	0.061	0.713	0.016	0.013	0.211	0.375	0.708	-0.069	0.054	0.197
rs6733839 (rs744373)	*BIN1*	2:127892810	-1.943	1.862	0.297	-0.07	0.052	0.183	-0.024	0.011	0.027	-0.168	0.867	0.079	0.043	0.064
rs4147929 (rs3752246)	*ABCA7*	19:1063443	0.103	2.342	0.965	-0.018	0.065	0.786	-0.017	0.014	0.226	NA	NA	0.017	0.058	0.773
rs983392 (rs11230161)	*MS4A6A*	11:59923508	-3.093	1.675	0.065	-0.059	0.047	0.214	-0.023	0.01	0.021	-1.42	0.156	-0.012	0.043	0.782
rs10948363	*CD2AP*	6:47487762	1.537	1.845	0.405	-0.017	0.052	0.742	0.003	0.011	0.87	1.089	0.276	-0.035	0.044	0.433
rs11771145	*EPHA1*	7:143110762	3.353	1.901	0.078	-0.026	0.053	0.625	0.003	0.011	0.912	NA	NA	-0.023	0.042	0.592
rs3865444	*CD33*	19:51727962	-5.209	1.886	0.0058	0.025	0.053	0.638	-0.019	0.011	0.087	-0.362	0.717	-0.088	0.045	0.048
rs9271192	*HLA-DRB1*[e]	6:32578530	NA	NA	NA	NA	NA	NA	NA	NA	NA	NA	NA	NA	NA	NA
rs28834970 (rs2322599)	*PTK2B*	8:27195121	3.675	1.67	0.028	-0.006	0.047	0.898	-0.003	0.01	0.762	-0.824	0.41	-0.006	0.04	0.89

Table 1 continued.

rs11218343 (rs7939826)	*SORL1*	11:121435587	4.525	6.239	0.468	-0.165	0.174	0.341	0.011	0.037	0.768	NA	NA	0.316	0.155	0.041
rs10498633	*SLC24A4*	14:92926952	-2.052	2.042	0.315	0.01	0.057	0.858	-0.012	0.012	0.329	0.363	0.717	0.049	0.048	0.304
rs35349669 (rs7607736)	*INPP5D*	2:234068476	-3.625	1.723	0.035	-0.063	0.048	0.196	-0.01	0.01	0.313	0.856	0.392	-0.003	0.041	0.935
rs190982	*MEF2C*	5:88223420	-1.611	1.918	0.401	0.034	0.054	0.525	0.005	0.011	0.687	0.545	0.586	0.046	0.044	0.3
rs2718058 (rs12155159)	*NME8*	7:37841534	2.168	1.762	0.218	0	0.05	0.994	0.012	0.01	0.271	-0.438	0.662	0.027	0.042	0.523
rs1476679	*ZCWPW1*	7:100004446	-0.22	1.8	0.903	-0.017	0.051	0.738	-0.01	0.011	0.36	-0.053	0.958	-0.014	0.044	0.754
rs10838725 (rs10838726)	*CELF1*	11:47557871	-0.433	1.795	0.809	0.085	0.05	0.092	0	0.011	0.992	-1.012	0.312	-0.068	0.043	0.115
rs17125944	*FERMT2*	14:53400629	0.465	2.767	0.867	-0.025	0.078	0.744	0.015	0.016	0.347	-0.574	0.566	0.069	0.071	0.332
rs7274581 (rs927174)	*CASS4*	20:55018260	-0.435	2.956	0.883	-0.119	0.083	0.152	-0.014	0.017	0.421	0.055	0.956	0.084	0.07	0.228

Key: β, beta (meta-analysis effect estimate) per allele increase of the risk allele; Z-statistic, meta-analysis of Z-statistics (beta/SE) from each study, weighted by effective sample size (product of the sample size and the ratio of the empirically observed dosage variance to the expected binomial dosage variance for imputed SNPs); WMH, white matter hyperintensities; SE, standard error

[a] Index SNP was defined as the SNP with the lowest p at the locus.

[b] Chr:position has been provided for the index SNP as per NCBI build 37 (GRCh37.p10).

[c] Distance from gene start or end (whichever is shortest) is provided in kilo bases (kb) and if within gene, wg notation used.

[d] expressed in cm^3 or on a semi-quantitative 10-point scale in the original study.

[e] Neither the index SNP nor any SNP in LD with index SNP is available in the HapMap based imputed data meta-analysis results p<0.0025 (α=0.05/20) was considered significant after correcting for number of independent loci tested

Table 2 | Gene-based associations (P<0.05) with MRI markers of brain aging for genes lying within 50kb of AD risk loci

Index-SNP (closest gene)	Gene	Chr	Start	Stop	p (Intra-cranial volume)	p (Total brain volume)	p (Hippocampal volume)	p (WMH burden)	p (brain infarcts)
rs6656401 (CR1)	*CR1*	1	207619472	207865110	0.271	0.0033	0.237	0.069	0.562
rs744373 (BIN1)	*BIN1*	2	127755598	127914903	0.612	0.782	0.00089	0.700	0.072
rs190982 (MEF2C)	*MEF2C*	5	87964057	88249922	0.020	0.815	0.134	0.180	0.033
rs9271192 (HLA-DRB1)	*HLA-DRB1*	6	32496546	32607613	0.467	0.00060	0.170	0.226	0.277
rs9271192 (HLA-DRB1)	*HLA-DQA1*	6	32555182	32661429	0.263	0.0014	0.108	0.059	0.310
rs9271192 (HLA-DRB1)	*HLA-DQB1*	6	32577240	32684466	0.179	0.0057	0.114	0.010	0.208
rs75932628 (TREM2)	*TREML1*	6	41066998	41172087	0.337	0.367	0.048	0.315	0.582
rs12155159 (NME8)	*NME8*	7	37838198	37990002	0.010	0.400	0.138	0.755	0.985
rs1476679 (ZCWPW1)	*PILRB*	7	99905625	100015454	0.0082	0.694	0.162	0.271	0.701
rs1476679 (ZCWPW1)	*PILRA*	7	99921067	100047722	0.0078	0.702	0.183	0.309	0.712
rs1476679 (ZCWPW1)	*ZCWPW1*	7	99948494	100076431	0.0078	0.672	0.196	0.363	0.751
rs1476679 (ZCWPW1)	*MEPCE*	7	99976412	100081749	0.0099	0.626	0.246	0.348	0.739
rs1476679 (ZCWPW1)	*PPP1R35*	7	99982911	100084094	0.0093	0.637	0.291	0.342	0.767
rs1476679 (ZCWPW1)	*C7orf61*	7	100004237	100111894	0.011	0.668	0.320	0.321	0.811
rs11771145 (EPHA1)	*TAS2R60*	7	143090545	143191502	0.931	0.012	0.393	0.086	0.049
rs2279590 (CLU)	*SCARA3*	8	27441576	27584286	0.060	0.031	0.367	0.440	0.651
rs11230161 (MS4A6A)	*MS4A6A*	11	59889079	60002139	0.035	0.375	0.030	0.358	0.804
rs11870474 (ATP5H/KCTD2)	*ICT1*	17	72958779	73067356	0.138	0.047	0.434	0.697	0.195
rs3752246 (ABCA7)	*ABCA7*	19	990101	1115570	0.497	0.589	0.799	0.049	0.301
rs3752246 (ABCA7)	*HMHA1*	19	1015921	1137830	0.337	0.577	0.724	0.046	0.128

Table 2 continued.

rs2075650 (APOE)	*PVRL2*	19	45299392	45442485	0.033	0.470	0.069	0.163	0.056
rs2075650 (APOE)	*TOMM40*	19	45344476	45456946	0.027	0.370	0.084	0.202	0.155
rs2075650 (APOE)	*APOE*	19	45359038	45462650	0.040	0.378	0.118	0.252	0.133
rs2075650 (APOE)	*APOC1*	19	45367920	45472606	0.030	0.488	0.106	0.274	0.163
rs3865444 (CD33)	*CD33*	19	51678334	51793274	0.179	0.046	0.463	0.968	0.100
rs927174 (CASS4)	*AURKA*	20	54894444	55017351	0.262	0.690	0.415	0.771	0.041
rs927174 (CASS4)	*CSTF1*	20	54917426	55029582	0.400	0.526	0.550	0.823	0.047

Key: WMH, white matter hyperintensities

p<0.0025 (α=0.05/20) was considered significant after correcting for number of independent loci tested; significant p-values after correcting for multiple testing are in bold; Gene-based association analysis was performed for genes within 50kB of index SNP. Only gene-based associations for those genes with p<0.05 with at least one MRI marker is presented. A complete list is presented in Supplementary Table 4.

Gene-based associations

Out of the 24 loci investigated, 23 had at least one protein coding gene within 50kb distance. Only rs3851179 (11q14) had no protein coding gene within 50kb and was not represented in the gene-based association analysis (nearest genes: *PICALM* 87.72kb downstream and *EED* 86.95kb upstream). In total, 65 protein coding genes from 23 independent loci were assessed for gene-based association analyses (Supplementary Table 4).

A total of 27 protein coding genes within 50kb of 15 index SNPs were associated with ICV, TBV, HV or brain infarcts at p<0.05 (Table 2). For ICV we observed association with 13 genes within 50kb of five index SNPs (*MEF2C, NME8, PILRB, PILRA, ZCWPW1, MEPCE, PPP1R35, C7orf61, MS4A6A, PVRL2, TOMM40, APOE, APOC1*; p-range: 0.04-0.0078). Eight genes within 50kB of six index SNPs were associated with TBV (*CR1, HLA-DRB1, HLA-DQA1, HLA-DQB1, TAS2R60, SCARA3, ICT1, CD33*; p-range: 0.047-0.0006). *BIN1, TREML1* and *MS4A6A* were associated with HV (p=0.00089, 0.03 and 0.048, respectively) while *MEF2C, AURKA, CSTF1 and TAS2R60*showed association with brain infarcts (p-range: 0.049-0.033). For WMH burden we observed association with three genes from two loci (*HLA-DQB1, HMHA1* and *ABCA7*; p=0.01, 0.046 and 0.049 respectively). If we correct for the number of genes tested the association of HLA-DRB1 with TBV remains significant but if we additionally correct for the number of phenotypes tested this association is not significant.

Genetic risk score based associations

The AD genetic risk score was associated with smaller HV (beta±SE=-0.047±0.013, p=0.00041) (Table 3). This association was also observed after removing the *APOE* locus from the AD genetic score (beta±SE=-0.050±0.023, p=0.029). There was also nominal association of the AD genetic risk score with smaller TBV (beta±SE =-0.127±0.064, P=0.046) but this association was not significant after excluding the *APOE* locus from the genetic risk score (P=0.13). Only association of the AD genetic risk score with HV including *APOE* locus was significant after correcting for the number of independent phenotypes tested.

Table 3 | Genetic risk score based association of the AD loci with MRI-markers of brain aging

	With *APOE*			Without *APOE*		
	Beta	SE	p	Beta	SE	p
Intra-cranial volume (in cm^3)	1.179	2.174	0.59	-6.224	3.945	0.11
Total brain volume (in % ICV)	-0.120	0.061	0.048	-0.166	0.111	0.13
Hippocampal volume (in cm^3)	-0.044	0.013	0.00042	-0.050	0.023	0.029
WMH burden[a]	0.013	0.020	0.52	-0.019	0.038	0.61
Brain infarcts (yes/no)	-0.039	0.052	0.45	0.055	0.094	0.56

Key: Beta, effect estimate, per allele increase of the risk allele; SE, standard error; WMH, white matter hyperintensities

[a] for WMH burden betas and SEs were estimated from the Z-statistics obtained in the WMH burden meta-analysis and do not reflect an interpretable effect size (as the WMH burden was estimated using different scales in participating studies) [24].

DISCUSSION

We investigated associations of 24 genome-wide significant AD risk loci with five MRI-markers of brain structure and aging (ICV, TBV, HV, WMH burden and brain infarcts), in over 8,000 dementia free older community participants from the CHARGE consortium. Although no single SNP-based association met the significance threshold after correction for multiple testing, index AD risk variants mapping to eight of the 21 AD risk loci showed nominal association with at least one MRI-marker, the most interesting being association for *APOE* (rs2075650) with smaller HV and for *CD33* (rs3865444) with smaller ICV. In gene-based association analyses *HLA-DRB1* was significantly associated with TBV after correction for number of genes tested. A weighted AD genetic risk score was significantly associated with smaller HV.

In Single-SNP based associations none of the associations were significant after correcting for multiple testing. Nominally significant associations of an *APOE* risk variant with HV (P=0.0054) and a *CD33* variant with ICV (P=0.0058) were observed. Since the mid 1990's (Supplementary Table 5) some studies have described significant associations between the *APOE*-ε4 allele and smaller HV [32-41], however other studies did not find such an association [42-45]. Using the largest sample size to date (N=11,550), as previously reported by our group, our findings are supportive of an association of the *APOE*-ε4 locus with smaller HV [23]. The rs3865444 (*CD33*) AD risk allele association with smaller ICV could perhaps be suggestive of an involvement of this locus in brain maturation and brain reserve. Recent reports suggest that rs3865444 influences *CD33* expression, including in young adults in their twenties [26], and is associated with diminished internalization of amyloid β_{42} peptide, and accumulation of neuritic amyloid pathology and fibrillar amyloid in vivo [26].

Gene-based analyses revealed significant associations of *HLA-DRB1* (index SNP rs9271192) with TBV. The *HLA-DRB1* locus was recently identified to be associated with AD in the largest meta-analysis of AD [15]. This locus is part of the major histocompatibility complex, class II, and our findings add support to the role of

autoimmunity in AD. The findings also suggest that the locus may be playing a role in pre-symptomatic stages of the disease, as we observe association with smaller brain volumes in non-demented older community persons.

When combined in a weighted genetic risk score, AD risk variants were associated cumulatively with decreased HV. Interestingly the association was maintained with a similar effect size, although less significant, after removing the *APOE* locus from the analysis, suggesting that, in aggregate, novel AD risk loci are associated with smaller HV in non-demented older community persons. The AD genetic risk score also showed nominal association with smaller TBV. Although this association was no longer significant after removing the *APOE* locus, other loci were contributing to this association, as the *APOE* risk variant alone was not significantly associated with TBV.

There were fewer associations with WMH burden and brain infarcts. Most associations with AD risk variants were observed for ICV, TBV, and HV. This may indicate that, even though they are strong predictors of dementia risk,[5, 6] MRI-markers of vascular brain injury could have less shared genetic determinants with AD than MRI-markers of brain growth and brain atrophy, as suggested by others [20]. Noteworthy, our study only tested for overlap of genome-wide significant AD risk variants, did not explore shared heritability and may have been underpowered for less common variants with smaller effect size (Supplementary Figure 1).

Our study has limitations. The 24 AD risk loci do not reflect the full spectrum of genetic susceptibility to AD and the index SNPs used may not be causal variants. The five GWAS of MRI-markers, although the largest of their kind, have fewer samples compared to the AD GWAS from which the loci have been obtained [15, 22-25]. These five GWAS of MRI-markers were performed using imputed genotypes based on the HapMap2 panel, which does not cover rare variants and has lower imputation accuracy, especially for lower allele frequencies, compared to the more recent 1000 genomes reference panels. We therefore couldn't analyze rare AD risk variants in the present study. In addition, despite major efforts to harmonize phenotype definitions across studies, there may be some residual heterogeneity in

methods for quantifying MRI-markers of brain aging. These elements could have reduced our power to detect associations of AD GWAS loci with MRI-markers of brain aging. The choice of 50 KB window for a gene based test does not account for potential regulatory effects on more distant genes. Our findings cannot be generalized to populations of non-European ancestry. Ongoing, larger multi-ethnic GWAS of MRI-markers of brain aging, as well as sequencing projects searching for rare variants associated with AD risk and MRI phenotypes may enable us to expand our findings in the future.

CONCLUSION

In conclusion, we have shown that novel AD genetic risk variants are associated with MRI-markers of structural brain aging in older, non-demented community persons. In aggregate, novel AD genetic risk variants were associated with smaller brain volumes, especially HV. Significant gene-based associations and suggestive single SNP-based associations with ICV, TBV and HV also provide interesting hypotheses for mechanisms underlying genetic associations with AD

REFERENCES

1. Ballard C, Gauthier S, Corbett A, Brayne C, Aarsland D, Jones E. Alzheimer's disease. *Lancet*. 2011;377:1019-1031
2. Sperling RA, Aisen PS, Beckett LA, Bennett DA, Craft S, Fagan AM, et al. T. *Alzheimers Dement*. 2011;7:280-292
3. Jack CR, Jr., Knopman DS, Jagust WJ, Petersen RC, Weiner MW, Aisen PS, et al.. *Lancet Neurol*. 2013;12:207-216
4. Kaye JA, Swihart T, Howieson D, Dame A, Moore MM, Karnos T, et al.. *Neurology*. 1997;48:1297-1304
5. Debette S, Markus HS.. *BMJ*. 2010;341:c3666
6. Vermeer SE, Longstreth WT, Jr., Koudstaal PJ. S: A systematic review. *Lancet Neurol*. 2007;6:611-
7. Jack CR, Jr., Knopman DS, Jagust WJ, Shaw LM, Aisen PS, Weiner MW, et al. *Lancet Neurol*. 2010;9:119-128
8. Negash S, Xie S, Davatzikos C, Clark CM, Trojanowski JQ, Shaw LM, et al. C. *Alzheimer's & dementia : the journal of the Alzheimer's Association*. 2013;9:e89-95
9. Carrasquillo MM, Zou F, Pankratz VS, Wilcox SL, Ma L, Walker LP, et al. *Nat Genet*. 2009;41:192-198
10. Harold D, Abraham R, Hollingworth P, Sims R, Gerrish A, Hamshere ML, et al.. *Nat Genet*. 2009;41:1088-1093
11. Lambert JC, Heath S, Even G, Campion D, Sleegers K, Hiltunen M, et al.. *Nat Genet*. 2009;41:1094-1099
12. Seshadri S, Fitzpatrick AL, Ikram MA, DeStefano AL, Gudnason V, Boada M, et al. Genome-wide analysis of genetic loci associated with alzheimer disease. *JAMA*. 2010;303:1832-1840
13. Hollingworth P, Harold D, Sims R, Gerrish A, Lambert JC, Carrasquillo MM, et al.. *Nat Genet*. 2011;43:429-435
14. Naj AC, Jun G, Beecham GW, Wang LS, Vardarajan BN, Buros J, et al. e. *Nat Genet*. 2011;43:436-441
15. Lambert JC, Ibrahim-Verbaas CA, Harold D, Naj AC, Sims R, Bellenguez C, et al.. *Nature genetics*. 2013;45:1452-1458
16. Boada M, Antunez C, Ramirez-Lorca R, Destefano AL, Gonzalez-Perez A, Gayan J, et al. Atp5h/kctd2 locus is associated with alzheimer's disease risk. *Molecular psychiatry*. 2013
17. Jonsson T, Atwal JK, Steinberg S, Snaedal J, Jonsson PV, Bjornsson S, et al. . *Nature*. 2012;488:96-99
18. Jonsson T, Stefansson H, Steinberg S, Jonsdottir I, Jonsson PV, Snaedal J, et al. Variant of trem2 associated with the risk of alzheimer's disease. *N Engl J Med*. 2013;368:107-116
19. Carrasquillo MM, Khan QU, Murray ME, Krishnan S, Aakre J, Pankratz VS, et al. Late-onset alzheimer disease genetic variants in posterior cortical atrophy and posterior ad. *Neurology*. 2014;82:1455-1462
20. Biffi A, Anderson CD, Desikan RS, Sabuncu M, Cortellini L, Schmansky N, et al. *Arch Neurol*. 2010;67:677-685
21. Furney SJ, Simmons A, Breen G, Pedroso I, Lunnon K, Proitsi P, et al. e. *Molecular psychiatry*. 2011;16:1130-1138
22. Ikram MA, Fornage M, Smith AV, Seshadri S, Schmidt R, Debette S, et al. *Nat Genet*. 2012;44:539-544
23. Bis JC, DeCarli C, Smith AV, van der Lijn F, Crivello F, Fornage M, et al. Common variants at 12q14 and 12q24

are associated with hippocampal volume. *Nat Genet*. 2012;44:545-551
24. Fornage M, Debette S, Bis JC, Schmidt H, Ikram MA, Dufouil C, et al. *Ann Neurol*. 2011;69:928-939
25. Debette S, Bis JC, Fornage M, Schmidt H, Ikram MA, Sigurdsson S, et al. *Stroke*. 2010;41:210-217
26. Bradshaw EM, Chibnik LB, Keenan BT, Ottoboni L, Raj T, Tang A, et al. Cd33 alzheimer's disease locus: Altered monocyte function and amyloid biology. *Nature neuroscience*. 2013;16:848-850
27. Gauderman WJ. Sample size requirements for association studies of gene-gene interaction. *Am J Epidemiol*. 2002;155:478-484
28. Gauderman WJ. Sample size requirements for matched case-control studies of gene-environment interaction. *Stat Med*. 2002;21:35-50
29. Nyholt DR. A *American journal of human genetics*. 2004;74:765-769
30. Liu JZ, McRae AF, Nyholt DR, Medland SE, Wray NR, Brown KM, et al. A versatile gene-based test for genome-wide association studies. *Am J Hum Genet*. 2010;87:139-145
31. Dastani Z, Hivert MF, Timpson N, Perry JR, Yuan X, Scott RA, et al. Nls. *PLoS genetics*. 2012;8:e1002607
32. Lehtovirta M, Laakso MP, Soininen H, Helisalmi S, Mannermaa A, Helkala EL, et al.. *Neuroscience*. 1995;67:65-72
33. Lehtovirta M, Soininen H, Laakso MP, Partanen K, Helisalmi S, Mannermaa A, et al. *J Neurol Neurosurg Psychiatry*. 1996;60:644-649
34. Plassman BL, Welsh-Bohmer KA, Bigler ED, Johnson SC, Anderson CV, Helms MJ, et al.. *Neurology*. 1997;48:985-989
35. Soininen H, Partanen K, Pitkanen A, Hallikainen M, Hanninen T, Helisalmi S, et al.. *Neurology*. 1995;45:391-392
36. Lind J, Larsson A, Persson J, Ingvar M, Nilsson LG, Backman L, et al. *Neurosci Lett*. 2006;396:23-27
37. Lu PH, Thompson PM, Leow A, Lee GJ, Lee A, Yanovsky I, et al. *J Alzheimers Dis*. 2011;23:433-442
38. Morra JH, Tu Z, Apostolova LG, Green AE, Avedissian C, Madsen SK, et al. *Neuroimage*. 2009;45:S3-15
39. Schuff N, Woerner N, Boreta L, Kornfield T, Shaw LM, Trojanowski JQ, et al. Mri of hippocampal volume loss in early alzheimer's disease in relation to apoe genotype and biomarkers. *Brain*. 2009;132:1067-1077
40. O'Dwyer L, Lamberton F, Matura S, Tanner C, Scheibe M, Miller J, et al. Reduced hippocampal volume in healthy young apoe4 carriers: An mri study. *PLoS One*. 2012;7:e48895
41. Liu Y, Yu JT, Wang HF, Han PR, Tan CC, Wang C, et al. Apoe genotype and neuroimaging markers of alzheimer's disease: Systematic review and meta-analysis. *J Neurol Neurosurg Psychiatry*. 2014
42. Ferencz B, Laukka EJ, Lovden M, Kalpouzos G, Keller L, Graff C, et al. *Front Hum Neurosci*. 2013;7:198
43. Schmidt H, Schmidt R, Fazekas F, Semmler J, Kapeller P, Reinhart B, et al. Apolipoprotein e e4 allele in the normal elderly: Neuropsychologic and brain mri correlates. *Clin Genet*. 1996;50:293-299
44. Khan W, Giampietro V, Ginestet C, Dell'Acqua F, Bouls D, Newhouse S, et al. *J Alzheimers Dis*. 2014;40:37-43
45. Reiman et al. Hippocampal volumes in cognitively normal persons at genetic risk for alzheimer's disease. *Ann Neurol*. 1998;44:288-291

Chapter 4.1.2

Genetic determinants of unruptured intracranial aneurysms

ABSTRACT

Background and Purpose: Genome-wide association studies have identified single nucleotide polymorphisms (SNPs) for intracranial aneurysms in clinical samples. Additionally, SNPs have been discovered for blood pressure, one of the strongest risk factors for intracranial aneurysms. We studied the role of these genetic variants on occurrence and size of unruptured intracranial aneurysms, discovered incidentally in a general community-dwelling population.

Methods: In 4,890 asymptomatic participants from the Rotterdam Study, 120 intracranial aneurysms were identified on brain imaging and segmented for maximum diameter and volume. Genetic risk scores (GRS) were calculated for intracranial aneurysms (10 SNPs), systolic blood pressure (33 SNPs) and diastolic blood pressure (41 SNPs).

Results: The GRS for intracranial aneurysms was not statistically significantly associated with presence of aneurysms in this population (OR: 1.16; 95%CI, 0.96-1.40; P=0.119), but showed a significant association with both maximum diameter (difference in log-transformed mm per SD increase of GRS: 0.10; 95%CI, 0.02-0.19; P=0.018) and volume (difference in log-transformed µl per SD increase of GRS: 0.21; 95%CI, 0.01-0.41; P=0.040) of aneurysms. GRSs for blood pressures were associated with neither presence nor size of aneurysms.

Conclusions: Genetic variants previously identified for intracranial aneurysms in clinical studies relate to the size rather than the presence of incidentally discovered, unruptured intracranial aneurysms in the general population.

INTRODUCTION

Unruptured intracranial aneurysms are incidentally discovered in imaging studies in approximately 2% of the general population.[1] Rupture of an intracranial aneurysm can result in a non-traumatic subarachnoid hemorrhage (SAH), an acute condition with high morbidity and mortality rates. For early risk stratification and potential treatment, it is therefore important to better understand the pathophysiology of aneurysm development.

Several risk factors for ruptured intracranial aneurysms have been identified, including age, gender, smoking, aneurysm size and location.[2-4] In addition, an important modifiable risk factor for ruptured intracranial aneurysms is hypertension.[5] Less is known about risk factors for development of intracranial aneurysms, although there is some overlap with risk factors for rupture, including gender, smoking and hypertension.[6, 7] Genetic factors also play an important role in intracranial aneurysms, which is evidenced by the fact that persons with a positive family history have a higher risk of developing intracranial aneurysms compared to the general population.[8] More recently, genome-wide association studies have identified multiple single nucleotide polymorphisms (SNPs) associated with intracranial aneurysms.[9] Importantly, most studies investigating genetics of intracranial aneurysms have done so in a clinical setting, thereby typically including patients presenting with ruptured aneurysms or persons screened for high familial risk. In such settings, it cannot be discerned whether these SNPs affect the development of intracranial aneurysms or lead to growth and rupture of already present aneurysms. A population-based setting provides a unique opportunity to study the effect of these SNPs on unselected unruptured aneurysms.

We investigated in a community-dwelling population the association of SNPs for intracranial aneurysms with the occurrence and size of unruptured aneurysms, incidentally detected on research imaging. Furthermore, we also studied SNPs for high blood pressure and their association with presence and size of unruptured intracranial aneurysms.

METHODS

The online-only Data Supplement provides further details on the methods.

Setting and study population

This study was embedded in the prospective Rotterdam Study[10], a population-based cohort study in the Netherlands. Between 2005 and 2014, 5,832 unique persons have undergone magnetic resonance imaging (MRI) of the brain.[11] The study cohort was genotyped across the whole genome, with genotype data available for 4,890 out of 5,832 subjects.

Assessment intracranial aneurysms on MRI

Reported incidental findings by research physicians were reassessed by a neuroradiologist and categorized accordingly. None of the participants had a history of SAH. Detected intracranial aneurysms were manually segmented. A 3D-model of the aneurysm was reconstructed, enabling us to calculate maximum diameter and volume of saccular intracranial aneurysms.

Construction of the Genetic Risk Score

Due to the small effects of individual SNPs and the relatively small number of aneurysms in our population-based setting, we constructed a genetic risk score to leverage the cumulative effect of all SNPs, allowing us to achieve higher power. For primary analyses we restricted to SNPs reaching a genome-wide significance ($P < 5 \times 10^{-8}$) in Caucasian populations, but in secondary analyses we included SNPs from non-Caucasian populations. The extracted SNP data is described in Supplementary Table 1.

Statistical analysis

We used logistic regression to associate genetic risk scores with presence of intracranial aneurysms (yes/no). Among persons with aneurysms we used linear regression to associate genetic risk scores with size of saccular intracranial aneurysms. Size was defined in both maximum diameter (mm) and volume (µl). For subjects with multiple saccular aneurysms, we calculated total aneurysm size by summing up the size of all the

Table 1 | Study Characteristics

Variables	Persons with intracranial aneurysms (n=109)	Persons without intracranial aneurysms (n=4781)
Women	73(67.0%)	2610(54.6%)
Age, years	65.4±11.9	65.2±10.9
Smoking		
Never	17(15.6%)	1380(28.8%)
Past	50(45.9%)	2427(50.8%)
Current	42(38.5%)	974(20.4%)
Systolic blood pressure, mmHg	140.3±23.1	140.0±21.4
Diastolic blood pressure, mmHg	82.9±11.6	82.4±10.9
Blood pressure-lowering medication	50(45.9%)	1712(35.8%)
Hypertension*	64(58.7%)	2427(50.8%)
Number of aneurysms	120	—
Fusiform aneurysms	7(5.8%)	—
Saccular aneurysms	113(94.2%)	—
Maximum diameter, mm†	5.5(4.3-7.4)	—
Volume, µL†	52.8(27.6-125.6)	—

**Defined as systolic blood pressure >= 140 or diastolic blood pressure >= 90.*
†Median with interquartile range.

saccular aneurysms. In all analyses we adjusted for age, sex and additionally for smoking status, systolic blood pressure, diastolic blood pressure and use of blood pressure-lowering medication (antihypertensives, diuretics, beta blocking agents, calcium channel blockers, and ACE-inhibitors). Because persons could have multiple saccular aneurysms, hence greatly determining total aneurysm size, we also adjusted for number of aneurysms when performing analyses for size.

RESULTS

In 4,890 MRI-scans we found 120 aneurysms in 109 unique persons (2%), with 10 persons having multiple aneurysms (max 3 per person). The persons with intracranial aneurysms had a mean age of 65.4 ± 11.9 years and 73 (67.0%) were women. Of the 120 aneurysms,

Table 2 | Association of Genetic Risk Score and presence of Intracranial Aneurysms

Genetic Risk Score (per SD increase)	OR (95%CI)	P
Model 1*		
Intracranial Aneurysm (10 SNPs)	1.16(0.96;1.40)	0.119
Systolic Blood Pressure (33 SNPs)	1.15(0.95;1.39)	0.166
Diastolic Blood Pressure (41 SNPs)	1.09(0.90;1.32)	0.386
Model 2†		
Intracranial Aneurysm (10 SNPs)	1.17(0.96;1.41)	0.112
Systolic Blood Pressure (33 SNPs)	1.14(0.94;1.38)	0.190
Diastolic Blood Pressure (41 SNPs)	1.06(0.88;1.29)	0.525

**Adjusted for: age, sex.*
†Adjusted for: age, sex, smoking, systolic blood pressure, diastolic blood pressure, blood pressure-lowering medication.

Table 3 | Association of Genetic Risk Score and Saccular Aneurysm Size

Genetic Risk Score (per SD increase)	Max. Diameter (95%CI)	P	Volume (95%CI)
Model 1*			
Intracranial Aneurysm (10 SNPs)	0.10(0.02;0.18)	0.018	0.21(0.01;0.41)
Systolic Blood Pressure (33 SNPs)	0.02(-0.07;0.10)	0.728	0.01(-0.20;0.22)
Diastolic Blood Pressure (41 SNPs)	-0.02(-0.11;0.07)	0.662	-0.06(-0.27;0.15)
Model 2†			
Intracranial Aneurysm (10 SNPs)	0.12(0.04;0.20)	0.006	0.26(0.06;0.46)
Systolic Blood Pressure (33 SNPs)	0.03(-0.06;0.13)	0.496	0.05(-0.18;0.27)
Diastolic Blood Pressure (41 SNPs)	-0.02(-0.11;0.08)	0.707	-0.06(-0.28;0.16)

**Adjusted for: age, sex, number of aneurysms.*
†Adjusted for: age, sex, number of aneurysms, smoking, systolic blood pressure, diastolic blood pressure, blood pressure-lowering medication.

114 (95%) were located in the anterior circulation and 113 (94.2%) were saccular with a median (interquartile range) maximum diameter of 5.5 mm (range 4.3-7.4) and volume of 52.8 µL (range 27.6-125.6). The 4,781 persons without aneurysms had a mean age of 65.2 ± 10.9 years and 2610 (54.6%) were women. Study characteristics are described in Table 1. We did not find any significant associations between genetic risk scores and presence of intracranial aneurysms (Table 2).In contrast, the genetic risk score for intracranial aneurysms showed a significant age-sex-adjusted association with maximum diameter (difference in log-transformed mm per SD increase of GRS: 0.10;

95%CI, 0.02-0.18; *P*=0.018) and volume (difference in log-transformed µl per SD increase of GRS: 0.21; 95%CI, 0.01-0.41; *P*=0.040) of saccular aneurysms. The association remained statistically significant after additional adjustment (Table 3). Creating a genetic risk score by including SNPs identified in non-Caucasian populations yielded slightly attenuated, but still statistically significant results (Supplementary Table 2 and 3). Individual analyses for each SNP of the risk score are shown in Supplementary Table 4. Two SNPs (rs1333040 and rs6475606) showed nominal significance with intracranial aneurysm size, but did not survive Bonferroni correction. Results for alternative methods of calculating aneurysm size are shown in Supplementary Table 5. No significant associations were found for the genetic risk scores of systolic blood pressure and diastolic blood pressure.

DISCUSSION

In this study of community-dwelling persons, genetic risk variants for intracranial aneurysms were not associated with presence of unruptured, incidentally discovered intracranial aneurysms. However, these genetic variants in combination were found to relate to larger size of incidental saccular aneurysms. Genetic risk variants for blood pressure were associated with neither presence nor size of intracranial aneurysms.

A major strength of our study is, that we obtained unruptured intracranial aneurysms in a population-based setting, allowing us to investigate the association between genetic risk factors and intracranial aneurysm presence in truly asymptomatic individuals. Another strength is the manual segmentation of the entire aneurysm, enabling us to calculate saccular aneurysm volume instead of only the diameter, thus representing actual aneurysm size more accurately. A limitation of our study is the relatively old age of participants. Although aneurysmal SAH incidence increases with age[12], a substantial portion of patients presenting with SAH are young adults. Due to the high morbidity and mortality associated with rupture of aneurysms, these patients were probably not included in our cohort of elderly persons. Combined with the limited statistical power considering a total of 109 cases, this could also explain why we did not find a statistically significant association for presence of aneurysms. Furthermore, the incidental aneurysms in the current study were typically small (median volume = 52.8 µL), which could make measurements inaccurate. However, inter-rater agreement was excellent for

both the maximum diameter and volume, indicating that the estimated aneurysm size was reliable. Also, intracranial aneurysms are more prevalent in persons with rare genetic diseases such as Loeys-Dietz Syndrome and Polycystic Kidney Disease. Even though information about the occurrence of these diseases was not available in our population, we expect the influence to be minimal in our cohort of healthy persons.

Most genetic variants for aneurysms have been identified using cases from a clinical setting, i.e., patients with rupture of intracranial aneurysms. In such a setting, it cannot be discerned whether these genetic variants affect the development of intracranial aneurysms or lead to growth and rupture of already present aneurysms. In our community-dwelling population, we did not find a statistically significant association between these genetic variants and the presence of incidental intracranial aneurysms, although the confidence interval for the odds ratio included values that would indicate a potentially important association (OR as large as 1.40). The absence of a statistically significant association may thus reflect low statistical power. Interestingly, despite the small numbers of persons with aneurysms, we did find an association between these genetic variants combined and the size of intracranial aneurysms, which is one of the strongest risk factors for rupture.[13] In addition, large aneurysms also have an increased risk of further enlargement.[14] Taken together, our findings suggest that SNPs previously associated with intracranial aneurysms in a clinical setting are likely associated with the aneurysm size in the general population and thus, potentially with their subsequent rupture.

A previous study in patients presenting with SAH did not find any association between similar genetic variants and diameter of aneurysms at the time of rupture[15], using 7 of the 10 SNPs we used. Possible explanations for the difference in results between studies are the difference in study population, and the fact that aneurysm rupture may potentially affect the observed aneurysm size.

Further research could explore the predictive ability of genetic risk scores, identifying additional SNPs to enhance discrimination and rupture risk classification in persons with intracranial aneurysms. We specifically created genetic risk scores for blood pressure genes because hypertension is one of the strongest modifiable risk factors associated

with aneurysm rupture. However smoking and heavy alcohol consumption, among other risk factors, are also strongly associated with aneurysm formation and rupture,[5] and future research should focus on these as well.

CONCLUSION

We demonstrated that genetic risk variants identified for intracranial aneurysms from a clinical setting were not associated with aneurysm presence in the general population. However we did show that these genetic risk variants affect aneurysm size, known to be one of the strongest risk factors for rupture. This possibly suggests that the clinically identified SNPs are mainly associated with aneurysm rupture, rather than with the presence of aneurysms in a general population.

REFERENCES

1. Vernooij MW, Ikram MA, Tanghe HL, Vincent AJ, Hofman A, Krestin GP, et al.. *The New England journal of medicine*. 2007;357:1821-1828
2. Rinkel GJ, Djibuti M, Algra A, van Gijn J.. *Stroke; a journal of cerebral circulation*. 1998;29:251-256
3. Vlak MH, Rinkel GJ, Greebe P, Algra A.. *Stroke; a journal of cerebral circulation*. 2013;44:1256-1259
4. Nahed BV, DiLuna ML, Morgan T, Ocal E, Hawkins AA, Ozduman K, et al. Hypertension, age, and location predict rupture of small intracranial aneurysms. *Neurosurgery*. 2005;57:676-683; discussion 676-683
5. Andreasen TH, Bartek J, Jr., Andresen M, Springborg JB, Romner B. *Stroke; a journal of cerebral circulation*. 2013;44:3607-3612
6. Juvela S, Poussa K, Porras M. *Stroke; a journal of cerebral circulation*. 2001;32:485-491
7. Daou MR, El Ahmadieh TY, El Tecle NE, Bohnen AM, Bendok BR. Unruptured intracranial aneurysms: Risk factors and their interactions. *Neurosurgery*. 2013;73:N14-15
8. Ronkainen A, Hernesniemi J, Puranen M, Niemitukia L, Vanninen R, Ryynanen M, et al. Familial intracranial aneurysms. *Lancet*. 1997;349:380-384
9. Bilguvar K, Yasuno K, Niemela M, Ruigrok YM, von Und Zu Fraunberg M, van Duijn CM, et al.. *Nature genetics*. 2008;40:1472-1477
10. Hofman A, Darwish Murad S, van Duijn CM, Franco OH, Goedegebure A, Ikram MA, et al. *European journal of epidemiology*. 2013;28:889-926

11. Ikram MA, van der Lugt A, Niessen WJ, Krestin GP, Koudstaal PJ, Hofman A, et al. *European journal of epidemiology*. 2011;26:811-824
12. de Rooij NK, Linn FH, van der Plas JA, Algra A, Rinkel GJ. *Journal of neurology, neurosurgery, and psychiatry*. 2007;78:1365-1372
13. Wermer MJ, van der Schaaf IC, Algra A, Rinkel GJ.. *Stroke; a journal of cerebral circulation*. 2007;38:1404-1410
14. Burns JD, Huston J, 3rd, Layton KF, Piepgras DG, Brown RD, Jr.*Stroke; a journal of cerebral circulation*. 2009;40:406-411
15. Kleinloog R, van 't Hof FN, Wolters FJ, Rasing I, van der Schaaf IC, Rinkel GJ, et al. *Neurosurgery*. 2013;73:705-

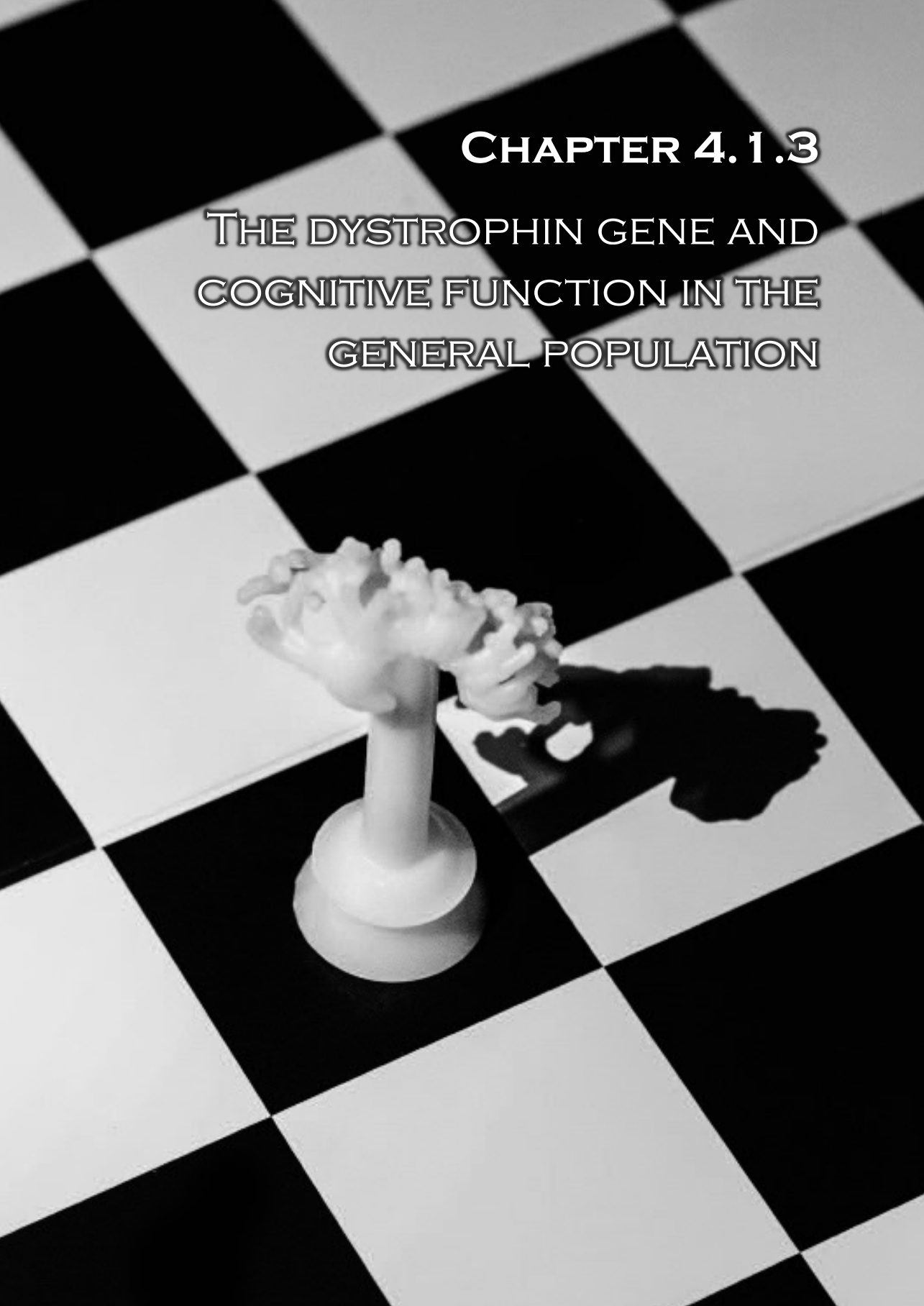

Chapter 4.1.3

The dystrophin gene and cognitive function in the general population

ABSTRACT

The aim of our study is to investigate whether single nucleotide dystrophin gene (DMD) variants associate with variability in cognitive functions in healthy populations. The study included 1,240 participants from the Erasmus Rucphen family (ERF) study and 1,464 individuals from the Rotterdam Study (RS). The participants whose exomes were sequenced and who were assessed for various cognitive traits were included in the analysis. To determine the association between DMD variants and cognitive ability linear (mixed) modeling with adjustment for age, sex and education was used. Moreover Sequence Kernel Association Test (SKAT) was used to test the overall association of the rare genetic variants present in the DMD with cognitive traits. Although no DMD variant surpassed the pre specified significance threshold ($p < 1*10^{-4}$), rs147546024:A>G showed strong association ($\beta = 1.786$, p-value = $2.56*10^{-4}$) with block design test in the ERF study, while another variant rs1800273:G>A showed suggestive association ($\beta = -0.465$, p-value = 0.002) with Mini-mental state examination test in the RS. Both variants are highly conserved, although rs147546024:A>G is an intronic variant, whereas, rs1800273:G>A is a missense variant in the DMD which has a predicted damaging effect on the protein. Further gene based analysis of DMD revealed suggestive association (p-values = 0.087 and 0.074) with general cognitive ability in both cohorts. In conclusion, both single variant and gene based analyses suggest the existence of variants in the DMD which may effect cognitive functioning in the general populations.

INTRODUCTION

The dystrophin gene (*DMD*) is localized on the X chromosome. Variants in *DMD* have been recognized as a cause of the most common form of muscular dystrophy during childhood, Duchenne muscular dystrophy (DMD).[1] This disorder leads to progressive muscle weakness and less well described non-progressive central nervous system manifestations.[2]

A consistent finding among patients with DMD is the reduction in Full-Scale intelligence quotient. Although most individuals are not intellectually disabled, risk for cognitive impairment is increased among affected males and up to 30 % of patients have intellectual disability.[3-5] Apart from intellectual abilities, frequently reported neurocognitive function impairment has been published.[6] Deficits in short-term memory, executive functions, visuospatial ability, as well as deficits in some aspect of attention, problems with narrative, linguistic and reading skills have been described, irrespective of general intelligence.[7-12] Moreover, a higher incidence of different neuropsychiatric disorders, such as autism spectrum, attention deficit hyperactivity disorder, obsessive-compulsive disorders and social behavior problems has been revealed among affected males.[13-17]

The impact of *DMD* on cognitive ability in cognitively healthy populations has not been studied to the best of our knowledge, therefore in the current study we aim to investigate whether single nucleotide *DMD* variants associate with variability in cognitive functions in general populations, suggesting loci in the *DMD* contributing to cognition, besides genuine *DMD* variants.

METHODS

Study populations

Our study population consisted of subjects from Erasmus Rucphen Family (ERF) and Rotterdam Study (RS). Erasmus Rucphen Family is a family based study that includes inhabitants of a genetically isolated community in the South-West of the Netherlands, studied as part of the Genetic Research in Isolated Population (GRIP) program.[18] Study population includes approximately 3,000 individuals who are

living descendants of 22 couples who had at least six children baptized in the community church. All data were collected between 2002 and 2005. The population shows minimal immigration and high inbreeding, therefore frequency of rare alleles is increased in this population. All participants gave informed consent, and the Medical Ethics Committee of the Erasmus University Medical Centre approved the study.

The Rotterdam study (RS) is a prospective, population-study from a well-defined Ommoord district in the Rotterdam city that investigates the occurrence and determinants of diseases in the elderly.[19] The cohort was initially defined in 1990 among approximately 7,900 persons who underwent a home interview and extensive physical examination at the baseline and during follow-up rounds every 3-4 years. Cohort was extended in 2000 and 2005.[19] RS is an outbred population, predominantly of Dutch origin. The Medical Ethics Committee of the Erasmus Medical Center, Rotterdam, approved the study. Written informed consent was obtained from all participants.

Data collection procedure

Participants from both cohorts underwent extensive neuropsychological examination. In ERF study different cognitive domains were assessed using Dutch validated battery of neuropsychological tests.[20,21] We focused on neurocognitive domains which are known to be affected in patients with DMD.[8-12] General cognitive ability was assessed with the Dutch Adult Reading Test (DART). Memory function was measured with a word learning test from which immediate recall and learning scores were derived while executive function was assessed with the Trail Making Test parts A and B (TMT)[22] and verbal fluency tests.[22] Visuospatial ability was assessed with the WAIS-III block-design subtest.

In the RS global cognitive function was assessed with the Mini-mental state examination test (MMSE), while executive function and information processing speed were assessed with the Letter-Digit Substitution Task (LDST)[23], the Word Fluency Test (WFT)[24], and the abbreviated Stroop test.[25] Examination was performed at baseline (MMSE) and during follow up rounds (MMSE, LDST,

WTF).Participants from the both cohorts who had dementia or clinical stroke were excluded from the analysis as these conditions can influence neuropsychological assessment.

Genotyping/Sequencing

The exomes of 1,336 individual from the ERF population were sequenced "in-house" at the Center for Biomics of the Cell Biology department of the Erasmus MC, The Netherlands, using the Agilent version V4 capture kit on an Illumina Hiseq2000 sequencer using the TruSeq Version 3 protocol. The sequence reads were aligned to the human genome build 19 (hg19) using BWA and the NARWHAL pipeline.[26,27] The aligned reads were processed further using the IndelRealigner, MarkDuplicates and TableRecalibration tools from the Genome Analysis Toolkit (GATK) and Picard (http://picard.sourceforge.net). Genetic variants were called using the Unified Genotyper tool of the GATK. About 1.4 million Single Nucleotide Variants (SNVs) were called and after removing the low quality variants (QUAL < 150) we retrieved 577,703 SNVs in 1,309 individuals. Further, for prediction of the functionality of the variants, annotations were performed using the SeattleSeq database (http://snp.gs.washington.edu/SeattleSeq Annotation131).

In the Rotterdam study exomes of 1,764 individuals from the RS-I population were sequenced using the Nimblegen SeqCap EZ V2 capture kit on an Illumina Hiseq2000 sequencer and the TrueSeq Version 3 protocol. The sequences reads were aligned to the human genome build 19 (hg19) using Burrows-Wheeler Aligner.[27] Subsequently, the aligned reads were processed further using Picard (http://picard.sourceforge.net), SAMtools[28] and Genome Analysis Toolkit (GATK).[29] Genetic variants were called using Unified Genotyper Tool from GATK. Samples with low concordance to genotyping array (< 95%), low transition/transversion ratio (< 2.3) and high heterozygote to homozygote ratio (> 2.0) were removed from the data. The final dataset consisted of 903,316 SNVs in 1,524 individuals.

Statistical analysis

Baseline descriptive analysis was performed with SPSS version 17. Deviation from

normality of cognitive functions was assessed by histograms and P-P plots. As the ERF study includes related individuals, all single variants in *DMD* were tested for association applying additive linear-mixed modeling with the „mmscore" function adjusting for age, sex and education in the GenABEL library of the R software.[30] The „mmscore" function uses the relationship matrix estimated from genomic data in the linear mixed model to correct for relatedness among the samples. Additionally, for the most interesting results gender stratified analysis was also performed. As most of these cognitive tests are correlated (the

Pearson correlation coefficient ranged from 0.219 to 0.670), in order to adjust for multiple testing we first calculated the effective number of independent tests using the eigenvalues of a correlation matrix using Matrix Spectral Decomposition (matSpDlite) software[31], finally Bonferroni correction was applied for the effective number of independent tests. The same strategy was also adopted for modeling linkage disequilibrium between the SNVs of the *DMD*. Considering the number of independent cognitive tests and independent variants, the significance threshold was set to 0.05/(4 independent cognitive tests*124 independent variants) = $1.00*10^{-04}$, whereas suggestive threshold was set to 1/(4 independent cognitive tests*124 independent variants) = $2*10^{-3}$. SNVs were coded 0, 1, 2 for genotypes AA, AB, BB in females respectively and 0, 2 for genotypes A, B in males. Since sequencing is likely to reveal several variants that may be population specific, we also performed the gene-based Sequence Kernel Association Test (SKAT), a test specifically designed to analyze rare sequence variation in a specific gene/region.[32] Assessing the joint effect of multiple variants within the gene/region, the SKAT is proposed as a more powerful approach for rare variants than a classical single variant analysis and several burden tests.[32] The significance threshold for gene-wise analysis was set to 0.05/4 independent cognitive tests = 0.0125, while the suggestive threshold was set to ¼ independent test = 0.25.

To assess the relationship between the SNVs variants outside the protein-coding regions with gene expression in the tissue we used the Genotype-Tissue Expression (GTEx) project database.[33] The data were deposited in GWAS Central (HGVST1824).

RESULTS

General characteristics of the studied populations are shown in Table 1. The mean age in ERF was 48 years and 39 % of the participants were males while mean age in RS was around 68 years and 44 % of the participants were males. Around 30 % of participants in the ERF study had only primary education compared to around 36 % subjects in the RS.

Number of SNVs in the *DMD* discovered by exome sequencing was 165 in the ERF and 482 in the RS (Supplementary Table 1). Around 70 % of variants in the *DMD* had minor allele frequency (MAF) lower than 0.05 in ERF compared to around 98 % of variants in the RS. The results of the association analysis between SNVs in the *DMD* and cognitive functions with nominal level of significance in ERF study are presented in Table 2. Although none of the findings surpassed multiple testing correction using a Bonferroni threshold of $1.00*10^{-04}$, strong association was observed between rs147546024:A>G ($\beta = 1.786$, *p-value* = $2.56*10^{-04}$) and the block design test. Gender

Table 1 | Descriptive statistics of the study populations.

	ERF	RS baseline	RS follow up
N	1241	1464	902
Age	47.9 (14.4)	68.1 (9.4)	72.0 (7.1)
Gender (% of males)	39.3%	44.3%	44.8%
Education (% of only primary education)	29.8%	35.6%	29.3%
Cognitive tests			
Dutch Adult Reading Test, mean (sd)	58.56 (20.31)		
AVLT - Immediate recall, mean (sd)	4.37 (1.69)		
AVLT - Learning, mean (sd)	33.55 (9.01)		
Ratio TMT-B / TMT-A, mean (sd)	2.68 (1.02)		
Verbal fluency, mean (sd)	61.66 (18.21)		
Block design test, mean (sd)	8.24 (2.77)		
Mini-mental state examination, mean (sd)		27.7 (1.8)	27.7 (2.0)
Letter-Digit Substitution Task, mean (sd)			27.0 (7.2)
Word Fluency Test, mean (sd)			21.3 (5.5)

ERF – Erasmus Rucphen family study; RS - Rotterdam study; N - number of participants; AVLT - Auditory Verbal Learning Test; TMT- A, TMT- B - Trail Making Test parts A and B;

Table 2 | Association of *DMD* variants with cognitive abilities in ERF study

Cognitive test	Name	Genomic position*	Ref allele	Variant allele	N	Effect	SE	Nominal *p-value*	MAF	HWE *p*	PolyPhen prediction	GERP
General cognitive ability												
Dutch	rs72470515	32716133	G	C	1222	3.839	1.456	8.59E-03	0.042	0.392	unknown	0.018
Adult	rs72470514	32716132	G	T	1225	3.226	1.419	2.35E-02	0.043	0.392	unknown	-1.75
Reading	rs1800278	31496426	T	C	1225	-3.448	1.528	2.45E-02	0.035	1	0.281	1.66
Test	rs41305353	31496431	T	A	1225	-3.448	1.528	2.45E-02	0.035	1	0.981	5.4
	rs183429765	31838024	C	T	1225	-9.496	4.213	2.47E-02	0.004	1	unknown	-1.47
	rs17338590	31497369	T	C	1146	-3.246	1.530	3.44E-02	0.034	0.006	unknown	-0.067
	rs16989970	31950056	G	A	1215	-3.053	1.460	3.72E-02	0.038	0.161	unknown	4.25
	rs17309542	32614065	A	G	1225	-1.815	0.882	4.03E-02	0.124	0.081	unknown	2.76
	rs5927082	32591811	A	G	1225	-1.639	0.798	4.07E-02	0.160	0.499	unknown	2.12
	rs5927083	32591931	T	C	1225	-1.639	0.798	4.07E-02	0.160	0.499	unknown	-1.32
	rs72468656	32459449	A	G	1221	-8.105	4.089	4.82E-02	0.006	1	unknown	3.9
	rs72466537	31165350	G	C	1225	-2.814	1.428	4.96E-02	0.042	0.105	unknown	2.83
Memory												
AVLT -	rs1800279	31496398	T	C	1228	0.311	0.138	3.04E-02	0.035	0.282	0.01	2.92
Immediate	23:32715801	32715801	G	A	1221	0.836	0.408	4.85E-02	0.003	1	unknown	2.84
AVLT -	23:32715801	32715801	G	A	1221	6.139	2.015	2.93E-03	0.003	1	unknown	2.84
Learning	rs2293667	31224881	A	G	1228	1.161	0.472	1.62E-02	0.076	0.467	unknown	1.29
	rs2293668	31224684	G	A	1228	1.161	0.472	1.62E-02	0.076	0.467	unknown	3.96
	rs2293666	31224994	G	A	1194	1.145	0.468	1.70E-02	0.077	0.141	unknown	3.65
	23:31838262	31838262	A	G	1228	-7.458	3.541	3.97E-02	0.001	1.000	unknown	-1.35
	rs1800279	31496398	T	C	1228	1.419	0.685	4.30E-02	0.035	0.282	0.01	2.92

Table 2 continued.

Executive												
Ratio TMT-B / TMT-A	rs7891425	32361033	C	T	1223	-0.101	0.048	3.99E-02	0.140	0.072	unknown	5.36
	rs56094071	32430503	A	T	1202	-0.098	0.048	4.55E-02	0.149	0.570	unknown	5.15
Verbal fluency	rs72468668	32486917	T	G	1225	7.426	3.124	2.12E-02	0.007	1	unknown	2.06
	rs72470511	32663417	G	A	1229	-8.246	3.758	3.34E-02	0.004	1	unknown	2.15
	rs12837503	32404249	A	G	1229	-4.038	1.993	4.95E-02	0.018	1	unknown	-5.13
Visuospatial												
Block design test	rs147546024	33146086	A	G	1211	1.786	0.470	2.56E-04	0.011	1	unknown	4.08
	rs72470511	32663417	G	A	1218	-2.144	0.629	1.01E-03	0.004	1	unknown	2.15
	rs183429765	31838024	C	T	1220	-1.673	0.650	1.32E-02	0.004	1	unknown	-1.47
	23:32834523	32834523	A	G	1220	-2.513	1.043	2.03E-02	0.002	1	unknown	0.531

*DMD – dystrophin gene; N - number of individuals; SE – standard error; MAF - minor allele frequency; HWE – Hardy-Weinberg equilibrium; GERP – the program that generates the conservation score; AVLT - Auditory Verbal Learning Test; TMT- A, TMT- B - Trail Making Test parts A and B; *Genomic positions are according hg19 assembly;*

Table 3 | Overlapping variant in both cohorts

	Name	Genomic position*	N	Reference allele	Variant allele	Effect	SE	*p*-	MAF	PolyPhen prediction	GERP conservation
ERF Block design	rs1800273	31986607	1220G		A	-	0.222	0.066	0.038	0.999	2.52
RS MMSE	rs1800273	31986607	1418G		A	-	0.151	0.002	0.033	0.999	2.52

N - number of individuals, SE - standard error; MAF - minor allele frequency; GERP - the program that generates the conservation score; ERF – Erasmus Rucphen family study; RS - Rotterdam study; MMSE – Mini-mental state examination test;
**Genomic positions are according to hg19 assembly.*

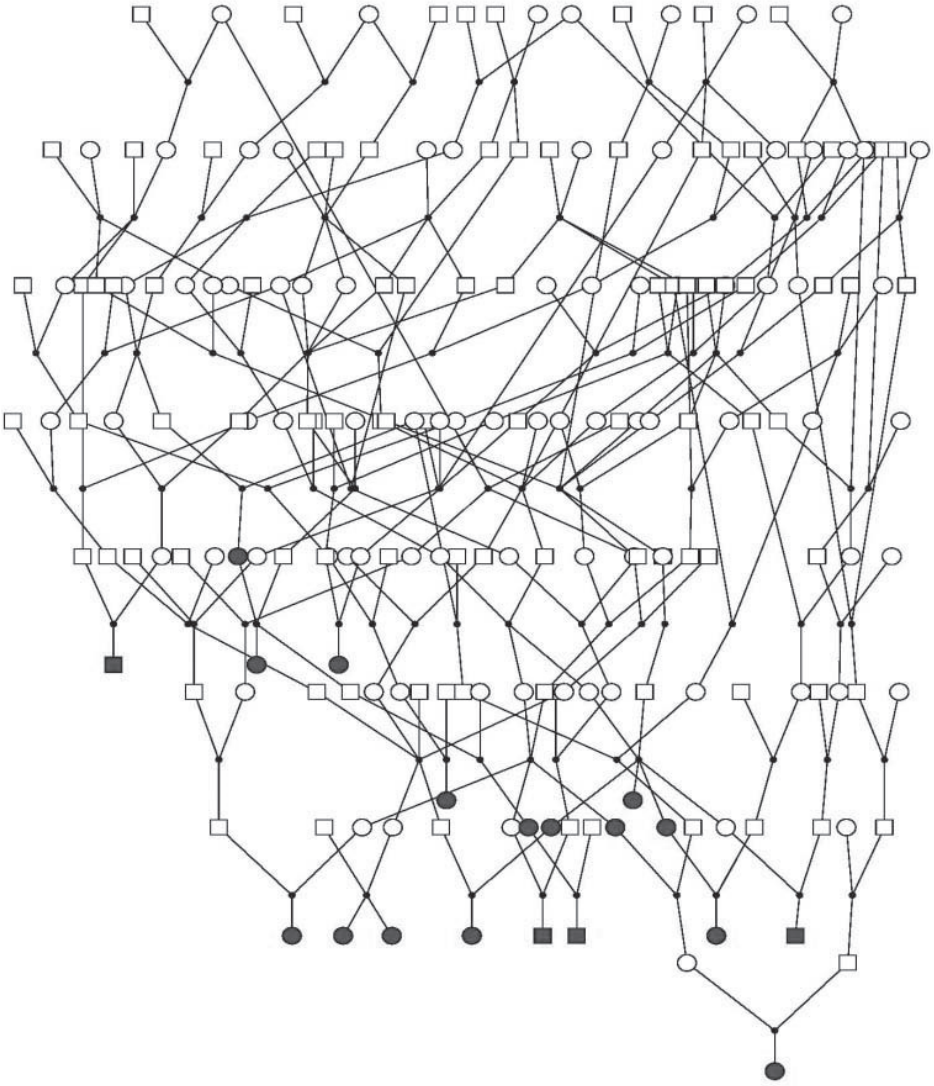

Figure 1. Carriers of the SNV that achieved the strongest association in the ERF study
Carriers are indicated in gray.

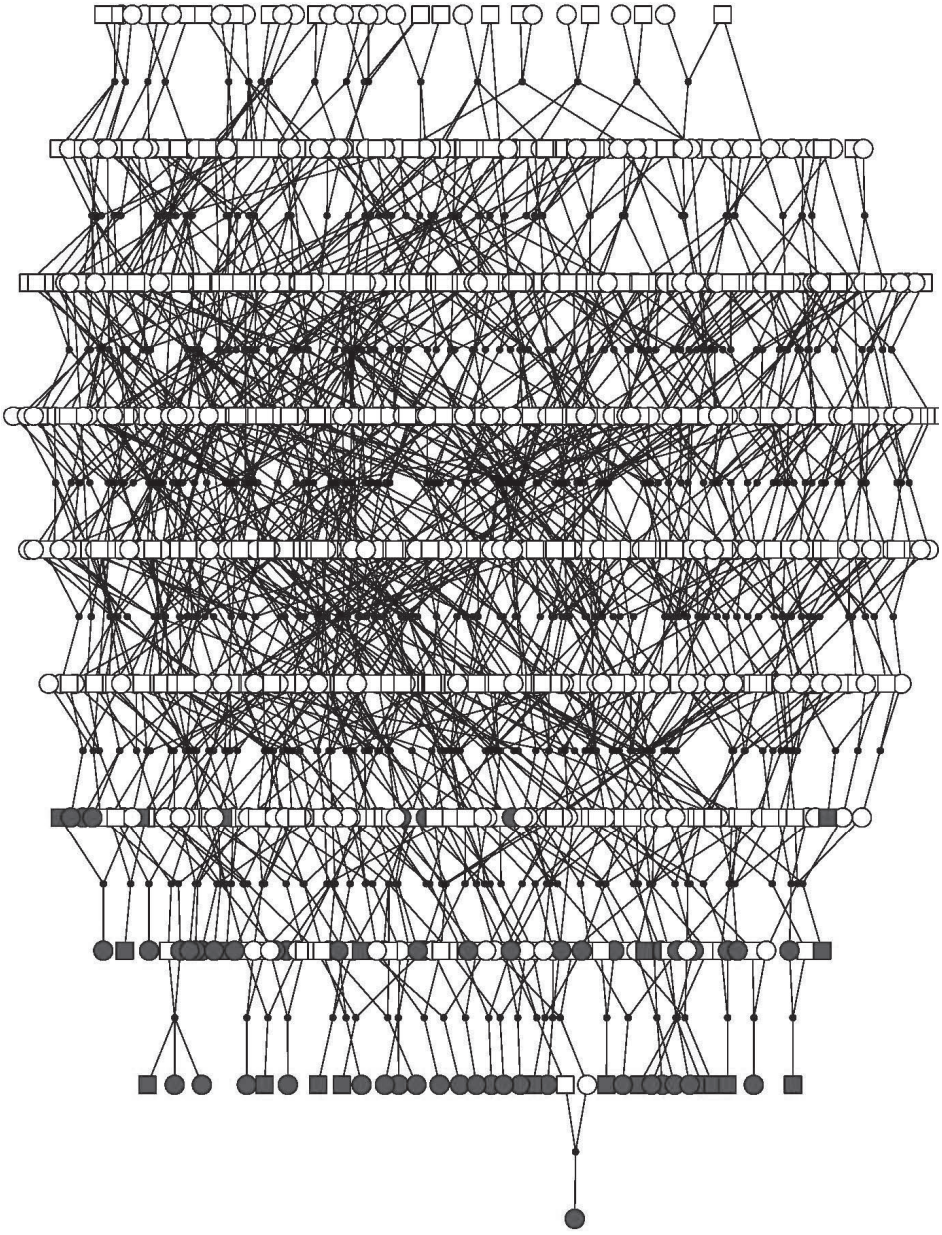

Figure 2. Carriers of the overlapping SNV in the ERF study.
Carriers are indicated in gray.

stratified analysis showed nominally significant association in both genders (β = 1.796, *p-value* = 0.009 in males and β = 1.623, *p-value* = 0.018 in females). This rare (*A G*) variant with MAF of 0.011 was localized in the intron 1 of the *DMD* (chrX.hg19:g.33146086A>G) and although being highly conserved over species (Conservation score GERP = 4.08) has an unknown effect on the protein. Based on localization, we studied the relationship of this variant with gene expression in human tissues GTEx database but no significant eQTLs were found for this variant.

The family-based design of the ERF study allowed us to check if all the carriers (*n* = 24) of this variant were closely related. All carriers were connected to each other in 10 generations (Figure 1).

Next, we explored the association of rs147546024:A>G in the population based study (RS). Even though rs147546024:A>G is a previously identified genetic variation in dbSNP database (present in six copies in 1000 Genomes with a MAF of 0.004) it was not present in RS and was not in linkage disequilibrium with any of the other SNVs of *DMD*. This prompted us to look for overlapping variants between the two studies. Among 34 overlapping variants we identified the most interesting overlapping finding that is shown in Table 3. Among these variants rs1800273 (chrX.hg19:g.31986607G>A), had similar MAF in both studies (0.038 in the ERF and 0.033 in the RS), similar effect size and same direction of the effect in both cohorts and was suggestively associated with Block design test in the ERF study (β = -0.424, *p-value* = 0.066) and with MMSE in RS (β = -0.465, *p- value* = 0.002) (Table 3). This G>A variant is localized in exon 45 of the *DMD* and is classified as a missense variant with a predicted damaging effect on the protein (POLYPHEN score = 0.99, conservation score GERP = 2.52). This variant is present in 23 copies in 1000 Genomes with a MAF of 0.014. All carriers of the variant in the ERF were connected to each other (Figure2).

In the gene based analysis using SKAT suggestive associations (*p-values* 0.087 and 0.074) were also observed both in ERF and RS for DART and MMSE respectively.

DISCUSSION

The aim of this study was to investigate possible impact of genetic variants in the *DMD* on cognitive ability in the general population. Even though none of the *DMD* variants surpassed the pre specified significance threshold, rs147546024:A>G was suggestively associated with block design test in ERF, whereas rs1800273:G>A was nominally associated with Mini-mental state examination test in the RS and marginally associated with block design test in ERF.

rs147546024:A>G is localized in the intron 1, 196 bp far from the promoter of full-length protein isoform (Dp427p) which is expressed predominantly in the Purkinje cells of the hippocampus. The frequency of this variant in 1000 Genomes was observed to be 0.005 in individuals of European origin compared to ERF where the frequency was 0.011. This enrichment is expected due to genetic drift and isolation of the ERF population.[18] Functional prediction of this variant showed high conservation score and unknown effect on the protein while gene expression analysis found no significant eQTLs in various human tissues. Interestingly, the rare allele of rs147546024:A>G was associated with better cognitive performance on block design test which is designed to assess visuospatial ability. Similar to some studies which have described a sex differences in cognitive ability with a male advantage on the spatial domains[34], our study confirmed slight, but not significant, higher scoring of males on block design test. It is known that better performance on block design test is associated with autistic spectrum disorder[35-37] and *DMD* is recognized as one of susceptibility genes for autism disorder.[38,39] Suppression of the global configuration in order to process the information in a detailed fashion, essential for this test, is described as a main characteristic of autistic patients.[40-43]

Another biologically interesting finding while searching for overlapping variants in both studies was the missense G A variant, rs1800273:G>A, which we found associated with block design test in ERF and the test of global cognitive ability (MMSE) in RS. This variant was observed at a frequency of 0.033 in the individuals of European origin and absent in those of African and Asian origin. Localized in exon 45 of the *DMD*, this variant was classified as a missense variant with a predicted

damaging effect on the protein. Since the *DMD* has three upstream and four intragenic promoters which control expression of full-length (Dp427c, Dp427m, Dp427p) and short protein isoforms (Dp260, Dp140, Dp116, Dp71), exon 45 is present in the four different isoforms (Dp427c, Dp427m, Dp427p, Dp260) among which Dp427c and Dp427p are expressed in the brain.[44] The Dp427c is expressed predominantly in neurons of the cortex and the CA regions of the hippocampus. It has been shown that this form of protein dystrophin colocalizes with inhibitory GABA receptor clusters at the postsynaptic membranes of hippocampal and neocortical pyramidal neurons where modulate synapse function.[45-48] According to various studies this dystrophin isoform has a stabilizing effect on the GABA receptors by limiting their lateral diffusion outside the synapse.[49,50] Importance of GABA receptors for the regulation of cognition, emotion and memory is increasingly being recognized.[51,52] The Dp427p is expressed in the cerebellar and hippocampal Purkinje cells and in the cortical brain.[53,54] However, exon 45 does not affect three shorter *DMD* isoforms (Dp140, Dp116 and Dp71) which are known to be associated with cognitive function in DMD.[55,56] rs1800273:G>A was detected earlier in DMD patients and is present in the Leiden Muscular dystrophy database.[57] Since majority of DMD patients have cognitive impairment, the association of rs1800273:G>A with DMD may represent association with cognitive impairment. However presence of this variant and lack of the dystrophin protein - which can by itself lead to cognitive impairment - would make it difficult to study the separate effect of this variant in DMD patients.

One of the difficulties that our study had to deal with is heterogeneity in classification of phenotypes. Even though various cognitive tests are used in the studied populations, different cognitive domains can be compared since they are correlated. Therefore, moderate correlation (the Pearson correlation coefficient 0.429, *p-value* < 0.0001) between visuospatial ability and global cognition ability in the ERF, as well as correlation (the Pearson correlation coefficient 0.460, *p-value* < 0.0001) between visuospatial ability and executive function which is recognized as a central domain of cognitive functioning[58,59] allow us to compare association of the most interesting overlapping variant with block design test in

the ERF and MMSE test in the RS.

The majority of variants called in our study were rare variants. Even though there is growing evidence that rare variants contribute to etiology of different complex traits, the search for rare variants is very difficult and challenging. Standard methods used to test for association with single common genetic variants are not powerful enough for the analysis of rare variants.[60-62] Therefore with the available sample size, our study had limited power to detect association. This we attempted to overcome using the recently proposed gene based analysis (SKAT) design for rare variant analysis.[32] Assessing the cumulative effect of multiple variants in *DMD* implied only suggestive *p-value* for both cohorts. Still like other approaches that deal with rare variants this approach also has limitations in terms of power but suggestive *p-values* generated by SKAT pointed out that variants in the *DMD* may effect cognitive functioning in healthy populations.

In conclusion, analyzing the sequence variants in the exon of *DMD* in two cognitively healthy cohorts we find evidence of association of *DMD* with cognitive functioning in healthy individuals. Larger studies are required for confirmation.

SUPPLEMENTARY MATERIAL

Supplementary Information is available at European Journal of Human Genetics website (http://www.nature.com/ejhg)

REFERENCES

1. Hoffman EP*, et al.* Cell.1987;51:919-928
2. Anderson JL*, et al.* Brain. 2002;125:4-13
3. Cotton S*, et al.*Dev Med Child Neurol.2001;43:497-501
4. Emery AEH. *Duchenne muscular dystrophy*. Oxford ; New York: Oxford University Press; 2003.
5. Cotton SM*, et al.*Dev Med Child Neurol.2005;47:257-265
6. Sollee ND*, et al.*J Clin Exp Neuropsychol.1985;7:486-496
7. Cyrulnik SE*, et al.*J Pediatr.2007;150:474-478
8. Wicksell RK*, et al.*D1. Hoffman EP*, et al.*Cell.1987;51:919-928
2. Anderson JL*, et al.*Brain.2002;125:4-13
3. Cotton S*, et al.*Dev Med Child Neurol.2001;43:497-501
4. Emery AEH. *Duchenne muscular dystrophy*. Oxford ; New York: Oxford University Press; 2003.
5. Cotton SM*, et al.*Dev Med Child Neurol.2005;47:257-265
6. Sollee ND*, et al.*J Clin Exp Neuropsychol.1985;7:486-496
7. Cyrulnik SE*, et al.*J Pediatr.2007;150:474-478
8. Wicksell RK*, et al.*Dev Med Child Neurol.2004;46:154-159
9. Hinton VJ*, et al.*Neurology.2000;54:2127-2132
10. Hinton VJ*, et al.*Dev Med Child Neurol.2007;49:123-128
11. Mento G*, et al.*Clin Neuropsychol.2011;25:1359-1377
12. D'Angelo MG*, et al.*Pediatr Neurol.2011;45:292-299
13. Perronnet C*, et al.*J Biomed Biotechnol.2010;2010:849426
14. Hendriksen JG*, et al.*J Child Neurol.2008;23:477-481
15. Wu JY*, et al.*J Child Neurol.2005;20:790-795
16. Kohane IS*, et al.*PLoS One.2012;7:e33224
17. Nakamura A MY, Kumagai T, Suzuki Y, Miura K.No To Hattatsu.2008;40:10-14
18. Pardo LM*, et al.*Ann Hum Genet.2005;69:288-295
19. Hofman A*, et al.*Eur J Epidemiol.2013;28:889-926
20. Sleegers K*, et al.*Brain.2004;127:1641-1649
21. Liu F*, et al.*Neurobiol Aging.2010;31:1831-1833
22. Reitan RM.J Consult Psychol.1955;19:393-394
23. Lezak MD HD, Loring DW.2004
24. Welsh KA*, et al.*Neurology.1994;44:609-614
25. Golden CJ.J Clin Psychol.1976;32:654-658
26. Brouwer RW*, et al.*Bioinformatics.2012;28:284-285
27. Li H*, et al.*Bioinformatics.2009;25:1754-1760
28. Li H*, et al.*Bioinformatics.2009;25:2078-2079
29. McKenna A*, et al.*Genome Res.2010;20:1297-1303
30. Aulchenko YS*, et al.*Bioinformatics.2007;23:1294-1296
31. Li J*, et al.*Heredity (Edinb).2005;95:221-227
32. Wu MC*, et al.*Am J Hum Genet.2011;89:82-93
33. Consortium TG.Nat Genet.2013;45:580-585
34. Voyer D*, et al.*Psychol Bull.1995;117:250-270
35. Lord C*, et al.*J Autism Dev Disord.1989;19:185-212
36. Caron MJ*, et al.*Brain.2006;129:1789-1802

37. Shah A FU.J Child Psychol Psychiatry.1993;34:1351–1364
38. Pagnamenta AT*, et al.*J Neurodev Disord.2011;3:124-131
39. Chung RH*, et al.*Mol Autism.2011;2:18
40. Pellicano E*, et al.*Dev Psychopathol.2006;18:77-98
41. Ropar D*, et al.*J Child Psychol Psychiatry.2001;42:539-549
42. Rumsey JM*, et al.*J Clin Exp Neuropsychol.1988;10:201-221
43. Happe F*, et al.*J Autism Dev Disord.2006;36:5-25
44. Muntoni F*, et al.*Lancet Neurol.2003;2:731-740
45. Lidov HG*, et al.*Nature.1990;348:725-728
46. Sekiguchi M*, et al.*Brain.2009;132:124-135
47. Kueh SL*, et al.*Clin Exp Pharmacol Physiol.2008;35:207-210
48. Vaillend C*, et al.*Hippocampus.2002;12:713-717
49. Fritschy JM*, et al.*Biochem Soc Trans.2003;31:889-892
50. Craig AM*, et al.*Curr Opin Neurobiol.2007;17:43-52
51. Mohler H.Biochem Soc Trans.2009;37:1328-1333
52. Millan MJ*, et al.*Nat Rev Drug Discov.2012;11:141-168
53. Holder E*, et al.*Hum Genet.1996;97:232-239
54. Gorecki DC*, et al.*Hum Mol Genet.1992;1:505-510
55. Daoud F*, et al.*Hum Mol Genet.2009;18:3779-3794
56. Taylor PJ*, et al.*PLoS One.2010;5:e8803
57. Aartsma-Rus A*, et al.*Muscle Nerve.2006;34:135-144
58. Miyake A FN, Rettinger DA, Shah P, Ph.D., Hegarty M.Journal of Experimental Psychology - General.2005;130:532–545
59. Salthouse T.Neuropsychology.2005;19:532-
60. Ladouceur M*, et al.*PLoS Genet.2012;8:e1002496
61. Li B*, et al.*Am J Hum Genet.2008;83:311-321
62. Madsen BE*, et al.*PLoS Genet.2009;5:e1000384
ev Med Child Neurol.2004;46:154-

Chapter 4.2

Brain-wide searches

Chapter 4.2.1

Alzheimer's disease genes and the brain

ABSTRACT

Background: The neural substrate of genetic risk variants for Alzheimer's disease (AD) remains unknown. We studied their effect on healthy brain morphology to provide insight into disease etiology in the pre-clinical phase.

Methods: We included 4071 non-demented, elderly participants of the population-based Rotterdam Study who underwent brain MRI and genotyping. We performed voxel-based morphometry (VBM) on all gray matter voxels for 19 previously identified, common AD risk variants. Whole-brain expression data from the Allen Human Brain Atlas was used to examine spatial overlap between VBM association results and expression of genes in AD risk loci regions.

Results: Brain regions most significantly associated with AD risk variants were the left postcentral gyrus with ABCA7 (rs4147929, $p = 4.45 \times 10^{-6}$), right superior frontal gyrus by ZCWPW1 (rs1476679, $p = 5.12 \times 10^{-6}$), and right postcentral gyrus by APOE ($p = 6.91 \times 10^{-6}$). Though no individual voxel passed multiple testing correction, we found significant spatial overlap between the effects of AD risk loci on VBM and the expression of genes (MEF2C, CLU, SLC24A4) in the Allen Brain Atlas. Results are available online on www.imagene.nl/ADSNPs/.

Conclusion: In this single largest imaging genetics dataset worldwide, we found that AD risk loci affect cortical gray matter in several brain regions known to be involved in AD, as well as regions that have not been implicated before.

INTRODUCTION

Alzheimer's disease (AD) is a complex neurodegenerative disease and the most common cause of dementia. It has a long preclinical phase, during which there are no symptoms but structural brain changes can already be detected, such cortical atrophy and localized atrophy of the hippocampus [1,2].

In recent years, common genetic risk factors for AD have been discovered through large meta-analyses of genome-wide association studies (GWAS) [3]. However, the underlying neurobiological substrate leading to AD for the genes assigned to these risk loci remains to be uncovered. Identifying the brain structures affected by these genes can increase our understanding of AD and aid future functional studies. Previous studies have investigated some of the AD risk loci in relation to neuroimaging measures [4–7]. However, they were generally focused on candidate regions that are known to play a role in AD, such as the hippocampus [6,7] or did not investigate all known risk loci [4,5]. Unbiased approaches for analyzing brain images have great potential to give novel insights that would not have been considered a priori. Voxel-based morphometry (VBM) is a hypothesis-free technique for analyzing brain imaging data that characterizes regional tissue concentration differences across the whole brain, without the need to predefine regions of interest [8]. Using VBM, we studied the association of 19 AD genetic risk loci with gray matter morphology at the voxel level in 4071 non-demented elderly from the Rotterdam study. This study provides insight into non-diseased brain morphology. Such knowledge is complementary and intertwined with better understanding disease etiology in the pre-clinical phase. Subsequently, we co-localized our results with publicly available genetic expression data. We thus identified genetic associations with known as well as novel regions affected in AD.

Table 1 |The most significant voxel-wise association signals with p-values<10^{-5}. Brain region labeling based on the Hammer Atlas segmentation.

Risk variant	Gene*	Minimum p-value	Effect direction	Brain Region
rs4147929	ABCA7	$4.46x10^{-6}$	-	postcentral gyrus left
rs1476679	ZCWPW1	$5.12x10^{-6}$	+	superior frontal gyrus right
rs429358/rs7412	APOEε4	$6.91x10^{-6}$	+	postcentral gyrus right
rs11771145	EPHA1	$8.91x10^{-6}$	-	precentral gyrus right
rs190982	MEF2C	$9.55x10^{-6}$	+	lateral remainder of occipital lobe right
Genetic Risk Score	All	$8.02x10^{-6}$	+	postcentral gyrus right
Genetic Risk Score	Without APOE	$1.47x10^{-5**}$	+	lateral remainder of occipital lobe right

Effect direction indicates beta sign, and demonstrates risk loci associated with increasing gray matter tissue (+) or decreasing gray matter tissue (-).

** Assigned risk gene according to Lambert et al [1]*

*** P-value is not less than 10^{-5}, shown to compare with GRS without exclusion APOE.*

METHODS

Study Population

The Rotterdam Study is an ongoing population-based cohort study in the Netherlands investigating diseases in the elderly and currently consists of 14,926 residents of Rotterdam who were aged 45 years or more at baseline [9,10]. The initial cohort was started in 1990 and expanded in 2000 and 2005. The whole population is subject to a set of multidisciplinary examinations every four years. MRI was implemented in 2005 and 5430 persons scanned until 2011 were eligible for this study. We excluded individuals with incomplete acquisitions, scans with artifacts hampering automated processing, participants with MRI-defined cortical infarcts, and subjects with dementia or stroke at the time of scanning. This resulted in a final study population of 4071 non-demented persons with information available on both genome-wide genotyping and MRI data. The Rotterdam Study has been approved by the Medical Ethics Committee of the Erasmus MC and by the Ministry of Health, Welfare and Sport of the Netherlands , implementing the Wet Bevolkingsonderzoek: ERGO (Population Studies Act: Rotterdam Study). All participants provided written informed consent to participate in the study and to obtain information from their treating physicians.

Imputation of genotypes

The Illumina 550K and 550K duo arrays were used for genotyping. Samples with low call rate (<97.5%), with excess autosomal heterozygosity (>0.336) or with sex-mismatch were excluded, as were outliers identified by the identity-by-state clustering analysis (outliers were defined as being >3 standard deviation (SD) from population mean or having identity-by-state probabilities >97%). A set of genotyped input SNPs with call rate >98%, MAF >0.001 and Hardy–Weinberg equilibrium (HWE) P-value > 10^{-6} was used for imputation. The Markov Chain Haplotyping (MACH) package version 1.0 software (Imputed to plus strand of NCBI build 37, 1000 Genomes phase I version 3) and minimac version 2012.8.6 were used for imputation. *APOE* status was genotyped separately, using a polymerase chain reaction, as described in [11]. *APOE*ε4 was coded as the number of ApoEε4 alleles.

MRI acquisition and processing

From August 2005 onwards, a dedicated 1.5 Tesla MRI scanner (GE Healthcare, Milwaukee, Wisconsin, USA) is operational in the Rotterdam Study research center in Ommoord. This scanner is operated by trained research technicians and all imaging data are collected according to standardized image acquisition protocols [10]. Brain MRI scans included a high-resolution 3D T1-weighted fast RF spoiled gradient recalled acquisition in steady state with an inversion recovery pre-pulse (FASTSPGR-IR) sequence with thin slices (voxel size<1mm^3) [10].

Voxel based morphometry (VBM) was performed according to an optimized VBM protocol [12]. First, all T1-weighted images were segmented into supratentorial gray matter (GM), white matter (WM) and cerebrospinal fluid (CSF) using a previously described k-nearest neighbor (kNN) algorithm, which was trained on six manually labeled atlases [13]. FSL software [14] was used for VBM data processing. Then, all GM density maps were non-linearly registered to the standard GM probability template. For this study we chose the ICBM MNI152 GM template (Montreal Neurological Institute) with a 1x1x1 mm^3 voxel resolution. The MNI152 standard-space T1-weighted average structural template is derived from 152 structural images, which have been warped and averaged into the common MNI152 co-ordinate system after high-dimensional nonlinear registration. A spatial modulation procedure was used to avoid differences in absolute GM volume due to the registration. This involved multiplying voxel density values by the Jacobian determinants estimated during spatial normalization. All images were smoothed using a 3mm (FWHM 8mm) isotropic Gaussian kernel.

Statistical analysis

Linear regression models were fitted with voxel values of GM modulation density as the dependent variable and age, sex, and the number of reference alleles (risk alleles for Alzheimer's disease, Supplementary Table 5) as independent variables. In total 1,534,602 voxels were processed. To perform a nonparametric permutation test, we randomly shuffled the genotype data between persons and performed the VBM association analysis with all 1,534,602 voxels in gray matter. This was repeated 10,000

times and for every permutation we saved the minimum p-value. Subsequently, we took the 5th percentile of this minimum p-value distribution to compute FWE p-value threshold, which was 3.0×10^{-7} [15]. This was then divided by 19 to account for the number of independent SNPs, resulting in the final threshold of 1.66×10^{-8}.

Genetic Risk Score

Genetic risk scores (GRS) were constructed by multiplying the number of risk alleles by their reported odds ratio (after natural logarithm transformation) for the disease, and summing this weighted allele score of each variant up into a disease risk score for AD[16]. We tested a GRS based on all 19 AD SNPs and second GRS excluding APOEε4.

APOEε4 stratified analysis

To investigate whether it is possible to enrich association signal of AD variants on brain morphology we split our sample into groups with increased chance for AD pathology by stratifying it for APOEε4 status. In total there were 1168 carrier and 2903 non-carrier in our data set.

The Allen Human Brain gene expression analysis

The Allen Human Brain Atlas (http://human.brain-map.org) includes RNA microarray data collected from the postmortem brains of six donors, with no known neuropsychiatric or neuropathological history. Around 500 samples per subject, per hemisphere were tested for expression profiles of 29,191 genes represented by 58,692 pro bes. The expression profiles were normalized across samples and across different brains as described previously [17].In our analysis we used the three Caucasian donors. For each of these donors we extracted expression profiles of 216 genes, which are located within ± 500kb from AD risk loci and used the MNI coordinates to map the location of the samples. For each probe we derived z-score statistics, which represent deviation of gene expression in that sample relative to background expression. Next, using the VBM association results from all 19 tested AD SNPs, we formed clusters at the significance threshold of p-value<0.05 and identified all tissue samples localized inside these clusters or within 10 voxels from them.

We performed 10.000 random VBM analyses to generate p-value maps of null associations. We formed clusters, based on a p-value threshold of < 0.05, and linked these to probes as described above. For three donors and all probes in the 216 genes (in total 667) we calculated the t-test statistic with a null hypothesis that expression of the gene within clusters is not significantly different from background expression. We saved the minimum p-values for every random VBM map. Subsequently, we took the 5th percentile of this minimum p-value distribution to compute the FWE p-value threshold. The obtained threshold was $1.7x10^{-5}$. Then we performed the same t-test with the AD VBM maps. Thus, we compared expression of genes around AD risk loci in regions identified in the VBM analysis with their background expression in the brain.

Regional analysis

We used the Hammer atlas [18] to segment the gray matter into 36 regions for both hemispheres and compare effects on specific brain regions. We summed all voxels values inside segmented region to estimate gray matter volume. For every risk locus and brain region we run the same regression model as for the VBM analysis.

Visualization

To provide easy access to the study results, we developed an online interactive visualization tool (www.imagene.nl/ADSNPs/).

Table 2 | Results of spatial overlap between VBM risk loci association and gene expression profiles of 3 Caucasian donors from the Allen Human Brain Atlas.

Risk variant	Putative causal gene[a]	Genes showing significant overlap				
	Locus	Significant gene expression	Minimum p-value	Distance from risk loci, bp	Significant donors/ total number of donors	Significant probes/total number of probes
rs10498633	SLC24A4	SLC24A4	$1.50x10^{-5}$	138.027	1/3	1/2
rs190982	MEF2C	MEF2C	$1.41x10^{-5}$	44.275	1/3	1/3
rs9331896	CLU	CLU	$4.43x10^{-7}$	13.252	1/3	1/1
rs35349669	INPP5D	NGEF	$7.57x10^{-16}$	325.080	3/3	2/2
rs11771145	EPHA1	GSTK1	$1.01x10^{-5}$	169.576	2/3	3/4

The table shows genes in risk loci regions, for which expression differs significantly (at corrected threshold $1.7x10^{-5}$) from background expression in regions associated by VBM analysis.

[a] Assigned causal gene according to Lambert et al [1];

RESULTS

Voxel-based morphometry of AD risk loci to

The study population for VBM analysis consisted of 4071 non-demented persons with information available on both genome-wide genotyping and MRI data from the population-based Rotterdam Study. The mean age was 64.7 (± 10.7) years and 2251 (55%) subjects were women.

We studied the association of 19 AD risk loci with 1,534,602 voxels of gray matter. None of the associations reached the multiple-testing correction threshold $1.66x10^{-8}$. Table 1 shows all associations between AD risk loci and gray matter voxel density with suggestive evidence for association p-values < 1×10^{-5}. The strongest associations of gray matter voxel with AD risk loci were found in the left postcentral gyrus, right superior frontal gyrus, and right postcentral gyrus. In Figure 1 we show the three-dimensional maps of the nominally significant (p-value<0.05) associations for the APOE risk loci. The negative clusters of APOE are located close to the medial temporal lobe, in particular around the hippocampus, whereas positive clusters are mainly in the occipital lobe. The GRSs association also did not reach the correction threshold. The strongest signal for risk score with APOE was found in the postcentral gyrus right (p-value=$8.02x10^{-6}$) and for the risk score without APOE in the lateral remainder of the occipital lobe right (p-value=$1.47x10^{-5}$). On Supplementary Figure 1 are shown maps for all risk loci from Table 1. Supplementary Table 2 provides the full list of the top three associated clusters of voxels for each risk locus and more detailed statistical information. All study results are available and can interactively be explored on the ImaGene website: www.imagene.nl/ADSNPs/.

In APOEε4 stratified analysis none of the signals passed the threshold, however variant in MEF2C loci showed much more significant association compare to full sample size analysis (Supplementary Table 5). Additionally, the association signal for non-carrier was in general less significant (Supplementary Table 6).

Spatial overlap with gene expression

To investigate whether the effect of AD risk loci on VBM overlaps with gene expression in the brain, we used the Allen Human Brain Atlas data. We overlapped brain regions identified through our VBM analysis with the maps of samples from three Allen Human Brain Atlas donors (Figure 3). We compared expression within the identified voxel clusters with background expression. In total we tested the expression profiles of 216 protein-coding genes, located ± 500kb from the AD variants (Supplementary Table 1). We found that *MEF2C, CLU, SLC24A4* were significantly expressed (p-value<$1.7x10^{-5}$) in the identified voxel clusters compared to other genes at that particular locus. Interestingly, these were the genes that were previously assigned as the risk genes at each respective locus based on a review of the available literature [3] (Table 2). Additionally, we found genes showing significantly different expression, which are located in the risk loci but were previously not proposed as the causal gene for AD. These are: *NGEF* (p-value=$7.57x10^{-16}$) for the region around rs35349669 and *GSTK1* (p-value=$1.01x10^{-5}$) for the region around rs11771145. Supplementary Table 2 provides the full list of genes and more detailed statistical information.

Regional analysis

Figure 2 provides a heat map showing all AD risk loci and their effect on different brain regions sorted by lobe. None of the association signals passed Bonferroni correction, however several loci showed nominal significant association (p-value <0.05; cells with stars on Figure 2), among them variant in EPHA1 with less tissue in caudate and in insula, CELF1 with more tissue in accumbens and APOE with very strong positive effect in the occipital lobe. Variants in *APOE*, *FERMT2*, *PTK2B, CASS4* and *MS4A6A* showed the strongest effect on hippocampus and were associated with smaller gray matter volume. Risk variants in *EPHA1* and *SORL1* had the largest negative effect on deep gray matter structures: putamen, thalamus, and pallidum.

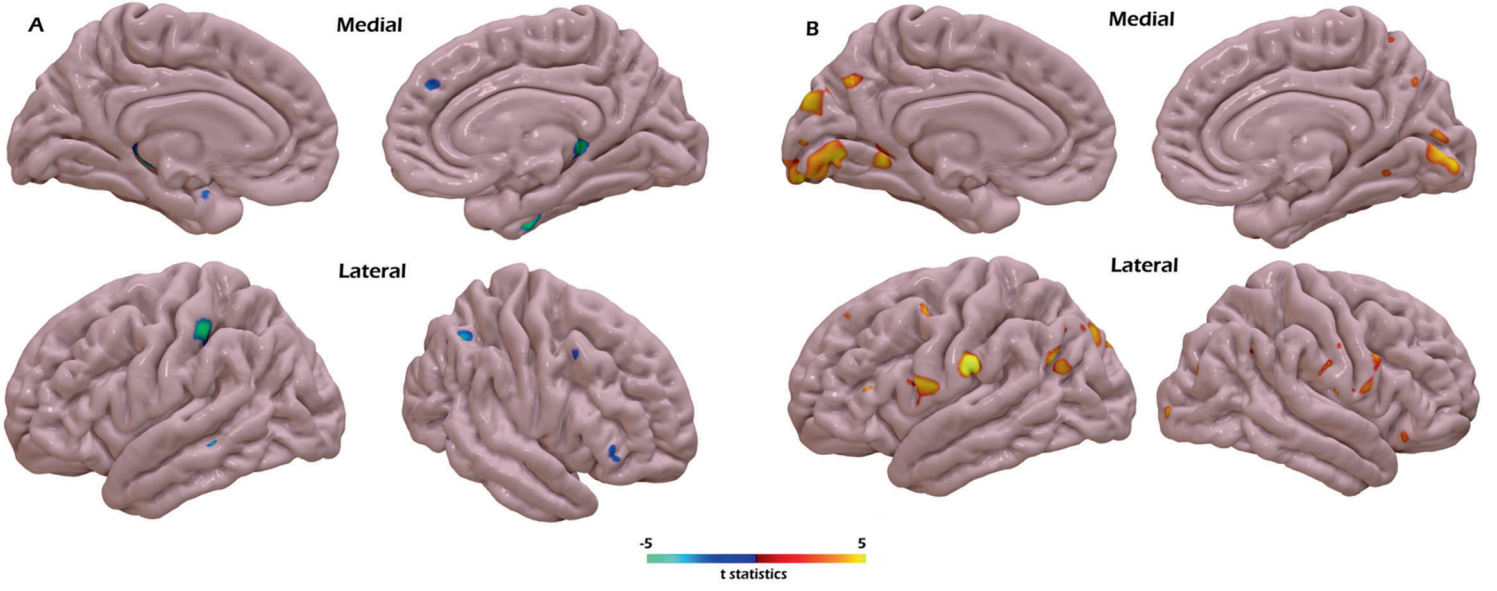

Figure 1 | Projection of APOE risk loci association clusters from VBM to cortical surface.
Colors reflect regression association: blue for negative (A), red for positive (B). Clusters formed based on nominal significant p-value threshold 0.05.

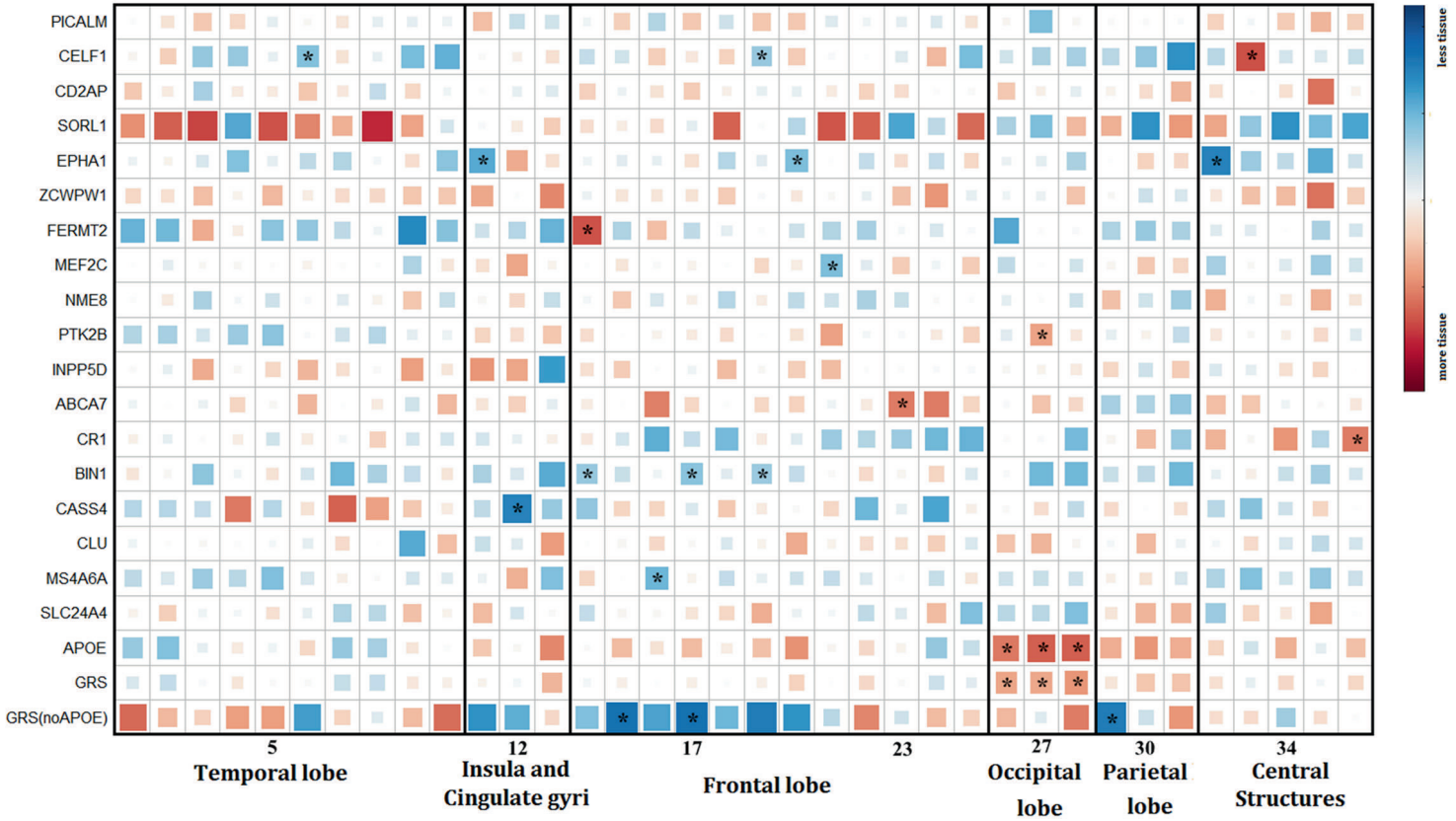

Figure 2 | Heatmap of AD risk loci[1] association effects from ROI analysis.

*The 19 AD risk loci are on the y-axis and brain regions, grouped by lobe, on the x-axis. Brain region labeling was based on the Hammer Atlas. Blue indicates that risk loci were associated with less gray matter tissue; red indicates association with more gray matter tissue. Supplementary Table 3 provides a coded structure list. Regions with nominal significant association (p-value < 0.05) marked with *.*

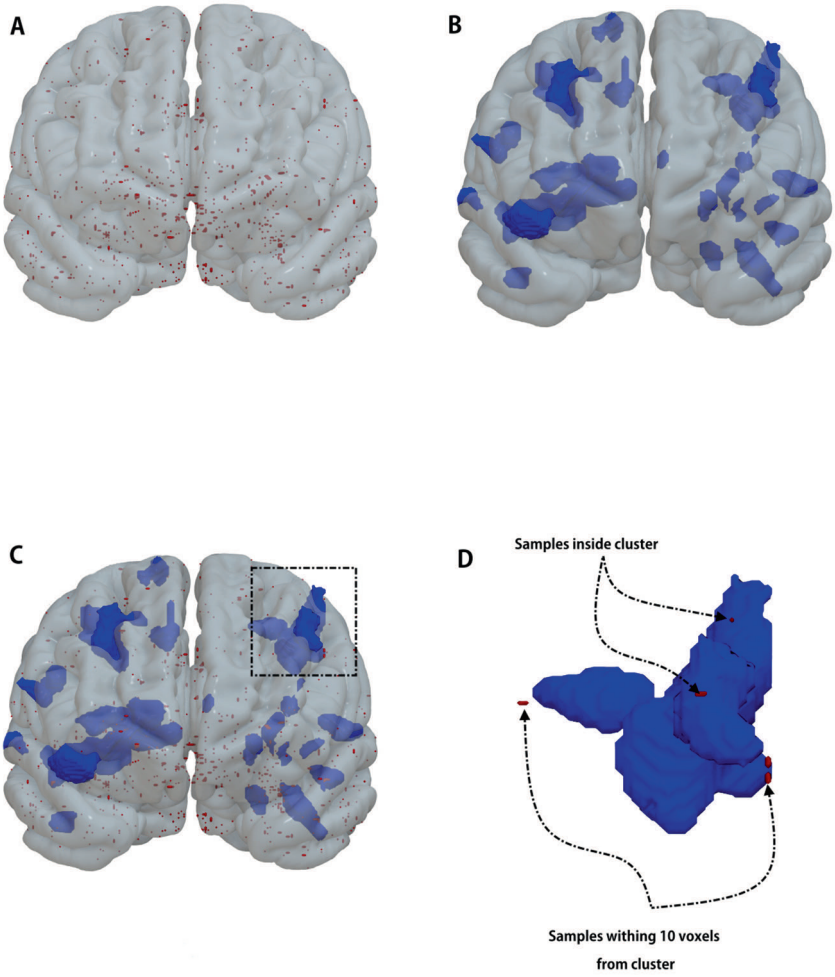

Figure 3 | Example of spatial overlap between VBM association map for the MEF2C risk variant and MEF2C gene expression probes from Allen Human Brain Atlas.
(A) –samples (red color) distribution from "donor9861" of Allen Human Brain Atlas; (B) – clusters of associated with MEF2C risk loci voxels (blue color) identified through VBM analysis formed using p-value threshold 0.05; (C) – Spatial overlap between Allen Brain probes and VBM clusters; (D) – example of VBM cluster and assigning sample location to them.

DISCUSSION

This study presents the association of 19 genome-wide significant AD risk loci [3] with VBM of the gray matter, among 4071 middle aged and elderly subjects from the population-based Rotterdam Study. The unprecedented sample size has enabled this unbiased whole grey matter investigation of established risk variants and their effect on brain morphology. We found nominally significant associations with the left postcentral gyrus, the right superior frontal gyrus and the right postcentral gyrus. Furthermore, through comparing our VBM results to the Allen Brain atlases of human gene expression, we found significant spatial overlap for genes previously assigned to be the causal gene in these loci (C*LU, SLC24A4* and *MEF2C*). Additionally, we identified two genes, not previously suggested to be the causal gene in AD (*GSTK1* and *NGEF*), of which the expression in the brain significantly overlaps with our VBM results.

There currently exists no consensus for voxel-wise genetics studies regarding the significance threshold for avoiding false positive findings while not to being too conservative [19,20]. A number of data processing and statistical analysis methods have been proposed in the literature to address this issue for neuroimaging analysis[21–23]. However, all these methods rely on a set of assumptions about the statistical structure of the data. Therefore, in our study we decided to use unbiased, but more conservative, non-parametric permutation methods to define the statistical threshold of significance. Although this is the largest genetic VBM study conducted to date, none of the voxels passed this conservative multiple testing correction. However, we have previously shown that AD risk loci are associated with cognitive functioning in the general population [11,16,24,25] as well as hippocampal volume in a larger sample (N= 9,232)[7]. This showed that subclinical effects of AD risk loci exist and that effects on gray matter could be expected. Additionally, we constructed genetic risk scores, to explore the combined effect of all AD SNPs on brain morphology. The association signal of GRSs also did not pass correction threshold and the strongest signal for GRS with APOE was driven by APOE variant, while for GRS without APOE by MEF2C variant (Supplementary Figure 2).

Furthermore, it is reasonable to assume that the effects of the risk loci are not restricted to a single voxel, but rather to a cluster of voxels spanning a certain brain region.

Therefore, we further explored the nominally significant associations we found by using the Allen Brain Human Atlas to analyze gene expression, and using Hammer brain atlas to estimate average effect on specific brain regions.

In Hammer regional analysis, we found that risk loci for Alzheimer's disease affect brain morphology in established regions such as the hippocampus (e.g. loci near *APOE, FERMT2, PTK2B*), putamen, thalamus (*SORL1, EPHA1*), as well as regions not often reported on including the insula (*EPHA1*) and occipital lobe (*APOE*). The heat map in Figure 2 summarizes the association results over the whole brain.

Alzheimer's disease is a complex disorder with multiple variants from different pathways involved in its etiology[26,27]. Therefore, as previously shown[6], the effect of these variants on brain morphology could also differ and have different directions. Figure 2 provides a detailed map of such heterogeneous effects. For example, large brain structures, such as the temporal lobe and central regions, are affected differently. Also, some risk loci have a different direction of effects, e.g. *FERMT2* is associated with less tissue and *SORL1* with more tissue in the temporal lobe. Of particular interest is that we found the positive association of APOE with the occipical lobe, which could possibly be explained by cerebral amyloid angiopathy (CAA). Indeed, CAA is linked to APOEε4 carriership [28,29] and has a predilection for the occipital neocortex [30]. Moreover, CAA is involved in Alzheimer's disease [31] and is characterized by ß-amyloid deposition in the media and adventitia of small and medium sized arteries. In healthy subjects, this may be observed as an increase in gray matter tissue density because of the influx of cells to clear the deposits. More research on the effects of AD risk loci on brain morphology is needed to further unravel the biological substrates involved in disease etiology.

Previous case-control studies showed ambiguous differential expression of putative causal genes for AD in the brain [32] or reported that the regional expression of each of the risk loci did not match the pattern of brain regional distribution in Alzheimer pathology [33]. Most of AD variants are non-coding and for the follow up studies would be very important to explore the potential roles of these intronic and intergenic regions in the regulation of gene expression. Confirmed functional variants underlying validated GWAS hits are still sparse in the literature[34,35], when considering all the diseases and traits

studied, but each of these is extremely valuable to the respective research and clinical environments. In our study, we found significant spatial overlap between VBM results in the Allen Human Brain atlas with some of the previously identified genes (C*LU, SLC24A4* and *MEF2C*). This could mean that genetic variability in these genes could act on gray matter density through differences in expression. This is also in line with the fact that most trait-specific GWAS signals are non-coding and probably act through modulation of gene expression[36]. Our results also suggest that VBM analysis combined with expression data could provide evidence for new candidate genes in genetic loci, where the causal gene has not been strongly established by biological experiments[37]. In AD loci, examples are *NGEF* for rs35349669 and *GSTK1* for rs11771145. Although the index variant rs35349669 is located within *INPP5D*, this gene is expressed at low levels in the brain [3] and the linkage peak spans multiple genes with suggestive signals, including *NGEF* [3]. Neuronal Guanine Nucleotide Exchange Factor *(NGEF)*, among its related pathway is signaling by G protein–coupled receptors (GPCRs), which are involved at many stages of AD disease progression, and this class of receptors is a potential therapeutic target for AD [38]. Glutathione S-transferase Kappa 1 (GSTK1) is member of the superfamily of enzymes that function in cellular detoxification. Interestingly, a significant decrease of glutathione transferase activity in different brain regions in patients with Alzheimer disease was previously reported [39], suggesting a possible link to Alzheimer through diabetes [40,41].

Our study also has several limitations. The 19 AD risk loci do not include all genetics variants associated with AD and the index variants used may not be the causal variants. Another consideration is that the cross-sectional nature of our analyses precludes us from inferring causality from the associations. Although reverse causality is unlikely for genetic variants, it remains unclear whether our findings represent developmental or degenerative effects. The absence of significant association, as we mentioned before, could be due to strict permutation threshold or lack of power of our study sample size compare to GWAS analysis where these risk loci were discovered. Additionally, in the experiment to determine spatial overlap between gene expression and regions identified through VBM, a number of considerations need to be taken into account. First, the threshold to form the clusters is a manual parameter and could be set to a different

threshold. However, with decreasing p-value threshold the number and size of the clusters goes down lnot enough clusters linked to samples to perform such analysis. Second, gene expression depends on the time of measurement and could be different over the lifespan and even during the day [42]. Second, the association between a risk locus and tissue density does not necessarily require the causative gene to be expressed in the same brain region, but could also be through a downstream effect of a functional pathway. Third, given the difficulties in obtaining brain tissue samples, these analyses are all based on relatively small samples.

CONCLUSION

Using a voxel-based morphometry study in over 4000 non-demented individuals, we provide a list of candidate brain regions that are potentially affected by AD risk loci and worthy of further study. Although detecting significant genetic effects on individual voxels will require even larger sample sizes, we show that data can be exploited by incorporating additional information in the analysis, such as gene expression data.

REFERENCES

1. Weiner, M. W. *et al.* The Alzheimer's Disease Neuroimaging Initiative: *Alzheimer's Dement.* **8,** S1-68 (2012).
2. Thompson, P. M. *et al.* Genetic influences on brain structure. *Nat. Neurosci.* **4,** 1253–8 (2001).
3. Lambert, J., Ibrahim-Verbaas, C. & Harold, D. Meta-analysis of 74,046 individuals identifies 11 new susceptibility loci for Alzheimer's disease. *Nat. Genet.* **45,** 1452–1458 (2013).
4. Liu, Y. *et al.* Association between NME8 Locus Polymorphism and Cognitive Decline, Cerebrospinal Fluid and Neuroimaging Biomarkers in Alzheimer's Disease. *PLoS One* **9,** e114777 (2014).
5. Morgen, K. *et al.* Genetic interaction of PICALM and APOE is associated with brain atrophy and cognitive impairment in Alzheimer's disease. *Alzheimers. Dement.* **10,** 1–8 (2014).
6. Chauhan, G. *et al.* Association of Alzheimer's disease GWAS loci with MRI markers of brain aging. *Neurobiol. Aging* **36,** 1765.e7-1765.e16 (2015).
7. Bis, J. C. *et al.* Common variants at 12q14 and 12q24 are associated with hippocampal volume. *Nat. Genet.* **44,** 545–551 (2012).
8. Wright, I. C. C. *et al.* A voxel-based method for the statistical analysis of gray and white matter density applied to schizophrenia. *Neuroimage* **2,** 244–52 (1995).
9. Hofman, A. *et al.* The Rotterdam Study: 2012 objectives and design update. *Eur. J. Epidemiol.* **26,** 657–86 (2011).
10. Ikram, M. & Lugt, A. van der. The Rotterdam Scan Study: design and update up to 2012. *Eur. J. Epidemiol.* **26,** 811–24 (2011).
11. Verhaaren, B. F. J. *et al.*. *Biol. Psychiatry* **73,** 429–434 (2013).
12. Good, C. D. *et al.* A voxel-based morphometric study of ageing in 465 normal adult human brains. *Neuroimage* **14,** 21–36 (2001).
13. Vrooman, H. A. *et al. Neuroimage* **37,** 71–81 (2007).
14. Smith, S. M. *et al.* Advances in functional and structural MR image analysis and implementation as FSL. *Neuroimage* **23 Suppl 1,** S208-19 (2004).
15. Churchill, G. A. & Doerge, R. W. Empirical threshold values for quantitative trait mapping. *Genetics* **138,** 963–71 (1994).
16. Adams, H. H. H. *et al. Alzheimer's Dement.* (2015). doi:10.1016/j.jalz.2014.12.00
17. ALLEN Human Brain Atlas Normalization, Microarray Data. 1–11 (2013).
18. Hammers, A. *et al.* . *Hum. Brain Mapp.* **19,** 224–47 (2003).
19. Medland, S. E., Jahanshad, N., Neale, B. M. & Thompson, P. M. *Nat. Publ. Gr.* **17,** 791–800 (2014).
20. Fritsch, V. *et al.* Robust regression for large-scale neuroimaging studies. *Neuroimage* **111,** 431–41 (2015).
21. Smith, S. M. & Nichols, T. E.

FMRIB Technical Report TR08SS1. **1,** 1–20

22. Jenkinson, M., Bannister, P., Brady, M. & Smith, S. *Neuroimage* **17,** (2002).
23. Bullmore, E. T. *et al.* Global, voxel, and cluster tests, by theory and permutation, for a difference between two groups of structural MR images of the brain. *IEEE Trans. Med. Imaging* **18,** 32–42 (1999).
24. Davies, G. *et al.* G *Mol. Psychiatry* 183–192 (2015). doi:10.1038/mp.2014.188
25. de Bruijn, R. F. A. G. *et al.* The potential for prevention of dementia across two decades: the prospective, population-based Rotterdam Study. *BMC Med.* **13** (2015).
26. Mattson, M. P. Pathways towards and away from Alzheimer's disease. *Nature* **430,** 631–639 (2004).
27. Jones, L. Convergent genetic and expression data implicate immunity in Alzheimer's disease. *Alzheimer's Dement.* **11,** 658–671 (2015).
28. Esiri, M. *et al. Brain Pathol.* **25,** 51–62 (2015).
29. Ringman, J. M. *et al*. *JAMA Neurol.* **71,** 878–83 (2014).
30. Nelson, P. T. APOE-ε2 and APOE-ε4 Correlate with Increased Amyloid Accumulation in Cerebral Vasculature. *J. Neuropathol. Exp. Neurol.* **72,** (2013).
31. Smith, E. E. & Greenberg, S. M. Amyloid, blood vessels, and brain function. *Stroke* **40,** 2601–2606 (2009).
32. Holton, P. *et al. Ann. Hum. Genet.* **77,** (2013).
33. Karch, C. M. *et al.* Expression of Novel Alzheimer's Disease Risk Genes in Control and Alzheimer's Disease Brains. *PLoS One* **7,** (2012).
34. Pandey, J. P. & Manolio, T. a. Genomewide association studies and assessment of the risk of disease. *N. Engl. J. Med.* **363,** 166–176 (2010).
35. Myers, A. J. *et al.* A survey of genetic human cortical gene expression. *Nat. Genet.* **39,** 1494–9 (2007).
36. Ramasamy, A. *et al.* Genetic variability in the regulation of gene expression in ten regions of the human brain. *Nat. Neurosci.* **17,** (2014).
37. Steinberg, S. *et al.* Loss-of-function variants in ABCA7 confer risk of Alzheimer's disease. *Nat. Genet.* **47**(2015).
38. Thathiah, A. & De Strooper, B. *Nat. Rev. Neurosci.* **12,** 73–87 (2011).
39. Lovell, M. A., Xie, C. & Markesbery, W. R. *Neurology* **51,** (1998).
40. Weyer, C. *et al. J. Clin. Endocrinol. Metab.* **86,** 1930–1935 (2001).
41. Shield, A. J., Murray, T. P., Cappello, J. Y., Coggan, M. & Board, P. G. *Genomics* **95,** 299–305 (2010).
42. Jaenisch, R. & Bird, A.. *Nat. Genet.* **33 Suppl,**(2003
).

Chapter 4.2.2

Frontotemporal lobar degeneration gene and the brain

ABSTRACT

Background: Frontotemporal lobar degeneration (FTLD) is a neurodegenerative disease characterized by brain atrophy of the frontal and anterior temporal lobes. The associated frontotemporal dementia syndromes are clinically heterogeneous and the pattern of affected cortical regions varies between subtypes. The TMEM106B rs1990622 polymorphism is associated with FTLD, but little is known about how it affects the brain.

Methods: We investigated the rs1990622 polymorphism in relation to regional brain volumes to identify potential structures through which TMEM106B confers risk for FTLD. In 4413 non-demented and stroke-free participants from the population-based Rotterdam Study, 150 cortical brain structures and 6 commissural regions were segmented from magnetic resonance imaging (MRI).

Results: We found a distinct pattern of association between rs1990622 and grey matter volume of left-sided temporal brain regions important for language processing, including the superior temporal gyrus (β = -88.8 µL per risk allele, $p = 7.64 \times 10^{-5}$), which contains Wernicke's area. The risk allele was also associated with a smaller anterior commissure cross-sectional area (β = -.167 mm^2, $p = 4.90 \times 10^{-5}$) and posterior part of the corpus callosum (β = -15.3, $p = 1.23 \times 10^{-5}$), both of which contain temporal lobe commissural tracts.

Conclusions: The asymmetric, predominantly left-sided involvement suggests an effect of TMEM106B on functions lateralized to the dominant hemisphere, such as language. These results show that, in non-demented persons, TMEM106B influences the volume of temporal brain regions which are important for language processing.

INTRODUCTION

Frontotemporal lobar degeneration (FTLD) is a heterogeneous pathological entity with the common feature being prominent frontal and anterior temporal lobe atrophy.[1] The diverse pathology that can be detected in the brains of patients serves as the basis of classification into more homogeneous subgroups.[2] These pathological subgroups correspond to clinically defined syndromes including behavioral-variant frontotemporal dementia, semantic dementia and progressive non-fluent aphasia, with strong relationships between certain pathological subgroups and clinical syndromes (e.g., between TDP-43 inclusions and semantic dementia).[3,4]

A recent genome-wide association study implicated single-nucleotide polymorphisms at the *TMEM106B-gene* in the risk of FTLD.[5] Although the initial discovery of *TMEM106B* was in the strictly defined subgroup of FTLD with TDP-43 inclusions,[5] it was replicated in a more heterogeneous patient group.[6] *TMEM106B* risk variants were subsequently associated with cognitive impairment in amyotrophic lateral sclerosis and the pathological presentation of Alzheimer's disease.[7,8] *TMEM106B* encodes a glycoprotein that co-localizes with progranulin, another FTLD risk factor, in late endo-lysosomes.[9] FTLD-associated variant rs1990622 is in complete linkage disequilibrium with the potential functional coding variant p.T185S, and has been suggested to affect progranulin levels and function.[10]

The rs1990622 risk allele A is common (~60%) and only increases susceptibility for FTLD marginally (odds ratio = 1.3), leaving the majority of carriers free of clinical disease.[5,6] It is currently unknown if carriers of the risk variant do have subclinical, structural brain changes in regions relevant to the pathophysiology of FTLD. Frontal and temporal cortical atrophy is a hallmark of FTLD and the patterns of cortical involvement are part of the diagnostic criteria used for differentiating between subtypes.[1,2,11-14] The regional atrophy reflects neuronal loss, mostly of cortical layer III, which contains the commissural fibers.[15-17] The corpus callosum (CC) and anterior commissure (AC) are reduced in size in FTLD patients, with the distribution of atrophy in these commissural tracts corresponding to the cortical damage.[11,16,18-20]

Table 1 | Study population characteristics.

Characteristic	Total (n=4413)
Demographics	
Age, years, mean (SD)	64.7 (10.8)
Women, n (%)	2446 (55.4%)
Brain volumetry	
Intracranial volume, mL, mean (SD)	1487.1 (160.3)
Grey matter volume, mL, mean (SD)	605.5 (58.3)
White matter volume, mL, mean (SD)	438.9 (62.4)
Rs1990622 genotype	
AA carriers, n (%)	1546 (35.0%)
AG carriers, n (%)	2089 (47.3%)
GG carriers, n (%)	778 (17.6%)

Here we investigated the relation of rs1990622 with cortical grey matter and interhemispheric white matter within the Rotterdam Study,[21] a large population-based study of the elderly, to identify potential brain structures through which *TMEM106B* confers risk for FTLD.

MATERIALS AND METHODS

Subjects

The Rotterdam Study is an ongoing prospective cohort study that aims to investigate causes and determinants of diseases in the elderly.[21] Residents of Rotterdam, a city in The Netherlands, were recruited from 1990 onwards and the current study population consists of 14,926 subjects aged 45 years or over at baseline.[21] The Medical Ethics Committee of the Erasmus Medical Center and the review board of The Netherlands Ministry of Health, Welfare and Sports both approved the study. Informed consent was obtained from all subjects.

Genotyping and quality control

In 11,496 participants of the Rotterdam Study, genotyping was performed on 550K and 610K Illumina arrays.[21] The genotyped dataset was restricted to persons who reported that they were from European descent. Ethnic outliers were further excluded using IBS distances > 4SD. Duplicates and/or 1st or 2nd degree relatives were excluded using IBS probabilities >97%, as well as samples with gender mismatch and excess autosomal heterozygosity. Variants with call rate below 95.0%, those failing missingness test, with a Hardy–Weinberg equilibrium p-value<10-6, and minor allele frequency<1% were also removed.

MRI data acquisition and image processing

To study early structural brain changes of neurodegenerative disease, magnetic resonance imaging (MRI) was introduced into the core protocol of the Rotterdam Study from 2005 onwards.[22] Brain MRI data were acquired with a dedicated 1.5T MR unit (GE, Milwaukee, USA) during a 30 minute imaging protocol that was previously described in detail.[22] This protocol included high resolution axial fluid-attenuated inversion recovery (FLAIR), T1- and T2-weighted sequences. Of the 5637 participants with MRI scans available, genotyping was performed in a random subset of 4735 persons. Volumetric measures of the cortical grey matter and CC were successfully acquired in 4699 (99.2%) MRI scans (remaining 36 scans failed due to technical issues) with the FreeSurfer

software (version 4.5.0): cortical grey matter was automatically segmented and parcellated into 75 regions per hemisphere,[23] whereas the CC was divided into five parts, namely anterior, mid-anterior, central, mid-posterior and posterior.[24] The AC cross-sectional area was manually segmented in 4732 (99.9%) scans in the mid-sagittal plane with high intra-rater reliability (intra-class correlation coefficient = 0.91 in 100 scans) using an in-house developed MeVisLab extension which has been made available online (see Supplementary Material and http://www.mevislab.de). Outliers, which were defined as brain structure volumes falling outside of $\mu \pm 2.5\sigma$, were visually inspected and removed if necessary. Trained raters viewed all scans to determine presence of brain infarcts using FLAIR, T1- and T2-weighted sequences, and these were classified as cortical infarcts in case of grey matter involvement.[25]

Data analysis

Excluded from analyses were people with dementia (according to DSM-III-R[26], n=55), clinical stroke (baseline medical history and continuous monitoring[27], n=162) and MRI-defined cortical infarcts (n=105), leaving 4413 participants with successful segmentation of FreeSurfer structures and/or the AC. Multiple linear regression models, with age and sex as covariates, were used to examine associations between rs1990622 and the left and right volume of the 75 cortical regions and CC and AC commissural tracts. Additionally, the effects on the significant structures were investigated for four previously reported *TMEM106B* variants that are in high linkage disequilibrium with rs1990622 and potentially functional (p.T185S and rs1042949)[28] or have also been genome-wide significantly associated with FTLD (rs6966915 and rs1020004)[5]. The Sidak corrected significance level to maintain $\alpha=0.05$ for testing 156 correlated outcomes (mean correlation $\rho=0.25$) was determined at $p<1.14 \times 10^{-3}$ (see Supplementary Methods).[29] For the significant structures, we additionally adjusted for the first four principal components to control for potential population stratification. The explained variance was calculated by squaring the semipartial correlation coefficients between rs1990622 and the brain structures. All analyses were performed with SPSS version 21 (IBM).

Table 2 | Nominally significant associations of rs1990622 with cortical grey matter volumes and commissural tracts.

Brain structure	Beta (95% CI)	P-value	R^2
Left hemisphere			
Superior temporal sulcus	*-88.8 (-44.8;-132.8)*	*7.64×10^{-5}*	0.29%
Angular gyrus	*-66.1 (-27.1;-105.2)*	*9.14×10^{-4}*	0.21%
Middle temporal gyrus	*-76.9 (-31.1;-122.8)*	*1.00×10^{-3}*	0.18%
Intraparietal sulcus and transverse parietal sulci	-36.4 (-9.9;-62.9)	7.15×10^{-3}	0.15%
Precuneus	-42.0 (-10.7;-73.4)	8.60×10^{-3}	0.14%
Central sulcus	-26.5 (-5.0;-47.9)	1.55×10^{-2}	0.11%
Middle-posterior cingulate gyrus and sulcus	-16.1 (-2.5;-29.6)	2.02×10^{-2}	0.10%
Lateral aspect of the superior temporal gyrus	-38.7 (-4.8;-72.5)	2.51×10^{-2}	0.09%
Supramarginal gyrus	-43.5 (-3.9;-83.2)	3.13×10^{-2}	0.09%
Subparietal sulcus	-15.1 (-0.8;-29.5)	3.82×10^{-2}	0.09%
Precentral gyrus	-31.8 (-1.2;-62.4)	4.14×10^{-2}	0.07%
Posterior transverse collateral sulcus	-5.7 (-0.2;-11.3)	4.29×10^{-2}	0.09%
Right hemisphere			
Supramarginal gyrus	*-64.3 (-26.9;-101.6)*	*7.51×10^{-4}*	0.22%
Vertical ramus of the lateral sulcus anterior segment	-7.3 (-2.7;-11.8)	1.91×10^{-3}	0.21%
Planum temporale of the superior temporal gyrus	-20.1 (-6.7;-33.4)	3.20×10^{-3}	0.17%
Precuneus	-42.5 (-13.6;-71.4)	3.96×10^{-3}	0.16%
Superior temporal sulcus	-67.1 (-20.2;-114.0)	5.08×10^{-3}	0.14%
Medial occipito-temporal and lingual sulcus	-22.7 (-6.3;-39.0)	6.52×10^{-3}	0.13%
Opercular part of the inferior frontal gyrus	-28.4 (-7.8;-49.0)	7.00×10^{-3}	0.15%
Subcentral gyrus (central operculum) and sulci	-23.3 (-5.4;-41.2)	1.08×10^{-2}	0.13%
Inferior temporal sulcus	-21.8 (-4.7;-38.9)	1.25×10^{-2}	0.11%
Transverse temporal sulcus	-5.2 (-1.0;-9.3)	1.46×10^{-2}	0.13%
Anterior part of the cingulate gyrus and sulcus	-31.0 (-4.7;-57.4)	2.09×10^{-2}	0.09%
Lateral orbital sulcus	-8.8 (-1.2;-16.4)	2.38×10^{-2}	0.11%

Table 2 continued.

Postcentral sulcus	-29.6 (-3.9;-55.2)	2.40 X 10^{-2}	0.11%
Lateral occipito-temporal gyrus	-39.1 (-5.1;-73.1)	2.43 X 10^{-2}	0.10%
Lateral occipito-temporal sulcus	-14.6 (-1.7;-27.6)	2.69 X 10^{-2}	0.09%
Long insular gyrus and central sulcus of the insula	-9.8 (-0.8;-18.7)	3.18 X 10^{-2}	0.10%
Middle-anterior cingulate gyrus and sulcus	-18.5 (-1.4;-35.6)	3.40 X 10^{-2}	0.08%
Inferior temporal gyrus	-50.5 (-2.2;-98.8)	4.04 X 10^{-2}	0.08%
Anterior occipital sulcus and preoccipital notch	-13.7 (-0.6;-26.8)	4.05 X 10^{-2}	0.09%
Commissural tracts			
Anterior commissure	*-.167 (-.087;-.248)*[†]	*4.90 X 10^{-5}*	0.34%
Corpus callosum, posterior	*-15.3 (-8.4;-22.1)*	*1.23 X 10^{-5}*	0.41%
Corpus callosum, mid-posterior	*-7.3 (-3.6;-11.1)*	*1.21 X 10^{-4}*	0.26%
Corpus callosum, central	*-6.9 (-3.4;-10.5)*	*1.20 X 10^{-4}*	0.27%
Corpus callosum, mid-anterior	-4.6 (-0.6;-8.5)	2.32 X 10^{-2}	0.09%
Corpus callosum, anterior	-8.5 (-2.0;-15.0)	1.01 X 10^{-2}	0.12%

Betas are in µl per risk allele of rs1990622.

Brain structures surviving multiple testing ($p<1.14 \times 10^{-3}$) are indicated in italic.

[†]Beta is in mm^2 per risk allele of rs1990622

R^2 is the variance of the brain structure that is explained by rs1990622, calculated by squaring the semipartial correlation coefficient.

RESULTS

Population characteristics

In the final sample of 4413 participants, mean (S.D.) age was 64.7 (10.8) years with 2446 (55.4%) women. The call rate of rs1990622 was high (>99.9%) with the minor allele (G) frequency corresponding to previous reports in healthy, non-demented populations (0.41) (see Table 1).[5,6]

Cortical grey matter

The risk allele A of rs1990622 was strongly associated with lower grey matter volume of the left superior temporal gyrus (β = -88.8 µL per allele, 95% confidence interval (CI) = -44.8 to -132.8, $p = 7.64 \times 10^{-5}$) and the directly neighboring angular gyrus (β = -66.1, 95% CI = -27.1 to -105.2, $p = 9.14 \times 10^{-4}$) and middle temporal gyrus (β = -76.9, 95% CI = -31.1 to -122.8, $p = 1.00 \times 10^{-3}$) (see Figure 1 and Table 2). The effect was less pronounced in the right superior temporal gyrus (β = -67.1, 95% CI = -20.2 to -114.0, $p = 5.08 \times 10^{-3}$) (see Figure 1 and Table 2). Post-hoc stratification for self-reported handedness revealed an opposite pattern in left-handed persons (n = 195), with a larger effect size for the right superior temporal gyrus, although this group was small (see Supplementary Table S1). After additional adjustments were made for the superior temporal gyrus volume of the contralateral side, the association between rs1990622 and left superior temporal gyrus volume remained significant ($p = 3.58 \times 10^{-3}$), but not for the right superior temporal gyrus ($p = 5.72 \times 10^{-1}$).

Furthermore, rs1990622 was associated with a lower volume of the right supramarginal gyrus (β = -64.3 µL per allele, 95% CI = -26.9 to -101.6, $p = 7.51 \times 10^{-4}$) (see Figure 1 and Table 2). Other nominally significant associations are reported in Table 1, with the full results for all cortical grey matter volumes per hemisphere provided in Supplementary Table S2. Adjustment for the first four principal components did not affect the associations between rs1990622 and the brain structures.

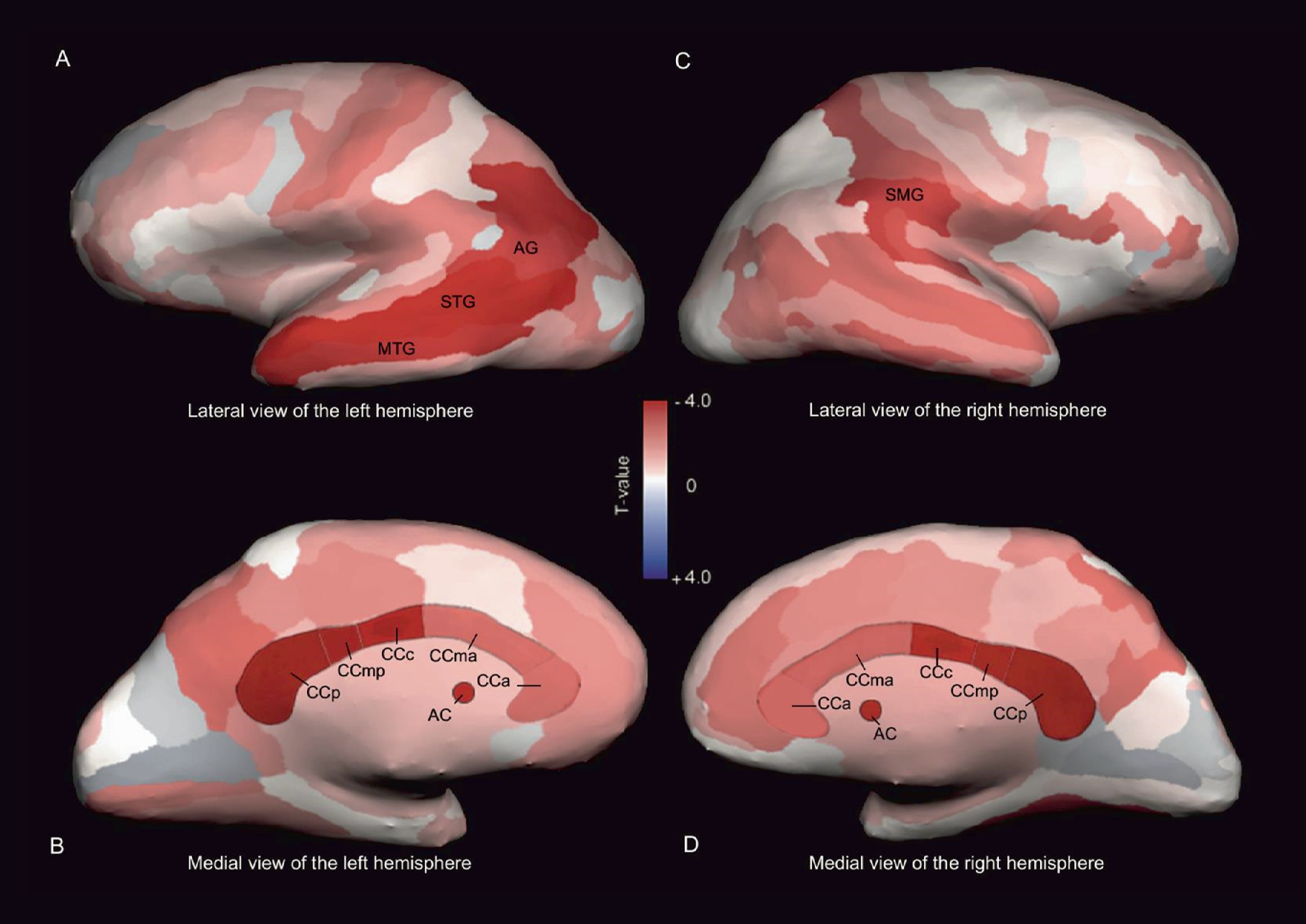
A
AG
STG
MTG
Lateral view of the left hemisphere
C
SMG
Lateral view of the right hemisphere
T-value
- 4.0
0
+ 4.0
CCp
CCmp
CCc
CCma
CCa
AC
B
Medial view of the left hemisphere
CCma
CCc
CCmp
CCa
CCp
AC
D
Medial view of the right hemisphere

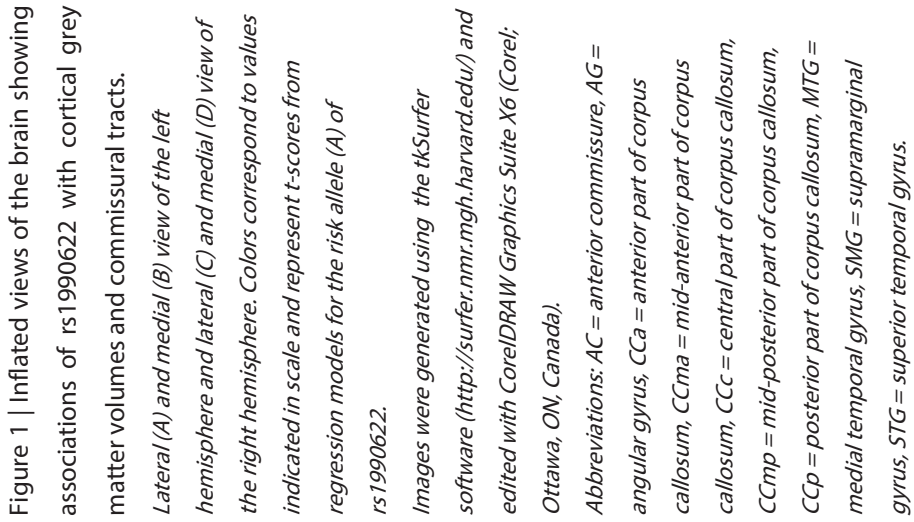

Figure 1 | Inflated views of the brain showing associations of rs1990622 with cortical grey matter volumes and commissural tracts. *Lateral (A) and medial (B) view of the left hemisphere and lateral (C) and medial (D) view of the right hemisphere. Colors correspond to values indicated in scale and represent t-scores from regression models for the risk allele (A) of rs1990622. Images were generated using the tkSurfer software (http://surfer.nmr.mgh.harvard.edu/) and edited with CorelDRAW Graphics Suite X6 (Corel; Ottawa, ON, Canada). Abbreviations: AC = anterior commissure, AG = angular gyrus, CCa = anterior part of corpus callosum, CCma = mid-anterior part of corpus callosum, CCc = central part of corpus callosum, CCmp = mid-posterior part of corpus callosum, CCp = posterior part of corpus callosum, MTG = medial temporal gyrus, SMG = supramarginal gyrus, STG = superior temporal gyrus.*

Commissural tracts

For the commissural tracts, we found rs1990622 to be associated with CC volume in an anterior-to-posterior gradient, with risk allele carriers having lower volumes towards the posterior pole (see Figure 1 and Table 2). Additionally, the risk allele was associated with a smaller AC cross-sectional area (β = -.167 mm^2 per allele, 95% CI = -.087 to -.248, p = 4.90 x 10^{-5}) (see Figure 1 and Table 2). Similarly, adjusting for the first four principal components made no difference on the associations.

Age x SNP interaction

An interaction term of 'age x rs1990622' for all structures that survived multiple testing correction showed a larger effect of rs1990622 with increasing age, but was only significant for the anterior commissure cross-sectional area (p=0.004).

Other TMEM106B variants

Additional variants in TMEM106B that have been reported to be associated with risk of FTLD (p.T185S, rs1042949, rs6966915 and rs1020004) were in high linkage disequilibrium with rs1990622 and showed a similar pattern of association (see Supplementary Table S3).

DISCUSSION

In this study we investigated *TMEM106B* in relation to structural brain measures in non-demented individuals and show that rs1990622 affects cortical regions and commissural tracts that are known to be important for semantic processing. This suggests that *TMEM106B* may increase the risk of FTLD by acting on this intermediate phenotype, which has particular relevance for the language-based dementia subtypes. We found that the risk allele of rs1990622 is associated with a smaller volume of the superior temporal gyrus, especially in the left hemisphere. This brain region includes structures such as Wernicke's area that are involved in language processing, a function which in the majority of right-handed persons is lateralized to the left (dominant) hemisphere.[30] Problems with language processing are an established clinical feature of frontotemporal dementia subtypes such as semantic dementia and progressive non-fluent aphasia. Brain atrophy is evident across the whole spectrum of FTLD, but the affected regions and pattern of progression varies between subtypes.[2,4] Semantic dementia patients typically have FTLD with type C TDP-43 inclusions, corresponding to asymmetric, predominantly left-sided temporal lobe atrophy.[2,4] In this light, it is worth noting that the original discovery of *TMEM106B* was in a strictly defined group of FTLD patients with TDP-43 inclusions.[5] Progressive non-fluent aphasia also causes left-sided superior temporal lobe atrophy, but regions more severely affected compared to semantic dementia include the right supramarginal gyrus.[31] Interestingly, this was the only right-sided cortical region that was significantly associated with rs1990622.

Patients with asymmetric temporal lobe atrophy have impairments in different functions depending on which side is affected and the hemispheric specialization.[32] The left-to-right hemispheric shift we observed within left-handed persons suggests that *TMEM106B* is not purely influencing anatomical variation of the left superior temporal gyrus, but rather plays a more important role in the actual cognitive functions within that structure that are also known to shift to the dominant hemispheres. However, although this reversed association is intriguing, it should be carefully interpreted since handedness itself is not a specific measure of language lateralization (only 30% of left-

handed persons are right-dominant),[30] and our assessment of handedness was based on self-reported data from participants.

We additionally showed that the risk allele of rs1990622 is associated with gradually smaller volumes towards the posterior pole of the CC and a smaller cross-sectional area of the AC. Commissural tracts facilitate the interhemispheric cross-talk of the brain and are known to be affected by neurodegenerative diseases such as Alzheimer's and FTLD.[16,20,33,34] *TMEM106B* might contribute to the interhemispheric disconnection of brain regions involved in the pathophysiology of FTLD. Moon *et al*. showed that the AC thickness measurement could be used to distinguish between AD, FTLD and healthy controls.[20] Interestingly, in their study, the AC was smallest in the semantic dementia subtype.[20] Northam *et al*. have shown that reductions in the temporal connections of the posterior CC result in language impairment in adolescents if the AC is also reduced in size.[35] Since our findings point to brain structures that are important for language, information on related phenotypes would be of interest. However, in the Rotterdam Study no cognitive tests measuring semantic processing are available, underlining the need for future studies to explore functional correlates of the neuroanatomical findings.

Although *TMEM106B* is a genetic risk factor for FTLD, we now observe anatomical brain differences in a population free of clinical neurodegenerative disease. The same allele that increases risk of FTLD was consistently associated with smaller brain volumes, with none of the 156 structures reaching even nominal significance in the opposite direction. *TMEM106B* explained less than 0.4% of the observed variance of the investigated brain structures, suggesting it does not severely affect (the volume of) structures such as the superior temporal gyrus by itself, but rather has a clinically significant impact in combination with other risk factors. Others suggested that disease might develop in patients who are vulnerable to additional genetic modifying factors such as *TMEM106B*.[10] This was compatible with reported roles of *TMEM106B* in patients with amyotrophic lateral sclerosis and Alzheimer's disease.[7,8] It was recently shown that *TMEM106B* might cause disease through interaction with *APOE*, the major genetic risk factor for Alzheimer's Disease.[36] Our study provides additional evidence for this 'increased susceptibility' hypothesis and specifically points to temporal lobe pathology.

However, even though we examine the effects of *TMEM106* in an aging population, we cannot firmly attribute the structural brain differences that we found to degenerative processes due to the cross-sectional nature of this study. Risk allele carriers could for example have a smaller anterior temporal lobe as a consequence of impaired development during brain growth in early life. Although we were not able to study association with brain volume longitudinally, we have performed additional analyses to evaluate a potential interaction effect between rs1990622 and age for the significant structures. We found a significant interaction term for the anterior commissure, which showed that the effect of rs1990622 was stronger with increasing age. This suggests that the effect could be attributed to a process later in life, e.g. neurodegeneration. However, because such age-interaction was not observed for the other brain structures, *TMEM106B* could also affect brain development earlier in life. Although *APOE's* role of in neurodegeneration is well-documented, developmental brain changes have now been found in infant carriers of the risk allele.[37] This adds to the complexity of neurodegenerative disorders and further emphasizes the role of our study in generating an agenda for future research, rather than making final conclusions based on our results. Longitudinal MRI studies are needed to investigate this relationship of *TMEM106B* with brain volumes.

Also, the smaller volumes of the CC and AC area suggest that interhemispheric connections are reduced, but it is possible that the number of neuronal fibers is similar but that they are more densely packed. Techniques that can specifically isolate fiber tracts within white matter structures, such as diffusion tensor imaging, can provide more insight into which specific white matter tracts are more affected and how *TMEM106B* influences the microstructural integrity.

To obtain valid measurements of brain volumes, with a balanced investment of manpower, we excluded persons with stroke and MRI-defined cortical infarcts, since these affect the grey matter of the brain and can distort the image post-processing. Additionally, we visually inspected scans when brain structure volumes fel out of 2.5σ and, if needed, excluded these outliers. Although this leaves the majority of scans uninspected, we note that any residual measurement error would only dilute the association between rs1990622 and the brain volumes.

The volumes of different brain structures are correlated and partly depend on shared environmental and genetic factors. The Sidak corrected significance level takes such interdependence into account using the correlation matrix across structures, thereby providing an adequate and data-driven adjustment. Even though our findings would even have survived the stringent Bonferroni correction, we chose to implement the appropriate Sidak correction for future reference by other studies, since using Bonferroni in similar situations could lead to false-negative findings in studies that are not as well-powered as ours.

In conclusion, our findings show that FTLD-associated *TMEM106B* variant rs1990622 influences the volume of temporal brain regions – in particular left hemispheric - and interconnectivity of the temporal lobes in an elderly population free of dementia. This indicates that the importance of *TMEM106B* extends outside of the realm of FTLD and mainly affects structures that are involved in language. Future studies should therefore investigate the effect of *TMEM106B* on the different aspects of semantic processing.

REFERENCES

1. Rosen HJ, *et al.*Neurology.2002;58:198-208
2. Mackenzie IR, *et al.*Acta Neuropathol.2011;122:111-113
3. Wolf H, *et al.*Int J Geriatr Psychiatry.2004;19:995-1007
4. Rohrer JD, *et al.*Neurology.2010;75:2204-2211
5. Van Deerlin VM, *et al.*Nat Genet.2010;42:234-239
6. van der Zee J, *et al.*Brain.2011;134:808-815
7. Vass R, *et al.*Acta Neuropathol.2011;121:373-380
8. Rutherford NJ, *et al.*Neurology.2012;79:717-718
9. Brady OA, *et al.*Hum Mol Genet.2013;22:685-695
10. Nicholson AM, *et al.*J Neurochem.2013
11. Kim EJ, *et al.*Journal of Neurology, Neurosurgery & Psychiatry.2007;78:1375-1378
12. Whitwell JL, *et al.*Neurology.2006;66:102-104
13. Whitwell JL, *et al.*Neurology.2009;72:813-820
14. Rohrer JD, *et al.*Neuroimage.2010;53:1070-
15. Hof P, *et al.*Alzheimer disease. Raven Press, New York.1994:197-
16. Yamauchi H, *et al.*JNNP .2000;69:623-629
17. Innocenti GM. General organization of callosal connections in the cerebral cortex. Springer; 1986:291-353.
18. Murray C, *et al.*American Journal of Alzheimer's Disease and Other Dementias.2006;21:37-43
19. Kaufer DI, *et al.*Neurology.1997;48:978-984
20. Moon WJ, *et al.*AJNR Am J Neuroradiol.2008;29:1308-1313
21. Hofman A, *et al.*Eur J Epidemiol.2011;26:657-686
22. Ikram MA, *et al.*Eur J Epidemiol.2011;26:811-824
23. Lu RC, *et al.*J Neural Transm.2013
24. Rosas HD, *et al.*Neuroimage.2010;49:2995-3004
25. Vernooij MW, *et al.*N Engl J Med.2007;357:1821-1828
26. Schrijvers EM, *et al.*Neurology.2012;78:1456-1463
27. Wieberdink RG, *et al.*Eur J Epidemiol.2012;27:287-295
28. Cruchaga C, *et al.*Arch Neurol.2011;68:581-586
29. Sankoh AJ, *et al.*Stat Med.1997;16:2529-2542
30. Knecht S, *et al.*Brain.2000;123 Pt 12:2512-2518
31. Rohrer JD, *et al.*Neurology.2009;72:1562-1569
32. Hersheson J, *et al.*Ann Neurol.2012
33. Hampel H, *et al.*Arch Neurol.1998;55:193-198
34. Teipel SJ, *et al.*Neurology.1998;51:1381-1385
35. Northam GB, *et al.*Brain.2012;135:3781-3798
36. Lu R-C, *et al.*Journal of Neural Transmission.2013:1-5
37. Dean DC, *et al.*JAMA neurology.2014;71:11-22

.

Chapter 4.2.3

Frontotemporal lobar degeneration gene recessive effect

ABSTRACT

We read with interest the article by Hernández et al. on the TMEM106B genetic variant rs1990622 that modifies the risk for frontotemporal dementia (FTD) [1]. Although the authors were underpowered to detect a significant association with FTD risk in their case-control study (n/N=146/381), the effect was concordant with the expected direction and slightly decreased in p-value under a recessive model. Similarly, meta-analysis of published data was more significant assuming a recessive effect for the rs1990622 CC genotype.

MAIN TEXT

Previously we showed that the additive effect of rs1990622 is not restricted to FTD but that this variant also affects brain structure in the general population free of dementia[2]. Given the findings of Hernández *et al.* we aimed to determine whether this recessive model also holds for the association of rs1990622 in the general population. In line with our previous publication, we investigated this question in 4413 non-demented and stroke-free participants from the population-based Rotterdam Study who underwent both genotyping and magnetic resonance imaging (MRI).[3,4] The eight brain structures that previously survived multiple testing correction were analyzed under three different models: additive (as published), recessive, and dominant.

As shown in Table 1, associations under both the recessive and dominant model were either in the same order of magnitude or less significant than the additive model. This does not support the notion of a recessive effect, as found by Hernández *et al.,* in our population-based sample in which we investigated brain structure. Rather, it seems to suggest that each T allele increase confers an additional risk. We agree with the authors that larger studies will provide us the definitive answer with regard to the genetic model under which rs1990622 predisposes to FTD.

REFERENCES

1. Hernández, Isabel, et al. "Association of TMEM106B rs1990622 Marker and Frontotemporal Dementia: Evidence for a Recessive Effect and Meta-Analysis." Journal of Alzheimer's Disease (2014).
2. Adams, Hieab HH, et al. "TMEM106B Influences Volume of Left-Sided Temporal Lobe and Interhemispheric Structures in the General Population." Biological psychiatry (2014).
3. Hofman, Albert, et al. "The Rotterdam Study: 2014 objectives and design update." European journal of epidemiology 28.11 (2013): 889-926.
4. Ikram, M. Arfan, et al. "The Rotterdam Scan Study: design and update up to 2012." European journal of epidemiology 26.10 (2011): 811-824.

Table 1 | Associations of the *TMEM106B* rs1990622 variants with brain structures surviving multiple testing correction in Adams *et al.* [2] under different genetic models.

	Association of rs1990622 with brain structures					
	Additive model		Dominant model		Recessive model	
Brain structure	Beta	P-value	Beta	P-value	Beta	P-value
Left hemisphere						
Superior temporal sulcus	-88.8	7.64×10^{-05}	-133.4	1.32×10^{-03}	-108.0	1.13×10^{-03}
Angular gyrus	-66.1	9.14×10^{-04}	-114.5	1.91×10^{-03}	-71.4	0.0153
Middle temporal gyrus	-76.9	1.00×10^{-03}	-137.0	1.54×10^{-03}	-81.0	0.0190
Right hemisphere						
Supramarginal gyrus	-64.3	7.51×10^{-04}	-68.8	0.0512	-96.3	6.20×10^{-04}
Commissural tracts						
Anterior commissure†	-.167	4.90×10^{-05}	-.165	0.0304	-.260	1.98×10^{-05}
Corpus callosum, posterior	-15.3	1.23×10^{-05}	-21.5	8.61×10^{-04}	-19.6	1.42×10^{-04}
Corpus callosum, mid-posterior	-7.3	1.21×10^{-04}	-9.9	4.96×10^{-03}	-9.7	5.69×10^{-04}
Corpus callosum, central	-6.9	1.20×10^{-04}	-8.1	0.0146	-9.9	1.91×10^{-04}

Betas are in µl per risk genotype(s) of rs1990622: per T allele under additive model, for the T/C and T/T genotypes under the dominant model, and for the T/T genotype under the recessive model.

† Betas are in mm2 per risk genotype(s) of rs1990622.

. All analyses were adjusted for age and sex.

Chapter 4.2.4

Multiple sclerosis genes and the brain

ABSTRACT

Background: Multiple sclerosis (MS) affects brain structure and cognitive function, and has a heritable component. Over a hundred common genetic risk variants have been identified, but most carriers do not develop MS. For other neurodegenerative diseases, risk variants have effects outside patient populations, but this remains uninvestigated for MS.

Objectives: To study the effect of MS-associated genetic variants on brain structure and cognitive function in the general population.

Methods: We studied middle-aged and elderly individuals (mean age=65.7 years) from the population-based Rotterdam Study. We determined 107 MS variants and additionally created a risk score combining all variants. Magnetic resonance imaging (N=4710) was performed to obtain measures of brain macrostructure, white matter microstructure, and grey matter voxel-based morphometry. A cognitive test battery (N=7556) was used to test a variety of cognitive domains.

Results: The MS risk score was associated with smaller grey matter volume over the whole brain ($\beta_{standardized}$ =-0.016;p=0.044), but region-specific analyses did not survive multiple testing correction. Similarly, no significant associations with brain structure were observed for individual variants. For cognition, rs2283792 was significantly associated with poorer memory (β=-0.064;p=3.4x10^{-5}).

Conclusion: Increased genetic susceptibility to MS may affect brain structure and cognition in persons without disease, pointing to a 'hidden burden' of MS.

INTRODUCTION

Multiple sclerosis (MS) is a multifactorial disease of the central nervous system, but the etiology has not been entirely unraveled. Magnetic resonance imaging (MRI) is an important cornerstone in detecting structural brain changes in MS patients, with the most striking features being the characteristic white matter lesions, which represent demyelination of nerve fibers.[1] These lesions are thought to be the end stage of various immunological mechanisms that results in the destruction of myelin in MS.[1] However, there is a long preclinical phase in which less severe white matter damage is already present but remains hidden on conventional MRI images. Diffusion tensor imaging (DTI) can capture such microstructural changes and it has shown that the normal-appearing white matter is in fact diffusively affected in patients.[2,3] More recently, the importance of grey matter pathology in MS has also been highlighted, possibly as a result of demyelination or secondary to axonal damage.[4] Grey matter damage is already detectable in the early phases of disease and can become quite severe.[5]

Not only are these structural brain changes important contributors to the motor and sensory deterioration seen in MS patients,[6] cognitive dysfunction is also a frequent and debilitating functional impairment among MS patients,[7,8] Such cognitive deficits are most common in verbal memory and processing speed, with over half of the patients showing impairment.[9] Other cognitive processes that are affected include information processing, executive functioning, and attention.[7]

The complexity of MS observed on imaging and in clinical presentation is mirrored in its genetics background. MS has a substantial genetic basis that is of a polygenic origin, with many common variants exerting modest effects on disease susceptibility.[10,11] Currently, over 100 MS risk variants have been discovered with high statistical confidence through large-scale association studies.[12-16] The major histocompatibility complex (MHC) region harbors some risk alleles with a relatively large effect (*DRB1*15:01*, odds ratio 2.92; *DLB1*13:03*, 2.66),[17] whereas the non-MHC variants only account for risk increases in the range of 1.03-1.34 times.[16] While these genetic variants are common (minor allele frequencies between 5% and 50%[16]), MS has a relatively low prevalence and incidence rate.[18] Thus, the majority of carriers of these variants do not

develop clinically diagnosed disease. The question therefore arises whether these risk variants might have a *subclinical* effect on the brains of apparently healthy individuals without MS.

Here, we aimed to investigate the potential effects of a genetically elevated risk of MS on the brain in the general population. Specifically, we determined whether MS-associated genetic variants are related to differences in brain structure and cognitive function in over 7000 middle-aged and elderly participants of the population-based Rotterdam Study.

METHODS

Study population

This work was performed in the Rotterdam Study,[19] a population-based cohort study in the Netherlands including a total of 14,926 participants (aged >=45 years at enrollment) that was initiated in 1990. The overall aim of the study is to investigate causes and determinants of chronic diseases in elderly people. Since 2002, an extensive cognitive test battery was implemented in the core protocol, and since 2005, all participants underwent brain MRI.[20] For this study, we excluded 29 participants with either definite/probable MS (N=27), or possible MS (N=2) based on records of general practitioners.

Genotyping and imputation

Of the 14,897 participants free of MS, genotyping was successfully performed in 11,481 using the Illumina 550K, 550K duo, and 610K quad arrays.[19] Samples were removed that had a call rate below 97.5%, gender mismatch, excess autosomal heterozygosity, duplicates or family relations and ancestry outliers, and variants were removed with call rate below 95.0%, failing missingness test, Hardy–Weinberg equilibrium p-value<10^{-6}, and minor allele frequency<1%. Genotypes were imputed using MACH/minimac software[21] to the 1000 Genomes reference panel.

Genetic risk score

We studied all variants reported at genome-wide significance in the most recent and largest genome-wide association study of the International Multiple Sclerosis Genetics Consortium (IMSGC).[16] Variants in the MHC region were not analyzed since these are not covered by standard genotyping arrays and, given the complexity of imputing classical alleles, require a dedicated effort. Of the 110 non-MHC variants, 3 could not be imputed in our dataset nor had reliable proxy variants.

Since the increase in risk of MS is small for individual variants, we calculated a combined genetic risk score to enable detection of the collective associations. This risk score was constructed by adding up all the risk alleles per individual weighted by their log-

transformed, reported effect size for the association with MS. A higher genetic risk score corresponds to more risk variants and thus a higher risk of MS. Furthermore, we calculated a second risk score that excluded all 31 variants with pleiotropic effects on other autoimmune disease (Table S8 from IMSGC GWAS[16]), leaving 76 MS-specific variants.

Image acquisition

Since the introduction of a dedicated MRI machine in the Rotterdam Study in 2005, MRI scanning was done in 4,917 on a 1.5-T MRI unit with a dedicated eight-channel head coil (Signa HD platform, GE Healthcare, Milwaukee, USA). The MRI protocol consisted of several high-resolution axial sequences, including a T1-weighted (slice thickness 0.8mm), T2-weighted (1.6mm), and fluid attenuated inversion recovery (FLAIR) sequence (2.5mm). The DTI sequence was a single shot, diffusion weighted spin echo EPI sequence (TR/TE 8000/68.7; ASSET factor 2; acquisition matrix 96×64; FOV 21cm, 38 contiguous slices with slice thickness of 3.5mm). A detailed description of the MRI protocol was presented previously.[20]

Image processing

Of the 4917 persons who came for MRI, we excluded 70 without a T1-weighted sequence. All T1-images were segmented into supratentorial gray matter, white matter and cerebrospinal fluid using a k-nearest neighbor (kNN) algorithm.[22] White matter lesions were segmented based on T1 tissue maps and an automatically detected threshold for the intensity of FLAIR scans.[23] To distinguish between the temporal, parietal, occipital, and frontal lobes, scans were non-rigidly registered to a template.[24] After visual inspection of all segmentations, an additional 137 persons were excluded because of poor quality, leaving 4710 for analysis.

Of these 4710 persons, voxel-based morphometry was performed with an optimized protocol using the FSL software.[25] Grey matter density maps were non-linearly registered to a the ICBM MNI152 template (Montreal Neurological Institute). The MNI152 standard-space T1-weighted average structural template has a 1x1x1 mm^3 voxel resolution and was derived from 152 structural images, which were averaged into the

common MNI152 co-ordinate system after high-dimensional nonlinear registration. To avoid effects of the registration step on the grey matter we implemented a spatial modulation procedure by multiplying voxel densities with the Jacobian determinants estimated during spatial normalization. Finally, images were smoothed using an isotropic Gaussian kernel of 3mm (FWHM 8mm). After quality control, 88 persons with insufficient registration quality were excluded, leaving 4622 persons for the voxel-based morphometry analyses.

Of the 4710 persons with successfully segmented tissues, 295 did not have DTI sequences. Preprocessing of DTI data was done using a standardized pipeline that includes eddy current and head-motion correction.[26] This data was combined with the tissue classification to obtain global values in the normal-appearing white matter for four DTI measures, namely fractional anisotropy, mean diffusivity, radial diffusivity, and axial diffusivity. Next, 27 white matter tracts were segmented using diffusion tractography to obtain tract-specific diffusion measures.[27] For 12 bilateral tracts, the mean of the left and right values was used, resulting in 15 tracts for analysis. We excluded persons with poor segmentation of a single (N=180) or multiple tracts (N=92), leaving 4143.

Cognitive function

Since the cognitive testing began in 2002, out of the 11,481 subjects, 7556 had cognitive function assessment. Cognitive function was assessed with the multiple neuropsychological test: a 15-word verbal learning test (based on the Rey's recall of words), the Stroop Color and Word Test, the Letter-Digit Substitution Task and a word fluency test (animal categories). A measure of general cognitive function ('G-factor') was obtained through principal component analysis.

Statistical analyses

We investigated the association of the genetic risk scores (per standard deviation increase) and individual variants (per risk allele increase) with neuroimaging and cognitive outcomes using linear regression models. All analyses were adjusted for age and sex, and additionally for intracranial volume in the macrostructural and DTI analyses.

For the 107 individual variants, the multiple testing threshold was set to $p<0.00047$ (0.05/107). Since the neuroimaging measures and cognitive tests consist of correlated data, the actual number of independent tests was calculated using 10,000 permutations. For $\alpha=0.05$ this yielded the following corrected significance thresholds: 0.0036 for the macrostructural measures, 0.0016 for the DTI tracts, 0.0055 for the cognitive tests, and 3.0×10^{-7} for the VBM analyses.

RESULTS

Study population

The characteristics of the study population are shown in Table 1, separately for participants with neuroimaging or cognition data available. The samples largely overlapped (N=4684) and were comparable with respect to age and sex.

Brain macrostructure

First, we investigated the relation between genetic risk for MS and gross volumetric measures of brain structure, across the whole brain and within individual lobes (Figure 1A). Nominally significant associations with smaller total grey matter volumes were detected for the risk score, which became stronger after restricting to MS-specific variants. When separated by lobe, the effects were most prominent for grey matter in the frontal lobe. For the single variant analyses, the five most significant associations are shown in Figure 1A. None of the individual variants survived multiple testing correction in the whole brain analyses, corrected for the number of variants ($p<4.7 \times 10^{-4}$), or the lobar analyses, additionally adjusted for the number of independent lobar volumes ($p<3.4 \times 10^{-5}$). There was no enrichment for association compared to the null distribution for any of the whole brain tissue volumes (Figure 1B). Table S1 contains all results.

Table 1 | Characteristics of the study population.

Characteristic	Neuroimaging sample (N = 4,710)	Cognition sample (N = 7,556)
Age, years	66.3 (10.3)	65.7 (11.1)
Female sex, n (%)	4,294 (56.8%)	2,599 (55.2%)
Brain volumes, cm^3		
White matter hyperintensities, median [IQR]	3.3 [1.8 – 7.2]	-
White matter	405.9 (61.6)	-
Grey matter	528.8 (54.9)	-
Cerebrospinal fluid	205.4 (55.1)	-
Cognitive tests		
Letter Digit Substitution Test	-	28.9 (7.4)
Stroop 1	-	17.7 (4.2)
Stroop 2	-	23.7 (5.4)
Stroop 3	-	51.7 (20.7)
Word fluency test	-	22.0 (5.9)
Word Learning Test immediate recall	-	17.7 (7.5)
Word Learning Test delayed recall	-	7.1 (2.9)
Purdue Pegboard Test left hand	-	12.3 (2.1)
Purdue Pegboard Test right hand	-	12.6 (2.1)
Purdue Pegboard Test both hands	-	10.1 (1.9)

All values are means (standard deviations), unless otherwise stated.

Abbreviation: IQR = interquartile range.

Voxel-based morphometry

For a more in depth investigation of grey matter, we performed voxel-based morphometry. Surface-based representations of the results of the genetic risk score are shown in Figure 2A, with the strongest association in the left superior parietal gyrus ($p=2.1x10^{-5}$). Of all variants, only rs212405 had voxel associations surviving the brain-wide significance level of $p<3.0x10^{-7}$ (Figure 2B), namely with larger grey matter volume in the right posterior temporal lobe ($p=1.5x10^{-7}$). This association was no longer significant after adjustment for all tested variants (threshold $p<2.8x10^{-9}$). The top VBM associations results are listed in Table S2.

White matter microstructure

Next, we studied measures of microstructural differences of the white matter in 15 white matter tracts using 4 diffusion tensor imaging parameters (Figure 3A-D). No significant effects were detected for the non-MHC risk score, while three associations were found with the MS-specific score. In the single variant analyses, two variants survived multiple testing correction for the number of genetic variants ($p<4.7x10^{-4}$), but not further adjustment for the tracts ($p<1.5x10^{-5}$). The variant rs1813375 showed nominal significance with 24 out of 60 tract measures (lowest $p=5.4x10^{-5}$, superior longitudinal fasciculus), and rs759648 was associated with 15 out of 60 tract measures (lowest $p=1.5x10^{-4}$, parahippocampal cingulum). Table S3 contains all DTI results.

Cognitive function

Finally, we explored functional differences in the sample with cognitive data (Figure 4). The MS-specific risk score was associated with poorer delayed recall ($p=0.039$). For the single variants, rs2283792 also associated with poorer delayed recall ($p=3.4x10^{-5}$), surviving multiple testing correction for both number of variants ($p<4.7x10^{-4}$) and also for the cognitive tests ($p<5.1x10^{-5}$). Table S4.contains all cognition result.

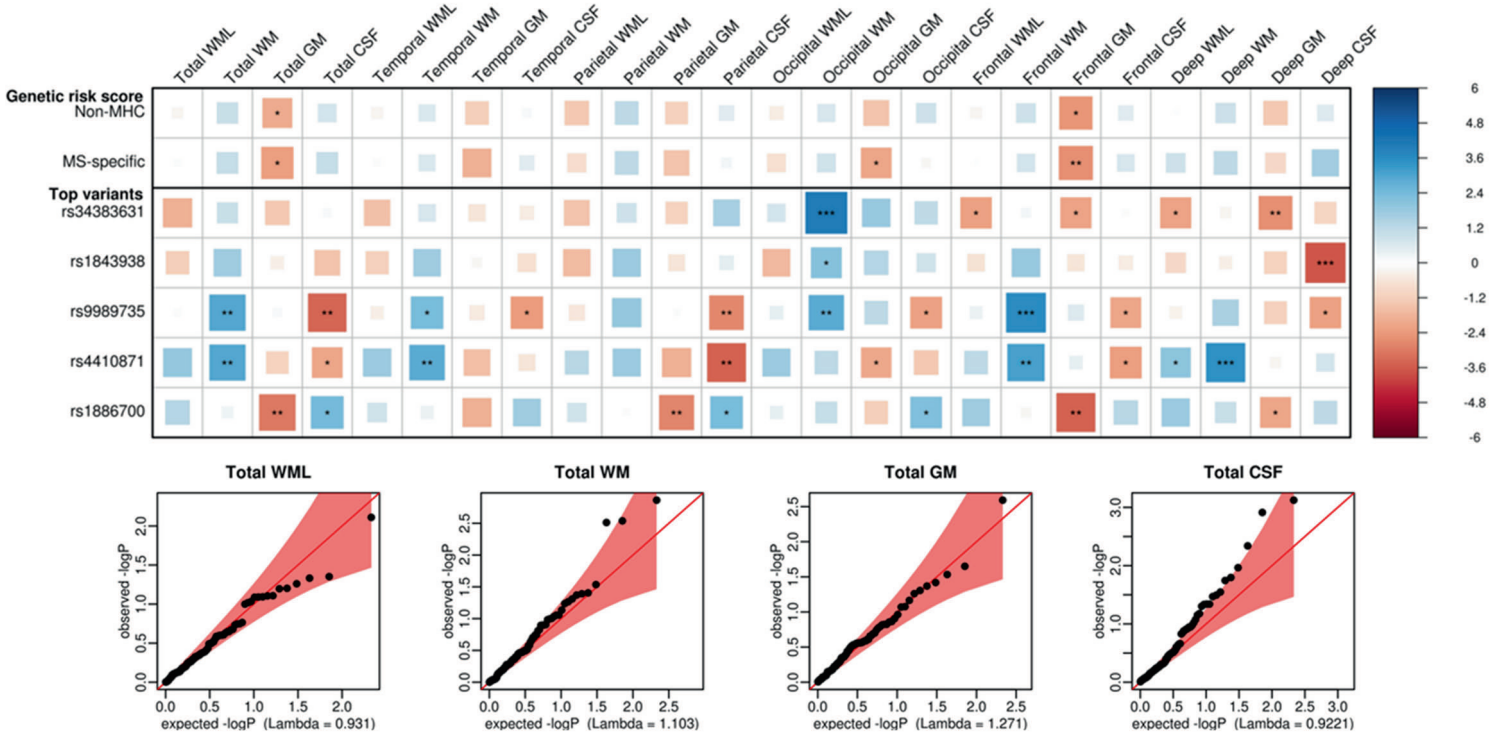

Figure 1 | Multiple sclerosis genetic variants and brain macrostructure (N = 4,710).

*Panel A: Heatmap of associations between genetic risk factors for MS with global and lobar tissue volumes. Colors and sizes of the blocks correspond to t-values, with blue and red indicating positive and negative associations, respectively. Larger blocks indicate stronger associations, and significance levels as indicated by asterisks: * p < 0.05 ** p < 0.01 *** p < 0.00047. Panel B: quantile-quantile plots for associations between single variants and global volumes. All WML volumes were natural-log transformed.*

Figure 2 | Voxel-based morphometry of multiple sclerosis genetic variants (N = 4,622).
Surface-based representation of the voxel-based morphometry results of the non-MHC risk score (panel A) and the most significant individual variants, rs212405 (panel B). From left to right, the figures depict the following four views: left side, right side, inferior, and superior. Colors correspond to t-values, with blue and red indicating positive and negative associations, respectively.

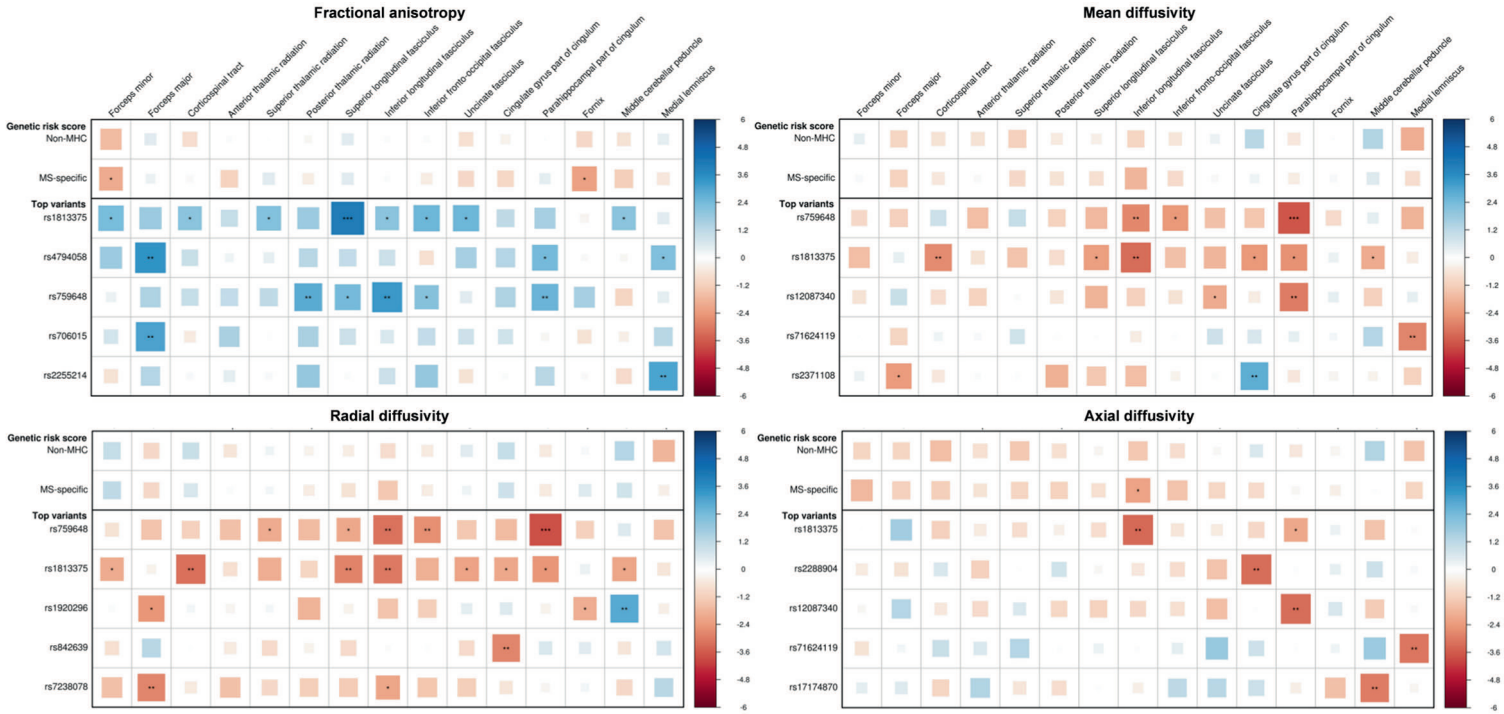

Figure 3 | Multiple sclerosis genetic variants and white matter tract integrity (N = 4,143).

*Heatmaps of associations between genetic risk factors for MS and 4 DTI parameters in 15 white matter tracts. Colors and sizes of the blocks correspond to t-values, with blue and red indicating positive and negative associations, respectively. Larger blocks indicate stronger associations, and significance levels as indicated by asterisks: * p < 0.05 ** p < 0.01 *** p < 0.00047. Tracts from left to right: 1) forceps minor, 2) forceps major, 3) corticospinal tract, 4) anterior thalamic radiation, 5) superior thalamic radiation, 6) posterior thalamic radiation, 7) superior longitudinal fasciculus, 8) inferior longitudinal fasciculus, 9) inferior fronto-occipital fasciculus, 10) uncinated fasciculus, 11) cingulum, cingulate gyrus, 12) cingulum, parahippocampus, 13) fornix, 14) middle cerebellar peduncle, 15) medial lemiscus.*

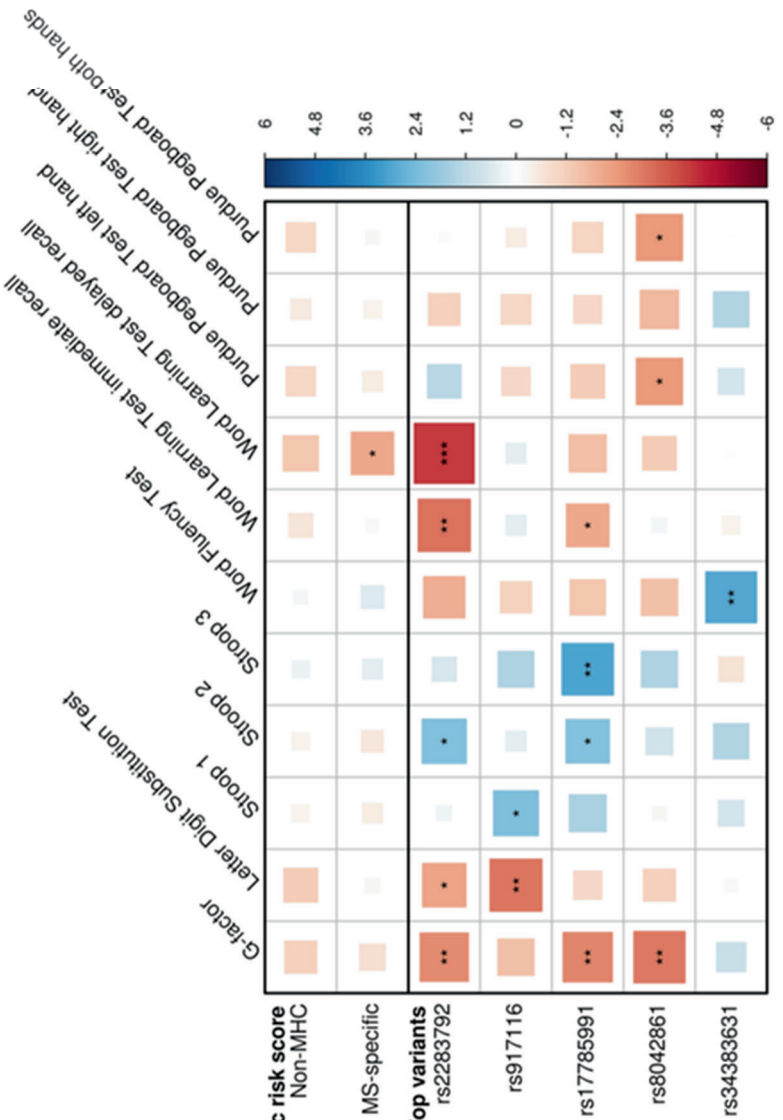

Figure 4 | Genetic susceptibility to multiple sclerosis and cognitive function (N = 7,556).
*Heatmap of associations between genetic risk factors for MS and cognitive tests. Higher scores indicate better cognitive performance, except for the Stroop tests. Colors and sizes of the blocks correspond to t-values, with blue and red indicating positive and negative associations, respectively. Larger blocks indicate stronger associations, and significance levels as indicated by asterisks: * $p < 0.05$ ** $p < 0.01$ *** $p < 0.00047$.*

DISCUSSION

Here we show the relation of genetically elevated risk for MS with brain structure and function in middle-aged and elderly individuals from the general population who are free of MS. Scores combining all common genetic risk variants were associated with smaller grey matter volumes, in particular in the frontal lobe. Single variant analyses revealed associations with white matter microstructure (rs1813375) and cognitive function (rs2283792), but only the latter survived multiple testing correction.

MS has traditionally been viewed as a heritable disease primarily affecting women of certain ages and geographic regions. However, genes involved in MS could exert more widespread detrimental effects in the general population than thus far suspected. We have previously shown that for other neurodegenerative diseases genetic risk variants can also affect cognitive function and brain structure in the general population,[28-30] which included Alzheimer's disease, Parkinson's disease, frontotemporal lobar degeneration, and amyotrophic lateral sclerosis. Others have suggested that schizophrenia risk variants are also associated with structural brain changes in persons without disease,[31] but such an effect was disputed in the general population.[32] Other found genetic overlap between MS and putamen volume on a genome-wide scale.[33]

Our study suggests that MS variants may also play a role outside of the MS population, but most findings do not reach pre-defined thresholds for statistical significance. Given that MS is a demyelinating disease, we put emphasis on white matter changes by investigating both its macro- and microstructure. Macrostructural MRI measures included both the volume of the white matter and the volume of T2-weighted hyperintensities, or 'white matter lesions', which are a marker of demyelinated white matter.[1] Furthermore, we quantified the white matter microstructural integrity using DTI, which has been shown to be decreased in MS patients.[1,2] Importantly, this loss of integrity picked up by DTI is seen earlier than macrostructural damage on conventional MRI,[1] making it particularly attractive for our research question. The top five variants for each of the four diffusion parameters showed consistent results across the white matter tracts: the risk alleles were associated with presumably better white matter integrity, i.e. higher FA but lower MD, RD, and AD. The strongest and most widespread effect was for

rs1813375, an intergenic variant without known function. However, not even this variant would survive additional multiple testing correction for the DTI tracts.

Since the role of grey matter in MS is increasingly apparent, we also examined the grey matter using macrostructural measures and voxel-based morphometry. For the global and lobar volumes, both risk scores were associated with smaller grey matter volumes over the whole brain and particularly in the frontal lobe. Frontal lobe atrophy is present in patients with MS and also correlates with the degree of cognitive dysfunction.[34] Contrary to the DTI analyses, the most significant individual variants did not show a similar pattern of association. We also attempted to map the effects of MS variants in detail using voxel-based morphometry, but no results surpassed multiple testing correction.

Besides structural measures, we also studied the effect of genetic risk of MS on cognitive outcomes. The significant risk variants were generally associated with worse cognition, but only rs2283792 survived multiple testing for all variants and cognitive tests. Each additional risk allele was associated with a 0.064 standard deviation decrease in the delayed recall test, which measures memory performance. Interestingly, memory impairment is among the most common cognitive deficits in persons suffering from MS.[9] This variant lies within *MAPK1*, but affects expression of multiple genes across various tissues. In the brain, the chromatin of this region contains H3K4me1, H3K27ac, and H3K9ac marks. This included tissue samples obtained from the hippocampus, an important brain structure for memory. If this finding is validated in other studies it could help understand the molecular mechanism underlying this association.

Overall, the combined impact of all genetic risk variants, as captured by the risk scores, was modest and suggests that MS variants do not have a large effect on the brain in the general population, but are instead restricted to MS patients. Such risk variants could exert their effect only when another environmental factor is present or through gene-by-gene interaction. Also, it is possible that the findings would have been stronger in a different population. Future studies might consider to study younger individuals, as the subclinical effects may have been obscured in our elderly population by the presence of age-related brain changes.

Another explanation is that we did not have enough power to detect any effects. However, the 110 MS variants explain almost 20% of the variance in disease susceptibility,[16] which is comparable to or even higher than many other complex diseases. The use of a genetic risk score further reduced the multiple testing burden, but this did not reveal any strong associations. The variants themselves might not have similar effects on the various neuroimaging measures and cognitive tests, and a combined score could thus have decreased power. Furthermore, other traits might need to be considered. Enlarged perivascular spaces are an emerging cerebrovascular disease marker and potentially related to inflammation.[35] Their enlargement is seen in MS and may captured other pathology.

While our focus was on brain structure and cognitive function, any subclinical effect of these variants need not be restricted to the brain. Another interesting line of research could be to study effects on the immune system. In this light, it should be noted that the IMSGC GWAS identifying and/or confirming the 110 MS risk variants employed the ImmunoChip for genotyping.[16] In its design, this genotyping platform was enriched for variants near immune-related genes and known autoimmune disease loci, thus making immune-related traits worthwhile for future studies on subclinical effects of MS variants. Conversely, this means that the current set of variants may be depleted for those primarily affecting the brain. Since many of the MS risk variants are indeed also associated with other autoimmune diseases, we constructed a second risk score that only included MS-specific variants, and is therefore potentially more related to brain-related traits. This MS-specific risk score showed a trend for more significant associations across the investigated traits, although the findings still did not surpass the multiple testing threshold.

In conclusion, this exploratory study suggests carriers of MS risk variants may at most have subtle differences with respect to brain structure and cognitive function, but further evidence is needed to confirm this.

REFERENCES

1. Werring DJ, *et al.* Brain. 2000
2. Werring DJ, *et al.* Neurology. 1999
3. Roosendaal SD, *et al.* Neuroimage. 2009
4. Geurts JJG, *et al.* The Lancet Neurology. 2008
5. Dalton CM, *et al.* Brain. 2004
6. Dineen RA, *et al.* Brain. 2009
7. Chiaravalloti ND, *et al.* The Lancet Neurology. 2008
8. Rao SM, *et al.* Neurology. 1991
9. Benedict RHB, *et al.* Journal of the International Neuropsychological Society. 2006
10. Sadovnick AD, *et al.* The Lancet. 1996
11. International Multiple Sclerosis Genetics C. The American Journal of Human Genetics. 2010
12. Fingerprinting G. N engl J med. 2007
13. Patsopoulos NA, *et al.* Annals of neurology. 2011
14. De Jager PL, *et al.* Nature genetics. 2009
15. Lill CM, *et al.* Journal of medical genetics. 2015
16. International Multiple Sclerosis Genetics C. Nature genetics. 2013
17. Patsopoulos NA, *et al.* PLoS Genet. 2013
18. Koch-Henriksen N, *et al.* The Lancet Neurology. 2010
19. Hofman A, *et al.* European journal of epidemiology. 2015
20. Ikram MA, *et al.* European journal of epidemiology. 2015
21. Howie B, *et al.* Nature genetics. 2012
22. Vrooman HA, *et al.* Neuroimage. 2007
23. De Boer R, *et al.* Neuroimage. 2009
24. Ikram MA, *et al.* Neurobiology of aging. 2010
25. Good CD, *et al.* A voxel-based morphometric study of ageing in 465 normal adult human brains. *Biomedical Imaging, 2002 5th IEEE EMBS International Summer School on*. 2002:16 pp.
26. Koppelmans V, *et al.* Human brain mapping. 2014
27. de Groot M, *et al.* Alzheimer's & Dementia. 2015
28. Adams HH, *et al.* Alzheimers Dement. 2015
29. Adams HH, *et al.* Biol Psychiatry. 2014
30. Chauhan G, *et al.* Neurobiol Aging. 2015
31. van Scheltinga AFT, *et al.* Biological psychiatry. 2013
32. Van der Auwera S, *et al.* Biological psychiatry. 2015
33. Rinker D, *et al.* Genetic pleiotropy between subcortical brain volumes and ms risk variants: A preliminary analysis. *Organization for Human Brain Mapping (OHBM)* 2015
34. Benedict RHB, *et al.* The Journal of neuropsychiatry and clinical neurosciences. 2002
35. Wuerfel J, *et al.* Brain. 2008

Chapter 5

Exploring clinical relevance

Chapter 5.1

Emerging markers

Chapter 5.1.1

Determinants of enlarged perivascular spaces

ABSTRACT

Enlarged perivascular spaces (ePVS) are emerging markers of cerebral small vessel disease, but research on their determinants has been hampered by conflicting results from small single-site studies that employ heterogeneous rating methods. We studied eight population-based cohort studies from the UNIVRSE consortium, totaling 6,844 subjects (age range 20-97 years). On MRI scans we counted ePVS in 4 brain regions (mesencephalon, hippocampus, basal ganglia, and centrum semi-ovale) according to a validated rating protocol. As potential determinants, we considered demographics, cardiovascular risk factors, APOE genotypes, and other MRI markers of cerebral small vessel disease. Negative biniomal regression models were used to examine the association between these determinants and ePVS counts. We found an increase in the average ePVS counts in the four regions from the age of 20 years (0-1 ePVS) to 90 years (2-8 ePVS). Men had more mesencephalon ePVS (OR [95%CI] = 1.11 [1.05-1.17] compared to women), but less hippocampal ePVS (0.84 [0.80–0.88]). Higher blood pressure, in particular diastolic pressure, was associated with more ePVS in all regions (ORs between 1.04-1.08). Hippocampal ePVS showed higher counts with higher LDL cholesterol levels (1.04 [1.01-1.07]), body mass index (1.03 [1.01-1.06]), and glucose levels (1.04 [1.01-1.07]), and APOE ε4-alleles (1.07 [1.02-1.13]). Furthermore, white matter hyperintensity volume and presence of lacunar infarcts associated with ePVS in multiple regions, but most strongly with the basal ganglia. In conclusion, The burden of ePVS is determined by various factors with considerable regional specificity, pointing to a multifactorial origin. Our consortium paves the way for collaborative research on ePVS.

INTRODUCTION

Perivascular spaces (PVS), also called Virchow-Robin spaces, are fluid-filled spaces encapsulating the penetrating vessels of the brain. These PVS can dilate so that they become large enough to become visible on magnetic resonance imaging (MRI) as spaces with a signal intensity similar to that of cerebrospinal fluid. Such enlarged PVS (ePVS) can occur throughout the brain but are more often seen in the white matter and deep grey matter.[1] These regional differences are thought to be partly due to morphological factors, such as regional differences in the composition of the membranes that enclose ePVS,[2] and the branching and caliber changes of the penetrating vessels.[3] Besides these morphological factors, however, it is thought that ePVS in various locations might reflect different etiologies.

While ePVS were originally thought to be an insignificant finding, in recent years they have been linked to many neurological diseases, including stroke,[4,5] Alzheimer's disease,[6,7] migraine,[8] and multiple sclerosis.[9] Reflecting the variety of associated diseases, studies have emerged on a broad range of determinants of ePVS. A major focus has been on aging, cardiovascular risk factors, and MRI markers of cerebral small vessel disease.[1,3,4,10-14] Additionally, some studies have investigated the relation with markers of inflammation and cerebral amyloid angiopathy.[5,15] However, all of these studies have in common that they assessed ePVS using heterogeneous methods and, combined with often small sample sizes, this has led to conflicting findings in the literature that are difficult to interpret. Furthermore, most studies only reported on one or two regions, mainly the basal ganglia and cerebral white matter. The mesencephalon and, to a lesser extent, the hippocampus are generally absent from rating scales even though they also frequently contain ePVS.

Here, we investigated the potential determinants of ePVS in four brain regions, namely the mesencephalon, hippocampus, basal ganglia, and centrum semi-ovale. We performed a pooled analysis of 8 population-based cohort studies with almost 7,000 individuals, all applying a uniform and validated rating method, and found region-specific associations of demographic factors, cardiovascular risk factors, *APOE* genotypes, and MRI markers of cerebral small vessel disease with ePVS burden.

METHODS

Study population

This study was performed as part of the Uniform Neuro-Imaging of Virchow-Robin Spaces Enlargement (UNIVRSE) consortium, a collaboration between several population-based cohort studies from Europe, North-America, and Asia.[16] The current study included subjects from the Austrian Stroke Prevention Study (ASPS), the ASPS Family study (ASPS-Family), the Epidemiology of Dementia In Singapore study (EDIS), the Rotterdam Study cohorts 1 and 2 (RS1 and RS2),[17,18] the Study of Health In Pomerania study (SHIP), and an extension cohort of SHIP (SHIP-Trend). Detailed information can be found in the references and Table 1.

Image acquisition

Various MRI scanners and protocols were used to acquire images in the participating cohorts, which have been thoroughly described in the consortium design paper.[16] Briefly, the field strength of the scanner in the EDIS study was 3T, whereas all other studies used a 1.5T scanner. All studies had T1-weighted, T2-weighted, and fluid-attenuated inversion recovery (FLAIR) sequences, except for the SHIP and SHIP-Trend studies, which did not have T2-weighted sequences available. The slice thickness of the primary rating sequence ranged between 1.0 and 5.5 mm.

ePVS rating

The ePVS rating was done in all cohorts according to a validated method.[19] We counted the ePVS taking into account their size, to be able to distinguish between 'normal' (< 1 mm) and 'enlarged' (between 1 and 3 mm) PVS. The ePVS that are larger than 3 mm are generally solitary lesions and were rated separately since they might represent a different etiology. The rating was done in four brain regions, namely the mesencephalon, hippocampus, basal ganglia, and centrum semi-ovale. For the latter two regions, which are large and can harbor hundreds of ePVS, only a single slice was rated. For the basal ganglia, this was at the height of the anterior commissure, and for the centrum semi-ovale this was 10 mm above the ventricles. Trained investigators rated

ePVS in ASPS, ASPSfam (C.G., P.K., P.S., R.S., T.P.), EDIS (S.H.), RS1, RS2, SHIP, and SHIP-Trend (H.H.H.A.). The primary rating sequence was the T2-weighted sequence for all studies except the SHIP and SHIP-Trend, in which the T1-weighted sequence was used. We have previously reported high reliability between use of T1-weighted or T2-weighted images as the primary rating sequence (mean ICC = 0.8).[16] The size and shape of lesions, as well as the presence of a hyperintense rim on FLAIR images, was used to differentiate ePVS from lacunes of ischemic origin.

Assessment of determinants

We investigated a range of potential determinants, including demographics, cardiovascular risk factors, *APOE* genotypes, and MRI markers of cerebral small vessel disease. We first looked at age at time of scanning, sex, and educational attainment. The cohort-specific education categories were recoded to years of education to make comparisons possible. We also measured systolic and diastolic blood pressure and calculated pulse pressure, the difference between the two. Blood samples were used to measure levels of total cholesterol, high-density lipoproteins (HDL) cholesterol, low-density lipoproteins (LDL) cholesterol, triglycerides, and glucose. Body mass index was calculated by dividing weight in kg / height in meters squared. Persons were coded according to their smoking status as never smokers, former smokers, or current smokers. *APOE* genotyping was performed using TaqMan assays, except for SHIP and SHIP-Trend, where it was imputed from a whole-genome genotyping chip. MRI markers that were investigated included lacunes of ischemic origin and cortical infarcts, which were rated visually according to established criteria.[20] Tissue volumes were automatically segmentated. For this, voxels were classified as grey matter, white matter, white matter hyperintensities, and cerebrospinal fluid. Given differences in segmentation methods, all volumes were first standardized within cohorts and subsequently pooled. Not all determinants were available in each cohort (Table 1)

Statistical analyses

The ePVS counts were analyzed as the dependent variables with zero-inflated negative binomial regression models, which take into account their discrete nature and excess of

zeros using a probability distribution. Each of the determinants was modelled as an independent variable along with other covariates. All analyses were adjusted for age and sex, but we also explored whether associations held after adjustment for cardiovascular risk factors. Volumetric measures were additionally adjusted for intracranial volume. Random effects for cohorts and individual raters were incorporated in the models. All analyses were performed in R (version 3.2.3) using the 'glmmADMB' package.

RESULTS

Study population

The population characteristics of the contributing sites are shown in Table 1. The 6,844 participants covered a wide age range, from 20 to 97 years old, and 3170 (46.31%) were men. Most participants were of European ancestry (91.5%), but the study population also included persons of Asian descent. The overall prevalence of ePVS was 90%, while region-specific prevalence estimates were 52% (mesencephalon), 69% (hippocampus), 64% (basal ganglia), and 73% (centrum semi-ovale).

Demographics

First, we investigated age, sex, and educational attainment in relation to ePVS. The age- and sex-specific trends of the number of ePVS in the four brain regions are shown in Figure 1. Higher age was associated with more ePVS in all four regions, with the largest effect in the basal ganglia (odds ratio per decade [95% confidence interval] = 1.39 [1.35 – 1.43]) compared to the other regions (odds ratios between 1.22-1.24). Men had more ePVS in the mesencephalon (1.11 [1.05 – 1.17]), whereas they had less in the hippocampus (0.84 [0.80 – 0.88]) and centrum semi-ovale (0.97 [0.92 – 1.01]), particularly at older age. There were no sex differences for the basal ganglia ePVS. Years of education was associated with more ePVS in the centrum semi-ovale (1.01 [1.00 – 1.02]).

Cardiovascular risk factors

Next, we studied the relation between cardiovascular risk factors and ePVS count per region (Table 2). Higher blood pressure was associated with more ePVS in all regions, with the largest effects for diastolic blood pressure compared to systolic blood pressure

(Figure 2). For the other cardiovascular risk factors, the significant associations were mostly for hippocampal ePVS, such as with LDL cholesterol levels (1.04 [1.01 – 1.07]), body mass index (1.03 [1.01 – 1.06]), and glucose levels (1.04 [1.01 – 1.07]). Furthermore, there was an association between higher levels of HDL cholesterol and centrum semi-ovale ePVS (1.03 [1.01 – 1.05]). After additional adjustment for all other cardiovascular risk factors, the association with diastolic blood pressure remained significant (Table S2).

APOE genotypes

We also investigated the effect of *APOE* genotypes on ePVS counts (Table 3). The most significant association was identified for ε3/ε4-carriers and hippocampal ePVS (1.10 [1.04 – 1.18]). Furthermore, there was a dose-dependent effects between ε4-alleles and ePVS in the hippocampus (1.07 [1.02 - 1.13]), but this was not significant for the basal ganglia (1.04 [0.99 – 1.10]) and centrum semi-ovale (1.04 [0.99 – 1.10])

MRI markers of cerebral small vessel disease

Finally, we explored MRI markers of cerebral small vessel disease in relation to ePVS counts (Table 4). White matter hyperintensity volume and presence of lacunar infarcts were both associated with more ePVS in multiple brain regions, with the strongest effects for the basal ganglia (1.20 [1.16 - 1.23] and 1.41 [1.33 - 1.50], respectively). Further associations were present between smaller grey matter volume and centrum semi-ovale ePVS (0.95 [0.91 - 0.98]), between larger cerebrospinal fluid volume and basal ganglia ePVS (1.03 [1.00 - 1.07]), and between larger white matter volume and ePVS in the mesencephalon (1.07 [1.02 - 1.12]) and centrum semi-ovale (1.08 [1.03 - 1.12]).

Table 1 | Characteristics of the study population.

Characteristic	ASPS	ASPS Family	EDIS Chinese	EDIS Malay	RS1	RS2	SHIP	SHIP-Trend
Sample size	670	354	284	299	1,184	884	1,116	2,053
Age, years	65.93 (8.23)	64.28 (10.46)	70.50 (6.33)	71.19 (7.04)	79.16 (4.85)	67.45 (5.47)	55.81 (12.86)	51.11 (14.09)
Male sex, n (%)	286 (42.68)	139 (39.26)	135 (47.53)	127 (42.47)	513 (43.32)	435 (49.2)	539 (48.29)	996 (48.51)
Education, years	11.04 (2.49)	11.63 (3.01)	5.68 (4.93)	4.46 (3.63)	11.61 (3.76)	12.77 (3.61)	12.30 (2.89)	11.74 (3.51)
Country	Austria	Austria	Singapore	Singapore	Netherlands	Netherlands	Germany	Germany
Ancestry	European	European	Chinese	Malay	European	European	European	European
Cardiovascular risk factors								
Systolic BP, mmHg	139.24 (20.53)	137.80 (21.20)	147.22 (18.79)	151.86 (20.80)	153.60 (21.75)	143.84 (18.54)	132.81 (18.29)	127.47 (17.32)
Diastolic BPe, mmHg	85.35 (9.37)	86.36 (9.31)	76.46 (10.43)	79.26 (11.59)	83.73 (11.37)	80.97 (10.19)	80.84 (9.92)	77.51 (9.67)
Glucose, mmol/L	-	-	6.66 (2.77)	7.11 (2.97)	5.77 (1.14)	5.63 (1.10)	5.64 (1.56)	5.62 (1.43)
Total cholesterol, mmol/L	5.87 (1.07)	5.48 (1.04)	4.89 (0.87)	5.19 (1.30)	5.29 (1.06)	5.71 (0.95)	-	5.51 (1.09)
HDL cholesterol, mmol/L	1.49 (0.46)	1.74 (0.55)	1.45 (0.38)	1.35 (0.39)	1.46 (0.39)	1.43 (0.39)	1.45 (0.39)	1.46 (0.37)
LDL cholesterol, mmol/L	3.70 (0.97)	3.18 (0.87)	2.85 (0.80)	3.14 (1.11)	-	-	3.36 (0.92)	3.41 (0.93)
Triglycerides, mmol/L	1.49 (0.81)	1.37 (0.84)	1.34 (0.81)	1.60 (0.88)	-	-	-	1.57 (1.09)
Body mass index, m/kg^2	26.57 (3.86)	26.43 (4.54)	18.98 (2.79)	20.44 (4.00)	27.26 (4.07)	27.52 (3.70)	27.63 (4.39)	27.63 (4.47)
Enlarged perivascular spaces								
Mesencephalon	1.81 (1.73)	2.95 (2.48)	0.73 (0.94)	1.05 (1.29)	1.65 (1.75)	1.83 (1.78)	0.62 (0.99)	0.51 (0.90)
Hippocampus	3.54 (2.51)	5.18 (3.19)	1.12 (1.31)	1.24 (1.64)	3.52 (3.03)	3.33 (3.07)	1.86 (2.26)	1.55 (2.05)
Basal ganglia	6.07 (3.27)	8.19 (3.79)	2.13 (2.08)	2.86 (2.88)	4.63 (4.08)	3.46 (2.96)	1.11 (2.11)	0.82 (1.59)
Centrum semi-ovale	13.04 (12.20)	13.27 (11.87)	3.56 (4.00)	4.46 (5.15)	7.73 (6.33)	7.57 (5.77)	2.39 (3.44)	1.89 (2.86)

Table 1 continued.

Other MRI markers								
White matter hyperintensities†	0.90 [1.60 – 9.31]	3.58 [1.60 – 9.31]	1.95 [1.60 – 9.31]	2.16 [1.60 – 9.31]	8.44 [1.60 – 9.31]	3.59 [1.60 – 9.31]	-	-
White matter, ml	716.77 (86.43)	513.95 (80.12)	364.66 (41.86)	357.41 (49.21)	375.02 (55.62)	404.38 (55.74)	615.24 (76.03)	612.09 (77.12)
Grey matter, ml	427.45 (44.92)	580.25 (64.24)	531.13 (62.41)	508.44 (60.54)	509.68 (52.40)	524.88 (51.28)	562.61 (66.85)	576.60 (68.21)
Cerebrospinal fluid, ml	1.59 (0.33)	1.62 (0.36)	200.63 (24.11)	192.86 (23.85)	247.96 (52.43)	207.23 (49.54)	252.98 (45.93)	246.46 (45.90)
Lacunar infarcts, n (%)	90 (13.71)	23 (6.7)	47 (16.54)	65 (21.73)	189 (15.96)	62 (7.01)	19 (1.7)	38 (1.85)
Cortical infarcts	15 (2.29)	15 (4.37)	7 (2.46)	11 (3.67)	76 (6.41)	21 (2.37)	20 (1.79)	31 (1.5)

All values are means (standard deviations), unless otherwise stated.

Abbreviation: BP = blood pressure, IQR = interquartile range.

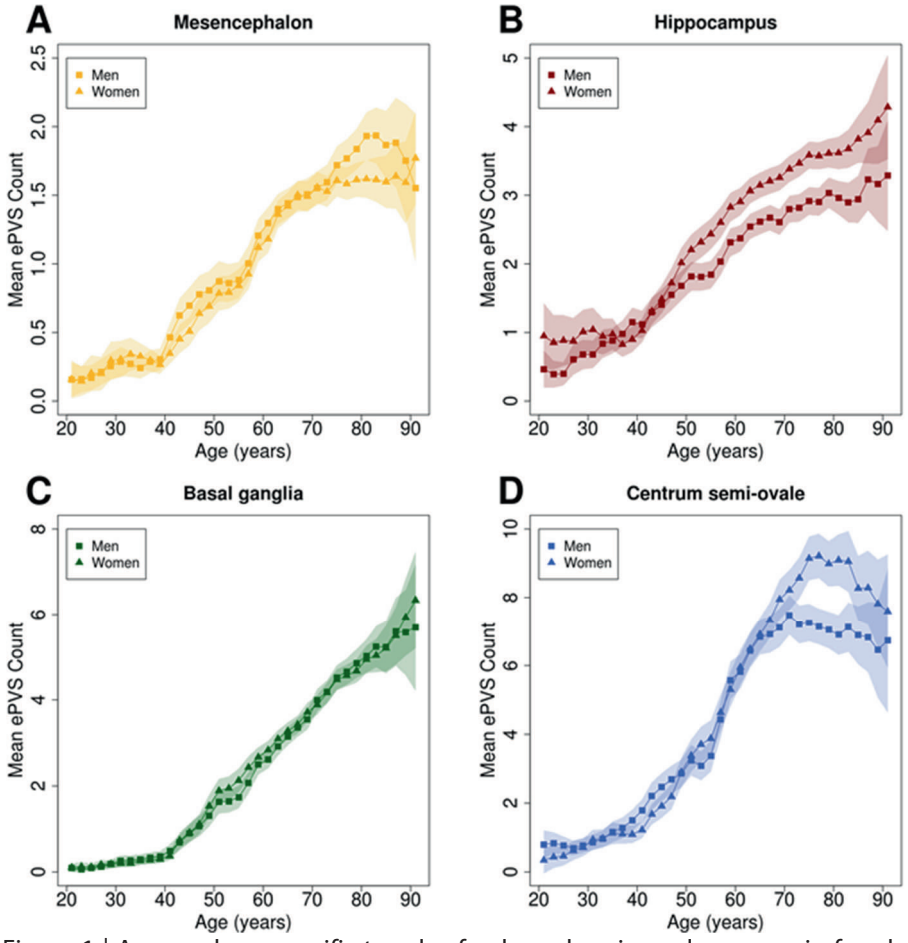

Figure 1 | Age- and sex-specific trends of enlarged perivascular spaces in four brain regions.

Mean counts of ePVS across the lifespan in the four brain regions: the mesencephalon (A), hippocampus (B), basal ganglia (C), and centrum semi-ovale (D).

Table 2 | Associations between cardiovascular risk factors and enlarged perivascular spaces.

Cardiovascular risk factor	Odds ratio (95% confidence interval)			
	Mesencephalon	Hippocampus	Basal ganglia	Centrum semi-ovale
Blood pressure				
Systolic blood pressure	1.03 (1.00 – 1.07)	1.07 (1.05 – 1.10)	1.02 (1.00 – 1.05)	1.04 (1.01 – 1.06)
Diastolic blood pressure	1.04 (1.01 – 1.08)	1.08 (1.06 – 1.11)	1.04 (1.02 – 1.07)	1.06 (1.04 – 1.09)
Pulse pressure	1.01 (0.98 - 1.05)	1.04 (1.01 - 1.07)	1.00 (0.97 - 1.02)	1.00 (0.98 - 1.03)
Lipid levels				
Total cholesterol	1.00 (0.97 - 1.03)	1.03 (1.00 - 1.05)	1.01 (0.99 - 1.04)	1.02 (1.00 - 1.05)
HDL cholesterol	1.03 (1.00 - 1.06)	1.01 (0.99 - 1.03)	1.00 (0.98 - 1.02)	1.03 (1.01 - 1.05)
LDL cholesterol	1.01 (0.97 - 1.05)	1.04 (1.01 - 1.07)	1.03 (1.00 - 1.06)	1.01 (0.98 - 1.04)
Triglycerides	0.99 (0.95 - 1.03)	1.03 (1.00 - 1.07)	0.99 (0.96 - 1.03)	0.97 (0.93 - 1.00)
Other factors				
Glucose	1.03 (1.00 - 1.07)	1.04 (1.01 - 1.07)	1.03 (1.00 - 1.05)	1.01 (0.99 - 1.04)
Body mass index	1.01 (0.97 - 1.04)	1.03 (1.01 - 1.06)	0.98 (0.95 - 1.00)	0.98 (0.96 - 1.01)

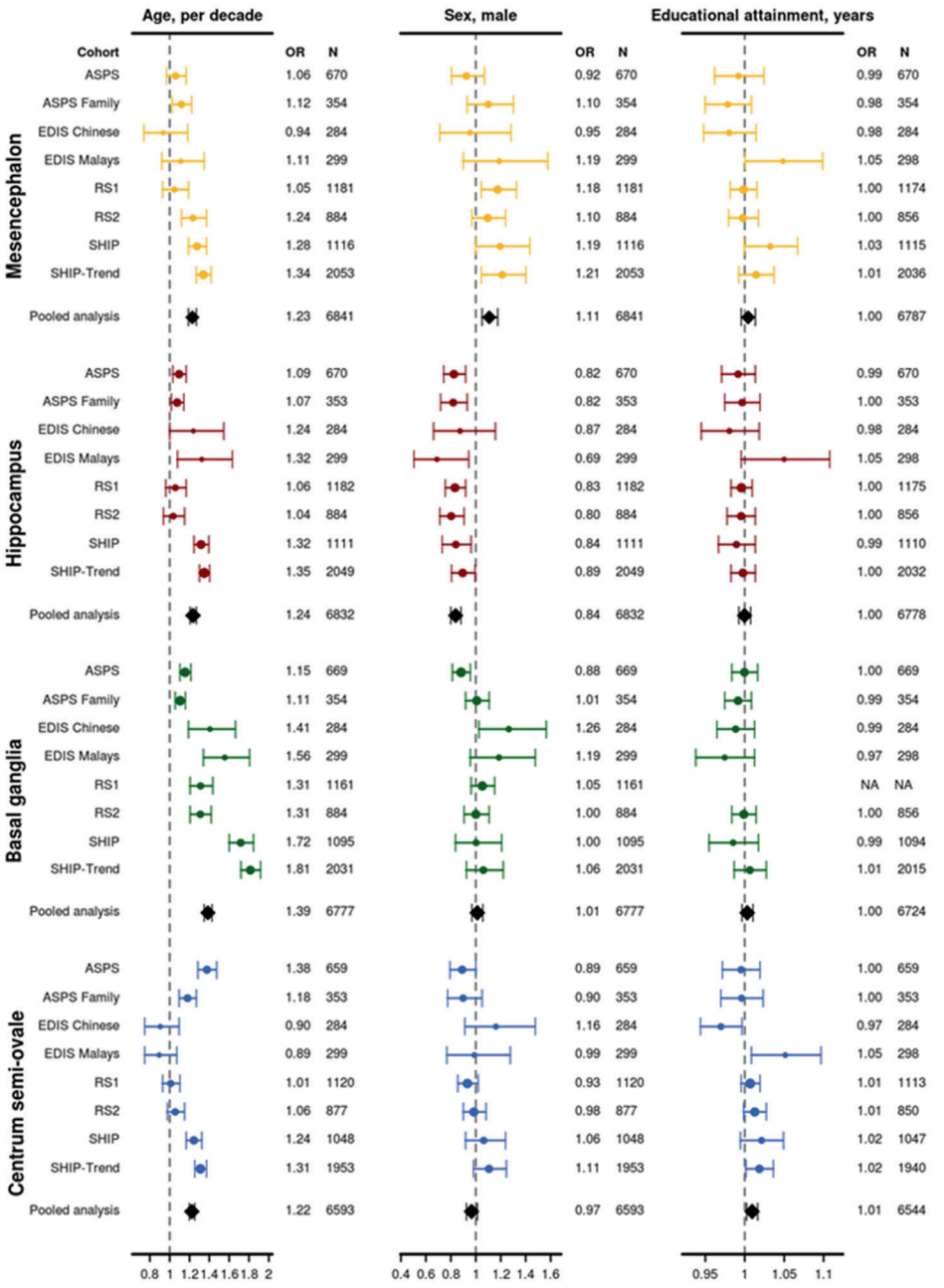

Figure 2 | Associations between demographic risk factors and enlarged perivascular spaces.

Odds ratios for demographic risk factor from the eight individual sites and the meta-analyzed result for counts of ePVS in the four brain regions: the mesencephalon (yellow), hippocampus (red), basal ganglia (green), and centrum semi-ovale (blue).

DISCUSSION

Enlargement of perivascular spaces has been hypothesized to arise in response to a variety of brain pathologies. In this multi-site analysis of population-based cohort studies, we investigated determinants of ePVS and found that increasing age was related to more ePVS throughout the brain. Other determinants were region-specific, including sex, cardiovascular risk factors, *APOE* genotypes, and MRI markers of cerebral small vessel disease. Our results support the notion that ePVS are indeed of a multifactorial origin, and furthermore highlight the power of collaborative efforts.

Of all investigated factors, higher age was among the most important determinants of ePVS. While ePVS could be seen even in the youngest participants, who were in their early twenties, a sharp increase in ePVS counts was apparent from the age of 40 onwards. The prevalence of ePVS in the various regions ranged between 11% to 93% depending on the age group, and from 47% to 100% across the whole brain. Three other population-based studies have reported prevalence estimates, namely the AGES-Reykjavik study (16%, mean age 76 years)[21], Northern Manhattan Study (NOMAS; 87.5%; mean age 72 years)[3], and the Three City Dijon study (3C; 100%; mean age 73 years).[1] These large differences likely reflect heterogeneity in methods, i.e. the choice of the rating scale and field strength of the MRI scanner. Different brain regions were rated in the various scales, making it difficult to compare these prevalence estimates.

Furthermore, no minimum threshold for the size of ePVS was defined,[1,3,21] resulting in higher prevalence estimates when high-resolution images were used.[1] We found that the effect of age was strongest for the basal ganglia (odds ratio per decade = 1.39) compared to the other regions (odds ratios between 1.22-1.24), representing an almost twofold larger increase of ePVS within the same time period. This is in line with a mouse study that found regional differences of PVS in response to aging.[2] This indicates that, rather than a shared process leading to more ePVS throughout the brain, there might be factors contributing specifically to pathology in certain regions. Since brain aging itself is complex and results from various forms of damage, we aimed to disentangle these individual components by investigating specific cardiovascular, genetic, and neuroimaging markers in relation to ePVS.

Table 3 | Associations between *APOE* genotypes and enlarged perivascular spaces.

APOE genotype	Odds ratio (95% confidence interval)			
	Mesencephalon	Hippocampus	Basal ganglia	Centrum semi-ovale
Per genotype				
ε3/ε3 (reference)	1	1	1	1
ε2/ε2	0.91 (0.64 - 1.29)	1.25 (0.97 - 1.60)	1.07 (0.83 - 1.38)	1.20 (0.94 - 1.55)
ε2/ε3	0.99 (0.91 - 1.09)	1.01 (0.94 - 1.09)	0.97 (0.90 - 1.04)	1.03 (0.96 - 1.11)
ε2/ε4	0.71 (0.54 - 0.93)	1.13 (0.94 - 1.35)	1.05 (0.89 - 1.26)	1.14 (0.96 - 1.36)
ε3/ε4	1.01 (0.94 - 1.10)	1.10 (1.04 - 1.18)	1.03 (0.97 - 1.10)	1.03 (0.97 - 1.10)
ε4/ε4	1.05 (0.81 - 1.38)	0.99 (0.80 - 1.23)	1.13 (0.94 - 1.36)	1.15 (0.95 - 1.39)
Additive				
Per ε2 allele	0.96 (0.88 - 1.03)	1.02 (0.96 - 1.09)	0.98 (0.93 - 1.04)	1.05 (0.99 - 1.11)
Per ε4 allele	1.00 (0.93 - 1.07)	1.07 (1.02 - 1.13)	1.04 (0.99 - 1.10)	1.04 (0.99 - 1.10)

Table 4 | Associations between MRI markers and enlarged perivascular spaces.

MRI marker	Odds ratio (95% confidence interval)			
	Mesencephalon	Hippocampus	Basal ganglia	Centrum semi-ovale
Volumetric measures				
White matter hyperintensities†	1.04 (1.00 - 1.08)	1.16 (1.12 - 1.19)	1.20 (1.16 - 1.23)	1.01 (0.98 - 1.04)
White matter	1.07 (1.02 - 1.12)	1.03 (0.99 - 1.08)	1.01 (0.97 - 1.05)	1.08 (1.03 - 1.12)
Grey matter	0.97 (0.93 - 1.02)	1.02 (0.98 - 1.06)	1.00 (0.96 - 1.04)	0.95 (0.91 - 0.98)
Cerebrospinal fluid	0.95 (0.91 - 0.99)	0.98 (0.95 - 1.02)	1.03 (1.00 - 1.07)	1.00 (0.97 - 1.04)
Focal measures				
Lacunar infarcts, n (%)	1.02 (0.99 - 1.04)	1.05 (1.03 - 1.07)	1.41 (1.33 - 1.50)	1.05 (1.03 - 1.07)
Cortical infarcts	1.02 (0.99 - 1.04)	1.02 (1.00 - 1.04)	1.14 (1.03 - 1.26)	1.02 (1.00 - 1.04)

One striking region-specific factor was sex, for which we report several novel findings. Men had more ePVS in the mesencephalon, a region where sex differences have been described with respect to both its structure and function.[22] The mesencephalon is important for motor control and cognition, but ePVS have remained understudied and are mostly the subject of extreme case reports. One anatomical study of 115 Japanese adults with neurologic complaints found no relation with age, but did not report on the effect of sex.[23] The NOMAS study did not find an association with sex, but pooled all infratentorial regions together.[3] In that study, they did find women had higher ePVS scores in the subcortical white matter, whereas a study in Chinese stroke patients reported higher scores in men.[10] We found no significant sex differences for the centrum semi-ovale, but we did see more hippocampal ePVS in women, as was observed earlier.[10] We also did not identify any sex differences in the basal ganglia, in line with most previous studies,[3,4,10] but contrary to the 3C study that found more ePVS in men.[1] The sex differences could be due to differences in brain development, but comparisons between men and women of morphological and functional aspects of PVS are lacking. Also, the differences were most apparent later at life, suggesting that there is differential susceptibility to age-related brain pathologies. In light of women's higher risk of Alzheimer's disease, it is interesting that they have more ePVS in the hippocampus, and to a lesser extent the centrum semi-ovale, since amyloid-β is disproportionately deposited here.

We also found that a higher systolic, and particularly diastolic, blood pressure was associated with more ePVS. High blood pressure has also been related to other markers of cerebral small vessel disease, including white matter hyperintensities, infarcts, and microbleeds; this included reports of differential associations between systolic and diastolic pressure.[24,25] The strong associations we found with diastolic pressure, rather than systolic, suggest the lower bound of blood pressure is more important for the enlargement of PVS. A possible explanation of this finding is that a continuously raised diastolic blood pressure leads to a greater extravasation of fluid into the spaces surrounding the small vessels, or alternatively prevents sufficient fluid from returning into the bloodstream (after a systolic pulse). Gutierrez *et al.*[3] suggested that ePVS might arise behind a large drop in vascular caliber that exposes the smaller vessels to greater

pulsatility and mechanical forces, which is the case for arteries in the basal ganglia and brainstem. While the 3C and NOMAS studies have previously reported high blood pressure as a determinant of ePVS severity in the basal ganglia,[3,11] our novel finding with mesencephalon ePVS provides further support for this hypothesis. However, pulse pressure, as a measure of the pulsatile component of blood pressure, was not strongly related to ePVS counts. Future studies should employ more extensive ways of measuring the compliance and distensibility of arteries, preferably in vessel beds relevant for the brain.

The association with diastolic blood pressure was strongest for hippocampal ePVS and this was similar for other cardiovascular risk factors, such as LDL cholesterol levels, body mass index, and glucose levels. There is some debate on whether these fluid-filled cavities in the hippocampus actually represent ePVS. Some define these lesions as hippocampal sulcal cavities that are thought to be a remnant from brain development,[26] Furthermore, it has recently been suggested that a subset of these, which appear hyperintense on FLAIR, might represent microinfarcts.[13] Nevertheless, others have observed characteristics of typical ePVS, namely the presence of a vessel within these lesions that is surrounded by a fluid-filled compartment without apparent damage to the surrounding tissue.[26] When studying their determinants, we found that cardiovascular risk was related to a higher ePVS count in the hippocampus, suggesting a potential vascular origin. Another finding that could add to this is the link with *APOE* ε4 genotypes, which influences lipid metabolism and increases risk of cardiovascular disease.[27] However, *APOE* ε4 is also an important risk factor for Alzheimer's disease and predisposes to amyloid pathology in the brain, particularly in the hippocampus.[28] Furthermore, *APOE* ε4 may disrupt perivascular drainage of soluble amyloid-β from the brain and thereby increase the risk for Alzheimer's disease.[29] It remains to be determined whether the association between *APOE* ε4 and hippocampal ePVS reflects a cardiovascular or amyloid-related pathway, or both.

The link between white matter hyperintensities and basal ganglia ePVS has been extensitvely described,[4,12] and our study convincingly confirms this. The mechanism underlying this association has not been elucidated but a possible explanation is that drainage from the (periventricular) white matter goes through the basal ganglia ePVS.

Alternatively, shared determinants could induce an association, but there was little influence by additional adjustment for cardiovascular risk factors and other MRI markers. Nonetheless, potential shared factors not assessed in this study, such as genetics, could well play a role. For the lacunar infarcts, another consideration is misclassificiation as ePVS or vice versa. However, we paid particular attention to differentiating ePVS from infarcts using their shape, size, and presence of a hyperintense rim on FLAIR images.[19] Furthermore, lacunar infarcts are per definition different lesions, since ePVS larger than 3mm were rated separately in our rating protocol,[19] and this is also the lower size bound of lacunar infarcts. Nevertheless, it remains possible that presence of lacunar infarcts might have influenced the counting of ePVS, but these visual ratings cannot be performed in a blinded fashion. However, we also find various associations with other MRI markers, including larger cerebrospinal fluid volume and basal ganglia ePVS as well as smaller grey matter volume and centrum semi-ovale ePVS, suggesting a relation with tissue loss. The ePVS could arise as part of the neurodegenerative process, e.g. insufficient clearance of neurotoxic proteins, but another explanation is that they simply become visible as a secondary consequence of neurodegeneration by filling up the empty space created by brain atrophy. Longitudinal studies are required to determine the temporal relation between ePVS and atrophy.

Strengths of the current study include 1) the large sample size resulting from a multi-site effort, 2) the rigorous harmonization of the rating protocol, including a minimal size criterion, which allowed the pooling of data, 3) the use of continuous measures (ePVS counts) instead of categorization (i.e. grades / severity scales), and the appropriate statistical handling with negative binomial regression models, and 4) the investigation of four different brain regions, which resulted in the identification of several region-specific associations. This study also has several limitations. For the two larger brain regions, where hundreds of ePVS can be present, only a single slice was used for rating to reduce the time needed for counting all ePVS. However, we have previously shown that this is sufficient to capture the burden across the whole region, with high correlations between the single-slice and whole-region approach.[16] All visual rating methods suffer from a substantial measurement error, with fully automated segmentation algorithms for ePVS still in development. Furthermore, although this is the

largest study on ePVS to date, we potentially did not have enough power to detect small effects and to explore any ethnic differences. Finally, the cross-sectional study design does not inform whether the determinants precede ePVS development or the other way around.

While the focus of the current study was on cardiovascular risk factors and MRI markers of cerebral small vessel disease, it would be interesting for future studies to investigate other potential determinants, to further disentangle potential differences in etiology of ePVS per region. These include relatively novel MRI markers, such a microbleeds, white matter microstructure measured through diffusion tensor imaging, and functional MRI. Also, it is possible that ePVS reflect a more systemic pathology. We and other have recently shown links with the retinal microvasculature[30] and inflammation,[15,31] but these findings have yet to be replicated. Furthermore, it is important to study the relation to clinical outcomes such as cognitive decline, stroke, and dementia.

In conclusion, factors related to enlargement of PVS include age, sex, cardiovascular risk factors, *APOE*, and other MRI markers. There seems to be important regional specificity to these associations, potentially reflecting heterogeneity in etiology.

REFERENCES

1. Zhu YC, *et al.* American Journal of Neuroradiology. 2011
2. Hawkes CA, *et al.* Aging cell. 2013
3. Gutierrez J, *et al.* American Journal of Neuroradiology. 2013
4. Doubal FN, *et al.* Stroke. 2010
5. Charidimou A, *et al.* Journal of Neurology, Neurosurgery & Psychiatry. 2013
6. Pappolla M, *et al.* Neurobiology of disease. 2014
7. Ramirez J, *et al.* Journal of Alzheimer's Disease. 2015
8. Schick S, *et al.* Neuroradiology. 1999
9. Achiron A, *et al.* American journal of neuroradiology. 2002
10. Zhang C, *et al.* PloS one. 2014
11. Zhu Y-C, *et al.* Stroke. 2010
12. MacLullich AMJ, *et al.* Journal of Neurology, Neurosurgery & Psychiatry. 2004
13. van Veluw SJ, *et al.* NeuroImage: Clinical. 2013
14. Yao M, *et al.* Neurobiology of aging. 2014
15. Satizabal CL, *et al.* Journal of Alzheimer's Disease. 2013
16. Adams HHH, *et al.* Alzheimer's & Dementia: Diagnosis, Assessment & Disease Monitoring. 2015
17. Hofman A, *et al.* European journal of epidemiology. 2015
18. Ikram MA, *et al.* European journal of epidemiology. 2015
19. Adams HH, *et al.* Stroke. 2013
20. Vermeer SE, *et al.* New England Journal of Medicine. 2003
21. van Sloten TT, *et al.* American Journal of Psychiatry. 2015
22. Sacher J, *et al.* Magnetic resonance imaging. 2013
23. Saeki N, *et al.* American journal of neuroradiology. 2005
24. Mast H, *et al.* Stroke. 1995
25. van Dijk EJ, *et al.* Hypertension. 2004
26. Sasaki M, *et al.* Radiology. 1993
27. Eichner JE, *et al.* American journal of epidemiology. 2002
28. Bales KR, *et al.* Molecular interventions. 2002
29. Hawkes CA, *et al.* PloS one. 2012
30. Mutlu U, *et al.* Stroke. 2016
31. Aribisala BS, *et al.* Stroke. 2014

Chapter 5.1.2

Retinal microvasculature and enlarged perivascular spaces

ABSTRACT

Background and Purpose: Perivascular enlargement in the brain is a putative imaging marker for microvascular brain damage, but this link has not yet been confirmed using direct in vivo visualization of small vessels. We investigated the relation between microvascular calibers on retinal imaging, and enlarged perivascular spaces [ePVSs] on brain MRI.

Methods: We included 704 participants from the Rotterdam Study. Retinal arteriolar and venular calibers were measured semi-automatically on fundus photographs. ePVSs were counted in the centrum semi-ovale, basal ganglia, hippocampus, and mesencephalon, using a standardized rating method. We determined the association between retinal vascular calibers and ePVS with negative binomial regression models, adjusting for age, sex, the other vascular caliber, structural brain MRI-markers, and cardiovascular risk factors.

Results: Both narrower arteriolar and wider venular calibers were associated with more ePVSs in the centrum semi-ovale and hippocampal region. Rate ratios (95% confidence interval) for arterioles in the centrum semi-ovale and hippocampus were 1.07 (1.01-1.14) and 1.13 (1.04-1.22), respectively, and for venules 1.08 (1.01-1.16) and 1.09 (1.00-1.18), respectively. These associations were independent from other brain MRI-markers, and cardiovascular risk factors.

Conclusions: Retinal microvascular calibers are related to ePVSs, confirming the putative link between microvascular damage and enlarged perivascular spaces.

INTRODUCTION

Enlarged perivascular spaces [ePVSs] in the brain, also known as Virchow-Robin spaces, have emerged as a promising imaging biomarker for vascular brain pathology.[1] These are spaces filled with interstitial fluid that surround the blood vessels as they extend into the brain. Increasing evidence suggests that ePVSs are affected by vascular risk factors, including high blood pressure and inflammation.[2] Additionally, ePVSs are strongly associated with other structural imaging markers, such as white matter lesions [WMLs] and lacunes, both hallmarks of cerebral small-vessel disease.[3] In histopathology, ePVSs and characteristics of microvascular diseases are often found concomitantly, further indicating that ePVSs might reflect damage to cerebral microvessels.[4] However, the link between microvascular damage and ePVSs has not yet been shown in vivo. The main difficulty is to directly assess the cerebral microvessels (<200 μm) in vivo with current brain imaging techniques. A robust alternative is visualization of the retinal microvasculature, as the retinal and cerebral microvasculature share anatomy, physiology and embryology.[5] Indeed, there is convincing evidence showing links between retinal microvascular damage and (sub)clinical vascular brain disease.[6] Here, we investigated the association of retinal microvasculature with ePVSs in the general population.

METHODS

See Supplemental Methods for detailed methods.

Setting and Study Population

This study was embedded within the population-based Rotterdam Study.[7] Between 2004-2006, we randomly invited 1,073 persons for brain MRI, of which 704 non-demented persons had complete scans and gradable fundus transparencies. The Rotterdam Study has been approved by the medical ethics committee according to the Population Study Act Rotterdam Study. Written informed consent was obtained from all participants.

Measurement of retinal vascular calibers

Fundus photographs centered on the optic disc were analyzed with a semi-automated system (Interactive Vessel ANalyzer (IVAN)) following standardized protocols.[8] For each participant one summary value was calculated for the arteriolar and venular calibers (in μm), and adjusted for possible magnification variations to approximate absolute measures.

Enlarged perivascular spaces rating

Perivascular enlargements were counted according to a previously published protocol[9] in the centrum semi-ovale, basal ganglia, hippocampus, and mesencephalon, areas in which ePVSs frequently occur. PVSs were identified by their linear, ovoid, or round shape, and considered enlarged when their diameter was ≥1 mm.[9]

Statistical analysis

We used negative binomial regression models to determine the association between retinal vascular calibers and count of ePVSs. Rate ratios (interpreted as ratios of ePVSs count) with 95% confidence intervals were estimated per SD decrease in arterioles, or increase in venules. We adjusted for age, sex, and the other vascular caliber, and additionally for structural brain MRI-markers (intracranial volume, WML volume, infarcts, and microbleeds), and for cardiovascular risk factors. We explored effect modification by stratifying for sex, hypertension, diabetes mellitus, and smoking. Analyses were performed using SPSS 21.0 (IBM corp., Armonk, New York).

RESULTS

Study population characteristics are reported in Table 1. Average age was 66.0 years, and 52% were females. We found that narrower arteriolar calibers and, to a lesser extent, wider venular calibers were significantly associated with more ePVSs in the hippocampus and centrum semi-ovale. Adjusting for structural brain MRI-markers and cardiovascular risk factors slightly attenuated these associations, but these remained statistically significant (Table 2). Excluding participants with a history of stroke (n=11) did not change the associations. Stratified analyses revealed no interactions ($p_{interaction}$ >0.05).

Table 1 | Characteristics of the study population, N=704

Characteristic	
Age, years	66.0 (5.1)
Female	365 (52%)
Systolic blood pressure, mmHg	143.1 (17.8)
Diastolic blood pressure, mmHg	81.0 (10.3)
Anti-hypertensive medication	249 (35%)
Body mass index, kg/m^2	27.5 (3.9)
Total cholesterol, mmol/L	5.7 (0.9)
High-density lipoprotein cholesterol, mmol/L	1.4 (0.4)
Diabetes mellitus	65 (9%)
C-reactive protein, mg/L	2.1 (3.7)
Carotid plaque score≥4	173 (25%)
Current smoker	89 (13%)
Intracranial volume, ml	1138.4 (115.5)
WML volume*, ml	3.5 (2.1-7.0)
Infarcts	58 (8%)
Cerebral microbleeds	111 (16)
Retinal arteriolar diameter, µm	149.3 (15.3)
Retinal venular diameter, µm	232.4 (22.1)
Regions of ePVSs *	
Centrum semi-ovale	6.0 (3.0-11.0)
Basal ganglia	3.0 (1.0-5.0)
Hippocampus	3.0 (1.0-5.0)
Mesencephalon	2.0 (0.0-3.0)

Values are presented as means (standard deviation) or as numbers.

**Values are presented as median (interquartile range), because of skewed distribution.*

Table 2 | The association between retinal vascular calibers and ePVSs.

Retinal vascular caliber	Centrum semi-ovale	Basal ganglia	Hippocampus	Mesencephalon
Arteriolar caliber, per SD decrease				
Model 1*	1.07 (1.01-1.14)	1.06 (0.99-1.13)	1.14 (1.05-1.24)	1.07 (0.99-1.16)
Model 2†	1.07 (1.01-1.14)	1.03 (0.97-1.10)	1.12 (1.04-1.22)	1.07 (0.99-1.15)
Model 3‡	1.07 (1.01-1.14)	1.05 (0.98-1.13)	1.13 (1.04-1.22)	1.06 (0.98-1.14)
Venular caliber, per SD increase				
Model 1	1.07 (1.00-1.15)	1.05 (0.97-1.12)	1.08 (1.00-1.17)	1.05 (0.97-1.15)
Model 2	1.07 (1.00-1.14)	1.03 (0.96-1.10)	1.06 (0.98-1.15)	1.05 (0.97-1.14)
Model 3	1.08 (1.01-1.16)	1.05 (0.98-1.13)	1.09 (1.00-1.18)	1.06 (0.98-1.16)

Values are rate ratios for count of ePVSs (95% CI).

**adjusted for age, sex, and the other vascular caliber.*

†as model 1, additionally adjusted for intracranial volume, WML volume, infarcts, and cerebral microbleeds.

‡as model 1, additionally adjusted for systolic blood pressure, diastolic blood pressure, antihypertensive medication, BMI, total cholesterol, HDL cholesterol, diabetes mellitus, C-reactive protein, carotid plaque score and smoking.

DISCUSSION

Here, we found that narrower arteriolar and wider venular calibers were associated with more ePVSs, independently of structural brain MRI-markers, and cardiovascular risk factors.

Previous studies showed that ePVSs are related to subclinical and clinical vascular brain disease,[1, 2] supporting that perivascular enlargements reflect microvascular damage. However, no study has directly investigated in vivo the association of PVSs with microvasculature. We provide the first in vivo evidence that microvascular calibers are related to ePVSs, but the mechanism remains undetermined.

First, PVSs drain interstitial and cerebrospinal fluid to the subarachnoid space, and eventually into cervical lymph nodes. Hence, a failure in this transmission may result in hemodynamic pressure differences that might manifest themselves in changed vascular calibers. Future studies are warranted to show how that would specifically lead to narrower arterioles. Second, narrower arterioles may lead to a state of cerebral hypoperfusion, eventually resulting in atrophy, and thus to perivascular enlargement. This ischemic mechanism is further supported by findings showing wider venular calibers to be associated with cerebral hypoxia.[10] Finally, it is also possible that shared risk factors explain the relation between retinal microvascular calibers and PVSs. Structural MRI-markers of cerebral small-vessel disease, or cardiovascular risk factors, are likely candidates as confounders, but these factors did not fully explain the association in our study, indicating that other processes also play a role. These include arteriolosclerosis, inflammation, venous collagenosis, and cerebral amyloid angiopathy. Interestingly, ePVSs in the brain regions most associated with the retinal vessels, namely the centrum semi-ovale and hippocampus, are related to cerebral amyloid angiopathy.[11] The perivascular drainage system in the basal ganglia is thought to process amyloid more efficiently and ePVSs there are associated more to vascular pathology. However, we did not find a significant association of retinal vascular calibers and ePVSs in the basal ganglia.

Strengths of our study are the population-based setting, the standardized rating protocol, and the extensive available data on brain MRI-markers and cardiovascular risk factors. A limitation is the cross-sectional design of our study, which precludes inferences on the temporal link between microvascular damage and ePVSs. Also, it is difficult to completely rule out misclassification of small infarcts as perivascular enlargements. This potential differential misclassification may have led to overestimation of our associations. However, since we used count data on PVSs as outcome, a single or even a few misclassified infarcts are unlikely to have majorly influenced our results. Finally, we used a static measure of the microcirculation instead of dynamic functional measures synchronized on the cardiac cycle. This may have caused random misclassification, leading to an underestimation of our associations.

In conclusion, our study shows that microvascular calibers are related to ePVSs, independent of structural MRI-markers of cerebral small-vessel disease, and cardiovascular risk factors.

REFERENCES

1. Groeschel S*, et al.* Neuroradiology. 2006
2. Zhu YC*, et al.* Stroke. 2010
3. Doubal FN*, et al.* Stroke. 2010
4. Adachi M*, et al.* Neuroradiology. 1998
5. Liew G*, et al.* Circ Cardiovasc Imaging. 2008
6. Heringa SM*, et al.* J Cereb Blood Flow Metab. 2013
7. Hofman A*, et al.* Eur J Epidemiol. 2015
8. Hubbard LD*, et al.* Ophthalmology. 1999
9. Adams HH*, et al.* Stroke. 2013
10. de Jong FJ*, et al.* Ophthalmology. 2008
11. Charidimou A*, et al.* Neurology. 2014

Chapter 5.2

Prediction of clinical outcomes

Chapter 5.2.1

Genetic risk of neurodegenerative diseases, MCI, and dementia

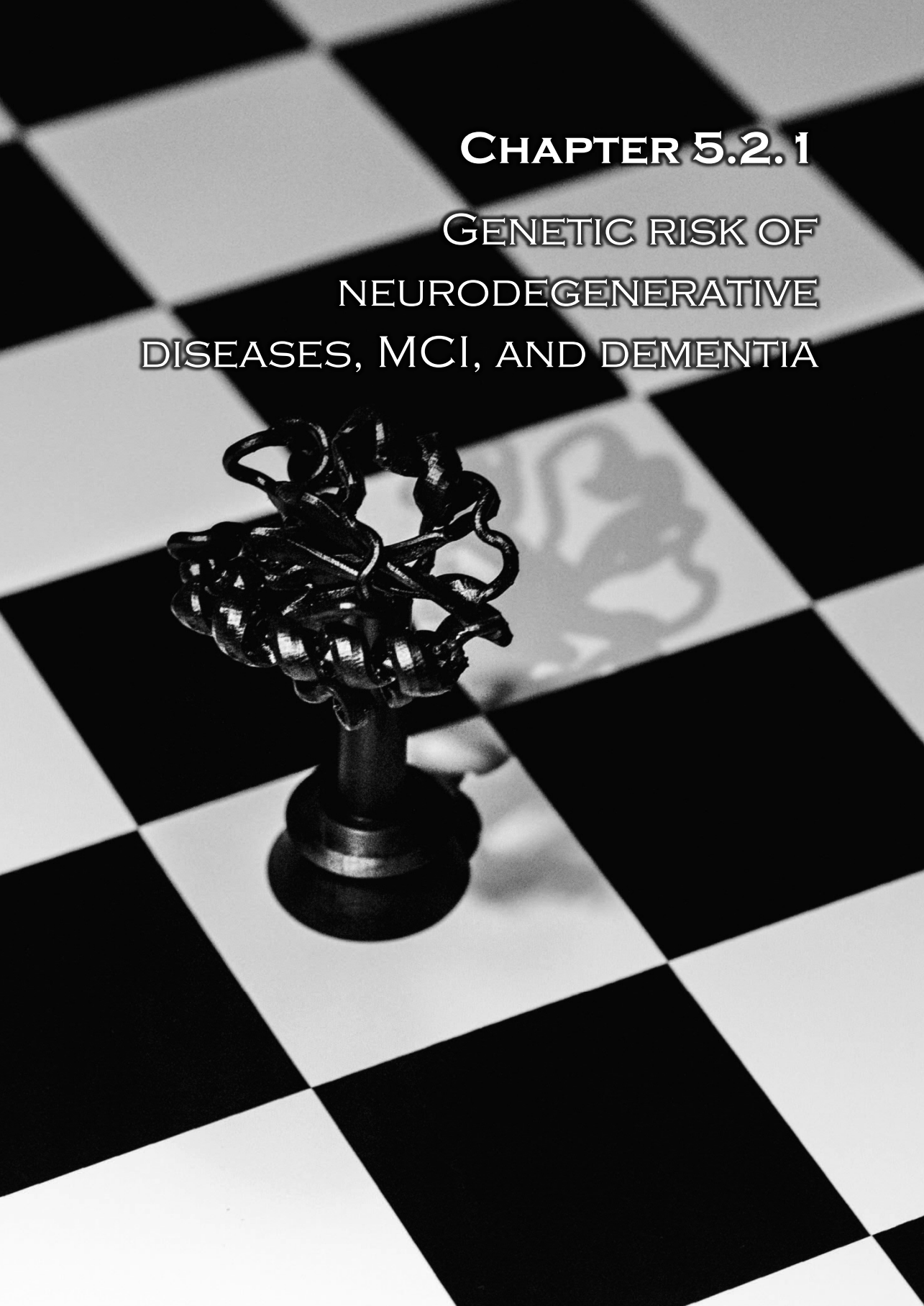

ABSTRACT

Background: Neurodegenerative diseases are a major cause of cognitive impairment and can ultimately lead to dementia. Genome-wide association studies have uncovered many genetic variants conferring risk of neurodegenerative diseases, but their role in cognitive impairment remains unexplored.

Methods: In the prospective, population-based Rotterdam Study, 3605 non-demented persons aged ≥55 years were genotyped, screened for MCI in 2002-2005 and underwent continuous follow-up for dementia until 2012. Weighted polygenic risk scores of genetic variants for Alzheimer's disease (AD), Parkinson's disease (PD), and the frontotemporal lobar degeneration/amyotrophic lateral sclerosis disease spectrum (FTLD/ALS) were constructed and investigated for association with mild cognitive impairment (MCI) and subsequent conversion to dementia.

Results: In total, 360 (10.0%) persons had MCI, of whom 147 (4.1%) amnestic and 213 (5.9%) non-amnestic. The AD risk score was associated with both MCI subtypes (odds ratio for all MCI 1.15 [95% CI, 1.03-1.28]), whereas PD and FTLD/ALS risk scores were associated only with non-amnestic MCI (odds ratios 1.15 [1.00-1.32] and 1.19 [1.03-1.37], respectively). The AD risk score, but not PD and FTLD/ALS risk scores, was associated with an increased risk of dementia (hazard ratio 1.55 [1.37-1.77]).

Conclusions: Genetic evidence supports the view that multiple neurodegenerative pathways lead to MCI and that subsequent conversion to dementia, primarily of the AD subtype, is mainly due to the AD pathway(s).

INTRODUCTION

Aging populations worldwide face an increasing burden of neurodegenerative diseases.[1] Major diseases, in terms of mortality, morbidity and health care costs, include Alzheimer's disease (AD), Parkinson's disease (PD), frontotemporal lobar degeneration (FTLD) and amyotrophic lateral sclerosis (ALS). Cognitive impairment is most prominent in AD[2,3] and FTLD[4], but it is also an important feature of PD[5] and ALS.[6] Our genetic understanding of these neurodegenerative diseases has improved considerably over the past years through large-scale genome-wide association studies that have identified a large number of novel risk variants.[7-12] However, due to the hypothesis-free design of genome-wide association studies, it remains largely unknown how these genetic variants lead to cognitive decline and ultimately clinical disease.

The severe deterioration in cognitive function seen in neurodegenerative diseases is often preceded by a pre-clinical stage with only subtle cognitive deficits that deteriorate over time. Mild cognitive impairment (MCI) describes this intermediate state and is variable in both its clinical presentation and conversion to dementia.[3] Given that MCI provides a window of opportunity for preventive or therapeutic interventions, it is important to uncover risk factors for MCI and factors that lead to conversion of MCI to dementia. The diagnosis of MCI is made on clinical grounds and, although cognitive abilities are highly heritable,[13] the genetic basis of MCI remains largely unknown.[2] APOE, the major risk gene in AD, is known to play a role in MCI,[14] but whether other, recently identified genetic variants for neurodegenerative diseases are also involved has yet to be determined.

In this study, we investigated the effect of genetic risk variants of AD, PD, FTLD and ALS on MCI status and subsequent conversion of MCI to dementia.

METHODS

Setting

The Rotterdam Study is an ongoing population-based cohort study in the Netherlands investigating diseases in the elderly and currently consists of 14 926 residents of Rotterdam who were aged 45 years or more at baseline.[15] The initial cohort was started in 1990 and expanded in 2000 and 2005. The whole population is subject to a set of multidisciplinary examinations every four years. Genotyping was performed in 11 496 participants at study entry. MCI status was assessed only between 2002 and 2005, and was available in 4198 participants. This resulted in a final study population of 3605 non-demented persons with information available on both genome-wide genotyping and MCI status, who were subsequently followed up for the development of dementia until 2012. The Rotterdam Study has been approved by the medical ethics committee according to the Population Study Act Rotterdam Study, executed by the Ministry of Health, Welfare and Sports of the Netherlands. A written informed consent was obtained from all participants.

Genotyping

The Illumina 550K and 550K duo arrays were used for genotyping. We removed samples with call rate below 97.5%, gender mismatch, excess autosomal heterozygosity, duplicates or family relations and ethnic outliers, and variants with call rate below 95.0%, failing missingness test, Hardy–Weinberg equilibrium p-value<10^{-6}, and minor allele frequency<1%. Genotypes were imputed using MACH/minimac software to the 1000 Genomes phase I version 3 reference panel (all population). *APOE*-ε4 genotyping was performed separately using polymerase chain reaction and was available in 3524 (97.8%) participants.[16]

Genetic risk scores

We searched the literature for genetic variants for AD, PD, FTLD and ALS. Given our population-based setting, we focused on sporadic mutations and therefore excluded mutations of familial disease (e.g., PS1, PS2 and APP in AD and PGN in FTLD). Since

various candidate gene studies have been performed that implicated hundreds of variants in these four neurodegenerative diseases, we have tried to minimize false-positives by including only those variants that were genome-wide significant in the largest meta-analysis of that disease. We chose to use this objective threshold and did not base decisions on functional work that potentially corroborated the findings. Notable loci that did not pass this strict threshold were CD33 and ACE. Other variants that were considered but not included were not genotyped nor imputed with sufficient quality (R^2<.5) in our dataset, and a suitable proxy variant was absent: these were typically rare (TREM2, PLD3, GBA) or in the poorly covered HLA-region (AD: rs111418223, PD: rs115736749, rs9275326).

For our analyses we identified 19 variants for AD, 25 variants for PD, 1 variant for FTLD and 2 variants for ALS (Table 1).[7-12,17-19] Since FTLD and ALS are considered extremes of the same disease spectrum, and the FTLD variant is also implicated in ALS, we decided to pool the three variants together for increased power. The variant rs3849943 is tagging the C9orf72 hexanucleotide expansion, which itself was not assessed in our study.[9]

Genetic risk scores were constructed by multiplying the number of risk alleles by their reported odds ratio (after natural logarithm transformation) for the disease, and summing this weighted allele score of each variant up into a disease risk score for AD, PD and FTLD/ALS. Similarly, a combined genetic risk score of all neurodegenerative disease variants was created.

MCI screening

From 2002-2005 onwards, we implemented extensive cognitive testing to allow for screening of MCI. All participants of the three Rotterdam Study sub-cohorts who were alive in 2002-2005 were invited to undergo these tests and assessed for MCI. However, as the third sub-cohort of the Rotterdam Study is comprised of relatively young participants (45 years and over), but still would yield a considerable number of screen-positives for MCI, it was not included in the current study population at risk. MCI was defined as the presence of both subjectively and objectively measured cognitive impairment, in the absence of dementia.[3]

Subjective cognitive impairment was considered present if persons reported complaints on any of three questions on memory (difficulty remembering, forgetting what one had planned to do, and difficulty finding words) or three questions on everyday functioning (difficulty managing finances, problems using a telephone, and difficulty getting dressed). Objective measures of cognitive functioning were neuropsychological tests (Letter-Digit Substitution Task, Stroop test, Verbal Fluency Test, and the 15-Word verbal Learning Test based on Rey's recall of words) that were incorporated into robust compound scores of memory function, information-processing speed, and executive function, as described previously.[20] Scores below 1.5 SD of the age- and education-adjusted means were considered indicative of objective cognitive impairment. MCI was further classified as 'amnestic' in case of an objective memory deficit (irrespective of other domains), or as 'non-amnestic' if only other cognitive domains were affected. The MCI assessment in the Rotterdam Study was previously described in more detail.[21]

Assessment of dementia

Participants were screened for dementia at each of the Rotterdam Study examination rounds and additionally by using information obtained from the general practitioners and regional outpatient care centers (follow-up completed until January 2012).[15] Mini-Mental State Examination (MMSE)[22] and the Geriatric Mental Schedule (GMS)[23] were used to identify high-risk individuals (MMSE<26 or GMS >0) for an additional interview with the Cambridge Examination for Mental Disorders in the Elderly (CAMDEX).[24] When required, further neuropsychological testing and neuroimaging were used by a consensus panel for diagnosis according to established criteria for dementia (Diagnostic and Statistical Manual of Mental Disorders, Third Edition, Revised (DSM-III-R)) and Alzheimer's Disease (National Institute of Neurological and Communicative Diseases and Stroke/Alzheimer's Disease and Related Disorders Association (NINCDS-ADRDA)).[25,26]

Statistical analyses

Genetic risk scores were transformed into z-scores to facilitate comparisons of their effect per standard deviation increase across each score. Logistic regression models were used to examine associations between the risk scores and MCI status. To evaluate

conversion of MCI to dementia and incident dementia in cognitively normal persons separately, Cox proportional hazard models stratified for MCI status were used. Additionally, the effects of individual variants were explored and considered significant after Bonferroni correction for the number of tested variants ($p=0.05/47=0.0011$). Regressions models were adjusted for age and sex, and additionally for vascular risk factors. Furthermore, potential interaction between the genetic risk scores and age-at-onset of MCI and dementia was examined.

To determine diagnostic and predictive accuracy of the genetic risk scores, the area under the receiver operating curve was calculated for a basic model including age and sex, and compared with a model additionally incorporating the genetic risk scores. All analyses were performed with SPSS version 22, IBM.

Table 1 | List of known genetic variants that increase risk of neurodegenerative diseases.

Disease	RS ID	Chr.	Position	Locus	Allele1	Allele2	OR
AD	rs6656401	1	207692049	CR1	A	G	1.18
AD	rs6733839	2	127892810	BIN1	T	C	1.22
AD	rs35349669	2	234068476	INPP5D	T	C	1.08
AD	rs190982	5	88223420	MEF2C	G	A	0.93
AD	rs10948363	6	47487762	CD2AP	G	A	1.10
AD	rs2718058	7	37841534	NME8	G	A	0.93
AD	rs1476679	7	100004446	ZCWPW1	C	T	0.91
AD	rs11771145	7	143110762	EPHA1	A	G	0.90
AD	rs28834970	8	27195121	PTK2B	C	T	1.10
AD	rs9331896	8	27467686	CLU	C	T	0.86
AD	rs10838725	11	47557871	CELF1	C	T	1.08
AD	rs983392	11	59923508	MS4A6A	G	A	0.90
AD	rs10792832	11	85867875	PICALM	A	G	0.87
AD	rs11218343	11	121435587	SORL1	C	T	0.77
AD	rs17125944	14	53400629	FERMT2	C	T	1.14
AD	rs10498633	14	92926952	SLC24A4	T	G	0.91
AD	rs4147929	19	1063443	ABCA7	A	G	1.15
AD	rs429358/rs7412	19	45411941/45412079	APOE	ε4	ε2/3	3.69
AD	rs7274581	20	55018260	CASS4	C	T	0.88
PD	rs114138760	1	154898185	GBA	C	G	1.57
PD	rs35749011	1	155135036	GBA	A	G	1.76
PD	rs823118	1	205723572	RAB7L1	T	C	1.13
PD	rs10797576	1	232664611	SIPA1L2	T	C	1.14
PD	rs6430538	2	135539967	ACMSD	T	C	0.87

Table 1 continued.

PD	rs1474055	2	169110394	STK39	T	C	1.21
PD	rs12637471	3	182762437	MCCC1	A	G	0.84
PD	rs34884217	4	944210	TMEM175	A	C	1.25
PD	rs34311866	4	951947	TMEM175	T	C	0.78
PD	rs11724635	4	15737101	BST1	A	C	1.12
PD	rs6812193	4	77198986	FAM47E	T	C	0.90
PD	rs356182	4	90626111	SNCA	A	G	0.74
PD	rs7681154	4	90763703	SNCA	A	C	0.84
PD	rs199347	7	23293746	GPNMB	A	G	1.12
PD	rs591323	8	16697091	FGF20	A	G	0.92
PD	rs117896735	10	121536327	INPP5F	A	G	1.77
PD	rs329648	11	133765367	MIR4697	T	C	1.10
PD	rs76904798	12	40614434	LRRK2	T	C	1.17
PD	rs11060180	12	123303586	CCDC62	A	G	1.10
PD	rs11158026	14	55348869	GCH1	T	C	0.89
PD	rs2414739	15	61994134	VPS13C	A	G	1.11
PD	rs14235	16	31121793	STX1B	A	G	1.09
PD	rs11868035	17	17715101	SREBF	A	G	0.94
PD	rs12456492	18	40673380	RIT2	A	G	0.91
PD	rs8118008	20	3168166	DDRGK1	A	G	1.11
FTLD	rs1990622	7	12283787	TMEM106B	G	A	0.61
ALS	rs3849943	9	27543382	C9ORF72	C	T	1.17
ALS	rs34517613	17	26610252	SARM1	T	C	0.83

Abbreviations: AD = Alzheimer's disease, ALS = Amyotrophic lateral sclerosis, FTLD = Frontotemporal lobar degeneration, Chr. = Chromosome, MCI = Mild cognitive impairment, OR = Odds ratio, PD = Parkinson's disease, RA = Risk allele.

Table 2 | Study population characteristics.

Characteristic	Total (N=3605)
Demographics	
Age, years	71.9 (7.2)
Females	2057 (58.2%)
Educational level	
Primary education	360 (10.1%)
Lower vocational education	1022 (28.7%)
Lower secondary education	585 (16.4%)
Intermediate vocational education	967 (27.1%)
General secondary education	145 (4.1%)
Higher vocational education	438 (12.3%)
University	49 (1.4%)
Vascular risk factors	
Hypertension	2912 (81.0%)
Diabetes mellitus	529 (14.7%)
Waist circumference, cm	93.6 (11.8)
Total cholesterol, mmol/L	5.61 (0.99)
HDL-cholesterol, mmol/L	1.45 (0.40)
Smoking	
Never	1054 (29.2%)
Former	1998 (55.4%)
Current	553 (15.3%)
Cognition	
Letter-digit substitution task, no. of items/min	27.1 (6.8)
Stroop test (color word interference), s	56.4 (21.0)
Verbal fluency test, no. of animals/min	20.9 (5.1)
15-word verbal learning test, no. of words	6.54 (2.69)
Diagnosis	
MCI	360 (10.0%)
Amnestic	147 (4.1%)
Non-amnestic	213 (5.9%)
Dementia	
Incident cases	191 (5.3%)
Follow-up time, years	6.04 (1.50)

Values are mean (SD) or number (percentage). Missing values are present in educational level (n=39), hypertension (n=9), waist circumference (n=9), and cholesterol levels (n=59).
Abbreviations: MCI = Mild cognitive impairment, HDL = High-density lipoprotein.

RESULTS

Population characteristics

Mean (SD) age was 71.9 (7.2) years and 2057 (57.1%) were women. A total of 360 (10.0%) participants met the criteria for MCI, of whom 147 (4.1%) with amnestic and 213 (5.9%) with non-amnestic MCI. Mean (SD) follow-up was 6.0 (1.5) years, during which 191 persons were diagnosed with dementia (156 with AD). More characteristics can be found in Table 2.

MCI status

The association with MCI status was significant for the genetic risk score of AD (OR=1.15 [1.03 - 1.28]) and suggestive for PD (1.10 [0.99 – 1.23]) and FTLD/ALS (1.09 [0.98 - 1.22]). Investigating subtypes of MCI separately, we found an association with amnestic MCI for the risk score of AD only (1.16 [0.99 - 1.36]) which attenuated after excluding *APOE* from the risk score (1.11 [0.94 - 1.31]). In contrast, risk scores of AD, PD and FTLD/ALS were all associated with the subtype of non-amnestic MCI (see Table 3). The combined risk score for all neurodegenerative diseases was significantly associated with MCI, particularly non-amnestic MCI. Results were similar after adjustment for education and vascular risk factors (see Table S1).

Investigating the objective and subjective complaints that make up the MCI diagnosis revealed that the AD score associated with subjective memory complaints (Table 4). The AD score without *APOE* as well as PD and FTLD/ALS affected objective measures of cognitive complaints, particularly information-processing speed and executive function, although PD also related to problems getting dressed. No significant interactions were detected between the risk scores and age-at-onset of MCI. In single variant analyses, AD risk variant rs6733839 near *BIN1* was associated with MCI after Bonferroni correction (Table S2 for all results).

Conversion to dementia

The risk score for AD, but not for PD and FTLD/ALS, was associated with incident dementia. This association was particularly strong for conversion from MCI (1.59 [1.23 -

2.05]). Exclusion of *APOE* attenuated the association of the AD risk score with incident dementia, remaining only borderline significant among persons without MCI (1.21 [1.02-1.43]). The combined genetic risk score was significantly associated with incident dementia. The associations were similar after additional adjustment for vascular risk factors (see Table S3). There was a significant interaction between the AD genetic risk score and age-at-onset of dementia (p=0.003), which indicated a stronger genetic effect when age at onset was lower.

Among all variants individually, only *APOE* survived multiple testing. Other AD variants that were related to incident dementia were rs983392 (*MS4A6A*), rs10948363 (*CD2AP*) and rs9331896 (*CLU*). Interestingly, rs6733839 (*BIN1*) which was associated with MCI, was not associated with incident dementia. The results of the genetic risk scores are in Table 5 and of single variants in Table S4. Additionally, the AD risk score without *APOE* was examined after stratification for *APOE* ε4 carrier status (Table S5).

Diagnosis and predictive accuracy

The addition of the genetic risk scores to models of age and sex for diagnosing MCI and predicting dementia resulted in small increases of <0.025 of the area under the receiver operating curve (see Table 6).

Table 3 | Associations of genetic risk scores for neurodegenerative diseases with mild cognitive impairment.

Genetic risk score, per SD	OR for MCI	p-value	OR for amnestic MCI	p-value	OR for non-amnestic MCI	p-value
Alzheimer disease	1.15 (1.03 - 1.28)	0.011	1.16 (0.99 - 1.36)	0.062	1.14 (0.99 - 1.31)	0.063
Alzheimer disease without APOE	1.19 (1.07 - 1.33)	0.002	1.11 (0.94 - 1.31)	0.223	1.25 (1.09 - 1.44)	0.002
Parkinson disease	1.10 (0.99 - 1.23)	0.081	1.02 (0.86 - 1.20)	0.830	1.16 (1.01 - 1.33)	0.037
FTLD/ALS	1.09 (0.98 - 1.22)	0.130	0.97 (0.82 - 1.14)	0.680	1.19 (1.03 - 1.37)	0.019
Combined risk score	1.20 (1.08 - 1.34)	0.001	1.13 (0.96 - 1.33)	0.142	1.26 (1.09 - 1.44)	0.001

Values are odds ratios with 95% confidence intervals per SD of genetic risk score, adjusted for age and sex.
Abbreviations: OR = odds ratio, SD = standard deviation, MCI = Mild cognitive impairment, FTLD/ALS = Frontotemporal lobar degeneration/amyotrophic lateral sclerosis.

Table 4 | Associations of genetic risk scores for neurodegenerative diseases with objective and subjective cognitive complaints.

Genetic risk score, per SD	OR (95% CI) for subjective memory complaints			OR (95% CI) for subjective everyday functioning complaints			OR (95% CI) for objective cognitive complaints		
	Difficulty remembering	Forgetting plans	Finding words	Managing finances	Using telephone	Getting dressed	Memory function	Information-processing	Executive function
Alzheimer disease	1.12 (1.05 - 1.20)	1.12 (1.04 - 1.20)	1.09 (1.01 - 1.17)	1.08 (0.96 - 1.21)	0.97 (0.60 - 1.59)	0.93 (0.74 - 1.15)	1.12 (0.98 - 1.28)	1.03 (0.90 - 1.18)	1.07 (0.94 - 1.22)
Alzheimer disease without APOE	1.08 (1.01 - 1.16)	1.05 (0.98 - 1.12)	1.01 (0.94 - 1.09)	1.12 (1.00 - 1.25)	0.86 (0.55 - 1.33)	1.01 (0.83 - 1.24)	1.10 (0.96 - 1.26)	1.22 (1.06 - 1.39)	1.13 (0.98 - 1.29)
Parkinson disease	0.97 (0.91 - 1.04)	1.01 (0.94 - 1.09)	0.97 (0.91 - 1.05)	0.98 (0.87 - 1.10)	0.80 (0.52 - 1.24)	1.32 (1.08 - 1.60)	1.04 (0.91 - 1.20)	1.16 (1.02 - 1.32)	1.11 (0.98 - 1.27)
FTLD/ALS	1.05 (0.98 - 1.12)	1.02 (0.95 - 1.09)	1.03 (0.96 - 1.10)	0.96 (0.85 - 1.07)	0.96 (0.62 - 1.49)	1.07 (0.87 - 1.31)	1.02 (0.89 - 1.17)	1.07 (0.94 - 1.23)	1.11 (0.97 - 1.28)
Combined risk score	1.10 (1.03 - 1.18)	1.11 (1.03 - 1.19)	1.07 (1.00 - 1.15)	1.02 (0.91 - 1.14)	0.88 (0.54 - 1.43)	1.12 (0.91 - 1.36)	1.13 (0.99 - 1.29)	1.13 (0.99 - 1.29)	1.15 (1.01 - 1.32)

Values are odds ratios with 95% confidence intervals per SD of genetic risk score, adjusted for age and sex.

Abbreviations: OR = odds ratio, SD = standard deviation, MCI = Mild cognitive impairment, FTLD/ALS = Frontotemporal lobar degeneration/amyotrophic lateral sclerosis.

Table 5 | Associations of genetic risk scores for neurodegenerative diseases with incident dementia in the total population and stratified by mild cognitive impairment status.

Genetic risk score, per SD	Hazard ratio for conversion to dementia, per SD increase of the genetic risk score (95% confidence interval)					
	Total population (n/N=191/3605)	p	Persons with MCI (n/N=55/360)	p	Cognitively normal persons (n/N=136/3245)	p
Alzheimer disease	1.56 (1.37 - 1.78)	<.001	1.59 (1.23 - 2.05)	<.001	1.53 (1.31 - 1.78)	<.001
Alzheimer disease without APOE	1.15 (1.00 - 1.32)	.058	1.03 (0.79 - 1.34)	.811	1.21 (1.02 - 1.43)	.027
Parkinson disease	0.90 (0.79 - 1.04)	.159	0.95 (0.74 - 1.21)	.669	0.89 (0.75 - 1.05)	.162
FTLD/ALS	0.92 (0.80 - 1.06)	.265	0.86 (0.66 - 1.12)	.264	0.96 (0.81 - 1.14)	.634
Combined risk score	1.34 (1.16 - 1.55)	<.001	1.35 (1.01 - 1.79)	.040	1.33 (1.12 - 1.57)	.001

All analyses are adjusted for age, sex and MCI-status if applicable.

Abbreviations: n=number of persons converting to dementia, N=cohort at risk, MCI = Mild cognitive impairment, FTLD/ALS = Frontotemporal lobar degeneration/amyotrophic lateral sclerosis.

Table 6a | Areas under the curve for diagnosing mild cognitive impairment with genetic risk scores for neurodegenerative diseases.

	Area under the curve for MCI status (95% Confidence interval)		
	All (n/N=360/3605)	Amnestic (n/N=147/3392)	Non-amnestic (n/N=213/3458)
Basic model: age and sex	.578 (.547 - .609)	.577 (.528 - .626)	.603 (.563 - .644)
+ Alzheimer's disease	.588 (.556 - .620)	.592 (.545 - .640)	.614 (.571 - .656)
+ Alzheimer's disease without APOE	.593 (.562 - .625)	.589 (.541 - .636)	.625 (.585 - .665)
+ Parkinson's disease	.582 (.551 - .613)	.577 (.529 - .625)	.612 (.573 - .651)
+ FTLD/ALS	.579 (.547 - .611)	.584 (.536 - .631)	.612 (.571 - .653)
+ Combined risk score	.594 (.562 - .626)	.590 (.543 - .637)	.627 (.585 - .669)

Abbreviations: n=number of persons with MCI, N=cohort at risk,

Table 6b | Areas under the curve for predicting dementia with genetic risk scores for neurodegenerative diseases.

	Area under the curve for conversion to dementia (95% Confidence interval)		
	Total population (n/N=191/3605)	Persons with MCI (n/N=55/360)	Cognitively normal persons (n/N=136/3245)
Basic model: age and sex	.783 (.751 - .815)	.734 (.666 - .802)	.781 (.744 - .818)
+ Alzheimer's disease	.801 (.770 - .833)	.744 (.676 - .813)	.803 (.767 - .838)
+ Alzheimer's disease without APOE	.785 (.752 - .817)	.735 (.667 - .803)	.782 (.745 - .819)
+ Parkinson's disease	.782 (.750 - .814)	.734 (.666 - .802)	.780 (.742 - .817)
+ FTLD/ALS	.785 (.753 - .817)	.743 (.678 - .808)	.782 (.745 - .819)
+ Combined risk score	.791 (.759 - .823)	.733 (.662 - .804)	.792 (.756 - .828)

Abbreviations: n=number of persons converting to dementia, N=cohort at risk, MCI = Mild cognitive impairment, FTLD/ALS = Frontotemporal lobar degeneration/amyotrophic lateral sclerosis.

DISCUSSION

We found in a population-based cohort study that a genetic risk score for AD was associated with amnestic and non-amnestic MCI, whereas genetic risk scores for PD and FTLD/ALS only associated with non-amnestic MCI. Furthermore, only the genetic risk score for AD was associated with incident dementia, which attenuated after exclusion of *APOE*. The diagnostic and predictive accuracy of these risk scores was only modest.

We found that genetic susceptibility to various neurodegenerative diseases associates with MCI. The clinical concept of MCI could therefore reflect an underlying heterogeneity of disease pathways leading to deterioration of cognitive functions. Amnestic MCI, the subtype which increases risk of AD, was associated with *APOE*, but the novel AD risk variants identified through GWAS were related more to the non-amnestic subtype. AD genes might thus influence different cognitive domains, with the common feature of (jointly) increasing risk of AD. The role *APOE* of in Alzheimer's disease is well-documented, and is often used as a model for 'typical' AD: neurodegeneration starting in the medial temporal lobe, giving episodic memory problems, amnestic MCI and then leading to dementia. It is therefore interesting to see that the novel genetic loci are acting differently from *APOE*, and the underlying pathophysiological mechanism(s) might also be different and thus result in this atypical presentation. Studying the novel loci separately and in combination could complement our current knowledge of the pathophysiology, and might eventually even warrant more detailed subtyping of the heterogeneous entity of AD. Non-amnestic MCI was associated with various genetic risk factors of PD and FTLD/ALS, which indicates that further characterization of MCI subgroups might also be appropriate.

Alternatively, these associations could be explained by persons with incipient disease who were classified as having MCI. However, all persons meeting criteria of dementia, including causes of AD, PD and FTLD, were excluded from the analyses with MCI, and a minimal contribution of ALS is expected due to our community-based setting. Unfortunately, family members or caregivers were generally not present during the center visits, and could therefore not be asked about subjective cognitive complaints of the participant. Also, visuospatial functions were not explicitly assessed. However, given

the extensive collection of both interview data and cognitive tests for each participant, it seems unlikely that this would results in a substantial number of undiagnosed MCI cases. Another consideration is that we were unable to assess incident MCI, since MCI screening was only performed at the baseline of our study. However, because genetic variants reflect life-long exposure, reverse causality or unmeasured confounding is highly unlikely.

A potential limitation is that we have not completed follow-up of participants until the end of their lifetimes, which would correspond to an expected 30 years of additional follow-up. Although mean age was already 72 years at baseline, and Cox proportional hazard models took the variation in starting age and follow-up time into account, we further evaluated whether age-at-onset modifies the association of the risk scores, which was true only for the AD risk score including *APOE*. Nonetheless, competing risks are a potential source of bias, and this bias remains even after following persons until the end of their lifetimes.

MCI is often called an intermediate stage, implicitly suggesting that it is merely an earlier form of dementia with more cognitive functions still remaining intact, but this might not be an adequate representation of MCI. Although risk factors between neurodegenerative diseases and MCI overlap, many people with MCI remain stable or can even return to normal.[2,3] In our study, the AD genetic risk score indeed associated with both MCI and incident dementia, but examining the individual risk variants separately suggests that each of these two processes could be driven by different factors; e.g., *BIN1* contributes more to initiating MCI (OR=1.32, p<.001) than to conversion to AD (OR=1.13, p=.31). If validated in other studies, these findings could help prioritize certain AD targets for early intervention. Since only part of the MCI population develops dementia, the heterogeneity of this group could therefore provide an explanation why some genes only predispose to MCI, namely that this factor for example mostly causes a stable MCI subtype. Also, the dementia trajectory spans decades, and even infant changes have recently been implicated.[27] Rather than a single process that is responsible for all dementia pathology across its various stages, different processes might either predispose to, initiate, or propagate cognitive decline. Which process is affected by a gene, and in particular **when** in the dementia trajectory this

process is relevant, might thus be reflected in stronger associations with MCI, that are less prominent later (conversion to dementia), such as with *BIN1*.

We note that the majority of our dementia cases were due to AD. Therefore, we were unable to detect any association of the other genetic risk scores with dementia due to PD or FTLD/ALS. It is possible that separate genetic risk scores increase the risk of disease-specific dementia subtypes only, but this needs to be studied further. An important consideration is that variant rs3849943 is tagging the GGGGCC expansion within open reading frame 72 (C9orf72), which was shown to be responsible for this GWAS signal on chromosome 9.[9] This expansion is present in 4-21% of sporadic ALS cases.[28,29] Phenotypes of neurodegenerative diseases are uncommon when less than 20 expansions are present, and it usually requires more than 50 expansions for ALS cases to develop dementia. Since we were unable to assess the exact number expansions, and given our population-based setting, it is possible that the average number of expansions was low in our current study. Future efforts should therefore investigate this locus in more detail to understand its role in MCI and subsequent conversion to dementia.

Our diagnostic and prediction models incorporating the genetic risk scores resulted in marginal improvement of diagnosing MCI and predicting dementia. This is in line with two previous studies that used a smaller set of variants.[30,31] It has been questioned if a sufficient level of accuracy will ever be achieved for complex diseases, as unraveling their complete causal pathways may be impossible.[32] However, further genetic discoveries in combination with other risk factors might eventually prove the clinical utility of polygenic risk scores, as has been shown for age-related macular degeneration and height.[33,34] Importantly, the genetic variants that are currently known explain only little of the variance in disease risk of AD, PD, FTLD and ALS. Uncovering the "missing heritability" through larger GWAS and the novel focus on rare variants could improve the clinical utility of genetic risk scores. Additionally, the current genetic variants could have a larger effect through gene-gene and gene-environment interaction. Stratification for *APOE* ε4 carrier status showed differences in associations of the various risk scores, but this needs to be explored further. Moreover, non-genetic factors could aid in more accurately diagnosing MCI and predicting dementia by themselves.

In conclusion, MCI is genetically heterogeneous, whereas dementia develops through disease-specific mechanisms. Future research should focus on disentangling different genetic causes of MCI and subsequent conversion to dementia.

REFERENCES

1. Organization WH. Dementia: A public health priority. WHO 2012
2. Winblad , *et al.* J Intern Med. 2004
3. Frank AR, *et al.* Handb Clin Neurol. 2008
4. Strong MJ, *et al.* Annals of neurology. 2003
5. Litvan I, *et al.* Movement disorders. 2011
6. Phukan J, *et al.* The Lancet Neurology. 2007
7. Lambert JC, *et al.* Nat Genet. 2013
8. Van Deerlin VM, *et al.* Nat Genet. 2010
9. Fogh I, *et al.* Hum Mol Genet. 2013
10. Lill CM, *et al.* PLoS Genet. 2012
11. Plagnol V, *et al.* PLoS genetics. 2011
12. Nalls MA, *et al.* Lancet. 2011
13. McClearn GE, *et al.* Science. 1997
14. Cherbuin N, *et al.* Dement Geriatr Cogn Disord. 2007
15. Hofman A, *et al.* Eur J Epidemiol. 2013
16. Ikram MA, *et al.* Biol Psychiatry. 2009
17. Hamza TH, *et al.* Nature genetics. 2010
18. Do CB, *et al.* PLoS genetics. 2011
19. Pankratz N, *et al.* Annals of neurology. 2012
20. Bos D, *et al.* Alzheimers Dement. 2012
21. de Bruijn RFAG, *et al.* Journal of Alzheimer's Disease. 2014
22. Folstein MF, *et al.* J Psychiatr Res. 1975
23. Copeland JR, *et al.* Psychol Med. 1976
24. Roth M, *et al.* Br J Psychiatry. 1986
25. *American psychiatric association: Diagnostic and statistical manual of mental disorders. 3rd rev. Ed.*: Washington, DC, American Psychiatric Association 1987.
26. McKhann G, *et al.* Neurology. 1984
27. Dean DC, *et al.* JAMA neurology. 2014
28. Sabatelli M, *et al.* Neurobiology of aging. 2012
29. Renton AE, *et al.* Neuron. 2011
30. Verhaaren BF, *et al.* Biol Psychiatry. 2013
31. Rodríguez-Rodríguez E, *et al.* Journal of Neural Transmission. 2013
32. Janssens A, *et al.* Human Molecular Genetics. 2008
33. Liu F, *et al.* Human genetics. 2013
34. Buitendijk GHS, *et al.* Ophthalmology. 2013

Chapter 5.2.2

Genetic risk of Parkinson disease in the general population

ABSTRACT

Introduction: We investigated whether a risk score based on genetic risk variants for Parkinson's disease (PD) is associated with the risk and improves prediction of incident PD, and whether the risk score is associated with basic activities of daily living (BADL) in healthy individuals.

Methods: Within the population-based Rotterdam Study, we genotyped 26 independent risk variants for PD and constructed a genetic risk score in 7167 participants who were free of parkinsonism and dementia at baseline (1990 or 2000). Participants were followed for a maximum of twenty years for the onset of parkinsonism, dementia or death until January 1, 2011 (median follow-up 12.1 years). We studied the relationship between the genetic risk score and incident PD with adjustment for age, sex, smoking and parental history. In an independent sample of 2997 persons free of parkinsonism and dementia, we studied whether the PD risk score was associated with BADL.

Results: During follow-up (median 12.1 years), 99 persons were diagnosed with incident PD. The genetic risk score was associated with incident PD (hazard ratio per standard deviation risk 1.25 [95% confidence interval=1.02;1.55]), but did not substantially improve prediction (change in C-statistic 0.687 [0.628; 0.745] to 0.698 [0.635; 0.760], ΔC=0.011 [-0.011;0.033]). The genetic risk score was associated with a higher probability of any impairment in BADL (odds ratio=1.11 [1.00;1.23]).

Conclusion: Genetic variants for PD are associated with the risk of incident PD in the general population and with impairment in daily functioning in individuals without clinical parkinsonism, but do not improve the clinical prediction of PD.

INTRODUCTION

Parkinson's disease (PD) is the second most common neurodegenerative disorder among the elderly.[1] Clinically, the disease is characterized by parkinsonism, an absence of markers suggestive of other causes, and supportive prospective criteria.[2] Clinical PD is preceded by a prodromal phase during which neurodegeneration has already started, but the signs defining parkinsonism are not present.[3] During this period, individuals often experience a combination of early motor and non-motor signs and symptoms that could affect their daily activities, ranging from subtle movement deficits under challenging conditions to autonomic dysfunction, rapid eye movement sleep behavior disorder, and depression.[4]

Several factors are associated with an altered risk of incident PD, such as environmental risk factors (e.g., smoking, exposure to pesticides) and early clinical features (e.g., anosmia, rapid eye movement behavior disorder).[1, 5] However, there is a lack of empirical data on whether these factors can identify a large group of persons at high risk for the disease from the general population. During the last decade, several studies have suggested a substantial genetic contribution to PD, including the identification of risk-increasing mutations in *GBA* and *LRRK2* that are common in PD patient populations,[6, 7] with a large proportion of contributing genes still to be identified.[8] In addition, genome-wide association studies have yielded a total of 28 independent risk variants that are common at a population level, 22 of which are genome-wide significant.[9] Recent case-control studies have shown a risk score based on these variants may contribute to discrimination of PD patients and healthy controls,[10, 11] and average genetic risk may be higher in patients with an early disease age at onset.[12] However, the clinical usefulness of these variants in prospectively predicting PD remains untested. Also, it is unclear whether these risk variants evoke symptoms related to PD in individuals without clinical parkinsonism, leading to subtle problems in daily functioning.

We hypothesized that a genetic risk score based on currently identified risk loci would be a risk factor for incident PD in the general population, and that the genetic risk score would improve prediction of PD. Furthermore, we hypothesized that PD genes affect daily activities in community-dwelling individuals without parkinsonism.

METHODS

Study design and setting

The study was embedded in the Rotterdam Study, a large, prospective, population-based study in the Netherlands.[13, 14] The original study cohort (RS-I) started in 1990 and consisted of 7983 community-dwelling people aged 55 years and older, residing in the suburb Ommoord, Rotterdam. They were re-examined every 4 years, with the last re-examination between 2009 and 2011. In 2000, the cohort was expanded with 3011 people aged 55 years and older (RS-II). The last follow-up examination for this subcohort took place between 2011 and 2012. The study was approved by the Medical Ethics Committee of Erasmus MC University Medical Center Rotterdam, the Netherlands. All participants provided written informed consent to participate in the study.

For PD prediction analyses, all participants in RS-I and RS-II free of parkinsonism and dementia at baseline with available genotype information on 26 risk loci for PD were eligible (n=7705). Of these persons, 7224 were interviewed at baseline on their smoking habits (never, past, current) and parental history of PD. Finally, 51 persons refused to provide informed consent, leaving 7167 participants (93.1%) for PD prediction analyses. We followed participants for a maximum of twenty years for onset of PD from baseline until the first of: onset of parkinsonism, onset of dementia, death or 1 January 2011.

For basic activities of daily living (BADL) analyses, we invited all participants (n=3855) who were still alive, free of parkinsonism as well as free of dementia at the time of the last center visit round of both cohorts (RS-I in 2009-2011 and RS-II in 2011-2012). Of these persons, 3046 (79.0%) agreed to participate and were able to participate. Twenty-five persons were excluded because of unknown smoking status at time of the BADL assessment and another twenty-four persons did not complete their BADL assessment, leaving 2997 persons for BADL analyses.

Genotyping

The Illumina 550K (RSI), 550K duo, and 610 quad (RSII) arrays were used for genotyping. We removed samples with call rate below 97.5%, gender mismatch, excess autosomal

heterozygosity, duplicates or family relations and ethnic outliers, and variants with call rate below 95.0%, failing missingness test, Hardy–Weinberg equilibrium p-value<10^{-6}, and minor allele frequency<1%. Genotypes were imputed using MACH/minimac software to the 1000 Genomes phase I version 3 reference panel (all population).

In the largest genome-wide association study of PD to date, 22 genome-wide significant primary variants, four secondary signals that remained significant in conditional analyses as well as two sub-genome-wide significant, potential risk variants were associated with the risk of disease at genome-wide significance in persons without known mutations in genes associated with mendelian forms of PD.[15] An overview of the of risk alleles as well as their reported effect size for the association with PD is presented in *Supplementary file 1*. Two of these variants were not genotyped in our dataset, nor reliably imputed (R2<.3), and also lacked a proxy variant (rs113579895, MAPT; rs115462410, HLA-DQB1), leaving 26 variants for analysis.

Ascertainment of parkinsonism and PD

At baseline, all participants were screened at the research center for signs of parkinsonism.[16] Individuals who screened positive received a structured clinical workup by a research physician specialized in neurologic disorders to establish parkinsonism. Persons who were suspected of having PD were further evaluated by an experienced neurologist.

During follow-up, we used four overlapping modalities to screen for potential parkinsonism: in-person screening (every 4 years), in-person interviews, use of antiparkinson medication, and clinical monitoring alerts.[17] Of all persons who screened positive in any of these methods, complete medical records were studied and case reports were drawn up covering all potentially relevant information to establish presence and subtype of parkinsonism. These case reports were evaluated by a panel led by an experienced neurologist. PD was only diagnosed after exclusion of parkinsonism associated with preexistent dementia, use of anti-dopaminergic drugs and cerebrovascular disease, multiple system atrophy, progressive supranuclear palsy and in the absence of evidence for other rare causes (e.g., corticobasal degeneration).[16] Persons

who first developed PD and then dementia within 1 year of the diagnosis of PD were also considered PD cases. After initial diagnosis, medical records of all incident parkinsonism cases (both PD and secondary) continued to be scrutinized until the end of the study period for new information that could lead to a revision of the diagnosis.

Ascertainment of dementia

Participants were screened for dementia at baseline and follow-up examinations using a three-step protocol,[18] comprising two brief tests of cognition to screen all subjects and the Cambridge Examination for Mental Disorders of the Elderly in individuals with positive screen results.[19] Additional information was obtained from in-person examination by a neuropsychologist, clinical monitoring and neuro-imaging . A consensus panel, led by a neurologist, decided on the final diagnosis in accordance with standard criteria using the DSM-III-R criteria for dementia.

Basic activities of daily living

Basic activities of daily living (BADL) was assessed based on the disability index from the Stanford Health Assessment Questionnaire, which consisted of 20 items constituting eight components: dressing and grooming, arising, eating, walking, hygiene, grip, reach, and activities.[20] In our study, two out of three items of eating (ability to lift a glass of milk and ability to cut meat) were combined into one. Items were scored from 0 to 3, as follows: 0=without difficulty, 1=with some difficulty, 2=with much difficulty, and 3=unable to. Component scores were calculated as the highest scored item per component.[20] The BADL score was calculated by summing all components, obtaining a score between 0 and 24. We considered scores from 0 to 8 as no to mild disability and from 8 to 24 as moderate to severe disability.[21]

Statistical analysis

We constructed a genetic risk score for each individual, by adding up their number of risk alleles weighted by the log-transformed, reported risk-increasing or risk-decreasing effect size for the association with PD.[9] Risk scores were transformed into z-scores to facilitate evaluation of their effect per standard deviation increase. A higher genetic risk

score corresponds to a larger weighted number of risk alleles and thus a higher risk of PD. We constructed two models: model I comprised age and sex for overall analyses, and only age for sex-stratified analyses. Model II comprised model I plus parental history of PD and smoking (never, past, current), and model III comprised model II plus the genetic risk score.

We investigated the association between the genetic risk score and incident PD by comparing each model using the method proposed by Fine and Gray, which takes into account the risk of competitive events (i.e., incident dementia or death).[22] In subanalyses, we separately added interaction terms between the genetic risk score and age, sex, smoking, and parental history to model III. The discriminative value of both models was expressed with Uno's C-statistic, which takes into account right-censoring.[15] Separately, we repeated the prediction analysis after addition of the *GBA* p.E326K variant to the risk score (its weight was calculated using the previously meta-analysed odds ratio of 1.71).[23] In other sensitivity analyses, we assessed the cross-sectional discriminative value of the risk score by combining prevalent PD cases with complete covariate data (n=68) and incident PD cases and performing logistic regression analyses.

To study the association between the genetic risk score and activities of daily living, we dichotomized BADL scores for having any difficulty in daily functioning or none. Because of the highly skewed distribution of BADL scores in our population,(*Supplementray file 2)* we used a binary logistic regression model to analyze the association of the genetic risk score with any difficulty in BADL, adjusting for age, sex and smoking. We report p-values based on 1000 permutations. In separate subanalyses, we added interaction terms between the genetic risk score and age, sex and smoking to the model. Furthermore, we used multinomial logistic regression models to examine the association of the genetic score with mild and moderate to severe BADL impairment separately. Also, we examined associations between the genetic risk score and impairment on each BADL domain separately using logistic regression models. Finally, we examined the association of each of the 26 single risk variants with any impairment in BADL, adjusting for age, sex, and smoking with a Bonferroni correction for 26 comparisons (p=0.05/26).

Table 1 | Population characteristics

Characteristic	At risk for PD*	BADL examination**
Number of individuals	7167	2,997
Women (%)	4135 (57.7)	1756 (58.6)
Age at baseline, mean, y (SD)	67.3 (8.4)	76.8 (6.6)
Smoking (%)		
Never	2353 (32.8)	1036 (34.6)
Past	3,237 (45.1)	1672 (55.8)
Current	1,580 (22.0)	289 (9.6)
Parental history (%)		
No	6,962 (97.1)	-
1 parent with PD	205 (2.9)	-
2 parents with PD	3 (<0.1)	-

PD, Parkinson's disease; BADL, activities of daily living; y, year; SD, standard deviation.
Smoking status was assessed at baseline for PD risk prediction analyses and during the last center visit for BADL analyses.
**Included in longitudinal association and prediction analyses for Parkinson's disease.*
***Included in cross-sectional association analyses for activities of daily living.*

RESULTS

Characteristics of the study population at risk for PD and the persons examined for daily activities are presented in Table 1. In *Supplementary file 3*, we present population characteristics stratified by incident PD case status. During follow-up (median 12.1 years), 99 (1.4%) individuals suffered from incident PD and 930 (13.0%) from incident dementia, while a total of 3286 (45.8%) persons died.

Table 2 | Prediction of incident Parkinson's disease in the general population

	HR (95% CI)	C-statistic (95% CI)
Model I		0.659 (0.599; 0.720)
Age	1.05 (1.03; 1.07)	
Female	0.66 (0.44; 0.98)	
Model II		0.687 (0.628; 0.745)
Age	1.05 (1.03; 1.07)	
Female	0.48 (0.30; 0.76)	
Smoking (past)	0.57 (0.35; 0.94)	
Smoking (current)	0.36 (0.18; 0.70)	
≥ 1 parent with PD	1.29 (0.40; 4.15)	
Model III		0.698 (0.635; 0.760)
Age	1.05 (1.02; 1.07)	
Female	0.48 (0.30; 0.76)	
Smoking (past)	0.57 (0.35; 0.93)	
Smoking (current)	0.36 (0.19; 0.71)	
≥ 1 parent with PD	1.25 (0.39; 4.03)	
Genetic risk score	1.25 (1.02; 1.55)	

HR, hazard ratio for incident Parkinson's disease per standard deviation increase in risk score. CI, confidence interval. For smoking, the reference category was never.

Table 3 | Genetic risk score and basic activities of daily living

BADL	N (%)	OR (95%CI)	P value
No impairment	461 (15.4)	1.000 (reference)	
Any impairment	2536 (84.6)	1.110 (1.002; 1.230)	0.016
Mild impairment	2017 (67.3)	1.123 (1.013; 1.246)	0.020
Moderate to severe impairment	519 (17.3)	1.020 (0.889; 1.171)	0.768

BADL, basic activities of daily living. N, number of persons. OR, odds ratio. 95%CI, 95% confidence interval.
Odds ratio per standard deviation increase in genetic risk score.
Reference category for both mild and moderate to severe impairment is no impairment.
All analyses were adjusted for age, sex and smoking.

In Table 2, we show that the genetic risk score was independently associated with the onset of PD. There was no significant interaction between the genetic risk score and any of the covariates in the model (p=0.57 for interaction with age; p=0.81 with sex; p=0.59 with smoking, p=0.88 with family history). Adding smoking and parental history to age and sex yielded borderline improvement in the prediction of incident PD (change in C=0.027 [-0.002; 0.056]), while addition of the genetic risk score to age and sex also produced improvement (change in C=0.038 [0.000; 0.076]). As shown in table 2, the genetic risk score did not improve prediction beyond age, sex, smoking and parental history (change in C =0.011 [-0.011; 0.033]). The *GBA* p.E326K variant had a minor allele frequency of 0.021 in our population, and incorporation of this variant in the genetic risk score did not affect its incremental predictive value (change in C = 0.009 [-0.009;0.026]).

The univariate C-statistic of the genetic risk score was 0.56 [0.48; 0.64]. In cross-sectional sensitivity analyses, the genetic risk score yielded a similarly small improvement of C-statistics beyond age, sex, smoking and parental history (C=0.663 to C=0.677).

The genetic risk score was associated with any impairment in BADL (p=0.016). There was no significant interaction of the genetic risk score with age, sex, or smoking (p>0.10 for all interaction terms). As shown in Table 3, the genetic risk score was significantly associated with mild impairment (p=0.020), but not with moderate to severe impairment (p=0.768) in separate analyses. In contrast to the overall BADL-score, the genetic risk score was not associated with any of the eight BADL domains separately (p>0.20 for each domain).

None of the 26 single risk variants was associated with impairment in BADL after Bonferroni correction. Interestingly, risk alleles in three PD loci were nominally borderline associated with any impairment BADL: *GCH1* (rs11158026; p=0.055), *CCDC62* (rs11060180; p=0.058) and *GBA-SYT11* (rs35749011; p=0.054). None of the remaining 23 variants was associated with any impairment in BADL (p>0.10 for each variant).

DISCUSSION

In this large population-based sample with a median of 12 years of follow-up, we found that a genetic risk score for PD based on the most recent set of genome-wide significant variants was associated with a modest but significant increase in the risk of PD. However,

in addition to age, sex, smoking status at baseline and parental history, the genetic risk score hardly improved the prediction of incident PD. In cross-sectional analyses, we further found that the genetic risk score was associated with any and with mild impairment in BADL.

As far as we know, only case–control studies have previously been employed to examine the use of a genetic risk score for PD to discriminate between PD cases and healthy controls.[10-12, 24] These studies showed that a risk score based on these variants may contribute to discrimination of PD patients and healthy controls,[10, 11] and average genetic risk may be higher in patients with an early disease age at onset.[12] In a recent diagnostic case-control study of PD, the univariate C-statistic of a genetic risk score that comprised 30 genetic variants including the 26 used in our study ranged from 0.62 to 0.64,[11] which was slightly higher than in our predictive study (C-statistic=0.56). This relatively small difference may be explained by the difference in study design: in case-control studies, controls are recruited with strict criteria that ensure maximal distinction from PD cases, whereas participants in prospective, population-based studies such as the Rotterdam Study are included irrespective of PD risk. The advantage of prospective population-based studies is that all participants were included and followed up using the same methodology, and following up persons in the general population presumably ensured a realistic estimate of the risk of incident PD. Several limitations of our study should be noted, however. We lacked histologic confirmation on PD diagnosis, suggesting that misclassification of PD cases occurred. The detailed in-person and clinical information on the presence and possible causes of parkinsonism throughout the study period make it unlikely that the misclassification was differential. Still, non-differential misclassification may underestimate the predictive ability of the genetic risk score for histologically confirmed PD. Also, part of the RS-I cohort used for prediction of PD was also among the discovery cohorts of the PD genes: the overlap comprised 44 incident PD cases (0.3%) and 5609 controls (5.9%).[9] We believe that it is unlikely that this small proportion of overlap influenced our findings. In addition, current effect estimates were based on a GWAS of PD cases across various Caucasian populations. It is possible that other variants have larger effects in the Dutch population than the published tagging SNPs. Including these population-specific variants in the risk score could

improve power. Furthermore, we were probably underpowered to a small improvement in PD prediction and, similarly, to detect interaction of the genetic risk score with traditional risk factors and parental history. In addition, we could only assess the predictive value of the risk score for incident PD in persons aged 55 years and older. Since high polygenic risk is associated with a lower age of onset of PD,[12] this probably led to a slight underestimate of the predictive value of the genetic risk score, considering the relatively small proportion of PD patients aged younger than 55 at a population level.[1]

The main motivation for learning how to predict PD is to identify PD patients as early as possible. At this time, although neuroprotective agents with sustainable effects remain elusive, PD manifestations can often be treated or delayed effectively, and surveillance could allow early symptomatic treatments, perhaps with long-term benefits on quality of life.[25, 26] As the pathological processes of PD advance, early clinical features become increasingly more prevalent in prediagnostic PD patients than in controls,[27] and discrimination of clinical PD patients and healthy controls can be accurately established (as reflected by high C-statistics) using just one early feature (impaired olfaction).[11] However, during the early pathological phase of PD, clinical differences between prediagnostic PD patients and controls are generally not yet overt, and discrimination between these groups is less accurate, as reflected by lower C-statistics. Early prediction is therefore based on basic demographics (e.g., age, sex, family history) and environmental risk factors (e.g., smoking, exposure to pesticides). The discriminative value of demographics is remarkably similar for long-term prediction (as in our study) and clinical diagnosis of PD as in diagnostic studies,[10, 11] with integrative demographic C-statistics typically ranging from 0.60 to 0.70. Smoking was previously included in a diagnostic model for PD,[10] but contributed insufficient independent information to be included in a recent integrative diagnostic algorithm for PD.[11] The latter was surprising for two reasons. First, smoking is common at a population level, and current smoking in particular is strongly inversely associated with PD in case-controls studies.[28] Second, PD patients who smoke are able to quit smoking more easily than controls,[29] making the discriminative value of smoking even higher for PD diagnosis than for PD prediction.

Over the past few years, genetic risk scores have been shown to be of marginal value in prediction of diseases with strong preexistent demographic and clinical factor-based predictive models.[30, 31] However, they have enabled improvement in prediction of diseases without such models,[32, 33] and in a recent diagnostic study of Alzheimer's disease, genetic risk scores based on GWAS variants and *APOE* variants improved diagnostic accuracy beyond age and sex.[34] In this study of more than 7000 individuals, we showed that addition of a genetic risk score for PD did not improve prediction beyond age, sex, smoking and parental history. Thus, our findings do not support a role for routine PD risk allele genotyping in a clinical setting at this time. This is similar to our previous observation of that genetic risk variants had limited predictive value for Alzheimer's disease and all-cause dementia.[35, 36] As more PD risk variants become known, however, their incorporation into the genetic risk score may explain more of the heritability that was first implied by familial aggregation of PD,[37] and is now estimated to be 0.27.[8] A recent meta-analysis showed that mild to severe GBA mutations are more common in PD populations than in controls.[6] For the carriers of the severe *GBA* mutations, it has been suggested that the high increase in risk of PD (OR 14.6 – 19.3) may warrant a closer clinical follow-up,[6] similar to carriers of the G2019S mutation in the *LRRK2* gene.[38] However, the predictive value of such rare variants at a population level remains undetermined, and we note that the current genetic risk score did not include the G2019S mutation in *LRKK2* and only focused on the p.E326K variant in *GBA*.

To our knowledge, this is the first study to investigate the relationship of a genetic risk score for PD with daily activities in the general population. The genetic risk score was associated with any impairment in BADL, suggesting that alleles with an established association with PD may also affect prodromal phenotypes linked with PD in the general PD-free population. Interestingly, we observed a clear association of the genetic risk score with mild impairment in BADL, but not with moderate to severe impairment. We offer two possible explanations for this observation. First, since we excluded individuals with parkinsonism and dementia from our analyses, the majority of persons with moderate to severe impairment probably comprised individuals with common, non-neurodegenerative diseases (e.g., locomotor diseases, COPD [39]). We note that we are unaware of substantial genetic overlap with PD for these diseases or of empirical

evidence for antagonistic pleiotropic effects of PD risk variants on BADL.. Second, we studied risk variants that are relatively common in the general population, and these variants may affect BADL more subtly than rarer risk variants with larger effect sizes on the risk of PD.

In conclusion, in this study in the general population, a genetic risk score based on 26 independent risk variants was associated with a higher risk of incident PD and a larger probability of impairment in BADL, but did not result in a substantially better prediction of PD beyond age, sex, smoking and parental history. Our results suggest that the use of this weighted combination of known risk loci is not yet as useful for the prediction of the risk of PD as it is for further elucidating the etiology of the disease. However, we were probably underpowered to detect a small improvement in PD prediction.

REFERENCES

1. de Lau LM, *et al.* Lancet Neurol. 2006
2. Lees AJ, *et al.* Lancet. 2009
3. Berg D, *et al.* Mov Disord. 2014
4. Berg D, *et al.* Lancet Neurol. 2013
5. Noyce AJ, *et al.* J Neurol Neurosurg Psychiatry. 2016
6. Gan-Or Z, *et al.* Neurology. 2015
7. Healy DG, *et al.* Lancet Neurol. 2008
8. Keller MF, *et al.* Hum Mol Genet. 2012
9. Nalls MA, *et al.* Nat Genet. 2014
10. Hall TO, *et al.* Genet Med. 2013
11. Nalls, *et al.* Lancet Neurol. 2015
12. Escott-Price V, *et al.* Ann Neurol. 2015
13. Hofman A, *et al.* Eur J Epidemiol. 1991
14. Hofman A, *et al.* Eur J Epidemiol. 2015
15. Uno H, *et al.* Statistics in Medicine. 2011
16. de Rijk MC, *et al.* Neurology. 1995
17. de Lau LM, *et al.* Neurology. 2004
18. Schrijvers EM, *et al.* Neurology. 2012
19. Roth M, *et al.* Br J Psychiatry. 1986
20. Fries JF, *et al.* J Rheumatol. 1982
21. Bruce B, *et al.* Health Qual Life Outcomes. 2003
22. Fine JP, *et al.* Journal of the American Statistical Association. 1999
23. Pankratz N, *et al.* Ann Neurol. 2012
24. Do CB, *et al.* PLoS Genet. 2011
25. Connolly BS, *et al.* JAMA. 2014
26. Castrioto A, *et al.* Lancet Neurol. 2014
27. Schrag A, *et al.* Lancet Neurol. 2015
28. Noyce AJ, *et al.* Ann Neurol. 2012
29. Ritz B, *et al.* Neurology. 2014
30. Meigs JB, *et al.* N Engl J Med. 2008
31. Paynter NP, *et al.* JAMA. 2010
32. Chen H, *et al.* PLoS One. 2011
33. Hageman GS, *et al.* Hum Genomics. 2011
34. Escott-Price V, *et al.* Brain. 2015
35. Verhaaren BF, *et al.* Biol Psychiatry. 2013
36. Adams HH, *et al.* Alzheimers Dement. 2015
37. Sveinbjornsdottir S, *et al.* N Engl J Med. 2000
38. Giladi N, *et al.* J Neurol Sci. 2011
39. Odding E, *et al.* Eur J Epidemiol. 2001

Chapter 6

General discussion

ABSTRACT

In this thesis I used genetics and neuroimaging to study complex neurological diseases. This chapter places the main findings into context and also includes a discussion of methodological considerations and clinical implications. I conclude by describing strategies for future research, also looking beyond neurodegenerative and cerebrovascular diseases.

GENETIC DISCOVERIES

Genetics play an important role in many neurological diseases.[1-4] Understanding which genetic factors are relevant for a particular disease can yield insight into the pathophysiology and potentially lead to novel therapies. Furthermore, it can improve diagnosis and prediction by removing part of the uncertainty of who has or will develop a disease. Genome-wide association studies (GWAS) in tens of thousands of individuals have identified hundreds of genetic risk variants for neurodegenerative and cerebrovascular diseases,[5-11] but the amount of variance in disease susceptibility that is explained by these variants is relatively small. The remaining unexplained variance is also called 'missing heritability',[12] and we aimed to uncover part of it in chapter 3 using an imaging genetics approach.

We studied the genetic determinants of imaging markers that are important for diseases. In contrast to dichotomous clinical diagnoses of healthy versus diseased, quantitative biomarkers obtained from imaging can classify individuals in a continuous and biologically more plausible manner (see Figure 1). These biomarkers take into account residual variation within groups of persons that are classified as healthy or diseased, thereby also capturing differences in *severity* of disease. Such information is lost by dichotomization, making continuous phenotypes statistically more powerful for detecting (genetic) effects. Furthermore, genetic effects on biomarkers might be larger, and thus easier to detect, compared to the effect sizes observed for neurological diseases: the multifactorial nature of most brain diseases means that there is heterogeneity in the underlying causes. Biomarkers that isolate specific disease processes would reduce the noise from other causes, assuming that this component is indeed genetically more homogeneous. Naturally, this raises the question: Which neuroimaging phenotypes should be used as biomarkers for which diseases?

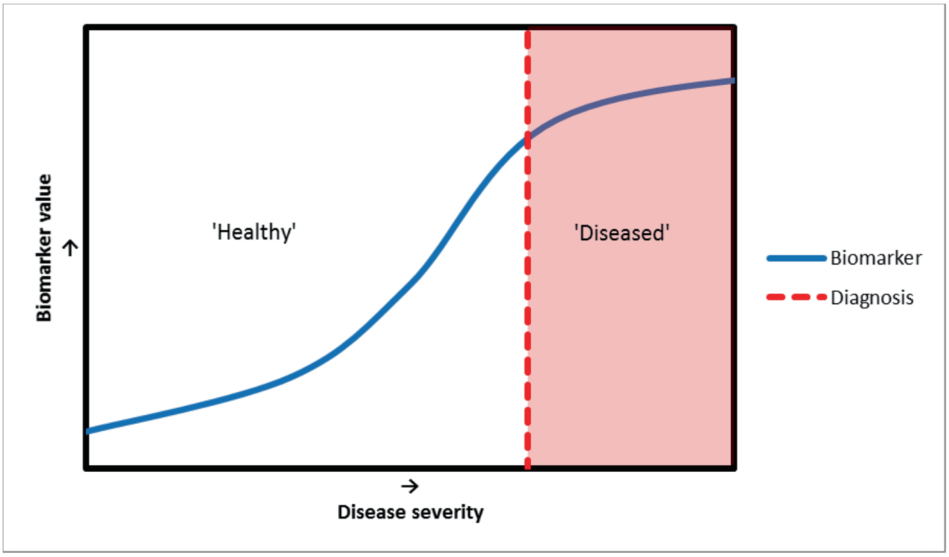

Figure 1 | The value of biomarkers beyond clinical diagnosis.

Plot illustrating the relation between biomarker values, disease severity, and clinical diagnosis. The blue line depicts values of a hypothetical biomarker in relation to disease severity. The red line indicates the point at which a sufficient amount of damage due to the disease leads to the clinical diagnosis. While labelling persons as 'healthy' or 'diseased' can successfully separate the most severe cases from those with less severe disease, the biomarker values provide additional information on the actual placement of an individual within the spectrum of

One criterion on which to select neuroimaging phenotypes is that they should capture part of the disease process. To this end, studies are necessary to determine their associations with diseases, with longitudinal studies being in the unique position to investigate disease as it develops. An informative marker has added value beyond the clinical diagnosis, and it should be noted that any link need not be causal: as long as the biomarker classifies individuals in a more meaningful way than 'healthy' versus 'diseased' it does not matter whether it is a causally related risk factor, a consequence of disease, or even a confounded association. The only prerequisite for identifying disease genes is that the underlying genetic determinants are shared between the biomarker and disease of interest (see section 6.4 about genetic correlation). Structural imaging markers have been widely investigated in relation to clinical outcomes and are the focus of chapter 3.1. Partly motivated by the high heritability, initial GWAS on these structural phenotypes have focused on intracranial volume,[13,14] a marker of brain reserve,[15] and the volumes of various subcortical structures,[14,16,17] which have been related to

neurodegenerative and psychiatric diseases.[18-20] The paucity of large-scale neuroimaging studies, however, has made current efforts underpowered. So far only 9 variants have been identified for these structural phenotypes and they fail to explain a substantial amount of the phenotypic variance. We found 33 additional loci for these and several novel traits, including the first genome-wide variants for the size of the brainstem, amygdala, pallidum, accumbens, and the anterior commissure. Furthermore, the additional loci identified for some phenotypes begin to highlight certain pathways. For intracranial volume, for example, we found that there is an enrichment for variants near genes involved in growth pathways. The most prominent was PI3K-AKT signaling: it is related to brain overgrowth disorders[21,22], with *AKT3* deletions causing microcephaly syndromes[23] and *AKT3* duplications cause macrocephaly.[24] Our results show that the effect of these genes is not restricted to persons who have severe syndromes, but also is of importance for determining brain size in the general population.

Besides genes implicated in human disease our GWAS are also informative for more fundamental biological research on brain development. We noted a striking overlap between studies of the anterior commissure in model organisms and the first investigation of genes influencing the human anterior commissure in chapter 3.3.1. Mouse and fruit fly experiments pointed to several gene families that are important for the development of commissural tracts and we now find genetic associations either within or very close to such genes: the Semaphorin *SEMA6A* and the Ephrin *EPHA3* loci are the two most significant loci in our anterior commissure GWAS, and they both belong to these major families of commissural genes. It is difficult to do experimental studies in humans that capture the complexity of the intricate network of commissural neurons, and approaches that capture part of this process (e.g., migration during development) are often not feasible for high-throughput. Our *in vivo* genetic analyses have now identified reliable candidate genes for further experimental studies to understand their exact function in interhemispheric communication.

Neuroimaging can also measure the extent of cerebrovascular disease, which is covered by chapter 3.2, and includes prominent imaging markers of small vessel disease, intracranial atherosclerosis, and cerebral blood flow.[25,26] Stroke patients typically have

subclinical cerebrovascular disease that can already be detected on MRI before a clinical event takes place.[27-29] In vascular dementia, imaging markers of cerebrovascular disease are part of the diagnostic criteria,[30] and their relevance for other types of dementia is increasingly being appreciated.[31,32] For intracranial carotid artery calcification, we reported the first GWAS and identified two significant loci, of which one was replicated in a sample of clinical stroke patients. GWAS have already identified 5 variants for white matter hyperintensities,[33] while efforts have been unsuccessful for brain infarcts,[34] and not yet undertaken for other markers of cerebrovascular disease. For enlarged perivascular spaces, such studies are complicated by the fact that heterogeneous methods exist for their assessment. In chapters 2.1 and 2.2 I described a reliable rating protocol for enlarged perivascular spaces to enable collaborative studies on these markers. These steps are the groundwork for facilitating multi-site genetic studies of such imaging markers, which will hopefully yield more insight into cerebrovascular disease in coming years.

Additionally, gene discovery is contingent on the imaging marker itself being genetically determined. Heritability studies can inform on the relative contribution of genes to the observed variation between individuals. Traditionally, such studies were done in families, but recently developed methods now also make this possible in samples of unrelated individuals.[35,36] In chapter 3 I report the first heritability studies for both established and emerging imaging markers and found that they have a considerable genetic component using studies of both related and unrelated individuals. We found most investigated imaging markers to be suitable for genetic studies. The volumes of subcortical brain structures and in particular the brainstem were highly heritable, and this was also the case for some of the vertex-wise and voxel-wise measures of subcortical grey matter structures. Other imaging markers also showed substantial heritability: the amount of intracranial carotid artery atherosclerosis, size of the anterior commissure, and certain gait parameters. How does this further our understanding of these traits? Here too it is good not to dichotomize traits into 'heritable' versus 'not heritable' since the degree of heritability varies a lot. The heritability analysis of the shape of subcortical structures in chapter 3.3.3 showed regions within the same structure with both high and low heritability. Partly this could be explained by the fact that some measures contain

more measurement error than others. However, even when focusing on those measures that were very reproducible there exists a large variation in heritability. This indicates that the influence of genes on brain structure really does vary and some regions of the brain are more determined by environmental factors. Depending on which regions are the most relevant for neurological diseases, research can refocus on either genetic or environmental risk factors. Another conceptual advance is illustrated by chapter 3.3.2: while some gait domains initially showed a quite promising heritability, we found that this was mainly driven by genes underlying height and weight. So although there are clinical correlates of these gait domains beyond height and weight, subsequent genetic studies do not seem promising for revealing novel associations besides those identified for these two anthropometric traits. Especially given the large sample sizes for height and weight GWAS,[37,38] it is unlikely that scarcely collected gait data could ever provide a meaningful contribution.

So far, the largest GWAS discovery sample of a neuroimaging marker comprised 13,171 individuals,[17] only 5% of the GWAS of height, another quantitative trait for which 697 variants were identified in a study of 253,288 individuals.[38] To work toward similar successes in imaging genetics, we undertook larger studies. In chapter 3, I describe GWAS of intracranial volume, hippocampal volume, and other subcortical brain structures in the largest discovery samples to date, identifying 33 novel genetic variants in 16,000-37,000 individuals. Similarly, for cerebrovascular disease markers we identified the first genome-wide significant variants for the amount of intracranial carotid artery atherosclerosis. We also studied, for the first time, emerging markers such as the anterior commissure and gait parameters. In total, we were able to report 42 significant novel associations for the various markers in chapter 3. Some of the identified variants were indeed related to clinical outcomes. Perhaps the best illustration of the biomarker approach comes from chapter 3.3.1, where I described a GWAS of the anterior commissure. Here, we were able to detect a strong association of genetic variants near the gene *TMEM106B* with the size of the anterior commissure. This particular gene was previously identified to increase the risk of frontotemporal lobar degeneration in a sample of 567 cases and 3,380 controls ($p = 2.7 \times 10^{-9}$). In the GWAS of the anterior commissure, however, we achieved a more significant signal in a smaller sample of the

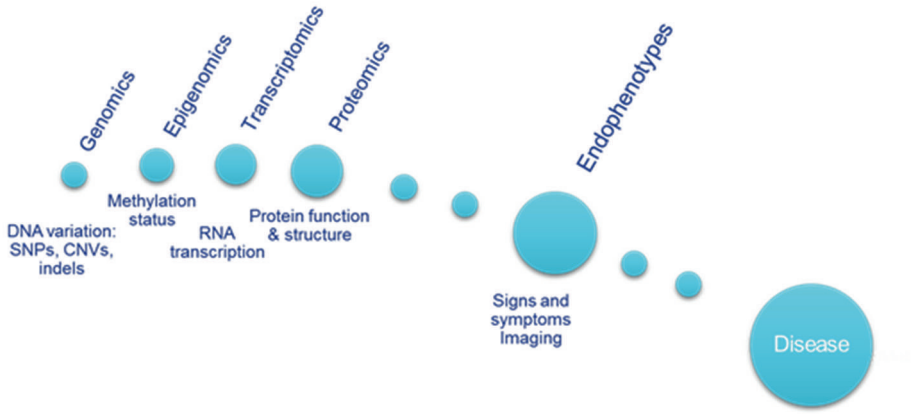

Figure 2 | From gene to disease: understanding the pathophysiological mechanism.
Schematic overview of DNA variation eventually causing clinical disease. The pathophysiological mechanism could lead to various subcellular effects such as altered methylation, gene expression, or protein function. This can in turn affect measurable endophenotypes, including neuroimaging markers.
Abbreviations: CNV = copy number variation, SNP = single nucleotide polymorphism

older cohorts (3,015 individuals; $p = 3.8 \times 10^{-11}$). In some way this can be seen as an intentional form of sampling bias: the associations in these older individuals are not representative of the general population. This approach is helpful when the goal is enrich for associations of a disease processes that occur in a certain population, but not if the goal is external validity.

While bigger may be better, another worthwhile approach is further refinement of the neuroimaging phenotype. For total brain volume, no genetic variants could be detected using sample sizes of almost 10,000 individuals.[13] While larger studies might indeed uncover some of its genetic determinants, it remains a rather crude phenotype that aggregates the entire brain into a single measure. Studying the volume of the hippocampus already gives better results, but also this is a crude phenotype. In chapter 2.4, we illustrated how further refinement of the hippocampal structure at a voxel-wise level can yield a stronger association. This chapter was aimed at solving the methodological problems that currently obstruct us from performing an actual genome-wide and brain-wide search for association signals.

UNDERSTANDING PATHOPHYSIOLOGY

Another avenue for combining neuroimaging and genetics is by exploring the effects of known disease genes on the changes that occur in the brain. While GWAS have identified genetic variants for disease, there is still a long way from genetic association to pathophysiological mechanism (see Figure 2). These variants have in common that they confer risk for a particular disease, but the pathophysiological mechanism is not necessarily the same. For complex diseases in particular, this potentially opens up research to several different pathways. Imaging genetics can shed light on which specific pathways are actually involved by studying known genetic variants for a disease in relation to the relevant imaging markers of that disease.

Since genetic variants primarily exert subcellular effects, a lot of efforts in recent years aimed to systematically map these: expression quantitative trait loci, predicted damaging effects on protein structure, and epigenetic modifications are among many characteristics that can inform on the potential functionality of genetic variants.[39-44] But these subcellular effects eventually translate into clinical disease by affecting the brain, and determining the type of changes can improve our understanding of the disease mechanism. Similar to the previous question on genetic discoveries, here too the question arises: which phenotypes to use?

One approach is to have the selection of phenotypes guided by prior knowledge of the presumed pathophysiological mechanism through which the gene leads to disease. Chapter 4.1 considered genetic disease variants in relation to such candidate phenotypes: Alzheimer's disease variants and several key vascular and degenerative markers (chapter 4.1.1), intracranial aneurysm variants and the presence and size of aneurysms (chapter 4.1.2), and the dystrophin gene and cognitive function (chapter 4.1.3). For example, when investigating the genetic variants for the occurrence symptomatic aneurysms in a sample from the general population, we found that these variants were associated with the size of the aneurysms rather than their presence per se. This was an interesting finding that suggested that these genetic variants for clinically relevant aneurysms were perhaps not leading to persons developing an aneurysm, but increasing the size of an existing aneurysm and thus risk of rupture.

Another approach to understand pathophysiology is to be unbiased towards certain hypotheses, to prevent any confirmation bias by only selecting phenotypes supporting prior beliefs, as is done in chapter 4.2. These studies can still be in line with patterns that would be expected *a priori*, such as the effects of risk variants for frontotemporal lobar degeneration being mainly on frontal and temporal brain regions (chapters 4.2.2 and 4.2.3), but they could also point to regions not implicated before as with brain-wide studies of Alzheimer's disease variants (chapter 4.2.1).

Another critical question in study design is which study population to use. The study of patients may be obvious, but is the effect of 'disease genes' really restricted to patients? One finding suggesting otherwise is that most of the risk variants are common in the general population, with minor allele frequencies between 1-50%.[5-11,13] Although it is possible that common risk variants only cause disease in a subset of carriers, e.g. because they exert an effect only in combination with other risk factors, there is also an alternative explanation: patients with a clinical diagnosis of disease are at the extreme end of a continuous spectrum, with non-diseased carriers of the risk variants showing less severe phenotypes. Knowledge on which of these explanations applies to risk variants can further our understanding of what causes disease. The studies in chapter 4 were all done in the general population to test this hypothesis. For variants of nearly all diseases we indeed found effects outside patient populations: Alzheimer's disease, intracranial aneurysms, frontotemporal lobar degeneration, Parkinson's disease, and amyotrophic lateral sclerosis. Only for multiple sclerosis (chapter 4.2.4) the effect of risk variants was not as apparent. In the field of psychiatry, research has been conflicting with regard to the effects of schizophrenia risk variants on structural brain changes in the general population.[45-47] However, while GWAS are generally done in a collaborative setting and include a replication stage, this is rarely a requirement for such follow up studies on potential pathophysiological mechanisms. For many of these findings, formal replication of the results could provide stronger evidence for the suspected role of disease variants in the general population.

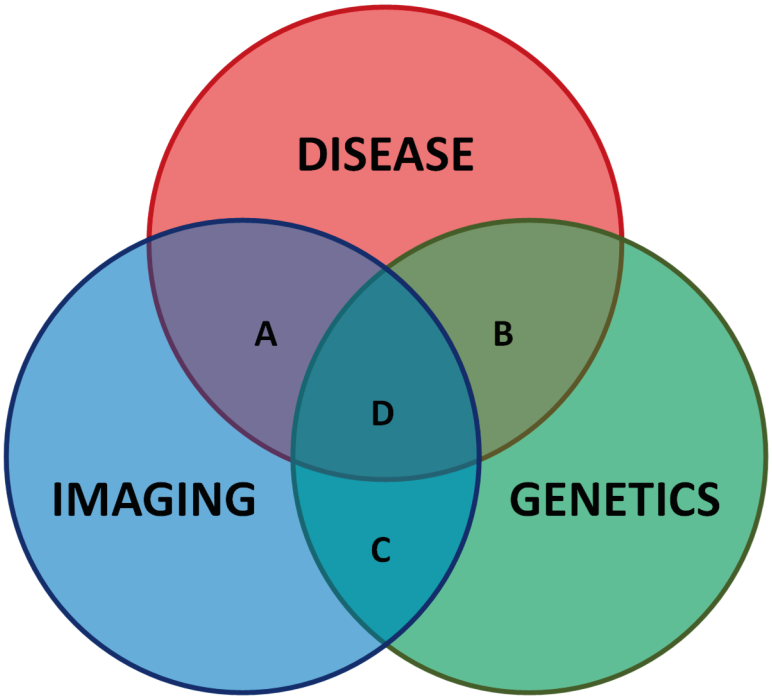

Figure 3 | Shared variance between neuroimaging, genetics, and disease susceptibility.

*Venn diagram of the variance in imaging, genetics, and disease, and their interrelations. The intersections (formally denoted by ∩) indicate shared variance between imaging and disease (**A**), genetics and disease (**B**), imaging and genetics (**C**), and variance that is common across all three traits (**D**).*

EXPLORING CLINICAL RELEVANCE

Besides genetic discoveries and understanding pathophysiology, imaging genetics ideally results in clinical translation. While insight into pathophysiology might reveal drug targets, such translations typically take decades before a treatment is actually implemented.[48] However, clinical utility does not only incorporate treatment, but also covers diagnosis and prediction. For this purpose, it is important to consider the variance observed in imaging, genetics, and disease (see Figure 3). Each of these three traits shows differences between individuals, corresponding to brain differences measurable on imaging, carrier status of genetic variants, or whether someone is diseased or not. The non-overlapping parts in Figure 3 consist of variance that is

restricted to one of these three traits. This includes both variance that is biologically unrelated to the other traits as well as measurement error (e.g. noise in image acquisition, genotyping errors, or misclassification of disease status). However, part of the variance is shared and can be leveraged to derive clinical value, forming the basis of chapter 5.

The intersection of imaging and disease, i.e. the shared variance between the two, is denoted by the letter A in Figure 3 (i.e., including D). This is part of the variance captured by imaging that is informative for disease. Given that many imaging markers are novel, their clinical relevance is yet unclear. In chapter 5.1, I determined clinical correlates of a variety of novel imaging markers. For enlarged perivascular spaces, there were associations with cardiovascular risk factors and cerebrovascular disease (chapter 5.1.1 and chapter 5.1.2). The number of enlarged perivascular spaces in the basal ganglia, for example, were related to hypertension beyond other risk factors or markers of cerebrovascular disease, suggesting that this might be a complementarily imaging marker for disease prediction. Similarly, intersection B represents the genetic variants that are associated with disease. Their clinical relevance was explored in chapter 5.2, specifically to determine whether these variants can improve individual prediction of symptoms and diseases. Genetic risk factors of four neurodegenerative diseases were related to mild cognitive impairment and incident dementia (chapter 5.2.1), and genetic risk of Parkinson's disease was related to basic activities of daily living and incident Parkinson's disease (chapter 5.1.2). However, the added predictive value of these genetic variants was low, in line with findings from recent studies.[49,50] This indicates that the currently identified variants for these neurodegenerative diseases do not yet have enough explanatory power to provide meaningful discrimination between individual who will develop disease versus those who will not.

FUTURE RESEARCH

In this section I describe future directions for research that I consider to have potential to move the field further forward beyond the work performed in my thesis.

For genetic discoveries, the most obvious approach is to **increase the sample size for discovery**. This has been successful for other complex traits,[11,37,38,51,52] and there is little doubt that this will also improve the power in genetic studies of imaging markers. The research I have presented in this thesis used data from the Cohorts for Heart and Aging Research in Genomic Epidemiology (CHARGE)[53] and Enhancing NeuroImaging Genetics through Meta-Analysis (ENIGMA)[54] consortia. These global collaborations incorporate the vast majority of studies with both neuroimaging and genetic data available. The research in chapter 3.1 shows that the current maximal sample size that can be attained is at most 35,000 individuals, which includes those of non-European descent. Large biobanks have been initiated in past years,[55,56] and the first batches of data have already become available for analysis.[57-62] Biobanks are likely to receive a prominent role in genetic discoveries within the coming years, and it is therefore imperative that their limitations are also acknowledged, such as potential bias in such large-scale data collection. For the UK Biobank, for example, 9.2 million persons were invited to participate, whereas only slightly over 5% were actually recruited.[63] From an epidemiological perspective this low participation rate is worrying because it has the potential to induce non-response bias and further complicate the generalizability of the obtained results. Replication of results across different population can alleviate those concerns, but will be increasingly difficult for effects that have been detected by pooling all available data together.

Statistical power can also be improved in ways other than adding more samples. One such approach is by **reducing the measurement error in both genetics and imaging**. The haplotype reference consortium has pooled together 65,000 human haplotypes to create a reference panel to which genotypes with minor allele frequencies as low as 0.1% can still be reliably imputed.[64] Advances in DNA sequencing and reductions in the associated costs also pave the way for obtaining whole genomes sequences.[65] This will enable the identification of the causal variants instead of tagging variants, where the

association signal is diluted. Similarly, imaging markers contain noise that is due to the equipment or subsequent image processing. While ultra-high field strength MRI scanners can provide more detail of the brain,[66-69] it also comes with drawbacks for participants in the form of longer scanning times and dizziness.[70] Furthermore, a large amount of data has already been acquired in the past decades and improved image processing can also reduce measurement error. In case persons have been scanned more than once, the additional images can be taken along to reduce the noise in the first image using longitudinal image processing techniques.[71-74] These techniques are employed to study changes in the brain in a longitudinal setting,[75-79] but they have not been applied to generate cross-sectional measures where the noise has been reduced and which are subsequently analyzed on their own. In a preliminary analysis within the Rotterdam Study of over 2000 individuals who have been scanned twice, I calculated the volume of the left hippocampus using two methods (Figure 4): extracting the hippocampus from each scan separately ('cross') for time point 1 (TP1) and time point 2 (TP2), or by extracting the hippocampus using a longitudinal image processing pipeline ('long'). Next, I determined which part of the variance in hippocampal volume is determined by genetics. For the cross-sectional measures of hippocampal volume the heritability was comparable for both time points at slight more than 30%. Intriguingly, the heritability was almost 55% when information from the other scan was taken along when determining the hippocampal volume. Since this analysis was done in the same set of individuals and scans, it suggests that the longitudinal processing helps extract true biological variance in hippocampal volume. Studies that have multiple scans available could thus boost power for genetic discoveries by using data from another time point. However, the advantages and disadvantages of such an approach needs to be carefully studied before large-scale application. While it might be reasonably argued that measurement error is random, recent research has suggested that, for example, the amount of head motion during resting state functional MRI is also heritable.[80] If image processing algorithms are affected by the presence of motion this will result in a differential misclassification, a form of information bias. Such factors resulting in measurement error are not specifically considered in imaging genetics studies (and to a

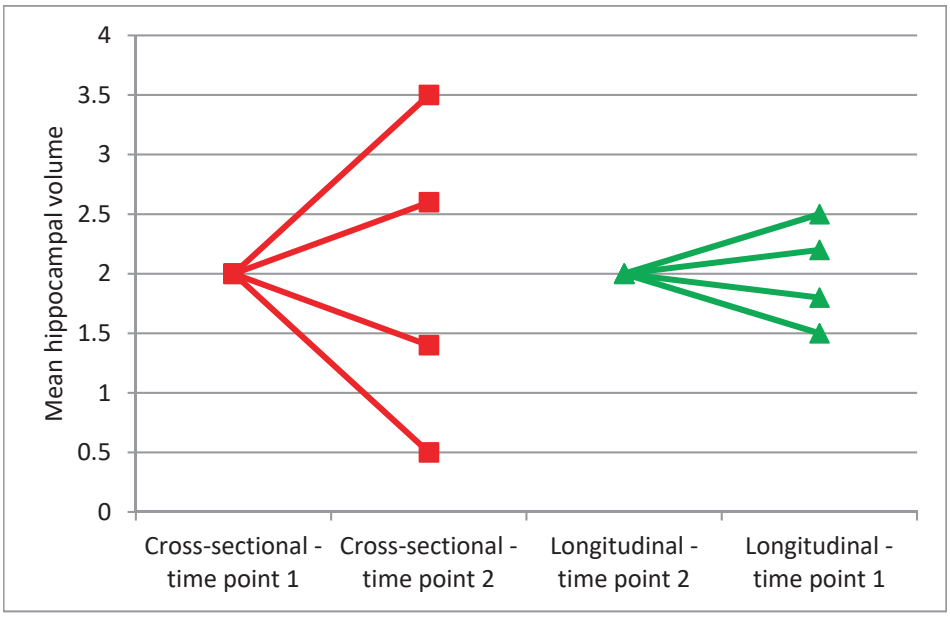

Heritability	33.5%	31.1%	54.6%	54.7%
P-value	0.02	0.03	0.0004	0.0004

Figure 4 | Noise between two scans for cross-sectional versus longitudinal processing.
Differences in hippocampal volume between the first and second scan using cross-sectional processing (red) versus longitudinal processing (green). TP = time point.

certain extent imaging studies in general), and it also remains to be determined how these influence longitudinal processing.

A final approach to maximize statistical power is by **using more powerful statistical techniques**. In chapter 2.3 I describe a novel meta-analytical technique that allows for combining results from multiple studies in a way that yields the same results as a pooled analysis, which is statistically the most powerful, but does not require the raw data to be shared. This is relevant for many collaborative settings where the individual participant data cannot be shared due to various including legal, ethical, and logistic reasons. Such collaborations currently resort to less powerful meta-analytical techniques, but implementation of our novel method can both adhere to restrictions of not sharing individual participant data without compromising on statistical power. It will also be possible to include studies with small sample sizes that would otherwise have been

excluded in a conventional meta-analysis. This not only reduces statistical power, but potentially leads to a selection bias. Furthermore, in this thesis I focus on univariate linear regression models for analyzing associations between genetic variants and imaging markers. Here too there is room for improvement with more sophisticated methods including machine learning algorithms, e.g. deep learning or support vector machines.[81-85]

The **selection of imaging markers** will have an important impact on future research in a more general sense. Even though we might be able to obtain a more accurate hippocampal volume, this by itself is a fairly gross measure and simplifies the complexity within this brain structure. Genes themselves might affect specific regions of the brain and the use of an aggregate measure can make such localized effects difficult to find. An illustration of this is a genetic locus that was associated with hippocampal volume in chapter 3.1.2, using a sample of over 30,000 individuals, and was also genome-wide significant in chapter 2.4 when performing GWAS of all 7,000 voxels in the hippocampus. The latter analysis was done in only 4,400 individuals, but the higher resolution provided by studying voxels was able to outweigh the smaller sample size. An important part of this thesis was to make such genome-wide association studies of many (imaging) traits possible, and that has now been successfully done as described in chapter 2.4. Future studies should therefore not be restricted by previous computational and logistic issues that prohibited the use of novel imaging markers that aim to measure the brain in more comprehensive and biologically meaningful ways, usually with thousands to even millions of values. Naturally, these refined imaging markers can be of benefit to genetic discoveries, but perhaps even more so for understanding the pathophysiology of neurological diseases. Emerging imaging markers that can be relevant for neurodegenerative diseases include cortical thickness, surface area, and gyrification.[86-91] For cerebrovascular diseases genetic studies are needed on enlarged perivascular spaces and brain microbleeds.[92-97] Phenotyping of the brain for genetic studies need not be restricted to conventional MRI imaging. Future studies can extend the scope of imaging genetics to other clinically relevant and heritable imaging markers, including the microstructural integrity of white matter as measured by diffusion tensor imaging and functional connectivity assessed by functional MRI. [98-112]

A further consideration is that while a phenotypic correlation may exist between imaging markers and neurological diseases, and both may be heritable, this does not necessarily mean that the underlying genes are also shared. The presence of a *genetic correlation* is thus also important when determining whether a certain imaging marker is relevant for a certain disease. Currently, there has not been a **systematic mapping of genetic correlations** between imaging markers and neurological diseases. Such a study would provide valuable information for researchers regarding which imaging markers they actually need to investigate, especially as novel imaging markers are constantly being developed.[113-129] Even when the most relevant markers for a disease of interest have been identified, the genetic correlation will never be perfect. A risk of using *markers* of diseases for genetic discoveries will thus be that the identified variants are not necessarily related to the disease outcome. However, I would like to describe how a genetic correlation is not a requirement per se for variants to have a clinical utility. I now return to Figure 3 and focus on the genetic variants influencing imaging markers which are in intersection C and can be divided into two groups: those also associated with disease, intersection D, or those only influencing the imaging markers, i.e. the remaining part of intersection C. The genetic variants in D explain part of the variance in disease susceptibility, likely because the effect of these variants is exerted through changes in the brain that are captured by these imaging markers. Identification of such variants, as described in chapter 3, can thus directly be used to investigate their clinical utility in predicting disease onset, severity, or specific symptoms. For the remaining part of intersection C, the added value for prediction is less direct. Since only part of the variance in imaging markers is related to disease (intersection A), methods to reduce the 'non-relevant' variance could results in neuroimaging phenotypes with a better predictive performance. Thus genetic variants that influence clinically relevant imaging markers, but are themselves not related to disease, could help accentuate the variance in imaging markers that can predict disease. So, even when a genetic correlation between an imaging marker and disease is lacking, the identified genetic variants might still harbor clinical value.

Eventually the goal is to map the effects of all genetic variants on the brain so that this information can be leveraged for understanding pathophysiology and determining their

clinical relevance, as described above. Ideally, as with GWAS summary statistics, we will have **publicly available repositories** with these neuroimaging maps. It will then be possible to link genetic profiles of neurological diseases to the accompanying brain differences or to see whether a certain radiological presentation has a genetic basis. Furthermore, **cross-investigations with other sources of biological data** (e.g., transcriptomics, proteomics, metabolomics, microbiomics) can amplify the synergistic value of imaging genetics. These data represent yet another dimension that can be added on top of imaging and genetics, and may therefore also require **novel methods** to be developed for facilitating such studies.

CONCLUSION

In this thesis, I have used an imaging genetics approach to report novel gene discoveries, add to our understanding of the pathophysiology of neurological diseases, and explore the clinical relevance of genetics and neuroimaging. Furthermore, I describe how future research can build upon this work. Genetic discoveries can be boosted with larger samples, particularly biobanks, but also by using more comprehensive genotyping, refined imaging markers, and smarter data analysis. With the surge of novel imaging markers, it will also be good to determine which are the most relevant for specific outcomes. For this, a systematic investigation is needed of the phenotypic and genetic correlations between these markers and neurological diseases. Also, there is promise in combining imaging genetics with other biological data, but come with their own methodological challenges. Novel genetic discoveries can eventually lead to clinical translation, but the life cycle of such translational research can span many decades.[48] Similarly, most advancements in this thesis will not have a direct impact on patients or their physicians. Rather, this research lays groundwork to enable tangible clinical translation in the future.

REFERENCES

1. Bevan S, *et al.* Stroke. 2012
2. Gatz M, *et al.* The Journals of Gerontology Series A: Biological Sciences and Medical Sciences. 1997
3. Keller MF, *et al.* Human molecular genetics. 2012
4. Sadovnick *et al.* The Lancet. 1996
5. Fogh I, *et al.* Human molecular genetics. 2013
6. Lambert J-C, *et al.* Nature genetics. 2013
7. Nalls *et al.* Nature genetics. 2014
8. of the Cohorts NWG, *et al.* The Lancet Neurology. 2016
9. International Multiple Sclerosis Genetics C. Nature genetics. 2013
10. Van Deerlin VM, *et al.* Nature genetics. 2010
11. Gormley P, *et al.* Nature Genetics. 2016
12. Manolio TA, *et al.* Nature. 2009
13. Ikram MA, *et al.* Nat Genet. 2012
14. Stein JL, *et al.* Nat Genet. 2012
15. Farias ST, *et al.* Neurobiology of aging. 2012
16. Bis JC, *et al.* Nat Genet. 2012
17. Hibar DP, *et al.* Nature. 2015
18. van Erp TGM, *et al.* Molecular psychiatry. 2015
19. Schmaal L, *et al.* Molecular Psychiatry. 2015
20. Laakso *et al.* Neurology. 1996
21. Hevner RF. Brain overgrowth in disorders of rtk–pi3k–akt signaling: A mosaic of malformations. *Seminars in perinatology*. 2015;39:36-43
22. Rivière J-B, *et al.* Nature genetics. 2012
23. Boland E, *et al.* The American Journal of Human Genetics. 2007
24. Wang D, *et al.* American Journal of Medical Genetics Part A. 2013
25. Wardlaw JM, *et al.* The Lancet Neurology. 2013
26. Mills S, *et al.* The British journal of radiology. 2014
27. Vermeer SE, *et al.* New England Journal of Medicine. 2003
28. Wong TY, *et al.* Jama. 2002
29. Bos D, *et al.* JAMA neurology. 2014
30. Román *et al.* Neurology. 1993
31. Toledo JB, *et al.* Brain. 2013
32. Bos D, *et al.* Alzheimer's & Dementia. 2015
33. Verhaaren BF, *et al.* Circ Cardiovasc Genet. 2015
34. Debette S, *et al.* Stroke. 2010
35. Yang J, *et al.* The American Journal of Human Genetics. 2011
36. Ge T, *et al.* Proceedings of the National Academy of Sciences. 2015
37. Justice A, *et al.* Circulation. 2013
38. Wood AR, *et al.* Nat Genet. 2014
39. Rosenbloom KR, *et al.* Nucleic acids research. 2013
40. Hoffman MM, *et al.* Nucleic acids research. 2012
41. Bahcall OG. Nature Reviews Genetics. 2015
42. Zhu *et al.* Nature genetics. 2016
43. Hu J, *et al.* PLoS One. 2013
44. MacArthur, *et al.* Nature. 2014
45. van Scheltinga AFT, *et al.* Biological psychiatry. 2013
46. Van der Auwera S, *et al.* Biological psychiatry. 2015
47. Papiol S, *et al.* Translational psychiatry. 2014
48. Contopoulos-Ioannidis DG, *et al.* Science. 2008
49. Chouraki V, *et al.* J Alzheimers Dis. 2016
50. Verhaaren BFJ, *et al.* Biological psychiatry. 2013
51. Ripke S, *et al.* Nature. 2014
52. Okbay A, *et al.* Nature. 2016

53. Psaty BM, *et al.* Circulation: Cardiovascular Genetics. 2009
54. Thompson PM, *et al.* Neuroimage. 2015
55. Elliott P, *et al.* International Journal of Epidemiology. 2008
56. Consortium GNCGNC. European journal of epidemiology. 2014
57. Davies G, *et al.* Molecular psychiatry. 2016
58. Wain LV, *et al.* The Lancet Respiratory Medicine. 2015
59. Lane JM, *et al.* Nature communications. 2016
60. Hagenaars SP, *et al.* Molecular psychiatry. 2016
61. Gale CR, *et al.* Translational psychiatry. 2016
62. Lyall DM, *et al.* PloS one. 2016
63. Allen N, *et al.* Health Policy and Technology. 2012
64. McCarthy S, *et al.* bioRxiv. 2016
65. Davies K. *The $1,000 genome: The revolution in DNA sequencing and the new era of personalized medicine*. Simon and Schuster; 2015.
66. Tallantyre *et al.* Neurology. 2008
67. Tallantyre *et al.* J of Magnetic resonance imaging. 2010
68. Abduljalil *et al.* J of Magnetic Resonance Imaging. 2003
69. Robitaille *et al.* J of computer assisted tomography. 2000
70. Theysohn JM, *et al.* Magnetic Resonance Materials in Physics, Biology and Medicine. 2008
71. Reuter *et al.* Neuroimage. 2012
72. Bernal-Rusiel JL, *et al.* NeuroImage. 2013
73. Smith *et al.* Neuroimage. 2002
74. Scahill RI, *et al.* Archives of neurology. 2003
75. Kim P, *et al.* Behavioral neuroscience. 2010
76. Ho B-C, *et al.* Archives of general psychiatry. 2011
77. Cannon TD, *et al.* Biological psychiatry. 2015
78. Fjell AM, *et al.* The Journal of Neuroscience. 2013
79. Zhou Y, *et al.* Radiology. 2013
80. Couvy-Duchesne B, *et al.* NeuroImage. 2014
81. Burges CJC. Data mining and knowledge discovery. 1998
82. LeCun Y, *et al.* Nature. 2015
83. Hardoon DR, *et al.* Neural computation. 2004
84. Freund Y, *et al.* The alternating decision tree learning algorithm. *icml*. 1999;99:124-133
85. Freund Y, *et al.* Experiments with a new boosting algorithm. *Icml*. 1996;96:148-156
86. Liu T, *et al.* PloS one. 2012
87. Cash DM, *et al.*. *International Conference on Medical Image Computing and Computer-Assisted Intervention*. 2012:289-296
88. Dickerson BC, *et al.* Neurobiology of aging. 2009
89. Lerch *et al.* Cerebral cortex. 2005
90. Jubault T, *et al.* Neuroimage. 2011
91. Lyoo CH, *et al.* Movement Disorders. 2010
92. Maxwell SS, *et al.* Neurology. 2011
93. Cordonnier C, *et al.* Brain. 2011
94. Poels MMF, *et al.* Neurology. 2012
95. Brundel M, *et al.* Journal of Alzheimer's Disease. 2012
96. Weller R, *et al.* Brain pathology. 2008
97. Preston SD, *et al.* Neuropathology and applied neurobiology. 2003
98. Chua TC, *et al.* Current opinion in neurology. 2008
99. Douaud G, *et al.* Neuroimage. 2011
100. Nir TM, *et al.* NeuroImage: Clinical. 2013
101Jahanshad N, *et al.* Neuroimage. 2013
102Brouwer RM, *et al.* Neuroimage. 2010

103. Kochunov P, *et al.* Neuroimage. 2015
104. Jahanshad N, *et al.* Neuroimage. 2010
105. Sinclair B, *et al.* Neuroimage. 2015
106. Blokland GAM, *et al.* Biological psychology. 2008
107. Park J, *et al.* Neuroimage. 2012
108. Meyer-Lindenberg A. NeuroImage. 2012
109. Chen X, *et al.* Organization of Human Brain Mapping, Seattle, WA. 2013
110. Rombouts SARB, *et al.* Human brain mapping. 2005
111. Wang L, *et al.* Neuroimage. 2006
112. Grossman M, *et al.* Brain. 2003
113. Mitsumoto H, *et al.* Neurology. 2007
114. Meyer Clinical Pharmacology & Therapeutics. 2012
115. Ewers M, *et al.* Trends in neurosciences. 2011
116. de Almeida JRC, *et al.* Biological psychiatry. 2013
117. Nouretdinov I, *et al.* Neuroimage. 2011
118. Luckhaus C, *et al.* European Journal of Neurology. 2010
119. Saykin AJ, *et al.* Alzheimer's & Dementia. 2010
120. Kohannim O, *et al.* Neurobiology of aging. 2010
121. Hua X, *et al.* Neuroimage. 2013
122. Adams HH, *et al.* Biol Psychiatry. 2014
123. Gutman BA, *et al.*. In: Shen L, Liu T, Yap P-T, Huang H, Shen D, Westin C-F, eds. *Multimodal brain image analysis*. Springer International Publishing; 2013:246-257.
124. Gutman BA, *et al. Biomedical Imaging (ISBI), 2012 9th IEEE International Symposium on*. 2012:716-719
125. Adams HH, *et al.* Stroke. 2013
126. van Veluw SJ, *et al.* NeuroImage: Clinical. 2013
127. Charidimou A, *et al.* JNNP 2013
128. Fischl B, *et al.* Proc Natl Acad Sci U S A. 2000
129. Fischl *et al.* Cereb Cortex. 2004

.

Chapter 7

Summary / Samenvatting

ENGLISH SUMMARY

In this thesis I studied complex neurological diseases and focused on those of a neurodegenerative or cerebrovascular nature, which include very common and debilitating diseases. I have used genetics and neuroimaging to further our understanding of these diseases and the main findings, described in chapters 2 through 5, are summarized here.

Chapter 2 deals with methodological aspects related to genetics and neuroimaging. Chapter 2.1 describes a method for assessing a novel neuroimaging marker, enlarged perivascular spaces on MRI – an emerging marker of cerebrovascular disease – whereas chapter 2.2 presents a newly initiated global consortium to systematically investigate the clinical relevance of this marker. In chapter 2.3 we present a novel meta-analysis method for increased power and flexibility when individual participant data cannot be shared between sites. This is a common issue in multi-site studies, which are routinely performed in the field of genetics and increasingly so in neuroimaging. Building further upon this method, we developed a novel software in chapter 2.4 that enables genome-wide and brain-wide association studies, overcoming the huge computational and logistic limitations. Finally, chapter 2.5 highlights potential biases in a recent study on the transmissibility of amyloid-β , which illustrates how causal inference can be affected in observational studies.

Chapter 3 reports genetic discoveries of imaging markers, including those linked to neurodegeneration (chapter 3.1), cerebrovascular disease (chapter 3.2), and emerging imaging markers that are not as well established (chapter 3.3). In the largest discovery samples to date, we identified a total of 33 novel genetic variants in studies of 25,000 to 34,000 individuals. We describe studies of intracranial volume (chapter 3.1.1) , hippocampal volume (chapter 3.1.2), and the volumes of other subcortical brain structures (chapter 3.1.3). We further found genetic overlap between some of these markers and neurodegenerative diseases, which can aid in the discovery of disease genes. In chapter 3.2.1 I review our current knowledge of the genetics of cerebrovascular disease, which remains limited compared to other fields within neurology. Chapter 3.2.2 then describes the first estimates of the heritability of intracranial carotid artery

calcification and also identifies its first genetic determinants. In chapter 3.3.1, I studied the anterior commissure, a recently proposed imaging marker for neurodegeneration, and present the first heritability and genetic association analyses. Similarly, chapter 3.3.2 describes the first comprehensive investigation of the genetic determinants of human gait, which was imaged using an electronic walkway. Next, I focus on two emerging neuroimaging phenotypes: the shape of subcortical brain structures (chapter 3.3.3) and the grey matter density (chapter 3.3.4). These markers describe the structure of the brain with greater detail than the established markers by using thousands to millions of measures. We found both to be promising for genetic studies with high heritabilities, but also with regional variability in the extent of the genetic contribution.

Chapter 4 covers known disease genes and their effects on the brain, using candidate imaging markers (chapter 4.1) and unbiased searches of the brain (chapter 4.2). In chapter 4.1.1 we studied Alzheimer's disease genetic variants in relation to several key vascular and neurodegenerative markers and found these variants contribute to structural brain aging. In chapter 4.1.2, we report that variants for clinically diagnosed intracranial aneurysms relate to the size rather than the presence of aneurysms that were discovered incidentally in the general population. Chapter 4.1.3 describes a study of dystrophin gene variants and cognitive function, where no significant association was found. In the subsequent chapters, we report brain-wide studies of genetics variants that increase the risk of Alzheimer's disease (chapter 4.2.1), frontotemporal lobar degeneration (chapter 4.2.2 and chapter 4.2.3), and multiple sclerosis (chapter 4.2.4). We found that 'disease variants' also have subclinical effects on the brains of non-diseased individuals from the general population.

Chapter 5 focuses on the clinical relevance of neuroimaging and genetics for neurological disease, which is yet to be established for novel imaging markers (chapter 5.1) and recently identified genetic variants (chapter 5.2). In chapter 5.1.1, we study demographic and cardiovascular determinants of enlarged perivascular spaces and find that their burden is determined by various factors with considerable regional specificity, pointing towards a multifactorial origin. In chapter 5.1.2 we further find that enlarged perivascular spaces are related to the retinal microvasculature, providing strong evidence that these represent small vessel disease. Chapter 5.2.1 covers a study of

genetic risk factors for four neurodegenerative diseases in relation to mild cognitive impairment and incident dementia, and chapter 5.1.2 investigates the genetic risk of Parkinson's disease in relation to basic activities of daily living and incident Parkinson's disease. While both studies showed associations of the genetic variants with clinical endpoints there was little improvement in the ability to predict symptoms and disease at an individual level.

DUTCH SUMMARY

In dit proefschrift heb ik complexe neurologische ziektebeelden bestudeerd met een nadruk op neurodegeneratieve en cerebrovasculaire aandoeningen, welke veelvoorkomend zijn en slopende gevolgen kunnen hebben. Ik heb gebruik gemaakt van genetica en beeldvorming van de hersenen om ons begrip van deze ziektebeelden te bevorderen. De voornaamste bevindingen uit hoofdstukken twee tot en met vijf worden hier samengevat.

Hoofdstuk 2 behandelt methodologische aspecten die belangrijk zijn voor genetica en hersenbeeldvorming. Hoofdstuk 2.1 beschrijft een methode voor het bepalen van een nieuwe marker op hersenbeeldvorming, vergrote perivasculaire ruimtes op MRI – een opkomende marker van cerebrovasculaire aandoeningen – terwijl hoofdstuk 2.2 een recent geïnitieerd globaal consortium presenteert om systematisch te bestuderen wat de klinische relevantie is van deze marker. In hoofdstuk 2.3 presenteren we een nieuwe meta-analyse methode: deze methode verbetert de statistische kracht en flexibiliteit wanneer data van individuele deelnemers niet gedeeld kan worden tussen verschillende onderzoeksgroepen. Dit is een vaak voorkomend probleem in studies met meerder groepen, welke routinematig worden uitgevoerd binnen de genetica en ook steeds vaker in het veld van hersenbeeldvorming. Voortbouwend op deze methode hebben wij een nieuwe software ontwikkeld in hoofdstuk 2.4 die het mogelijk maakt om genoom-wijde en brein-wijde associatie studies uit te voeren door het wegnemen van beperkingen in de rekenkracht en logistiek. Tot slot benadrukt hoofdstuk 2.5 mogelijke aanwezigheid van bias in een recente studie over de overdraagbaarheid van het amyloid-β eiwit, wat illustreert hoe de causale gevolgtrekking kan worden beïnvloed in observationele studies.

Hoofdstuk 3 rapporteert genetische ontdekkingen van markers uit de beeldvorming, met inbegrip van markers die verband houden met neurodegeneratie (hoofdstuk 3.1), cerebrovasculaire aandoeningen (hoofdstuk 3.2), en opkomende markers welke nog niet gangbaar zijn (hoofdstuk 3.3). In de grootste ontdekkingsstudies tot nu toe hebben wij in totaal 33 nieuwe genetische varianten ontdekt door het onderzoeken van 25.000 tot 34.000 deelnemers. We beschrijven studies van het intracraniële volume (hoofdstuk

3.1.1) , het volume van de hippocampus (hoofdstuk 3.1.2), en het volume van andere subcorticale hersenstructuren (hoofdstuk 3.1.3). We hebben verder gevonden dat er genetische overlap is tussen deze markers en neurodegeneratieve aandoeningen, wat kan helpen bij het ontdekken van nieuwe ziektegenen. In hoofdstuk 3.2.1 geef ik een overzicht van onze huidige kennis van de genetica van cerebrovasculaire aandoeningen, die relatief beperkt blijft in vergelijking met andere gebieden binnen de neurologie. Hoofdstuk 3.2.2 beschrijft vervolgens de eerste schattingen van de erfelijkheid van calcificaties van de intracraniële halsslagader en identificeert ook de eerste genetische determinanten. In hoofdstuk 3.3.1 bestudeerden we de grootte van de commissura anterior, een recent voorgestelde marker van neurodegeneratie, en presenteren we de eerste erfelijkheid en genetische associatie analyses. Evenzo hoofdstuk 3.3.2, welke het eerste uitgebreide onderzoek beschrijft naar de genetische determinanten van het menselijke looppatroon, wat werd afgebeeld met behulp van een elektronische loopmat. Vervolgens richt ik me op twee opkomende hersenbeeldvorming markers: de vorm van de subcorticale hersenstructuren (hoofdstuk 3.3.3) en de grijzestofdichtheid (hoofdstuk 3.3.4). Deze markers beschrijven de hersenstructuur in groter detail dan de gangbare markers door duizenden tot miljoenen maten te gebruiken. Wij vonden beide markers veelbelovend te zijn voor genetische studies vanwege de hoge erfelijkheid, maar er was ook regionale variabiliteit in de mate waarin genen bijdragen.

Hoofdstuk 4 bestudeert bekende ziektegenen en hun effect op de hersenen, gebruikmakend van kandidaat beeldvormingsmarkers (hoofdstuk 4.1) en studies vrij van bias (hoofdstuk 4.2). In hoofdstuk 4.1.1 onderzochten we genetische varianten voor de ziekte van Alzheimer in relatie tot enkele belangrijke vasculaire en neurodegeneratieve markers en vonden dat deze varianten bijdragen aan structurele hersenveroudering. In hoofdstuk 4.1.2 rapporteren wij dat genetische varianten voor klinisch gediagnosticeerde intracraniële aneurysmata meer samenhangen met de grootte dan de aanwezigheid van aneursmata die onvoorzien zijn ontdekt in de algemene bevolking. Hoofdstuk 4.1.3 beschrijft een studie van genetische variatie in het dystrofine gen en cognitieve functie, waarin geen significante associatie was gevonden. In de volgende hoofdstukken rapporteren wij breinwijde studies van genetische varianten die het risico verhogen op de ziekte van Alzheimer (hoofdstuk 4.2.1), frontotemporale

lobaire degeneratie (hoofdstuk 4.2.2 en hoofdstuk 4.2.3), en multiple sclerosis (hoofdstuk 4.2.4). We vonden dat 'ziektegenen' ook subklinische effecten hebben op de hersenen van personen zonder ziekte uit de algemene bevolking.

Hoofdstuk 5 richt zich op de klinische relevantie van hersenbeeldvorming en genetica voor neurologische aandoeningen, wat nog moet worden vastgesteld voor nieuwe markers uit de beeldvorming (hoofdstuk 5.1) en recent geïdentificeerde genetische varianten (hoofdstuk 5.2). In hoofdstuk 5.1.1 bestuderen we demografische en cardiovasculaire determinanten van vergrote perivasculaire ruimten en vinden we dat hun ernst bepaald wordt door meerder factoren met een aanzienlijke specificiteit per hersengebied, wat wijst op een multifactoriële oorsprong. In hoofdstuk 5.1.2 zien we verder dat vergrote perivasculaire ruimten gerelateerd zijn met de retinale microvasculatuur, een sterke aanwijzing dat deze een vaatlijden vertegenwoordigen van de kleine hersenvaten. Hoofdstuk 5.2.1 heeft betrekking op een studie naar genetische risicofactoren voor vier neurodegeneratieve aandoeningen en hun relatie met milde cognitieve stoornissen en het ontwikkelen van dementie in de toekomst, en hoofdstuk 5.1.2 onderzoekt het genetisch risico op de ziekte van Parkinson met betrekking tot het uitvoeren van dagelijkse activiteiten en het ontwikkelen van de ziekte van Parkinson in de toekomst. Hoewel beide studies associaties tonen tussen genetische varianten en klinische eindpunten was er weinig verbetering in het vermogen om de symptomen en ziekten op individueel niveau te voorspellen.

Chapter 8

Epilogue

EPILOGUE

Epidemiology aims to answer one of the key questions humans currently face: what causes disease?

It is clear that for the numerous diseases that can befall us, the culprits can take various forms: they might be genes, what you eat and drink, or your environment. Consequently, an epidemiologist must become fluent in the relevant subject matter of a particular disease if he or she truly wishes to understand it. This is why epidemiologists can be seen asking you to fill out questionnaires, measuring your local water quality, or taking blood samples for further analysis in lab. The required skills and knowledge cannot be set in stone, making it a truly remarkable discipline. The drive to understand disease therefore leads to considerable heterogeneity between epidemiologists, but it is also what binds them.

The work in this thesis, where I investigated complex neurological diseases, underlines these characteristics of epidemiology. The chapters describe 'classic epidemiology', but also mathematics, bioinformatics, neuroimaging, genetics, and cell biology. Beyond the contents of these chapters, this thesis is also built upon friendship, collaboration, politics, anger management, business, and a healthy dose of mind games.

Although genetics is a key part of my thesis, it is important to realize the impact of your environment. During the past years, I was able to get a lot done, meaning I am indebted to a lot of people.

Guiding me through this journey, my supervisors have been crucial along the way.

My promotors **Prof.dr. Hofman** and **Prof.dr. Van der Lugt**:
Bert, thank you for the opportunity to be part of your department. Our first conversation was during my interview where I applied for the NIHES research master, and requested to do this in parallel to medical school and another research master. From all the people I had spoken to about this triple degree idea, you were literally the only person who supported me from the beginning. I have tried to repay this faith with my grades and master theses, and this doctorate thesis is the first fruit that was grown on this diverse education. Also, I would like to thank you for tempering two of my fears of growing old:

losing my passion and losing my hair. Although you don't believe in the term yourself, I think you are a great example of 'healthy aging'.

Aad, thank you for your contributions to the various manuscripts. I appreciate your attention to detail and also enjoyed our conversations about the 'big picture'. Your passion for radiology has definitely rubbed off on me during the past years.

My co-promotors **(Prof.)Dr. Ikram** and **Dr. Vernooij**:

You are both principal investigators at the Rotterdam Study, an impressive population-based study that is very suitable to investigate the central question of my thesis. However, larger studies are constantly being initiated, newer MRI scanners are becoming available, and the genetic technologies are revolutionized every few years. Why then choose to do my doctorate research here? More important than all these factors are the people you work with. I can honestly say that without you being my co-promotores, I would have probably even passed up the beautiful Rotterdam Study.

Arfan, you would typically be late to meetings, but compensate by immediately having great input. I joined the department around your thesis defence and it gives me joy that you are now becoming professor when I am defending mine. While you scientific achievements have been widely recognized, I also admire your broad interest and in-depth knowledge of other fields, whether it is physics, religion, or music.

Meike, your work ethic is unparalled. I often forget that besides running a successful research group you are also working in the clinic, and additionally have an active life beyond the Erasmus MC. It is amazing that you remain so approachable for your students and are always looking out for their best interests. It certainly explains why are loved by all who know you, and I feel lucky for having you as a co-promotor.

They say that the greatest compliment you can give your teachers is to surpass them, so I would like to thank you both for setting the bar extremely high for my PhD. I am sure your accomplishments will continue to motivate me during the rest of my career.

I'm also honered to have as part of my reading committee Prof.dr. Kushner, Prof.dr. Franke, and Prof.dr. Grabe. Steven, you're an inspiration for every young researcher and for me in particular for combining basic science with population level research. Barbara, you do wonderful work and I look forward to seeing Nijmegen and Rotterdam become

closer partners. Hans, it's inspiring to see you involved in so many endeavors but still managing to stay (or appear☺) relaxed at the same time.

I would also like to thank the Prof.dr. Tiemeier, Prof.dr. Uitterlinden, and Dr. White for being part of my committee:
Henning, while collaborations are usually initiated with a research question in mind, I can say that for me working with you is actually a goal by itself. André, thank you for your input on the various papers, especially when there was strict submission deadline! Tonya, it's great to see someone in your position who has retained a thorough understanding of all aspects of her field of research.

Given the impressive committee, I obvisously was left with no choice but to intimidate them with my paranymphs **Sirwan Darweesh** and **Gennady Roshchupkin**. This does not only apply to your physical prowess, but also your academic achievements.
Sirwan, before everything, you are truly an amazing friend. I cherish the valuable time we have spent together during past years, which have had a unique impact on me. I was excited that you decided to join our department and not at all surprised to see your rise to the top in such a short period. You surely have an amazing future ahead of you, which I will be following with the utmost interest.
Gena, I couldn't have wished for a better intellectual sparring partner during my PhD than you. From day one it felt like you were a longtime friend and this feeling has only become stronger after all the papers, 'short' stories, and discussions of various scientific and non-scientific topics. I look forward to our secret plan to take over Rotterdam.
Thank you both for having my back and let's continue the paranymph outings! While our marital status allows this, of course.

Next I would like to thank the participants of the Rotterdam Study, whose selflessness made this research possible. I feel connected with the Rotterdam Study, as we both had our conception in 1989 and actual birth in 1990. Many people have contributed to make this effort as successful as it is, which I couldn't possibly all name here, but I would like to mention at least a few of them. Frank, Yolande, and Nano, your continuous support of researchers is much appreciated. Also, I'm very grateful to the MRI personnel, including Charlotte, Pauli and Lydia: your dedication lies at the basis of all the data we publish on.

Furthermore, the former and current principal investigators of the Rotterdam Study for their vision and hard work. In particular, I would like to mention **Prof.dr. Breteler**, Prof.dr. Van Duijn, and Prof.dr. Franco:
Monique, I couldn't have wished for a better introduction to science. Your cirtical and results-oriented thinking have taught me a lot. I have to admit that as a teenager I was surprised that, instead of a textbook on the principles of epidemiology, your first suggested piece of literature was 'The Art of War' by Machiavelli. However, it makes sense now. Good luck with the new RS, I'm sure it will make a big impact on the field!
Cornelia, thank you for your valuable comments on manuscripts during the past years. Oscar, your positive energy is contagious and this effect is noticeable department-wide.

Making sure that all runs smoothly, there were Hetty, Jacqueline, Erica, and Gabrielle. I am very thankful for the secretarial support over the past years!

Leading up to my PhD, I have been lucky to receive an extraordinary scientific training. From NIHES, I would like to thank Astrid, Annet, Koos, Lenie, and Neetlje. From MolMed, my gratitude goes out to Prof.dr. Grootegoed, Benno, **Dr. Poot**, and Dr. Moen:
Raymond, while your track record initially attracted me to work in your lab, it was your mentorship that made me request an exception to stay there for a prolonged period. I greatly appreciate your advice on research projects, career choices, and personal matters. I hope we can build on the cellular epidemiology concept in the coming years.
Maaike, I've learned a lot from you about labwork, going from holding a pipet wrongly to performing elaborate experiments. You perfectly balanced out Raymond with your orderliness.☺ Although our years of work is represented by 'only' a single paper in my publication list, it holds a special place in my heart.

I would further like to thank **Prof.dr. Frens** and Prof.dr. Themmen. Maarten, you did an amazing job with the Honours Class. The program resulted in the connections that ultimately led to this thesis, and it was a great platform to meet and befriend likeminded students. I am proud to have been a part of it and hear similar things about the Erasmus University College. Good luck on your next steps!

Over the course of my PhD, I have shared offices with fantastic colleagues: Ben, thanks for your warm welcome into the group. I'm glad we could work together and wish you

all the best in the clinic and with the family life.

Vincent, thank you for some of the most unproductive times at the office, which is one of the dangers of having a similar (i.e., great) sense of humor. But I also should thank you for some of the most productive times, when discussing ideas for new projects, statistical or epidemiological concepts, or splitting the helpdesk work. It was a priviledge to be your paranymph and I can't wait to be there to celebrate your next achievements.

Saloua, oh Saloua. How I miss you. You inspired one of my candidate 11th propositions: "If there was a *SPSS* gene, it would be located on the Y chromosome." All kidding aside though, your hard work and pragmatic mindset are truly an inspiration.

Rens, I miss walking into an office filled with pictures of legs. I hope you will be able to satisfy your needs as a neurologist. Please come back every now and then for a match! And a rematch!

Liz! What can I say, we really had a  of a time. I wish you all the best at Harvard with Carlo. Thanks for staying in touch. You will probably be hearing about the great postdoc positions that Rotterdam is offering.☺

Daniel, I always had difficulty to determine what I enjoyed more: your presence, or the sound of your computer. Even though your stay in Boston made me realize I probably got the better half of the deal, I'm still looking forward to having you back.

Ryan, the most popular person of Erasmus MC. It's unbelievable how much work you got done, given that you were always helping out others, not least of all myself. Thanks for feeding me lots of sweets and always being available!

Tavia, you might be perfect. I'm pretty sure you are. I didn't think I could ever love someone as much as I love food, and you proved me right. Our lunches and dinners were amazing, and I can't wait to finish the ever-growing to-do list. Plus thanks for the geese! They look oriental. And yes, you're perfect.

Eline and Jory, I enjoyed your short but pleasant company in the office.

Next, my colleagues from the neuro-epi group:

Kamran, I'm glad you decided to return to Rotterdam, the city where everything happens (except for our lunch meetings). I'm looking forward to continue seeing you do great things.

Hazel, you were an adequate colleague. Other people that I would like to thank are

… hihi ☺ Oh Hazel, where to start? One of the first things I found out about you is that you also love sushi. It wasn't long before it became clear that we have much more in common: a geeky attraction to scripting, never closing a single web page (since you might need it some day), germophobia, other obsessive compulsive behaviours, and our favorite hobby – incidental finding ratings. However, there obviously are some differences too. For example, you would be much happier than me if the *KRTHAP1* gene was suddenly reactivated in humans. While this hasn't changed for me, other things have. I want to thank you for loosening me up a bit, or perhaps even too much: I think we can agree we were both quite successful in exploring the limits of what can and cannot be said (that's why they invented chocolate, right?). Hazel, thanks forever.

Saira, I can't wait to see you the 22nd of November! Thanks so much for booking a last minute flight, it wouldn't be the same without you! ☺ If however this does not make you feel guilty enough to fly across the Atlantic, please know that for me you never left – I still want to jump in and talk to you when I walk by your old office.

Abbas and Jasper, I'm very glad to have had such talented students. While you are both completing your medical studies now and considering to specialize afterwards, I think it is clear you would also have promising careers in research.

Frank, your research topic made you the centre of our group and I think we've learnt a lot from your healthy scepticism during the neuro meetings. It's too bad you will be travelling during my defence! Also, given your sense of humour, you might have realised there is a reason this is the only part of my thesis written in British English.

Lotte!! When people say 'Guess what?' my standard reply is 'You're pregnant?'. I was so happy that one day when I guessed correctly! I'm jealous of Vinz because he gets to spend more time with such a loving, talented, and energetic person.

Sanaz, how I enjoyed our shared interests. You are into self-mockery, and I'm also a big fan of mocking you. It's also not a coincidence that we both have a Dr. Phil seat / gossip-chair in our room. Thanks for the good times and for making me feel normal!

Sven, as a member of the three STW-musketeers you were essential for the scientific output. Besides this, you're also politically savvy and a very likable person. I can't wait for the moment a mini-Sven appears at our department!

Vanja, pile moje lepo! I always wondered what was under those bangs and I'm glad I

found out it was a dedicated and generous mind. Thanks for all the edible gifts from your trips, I'm pretty sure I can still smell one of them.☺ I'm hopeful you will still come by quite often when you're doing your PhD!
Unal, I've rarely seen someone so focused on getting results and I admire how much time and effort you spent on self improvement. But enough on foosball.
I also shared many moments with other colleagues from the neuro-epi: Ana, Ayesha, Eline, Elisabeth, Hoyan, Marielle, Marileen, Pauline, Pinar, Renée, Renske, Sander, Silvan, Sonja, Thom, Unal, and Vincent K.

My thanks also go out to others in our department, in particular the genetic epidemiology unit with Najaf, Dina, Adriana, Shazad, Ashley, and Ivana. For the cluster support, this includes Maarten and Lennart: thank you for the quick responses to my queries. Lennart, luckily my thesis is already written in English, so I don't need to translate it for you :).
Furthermore, I thank **Natalie** for the ups and downs of debugging PLINK, experimenting with our favorite function, and the discussions about ALBI and other new software. Your unquenchable thirst for improvement is admirable and I foresee a great career ahead of you. Maybe in the field of neuro?☺ Abbas, it has been great to see you grow over the years at our department and I envy your colleagues in London. Others I would like to mention are Carolina, Fernando, Janine, Symen, and Paul.

Much of the work in this thesis wouldn't have been possible without our close collaboration with BIGR, headed by **Prof.dr. Niessen**: Wiro, you have set up an amazing department and the many honors and prizes are a testimony to this. The team you have established is simply amazing.
Marius, you rock! I was really excited when, after sharing a lot of laughs, we finally also got to work together. While you now moved to Cambridge, it's luckily only a short fly away hihi. ;)
I'm also grateful for all the hard work of others, including: Annereet, Fedde, Florian, Hakim, Henri, Marcel, Marleen, Raimon, Wyke, and Yuan.

I have been privileged to work with many international collaborators as well through the CHARGE, UNIVRSE, and ENIGMA consortia. With great sample size comes great statistical

power and responsibility. My experiences gave me the fullest confidence that the future is in able hands, only a few of which I mention here: **Sudha Seshadri**, Lenore Launer, Myriam Fornage, Will Longstreth, Helena Schmidt, Josha Bis, Paul Nyquist, Stephanie Debette, Joanna Wardlaw, Ganesh Chauhan, Vincent Chouraki, Claudia Satizabal, Albert Smith, Edith Hofer, Charles DeCarli, Bernard Mazoyer, Reinhold Schmidt, Alexander Teumer, Tomáš Paus, Katharina Wittfeld, Mohamad Habes, Michelle Luciano, Christopher Chen, **Paul Thompson**, Derrek Hibar, Neda Jahanshad, and Boris Gutman.

Sudha, I have met people who were either very smart, friendly, strong, or huggable, but is so rare to all these traits in a single person. You continue to inspire me and undoubtledly many others.

Paul, it's truly amazing to work with the busiest person I know. When I visited your lab for half a year, I think there were two weeks where you weren't traveling. Nonetheless, you always make time for everyone and you still pay attention to details when reviewing a paper. LONI is very successful and an important reason for this is its excellent team:

Derrek, I miss you! Neda, I miss you more! Boris, I miss you even… ok, I definitely miss Neda the most. I really enjoyed working with you guys and I'm happy that you visited Rotterdam a few times. You are always welcome again, and the same goes for Adam, Jason, Josh, Madeleine, Priya, and Sarah, as well as the other LONI peeps.

I am also grateful to Alfred Aho, Peter Weinberger and Brian Kernighan.

I feel lucky to have such great **friends** who value the quality of our contact above the quantity. I hope that this thesis serves as a good alibi for the past years.

Spring, the ostrich delivery always was the highlight of my week. Two pistachios fighting (in) a nuclear reactor. Thank you so much for never delivering an ostrich.

Sinan, every now and then when work gets too stressful I think about your helmets. I hope you will continue to grow the collection in the future to reach your final goal of having approximately three helmets.

Michael, your charitable work is an inspiration to all of us, but especially to Martinox.

Evgeny, one of my fondest memories is of the day when someone we don't know settled a lawsuit. I wish you could have been there!

Rick, I would love to do a genetic study on you about stress resilience. Thanks for the great times and for giving me something to look forward to during my internships!

Nevertheless, genetics remain important, so I'd like to end by thanking my family.

أول الشجرة بذرة

At the first place my parents:

Thank you for planting the seed that would would turn into this thesis.

Pipi, you taught me to set big goals and work harder than everyone else to achieve them. I'm glad I inherited some of your appetite for knowledge and critical thinking, and I'm relieved you are not part of my committee. Thank you for raising me to be independent, but also for letting me know (very often) that you are there for me if I need anything.

Mimi, you taught me important lessons on dedication, compassion, and respect. Furthermore, I learned a lot about cooking, crocheting, and fashion design. Although I was often immersed in my laptop, your presence brought me a lot of joy and motivation, even though I might not have always shown this. Thank you for making me understand the value of family and for keeping us together.

I also owe a lot to my brothers, who nurtured this seed further:

Hu, you repeatedly reminded me that relaxing is just as important as work, if not more so. Looking back, I regret not taking you up on more offers to do things together because of a deadline, but we will compensate this surely! Thank you for being who you are, but above all, thank you for expanding our family: Hanin, I couldn't have wished for a sweeter sister.

Ha, all the pages in this book would not suffice to thank you for what you have done for me. You cultivated my creativity (HiHa-ballen), passion to save lives (the 'kussen'-incident), work ethic (Pokémon), scientific thinking ('leuk' discussiëren), and you taught me to live life to the fullest (the legendary CTCT trip). You are incontestably the smartest person I know, and your guidance is the foundation of this thesis and all my achievements. While it is an unreachable goal, I motivate myself by aiming to catch up to you one day. Thank you.

"Congratulations! Now, you found the most important magic in the world. It is love and friendship and mmhvummduokbm!".

Appendix

List of publications and manuscripts

This thesis

1. **Adams HH**, Cavalieri M, Verhaaren BF, Bos D, van der Lugt A, Enzinger C, Vernooij MW, Schmidt R, Ikram MA. Rating method for dilated virchow-robin spaces on magnetic resonance imaging. *Stroke*. 2013;44:1732-1735
2. **Adams HH**, Hilal S, Schwingenschuh P, Wittfeld K, van der Lee SJ, DeCarli C, Vernooij MW, Katschnig-Winter P, Habes M, Chen C, Seshadri S, van Duijn CM, Ikram MK, Grabe HJ, Schmidt R, Ikram MA. A priori collaboration in population imaging: The uniform neuro-imaging of virchow-robin spaces enlargement consortium. *Alzheimers Dement (Amst)*. 2015;1:513-520
3. **Adams HH**, Adams H, Launer LJ, Seshadri S, Schmidt R, Bis JC, Debette S, Nyquist PA, Van der Grond J, Mosley TH, Yang J, Teumer A, Hilal S, Roshchupkin GV, Wardlaw JM, Satizabal CL, Hofer E, Chauhan G, Smith AV, Yanek LR, Van der Lee SJ, Trompet S, Chouraki V, Arfanakis KA, Becker JT, Niessen WJ, De Craen AJ, Crivello FF, Lin LA, Fleischman DA, Wong TY, Franco OH, Wittfeld K, Jukema JW, De Jager PL, Hofman A, DeCarli C, Rizopoulos D, Longstreth WT, Mazoyer BM, Gudnason V, Bennett DA, Deary IJ, Ikram MK, Grabe HJ, Fornage M, Van Duijn CM, Vernooij MW, Ikram MA. Partial derivatives meta-analysis: Pooled analyses when individual participant data cannot be shared. *bioRxiv*. 2016:038893
4. Roshchupkin G, **Adams HH**, Vernooij M, Hofman A, van Duijn C, Ikram MA,** Niessen W.** Hase: Framework for efficient high-dimensional association analyses. *Scientific reports*. In press.
5. **Adams HH**, Swanson SA, Hofman A, Ikram MA. Amyloid-β transmission or unexamined bias [quest]. *Nature*. 2016;537:E7-E9
6. **Adams HH**,* Hibar DP,* Chouraki V,* Stein JL,* Nyquist PA,* Renteria ME,* Trompet S,* Arias-Vasquez A,* Seshadri S, Desrivieres S, Beecham AH, Jahanshad N, Wittfeld K, Van der Lee SJ, Abramovic L, Alhusaini S, Amin N, Andersson M, Arfanakis K, Aribisala BS, Armstrong NJ, Athanasiu L, Axelsson T, Beiser A, Bernard M, Bis JC, Blanken LM, Blanton SH, Bohlken MM, Boks MP, Bralten J, Brickman AM, Carmichael O, Chakravarty MM, Chauhan G, Chen Q, Ching CR, Cuellar-Partida G, Braber AD, Doan NT, Ehrlich S, Filippi I, Ge T, Giddaluru S, Goldman AL, Gottesman RF, Greven CU, Grimm O, Griswold ME, Guadalupe T, Hass J, Haukvik UK, Hilal S, Hofer E, Hoehn D, Holmes AJ, Hoogman M, Janowitz D, Jia T, Kasperaviciute D, Kim S, Klein M, Kraemer B, Lee PH, Liao J, Liewald DC, Lopez LM, Luciano M, Macare C, Marquand A, Matarin M, Mather KA, Mattheisen M, Mazoyer B, McKay DR, McWhirter R, Milaneschi Y, Mirza-Schreiber N, Muetzel RL, Maniega SM, Nho K, Nugent AC, Loohuis LM, Oosterlaan J, Papmeyer M, Pappa I, Pirpamer L, Pudas S, Putz B, Rajan KB, Ramasamy A, Richards JS, Risacher SL, Roiz-Santianez R, Rommelse N, Rose EJ, Royle NA, Rundek T, Samann PG, Satizabal CL, Schmaal L, Schork AJ, Shen L, Shin J, Shumskaya E, Smith AV, Sprooten E, Strike LT, Teumer A, Thomson R, Tordesillas-Gutierrez D,

Toro R, Trabzuni D, Vaidya D, Van der Grond J, Van der Meer D, Van Donkelaar MM, Van Eijk KR, Van Erp TG, Van Rooij D, Walton E, Westlye LT, Whelan CD, Windham BG, Winkler AM, Woldehawariat G, Wolf C, Wolfers T, Xu B, Yanek LR, Yang J, Zijdenbos A, Zwiers MP, Agartz I, Aggarwal NT, Almasy L, Ames D, Amouyel P, Andreassen OA, Arepalli S, Assareh AA, Barral S, Bastin ME, Becker DM, Becker JT, Bennett DA, Blangero J, van Bokhoven H, Boomsma DI, Brodaty H, Brouwer RM, Brunner HG, Buckner RL, Buitelaar JK, Bulayeva KB, Cahn W, Calhoun VD, Cannon DM, Cavalleri GL, Chen C, Cheng CY, Cichon S, Cookson MR, Corvin A, Crespo-Facorro B, Curran JE, Czisch M, Dale AM, Davies GE, De Geus EJ, De Jager PL, de Zubicaray GI, Delanty N, Depondt C, DeStefano AL, Dillman A, Djurovic S, Donohoe G, Drevets WC, Duggirala R, Dyer TD, Erk S, Espeseth T, Evans DA, Fedko IO, Fernandez G, Ferrucci L, Fisher SE, Fleischman DA, Ford I, Foroud TM, Fox PT, Francks C, Fukunaga M, Gibbs JR, Glahn DC, Gollub RL, Goring HH, Grabe HJ, Green RC, Gruber O, Gudnason V, Guelfi S, Hansell NK, Hardy J, Hartman CA, Hashimoto R, Hegenscheid K, Heinz A, Le Hellard S, Hernandez DG, Heslenfeld DJ, Ho BC, Hoekstra PJ, Hoffmann W, Hofman A, Holsboer F, Homuth G, Hosten N, Hottenga JJ, Pol HE, Ikeda M, Ikram MK, Jr CR, Jenkinson M, Johnson R, Jonsson EG, Jukema JW, Kahn RS, Kanai R, Kloszewska I, Knopman DS, Kochunov P, Kwok JB, Lawrie SM, Lemaitre H, Liu X, Longo DL, Jr WT, Lopez OL, Lovestone S, Martinez O, Martinot JL, Mattay VS, McDonald C, McIntosh AM, McMahon KL, McMahon FJ, Mecocci P, Melle I, Meyer-Lindenberg A, Mohnke S, Montgomery GW, Morris DW, Mosley TH, Muhleisen TW, Muller-Myhsok B, Nalls MA, Nauck M, Nichols TE, Niessen WJ, Nothen MM, Nyberg L, Ohi K, Olvera RL, Ophoff RA, Pandolfo M, Paus T, Pausova Z, Penninx BW, Pike GB, Potkin SG, Psaty BM, Reppermund S, Rietschel M, Roffman JL, Romanczuk-Seiferth N, Rotter JI, Ryten M, Sacco RL, Sachdev PS, Saykin AJ, Schmidt R, Schofield PR, Sigurdsson S, Simmons A, Singleton A, Sisodiya SM, Smith C, Smoller JW, Soininen H, Srikanth V, Steen VM, Stott DJ, Sussmann JE, Thalamuthu A, Tiemeier H, Toga AW, Traynor BJ, Troncoso J, Turner JA, Tzourio C, Uitterlinden AG, Hernandez MC, Van der Brug M, Van der Lugt A, Van der Wee NJ, Van Duijn CM, Van Haren NE, Van TED, Van Tol MJ, Vardarajan BN, Veltman DJ, Vernooij MW, Volzke H, Walter H, Wardlaw JM, Wassink TH, Weale ME, Weinberger DR, Weiner MW, Wen W, Westman E, White T, Wong TY, Wright CB, Zielke HR, Zonderman AB, Deary IJ, DeCarli C, Schmidt H, Martin NG, De Craen AJ, Wright MJ, Launer LJ,** Schumann G,** Fornage M,** Franke B,** Debette S,** Medland SE,** Ikram MA,** Thompson PM.** Novel genetic loci underlying human intracranial volume identified through genome-wide association. *Nat Neurosci*. 2016

7. Hibar DP,* **Adams HH**,* Jahanshad N,* Chauhan G,* Stein JL,* Hofer E,* Renteria ME,* Bis JC,* Arias-Vasquez A, Ikram MK, Desrivieres S, Vernooij MW, Abramovic L, Alhusaini S, Amin N, Andersson M, Arfanakis K, Aribisala BS, Armstrong NJ,

Athanasiu L, Axelsson T, Beecham AH, Beiser A, Bernard M, Blanton SH, Bohlken MM, Boks MP, Bralten J, Brickman AM, Carmichael O, Chakravarty MM, Chen Q, Ching CR, Chouraki V, Cuellar-Partida G, Braber AD, Doan NT, Ehrlich S, Filippi I, Ge T, Giddaluru S, Goldman AL, Gottesman RF, Greven CU, Grimm O, Griswold ME, Guadalupe T, Hass J, Haukvik UK, Hilal S, Hoehn D, Holmes AJ, Hoogman M, Janowitz D, Jia T, Kasperaviciute D, Kim S, Klein M, Kraemer B, Lee PH, Liao J, Liewald DC, Lopez LM, Luciano M, Macare C, Marquand A, Matarin M, Mather KA, Mattheisen M, Mazoyer B, McKay DR, McWhirter R, Milaneschi Y, Mirza-Schreiber N, Maniega SM, Nho K, Nugent AC, Nyquist PA, Loohuis LM, Oosterlaan J, Papmeyer M, Pirpamer L, Pudas S, Putz B, Rajan KB, Ramasamy A, Richards JS, Risacher SL, Roiz-Santianez R, Rommelse N, Rose EJ, Royle NA, Rundek T, Samann PG, Satizabal CL, Schmaal L, Schork AJ, Shen L, Shin J, Shumskaya E, Smith AV, Sprooten E, Strike LT, Teumer A, Thomson R, Tordesillas-Gutierrez D, Toro R, Trabzuni D, Trompet S, Vaidya D, Van der Grond J, Van der Lee SJ, Van der Meer D, Van Donkelaar MM, Van Eijk KR, Van Erp TG, Van Rooij D, Walton E, Westlye LT, Whelan CD, Windham BG, Winkler AM, Wittfeld K, Woldehawariat G, Wolf C, Wolfers T, Yanek LR, Yang J, Zijdenbos A, Zwiers MP, Agartz I, Aggarwal NT, Almasy L, Ames D, Amouyel P, Andreassen OA, Arepalli S, Assareh AA, Barral S, Bastin ME, Becker DM, Becker JT, Bennett DA, Blangero J, van Bokhoven H, Boomsma DI, Brodaty H, Brouwer RM, Brunner HG, Buckner RL, Buitelaar JK, Bulayeva KB, Cahn W, Calhoun VD, Cannon DM, Cavalleri GL, Chen C, Cheng CY, Cichon S, Cookson MR, Corvin A, Crespo-Facorro B, Curran JE, Czisch M, Dale AM, Davies GE, De Craen AJ, De Geus EJ, De Jager PL, de Zubicaray GI, Deary IJ, Debette S, DeCarli C, Delanty N, Depondt C, DeStefano AL, Dillman A, Djurovic S, Donohoe G, Drevets WC, Duggirala R, Dyer TD, Erk S, Espeseth T, Evans DA, Fedko IO, Fernandez G, Ferrucci L, Fisher SE, Fleischman DA, Ford I, Fornage M, Foroud TM, Fox PT, Francks C, Fukunaga M, Gibbs JR, Glahn DC, Gollub RL, Goring HH, Green RC, Gruber O, Gudnason V, Guelfi S, Hansell NK, Hardy J, Hartman CA, Hashimoto R, Hegenscheid K, Heinz A, Le Hellard S, Hernandez DG, Heslenfeld DJ, Ho BC, Hoekstra PJ, Hoffmann W, Hofman A, Holsboer F, Homuth G, Hosten N, Hottenga JJ, Pol HE, Ikeda M, Jr CR, Jenkinson M, Johnson R, Jonsson EG, Jukema JW, Kahn RS, Kanai R, Kloszewska I, Knopman DS, Kochunov P, Kwok JB, Lawrie SM, Lemaitre H, Liu X, Longo DL, Lopez OL, Lovestone S, Martinez O, Martinot JL, Mattay VS, McDonald C, McIntosh AM, McMahon KL, McMahon FJ, Mecocci P, Melle I, Meyer-Lindenberg A, Mohnke S, Montgomery GW, Morris DW, Mosley TH, Muhleisen TW, Muller-Myhsok B, Nalls MA, Nauck M, Nichols TE, Niessen WJ, Nothen MM, Nyberg L, Ohi K, Olvera RL, Ophoff RA, Pandolfo M, Paus T, Pausova Z, Penninx BW, Pike GB, Potkin SG, Psaty BM, Reppermund S, Rietschel M, Roffman JL, Romanczuk-Seiferth N, Rotter JI, Ryten M, Sacco RL, Sachdev PS, Saykin AJ, Schmidt H, Schmidt R, Schofield PR, Sigurdsson S, Simmons A, Singleton A, Sisodiya SM,

Smith C, Smoller JW, Soininen H, Srikanth V, Steen VM, Stott DJ, Sussmann JE, Thalamuthu A, Toga AW, Traynor BJ, Troncoso J, Turner JA, Tzourio C, Uitterlinden AG, Hernandez MC, Van der Brug M, Van der Lugt A, Van der Wee NJ, Van Haren NE, Van TED, Van Tol MJ, Vardarajan BN, Veltman DJ, Volzke H, Walter H, Wardlaw JM, Wassink TH, Weale ME, Weinberger DR, Weiner MW, Wen W, Westman E, White T, Wong TY, Wright CB, Zielke HR, Zonderman AB, Martin NG, Van Duijn CM, Wright MJ, Longstreth Jr WT, Schumann G,** Grabe HJ,** Franke B,** Launer LJ,** Medland SE,** Seshadri S,** Thompson PM,** Ikram MA.** Novel genetic loci underlying human intracranial volume identified through genome-wide association. *Nat Comm*. In press.

8. Satizabal CL*, **Adams HH***, Hibar DP, CHARGE consortium, ENIGMA consortium, Thompson PM, Seshadri S**, Ikram MA**. Genetic Determinants of MRI subcortical brain structures: 20 novel loci identified through GWAS in 26,000 persons. *In preparation*.
9. Ikram MA, Bersano A, Manso-Calderón R, Jia J, Schmidt H, Middleton L, Nacmias B, Siddiqi S, **Adams HH**. Genetics of Vascular Dementia: Consensus Report from the ICVD Working Group. *Submitted*.
10. **Adams HH**, Ikram MA, Vernooij MW, van Dijk AC, Hofman A, Uitterlinden AG, van Duijn CM, Koudstaal PJ, Franco OH, van der Lugt A, Bos D. Heritability and genome-wide association analyses of intracranial carotid artery calcification: The rotterdam study. *Stroke*. 2016;47:912-917
11. **Adams HH***, Teumer A*, Hibar DP*, Roshchupkin GV*, Amouyel P, Chauhan G, Debette S, Mazoyer B, Tzourio C, Davis KL, Parva P, DeCarli C, Huizinga W, Mahfouz A, Lelieveldt BPF, Kolovos P, Grosveld F, Poot A, Beiser A, Li S, Romero JR, Satizabal CL, Yang Q, Gudnason V, Launer LJ, Sigursson S, Smith A, Zijdenbos A, Fornage M, Gottesman RF, Griswold ME, Knopman DS, Mosley TH, Windham BG, Hofer E, Pirpamer L, Schmidt H, Schmidt R, Becker JT, Bis JT, Carmichael O, Longstreth, Jr WT, Lopez OL, Psaty BM, Rotter JI, Becker DM, Nyquist P, Vaidya D, Yanek LR, Aribisala BS, Bastin ME, Deary IJ, Liewald DC, Lopez LM, Luciano M, Muñoz Maniega S, Royle NA, Wardlaw JA, De Craen A, Ford I, Jukema JW, Stott DJ, Trompet S, Van der Grond J, Hegenscheid K, Hoffmann W, Homuth G, Hosten N, Janowitz D, Nauck M, Völzke H, Jahanshad N, Vernooij MW, Seshadri S, Niessen WJ**, Paul M Thompson**, Grabe HJ**, Ikram MA**. Genetic architecture of the human anterior commissure. *In preparation*.
12. **Adams HH***, Verlinden VJ*, Callisaya ML, van Duijn CM, Hofman A, Thomson R, Uitterlinden AG, Vernooij MW, van der Geest JN, Srikanth V, Ikram MA. Heritability and genome-wide association analyses of human gait suggest contribution of common variants. *J Gerontol A Biol Sci Med Sci*. 2016;71:740-746
13. Roshchupkin GV*, Gutman BA*, Vernooij MW, Jahanshad N, Martin NG, Hofman A, McMahon KL, Van der Lee S, Van Duijn CM, De Zubicaray G, Uitterlinden AG, Wright MJ, Niessen WJ, Thompson PM, Ikram MA**, **Adams HH****. Heritability of

the shape of subcortical brain structures in the general population. *Nat Comm*. In press.

14. Van der Lee S*, Roshchupkin GV*, **Adams HH***, Schmidt H, Hofer E, Saba Y, Schmidt R, Hofman A, Amin N, Van Duijn CM, Vernooij MW, Ikram MA, Niessen WJ. Grey matter heritability in family-based and population-based studies using voxel-based morphometry. *Submitted*.
15. Chauhan G*, **Adams HH***, Bis JC, Weinstein G, Yu L, Toglhofer AM, Smith AV, van der Lee SJ, Gottesman RF, Thomson R, Wang J, Yang Q, Niessen WJ, Lopez OL, Becker JT, Phan TG, Beare RJ, Arfanakis K, Fleischman D, Vernooij MW, Mazoyer B, Schmidt H, Srikanth V, Knopman DS, Jack CR, Jr., Amouyel P, Hofman A, DeCarli C, Tzourio C, van Duijn CM, Bennett DA, Schmidt R, Longstreth WT, Jr., Mosley TH, Fornage M, Launer LJ, Seshadri S, Ikram MA, Debette S. Association of alzheimer's disease gwas loci with mri markers of brain aging. *Neurobiol Aging*. 2015;36:1765 e1767-1716
16. Peymani A, **Adams HH**, Cremers LG, Krestin G, Hofman A, van Duijn CM, Uitterlinden AG, van der Lugt A, Vernooij MW, Ikram MA. Genetic determinants of unruptured intracranial aneurysms in the general population. *Stroke*. 2015;46:2961-2964
17. Vojinovic D, **Adams HH**, van der Lee SJ, Ibrahim-Verbaas CA, Brouwer R, van den Hout MC, Oole E, van Rooij J, Uitterlinden A, Hofman A, van IWF, Aartsma-Rus A, van Ommen GB, Ikram MA, van Duijn CM, Amin N. The dystrophin gene and cognitive function in the general population. *Eur J Hum Genet*. 2015;23:837-843
18. Roshchupkin GV*, **Adams HH***, van der Lee SJ*, Vernooij MW, van Duijn CM, Uitterlinden AG, van der Lugt A, Hofman A, Niessen WJ, Ikram MA. Fine-mapping the effects of alzheimer's disease risk loci on brain morphology. *Neurobiol Aging*. 2016;48:204-211
19. **Adams HH**, Verhaaren BF, Vrooman HA, Uitterlinden AG, Hofman A, van Duijn CM, van der Lugt A, Niessen WJ, Vernooij MW, Ikram MA. Tmem106b influences volume of left-sided temporal lobe and interhemispheric structures in the general population. *Biol Psychiatry*. 2014;76:503-508
20. **Adams HH**, Vernooij MW, Ikram MA. No evidence for a recessive effect of tmem106b rs1990622 variant in the general population. *Journal of Alzheimer's Disease*. 2015
21. Ikram MA, Vernooij MW, Roshchupkin GV, *, Hofman A, Van Duijn CM, Uitterlinden AG, Niessen WJ, Hintzen RQ, **Adams HH**. Genetic susceptibility to multiple sclerosis: brain structure and cognitive function in the general population. *Submitted*.
22. **Adams HH**, Schwingenschuh P, Wittfeld K, Hilal S, Ikram MA, Katschnig-Winter P, Habes M, Chen C, Seshadri S, van Duijn CM, Ikram MK, Grabe HJ, Schmidt R, Vernooij MW. Determinants of enlarged perivascular spaces in the general

population: a pooled analysis of individual participant data in the UNIVRSE consortium**.** *In preparation*.

23. Mutlu U, **Adams HH**, Hofman A, Lugt A, Klaver CC, Vernooij MW, Ikram MK, Ikram MA. Retinal microvascular calibers are associated with enlarged perivascular spaces in the brain. *Stroke*. 2016;47:1374-1376
24. **Adams HH**, de Bruijn RF, Hofman A, Uitterlinden AG, van Duijn CM, Vernooij MW, Koudstaal PJ, Ikram MA. Genetic risk of neurodegenerative diseases is associated with mild cognitive impairment and conversion to dementia. *Alzheimers Dement*. 2015;11:1277-1285
25. Darweesh SK*, Verlinden VJ*, **Adams HH***, Uitterlinden AG, Hofman A, Stricker BH, van Duijn CM, Koudstaal PJ, Ikram MA. Genetic risk of parkinson's disease in the general population. *Parkinsonism Relat Disord*. 2016;29:54-59

Other publications

26. Adams H, **Adams HH**, Jackson C, Rincon-Torroella J, Jallo GI, Quinones-Hinojosa A. Evaluating extent of resection in pediatric glioblastoma: A multiple propensity score-adjusted population-based analysis. *Childs Nerv Syst*. 2016;32:493-503
27. Gormley P, Anttila V, Winsvold BS, Palta P, Esko T, Pers TH, Farh KH, Cuenca-Leon E, Muona M, Furlotte NA, Kurth T, Ingason A, McMahon G, Ligthart L, Terwindt GM, Kallela M, Freilinger TM, Ran C, Gordon SG, Stam AH, Steinberg S, Borck G, Koiranen M, Quaye L, **Adams HH**, Lehtimaki T, Sarin AP, Wedenoja J, Hinds DA, Buring JE, Schurks M, Ridker PM, Hrafnsdottir MG, Stefansson H, Ring SM, Hottenga JJ, Penninx BW, Farkkila M, Artto V, Kaunisto M, Vepsalainen S, Malik R, Heath AC, Madden PA, Martin NG, Montgomery GW, Kurki MI, Kals M, Magi R, Parn K, Hamalainen E, Huang H, Byrnes AE, Franke L, Huang J, Stergiakouli E, Lee PH, Sandor C, Webber C, Cader Z, Muller-Myhsok B, Schreiber S, Meitinger T, Eriksson JG, Salomaa V, Heikkila K, Loehrer E, Uitterlinden AG, Hofman A, van Duijn CM, Cherkas L, Pedersen LM, Stubhaug A, Nielsen CS, Mannikko M, Mihailov E, Milani L, Gobel H, Esserlind AL, Christensen AF, Hansen TF, Werge T, International Headache Genetics C, Kaprio J, Aromaa AJ, Raitakari O, Ikram MA, Spector T, Jarvelin MR, Metspalu A, Kubisch C, Strachan DP, Ferrari MD, Belin AC, Dichgans M, Wessman M, van den Maagdenberg AM, Zwart JA, Boomsma DI, Smith GD, Stefansson K, Eriksson N, Daly MJ, Neale BM, Olesen J, Chasman DI, Nyholt DR, Palotie A. Meta-analysis of 375,000 individuals identifies 38 susceptibility loci for migraine. *Nat Genet*. 2016;48:856-866
28. Chouraki V, Reitz C, Maury F, Bis JC, Bellenguez C, Yu L, Jakobsdottir J, Mukherjee S, **Adams HH**, Choi SH, Larson EB, Fitzpatrick A, Uitterlinden AG, de Jager PL, Hofman A, Gudnason V, Vardarajan B, Ibrahim-Verbaas C, van der Lee SJ, Lopez O, Dartigues JF, Berr C, Amouyel P, Bennett DA, van Duijn C,

DeStefano AL, Launer LJ, Ikram MA, Crane PK, Lambert JC, Mayeux R, Seshadri S, International Genomics of Alzheimer's P. Evaluation of a genetic risk score to improve risk prediction for alzheimer's disease. *J Alzheimers Dis*. 2016;53:921-932

29. Hibar DP, Stein JL, Renteria ME, Arias-Vasquez A, Desrivieres S, Jahanshad N, Toro R, Wittfeld K, Abramovic L, Andersson M, Aribisala BS, Armstrong NJ, Bernard M, Bohlken MM, Boks MP, Bralten J, Brown AA, Chakravarty MM, Chen Q, Ching CR, Cuellar-Partida G, den Braber A, Giddaluru S, Goldman AL, Grimm O, Guadalupe T, Hass J, Woldehawariat G, Holmes AJ, Hoogman M, Janowitz D, Jia T, Kim S, Klein M, Kraemer B, Lee PH, Olde Loohuis LM, Luciano M, Macare C, Mather KA, Mattheisen M, Milaneschi Y, Nho K, Papmeyer M, Ramasamy A, Risacher SL, Roiz-Santianez R, Rose EJ, Salami A, Samann PG, Schmaal L, Schork AJ, Shin J, Strike LT, Teumer A, van Donkelaar MM, van Eijk KR, Walters RK, Westlye LT, Whelan CD, Winkler AM, Zwiers MP, Alhusaini S, Athanasiu L, Ehrlich S, Hakobjan MM, Hartberg CB, Haukvik UK, Heister AJ, Hoehn D, Kasperaviciute D, Liewald DC, Lopez LM, Makkinje RR, Matarin M, Naber MA, McKay DR, Needham M, Nugent AC, Putz B, Royle NA, Shen L, Sprooten E, Trabzuni D, van der Marel SS, van Hulzen KJ, Walton E, Wolf C, Almasy L, Ames D, Arepalli S, Assareh AA, Bastin ME, Brodaty H, Bulayeva KB, Carless MA, Cichon S, Corvin A, Curran JE, Czisch M, de Zubicaray GI, Dillman A, Duggirala R, Dyer TD, Erk S, Fedko IO, Ferrucci L, Foroud TM, Fox PT, Fukunaga M, Gibbs JR, Goring HH, Green RC, Guelfi S, Hansell NK, Hartman CA, Hegenscheid K, Heinz A, Hernandez DG, Heslenfeld DJ, Hoekstra PJ, Holsboer F, Homuth G, Hottenga JJ, Ikeda M, Jack CR, Jr., Jenkinson M, Johnson R, Kanai R, Keil M, Kent JW, Jr., Kochunov P, Kwok JB, Lawrie SM, Liu X, Longo DL, McMahon KL, Meisenzahl E, Melle I, Mohnke S, Montgomery GW, Mostert JC, Muhleisen TW, Nalls MA, Nichols TE, Nilsson LG, Nothen MM, Ohi K, Olvera RL, Perez-Iglesias R, Pike GB, Potkin SG, Reinvang I, Reppermund S, Rietschel M, Romanczuk-Seiferth N, Rosen GD, Rujescu D, Schnell K, Schofield PR, Smith C, Steen VM, Sussmann JE, Thalamuthu A, Toga AW, Traynor BJ, Troncoso J, Turner JA, Valdes Hernandez MC, van 't Ent D, van der Brug M, van der Wee NJ, van Tol MJ, Veltman DJ, Wassink TH, Westman E, Zielke RH, Zonderman AB, Ashbrook DG, Hager R, Lu L, McMahon FJ, Morris DW, Williams RW, Brunner HG, Buckner RL, Buitelaar JK, Cahn W, Calhoun VD, Cavalleri GL, Crespo-Facorro B, Dale AM, Davies GE, Delanty N, Depondt C, Djurovic S, Drevets WC, Espeseth T, Gollub RL, Ho BC, Hoffmann W, Hosten N, Kahn RS, Le Hellard S, Meyer-Lindenberg A, Muller-Myhsok B, Nauck M, Nyberg L, Pandolfo M, Penninx BW, Roffman JL, Sisodiya SM, Smoller JW, van Bokhoven H, van Haren NE, Volzke H, Walter H, Weiner MW, Wen W, White T, Agartz I, Andreassen OA, Blangero J, Boomsma DI, Brouwer RM, Cannon DM, Cookson MR, de Geus EJ, Deary IJ, Donohoe G, Fernandez G, Fisher SE, Francks C, Glahn DC, Grabe HJ, Gruber O, Hardy J, Hashimoto R, Hulshoff Pol HE, Jonsson

EG, Kloszewska I, Lovestone S, Mattay VS, Mecocci P, McDonald C, McIntosh AM, Ophoff RA, Paus T, Pausova Z, Ryten M, Sachdev PS, Saykin AJ, Simmons A, Singleton A, Soininen H, Wardlaw JM, Weale ME, Weinberger DR, **Adams HH**, Launer LJ, Seiler S, Schmidt R, Chauhan G, Satizabal CL, Becker JT, Yanek L, van der Lee SJ, Ebling M, Fischl B, Longstreth WT, Jr., Greve D, Schmidt H, Nyquist P, Vinke LN, van Duijn CM, Xue L, Mazoyer B, Bis JC, Gudnason V, Seshadri S, Ikram MA, Alzheimer's Disease Neuroimaging I, Consortium C, Epigen, Imagen, Sys, Martin NG, Wright MJ, Schumann G, Franke B, Thompson PM, Medland SE. Common genetic variants influence human subcortical brain structures. *Nature*. 2015;520:224-229

30. Hofer E, Cavalieri M, Bis JC, DeCarli C, Fornage M, Sigurdsson S, Srikanth V, Trompet S, Verhaaren BF, Wolf C, Yang Q, **Adams HH**, Amouyel P, Beiser A, Buckley BM, Callisaya M, Chauhan G, de Craen AJ, Dufouil C, van Duijn CM, Ford I, Freudenberger P, Gottesman RF, Gudnason V, Heiss G, Hofman A, Lumley T, Martinez O, Mazoyer B, Moran C, Niessen WJ, Phan T, Psaty BM, Satizabal CL, Sattar N, Schilling S, Shibata DK, Slagboom PE, Smith A, Stott DJ, Taylor KD, Thomson R, Toglhofer AM, Tzourio C, van Buchem M, Wang J, Westendorp RG, Windham BG, Vernooij MW, Zijdenbos A, Beare R, Debette S, Ikram MA, Jukema JW, Launer LJ, Longstreth WT, Jr., Mosley TH, Seshadri S, Schmidt H, Schmidt R, Cohorts for H, Aging Research in Genomic Epidemiology C. White matter lesion progression: Genome-wide search for genetic influences. *Stroke*. 2015;46:3048-3057
31. Akoudad S, Ikram MA, Portegies ML, **Adams HH**, Bos D, Hofman A, Koudstaal PJ, Uitterlinden AG, van der Lugt A, van Duijn CM, Vernooij MW. Genetic loci for serum lipid fractions and intracerebral hemorrhage. *Atherosclerosis*. 2016;246:287-292
32. Amin N, Jovanova O, **Adams HH**, Dehghan A, Kavousi M, Vernooij MW, Peeters RP, de Vrij FM, van der Lee SJ, van Rooij JG, van Leeuwen EM, Chaker L, Demirkan A, Hofman A, Brouwer RW, Kraaij R, Willems van Dijk K, Hankemeier T, van Ijcken WF, Uitterlinden AG, Niessen WJ, Franco OH, Kushner SA, Ikram MA, Tiemeier H, van Duijn CM. Exome-sequencing in a large population-based study reveals a rare asn396ser variant in the lipg gene associated with depressive symptoms. *Mol Psychiatry*. 2016
33. Bos D, Poels MM, **Adams HH**, Akoudad S, Cremers LG, Zonneveld HI, Hoogendam YY, Verhaaren BF, Verlinden VJ, Verbruggen JG, Peymani A, Hofman A, Krestin GP, Vincent AJ, Feelders RA, Koudstaal PJ, van der Lugt A, Ikram MA, Vernooij MW. Prevalence, clinical management, and natural course of incidental findings on brain mr images: The population-based rotterdam scan study. *Radiology*. 2016:160218
34. Verhaaren BF, Debette S, Bis JC, Smith JA, Ikram MK, **Adams HH**, Beecham AH, Rajan KB, Lopez LM, Barral S, van Buchem MA, van der Grond J, Smith AV,

Hegenscheid K, Aggarwal NT, de Andrade M, Atkinson EJ, Beekman M, Beiser AS, Blanton SH, Boerwinkle E, Brickman AM, Bryan RN, Chauhan G, Chen CP, Chouraki V, de Craen AJ, Crivello F, Deary IJ, Deelen J, De Jager PL, Dufouil C, Elkind MS, Evans DA, Freudenberger P, Gottesman RF, Guethnason V, Habes M, Heckbert SR, Heiss G, Hilal S, Hofer E, Hofman A, Ibrahim-Verbaas CA, Knopman DS, Lewis CE, Liao J, Liewald DC, Luciano M, van der Lugt A, Martinez OO, Mayeux R, Mazoyer B, Nalls M, Nauck M, Niessen WJ, Oostra BA, Psaty BM, Rice KM, Rotter JI, von Sarnowski B, Schmidt H, Schreiner PJ, Schuur M, Sidney SS, Sigurdsson S, Slagboom PE, Stott DJ, van Swieten JC, Teumer A, Toglhofer AM, Traylor M, Trompet S, Turner ST, Tzourio C, Uh HW, Uitterlinden AG, Vernooij MW, Wang JJ, Wong TY, Wardlaw JM, Windham BG, Wittfeld K, Wolf C, Wright CB, Yang Q, Zhao W, Zijdenbos A, Jukema JW, Sacco RL, Kardia SL, Amouyel P, Mosley TH, Longstreth WT, Jr., DeCarli CC, van Duijn CM, Schmidt R, Launer LJ, Grabe HJ, Seshadri SS, Ikram MA, Fornage M. Multiethnic genome-wide association study of cerebral white matter hyperintensities on mri. *Circ Cardiovasc Genet*. 2015;8:398-409

35. Chauhan G*, Arnold CR*, Chu AY*, Fornage M*, Reyahi A*, Bis JC*, Havulinna AS*, Sargurupremraj M, Smith AV, **Adams HH**, Choi SH, Pulit SL, Trompet S, Garcia ME, Manichaikul A, Teumer A, Gustafsson S, Bartz TM, Bellenguez C, Vidal JS, Jian X, Kjartansson O, Wiggins KL, Satizabal CL, Xue F, Ripatti S, Liu Y, Deelen J, Hoed Md, Bevan S, Hopewell JC, Malik R, Heckbert SR, Rice K, Smith NL, Levi C, Sharma P, Sudlow CL, Nik AM, Cole JW, Schmidt R, Meschia J, Thijs V, Lindgren A, Melander O, Grewal RP, Sacco RL, Rundek T, Rothwell PM, Arnett DK, Jern C, Johnson JA, Benavente OR, Wassertheil-Smoller S, Lee J, Wong Q, Aparicio HJ, Engelter ST, Kloss M, Leys D, Pezzini A, Buring JE, Ridker PM, Berr C, Dartigues J, Hamsten A, Magnusson PK, Traylor M, Pedersen NL, Lannfelt L, Lind L, Lindgren CM, Morris AP, Jimenez-Conde J, Montaner J, Radmanesh F, Slowik A, Woo D, Hofman A, Koudstaal PJ, Portegies ML, Uitterlinden AG, De Craen AJ, Ford I, Jukema JW, Stott DJ, Allen NB, Sale MM, Johnson AD, Bennett DA, De Jager PL, White CC, Grabe HJ, Markus MR, Schminke U, Boncoraglio GB, Clarke R, Kamatani Y, Dallongeville J, Lopez OL, Rotter JI, Nalls MA, Gottesman RF, Griswold ME, Knopman DS, Windham BG, Beiser A, Markus HS, Vartiainen E, French CR, Dichgans M, Pastinen T, Lathrop M, Gudnason V, Kurth T, Psaty BM, Harris TB, Rich SS, deStefano AL, Schmidt CO, Worrall BB, Rosand J, Salomaa V, Mosley TH, Ingelsson E, Van Duijn CM, Tzourio C, Rexrode KM, Lehmann OJ**, Launer LJ**, Ikram MA**, Carlsson P**, Chasman DI**, Childs SJ**, Longstreth Jr WT**, Seshadri S**, Debette. S**. Identification of additional risk loci for stroke and small vessel disease: A meta-analysis of genome-wide association studies. *The Lancet Neurology*. 2016;15:695-707

36. Davies G, Armstrong N, Bis JC, Bressler J, Chouraki V, Giddaluru S, Hofer E, Ibrahim-Verbaas CA, Kirin M, Lahti J, van der Lee SJ, Le Hellard S, Liu T, Marioni

RE, Oldmeadow C, Postmus I, Smith AV, Smith JA, Thalamuthu A, Thomson R, Vitart V, Wang J, Yu L, Zgaga L, Zhao W, Boxall R, Harris SE, Hill WD, Liewald DC, Luciano M, **Adams HH**, Ames D, Amin N, Amouyel P, Assareh AA, Au R, Becker JT, Beiser A, Berr C, Bertram L, Boerwinkle E, Buckley BM, Campbell H, Corley J, De Jager PL, Dufouil C, Eriksson JG, Espeseth T, Faul JD, Ford I, Generation S, Gottesman RF, Griswold ME, Gudnason V, Harris TB, Heiss G, Hofman A, Holliday EG, Huffman J, Kardia SL, Kochan N, Knopman DS, Kwok JB, Lambert JC, Lee T, Li G, Li SC, Loitfelder M, Lopez OL, Lundervold AJ, Lundqvist A, Mather KA, Mirza SS, Nyberg L, Oostra BA, Palotie A, Papenberg G, Pattie A, Petrovic K, Polasek O, Psaty BM, Redmond P, Reppermund S, Rotter JI, Schmidt H, Schuur M, Schofield PW, Scott RJ, Steen VM, Stott DJ, van Swieten JC, Taylor KD, Trollor J, Trompet S, Uitterlinden AG, Weinstein G, Widen E, Windham BG, Jukema JW, Wright AF, Wright MJ, Yang Q, Amieva H, Attia JR, Bennett DA, Brodaty H, de Craen AJ, Hayward C, Ikram MA, Lindenberger U, Nilsson LG, Porteous DJ, Raikkonen K, Reinvang I, Rudan I, Sachdev PS, Schmidt R, Schofield PR, Srikanth V, Starr JM, Turner ST, Weir DR, Wilson JF, van Duijn C, Launer L, Fitzpatrick AL, Seshadri S, Mosley TH, Jr., Deary IJ. Genetic contributions to variation in general cognitive function: A meta-analysis of genome-wide association studies in the charge consortium (n=53949). *Mol Psychiatry*. 2015;20:183-192

37. Atzmon G, Ben-Avraham D, Karasik D, Verghese J, Lunetta K, Smith J, Eicher J, Vered R, Deelen J, Arnold A, Buchman A, Tanaka T, Faul J, Nethander M, Fornage M, **Adams HH**, Matteini A, Callisaya M, Smith A, Yu L, De Jager P, Evans D, Gudnason V, Hofman A, Pattie A, Corley J, Launer L, Knopman D, Parimi N, Turner S, Bandinelli S, Beekman M, Mooijaart S, Liewald D, Houwing-Duistermaat J, Ohlsson C, Moed M, Verlinden V, Mellström D, Van der Geest J, Karlsson M, Hernandez D, McWhirter R, Liu Y, Thomson R, Tranah G, Uitterlinden A, Weir D, Zhao W, Starr J, Johnson A, Ikram MA, Bennett D, Cummings S, Deary I, Harris T, Kardia S, Mosley T, Srikanth V , Windham B, Newman A, Walston J, Davies G, Evans D, Slagboom E, Ferrucci L, Kiel D, Murabito J. The complex genetics of gait speed: genome-wide meta-analysis approach. *Aging*. In press.

38. Jahanshad N, Roshchupkin G, Faskowitz J, Hibar DP, Gutman BA, **Adams HH,** Niessen WJ, Vernooij MW, Ikram MA, Zwiers MP, Vasquez AA, Franke B, Ing A, Desrivieres S, Schumann G, de Zubicaraya GI, McMahonb KL, Medlandc SE, Wrightc MJ, Thompson PM. Multi-site meta-analysis of image-wide genome-wide associations of morphometry. *MICCAI Imaging Genetics Workshop*. 2015;2015

39. Moen M, **Adams HH***, Brandsma J*, Dekkers D, Akinci U, Karkampouna S, Kockx C, Ozgur Z, Van IJcken WFJ, Demmers J, Poot RA. An interaction network of mental disorder proteins in neural stem cells. *Submitted*.

40. Luik AI*, **Adams HH***, Zuurbier LA, Tiemeier H, Niessen WJ, Whitmore H, Ikram MA, Vernooij WM. Brain structure, EEG activity during sleep and sleep quality a population-based study of middle-aged and elderly persons. *Submitted.*
41. Sims R*, Van der Lee S*, Naj A*, Bellenguez C*, Badarinarayan N, Jakobsdottir J, Kunkle B, Boland A, Raybould R, Bis J, Martin E, Grenier-Boley B, Heilmann-Heimbach S, Chouraki V, Partch A, Sleegers K, Vronskaya M, Ruiz A, Graham R, Aloso R, Hoffmann P, Grove M, Hamilton-Nelson K, Hiltunen M, Nöthen M, White C, Beecham G, Epelbaum J, Maier W, Choi S, Valladares O, Dulary C, Herms S, Smith A, Qu L, Derbois C, Forstner A, Ahmad S, Zhao Y, Bacq D, Harold D, Satizabal C, Malamon J, Squassina A, Thomas R, Brody J, Dombroski B, Mateo I, Morgan T, Wolters F, Whitehead P, Garcia F, Denning N, Fornage M, Mukherjee S, Naranjo M, Majounie E, Mosley T, Cantwell L, Wallon D, Lupton M, Dupuis J, Crane P, Fratiglioni L, Medway C, Jian X, Keller L, Brown K, Lin H, Panza F, McGuinness B, Moreno-Grau S, Solfrizzi V, Proitsi P, **Adams HH**, Seripa D, Pastor P, Cupples L, Hannequin D, Frank-García A, Levy D, Caffarra P, Giegling I, Beiser A, Giedraitis V, Hampel H, Garcia M, Lannfelt L, Mecocci P, Eiriksdottir G, Pasquier F, Boccardi V, Henández I, Scherer M, Tarraga L, Leber M, Chen Y, Riedel-Heller S, Emilsson V, Braae A, Schmidt R, Masullo C, Schmidt H, Spalletta G, Jr W, Bossù P, Lopez O, Sacchinelli E, Boada M, Sánchez-Juan P, Yang Q, Jessen F, Li S, Morris J, Sotolongo-Grau O, Corcoran C, Himali J, Tschanz J, Fitzpatrick A, Norton M, Aspelund T, Munger R, Rotter J, Bullido M, Hofman A, Coto E, Boerwinkle E, Alvarez V, Rivadeneira F, GERAD/PERADES G, O'Donnell C, Gallo M, CHARGE C, ADGC A, EADI E, Bruni A, Dichgans M, Galimberti D, Scarpini E, Mancuso M, Bonuccelli U, Daniele A, Peters O, Nacmias B, Riemenschneider M, Heun R, Brayne C, Rubinsztein D, Bras J, Guerreiro R, Hardy J, Al-Chalabi A, Shaw C, Collinge J, Mann D, Tsolaki M, Clarimón J, Sussams R, Lovestone S, O'Donovan M, Owen M, Mead S, Uitterlinden A, Holmes C, Ingelsson M, Bennett D, Powell J, Graff C, De Jager P, Morgan K, Cambarros O, Psaty B, Passmore P, Behrens T, Berr C, Gudnason V, Rujescu D, Goate A, Dartigues J, DeStefano A, Ortega-Cubero S, Farrer L, campion D, Boada M, Kauwe J, Haines J, Van Broeckhoven C, Ikram M, Jones L, Mayeux R, Tzourio C, Launer L, Escott-Price V, Cruchaga C, Deleuze J, Amin N, Holmans P, Pericak-Vance M, Amouyel P**, van Duijn C**, Wang L**, Ramirez A**, Lambert J**, Seshadri S**, Williams J**, Schellenberg G**. Novel rare coding variants in PLCG2, ABI3 and TREM2 implicate microglial-mediated innate immunity in Alzheimer's disease. *Submitted.*
42. Verbruggen JG, Ikram MA, Roshchupkin GV, Verlinden VJA, Vrooman HA, Jaspers L, Niessen WJ, Vernooij MW, **Adams HH**. Asymptomatic intracranial meningiomas in the general population: spatial distribution and determinants. *In preparation*.
43. Evans TE, **Adams HH**, Licher S, Wolters FJ, Van der Lugt A, Ikram MK, O'Sullivan M, Vernooij MW, Ikram MA. Hippocampal Subregions Provide Information

Beyond Gross Hippocampal Volume for Cognitive Function and Risk of Dementia. *In preparation*.

44. Chauhan G*, **Adams HH***, Satizabal CL*, Bis JC*, Teumer A*, Hofer E, Trompet S, Hilal S, Smith AV, Jian X, Malik R, Traylor M, Pulit SL, Tzourio C, Amouyel P, Mazoyer B, Zhu Y, Dufouil C, Sargurupremraj M, Kaffashian S, Beecham GW, Montine TJ, Schellenberg GD, Kjartansson O, Gudnason V, Knopman DS, Griswold ME, Windham BG, Gottesman RF, Mosley TH, Schmidt R, Saba Y, Schmidt H, Takeuchi F, Yamaguchi S, Nabika T, Kato N, Rajan KB, Aggarwal NT, De Jager PL, Evans DA, Psaty BM, Rotter JI, Rice K, Lopez OL, Liao J, Chen C, Cheng CYu, Wong TY, Ikram MK, Van der Lee SJ, Amin N, Chouraki V, DeStefano AL, Aparicio HJ, Romero JR, Maillard P, DeCarli C, Wardlaw JM, Valdés Hernández M, Luciano M, Liewald D, Deary IJ, Slagboom PE, Beekman M, Deelen J, Uh H, Boncoraglio GB, Hopewell J, Beecham AH, Blanton SH, Wright CB, Sacco RL, Wen W, Thalamuthu A, Armstrong NJ, Chong E, De Craen AJM, Van der Grond J, Stott DJ, Ford I, Jukema JW, Vernooij MW, Hofman A, Uitterlinden AG, Van der Lugt A, Wittfeld K, Grabe HJ, Hosten N, Von Sarnowski B, Völker U, Levi C, Jimenez-Conde J, Sharma P, Sudlow CLM, Rosand J, Woo D, Cole JW, Meschia J, Słowik A, Thijs V, Lindgren A, Melander O, Grewal RP, Rundek T, Rexrode K, Rothwell PM, Arnett DK, Jern C, Johnson JA, Benavente OR, Wasssertheil-Smoller S, Lee J, Wong Q, Mitchell B, Rich SS, McArdle P, Geerlings MI, Van der Graag Y, De Bakker PIW, Asselbergs FW, Srikanth V, Thomson R, McWhirter R, Moran C, Callisaya M, Phan T, Rutten-Jacobs LCA, Bevan S, Mather KA, Sachdev PS, Van Duijn CM, Worrall BB, Dichgans M, Kittner SJ, Markus HS, Ikram MA**, Fornage M**, Launer LJ**, Seshadri S**, Longstreth WT**, Debette S**. Trans-ethnic gwas of mri-defined brain infarcts: Charge consortium. *In preparation*.

45. van der Lee SJ, **Adams HH**, Chouraki V, Satizabal CL, Yang Q, Li S, Debette SA, Yanek LR, DeCarli C, Hofer E, Yu L, Smith AV, Amin N, Seshadri S, Launer LJ, Tzourio C, Mazoyer B, Chauhan G, de Jager P, Arfanakis K, Fleischman DA, Bennett DA, Ikram MA, van Duijn CM. Genome-wide association study of lobar brain volumes. *In preparation*.

46. Chouraki VA, Jakobsdottir J, Mather K, **Adams HH,** Mollon J, Oldmeadow C, Thalamuthu A, Tanaka T, Scott R, Levy D, Holliday L, Song F, Thambisetty M, Poljak A, Eiriksdottir G, Sachdev PS, Gupta VB, Martins R, Launer L, Dobson R, Brodaty H, Attia J, Lovestone S, Gudnason V, Ikram M, Seshadri S. A genome-wide meta-analysis of plasma clusterin levels in the charge consortium. *In preparation*.

47. Fornage M, Jian X, Chouraki V, Bis JC, **Adams HH**, DeStefano A, Brody JA, Psaty BM, Gibbs RA, Ikram MA, DeCarli C, Mosley T, Longstreth W, van Duijn CM, Boerwinkle E, Seshadri S. Whole exome sequence analysis of white matter hyperintensities on cranial mri. *In preparation*.

48. Ikram MA, Zonneveld HI, Hofman A, Van Duijn CM, Uitterlinden AG, Vernooij MW, **Adams HH**. Genome-wide associations studies of cerebral blood flow. *In preparation.*
49. Van der Auwera S, Wittfeld K, **Adams HH**, Roshchupkin GV, Van Meurs J, Uitterlinden AG, Hofman A, Vernooij MW, Ikram MA, Homuth H Schurmann C, Völker U, Völzke H, Teumer A, Hosten N, Nauck M, Grabe HJ. The impact of whole-blood gene expression on brain white matter volume variation in two general population samples. *In preparation.*
50. **Adams HH**, Wen KX, Zonneveld HI, Hofman A, Van Duijn CM, Uitterlinden AG, Vernooij MW, Ikram MA. Migraine genetic variants influence cerebral blood flow. *In preparation.*
51. Zonneveld HI*, Roshchupkin GV*, **Adams HH**, Niessen WJ, Ikram MA, Vernooij MW. The neural substrate of cognition: an approach using voxel-based morphometry. *In preparation.*

**Contributed equally*

***Jointly directed the work*

PhD Portfolio

Name PhD student:	Hieab Adams
Research School:	Netherlands Institute for Health Sciences (NIHES)
Erasmus MC Departments:	Epidemiology
	Radiology and Nuclear Medicine
PhD period:	July 2013 – July 2016
Promotors:	Prof.dr. A. Hofman
	Prof.dr. A. van der Lugt
Copromotors:	Dr. M.A. Ikram
	Dr. M.W. Vernooij

	Year	Workload
1.) PhD Training		
General courses		
Master of Science in Health Sciences (NIHES)	2010-2013	120
Master of Science in Molecular Medicine (MolMed)	2010-2013	120
Research Integrity	2015	0.3
International Conferences		
CHARGE consortium meeting (Rotterdam, the Netherlands)	2013	0.5
Cognomics (Nijmegen, the Netherlands)	2013	1.1
Alzheimer's Association International Conferences (Copenhagen, Denmark)	2014	2.2
CHARGE consortium meeting (Washington, DC, USA)	2014	1.1
CHARGE consortium meeting (Los Angeles, CA, USA)	2014	1.1
HD-READy consortium meeting (Rotterdam, the Netherlands)	2014	2.0
International CAA conference (London, UK)	2014	1.2
CHARGE consortium meeting (Jackson, MS, USA)	2014	0.5
Congress of the European Academy of Neurology (Berlin, Germany)	2015	1.2
HD-READy consortium meeting (Rotterdam, the Netherlands)	2015	2.0
International Conference on Vascular Dementia (Ljubljana, Slovenia)	2015	1.1
VasCog conference (Tokyo, Japan)	2015	1.6
Alzheimer's Association International Conferences (Toronto, Canada)	2016	2.8
BRIDGET consortium meeting (Bordeaux, France)	2016	0.5
CHARGE consortium meeting (Charlottesville, VA, USA)	2016	1.1
VasCog conference (Amsterdam, the Netherlands)	2016	0.6
Research visits		
SHIP Study (Greifswald, Germany)	2013	
Laboratory Of NeuroImaging (Los Angeles, CA, USA)	2014-2015	
AGES Study (Reykyavik, Iceland)	2015	
Framingham Heart Study (Boston, MA, USA)	2015	

Workshops, Meetings, and Symposia		
Epidemiology research seminars	2012-2016	2.0
Genetic epidemiology research meetings	2013-2016	1.0
Molecular epidemiology research meetings	2013-2016	1.0
Workshop media contacts for researchers	2015	0.1

2.) Teaching Activities		
Supervision		
Abbas Peymani (master thesis): *Genetic Determinants of Unruptured Intracranial Aneurysms in the General Population*	2014-2015	3.0
Jasper Verbruggen (master thesis): *Asymptomatic intracranial meningiomas in the general population: spatial distribution and determinants , volume*	2014-2016	3.0
André Mamede Soares Braga (capstone thesis): *Pituitary gland volume and cortisol levels in elderly depressed individuals: the Rotterdam Study*	2015-2016	2.0
Junior Med School: *Hyperostosis Frontalis Interna in de algemene bevolking: prevalentie, risicofactoren en gevolgen*	2014	1.5
Junior Med School: *Gyrificatie: De vingerafdruk van het menselijk brein?*	2016	1.5
Geneeskunde KOW2: *Research proposal for identifying clinical indicators of intracranial arachnoid cyst diagnosis and prognosis with neuroimaging*	2014	0.8
Other Teaching Activities		
Coordinator, Scientific Speedreading – SC18	2015-2016	3.0
Teaching Assistant, Biostatistical Methods – CC02	2013-2015	0.6
Teaching Assistant, Erasmus Summer Program - ESP01	2015	0.2
Teaching Assistant, Erasmus Summer Program - ESP65	2012	0.2

3.) Other Activities		
Peer Review	2012-2016	3.0

1 ECTS (European Credit Transfer System) is equal to a workload of 28 hours

About the author

Hieab Adams was born on April 7th 1990 in Heerlen, the Netherlands. After graduating from the Erasmiaans Gymnasium, he went on to study Medicine at the Erasmus MC in Rotterdam and participated in the Honours Class program. From his second year onward, he was concurrently enrolled in two research master programs: one in Health Sciences and one in Molecular Medicine. For the former, he initiated his first epidemiological study under the supervision of Prof.dr. Monique Breteler and also received training at the Harvard School of Public Health. For the Molecular Medicine program, he performed basic science research on neural stem cell transcriptional regulation under the supervision of Dr. Raymond Poot. Furthermore, he committed during his studies to additional courses in Business Administration (Rotterdam School of Management) and microelectronics (Technical University Delft).

After obtaining his master degrees in 2013, Hieab initiated the genetic and neuroimaging studies on complex neurological diseases that culminated into his doctorate thesis. This work was primarily done at the departments of Epidemiology (Chair: Prof.dr. Hofman) and Radiology and Nuclear Medicine (Chair: Prof.dr. Krestin) of the Erasmus MC under the supervision of Dr. Arfan Ikram and Dr. Meike Vernooij. Additionally, he visited leading research centers including the Study of Health in Pomerania (Greifswald, Germany), the Age, Gene/Environment Susceptibility–Reykjavik Study (Reykyavik, Iceland), and the Framingham Heart Study (Boston, MA, USA). Notably, support by the Van Leersum Grant of the Royal Netherlands Academy of Arts and Sciences allowed him to work at the Laboratory Of Neuro Imaging (Los Angeles, CA, USA) in the group of Prof.dr. Paul Thompson.

In 2014, he received the Gerrit-Jan Mulder prize for best research master thesis, and won the Young Investigator's Award at the 2015 World Congress of the International Society for Vascular Behavioural and Cognitive Disorders (Tokyo, Japan). At the 2016 Cohorts for Heart and Aging Research in Genomic Epidemiology Consortium meeting (Charlottesville, VA, USA), Hieab was awarded a Golden Tiger for early career achievements.

Hieab will continue working at the department of Epidemiology (Chair: Prof.dr. Arfan Ikram) and concurrently finish his medical studies.